ISSN 1007-9327 (print)
ISSN 2219-2840 (online)

World Journal of *Gastroenterology*

World J Gastroenterol 2018 January 14; 24(2): 161-314

Published by Baishideng Publishing Group Inc

World Journal of Gastroenterology

Contents

Weekly Volume 24 Number 2 January 14, 2018

MINIREVIEWS

ORIGINAL ARTICLE

Basic Study

Case Control Study

Contents

World Journal of Gastroenterology
Volume 24 Number 2 January 14, 2018

Contents

World Journal of Gastroenterology
Volume 24 Number 2 January 14, 2018

ABOUT COVER

Editorial board member of *World Journal of Gastroenterology*, Gianluca Pellino, MD, Research Fellow, Surgeon, Unit of General and Geriatric Surgery, Università degli Studi della Campania "Luigi Vanvitelli", Naples 80138, Italy

AIMS AND SCOPE

World Journal of Gastroenterology (*World J Gastroenterol*, *WJG*, print ISSN 1007-9327, online ISSN 2219-2840, DOI: 10.3748) is a peer-reviewed open access journal. *WJG* was established on October 1, 1995. It is published weekly on the 7th, 14th, 21st, and 28th each month. The *WJG* Editorial Board consists of 642 experts in gastroenterology and hepatology from 59 countries.

The primary task of *WJG* is to rapidly publish high-quality original articles, reviews, and commentaries in the fields of gastroenterology, hepatology, gastrointestinal endoscopy, gastrointestinal surgery, hepatobiliary surgery, gastrointestinal oncology, gastrointestinal radiation oncology, gastrointestinal imaging, gastrointestinal interventional therapy, gastrointestinal infectious diseases, gastrointestinal pharmacology, gastrointestinal pathophysiology, gastrointestinal pathology, evidence-based medicine in gastroenterology, pancreatology, gastrointestinal laboratory medicine, gastrointestinal molecular biology, gastrointestinal immunology, gastrointestinal microbiology, gastrointestinal genetics, gastrointestinal translational medicine, gastrointestinal diagnostics, and gastrointestinal therapeutics. *WJG* is dedicated to become an influential and prestigious journal in gastroenterology and hepatology, to promote the development of above disciplines, and to improve the diagnostic and therapeutic skill and expertise of clinicians.

INDEXING/ABSTRACTING

World Journal of Gastroenterology (*WJG*) is now indexed in Current Contents®/Clinical Medicine, Science Citation Index Expanded (also known as SciSearch®), Journal Citation Reports®, Index Medicus, MEDLINE, PubMed, PubMed Central and Directory of Open Access Journals. The 2017 edition of Journal Citation Reports® cites the 2016 impact factor for *WJG* as 3.365 (5-year impact factor: 3.176), ranking *WJG* as 29th among 79 journals in gastroenterology and hepatology (quartile in category Q2).

NAME OF JOURNAL
World Journal of Gastroenterology

ISSN
ISSN 1007-9327 (print)
ISSN 2219-2840 (online)

LAUNCH DATE
October 1, 1995

FREQUENCY
Weekly

EDITORIAL OFFICE
Ze-Mao Gong, Director
World Journal of Gastroenterology
Baishideng Publishing Group Inc
7901 Stoneridge Drive, Suite 501,
Pleasanton, CA 94588, USA
Telephone: +1-925-2238242
Fax: +1-925-2238243
E-mail: editorialoffice@wjgnet.com
Help Desk: http://www.f6publishing.com/helpdesk
http://www.wjgnet.com

PUBLISHER
Baishideng Publishing Group Inc
7901 Stoneridge Drive, Suite 501,
Pleasanton, CA 94588, USA
Telephone: +1-925-2238242
Fax: +1-925-2238243
E-mail: bpgoffice@wjgnet.com
Help Desk: http://www.f6publishing.com/helpdesk
http://www.wjgnet.com

PUBLICATION DATE
January 14, 2018

INSTRUCTIONS TO AUTHORS
Full instructions are available online at http://www.wjgnet.com/bpg/gerinfo/204

ONLINE SUBMISSION
http://www.f6publishing.com

World Journal of Gastroenterology

Submit a Manuscript: http://www.f6publishing.com

World J Gastroenterol 2018 January 14; 24(2): 161-169

DOI: 10.3748/wjg.v24.i2.161

ISSN 1007-9327 (print) ISSN 2219-2840 (online)

MINIREVIEWS

Drug-eluting beads transarterial chemoembolization for hepatocellular carcinoma: Current state of the art

Antonio Facciorusso

Antonio Facciorusso, Gastroenterology Unit, Department of Medical Sciences, University of Foggia, Foggia 71122, Italy

ORCID number: Antonio Facciorusso (0000-0002-2017-2156).

Author contributions: Facciorusso A designed the study and wrote the paper.

Conflict-of-interest statement: None of the authors have received fees for serving as a speaker or are consultant/advisory board member for any organizations. None of the authors have received research funding from any organizations. None of the authors are employees of any organizations. None of the authors own stocks and/or share in any organizations. None of the authors own patents.

Manuscript source: Invited manuscript

Correspondence to: Antonio Facciorusso, MD, PhD, Assistant Professor, Gastroenterology Unit, Department of Medical Sciences, University of Foggia, Viale L.Pinto 1, Foggia 71100, Italy. antonio.facciorusso@virgilio.it
Telephone: +39-88-1732154
Fax: +39-88-1732135

Received: October 26, 2017
Peer-review started: October 27, 2017
First decision: November 21, 2017
Revised: December 16, 2017
Accepted: December 20, 2017
Article in press: December 20, 2017
Published online: January 14, 2018

Abstract

Transarterial chemoembolization (TACE) represents the current gold standard for hepatocellular carcinoma (HCC) patients in intermediate stage. Conventional TACE (cTACE) is performed with the injection of an emulsion of a chemotherapeutic drug with lipiodol into the artery feeding the tumoral nodules, followed by embolization of the same vessel to obtain a synergistic effect of drug cytotoxic activity and ischemia. Aim of this review is to summarize the main characteristics of drug-eluting beads (DEB)-TACE and the clinical results reported so far in the literature. A literature search was conducted using PubMed until June 2017. In order to overcome the drawbacks of cTACE, namely lack of standardization and unpredictability of outcomes, non-absorbable embolic microspheres charged with cytotoxic agents (DEBs) have been developed. DEBs are able to simultaneously exert both the therapeutic components of TACE, either drug-carrier function and embolization, unlike cTACE in which applying the embolic agent is a second moment after drug injection. This way, risk of systemic drug release is minimal due to both high-affinity carrier activity of DEBs and absence of a time interval between injection and embolization. However, despite promising results of preliminary studies, clear evidence of superiority of DEB-TACE over cTACE is still lacking. A number of novel technical devices are actually in development in the field of loco-regional treatments for HCC, but only a few of them have entered the clinical arena. In absence of well-designed randomized-controlled trials, the decision on whether use DEB-TACE or cTACE is still controversial.

Key words: Embolization; Doxorubicin; Conventional; Hepatocarcinoma; Liver cancer; Survival

Core tip: Aim of this review is to summarize the main characteristics and the clinical results of drug-eluting beads (DEB)-transarterial chemoembolization (TACE). To obviate to the limitations of cTACE, non-absorbable embolic microspheres charged with cytotoxic agents (DEBs) have been developed. DEBs are able to simultaneously exert both the therapeutic components of TACE, either drug-carrier function and embolization. This way, risk of systemic drug release is minimal. However, despite promising results of preliminary studies, clear evidence of superiority of DEB-TACE over cTACE is still lacking. In absence of well-designed randomized-controlled trials, the decision on whether use DEB-TACE or cTACE is still controversial.

Facciorusso A. Drug-eluting beads transarterial chemoembolization for hepatocellular carcinoma: Current state of the art. *World J Gastroenterol* 2018; 24(2): 161-169 Available from: URL: http://www.wjgnet.com/1007-9327/full/v24/i2/161.htm DOI: http://dx.doi.org/10.3748/wjg.v24.i2.161

INTRODUCTION

Transarterial chemoembolization (TACE) constitutes the gold standard for patients in intermediate stage according to the Barcelona Clinic Liver Cancer (BCLC) staging system, specifically those presenting with large or multifocal hepatocellular carcinoma (HCC) with preserved liver function, deteriorated performance status, and neoplastic portal vein thrombosis (PVT) or extrahepatic metastases[1,2]. By the way, TACE may constitute a valuable therapy also in early stage patients unsuitable to curative treatments, such as hepatic resection, liver transplantation (LT) or ablative therapy[3]. TACE is performed through the injection of a chemotherapeutic drug (mainly doxorubicin or cisplatin) selectively into the artery feeding the target tumoral nodules, followed by embolization of the same vessel to obtain a synergistic effect of either cytotoxic activity and ischemia[4]. Injection should be continued until the contrast column clears within 2-5 heartbeats (so called "near stasis") and a number of different embolic agents may be used (see below) to avoid drug release into the systemic circulation[5].

The different post-treatment outcomes are probably due to the fact that TACE is a not well standardized procedure widely varying as for chemotherapeutic agents injected, treatment devices used and therapeutic schedule. In fact, overall survival (OS) of patients treated with TACE ranges from 3.4 up to beyond 40 mo (median 16.5 mo[6]). The best survival median reported is 48 mo in a series recently published by the Barcelona group[7].

INDICATIONS AND SAFETY

Current guidelines consider as optimal candidates to TACE patients with preserved liver function, namely under or equal to Child-Pugh (CP) B7 stage without ascites in accordance with European Association for the Study of the Liver (EASL) guidelines[2] or CP A stage according to American Association for the Study of Liver Diseases (AASLD) guidelines[1].

Table 1 reports main absolute and relative contraindications to TACE.

Despite decompensated cirrhosis is commonly considered an absolute contraindication to TACE, some authors still consider chemoembolization as an option in cases of impaired portal blood flow[3].

Indeed, both EASL and AASLD guidelines strongly stand against use of TACE in PVT patients (defined as "advanced" according to BCLC staging system) because of the considerably increased risk of liver failure and consider sorafenib as the only validated option in attendance of definitive results of transarterial radioembolization (TARE) in such patients[8-10]. However, survival benefit of TACE over Best Supportive Care (BSC) has been observed in some small Asian RCTs and in a recent meta-analysis of 8 studies (of which 3 prospective) conducted in advanced HCC patients with PVT[11-13]. However, these results should be interpreted with caution since subjects with better liver function were preferably recruited in the TACE group while decompensated patients tended to be treated with BSC. The only published head-to-head comparison between TACE and sorafenib is a retrospective Austrian study which reported similar survival outcomes with a very competitive role of TACE in selected advanced patients (CP A and segmental PVT), as further confirmed in other observational studies[14,15]. By the way, the same selection bias can be detected in the Austrian study since thrombosis of the main trunk of portal vein (at more dismal prognosis) was more frequently observed in patients treated with sorafenib than in those who underwent TACE (25% *vs* 3%), thus claiming for great caution in interpreting this finding, and significantly higher severe adverse event (SAE) rate was experienced by TACE patients[14].

Hence, TACE may represent a valuable option for a specific subset of BCLC C patients (segmental PVT and CP A) who do not have access or are intolerant/unsuitable to sorafenib or TARE, however safety could represent an issue in these subjects and this therapeutic opportunity should be limited to highly-experienced centers[3].

Experts suggest also high tumor burden with massive replacing of both hepatic lobes as other absolute contraindication, whereas huge tumor nodule $\geqslant$ 10 cm, bile-duct occlusion, and untreated high-risk varices constitute relative contraindication rather than

Table 1 Absolute and relative contraindications to transarterial chemoembolization

Contraindications	
Absolute contraindications	Decompensated cirrhosis (Child-Pugh ⩾ B8)
	Extensive tumor with massive replacement of both entire lobes
	Severely reduced portal vein flow
	Technical impediments to hepatic intra-arterial treatment
Relative contraindications	Kidney failure
	Severe cardiopulmonary comorbidities
	Tumor size ⩾ 10 cm
	Untreated varices at high risk of bleeding
	Bile-duct occlusion

absolute ones[6].

A considerable number of patients treated with conventional TACE (cTACE) experience a transient episode of post-embolization syndrome (characterized by abdominal pain, fever and nausea), reported in 35% up to 100% of cases[16,17]. Treatment-related deaths are observed in ⩽ 2% of cases if proper selection of candidates is adopted[3,18].

Hence, according to current guidelines, TACE represents a safe treatment in selected subjects.

TREATMENT SCHEDULE

A single cycle of TACE is usually insufficient for effective treatment of intermediate-stage HCC and repeating TACE is widely recognized to prolong OS; however, guidelines do not specify the criteria for treatment repetition and current clinical practice relies only on expert opinions which suggest "on-demand" TACE (*i.e.*, number of sessions on the basis of tumor response after each TACE cycle) up to 3 to 4 times per year and switching to other therapeutic options in absence of response to at least 2 sessions[6,19].

As a consequence of the lack of sturdy and definitive data, there is great heterogeneity in applying TACE repetition in the common clinical practice, although a systematic review of observational and randomized trials reported a mean number of TACE sessions worldwide of 2.5 ± 1.5 per patient[20].

Many prognostic systems have been proposed to help the clinician in selecting appropriate candidates for starting or repeating TACE, but none of them achieved an universal validation mainly due to overfitting[21-23].

USEFULNESS OF DRUG INJECTION

Robust data in favor of a clear superiority of TACE (with chemotherapy injection) over TAE (bland embolization) is still lacking[24].

In fact, while the well-known hypervascularization of HCC nodules provides the rationale for the occlusion by embolic particles which results in tumour hypoxia and necrosis, on the other hand whether adding a local chemotherapeutic agent could determine a synergistic anti-tumor effect is still matter of debate[3,24].

A landmark RCT conducted in early 2000s comparing cTACE, TAE and BSC was prematurely terminated because such was the superiority of cTACE over BSC that keeping enrolling patients resulted unethical[25]. Unfortunately, this prevented the possibility to verify the competitive efficacy of TAE and only a comparable trend in OS with respect to TACE could be observed[25]. Similarly, no difference in terms of survival rates and safety was reported in another important multicentric American RCT published this year[26]. However, positive results by adding doxorubicin to drug-eluting bead (DEB)-TACE over bland embolization has been recently found in a Greek trial[27] and in a retrospective Italian report assessing as primary endpoint the degree of necrosis in explanted livers during OLT[28].

To make even more complicated this matter, there is no univocal agreement on the optimal chemotherapy to use in TACE. Worldwide, the most commonly used agent is doxorubicin administered at a dose ranging from 30 to 75 mg/m^2 (to a maximum of 150 mg)[3,5]. However, robust data provided by properly conducted RCTs are needed in order to deliver definitive indications in this regard.

DEVELOPMENT OF DEB-TACE AND TECHNICAL ASPECTS

Despite its well-proved efficacy and superiority over BSC, cTACE presents several unsolved issues. In fact, although lipiodol acts as a carrier of doxorubicin to the target nodules, release of the injected drug into systemic circulation has been demonstrated maybe due to the non-concomitant embolization, thus allowing release of a certain amount of doxorubicin in the interval time between injection and embolization[29]. Other important limitation of cTACE is the lack of standardization as the injected particles are prepared extemporaneously, therefore is operator-dependent (not standardized) and unstable[3,29].

The optimal procedure should be able to selectively deliver the injected chemotherapeutic into the target tumor where the drug should be retained with no passage into blood stream to avoid systemic toxicity[3].

In order to obviate to the aforementioned limitations of conventional TACE, non-absorbable embolic microspheres charged with cytotoxic agents (DEBs) have been developed.

DEBs are composed of a hydrophilic, ionic polymer that can bind anthracyclines via an ion exchange mechanism. The drug is usually loaded into DEBs prior to the TACE procedure creating a solution at a pre-defined concentration and then merging it into a vial with a slurry of DC Bead from which the packing solution has been removed[30]. The drug takes from 30 min to 2 h (depending on bead size) to be loaded

with small beads loading faster because of surface area effects. The maximum drug loading capacity is determined by the quantity of drug-binding sites in the beads, thus being the maximum dose dependent on drug molecular mass[30,31]. This is why a group of experts in the field has suggested in a recent review a dosage of 75 mg doxorubicin loaded into one vial of DC Bead for disease within the Milan criteria and up to 150 mg doxorubicin loaded into two vials of DC Bead in the case of Milan-out patients[5].

DEBs are able to simultaneously exert both the therapeutic components of TACE, either drug-carrier function and embolization, unlike cTACE in which applying the embolic agent is a second moment after drug injection. This way, risk of systemic drug release is minimal due to both high-affinity carrier activity of DEBs and absence of a time interval between injection and embolization.

An *in vitro* analysis showed that DEB spheres could be easily loaded with doxorubicin way better than other commercial embolic microspheres[32]. Furthermore, drug loading led to a decrease in the average size of the beads in function of the bead size and drug dose [32]. Interestingly, the same study calculated half-lives of drug-elution of 150 h for the 100-300-mc range to a maximum of 1730 h for the 700-900-mc size range while there was a fast release of the chemotherapeutic agent from the unstable Lipiodol emulsion with a half-life of approximately 1 h[32]. Authors then concluded that DEBs lead to an accurate dosage of drug per unit volume of beads and drug release is predictable and sustained, unlike Lipiodol. In addition to all of these advantages, beads are easy to handle and to deliver thus making them a valuable option for superselective TACE[32].

Plasma concentration of doxorubicin resulted very low (0.009-0.05 mmol/L at different consecutive time-points) after DEB-TACE in an in-animal study conducted in a rabbit model, suggesting considerable doxorubicin retention into the tumor[33]. This was significantly lower (70%-85% decrease in plasma concentration) than control animals treated with doxorubicin intra-arterially[33]. Of note, doxorubicin concentration into the nodule had a peak at 3 d (413.5 nmol/g), remaining high to 7 d (116.7 nmol/g) and then declining at 14 d (41.76 nmol/g), indicating continuous release of the drug from the microparticles[33]. As a consequence of this slower release of doxorubicin, maximal tumor necrosis was observed at 7 d, with limited local complications[33].

In vivo demonstration of the aforementioned strengths of DEBs has been provided by a French study conducted in 6 HCC patients who had undergone DEB-TACE before OLT[34]. Doxorubicin was detected on the explanted livers in an area of at least 1.2 mm in diameter around the occluded vessel. The tissue concentration of drug ranged from 5 μmol/L at 8 h to 0.65 μmol/L at 1 mo[34]. Necrotic tissue was characterized by a more profound penetration and a higher concentration of the drug than non necrotized areas. Authors concluded that DEBs provide a sustained delivery of drug for a period of 1 mo and local tissue concentrations above cytotoxic into the target nodules[34].

The first clinical study reporting the efficacy of DEB-TACE was a phase II study by the Barcelona group[35]. In this pivotal paper conducted on 27 CP A HCC treated with DEB-TACE (500-700 μm particles), objective response rate (ORR) was 66.6% (of which 26% complete responses) after two consecutive sessions performed 2 mo apart[35]. Doxorubicin maximal concentration (Cmax) and area under the curve were considerable inferior in DEB-TACE patients in comparison with a previous cohort of cTACE patients (P = 0.00002 and P = 0.001, respectively)[35]. Moreover, SAE rate was very low with only two cases of liver abscesses experienced by treated patients[35]. These findings were reproduced by Poon *et al*[36] with the maximal dose of doxorubicin (150 mg). Noteworthy, no patients in both studies experienced doxorubicin-related systemic adverse events (alopecia, bone marrow toxicity, dyspnea or pulmonary embolism)[35,36].

In light of the aforementioned in-animal studies[32,37], 100-300 μm beads became the most frequently used particles and are still actually recommended[5].

In early 2010s, two retrospective European studies reported striking survival results in unresectable HCC patients treated with 100-300 μm DEB-TACE, particularly 43.8 mo in a Greek series[38] and 48 mo of median OS in the Barcelona group's article[7]. These findings, really of note considering that TACE represents only a palliative therapy, paved the way to a wide use of DEB-TACE in the clinical practice.

COMPARATIVE EFFECTIVENESS OF DEB-TACE AND cTACE

In spite of the interesting findings of the aforementioned studies[35,36], data on comparative efficacy between cTACE and DEB TACE is still matter of debate. In fact, the 4 comparative RCTs and several retrospective studies report conflicting results.

The PRECISION V trial, a broad multicentric RCT published in 2010, enrolled 212 patients (75% BCLC B, 25% A; 80% CP A, 20% B) treated at 2-monthly intervals according a pre-defined schedule up to a maximum of three sessions[39,40]. Higher complete response, objective response, and disease control rates were registered in the DEB-TACE group (300-500 and 500-700 μm) as compared to cTACE (27% *vs* 22%, 52% *vs* 44%, and 63% *vs* 52%, respectively) but the hypothesis of superiority was not supported (one-sided P = 0.11)[40]. Primary endpoint (tumor response) was reached only in the subgroup of more advanced patients, namely those CP B, Eastern Cooperative Oncology Group (ECOG), bilobar and recurrent disease,

Table 2 Clinical studies comparing drug-eluting beads and conventional transarterial chemombolization

Study	Arm	Sample size	Study design	Region	CP (A/B/C)	BCLC (A/B/C)	1-yr survival
Lammer *et al*[40] 2010	DEB-TACE	93	RCT	Europe	77/16/0	24/69/0	NA
	cTACE	108			89/19/0	29/79/0	
Song *et al*[43] 2012	DEB-TACE	60	R	South Korea	56/4/0	27/33/0	88%
	cTACE	69			62/6/0	28/41/0	67%
Sacco *et al*[41] 2011	DEB-TACE	33	RCT	Italy	29/4/0	22/11/0	94.10%
	cTACE	34			25/9/0	22/12/0	90%
Van Malenstein *et al*[44] 2011	DEB-TACE	16	RCT	Belgium	14/2/0	9/5/2002	NA
	cTACE	14			14/0/0	10/3/2001	
Golfieri *et al*[42] 2014	DEB-TACE	89	RCT	Italy	75/14/0	41/26/22	86.20%
	cTACE	88			77/11/0	41/23/24	83.50%
Ferrer *et al*[45] 2011	DEB-TACE	47	P	Spain	NA	NA	88%
	cTACE	25			NA	NA	90%
Dhanasekaran *et al*[46] 2010	DEB-TACE	45	R	United States	11/12/2022	NA	58%
	cTACE	26			11/4/2011	NA	31%
Wiggermann *et al*[47] 2011	DEB-TACE	22	R	Germany	22/0/0	1/17/3	70%
	cTACE	22			22/0/0	4/15/2	55%
Recchia *et al*[48] 2012	DEB-TACE	35	P	Italy	NA	NA	63.40%
	cTACE	70			NA	NA	49.30%
Facciorusso *et al*[49] 2015	DEB-TACE	145	R	Italy	129/16/0	58/81/6	85%
	cTACE	104			93/11/0	41/63/0	92%
Arabi *et al*[50] 2015	DEB-TACE	35	R	Saudi Arabia	24/11/0	NA	72.70%
	cTACE	19			17/2/0	NA	74.50%
Kloeckner *et al*[51] 2015	DEB-TACE	76	R	Germany	51/22/3	8/34/34	45%
	cTACE	174			103/64/7	30/59/85	52%
Megias *et al*[52] 2015	DEB-TACE	30	R	Spain	46.7%[a]	NA	68%
	cTACE	30			63.3%[a]		58%
Liu *et al*[53] 2015	DEB-TACE	53	R	Taiwan	53/0/0	0/53/0	NA
	cTACE	64			64/0/0	6/58/0	
Scartozzi *et al*[54] 2010	DEB-TACE	64	R	Italy	57.1%[a]	NA	74%
	cTACE	87			58.6%[a]		93%

Percentage of CP A patients. CP: Child-Pugh; BCLC: Barcelona clinic liver cancer; DEB-TACE: Drug-eluting beads transarterial chemoembolization; cTACE: Conventional transarterial chemoembolization; RCT: Randomized controlled trial; P: Prospective non-randomized study; R: Retrospective study, [a]$P < 0.05$.

where DEB-TACE outperformed cTACE[40]. The sole result clearly in favor of DEB-TACE was a better safety profile with significant decrease in serious liver-related adverse events ($P < 0.001$) and systemic side effects (particularly alopecia) ($P = 0.0001$), while the incidence of post embolization syndrome was comparable in the treatment groups[40]. Unfortunately, the short follow-up time prevented assessment of OS and Time-to-Progression (TTP).

Two Italian RCTs failed to find any significant difference in tumor response and survival between the two TACE regimens[41,42]. In particular, the broad PRECISION ITALIA trial, a multicentre, RCT comparing "on demand" cTACE (with epirubicin injection) and DEB-TACE (100-300 μm loaded with 50 mg of doxorubicin), was stopped for futility at the second interim analysis when only 83% of the original planned sample size had been enrolled[42]. Of note, 46 (26%) patients were classified as BCLC C due to ECOG-1 status. Tumor response was similar between the two groups with the only difference registered as for complete response at 1 mo which resulted significantly higher after cTACE likely due to the lipiodol "staining" effect on CT-scan. In fact, at successive response assessments in concomitance with lipiodol discharge from the target nodule, this difference disappeared[42]. No difference neither in median TTP (9 mo in both treatment groups, $P = 0.766$) nor in 2-year survival rate (primary endpoint: 55.4% after cTACE and 56.8% after DEB-TACE, $P = 0.949$) was observed, hence the decision to prematurely stop the trial because the primary endpoint would have not been met[42]. Unlike the PRECISION trial, there was no significant difference in the incidence of AEs[42].

Retrospective studies reported discordant results, with only a single outlier Korean series clearly in favor of DEB-TACE[43].

Table 2 reports clinical studies comparing DEB-TACE and cTACE published so far[40-54].

A recent meta-analysis of 12 studies (4 RCTs and 8 observational) performed by my group reported similar pooled odds ratios of survival rate at 1, 2 and 3 years with a decreasing trend in favor of DEB-TACE (0.76, 0.68 and 0.57, respectively)[55]. This result was mainly determined by the difference in follow-up length between the two treatment groups in the retrospective reports since DEB-TACE patients, being DEBs recently introduced in the clinical practice, reported more frequent censored data and more limited absolute number of deaths[55]. In order to partially obviate to this bias, we plotted relative hazard ratios which are less sensitive to follow-up time bias and final result was a ratio close to 1 with no difference between the

two groups and low evidence of heterogeneity[55]. In particular, when restricting the analysis to only RCTs, the efficacy between the two techniques was absolutely comparable[55].

Our findings updated those of previous meta-analyses which had concluded that DEB-TACE is superior to cTACE as for objective response; by the way, these systematic reviews included a limited number of studies and were underpowered to properly explore the sources of the high heterogeneity found in their results[56,57]. Instead, no difference concerning neither tumor response nor safety profile was found in our meta-analysis which is in keeping with another recent systematic review[58].

In conclusion, as clearly stated in the editorial to this paper, no evidence enough to support the current extensive use of DEB-TACE exists[59]. The same editorial, commenting a cost-effective analysis published by the Bologna group[60], stated that the suggested cost-effectiveness advantage of DEB-TACE requires further trials conducted in countries other than Italy and with standardized procedures and clinical settings[59].

LATEST ADVANCEMENTS IN THE FIELD OF TRANSARTERIAL CHEMOEMBOLIZATION

Although a clear evidence of the superiority of DEB-TACE is still lacking, novel beads have been recently developed and clinically tested. As previously described, small microparticles have been found to determine necrosis of the target lesion as they lead to a more distal embolization, thus also obstructing collateral vessels[32,36,37]. Some concerns have been initially raised on the potential extrahepatic toxicity of these micro-particles due to the theoretical risk of their extrahepatic passage via collateral small vessels[61,62], but successive clinical reports have debunked this issue since smaller particles have been proved as safe if not more than conventional 100-300 μm and 300-500 μm[63-65]. In fact, Larger particles results in more proximal embolization and consequently in broader area of ischemia, thus increasing the risk of liver damage.

An Italian prospective series from Milan showed interesting results with DEBs 70-150 μm (M1®, BTG, United Kingdom)[66]. In this study conducted on 45 HCC early/intermediate patients, complete response was achieved in one third of them (33.3%) whereas other 20 (44.4%) reached partial response, accounting for a 77.7% ORR[66]. The histological analysis of 28 nodules in 13 explanted livers showed 100% necrosis (complete pathologic necrosis) in 7 cases and 90%-99% necrosis in 3 cases[66]. Noteworthy, only one SAE (grade 3) was reported, namely a case of bleeding from esophageal varices caused by the worsening of the portal hypertension[66]. These findings have been later confirmed in other retrospective studies[64,65].

HepaSphere microspheres 30-60 μm (Biosphere®, Merit, United States) constitute another promising device. HepaSphere 30-60 μmol/L is a new size of a loadable microsphere that has a dry caliber of 30-60 μmol/L that expands to 166-242 (197 ± 31) μmol/L in saline and 145-213 (148 ± 45) μmol/L after loading with doxorubicin[67]. In addition, doxorubicin was found to be released by the beads over 1 mo after TACE. Moreover, the concentration of doxorubicin in the treated tissue was high with very low plasma levels of the drug[67,68]. A recent Greek study enrolling 45 patients treated with HepaSphere microspheres 30-60 μmol/L found a complete response rate of 22.2% for the target lesions and ORR of 68.9%[69]. No patient died in the first year after TACE and no SAE was registered[69].

By the way, in absence of RCTs comparing these novel microspheres, no definitive indication can be released on which DEB should be used in the common clinical practice, and the decision still relies on local expertise or availability of device.

CONCLUSION

A number of novel technical devices are actually in development in the field of loco-regional treatments for HCC[70,71], but only a few of them have entered the clinical arena. Beside the lack of RCTs, many other issues remain unsolved, such as understanding the real balance between the two components of the therapy (*i.e.*, ischemia and cytotoxicity), further defining the several steps of hepatocarcinogenesis which could be targeted by combined pharmacological and interventional therapy[72-75], and identifying reliable prognostic markers in order to deliver a more precise oncology in patients really amenable of loco-regional treatments[76,77].

REFERENCES

1 **Heimbach JK**, Kulik LM, Finn RS, Sirlin CB, Abecassis MM, Roberts LR, Zhu AX, Murad MH, Marrero JA. AASLD guidelines for the treatment of hepatocellular carcinoma. *Hepatology* 2018; **67**: 358-380 [PMID: 28130846 DOI: 10.1002/hep.29086]

2 **European Association For The Study Of The Liver.**; European Organisation For Research And Treatment Of Cancer. EASL-EORTC clinical practice guidelines: management of hepatocellular carcinoma. *J Hepatol* 2012; **56**: 908-943 [PMID: 22424438 DOI: 10.1016/j.jhep.2011.12.001]

3 **Facciorusso A**, Licinio R, Muscatiello N, Di Leo A, Barone M. Transarterial chemoembolization: Evidences from the literature and applications in hepatocellular carcinoma patients. *World J Hepatol* 2015; **7**: 2009-2019 [PMID: 26261690 DOI: 10.4254/wjh.v7.i16.2009]

4 **Lencioni R**, Petruzzi P, Crocetti L. Chemoembolization of hepatocellular carcinoma. *Semin Intervent Radiol* 2013; **30**: 3-11 [PMID: 24436512 DOI: 10.1055/s-0033-1333648]

5 **Lencioni R**, de Baere T, Burrel M, Caridi JG, Lammer J, Malagari K, Martin RC, O'Grady E, Real MI, Vogl TJ, Watkinson A, Geschwind JF. Transcatheter treatment of hepatocellular carcinoma with Doxorubicin-loaded DC Bead (DEBDOX): technical recommendations. *Cardiovasc Intervent Radiol* 2012; **35**: 980-985 [PMID: 22009576 DOI: 10.1007/s00270-011-0287-7]

6 **Raoul JL**, Sangro B, Forner A, Mazzaferro V, Piscaglia F, Bolondi L, Lencioni R. Evolving strategies for the management of intermediate-stage hepatocellular carcinoma: available evidence and expert opinion on the use of transarterial chemoembolization. *Cancer Treat Rev* 2011; **37**: 212-220 [PMID: 20724077 DOI: 10.1016/j.ctrv.2010.07.006]

7 **Burrel M**, Reig M, Forner A, Barrufet M, de Lope CR, Tremosini S, Ayuso C, Llovet JM, Real MI, Bruix J. Survival of patients with hepatocellular carcinoma treated by transarterial chemoembolisation (TACE) using Drug Eluting Beads. Implications for clinical practice and trial design. *J Hepatol* 2012; **56**: 1330-1335 [PMID: 22314428 DOI: 10.1016/j.jhep.2012.01.008]

8 **Salem R**, Mazzaferro V, Sangro B. Yttrium 90 radioembolization for the treatment of hepatocellular carcinoma: biological lessons, current challenges, and clinical perspectives. *Hepatology* 2013; **58**: 2188-2197 [PMID: 23512791 DOI: 10.1002/hep.26382]

9 **Facciorusso A**, Serviddio G, Muscatiello N. Transarterial radioembolization vs chemoembolization for hepatocarcinoma patients: A systematic review and meta-analysis. *World J Hepatol* 2016; **8**: 770-778 [PMID: 27366304 DOI: 10.4254/wjh.v8.i18.770]

10 **Rognoni C**, Ciani O, Sommariva S, Facciorusso A, Tarricone R, Bhoori S, Mazzaferro V. Trans-arterial radioembolization in intermediate-advanced hepatocellular carcinoma: systematic review and meta-analyses. *Oncotarget* 2016; **7**: 72343-72355 [PMID: 27579537 DOI: 10.18632/oncotarget.11644]

11 **Luo J**, Guo RP, Lai EC, Zhang YJ, Lau WY, Chen MS, Shi M. Transarterial chemoembolization for unresectable hepatocellular carcinoma with portal vein tumor thrombosis: a prospective comparative study. *Ann Surg Oncol* 2011; **18**: 413-420 [PMID: 20839057 DOI: 10.1245/s10434-010-1321-8]

12 **Niu ZJ**, Ma YL, Kang P, Ou SQ, Meng ZB, Li ZK, Qi F, Zhao C. Transarterial chemoembolization compared with conservative treatment for advanced hepatocellular carcinoma with portal vein tumor thrombus: using a new classification. *Med Oncol* 2012; **29**: 2992-2997 [PMID: 22200992 DOI: 10.1007/s12032-011-0145-0]

13 **Xue TC**, Xie XY, Zhang L, Yin X, Zhang BH, Ren ZG. Transarterial chemoembolization for hepatocellular carcinoma with portal vein tumor thrombus: a meta-analysis. *BMC Gastroenterol* 2013; **13**: 60 [PMID: 23566041 DOI: 10.1186/1471-230X-13-60]

14 **Pinter M**, Hucke F, Graziadei I, Vogel W, Maieron A, Königsberg R, Stauber R, Grünberger B, Müller C, Kölblinger C, Peck-Radosavljevic M, Sieghart W. Advanced-stage hepatocellular carcinoma: transarterial chemoembolization versus sorafenib. *Radiology* 2012; **263**: 590-599 [PMID: 22438359 DOI: 10.1148/radiol.12111550]

15 **Kalva SP**, Pectasides M, Liu R, Rachamreddy N, Surakanti S, Yeddula K, Ganguli S, Wicky S, Blaszkowsky LS, Zhu AX. Safety and effectiveness of chemoembolization with drug-eluting beads for advanced-stage hepatocellular carcinoma. *Cardiovasc Intervent Radiol* 2014; **37**: 381-387 [PMID: 23754191 DOI: 10.1007/s00270-013-0654-7]

16 **Bruix J**, Llovet JM, Castells A, Montañá X, Brú C, Ayuso MC, Vilana R, Rodés J. Transarterial embolization versus symptomatic treatment in patients with advanced hepatocellular carcinoma: results of a randomized, controlled trial in a single institution. *Hepatology* 1998; **27**: 1578-1583 [PMID: 9620330 DOI: 10.1002/hep.510270617]

17 **Bayraktar Y**, Balkanci F, Kayhan B, Uzunalimoglu B, Gokoz A, Ozisik Y, Gurakar A, Van Thiel DH, Firat D. A comparison of chemoembolization with conventional chemotherapy and symptomatic treatment in cirrhotic patients with hepatocellular carcinoma. *Hepatogastroenterology* 1996; **43**: 681-687 [PMID: 8799415]

18 **Lencioni R**. Chemoembolization for hepatocellular carcinoma. *Semin Oncol* 2012; **39**: 503-509 [PMID: 22846867 DOI: 10.1053/j.seminoncol.2012.05.004]

19 **Bolondi L**, Burroughs A, Dufour JF, Galle PR, Mazzaferro V, Piscaglia F, Raoul JL, Sangro B. Heterogeneity of patients with intermediate (BCLC B) Hepatocellular Carcinoma: proposal for a subclassification to facilitate treatment decisions. *Semin Liver Dis* 2012; **32**: 348-359 [PMID: 23397536 DOI: 10.1055/s-0032-1329906]

20 **Forner A**, Ayuso C, Varela M, Rimola J, Hessheimer AJ, de Lope CR, Reig M, Bianchi L, Llovet JM, Bruix J. Evaluation of tumor response after locoregional therapies in hepatocellular carcinoma: are response evaluation criteria in solid tumors reliable? *Cancer* 2009; **115**: 616-623 [PMID: 19117042 DOI: 10.1002/cncr.24050]

21 **Sieghart W**, Hucke F, Pinter M, Graziadei I, Vogel W, Müller C, Heinzl H, Trauner M, Peck-Radosavljevic M. The ART of decision making: retreatment with transarterial chemoembolization in patients with hepatocellular carcinoma. *Hepatology* 2013; **57**: 2261-2273 [PMID: 23316013 DOI: 10.1002/hep.26256]

22 **Adhoute X**, Penaranda G, Naude S, Raoul JL, Perrier H, Bayle O, Monnet O, Beaurain P, Bazin C, Pol B, Folgoc GL, Castellani P, Bronowicki JP, Bourlière M. Retreatment with TACE: the ABCR SCORE, an aid to the decision-making process. *J Hepatol* 2015; **62**: 855-862 [PMID: 25463541 DOI: 10.1016/j.jhep.2014.11.014]

23 **Facciorusso A**, Bhoori S, Sposito C, Mazzaferro V. Repeated transarterial chemoembolization: An overfitting effort? *J Hepatol* 2015; **62**: 1440-1442 [PMID: 25678386 DOI: 10.1016/j.jhep.2015.01.033]

24 **Facciorusso A**, Bellanti F, Villani R, Salvatore V, Muscatiello N, Piscaglia F, Vendemiale G, Serviddio G. Transarterial chemoembolization vs bland embolization in hepatocellular carcinoma: A meta-analysis of randomized trials. *United European Gastroenterol J* 2017; **5**: 511-518 [PMID: 28588882 DOI: 10.1177/2050640616673516]

25 **Llovet JM**, Real MI, Montaña X, Planas R, Coll S, Aponte J, Ayuso C, Sala M, Muchart J, Solà R, Rodés J, Bruix J; Barcelona Liver Cancer Group. Arterial embolisation or chemoembolisation versus symptomatic treatment in patients with unresectable hepatocellular carcinoma: a randomised controlled trial. *Lancet* 2002; **359**: 1734-1739 [PMID: 12049862 DOI: 10.1016/S0140-6736(02)08649-X]

26 **Brown KT**, Do RK, Gonen M, Covey AM, Getrajdman GI, Sofocleous CT, Jarnagin WR, D'Angelica MI, Allen PJ, Erinjeri JP, Brody LA, O'Neill GP, Johnson KN, Garcia AR, Beattie C, Zhao B, Solomon SB, Schwartz LH, DeMatteo R, Abou-Alfa GK. Randomized Trial of Hepatic Artery Embolization for Hepatocellular Carcinoma Using Doxorubicin-Eluting Microspheres Compared With Embolization With Microspheres Alone. *J Clin Oncol* 2016; **34**: 2046-2053 [PMID: 26834067 DOI: 10.1200/JCO.2015.64.0821]

27 **Malagari K**, Pomoni M, Kelekis A, Pomoni A, Dourakis S, Spyridopoulos T, Moschouris H, Emmanouil E, Rizos S, Kelekis D. Prospective randomized comparison of chemoembolization with doxorubicin-eluting beads and bland embolization with BeadBlock for hepatocellular carcinoma. *Cardiovasc Intervent Radiol* 2010; **33**: 541-551 [PMID: 19937027 DOI: 10.1007/s00270-009-9750-0]

28 **Nicolini A**, Martinetti L, Crespi S, Maggioni M, Sangiovanni A. Transarterial chemoembolization with epirubicin-eluting beads versus transarterial embolization before liver transplantation for hepatocellular carcinoma. *J Vasc Interv Radiol* 2010; **21**: 327-332 [PMID: 20097098 DOI: 10.1016/j.jvir.2009.10.038]

29 **de Baere T**, Arai Y, Lencioni R, Geschwind JF, Rilling W, Salem R, Matsui O, Soulen MC. Treatment of Liver Tumors with Lipiodol TACE: Technical Recommendations from Experts Opinion. *Cardiovasc Intervent Radiol* 2016; **39**: 334-343 [PMID: 26390875 DOI: 10.1007/s00270-015-1208-y]

30 **Hecq JD**, Lewis AL, Vanbeckbergen D, Athanosopoulos A, Galanti L, Jamart J, Czuczman P, Chung T. Doxorubicin-loaded drug-eluting beads (DC Bead®) for use in transarterial chemoembolization: a stability assessment. *J Oncol Pharm Pract* 2013; **19**: 65-74 [PMID: 22801955 DOI: 10.1177/1078155212452765]

31 **Lewis AL**. DC Bead: a major development in the toolbox for the interventional oncologist. *Expert Rev Med Devices* 2009; **6**: 389-400 [PMID: 19572794 DOI: 10.1586/erd.09.20]

32 **Lewis AL**, Taylor RR, Hall B, Gonzalez MV, Willis SL, Stratford

PW. Pharmacokinetic and safety study of doxorubicin-eluting beads in a porcine model of hepatic arterial embolization. *J Vasc Interv Radiol* 2006; **17**: 1335-1343 [PMID: 16923981 DOI: 10.1097/01.RVI.0000228416.21560.7F]

33 **Hong K**, Khwaja A, Liapi E, Torbenson MS, Georgiades CS, Geschwind JF. New intra-arterial drug delivery system for the treatment of liver cancer: preclinical assessment in a rabbit model of liver cancer. *Clin Cancer Res* 2006; **12**: 2563-2567 [PMID: 16638866 DOI: 10.1158/1078-0432.CCR-05-2225]

34 **Namur J**, Citron SJ, Sellers MT, Dupuis MH, Wassef M, Manfait M, Laurent A. Embolization of hepatocellular carcinoma with drug-eluting beads: doxorubicin tissue concentration and distribution in patient liver explants. *J Hepatol* 2011; **55**: 1332-1338 [PMID: 21703190 DOI: 10.1016/j.jhep.2011.03.024]

35 **Varela M**, Real MI, Burrel M, Forner A, Sala M, Brunet M, Ayuso C, Castells L, Montañá X, Llovet JM, Bruix J. Chemoembolization of hepatocellular carcinoma with drug eluting beads: efficacy and doxorubicin pharmacokinetics. *J Hepatol* 2007; **46**: 474-481 [PMID: 17239480 DOI: 10.1016/j.jhep.2006.10.020]

36 **Poon RT**, Tso WK, Pang RW, Ng KK, Woo R, Tai KS, Fan ST. A phase I/II trial of chemoembolization for hepatocellular carcinoma using a novel intra-arterial drug-eluting bead. *Clin Gastroenterol Hepatol* 2007; **5**: 1100-1108 [PMID: 17627902 DOI: 10.1016/j.cgh.2007.04.021]

37 **Lee KH**, Liapi E, Ventura VP, Buijs M, Vossen JA, Vali M, Geschwind JF. Evaluation of different calibrated spherical polyvinyl alcohol microspheres in transcatheter arterial chemoembolization: VX2 tumor model in rabbit liver. *J Vasc Interv Radiol* 2008; **19**: 1065-1069 [PMID: 18589321 DOI: 10.1016/j.jvir.2008.02.023]

38 **Malagari K**, Pomoni M, Moschouris H, Bouma E, Koskinas J, Stefaniotou A, Marinis A, Kelekis A, Alexopoulou E, Chatziioannou A, Chatzimichael K, Dourakis S, Kelekis N, Rizos S, Kelekis D. Chemoembolization with doxorubicin-eluting beads for unresectable hepatocellular carcinoma: five-year survival analysis. *Cardiovasc Intervent Radiol* 2012; **35**: 1119-1128 [PMID: 22614031 DOI: 10.1007/s00270-012-0394-0]

39 **Vogl TJ**, Lammer J, Lencioni R, Malagari K, Watkinson A, Pilleul F, Denys A, Lee C. Liver, gastrointestinal, and cardiac toxicity in intermediate hepatocellular carcinoma treated with PRECISION TACE with drug-eluting beads: results from the PRECISION V randomized trial. *AJR Am J Roentgenol* 2011; **197**: W562-W570 [PMID: 21940527 DOI: 10.2214/AJR.10.4379]

40 **Lammer J**, Malagari K, Vogl T, Pilleul F, Denys A, Watkinson A, Pitton M, Sergent G, Pfammatter T, Terraz S, Benhamou Y, Avajon Y, Gruenberger T, Pomoni M, Langenberger H, Schuchmann M, Dumortier J, Mueller C, Chevallier P, Lencioni R; PRECISION V Investigators. Prospective randomized study of doxorubicin-eluting-bead embolization in the treatment of hepatocellular carcinoma: results of the PRECISION V study. *Cardiovasc Intervent Radiol* 2010; **33**: 41-52 [PMID: 19908093 DOI: 10.1007/s00270-009-9711-7]

41 **Sacco R**, Bargellini I, Bertini M, Bozzi E, Romano A, Petruzzi P, Tumino E, Ginanni B, Federici G, Cioni R, Metrangolo S, Bertoni M, Bresci G, Parisi G, Altomare E, Capria A, Bartolozzi C. Conventional versus doxorubicin-eluting bead transarterial chemoembolization for hepatocellular carcinoma. *J Vasc Interv Radiol* 2011; **22**: 1545-1552 [PMID: 21849247 DOI: 10.1016/j.jvir.2011.07.002]

42 **Golfieri R**, Giampalma E, Renzulli M, Cioni R, Bargellini I, Bartolozzi C, Breatta AD, Gandini G, Nani R, Gasparini D, Cucchetti A, Bolondi L, Trevisani F; PRECISION ITALIA STUDY GROUP. Randomised controlled trial of doxorubicin-eluting beads vs conventional chemoembolisation for hepatocellular carcinoma. *Br J Cancer* 2014; **111**: 255-264 [PMID: 24937669 DOI: 10.1038/bjc.2014.199]

43 **Song MJ**, Chun HJ, Song DS, Kim HY, Yoo SH, Park CH, Bae SH, Choi JY, Chang UI, Yang JM, Lee HG, Yoon SK. Comparative study between doxorubicin-eluting beads and conventional transarterial chemoembolization for treatment of hepatocellular carcinoma. *J Hepatol* 2012; **57**: 1244-1250 [PMID: 22824821 DOI: 10.1016/j.jhep.2012.07.017]

44 **van Malenstein H**, Maleux G, Vandecaveye V, Heye S, Laleman W, van Pelt J, Vaninbroukx J, Nevens F, Verslype C. A randomized phase II study of drug-eluting beads versus transarterial chemoembolization for unresectable hepatocellular carcinoma. *Onkologie* 2011; **34**: 368-376 [PMID: 21734423 DOI: 10.1159/000329602]

45 **Ferrer Puchol MD**, la Parra C, Esteban E, Vaño M, Forment M, Vera A, Cosín O. [Comparison of doxorubicin-eluting bead transarterial chemoembolization (DEB-TACE) with conventional transarterial chemoembolization (TACE) for the treatment of hepatocellular carcinoma]. *Radiologia* 2011; **53**: 246-253 [PMID: 21295802 DOI: 10.1016/j.rx.2010.07.010]

46 **Dhanasekaran R**, Kooby DA, Staley CA, Kauh JS, Khanna V, Kim HS. Comparison of conventional transarterial chemoembolization (TACE) and chemoembolization with doxorubicin drug eluting beads (DEB) for unresectable hepatocelluar carcinoma (HCC). *J Surg Oncol* 2010; **101**: 476-480 [PMID: 20213741 DOI: 10.1002/jso.21522]

47 **Wiggermann P**, Sieron D, Brosche C, Brauer T, Scheer F, Platzek I, Wawrzynek W, Stroszczynski C. Transarterial Chemoembolization of Child-A hepatocellular carcinoma: drug-eluting bead TACE (DEB TACE) vs. TACE with cisplatin/lipiodol (cTACE). *Med Sci Monit* 2011; **17**: CR189-CR195 [PMID: 21455104 DOI: 10.12659/MSM.881714]

48 48 **Recchia F**, Passalacqua G, Filauri P, Doddi M, Boscarato P, Candeloro G, Necozione S, Desideri G, Rea S. Chemoembolization of unresectable hepatocellular carcinoma: Decreased toxicity with slow-release doxorubicin-eluting beads compared with lipiodol. *Oncol Rep* 2012; **27**: 1377-1383 [PMID: 22294036 DOI: 10.3892/or.2012.1651]

49 **Facciorusso A**, Mariani L, Sposito C, Spreafico C, Bongini M, Morosi C, Cascella T, Marchianò A, Camerini T, Bhoori S, Brunero F, Barone M, Mazzaferro V. Drug-eluting beads versus conventional chemoembolization for the treatment of unresectable hepatocellular carcinoma. *J Gastroenterol Hepatol* 2016; **31**: 645-653 [PMID: 26331807 DOI: 10.1111/jgh.13147]

50 **Arabi M**, BenMousa A, Bzeizi K, Garad F, Ahmed I, Al-Otaibi M. Doxorubicin-loaded drug-eluting beads versus conventional transarterial chemoembolization for nonresectable hepatocellular carcinoma. *Saudi J Gastroenterol* 2015; **21**: 175-180 [PMID: 26021777 DOI: 10.4103/1319-3767.157571]

51 **Kloeckner R**, Weinmann A, Prinz F, Pinto dos Santos D, Ruckes C, Dueber C, Pitton MB. Conventional transarterial chemoembolization versus drug-eluting bead transarterial chemoembolization for the treatment of hepatocellular carcinoma. *BMC Cancer* 2015; **15**: 465 [PMID: 26059447 DOI: 10.1186/s12885-015-1480-x]

52 **Megías Vericat JE**, García Marcos R, López Briz E, Gómez Muñoz F, Ramos Ruiz J, Martínez Rodrigo JJ, Poveda Andrés JL. Trans-arterial chemoembolization with doxorubicin-eluting particles versus conventional trans-arterial chemoembolization in unresectable hepatocellular carcinoma: A study of effectiveness, safety and costs. *Radiologia* 2015; **57**: 496-504 [PMID: 25857250 DOI: 10.1016/j.rx.2015.01.008]

53 **Liu YS**, Ou MC, Tsai YS, Lin XZ, Wang CK, Tsai HM, Chuang MT. Transarterial chemoembolization using gelatin sponges or microspheres plus lipiodol-doxorubicin versus doxorubicin-loaded beads for the treatment of hepatocellular carcinoma. *Korean J Radiol* 2015; **16**: 125-132 [PMID: 25598680 DOI: 10.3348/kjr.2015.16.1.125]

54 **Scartozzi M**, Baroni GS, Faloppi L, Paolo MD, Pierantoni C, Candelari R, Berardi R, Antognoli S, Mincarelli C, Risaliti A, Marmorale C, Antico E, Benedetti A, Cascinu S. Trans-arterial chemoembolization (TACE), with either lipiodol (traditional TACE) or drug-eluting microspheres (precision TACE, pTACE) in the treatment of hepatocellular carcinoma: efficacy and safety results from a large mono-institutional analysis. *J Exp Clin Cancer Res* 2010; **29**: 164 [PMID: 21159184 DOI: 10.1186/1756-9966-29-164]

55 **Facciorusso A**, Di Maso M, Muscatiello N. Drug-eluting beads versus conventional chemoembolization for the treatment of unresectable hepatocellular carcinoma: A meta-analysis. *Dig Liver Dis* 2016; **48**: 571-577 [PMID: 26965785 DOI: 10.1016/j.dld.2016.02.005]

56 **Huang K**, Zhou Q, Wang R, Cheng D, Ma Y. Doxorubicin-eluting beads versus conventional transarterial chemoembolization for the treatment of hepatocellular carcinoma. *J Gastroenterol Hepatol* 2014; **29**: 920-925 [PMID: 24224722 DOI: 10.1111/jgh.12439]

57 **Han S**, Zhang X, Zou L, Lu C, Zhang J, Li J, Li M. Does drug-eluting bead transcatheter arterial chemoembolization improve the management of patients with hepatocellular carcinoma? A meta-analysis. *PLoS One* 2014; **9**: e102686 [PMID: 25083860 DOI: 10.1371/journal.pone.0102686]

58 **Xie ZB**, Wang XB, Peng YC, Zhu SL, Ma L, Xiang BD, Gong WF, Chen J, You XM, Jiang JH, Li LQ, Zhong JH. Systematic review comparing the safety and efficacy of conventional and drug-eluting bead transarterial chemoembolization for inoperable hepatocellular carcinoma. *Hepatol Res* 2015; **45**: 190-200 [PMID: 25388603 DOI: 10.1111/hepr.12450]

59 **Angelico M**. TACE vs DEB-TACE: Who wins? *Dig Liver Dis* 2016; **48**: 796-797 [PMID: 27257050 DOI: 10.1016/j.dld.2016.05.009]

60 **Cucchetti A**, Trevisani F, Cappelli A, Mosconi C, Renzulli M, Pinna AD, Golfieri R. Cost-effectiveness of doxorubicin-eluting beads versus conventional trans-arterial chemo-embolization for hepatocellular carcinoma. *Dig Liver Dis* 2016; **48**: 798-805 [PMID: 27263056 DOI: 10.1016/j.dld.2016.03.031]

61 **Nishikawa H**, Kita R, Kimura T, Osaki Y. Transcatheter arterial embolic therapies for hepatocellular carcinoma: a literature review. *Anticancer Res* 2014; **34**: 6877-6886 [PMID: 25503113]

62 **Minocha J**, Salem R, Lewandowski RJ. Transarterial chemoembolization and yittrium-90 for liver cancer and other lesions. *Clin Liver Dis* 2014; **18**: 877-890 [PMID: 25438288 DOI: 10.1016/j.cld.2014.07.007]

63 **Gholamrezanezhad A**, Mirpour S, Geschwind JF, Rao P, Loffroy R, Pellerin O, Liapi EA. Evaluation of 70-150-μm doxorubicin-eluting beads for transcatheter arterial chemoembolization in the rabbit liver VX2 tumour model. *Eur Radiol* 2016; **26**: 3474-3482 [PMID: 26780638 DOI: 10.1007/s00330-015-4197-y]

64 **Odisio BC**, Ashton A, Yan Y, Wei W, Kaseb A, Wallace MJ, Vauthey JN, Gupta S, Tam AL. Transarterial hepatic chemoembolization with 70-150 μm drug-eluting beads: assessment of clinical safety and liver toxicity profile. *J Vasc Interv Radiol* 2015; **26**: 965-971 [PMID: 25979305 DOI: 10.1016/j.jvir.2015.03.020]

65 **Deipolyi AR**, Oklu R, Al-Ansari S, Zhu AX, Goyal L, Ganguli S. Safety and efficacy of 70-150 μm and 100-300 μm drug-eluting bead transarterial chemoembolization for hepatocellular carcinoma. *J Vasc Interv Radiol* 2015; **26**: 516-522 [PMID: 25704226 DOI: 10.1016/j.jvir.2014.12.020]

66 **Spreafico C**, Cascella T, Facciorusso A, Sposito C, Rodolfo L, Morosi C, Civelli EM, Vaiani M, Bhoori S, Pellegrinelli A, Marchianò A, Mazzaferro V. Transarterial chemoembolization for hepatocellular carcinoma with a new generation of beads: clinical-radiological outcomes and safety profile. *Cardiovasc Intervent Radiol* 2015; **38**: 129-134 [PMID: 24870698 DOI: 10.1007/s00270-014-0907-0]

67 **Dinca H**, Pelage JP, Baylatry MT, Ghegediban SH, Pascale F, Manfait M. Why do small size doxorubicin-eluting microspheres induce more tissue necrosis than larger ones? A comparative study in healthy pig liver (oral communication 2206-2). CIRSE Annual meeting, Lisbon 2012

68 **Liu DM**, Kos S, Buczkowski A, Kee S, Munk PL, Klass D, Wasan E. Optimization of doxorubicin loading for superabsorbent polymer microspheres: in vitro analysis. *Cardiovasc Intervent Radiol* 2012; **35**: 391-398 [PMID: 21567274 DOI: 10.1007/s00270-011-0168-0]

69 **Malagari K**, Pomoni M, Moschouris H, Kelekis A, Charokopakis A, Bouma E, Spyridopoulos T, Chatziioannou A, Sotirchos V, Karampelas T, Tamvakopoulos C, Filippiadis D, Karagiannis E, Marinis A, Koskinas J, Kelekis DA. Chemoembolization of hepatocellular carcinoma with HepaSphere 30-60 μm. Safety and efficacy study. *Cardiovasc Intervent Radiol* 2014; **37**: 165-175 [PMID: 24263774 DOI: 10.1007/s00270-013-0777-x]

70 **Kumar Y**, Sharma P, Bhatt N, Hooda K. Transarterial Therapies for Hepatocellular Carcinoma: a Comprehensive Review with Current Updates and Future Directions. *Asian Pac J Cancer Prev* 2016; **17**: 473-478 [PMID: 26925630 DOI: 10.7314/APJCP.2016.17.2.473]

71 **Greco G**, Cascella T, Facciorusso A, Nani R, Lanocita R, Morosi C, Vaiani M, Calareso G, Greco FG, Ragnanese A, Bongini MA, Marchianò AV, Mazzaferro V, Spreafico C. Transarterial chemoembolization using 40 μm drug eluting beads for hepatocellular carcinoma. *World J Radiol* 2017; **9**: 245-252 [PMID: 28634515 DOI: 10.4329/wjr.v9.i5.245]

72 **Facciorusso A**, Villani R, Bellanti F, Mitarotonda D, Vendemiale G, Serviddio G. Mitochondrial Signaling and Hepatocellular Carcinoma: Molecular Mechanisms and Therapeutic Implications. *Curr Pharm Des* 2016; **22**: 2689-2696 [PMID: 26861645 DOI: 10.2174/1381612822666160209153624]

73 **Facciorusso A**, Antonino M, Del Prete V, Neve V, Scavo MP, Barone M. Are hematopoietic stem cells involved in hepatocarcinogenesis? *Hepatobiliary Surg Nutr* 2014; **3**: 199-206 [PMID: 25202697 DOI: 10.3978/j.issn.2304-3881.2014.06.02]

74 **Facciorusso A**. The influence of diabetes in the pathogenesis and the clinical course of hepatocellular carcinoma: recent findings and new perspectives. *Curr Diabetes Rev* 2013; **9**: 382-386 [PMID: 23845075 DOI: 10.2174/15733998113099990068]

75 **Lencioni R**, Llovet JM, Han G, Tak WY, Yang J, Guglielmi A, Paik SW, Reig M, Kim DY, Chau GY, Luca A, Del Arbol LR, Leberre MA, Niu W, Nicholson K, Meinhardt G, Bruix J. Sorafenib or placebo plus TACE with doxorubicin-eluting beads for intermediate stage HCC: The SPACE trial. *J Hepatol* 2016; **64**: 1090-1098 [PMID: 26809111 DOI: 10.1016/j.jhep.2016.01.012]

76 **Facciorusso A**, Del Prete V, Antonino M, Crucinio N, Neve V, Di Leo A, Carr BI, Barone M. Post-recurrence survival in hepatocellular carcinoma after percutaneous radiofrequency ablation. *Dig Liver Dis* 2014; **46**: 1014-1019 [PMID: 25085684 DOI: 10.1016/j.dld.2014.07.012]

77 **Facciorusso A**, Del Prete V, Antonino M, Neve V, Crucinio N, Di Leo A, Carr BI, Barone M. Serum ferritin as a new prognostic factor in hepatocellular carcinoma patients treated with radiofrequency ablation. *J Gastroenterol Hepatol* 2014; **29**: 1905-1910 [PMID: 24731153 DOI: 10.1111/jgh.12618]

P- Reviewer: Chen Z **S- Editor**: Chen K **L- Editor**: A
E- Editor: Ma YJ

World Journal of Gastroenterology

Submit a Manuscript: http://www.f6publishing.com

World J Gastroenterol 2018 January 14; 24(2): 170-178

DOI: 10.3748/wjg.v24.i2.170

ISSN 1007-9327 (print) ISSN 2219-2840 (online)

ORIGINAL ARTICLE

Basic Study

Antifibrogenic effects of vitamin D derivatives on mouse pancreatic stellate cells

Peter Wallbaum, Sarah Rohde, Luise Ehlers, Falko Lange, Alexander Hohn, Carina Bergner, Sarah Marie Schwarzenböck, Bernd Joachim Krause, Robert Jaster

Peter Wallbaum, Sarah Rohde, Luise Ehlers, Robert Jaster, Department of Medicine Ⅱ, Division of Gastroenterology, Rostock University Medical Center, Rostock 18057, Germany

Falko Lange, Oscar-Langendorff-Institute of Physiology, Rostock University Medical Center, Rostock 18057, Germany

Alexander Hohn, Carina Bergner, Sarah Marie Schwarzenböck, Bernd Joachim Krause, Department of Nuclear Medicine, Rostock University Medical Center, Rostock 18057, Germany

ORCID number: Peter Wallbaum (0000-0002-2270-6341); Sarah Rohde (0000-0002-6892-1565); Luise Ehlers (0000-0001-8565-0560); Falko Lange (0000-0001-8782-5205); Alexander Hohn (0000-0001-9637-6560); Carina Bergner (0000-0001-7346-8067); Sarah Marie Schwarzenböck (0000-0001-5138-7979); Bernd Krause (0000-0002-2572-4131); Robert Jaster (0000-0002-8220-4570).

Author contributions: Jaster R, Schwarzenböck SM and Krause BJ designed the study; Wallbaum P, Rohde S, Ehlers L, Lange F, Bergner C, Hohn A and Jaster R performed the experiments; all authors analyzed the data; and Jaster R wrote the manuscript.

Supported by FORUN program of the Rostock University Medical Center.

Conflict-of-interest statement: The authors declare that there is no conflict of interest.

Manuscript source: Unsolicited manuscript

Correspondence to: Robert Jaster, MD, Academic Research, Professor, Senior Scientist, Department of Medicine Ⅱ, Division of Gastroenterology, Rostock University Medical Center, E.-Heydemann-Str. 6, Rostock 18057, Germany. jaster@med.uni-rostock.de
Telephone: +49-381-4947349
Fax: +49-381-4947482

Received: October 10, 2017
Peer-review started: October 10, 2017
First decision: October 30, 2017
Revised: November 15, 2017
Accepted: November 27, 2017
Article in press: November 27, 2017
Published online: January 14, 2018

Abstract

AIM

To study the molecular effects of three different D-vitamins, vitamin D2, vitamin D3 and calcipotriol, in pancreatic stellate cells (PSCs).

METHODS

Quiescent PSCs were isolated from mouse pancreas and activated *in vitro* by seeding on plastic surfaces. The cells were exposed to D-vitamins as primary cultures (early-activated PSCs) and upon re-culturing (fully-activated cells). Exhibition of vitamin A-containing lipid droplets was visualized by oil-red staining. Expression of α-smooth muscle actin (α-SMA), a marker of PSC activation, was monitored by immunofluorescence and immunoblot analysis. The rate of DNA synthesis was quantified by 5-bromo-2′-deoxyuridine (BrdU) incorporation assays. Real-time PCR was employed to monitor gene expression, and protein levels of interleukin-6 (IL-6) were measured by ELISA. Uptake of proline was determined using ^{18}F-proline.

RESULTS

Sustained culture of originally quiescent PSCs induced

cell proliferation, loss of lipid droplets and exhibition of stress fibers, indicating cell activation. When added to PSCs in primary culture, all three D-vitamins diminished expression of α-SMA (to 32%-39% of the level of control cells; $P < 0.05$) and increased the storage of lipids (scores from 1.97-2.15 on a scale from 0-3; controls: 1.49; $P < 0.05$). No such effects were observed when D-vitamins were added to fully-activated cells, while incorporation of BrdU remained unaffected under both experimental conditions. Treatment of re-cultured PSCs with D-vitamins was associated with lower expression of IL-6 (-42% to -49%; $P < 0.05$; also confirmed at the protein level) and increased expression of the vitamin D receptor gene (209%-321% *vs* controls; $P < 0.05$). There was no effect of D-vitamins on the expression of transforming growth factor-β1 and collagen type 1 (chain α1). The lowest uptake of proline, a main component of collagen, was observed in calcipotriol-treated PSCs.

CONCLUSION

The three D-vitamins inhibit, with similar efficiencies, activation of PSCs *in vitro*, but cannot reverse the phenotype once the cells are fully activated.

Key words: Pancreatic stellate cells; Fibrosis; Vitamin D2; Vitamin D3; Calcipotriol

Core tip: Modulation of the stroma response by vitamin D has been suggested as a concept to treat chronic pancreatitis and pancreatic cancer. Here we show that three derivatives, vitamin D2, vitamin D3 and calcipotriol, with similar efficiencies prevented pancreatic stellate cell (PSC) activation *in vitro*. Once the cells were fully activated, vitamin D failed to induce a reversal of the myofibroblastic phenotype, but still exerted antifibrotic effects by diminishing the uptake of proline and secretion of interleukin-6, an autocrine mediator of PSC activation. Our findings encourage further studies on the potential of vitamin D derivatives as antifibrotic drugs.

Wallbaum P, Rohde S, Ehlers L, Lange F, Hohn A, Bergner C, Schwarzenböck SM, Krause BJ, Jaster R. Antifibrogenic effects of vitamin D derivatives on mouse pancreatic stellate cells. *World J Gastroenterol* 2018; 24(2): 170-178 Available from: URL: http://www.wjgnet.com/1007-9327/full/v24/i2/170.htm DOI: http://dx.doi.org/10.3748/wjg.v24.i2.170

INTRODUCTION

Pancreatic stellate cells (PSCs) were identified as the main source of extracellular matrix (ECM) proteins in the diseased pancreas, specifically in the context of cancer and chronic pancreatitis (CP), two decades ago. Since then, cellular interactions of PSCs and extracellular as well as intracellular regulators of PSC function have been studied in great detail (reported by Erkan *et al*[1]). In the healthy pancreas, PSCs exist in a quiescent state and are phenotypically characterized by the presence of abundant vitamin A-containing lipid droplets in their cytoplasm[2,3]. In response to mitogens (such as platelet-derived growth factor) and profibrogenic mediators (*e.g.*, transforming growth factor-β1), PSCs undergo an activation process that involves cell proliferation and an enhanced synthesis of ECM proteins[4]. The cells also lose their vitamin A storages and exhibit stress fibers containing α-smooth muscle actin (α-SMA) protein. *In vitro*, contact of PSCs with plastic surfaces induces phenotypic changes that mimic the activation process under *in vivo* conditions[2,3].

In the past years, it has become clear that PSCs play an active and complex role in the progression of pancreatic cancer (PC), a stroma-rich tumor with the worst prognosis of all common human malignancies[5-8]. Most recent publications in the field have shifted the main focus of attention from a stroma deletion, which even displayed deleterious effects in experimental models of PC[9,10], towards a modulation of the stroma response, with the aim to interrupt tumor-promoting interactions between PSCs and PC cells on one hand while preserving the barrier function of the stroma on the other hand[11]. In this regard, vitamin D and its receptor VDR have gained significant interest as master regulators of PSC function and mediators of a transcriptional reprogramming of the tumor stroma that enable an enhanced chemotherapeutic response[12]. Recently, suppression of cell proliferation and inhibition of ECM synthesis have been proposed as important mechanisms of vitamin D action in PSCs[13]. Nevertheless, to this end the precise molecular actions of vitamin D in stellate cells are not fully understood. Furthermore, relative efficiencies of different vitamin D derivatives have not been studied yet.

Here, we have compared the effects of vitamin D2, vitamin D3 and the synthetic vitamin D3 derivative calcipotriol on primary cultures of originally quiescent PSC as well as on fully-activated re-cultured cells. All D-vitamins inhibited PSC activation, but did not reverse the phenotype once the cells were fully activated. Interleukin-6 (IL-6) was identified as an important target of vitamin D action. Although the three D-vitamins displayed slightly different molecular effects in our studies, their general efficiency was found to be similar.

MATERIALS AND METHODS

Cell culture

Quiescent PSCs were isolated from the pancreas of healthy C57BL/6 mice (approximately 3 months old) by collagenase digestion followed by Nycodenz® (Nycomed, Oslo, Norway) density gradient centrifugation[14]. Afterwards, they were resuspended in cryopreservation

medium [fetal calf serum (FCS) supplemented with 10% dimethyl sulfoxide) and stored at -150 ℃ until required as previously described[15]. After thawing, the cells were cultured in Iscove's modified Dulbecco's medium supplemented with 17% FCS, 1% non-essential amino acids (dilution of a 100 × stock solution), 10^5 U/L penicillin and 100 mg/L streptomycin (all reagents from Merck Millipore, Darmstadt, Germany). Approximately on day 3 of primary culture, PSCs started to proliferate and reached subconfluency around day 8. Afterwards, the cells were harvested by trypsinization and re-cultured according to the experimental requirements.

Histochemical staining of intracellular fat

PSCs were grown on glass coverslips as primary cultures or cells of the first passage for the indicated periods of time. Subsequently, they were fixed for 30 min in 2.5% paraformaldehyde, and intracellular fat droplets were visualized by oil red O staining as described before[16]. Briefly, the coverslips were incubated with dye solution [three parts of an oil red O stock solution (1% wt/vol dissolved in isopropanol, mixed with two parts of distilled water)] for 15 min followed by counterstaining with Mayer's hemalum solution (Merck Millipore). The samples were evaluated by light microscopy and assessed, in a blinded manner, by two independent investigators on a semiquantitative scale from 0 (absence of lipid droplets) to 3 (large and numerous lipid droplets).

Quantification of DNA synthesis

DNA synthesis was quantified employing the 5-bromo-2'-deoxyuridine (BrdU) labelling and detection enzyme-linked immunosorbent assay kit (Roche Diagnostics, Mannheim, Germany). Therefore, quiescent or activated (proliferating) PSCs were plated in 96-well plates at equal seeding densities and allowed to adhere overnight. Afterwards, the cells were exposed to vitamin D2, vitamin D3 (both from Santa Cruz Biotechnologies, Heidelberg, Germany) or calcipotriol (Sigma-Aldrich, Deisenhofen, Germany) for the indicated periods of time. Twenty-four hours prior to cell harvesting, BrdU labelling was initiated by adding labelling solution at a final concentration of 10 μmol/L. Afterwards, labelling was stopped, and BrdU uptake was measured according to the manufacturer's instructions.

Immunoblotting

PSCs in primary culture were pretreated as indicated, and protein extracts were prepared and subjected to immunoblot analysis as described before[14], using polyvinylidene fluoride membrane (Merck Millipore) for protein transfer. Primary antibodies were obtained from the following sources: anti-α-SMA; Sigma-Aldrich (#A2547), and glyceraldehyde 3-phosphate dehydrogenase (GAPDH); New England Biolabs, Frankfurt am Main, Germany (#2118). To develop the blots, LI-COR reagents for an Odyssey® Infrared Imaging System (LI-COR Biosciences, Lincoln, NE, United States) were used as described before[17]. Signal intensities were quantified by means of the Image Studio Lite Version 5.2, and normalized to GAPDH by calculating the ratio α-SMA/GAPDH.

Immunofluorescence detection of α-SMA

Quiescent PSCs or cells of the first passage were seeded onto glass coverslips and allowed to adhere overnight before they were exposed to D-vitamins at 100 nmol/L. After the indicated periods of time, the cells were fixed with ice-cold methanol, followed by staining of the DNA with 4',6-diamidino-2-phenylindole. Next, the cells were incubated with a mouse monoclonal antibody to α-SMA (#A2547; Sigma-Aldrich). Antibody binding was determined by a fluorescein-labelled goat anti-mouse IgG (MoBiTec, Göttingen, Germany) and visualized employing a fluorescence microscope (Leica DFC320, Leica Microsystems, Wetzlar, Germany). For further evaluation, α-SMA expression in PSCs and organization of the protein in stress fibers were assessed in a semiquantitative manner, using a scoring system as previously established[18]. Therefore, blinded samples were scored by two independent investigators on a scale from 0 (low or undetectable α-SMA expression; absence of stress fibers) to 3 (high expression levels; extensive stress fiber bundles).

Quantitative reverse transcriptase-PCR using real-time TaqMan™ technology

PSCs of passage 1 were grown in 12-well plates and treated as indicated, before total RNA was isolated with TriFast reagent (PEQLAB Biotechnologie, Erlangen, Germany). Unless indicated otherwise, reagents from Thermo Fisher Scientific (Karlsruhe, Germany) were used for all subsequent procedures. Traces of genomic DNA were removed employing the DNA-free kit, and 250 ng of RNA per sample was reverse transcribed into cDNA by means of TaqMan™ Reverse Transcription Reagents and random priming. Target cDNA levels were quantified by real-time PCR, using a ViiA 7 sequence detection system (Thermo Fisher Scientific). Therefore, qPCR MasterMix (Eurogentec, Seraing, Liège, Belgium) and the following mouse-specific *TaqMan*™ gene expression assays with fluorescently labelled MGB probes were employed: Mm00446190_m1 (*Il6*), Mm01178820_m1 (*Tgfb1*), Mm00801666_m1 (α1 type Ⅰ collagen, Col1a1), Mm00437297_m1 (vitamin D receptor, *Vdr*) and Mm01545399_m1 (hypoxanthine guanine phosphoribosyl transferase; *Hprt*; housekeeping gene control). PCR conditions were: 95 ℃ for 10 min, followed by 40 cycles of 15 s at 95 ℃/1 min at 60 ℃. The relative amount of target mRNA in untreated PSCs (control) and all other samples was expressed as $2^{-(\Delta\Delta Ct)}$, where $\Delta\Delta Ct_{sample} = \Delta Ct_{sample} - \Delta Ct_{control}$.

IL-6 ELISA

IL-6 protein levels were determined using a mouse IL-6-specific ELISA (Thermo Fisher Scientific). Therefore, activated PSCs (passage 1) were grown in 24-well plates and treated with D-vitamins as indicated. Cell culture

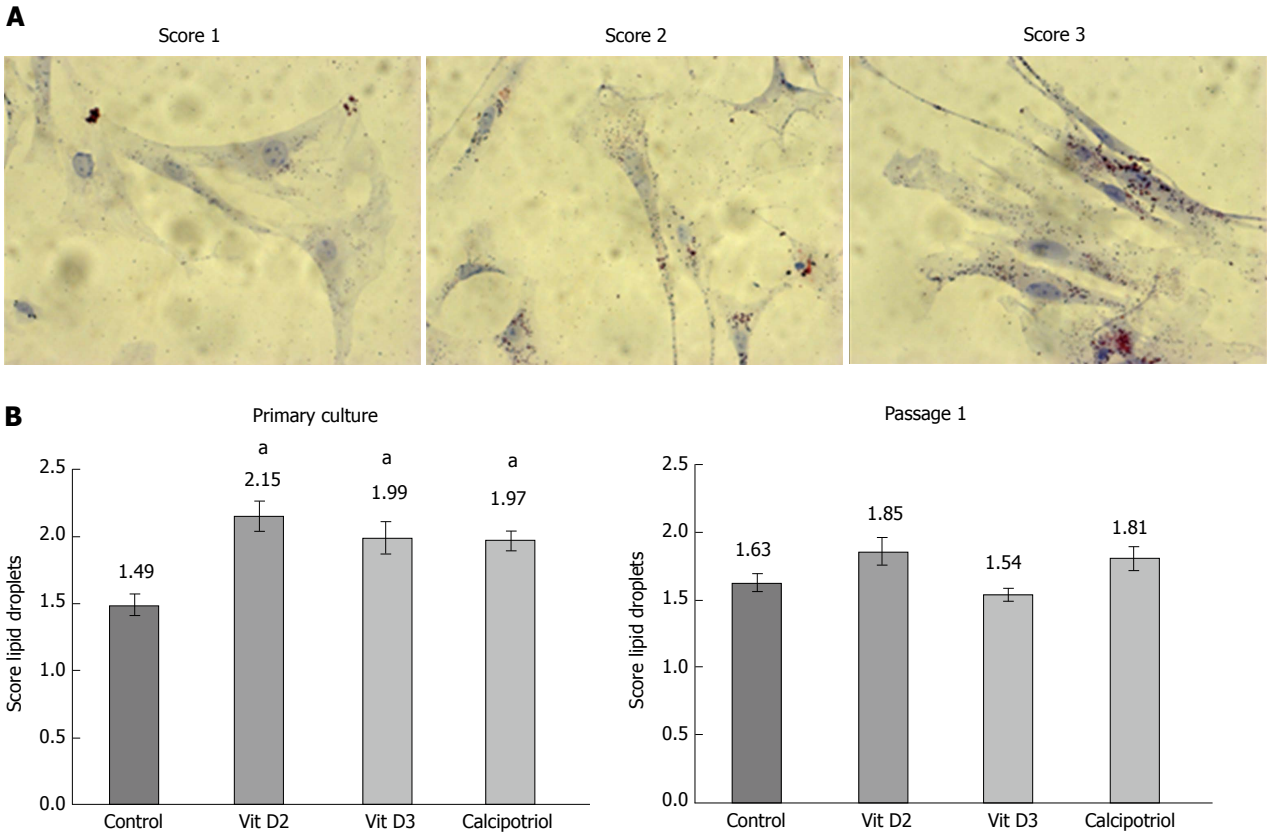

Figure 1 D-vitamins prevent loss of lipid droplets in quiescent pancreatic stellate cells. Pancreatic stellate cells in primary culture (days 1-4) and of passage 1 (days 1-3) were exposed to the indicated D-vitamins at 100 nmol/L each. Afterwards, intracellular lipids were stained with oil-red, and size/number of lipid droplets were assessed on a semiquantitative scale from 0 to 3. A: Exemplary stains for scores 1-3 (original magnification, × 400); B: Shown are the mean scores of $n \geqslant 14$ independent samples (mean ± SE) for primary cultures (left panel) and passaged cells (right panel). $^{a}P < 0.05$ *vs* untreated controls.

supernatants were collected and stored at -80 ℃ until assayed. The measurements were performed according to the manufacturer's instructions.

^{18}F-proline incorporation assay

For this investigation, PSCs were seeded at a low density and grown for a prolonged period of 12 d in primary culture. At this time, the cells, like re-cultured PSCs, displayed a fully activated, myofibroblastic phenotype. Experiments with cells of passage 1 yielded unsatisfactory results due to inconsistent growth rates and low proline uptake (data not shown). 2-[^{18}F] proline (^{18}F-proline) was synthesized according to literature[19] with a modification as described in[20]. After pretreatment with D-vitamins for 48 h, ^{18}F-proline (1.0 GBq/L culture medium) was added to each culture well. Two hours later, incubation was terminated by aspirating the medium and rinsing the cell layer two times with ice-cold PBS. PSCs were solubilized with 100 mmol/L NaOH, and incorporated ^{18}F activity was determined using an automated counter (Wizard 2470, Automatic Gamma Counter, PerkinElmer, Groningen, the Netherlands). The raw data were normalized to the protein content of the sample, which was determined using a commercial Bradford assay (Bio-Rad Laboratories, Munich, Germany).

Statistical analysis

All data were stored and analyzed using the IBM SPSS Statistics 22.0. Values were expressed as mean ± SE for the indicated number of samples (n) per experimental protocol. Mean group differences were checked using analysis of variance. If data did not meet the assumptions for ANOVA, nonparametric analysis of variance was performed employing the Kruskal-Wallis test or, in case of dependency of samples, the Friedman test, before subgroups were tested pairwise using the Mann-Whitney U test and the Wilcoxon rank sum test, respectively. Here, Bonferroni-adjusted P-values, otherwise $P < 0.05$ were considered to be statistically significant.

RESULTS

D-vitamins inhibit exhibition of a myofibroblastic PSC phenotype

In a first set of experiments, we analyzed the effects of D-vitamins on the activation status of cultured PSCs *in vitro*. Therefore, PSCs in early primary culture and cells of the first passage were incubated with vitamin D2, vitamin D3 or calcipotriol as indicated, and cytoplasmic lipid droplets (Figure 1) as well as stress fiber bundles of α-SMA (Figure 2) were used as surrogate markers of

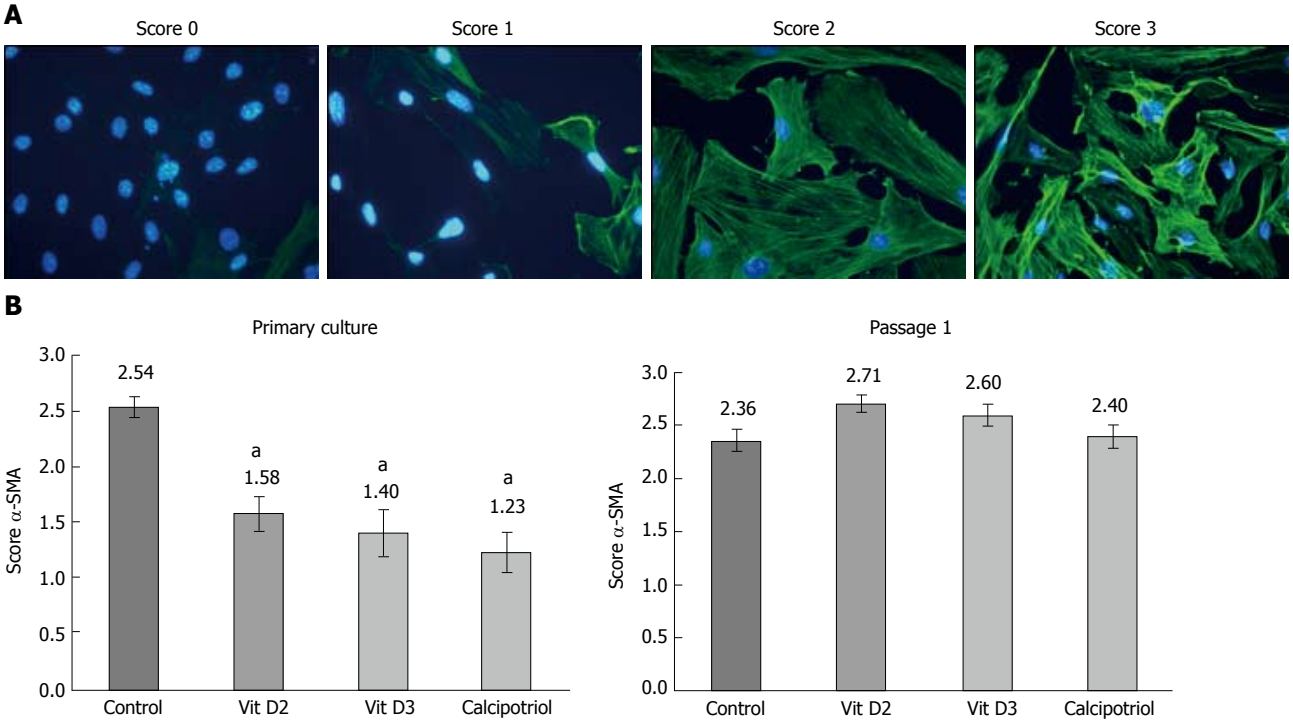

Figure 2 D-vitamins inhibit formation of stress fiber bundles. Pancreatic stellate cells in primary culture (days 1-4) and of passage 1 (days 1-3) were treated with the indicated D-vitamins at 100 nmol/L each. Subsequently, α-smooth muscle actin (α-SMA) fibres (green) were visualized by immunofluorescence staining; while nuclei were counterstained with DNA with 4',6-diamidino-2-phenylindole (blue). Expression of α-SMA and formation of stress fiber bundles were assessed on a semiquantitative scale from 0 to 3. Exemplary stains for each score are shown in (A) (original magnification, × 630). In (B), mean values of $n \geqslant 12$ independent samples ± SE for primary cultures (left panel) and passaged cells (right panel) are shown. $^{a}P < 0.05$ *vs* untreated controls.

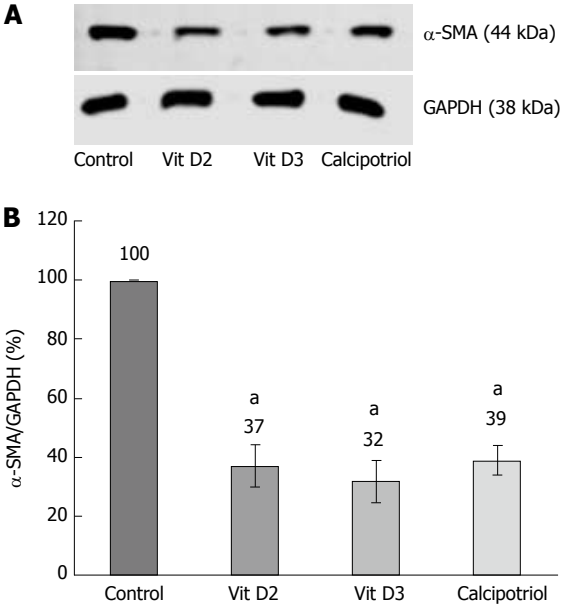

Figure 3 D-vitamins reduce protein levels of α-smooth muscle actin in primary cultured pancreatic stellate cells. Pancreatic stellate cells were treated with the indicated D-vitamins (100 nmol/L each) from day 1-4 of primary culture, before expression of α-smooth muscle actin (α-SMA) and the housekeeping protein GAPDH was assessed by Western blot analysis (see A for a typical experiment); B: Intensities of fluorescence signals were expressed as ratio α-SMA/GAPDH. Data of 5 independent experiments were used to calculate mean ± SE. $^{a}P < 0.05$ *vs* untreated controls.

the cellular phenotype. At the time of analysis, originally quiescent PSCs had undergone 4 d of primary culture on plastic and were considered as a model of early activated stellate cells. Accordingly, re-cultured PSCs corresponded to mature activated cells.

As shown in Figure 1, primary cultures of PSCs contained more lipid droplets after incubation with any of the three vitamin D derivatives than without this treatment. In passaged cells, no such effect was observed. In primary culture as well as upon re-culturing, untreated PSCs expressed high levels of α-SMA protein that was organized in stress fibers (Figure 2). All three D-vitamins significantly diminished the formation of stress fiber bundles in primary cultures, but not in re-cultured cells. The effects of D-vitamins on cells in primary culture were also confirmed by Western blot analysis of α-SMA expression (Figure 3).

High levels of lipid droplets and absence of stress fibers are characteristics of quiescent PSCs[2,3]. Therefore, our data suggest that D-vitamins support the maintenance of a quiescent state when added early in the course of primary culture, but cannot reverse the myofibroblastic phenotype (with high levels of α-SMA and a decline of lipid droplets) once the cells are fully activated.

Effects of D-vitamins on DNA synthesis

At concentrations of 100 nmol/L (Figure 4) and below, D-vitamins had no effect on the rate of DNA synthesis, independent of whether primary cultures or passaged

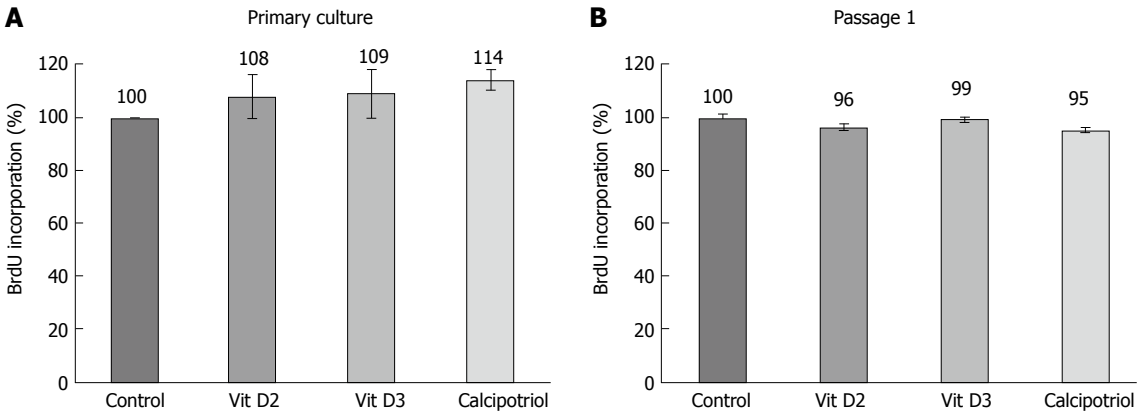

Figure 4 D-vitamins have no effect on DNA synthesis of pancreatic stellate cells. Pancreatic stellate cells (PSCs) (A) in primary culture (days 1-4) and (B) of passage 1 (days 1-3) were challenged with D-vitamins at 100 nmol/L each, and DNA synthesis was assessed employing the BrdU incorporation assay. One hundred percent BrdU incorporation corresponds to solvent-treated PSCs. Data are expressed as mean ± SE ($n \geqslant 6$ independent samples).

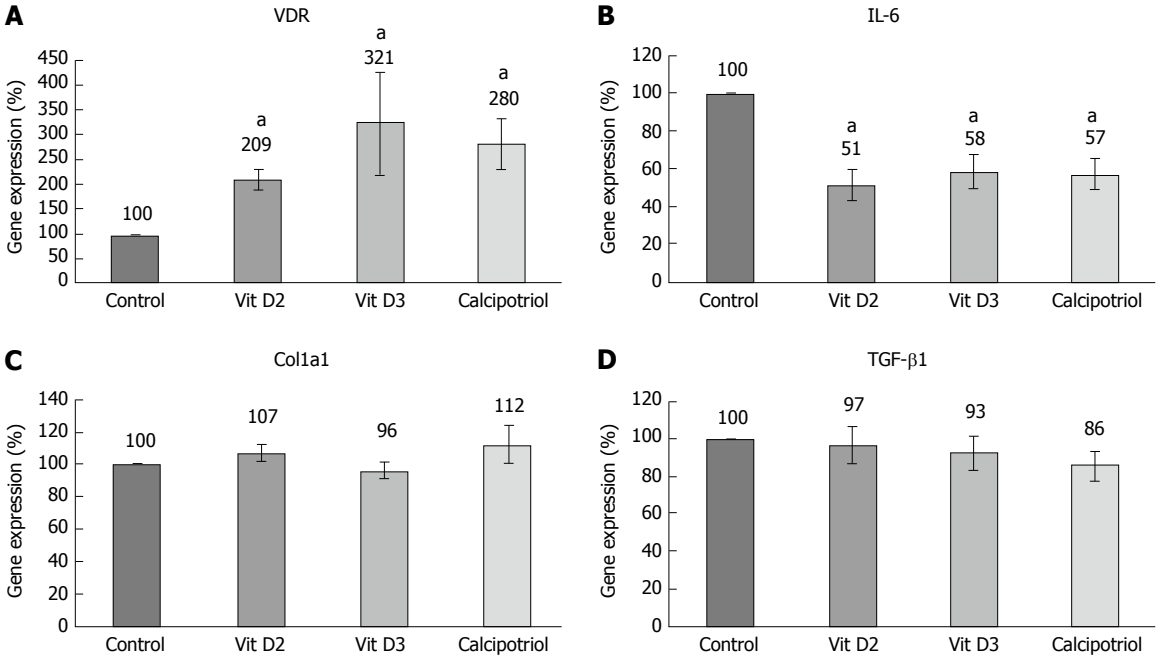

Figure 5 Effects of D-vitamins on pancreatic stellate cell gene expression (A-D). Pancreatic stellate cells of the first passage were treated for 48 h with the indicated D-vitamins at 100 nmol/L each. Subsequently, the mRNA expression of the indicated genes and the house-keeping control *Hprt* was analyzed by real-time PCR, and relative amounts of target mRNA were calculated as described in the methods section. One hundred percent mRNA expression of each gene corresponds to untreated cells. Data are presented as averaged mean ± SE ($n \geqslant 8$ independent samples). $^{a}P < 0.05$ *vs* untreated controls.

cells were exposed to the drugs.

D-vitamins reduce IL-6 expression and secretion

Effects of D-vitamins at the level of gene expression were studied in passaged PSCs only, since the mRNA yield from the small number of cells in primary culture proved too low for reproducible results. As expected, all D-vitamins enhanced the expression of *VDR* as a known target gene[21] (Figure 5A). Interestingly, vitamins D2 and D3 significantly diminished the mRNA and protein levels of IL-6, an autocrine mediator of PSC activation and major proinflammatory cytokine[22,23] (Figures 5B and 6). Calcipotriol showed similar effects, but only the inhibition of mRNA expression was statistically significant. None of the investigated derivatives inhibited the expression of collagen type 1 (α1-chain) and *Tgfb1* as the main profibrogenic cytokine[4,24] substantially (Figure 5C and D).

Effects of D-vitamins on proline uptake

In subsequent experiments, uptake of proline, a main component of collagen, by PSCs was measured. The lowest rate of proline incorporation was observed for calcipotriol-treated cells (Figure 7). Although a Friedman test yielded a *P* value of 0.007, the differences between treated cells and controls did not reach statistical significance.

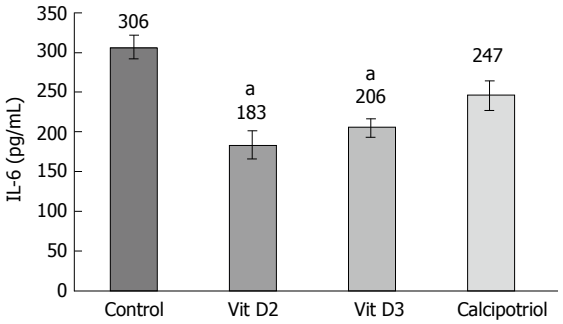

Figure 6 D-vitamins reduce interleukin-6 secretion. Pancreatic stellate cells of the first passage were incubated for 24 h with D-vitamins (at 100 nmol/L each) as indicated. Subsequently, interleukin-6 (IL-6) protein levels in cell culture supernatants were analyzed by ELISA. Mean values and SE were calculated from 6 independent samples. $^{a}P < 0.05$ *vs* untreated controls. For calcipotriol, the Bonferroni-adjusted *P*-value was 0.141.

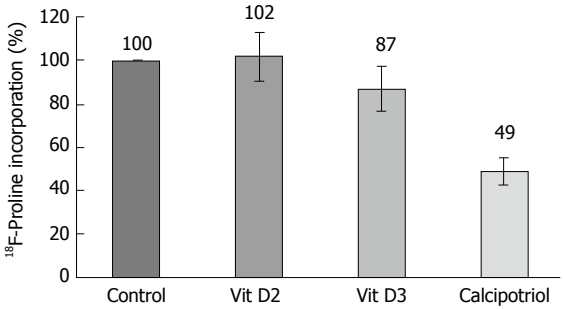

Figure 7 Effects of D-vitamins on ^{18}F-proline incorporation. Pancreatic stellate cells were treated for 48 h with the indicated D-vitamins at 100 nmol/L each. Afterwards, incorporation of ^{18}F-proline was determined as described in the materials and methods section. Raw data were normalized to the protein content of the samples. One hundred percent ^{18}F-proline incorporation corresponds to untreated PSCs. Data are expressed as mean ± SE (n = 5 samples). $P_{\text{Friedman test}}$ = 0.007, but no statistically significant differences between treated cells and the control group.

DISCUSSION

To this end, antifibrotic drugs that effectively inhibit the stroma response in the context of CP and PC are largely missing. Undoubtedly, their availability would also facilitate experimental studies on the role of fibrosis in the progression of both diseases, which remains unknown (CP) or controversial (PC). Currently, drugs that block pro-tumorigenic functions of the stroma but maintain, or even enhance, its anti-tumorigenic properties are considered most interesting with respect to their clinical potential. Recently, the vitamin D derivative calcipotriol has been suggested to exert such effects by inducing a transcriptional re-programming of the tumor stroma in PC, and PSCs have been suggested as important targets of vitamin D action[12,13].

The results of this study provide for the first time insights into the relative efficiencies of different vitamin D derivatives in the context of pancreatic fibrogenesis. Using primary cultures of quiescent murine PSCs, we found that vitamin D2, vitamin D3 and calcipotriol all significantly reduced the expression of α-SMA and prevented the loss of vitamin A-containing fat droplets. Once the cells were fully activated (upon re-culture), no such effects were detected anymore. Together, these data suggest that all three vitamin D derivatives inhibit activation of PSCs *in vitro*, but cannot reverse the myofibroblastic phenotype of fully activated PSCs. Nevertheless, the latter cells remained vitamin D-responsive. Specifically, all D-vitamins reduced the mRNA levels of IL-6. Moreover, vitamins D2 and D3 also significantly diminished IL-6 protein secretion. Here, the effect of calcipotriol was not significant, although this might be due to the small sample size. Furthermore, uptake of proline was affected by vitamin D-treatment. Somewhat unexpectedly, we did not observe significant effects of any vitamin D derivative on DNA synthesis, a finding that is in contrast to a previous report of antiproliferative effects of vitamin D3 on murine PSCs[13]. The possibility that methodological differences account for this discrepancy cannot be excluded at this stage. In the previous study, longer periods of treatment with vitamin D3 and a different assay to monitor cell growth were employed[13]. Interestingly, D-vitamins neither inhibited the expression of collagen type 1 (α1-chain) nor of *Tgfb1*. These findings suggest that both genes are no direct targets of vitamin D action in PSCs. Since D-vitamins interfered with the exhibition of a myofibroblastic PSC phenotype, we nevertheless suggest an antifibrotic net effect of the three derivatives.

In conclusion, despite small differences, the biological efficiencies of the three D-vitamins were similar. The inability of D-vitamins to reverse the activated PSC phenotype does not necessarily limit their potential as antifibrotic drugs, since (1) they may prevent the further recruitment of still quiescent PSCs; and (2) diminished secretion of the autocrine PSC activator IL-6[20,21]. The reduced uptake of proline, a main compound of collagen, is compatible with a preserved antifibrotic action of D-vitamins even upon completion of PSC activation. We therefore suggest follow-up studies in animal models not only of PC but also of CP to further evaluate the antifibrotic effects of vitamin D under *in vivo* conditions.

ARTICLE HIGHLIGHTS

Research background

Chronic pancreatitis and pancreatic cancer are accompanied by an extended fibrosis that plays an active role in disease progression. Pancreatic stellate cells (PSCs) are the main source of extracellular matrix proteins in the diseased organ. To this end, there is a lack of specific antifibrotic agents for preclinical evaluation and potential clinical applications.

Research motivation

Vitamin D has recently been suggested to modulate the pancreatic stroma in a way that pancreatitis is suppressed and pancreatic cancer therapy is enhanced. PSCs were identified as a target of vitamin D action. The molecular mechanisms of vitamin D action in PSCs are only partially understood, and the relative efficiencies of different vitamin D derivatives have not been elucidated yet.

Research objectives

The objective of this study was to analyze and to compare the biological and molecular effects of three different D-vitamins, vitamin D2, vitamin D3 and calcipotriol, in PSCs.

Research methods

Murine PSCs were exposed to D-vitamins as primary cultures (early activated PSCs) and upon re-culturing (fully-activated cells). Exhibition of vitamin A containing lipid droplets and expression of α-smooth muscle actin were used as surrogate markers of PSC activation. Therefore, oil red staining, immunofluorescence studies and immunoblot analyses were performed. Gene expression was monitored by real-time PCR, and interleukin-6 (IL-6) protein levels were quantified by ELISA. Furthermore, ^{18}F-proline was employed to measure the cellular uptake of proline.

Research results

The results of this study show for the first time that vitamin D exerts distinct effects on quiescent and activated PSCs *in vitro*. In quiescent PSCs, vitamin D prevented the exhibition of a myofibroblastic phenotype. Once the cells were fully activated, vitamin D failed to induce a complete reversal of the myofibroblastic phenotype, but still exerted antifibrotic effects on PSCs by inhibiting uptake of proline and expression of IL-6. Three vitamin D derivatives, vitamin D2, vitamin D3 and calcipotriol, displayed very similar biological effects.

Research conclusions

D-vitamins are efficient inhibitors of PSC activation *in vitro*, but cannot reverse the phenotype once the cells are fully activated. In line with other publications in the field, our findings encourage a further evaluation of vitamin D effects in pancreatic cancer and chronic pancreatitis. A modulation of the stroma response by vitamin D might hold potential as part of a multimodal concept for the treatment of both diseases.

Research perspectives

These investigations have shown that vitamin D2, vitamin D3 and calcipotriol are similarly effective with respect to the inhibition of PSC activation *in vitro*. Directions of future research should include both mechanistic studies on the molecular basis of vitamin D action in PSCs, and experimental studies on vitamin D efficiency in the context pancreatic cancer and chronic pancreatitis. Therefore, advanced cell culture models such as human stellate cells and animal models of pancreatic fibrosis need to be employed.

ACKNOWLEDGMENTS

We thank Mrs. Katja Bergmann for expert technical assistance and Dr. Änne Glass for help with the statistical evaluation of the data.

REFERENCES

1 **Erkan M**, Adler G, Apte MV, Bachem MG, Buchholz M, Detlefsen S, Esposito I, Friess H, Gress TM, Habisch HJ, Hwang RF, Jaster R, Kleeff J, Klöppel G, Kordes C, Logsdon CD, Masamune A, Michalski CW, Oh J, Phillips PA, Pinzani M, Reiser-Erkan C, Tsukamoto H, Wilson J. StellaTUM: current consensus and discussion on pancreatic stellate cell research. *Gut* 2012; **61**: 172-178 [PMID: 22115911 DOI: 10.1136/gutjnl-2011-301220]

2 **Bachem MG**, Schneider E, Gross H, Weidenbach H, Schmid RM, Menke A, Siech M, Beger H, Grünert A, Adler G. Identification, culture, and characterization of pancreatic stellate cells in rats and humans. *Gastroenterology* 1998; **115**: 421-432 [PMID: 9679048 DOI: 10.1016/S0016-5085(98)70209-4]

3 **Apte MV**, Haber PS, Applegate TL, Norton ID, McCaughan GW, Korsten MA, Pirola RC, Wilson JS. Periacinar stellate shaped cells in rat pancreas: identification, isolation, and culture. *Gut* 1998; **43**: 128-133 [PMID: 9771417 DOI: 10.1136/gut.43.1.128]

4 **Luttenberger T**, Schmid-Kotsas A, Menke A, Siech M, Beger H, Adler G, Grünert A, Bachem MG. Platelet-derived growth factors stimulate proliferation and extracellular matrix synthesis of pancreatic stellate cells: implications in pathogenesis of pancreas fibrosis. *Lab Invest* 2000; **80**: 47-55 [PMID: 10653002 DOI: 10.3748/wjg.15.4143]

5 **Vonlaufen A**, Joshi S, Qu C, Phillips PA, Xu Z, Parker NR, Toi CS, Pirola RC, Wilson JS, Goldstein D, Apte MV. Pancreatic stellate cells: partners in crime with pancreatic cancer cells. *Cancer Res* 2008; **68**: 2085-2093 [PMID: 18381413 DOI: 10.1158/0008-5472.CAN-07-2477]

6 **Hwang RF**, Moore T, Arumugam T, Ramachandran V, Amos KD, Rivera A, Ji B, Evans DB, Logsdon CD. Cancer-associated stromal fibroblasts promote pancreatic tumor progression. *Cancer Res* 2008; **68**: 918-926 [PMID: 18245495 DOI: 10.1158/0008-5472.CAN-07-5714]

7 **Müerköster S**, Wegehenkel K, Arlt A, Witt M, Sipos B, Kruse ML, Sebens T, Klöppel G, Kalthoff H, Fölsch UR, Schäfer H. Tumor stroma interactions induce chemoresistance in pancreatic ductal carcinoma cells involving increased secretion and paracrine effects of nitric oxide and interleukin-1beta. *Cancer Res* 2004; **64**: 1331-1337 [PMID: 14973050 DOI: 10.1158/0008-5472.CAN-03-1860]

8 **Bachem MG**, Schünemann M, Ramadani M, Siech M, Beger H, Buck A, Zhou S, Schmid-Kotsas A, Adler G. Pancreatic carcinoma cells induce fibrosis by stimulating proliferation and matrix synthesis of stellate cells. *Gastroenterology* 2005; **128**: 907-921 [PMID: 15825074 DOI: 10.1053/j.gastro.2004.12.036]

9 **Özdemir BC**, Pentcheva-Hoang T, Carstens JL, Zheng X, Wu CC, Simpson TR, Laklai H, Sugimoto H, Kahlert C, Novitskiy SV, De Jesus-Acosta A, Sharma P, Heidari P, Mahmood U, Chin L, Moses HL, Weaver VM, Maitra A, Allison JP, LeBleu VS, Kalluri R. Depletion of Carcinoma-Associated Fibroblasts and Fibrosis Induces Immunosuppression and Accelerates Pancreas Cancer with Reduced Survival. *Cancer Cell* 2015; **28**: 831-833 [PMID: 28843279 DOI: 10.1016/j.ccell.2015.11.002]

10 **Rhim AD**, Oberstein PE, Thomas DH, Mirek ET, Palermo CF, Sastra SA, Dekleva EN, Saunders T, Becerra CP, Tattersall IW, Westphalen CB, Kitajewski J, Fernandez-Barrena MG, Fernandez-Zapico ME, Iacobuzio-Donahue C, Olive KP, Stanger BZ. Stromal elements act to restrain, rather than support, pancreatic ductal adenocarcinoma. *Cancer Cell* 2014; **25**: 735-747 [PMID: 24856585 DOI: 10.1016/j.ccr.2014.04.021]

11 **Wang Z**, Li J, Chen X, Duan W, Ma Q, Li X. Disrupting the balance between tumor epithelia and stroma is a possible therapeutic approach for pancreatic cancer. *Med Sci Monit* 2014; **20**: 2002-2006 [PMID: 25327552 DOI: 10.12659/MSM.892523]

12 **Sherman MH**, Yu RT, Engle DD, Ding N, Atkins AR, Tiriac H, Collisson EA, Connor F, Van Dyke T, Kozlov S, Martin P, Tseng TW, Dawson DW, Donahue TR, Masamune A, Shimosegawa T, Apte MV, Wilson JS, Ng B, Lau SL, Gunton JE, Wahl GM, Hunter T, Drebin JA, O'Dwyer PJ, Liddle C, Tuveson DA, Downes M, Evans RM. Vitamin D receptor-mediated stromal reprogramming suppresses pancreatitis and enhances pancreatic cancer therapy. *Cell* 2014; **159**: 80-93 [PMID: 25259922 DOI: 10.1016/j.cell.2014.08.007]

13 **Bläuer M**, Sand J, Laukkarinen J. Physiological and clinically attainable concentrations of 1,25-dihydroxyvitamin D3 suppress proliferation and extracellular matrix protein expression in mouse pancreatic stellate cells. *Pancreatology* 2015; **15**: 366-371 [PMID: 26005021 DOI: 10.1016/j.pan.2015.05.044]

14 **Jaster R**, Sparmann G, Emmrich J, Liebe S. Extracellular signal regulated kinases are key mediators of mitogenic signals in rat pancreatic stellate cells. *Gut* 2002; **51**: 579-584 [PMID: 12235084 DOI: 10.1136/gut.51.4.579]

15 **Witteck L**, Jaster R. Trametinib and dactolisib but not regorafenib exert antiproliferative effects on rat pancreatic stellate cells. *Hepatobiliary Pancreat Dis Int* 2015; **14**: 642-650 [PMID: 26663013 DOI: 10.1016/S1499-3872(15)60032-7]

16 **Sparmann G**, Kruse ML, Hofmeister-Mielke N, Koczan D, Jaster R, Liebe S, Wolff D, Emmrich J. Bone marrow-derived pancreatic

stellate cells in rats. *Cell Res* 2010; **20**: 288-298 [PMID: 20101265 DOI: 10.1038/cr.2010.10]
17 **Rateitschak K**, Karger A, Fitzner B, Lange F, Wolkenhauer O, Jaster R. Mathematical modelling of interferon-gamma signalling in pancreatic stellate cells reflects and predicts the dynamics of STAT1 pathway activity. *Cell Signal* 2010; **22**: 97-105 [PMID: 19781632 DOI: 10.1016/j.cellsig.2009.09.019]
18 **Bülow R**, Fitzner B, Sparmann G, Emmrich J, Liebe S, Jaster R. Antifibrogenic effects of histone deacetylase inhibitors on pancreatic stellate cells. *Biochem Pharmacol* 2007; **74**: 1747-1757 [PMID: 17889833 DOI: 10.1016/j.bcp.2007.08.023]
19 **Hamacher K.** Synthesis of n.c.a. cis- and trans-4-[18F]Fluoro-L-proline, radiotracers for PET-investigation of disordered matrix protein synthesis. *J Label Compd Radiopharm* 1999; **42**: 1135-1144 [DOI: 10.1002/(SICI)1099-1344(199912)42:123.0.CO;2-3]
20 **Lavalaye J**, Grutters JC, van de Garde EM, van Buul MM, van den Bosch JM, Windhorst AD, Verzijlbergen FJ. Imaging of fibrogenesis in patients with idiopathic pulmonary fibrosis with cis-4-[(18)F]-Fluoro-L: -proline PET. *Mol Imaging Biol* 2009; **11**: 123-127 [PMID: 18665424 DOI: 10.1007/s11307-008-0164-1]
21 **Zella LA**, Kim S, Shevde NK, Pike JW. Enhancers located in the vitamin D receptor gene mediate transcriptional autoregulation by 1,25-dihydroxyvitamin D3. *J Steroid Biochem Mol Biol* 2007; **103**: 435-439 [PMID: 17218097 DOI: 10.1016/j.jsbmb.2006.12.019]
22 **Aoki H**, Ohnishi H, Hama K, Shinozaki S, Kita H, Yamamoto H, Osawa H, Sato K, Tamada K, Sugano K. Existence of autocrine loop between interleukin-6 and transforming growth factor-beta1 in activated rat pancreatic stellate cells. *J Cell Biochem* 2006; **99**: 221-228 [PMID: 16598747 DOI: 10.1002/jcb.20906]
23 **Mews P**, Phillips P, Fahmy R, Korsten M, Pirola R, Wilson J, Apte M. Pancreatic stellate cells respond to inflammatory cytokines: potential role in chronic pancreatitis. *Gut* 2002; **50**: 535-541 [PMID: 11889076 DOI: 10.1136/gut.50.4.535]
24 **Schneider E**, Schmid-Kotsas A, Zhao J, Weidenbach H, Schmid RM, Menke A, Adler G, Waltenberger J, Grünert A, Bachem MG. Identification of mediators stimulating proliferation and matrix synthesis of rat pancreatic stellate cells. *Am J Physiol Cell Physiol* 2001; **281**: C532-C543 [PMID: 11443052]

P- Reviewer: Chowdhury P, Ker CG **S- Editor**: Ma YJ **L- Editor**: A
E- Editor: Li D

World Journal of Gastroenterology

Submit a Manuscript: http://www.f6publishing.com

World J Gastroenterol 2018 January 14; 24(2): 179-194

DOI: 10.3748/wjg.v24.i2.179

ISSN 1007-9327 (print) ISSN 2219-2840 (online)

ORIGINAL ARTICLE

Basic Study

Metabolic and hepatic effects of liraglutide, obeticholic acid and elafibranor in diet-induced obese mouse models of biopsy-confirmed nonalcoholic steatohepatitis

Kirstine S Tølbøl, Maria NB Kristiansen, Henrik H Hansen, Sanne S Veidal, Kristoffer TG Rigbolt, Matthew P Gillum, Jacob Jelsing, Niels Vrang, Michael Feigh

Kirstine S Tølbøl, Maria NB Kristiansen, Henrik H Hansen, Sanne S Veidal, Kristoffer TG Rigbolt, Jacob Jelsing, Niels Vrang, Michael Feigh, Gubra Aps, Hørsholm DK-2970, Denmark

Kirstine S Tølbøl, Maria NB Kristiansen, Department of Biomedical Sciences, Faculty of Health Sciences, University of Copenhagen, Copenhagen DK-2200, Denmark

Kirstine S Tølbøl, Matthew P Gillum, Section for Metabolic Imaging and Liver Metabolism, The Novo Nordisk Foundation Center for Basic Metabolic Research, Faculty of Health Sciences, University of Copenhagen, Copenhagen DK-2200, Denmark

Niels Vrang, Department of Chemistry, Faculty of Science, University of Copenhagen, Copenhagen DK-2200, Denmark

ORCID number: Kirstine S Tølbøl (0000-0001-6817-7441); Maria NB Kristiansen (0000-0001-8732-3977); Henrik H Hansen (0000-0002-3732-0281); Sanne S Veidal (0000-0003-1240-2034); Kristoffer TG Rigbolt (0000-0002-9470-0993); Matthew P Gillum (0000-0003-4893-012X); Jacob Jelsing (0000-0002-4583-1022); Niels Vrang (0000-0002-7203-9532); Michael Feigh (0000-0001-5274-8799).

Author contributions: Tølbøl KS and Kristiansen MNB contributed equally to the work; Jelsing J, Vrang N and Feigh M designed the study; Tølbøl KS, Kristiansen MNB, Veidal SS and Rigbolt KTG acquired and analysed data; Tølbøl KS, Kristiansen MNB, Hansen HH, Veidal SS, Rigbolt KTG, Gillum MP, Jelsing J, Vrang N and Feigh M interpreted the data and contributed to writing the article, editing and reviewing, all authors approved the final version of the article.

Supported by Innovation Fund Denmark, KST; No. 5016-00168B; and MNBK, No. 5189-00040B.

Institutional animal care and use committee statement: All animal experiments conformed to the internationally accepted principles for the care and use of laboratory animals (Licence No. 2013-15-2934-00784, The Animal Experiments Inspectorate, Denmark).

Conflict-of-interest statement: The authors declare no conflict of interest.

Data sharing statement: No additional data are available.

Manuscript source: Unsolicited manuscript

Correspondence to: Kirstine S Tølbøl, MSc, Research Scientist, Gubra Aps, Hørsholm Kongevej 11B, Hørsholm DK-2970, Denmark. kst@gubra.dk
Telephone: +45-23-1522650

Received: September 25, 2017
Peer-review started: September 25, 2017
First decision: November 3, 2017
Revised: November 24, 2017
Accepted: December 5, 2017
Article in press: December 5, 2017
Published online: January 14, 2018

Abstract

AIM

To evaluate the pharmacodynamics of compounds in clinical development for nonalcoholic steatohepatitis (NASH) in obese mouse models of biopsy-confirmed

NASH.

METHODS

Male wild-type C57BL/6J mice (DIO-NASH) and Lep$^{ob/ob}$ (*ob/ob*-NASH) mice were fed a diet high in trans-fat (40%), fructose (20%) and cholesterol (2%) for 30 and 21 wk, respectively. Prior to treatment, all mice underwent liver biopsy for confirmation and stratification of liver steatosis and fibrosis, using the nonalcoholic fatty liver disease activity score (NAS) and fibrosis staging system. The mice were kept on the diet and received vehicle, liraglutide (0.2 mg/kg, SC, BID), obeticholic acid (OCA, 30 mg/kg PO, QD), or elafibranor (30 mg/kg PO, QD) for eight weeks. Within-subject comparisons were performed on changes in steatosis, inflammation, ballooning degeneration, and fibrosis scores. In addition, compound effects were evaluated by quantitative liver histology, including percent fractional area of liver fat, galectin-3, and collagen 1a1.

RESULTS

Liraglutide and elafibranor, but not OCA, reduced body weight in both models. Liraglutide improved steatosis scores in DIO-NASH mice only. Elafibranor and OCA reduced histopathological scores of hepatic steatosis and inflammation in both models, but only elafibranor reduced fibrosis severity. Liraglutide and OCA reduced total liver fat, collagen 1a1, and galectin-3 content, driven by significant reductions in liver weight. The individual drug effects on NASH histological endpoints were supported by global gene expression (RNA sequencing) and liver lipid biochemistry.

CONCLUSION

DIO-NASH and *ob/ob*-NASH mouse models show distinct treatment effects of liraglutide, OCA, and elafibranor, being in general agreement with corresponding findings in clinical trials for NASH. The present data therefore further supports the clinical translatability and utility of DIO-NASH and *ob/ob*-NASH mouse models of NASH for probing the therapeutic efficacy of compounds in preclinical drug development for NASH.

Key words: Nonalcoholic steatohepatitis; Disease models; Pathology; Fibrosis; Liver biopsy; Transcriptomics; Pharmacodynamics; Glucagon-like peptide-1 receptor; Peroxisome proliferator-activated receptor; Farnesoid X receptor

Core tip: The pharmacodynamics of three compounds in advanced clinical development for the treatment of nonalcoholic steatohepatitis (NASH), including liraglutide, elafibranor and obeticholic acid, were evaluated in wild-type and genetically (*ob/ob*) obese mouse models of NASH. Prior to treatment, all mice underwent liver biopsy for confirmation and stratification of liver steatosis and fibrosis. Within-subject comparisons were performed on changes in liver histopathology. Wild-type and *ob/ob*-NASH obese mice showed distinct treatment effects of liraglutide, OCA, and elafibranor, being in general agreement with corresponding findings in clinical trials for NASH. In conclusion, the two obese mouse models of NASH show clinical translatability with respect to disease etiology, histopathology and drug treatment effects, which supports their utility in preclinical drug development.

Tølbøl KS, Kristiansen MN, Hansen HH, Veidal SS, Rigbolt KT, Gillum MP, Jelsing J, Vrang N, Feigh M. Metabolic and hepatic effects of liraglutide, obeticholic acid and elafibranor in diet-induced obese mouse models of biopsy-confirmed nonalcoholic steatohepatitis. *World J Gastroenterol* 2018; 24(2): 179-194 Available from: URL: http://www.wjgnet.com/1007-9327/full/v24/i2/179.htm DOI: http://dx.doi.org/10.3748/wjg.v24.i2.179

INTRODUCTION

Nonalcoholic steatohepatitis (NASH) is characterized by varying degrees of hepatic steatosis, cytoskeletal damage, and lobular inflammation with or without fibrosis[1]. The pathogenesis of NASH is complex with current hypotheses involving fatty acid-mediated lipotoxicity exhausting hepatocyte adaptive and regenerative responses, whereby accumulating oxidative stress can trigger hepatocyte necroinflammation, fibrosis, and disruption of hepatic cytoarchitecture[2,3]. Immunopathological alterations likely also play a key role in NASH, presumably driven by maladaptive responses in the innate and adaptive immune system[4,5].

The primary drivers of NASH are obesity and diabetes, and the high prevalence of these major metabolic diseases is expected to make NASH one of the most common causes of advanced liver disorders in the coming decade[6]. NASH is therefore rapidly emerging as a major public health problem, however, with currently no evidence-based approved drug therapies. This has prompted substantial efforts to identify novel pharmacological concepts for correcting the underlying metabolic deficits and alleviate, or prevent, hepatic fibrosis in NASH[7,8]. To improve the understanding of NASH pathogenesis and facilitate the development of novel therapeutics for NASH, several mouse models have been employed[8]. A number of diet-induced obesity (DIO) models mimic the natural history of NASH and have demonstrated relatively good clinical translatability with respect to key metabolic and liver pathological changes with mild- to moderate-grade liver fibrosis, and these models have therefore been increasingly used in preclinical drug development[9-13]. In comparison, non-physiological diets that are low or devoid of certain essential amino acids promote more severe liver fibrosis, but also result in significant weight loss, making these NASH models more applicable for

probing drug treatment efficacy on hepatic injury and regeneration[13-16].

Notably, NASH show spontaneous and unpredictable onset with varying disease severity and different rates of progression[1]. Today, liver biopsy-confirmed pathology is the mainstay for clinical trials which allows for stratification of disease severity/stage and within-subject evaluation of endpoint liver histology[17,18]. In agreement with the clinical findings, DIO mouse models of NASH show variable disease severity. Recent reports have demonstrated that all stages of NASH are represented in mice fed Western-type obesogenic diets for any period ⩾ 20 wk, and a significant proportion of up to 30% of the animals fail to develop steatohepatitis and liver fibrosis[9,13,19], indicating that individual baseline disease stage is also a critical factor in the assessment of treatment effects in DIO mouse models of NASH. However, disease state heterogeneity is often overlooked in preclinical NASH studies which may result in unintentional large variability in endpoint histopathology and narrow the window for detection of therapeutic effects. Another factor to be considered in preclinical drug development for NASH is that drug treatment periods in mouse models of NASH have varied from subacute to chronic dosing settings with histological endpoints evaluated by different qualitative and quantitative methods. Comparison of preclinical treatment effects of potential anti-NASH compounds is therefore misleading in the absence of head-to-head pharmacological studies in experimental models of NASH.

We have recently reported liver biopsy-confirmed histopathology in wild-type (DIO-NASH) and genetically obese (*ob/ob*-NASH) mouse models of NASH[19]. Both models display hallmarks of NASH, *i.e.* steatosis, lobular inflammation, hepatocellular ballooning, but are distinguished histologically by the representation of mild (DIO-NASH) or moderate (*ob/ob*-NASH) grade hepatic fibrosis[9,19]. The present comparative study in the DIO-NASH and *ob/ob*-NASH mouse models of biopsy-confirmed histopathology aimed to characterize within-subject treatment responses of compounds in current advanced clinical development for NASH, including liraglutide[20], obeticholic acid (OCA, INT-747)[21], and elafibranor (GFT-505)[22]. Liraglutide is a long-acting glucagon-like peptide 1 (GLP-1) analogue with picomolar GLP-1 receptor binding potency[23], and is approved for the management of type 2 diabetes and obesity. Whereas liraglutide improves glycemia by stimulating pancreatic cell function, its anti-obesity effects are predominantly centrally mediated through suppression of hypothalamic appetite signaling[24,25]. OCA is a semi-synthetic bile acid currently approved for the treatment of primary biliary cholangitis[26]. OCA acts as a transcriptional activator through high-affinity binding to the nuclear farnesoid X receptor (FXR)[27] to regulate bile acid synthesis and transport, hepatic lipid and carbohydrate metabolism, as well as immune function[28]. Elafibranor is a selective dual agonist for peroxisome proliferator-activated α/δ receptors (PPAR-α/δ)[29], another group of ligand-activated nuclear receptors with particularly highly abundancy in the liver. As for OCA, elafibranor exerts its major effects through transcriptional regulation of key genes involved in hepatic lipid and glucose metabolism, but also modulates hepatic inflammation and collagen turnover[30]. Liraglutide, OCA and elafibranor therefore influences different disease mechanisms in NASH, making these compounds well-suited for comparing the treatment efficacy of different therapeutic concepts in the two mouse models of NASH.

MATERIALS AND METHODS

Animals

All animal experiments were conducted according to internationally accepted principles for the care and use of laboratory animals (licence no. 2013-15-2934-00784, The Animal Experiments Inspectorate, Denmark). The animal protocol was designed to minimize pain or discomfort to the animals. Male mice were obtained from Janvier Labs (Le Genest Saint Isle, France) and housed in a controlled environment (12 h light/dark cycle, light on at 3 AM, 21 ± 2 ℃, humidity 50% ± 10%). Each animal was identified by an implantable microchip (PetID Microchip, E-vet, Haderslev, Denmark). Mice had *ad libitum* access to tap water and either regular rodent chow (Altromin 1324, Brogaarden, Hoersholm, Denmark), or a diet high in fat (40%, containing 18% trans-fat), 40% carbohydrates (20% fructose) and 2% cholesterol (AMLN diet; D09100301, Research Diets, New Brunswick, NJ)[19]. Disease progression was characterized in wild-type DIO-NASH mice, 5 wk-old at the arrival at Gubra, and fed AMLN diet for up to 50 wk (n = 8-10 animals per time point). Effects of drug treatment were evaluated in wild-type C57BL/6J and B6.V-*Lep*^{ob}/JRj (*ob/ob*) mice 5-6 wk-old at the arrival at Gubra. C57BL/6J mice were fed chow (controls) or AMLN diet (DIO-NASH mice) for 30 wk prior to treatment start. *ob/ob* mice were fed chow (*ob/ob* controls) or AMLN diet (*ob/ob*-NASH mice) for 21 wk prior to treatment start. Body weight was measured daily during the treatment period.

Baseline liver biopsy

All animals included in the drug treatment experiments underwent liver biopsy, as described in detail previously[9,19]. In brief, the mice were anesthetized with isoflurane (Vetflurane®, Virbac, Kolding, Denmark) in atmospheric air. A midline abdominal incision was made to expose the left lateral lobe, and a cone-shaped biopsy of 50-100 mg liver tissue was collected and fixed in 4% paraformaldehyde overnight and subsequently used for histological assessment. The cut surfaces were electrocoagulated using an electrosurgicial unit (ERBE VIO 100C, ERBE, Marietta, GA, United States), whereupon the liver was returned to the abdominal

cavity, the abdominal wall was sutured and the skin was stapled. The animals received 5 mg/kg carprofen (Norodyl®, ScanVet, Fredensborg, Denmark) prior to surgery and on post-operative day 1 and 2. Animals were single-housed after the procedure and allowed to recover for 3 wk prior to treatment start. Only mice with fibrosis stage $\geqslant$ 1 and steatosis score $\geqslant$ 2, evaluated using the clinical criteria outlined by Kleiner *et al*[31], were included in the study.

Drug treatment

Liraglutide (Victoza™ pen) was from Novo Nordisk (Bagsvaerd, Denmark), elafibranor and OCA were from SunshineChem (Shanghai, China). Vehicles were 0.5% carboxymethyl cellulose with 0.01 % Tween-80 (PO dosing) or phosphate-buffered saline with 0.1% bovine serum albumin (SC dosing), administered in a dosing volume of 5 mL/kg. Animals were stratified (n = 9-12 per group) based on mean fibrosis and steatosis score, and treated for 8 wk with vehicle (PO, QD), liraglutide (0.2 mg/kg, SC, BID), OCA (30 mg/kg, PO, QD), or elafibranor (30 mg/kg, PO, QD). Vehicle-dosed chow-fed mice (PO, QD) served as additional controls. The compound doses used in the present study were within the dose range reported efficacious in other mouse models of diet-induced obesity and NASH[13,30,32-35]. A terminal blood sample was collected from the tail vein in non-fasted mice and used for plasma biochemistry. Animals were sacrificed by cardiac puncture under isoflurane anesthesia. Liver samples were processed as described below.

Biochemical and histological analyses

Biochemical and histological analyses were performed as reported previously[19]. Plasma analytes included alanine aminotransferase (ALT), aspartate aminotransferase (AST), triglycerides (TG) and total cholesterol (TC). Liver homogenates were analyzed for TG and TC. Paraformaldehyde-fixed liver pre- and post-biopsies were paraffin-embedded, sectioned, and stained with hematoxylin-eosin (Dako, Glostrup, Denmark), Picro-Sirius red (Sigma-Aldrich, Broendby, Denmark), anti-type I collagen (Col1a1; Southern Biotech, Birmingham, AL), or anti-galectin-3 (Biolegend, San Diego, CA, United States). The NAFLD activity score (NAS) and fibrosis staging system was applied to liver pre-biopies and terminal samples (drug treatment experiments) or only terminal samples (disease progression experiment) for scoring of steatosis, lobular inflammation, hepatocyte ballooning, and fibrosis outlined by Kleiner *et al*[31]. All histological assessments were performed by a pathologist blind to treatment. Because all treatment paradigms affected total liver weight, quantitative data on liver biochemistry (liver TG, TC) and histology (liver lipid, galectin-3, Col1a1) were expressed as whole-liver amounts by multiplying individual terminal liver weight with the corresponding liver lipid concentration (biochemistry data) or percent fractional area (histology data), respectively.

RNA sequencing

Hepatic transcriptome analysis was performed by RNA sequencing on RNA extracts from terminal liver samples (15 mg fresh tissue), as described in detail previously[19]. The RNA quantity was measured using Qubit® (Thermo Scientific, Eugene, OR, United States). The RNA quality was determined using a bioanalyzer with RNA 6000 Nano kit (Agilent, Waldbronn, Germany). RNA sequence libraries were prepared with NeoPrep (Illumina, San Diego, CA, United States) using Illumina TruSeq stranded mRNA Library kit for NeoPrep (Illumina, San Diego, CA, United States) and sequenced on the NextSeq 500 (Illumina, San Diego, CA, United States) with NSQ 500 hi-Output KT v2 (75 CYS, Illumina, San Diego, CA, United States). Reads were aligned to the GRCm38 v84 Ensembl *Mus musculus* genome using STAR v.2.5.2a with default parameters[36]. Differential gene expression analysis was performed with DEseq2[37]. Genes with a Benjamini and Hochberg adjusted $P \leqslant 0.05$ (5% False Discovery Rate) were regarded as statistically significantly regulated. Enrichment analysis of KEGG pathways were performed using the clusterProfiler package for R[38].

Statistical analyses

Except from RNA sequencing, data were analyzed using GraphPad Prism v5.02 software (GraphPad, La Jolla, CA, United States). All results are shown as mean ± SE. A two-way ANOVA with Bonferroni's post-hoc test was performed for body weight analysis. Fisher's exact test was used to test for within-subject changes in histology scores before and after treatment, compared to vehicle controls. A one-way ANOVA with Dunnett's post-hoc test was used for all other parameters. A P-value < 0.05 was considered statistically significant.

RESULTS

Disease progression in wild-type DIO-NASH mice

Terminal samples were assessed for analysis of plasma and liver biochemistry, as well as liver morphology and quantitative histology.

Metabolic data are shown in Supplemental Figure 1. Body weight in DIO-NASH mice gradually increased over the feeding period and reached a plateau (approximately 40 g) after approximately 35 wk of dieting (Supplemental Figure 1, panel A). DIO-NASH mice developed hepatomegaly and fatty liver from dietary week 10 and onwards (panel B, F). Plasma ALT and AST increased during the dieting period, with the effect on AST being transient (panel C, D). Onset of hypercholesterolemia was evident from dieting week 10 (panel E), and liver TC levels were elevated even earlier (panel G). Liver, but not plasma, TG levels were increased from dieting wk 10-50 (panel F, H).

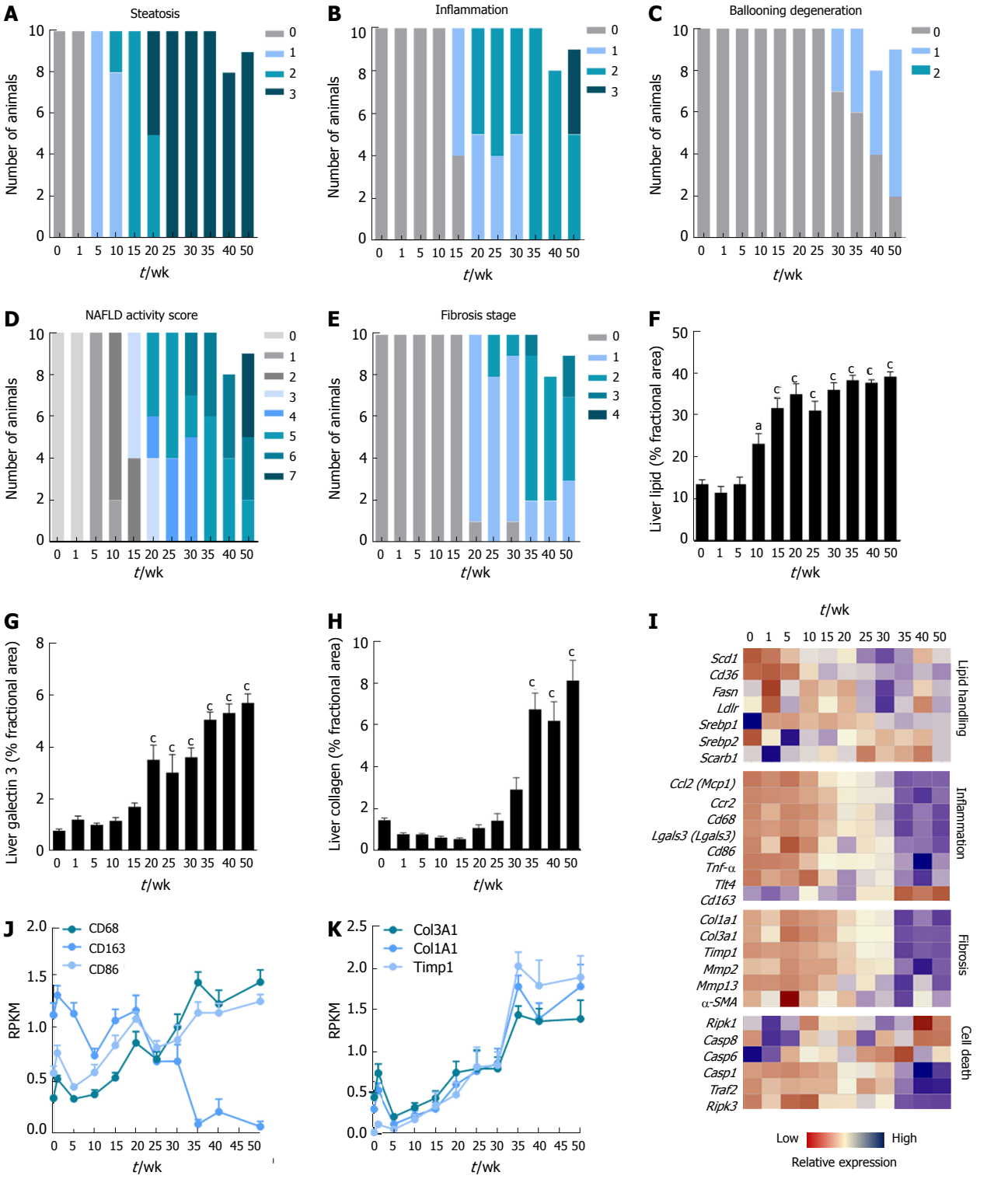

Figure 1 Disease progression in DIO-nonalcoholic steatohepatitis mice. A-E: Individual and composite NAFLD activity scores (NAS) and fibrosis stage; F-H: Quantitative analysis of liver lipid, galectin-3 and collagen 1a1 fractional area; I-K: Heatmap on liver transcriptome changes and expression of selected genes. $^{a}P < 0.05$, $^{c}P < 0.001$ *vs* week 0. NASH: Nonalcoholic steatohepatitis.

Histology data are presented in Figure 1. Steatosis developed gradually in DIO-NASH mice and became severe after 20-25 wk of dieting (panel A). Lobular inflammation was observed after 15 wk and progressed in severity with increasing dieting periods (panel B). Hepatocyte ballooning was detected in a few mice after 30 wk, increasing in prevalence over time, but did not progress beyond stage 1 (panel C). Manifest NASH (NAS 4-5) was consistently observed after 20-30 wk of dieting and increase in severity during the remainder of the monitoring period (panel D). Fibrosis (stage 1) was consistently detected from 20 wk of dieting. All DIO-NASH mice developed fibrosis after 35 wk (predominantly stage 2), but 20%-30% of the

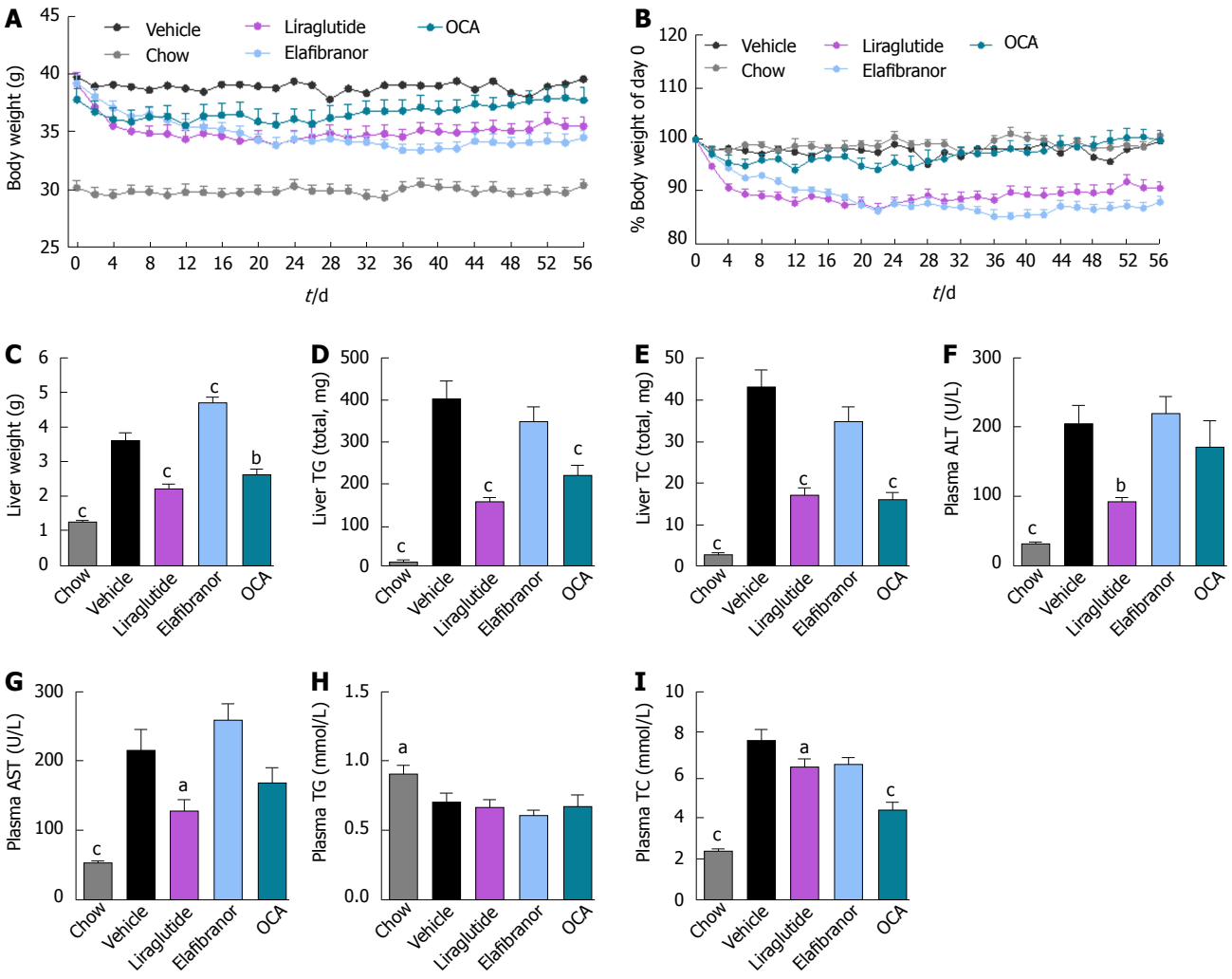

Figure 2 Metabolic effects of liraglutide, obeticholic acid, and elafibranor treatment in DIO-nonalcoholic steatohepatitis mice. $^{a}P < 0.05$, $^{b}P < 0.01$, $^{c}P < 0.001$ *vs* vehicle controls; OCA: Obeticholic acid; NASH: Nonalcoholic steatohepatitis.

mice remained at stage 1 after 50 wk of dieting (panel E). Hepatic lipid amounts significantly increased from dieting week 10 and reached a maximal level from week 15 (panel F). Liver galectin-3 immunoreactivity increased after 20 wk of dieting and progressed further with increasing dieting periods (panel G). Col1a1 immunoreactivity was elevated after 35 wk of dieting and did not change further (panel H). Late-stage complications were rare in DIO-NASH mice, and occurred only after ⩾ 40 wk on AMLN diet (cirrhosis and hepatic nodular formation, *n* = 1/19; extensive bile duct proliferation, *n* = 1/19, animals not included in data analysis).

A heatmap was generated for a panel of prototypical gene candidates associated with NASH pathology (Supplementary Figure 1, panel I). Signatures were markedly different during the study period, with an upregulation of genes involved in lipid handling, inflammation, fibrosis and cell death occurring over time. Expression of genes involved in lipid handling were gradually upregulated from week 20, with highest expression from week 35 wk and onwards. Gene groupings representative of monocyte/macrophage infiltration, inflammation, extracellular matrix (ECM) turnover, and apoptosis execution peaked at 35-50 wk of dieting (panel I-K).

Drug treatment in DIO-NASH mice

As expected, DIO-NASH mice gained more weight than chow-fed controls (Figure 2A). Treatment with liraglutide and elafibranor, but not OCA, resulted in weight loss (and loss of terminal whole-body fat, data not shown) which reached a maximal effect after approximately 2 wk of treatment (Figure 2A and B). Liraglutide and elafibranor, but not OCA, induced a transient reduction in daily food intake (from treatment d 1-3), whereupon food intake remained similar to vehicle-dosed DIO-NASH mice (data not shown). Whereas liraglutide and OCA reduced liver weight, elafibranor had the opposite effect (Figure 2C). Biochemical (plasma, liver) and quantitative histological (liver) analyses were applied. Liraglutide and OCA reduced total liver TG and TC content (Figure 2D and E). Only liraglutide significantly reduced plasma ALT and AST (Figure 2F and G). Liraglutide and OCA, but not

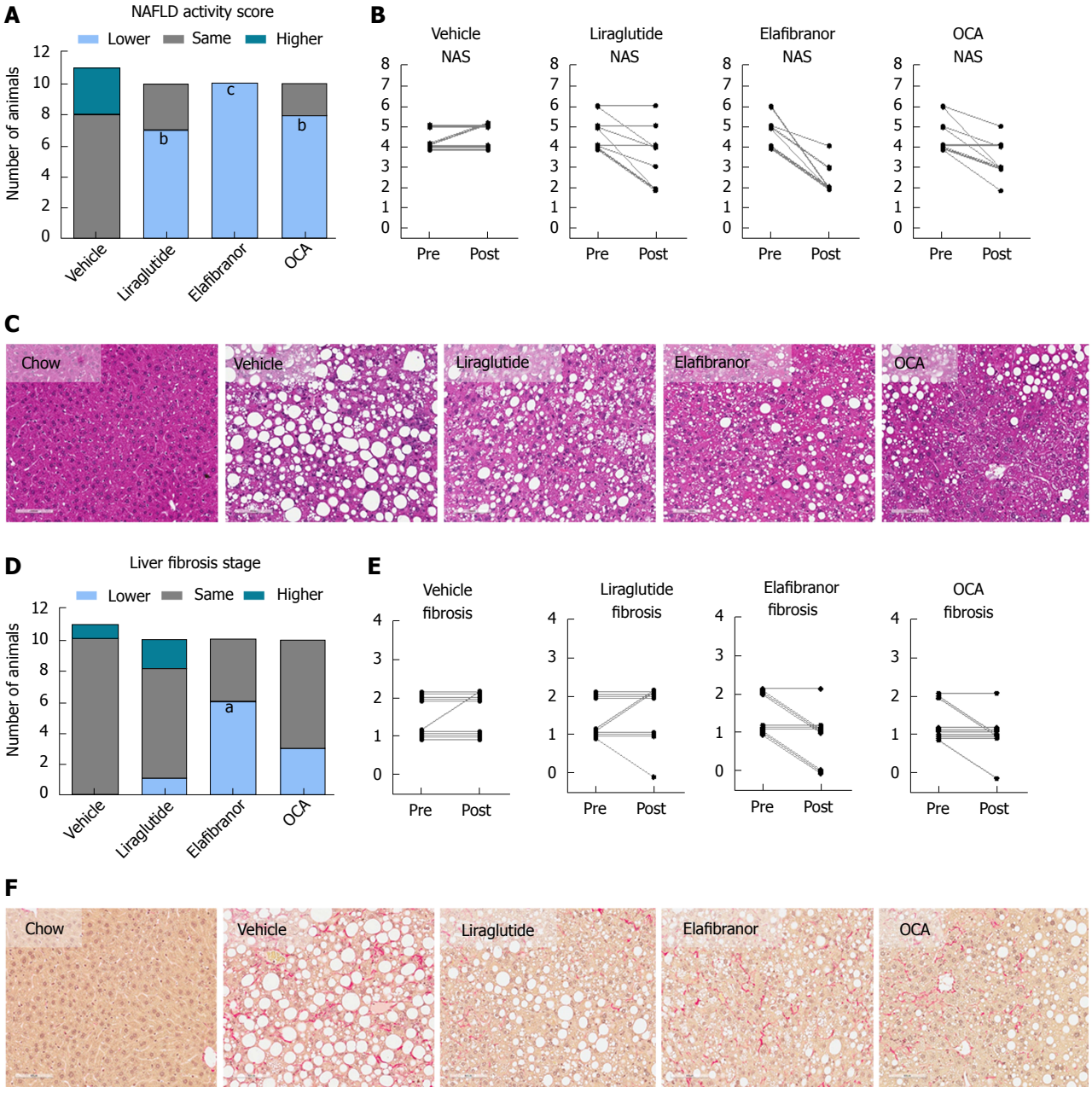

Figure 3 Histomorphological effects of liraglutide, obeticholic acid, and elafibranor treatment in DIO-nonalcoholic steatohepatitis mice. [a]$P < 0.05$, [b]$P < 0.01$, [c]$P < 0.001$ *vs* vehicle controls. OCA: Obeticholic acid; NASH: Nonalcoholic steatohepatitis.

elafibranor, reduced plasma TC levels (Figure 2I). None of the compounds affected plasma TG levels (Figure 2H). Liver morphometry was compared in pre- *vs.* post-treatment liver biopsies. All DIO-NASH mice included in the experiment showed pre-biopsy confirmed NASH (composite NAS 4-6) and liver fibrosis (stage 1-2), see Figure 3B and Supplementary Figure 2. All three compounds significantly improved NAS in DIO-NASH mice (Figure 3A and B), mainly due to reduced steatosis score (Supplementary Figure 2). In correspondence, all drug treatments also reduced total liver lipid content (Figure 4A and B). Only elafibranor improved fibrosis stage in pre- *vs*. post-treatment liver biopsies ($P < 0.05$, Figure 3D-F). In contrast, total galectin-3 and total Col1a1 levels were reduced following liraglutide and OCA, but not elafibranor, treatment (Figure 4C-F). Principal component analysis (PCA) indicated distinct uniform and stable gene transcriptional responses in the experimental groups. The major proportion of variance correlated with separation of the chow-fed and DIO-NASH controls (Figure 5A). PCA on the minor proportion of variance yielded a more mixed profile with partial separation of liraglutide and OCA effects (Figure 5B). Overall, liraglutide and OCA treatment resulted in transcriptome signatures partially resembling the lean control signature. Transcriptome changes also markedly overlapped between drug treatment groups. Notably, elafibranor induced the highest number of

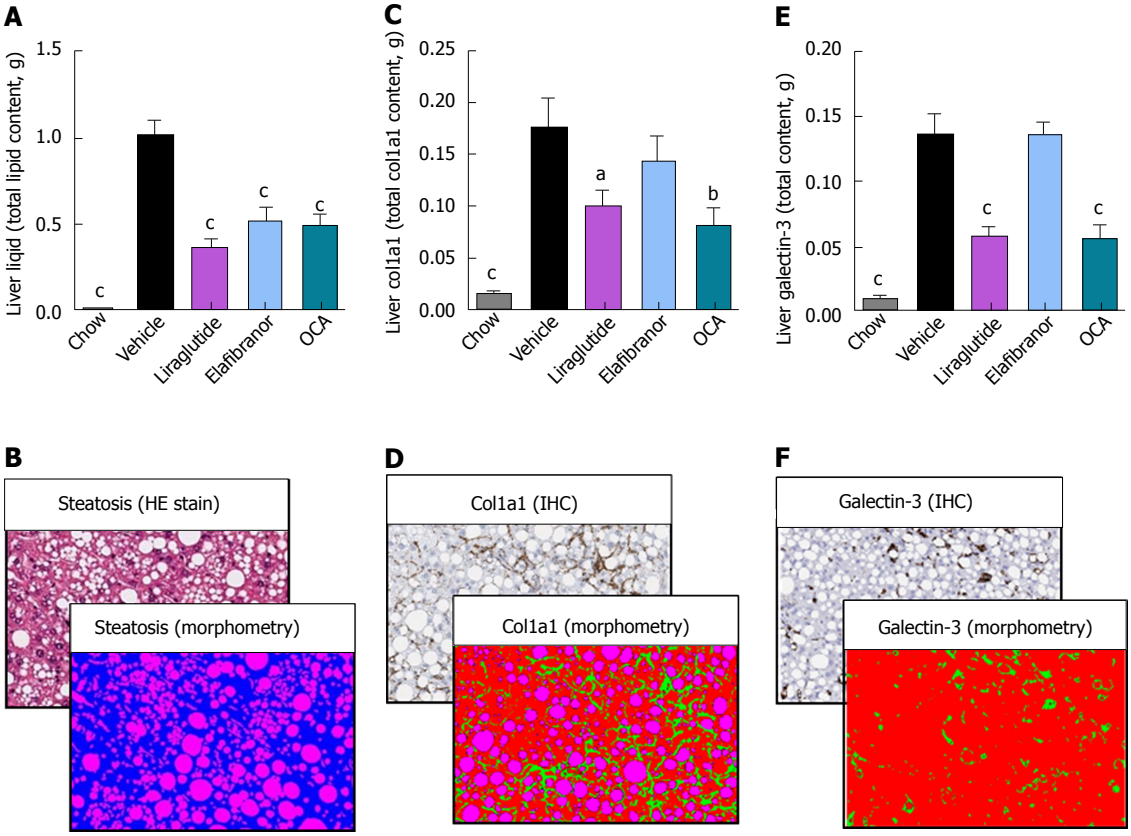

Figure 4 Quantitative histological assessment of liver lipids, collagen deposition and inflammation in DIO-nonalcoholic steatohepatitis mice. $^{a}P < 0.05$, $^{b}P < 0.01$, $^{c}P < 0.001$ *vs* vehicle controls. OCA: Obeticholic acid; NASH: Nonalcoholic steatohepatitis.

differentially expressed genes and evoked transcriptome modifications distinct from all other experimental groups (Figure 5A and C). Liraglutide induced conspicuous changes in transcriptional pathways associated with glucose metabolism, but had virtually no impact on gene groupings representing other liver metabolic pathways (Figure 5D). OCA modulated gene groupings linked to glucose metabolism, but also affected signaling pathways associated with NAFLD, ECM-receptor interaction, PI3 kinase signaling, and focal adhesion. Pathways perturbations promoted by elafibranor treatment mapped to NAFLD, lipid metabolism, oxidative phosphorylation, PPAR and peroxisome signaling. All drug treatments reduced expression of gene markers involved in inflammation, fibrogenesis, and apoptosis (Figure 5E and F).

Drug treatment in ob/ob-NASH mice

ob/ob-NASH controls were obese prior to treatment (51.7 ± 1.1 g, $n = 12$), but showed lower body weight compared to age-matched chow-fed *ob/ob* controls (60.1 ± 1.3 g, $n = 9$) (Figure 6A). Terminal liver weight was markedly higher in *ob/ob*-NASH control mice compared to chow-fed controls (Figure 6A-C). Liraglutide and elafibranor treatment progressively reduced body weight with a maximal weight loss of approximately 10% compared to baseline (approximately 20% *vs* vehicle-dosing), see Figure 6B. OCA did not affect body weight in *ob/ob*-NASH mice. Liraglutide, but not OCA and elafibranor, induced a transient reduction in daily food intake (from treatment d 1-7), whereupon food intake remained similar to vehicle-dosed *ob/ob*-NASH mice (data not shown). Liraglutide and OCA, but not elafibranor, reduced terminal liver weight (Figure 6C). Liraglutide reduced total liver TG content (Figure 6D) as well as plasma TG levels (Figure 6H), while elafibranor and OCA reduced total liver TC content (Figure 6E). All compounds lowered plasma TC levels (Figure 6I). Liraglutide and elafibranor, but not OCA, reduced plasma ALT and AST (Figure 6F and G). All *ob/ob*-NASH mice included in the experiment showed pre-biopsy confirmed NASH (composite NAS 4-7) and liver fibrosis (stage 2-3), see Figure 7B and Supplementary Figure 3. Elafibranor and OCA significantly reduced composite NAS, total liver fat and galectin-3 content in *ob/ob*-NASH mice (Figure 7A, B, E and F). Liver morphometry was compared in pre- *vs*. post-treatment liver biopsies. While elafibranor reduced NAS largely by improving steatosis and inflammation scores, OCA also consistently reduced ballooning (Supplementary Figure 3). Only elafibranor significantly reduced hepatic fibrosis stage (Figure 7C and D), but did not change total levels of Col1a1 (Figure 7F). Liraglutide had no effect on any individual NAS component, as well as composite NAS,

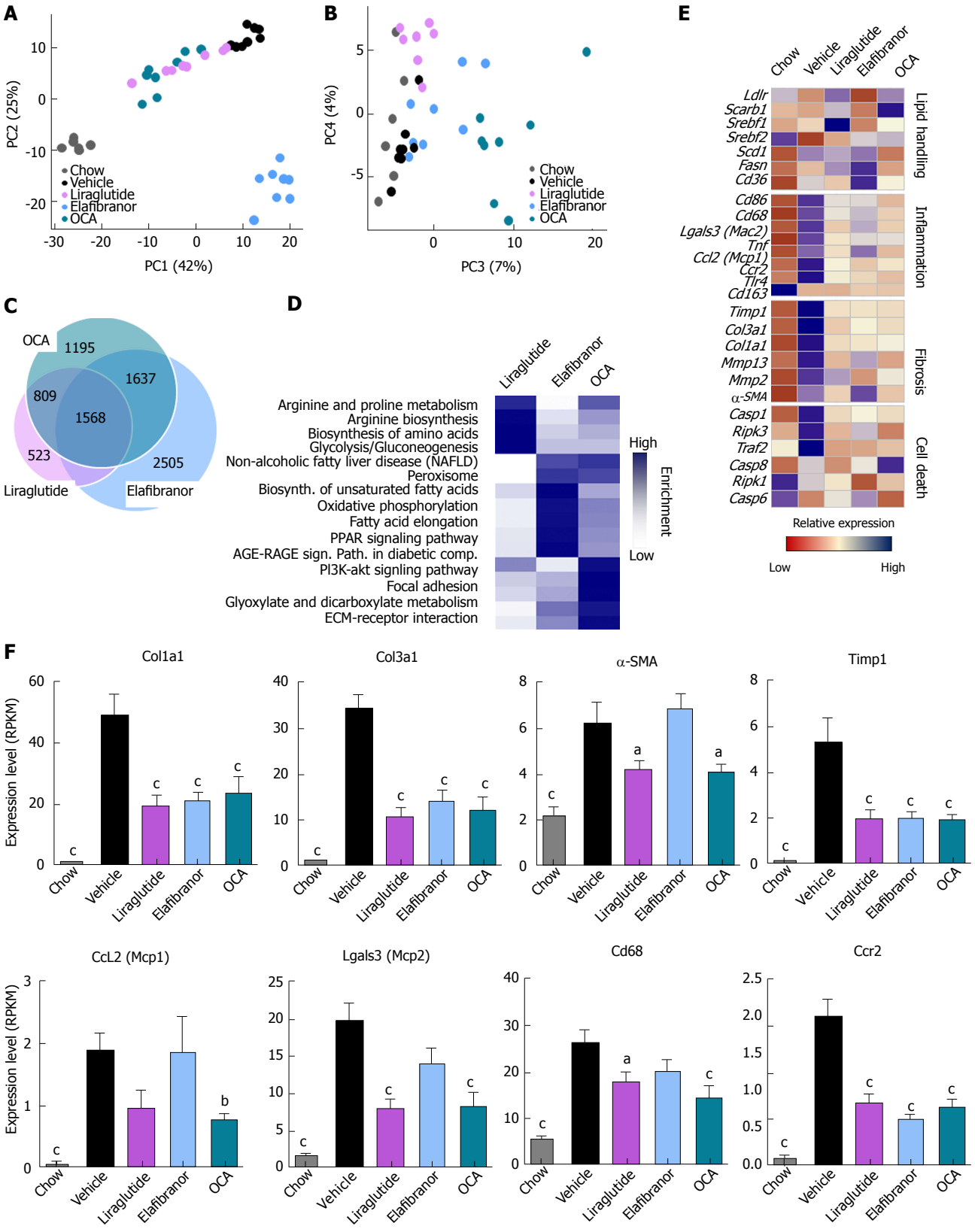

Figure 5 Hepatic global gene expression analysis in DIO-nonalcoholic steatohepatitis mice. A and B: Principal component analysis; C: Venn diagram of differentially expressed genes, compared to vehicle treatment; D: Overview of KEGG pathway-enriched gene groups; E: Relative expression of prototypic NASH genes; F: Relative expression of selected genes. $^{a}P < 0.05$, $^{b}P < 0.01$, $^{c}P < 0.001$ *vs* vehicle controls. OCA: Obeticholic acid; NASH: Nonalcoholic steatohepatitis.

and did not alter the fibrosis stage (Figure 7A and B, Supplementary Figure 3). In contrast, liraglutide significantly reduced total liver levels of lipids, galectin-3 and Col1a1 (Figure 7E-G).

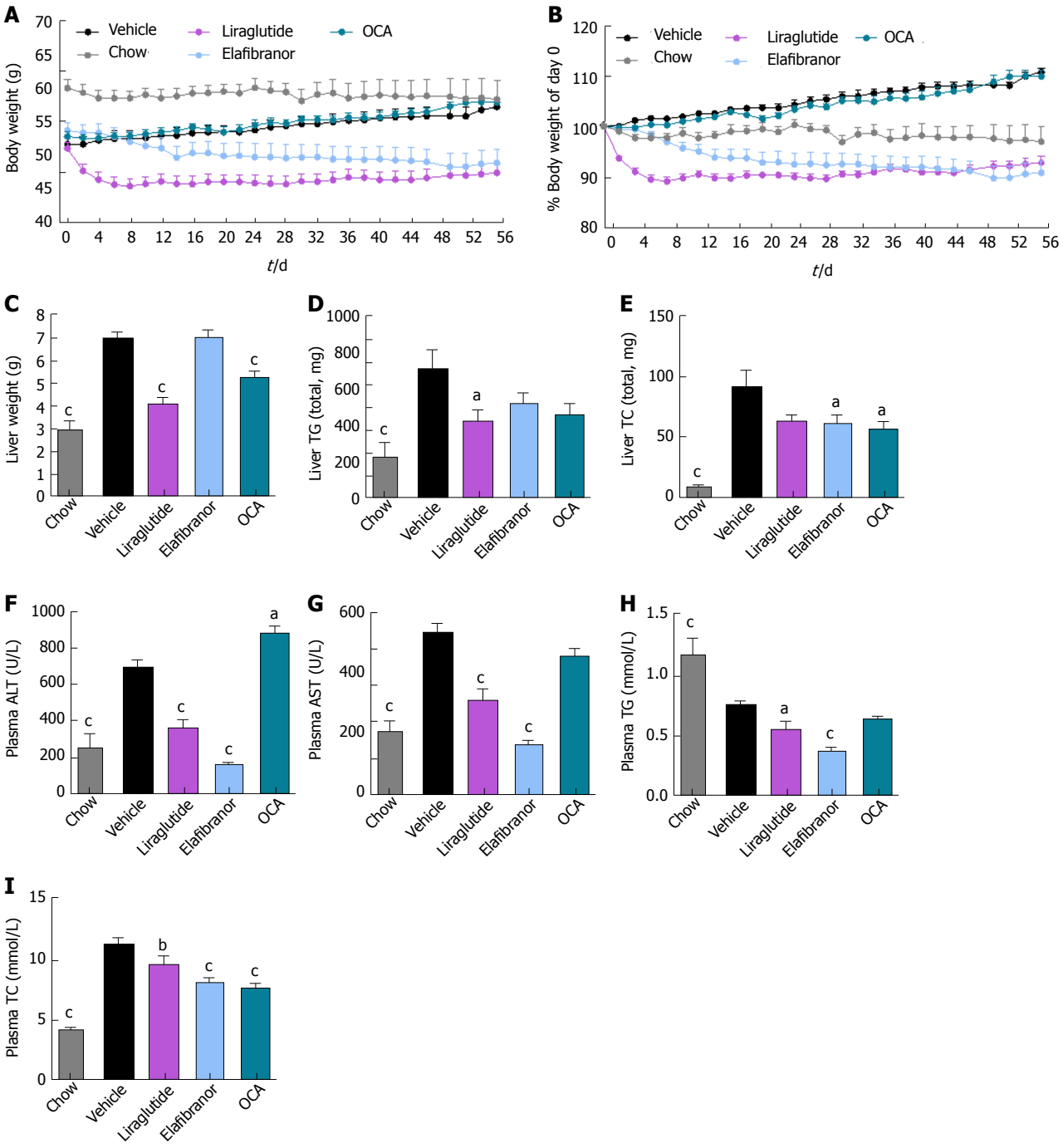

Figure 6 Metabolic effects of liraglutide, obeticholic acid, and elafibranor treatment in *ob/ob*-nonalcoholic steatohepatitis mice. $^{a}P < 0.05$, $^{b}P < 0.01$, $^{c}P < 0.001$ *vs* vehicle controls. OCA: Obeticholic acid; NASH: Nonalcoholic steatohepatitis.

DISCUSSION

We and others have previously reported that DIO-NASH mice develop low-grade liver fibrosis when maintained on a trans-fat containing obesogenic diet[9,19,39]. To obtain further information on the pathology in this translational mouse model of NASH we initially performed a detailed investigation on the disease onset and progression in DIO-NASH mice, followed by comparison of the treatment effects of liraglutide, OCA and elafibranor in both DIO-NASH and *ob/ob*-NASH mice.

DIO-NASH mice exhibited a relatively rapid onset of body weight gain with concurrent liver TG and TC accumulation and progressive development of hepatomegaly. DIO-NASH mice developed hypercholesterolemia, but not hypertriglyceridemia. This is a consistent finding DIO-NASH mice[9,19], as well as in *ob/ob*-NASH mice[10,19] and other Western diet-based mouse models of NASH[12,40]. In contrast, high-fat diets with lower cholesterol content (0.2%) are reported to induce combined hypertriglyceridemia and hypercholesterolemia in obese mice[11,41,42], suggesting

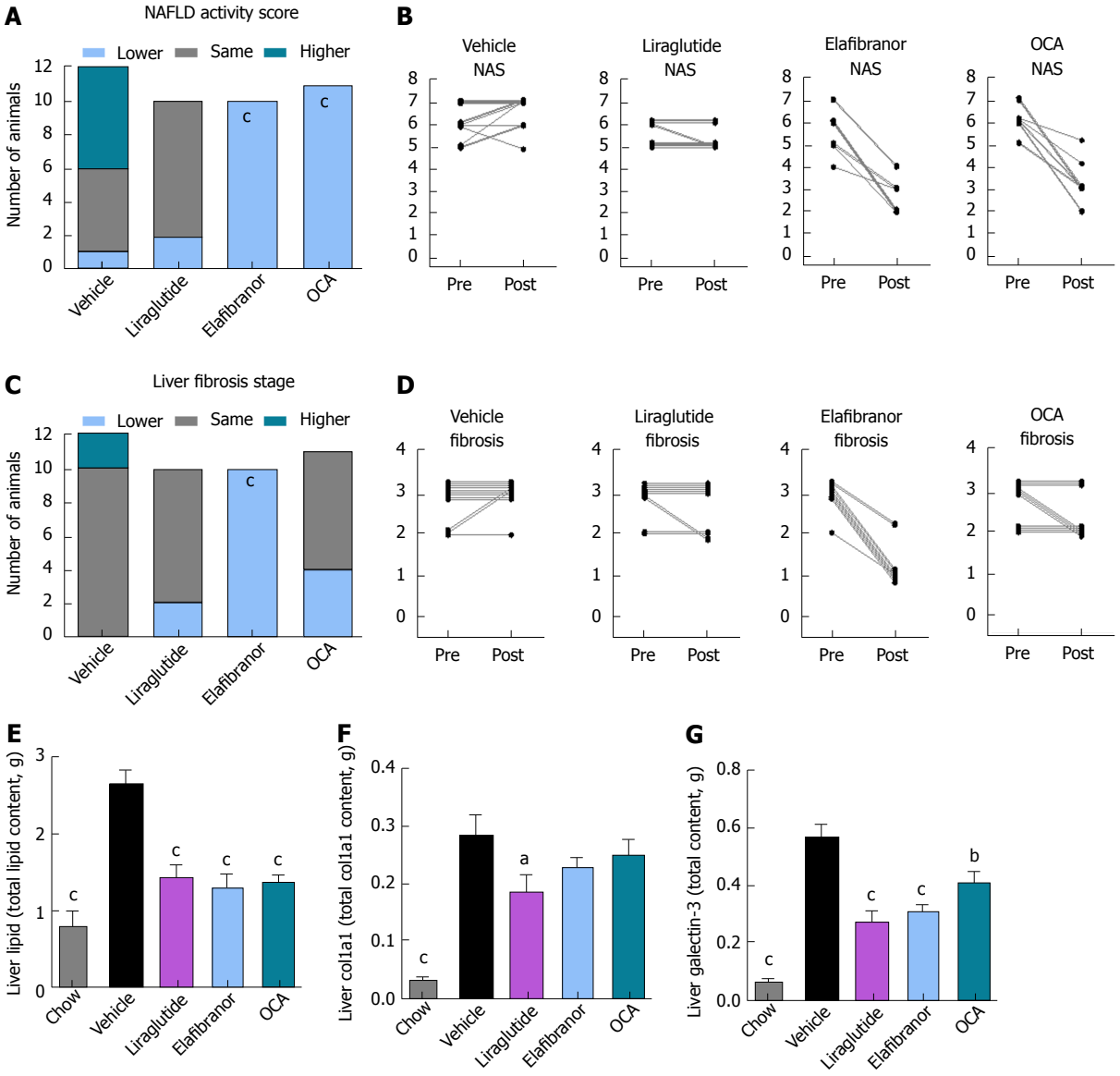

Figure 7 Histomorphological effects of liraglutide, obeticholic acid, and elafibranor treatment in *ob/ob*-nonalcoholic steatohepatitis mice. [a]$P < 0.05$, [b]$P < 0.01$, [c]$P < 0.001$ *vs* vehicle controls. OCA: Obeticholic acid; NASH: Nonalcoholic steatohepatitis.

that elevated dietary cholesterol influences hepatocyte TG secretion, perhaps by modifying cholesterol ester and lipoprotein synthesis[40,43]. Hepatopathology was further indicated by increased levels of plasma transaminases, most consistently observed for ALT. As persistently elevated ratios of AST:ALT has been reported to associate to advanced fibrotic NASH but not at milder disease stages[44], the moderate changes in ALT and AST levels in DIO-NASH (and *ob/ob*-NASH) mice presumably reflects the mild-to-moderate disease severity in these two models. Histological morphometry suggested a sequential onset of NASH pathology in DIO-NASH mice, with initial steatosis progressing to inflammation and ballooning degeneration (from week 30). Quantitative histology on steatosis (HE staining), inflammation (galectin-3) and fibrosis (Col1a1) supported a distinct temporal sequence of hepatopathological events in DIO-NASH mice. In correspondence, transcriptome pathway analyses revealed initial gene signatures of upregulated hepatic lipid synthesis and handling, over enhanced inflammation signaling to recruitment of monocytes/myofibroblasts, stimulation of fibrogenesis and extracellular matrix turnover. These findings are in general concordance with recent hypotheses that mounting lipotoxicity constitutes a triggering event for progression of NAFLD into NASH[45,46].

In agreement with previous findings[9,19], all morphological hallmarks of NASH were consistently present in DIO-NASH mice at ⩾ 25 wk of dieting (NAS ⩾ 4-5, corresponding to the clinical criteria for NASH[31]). NAS was largely driven by progressive changes in hepatosteatosis and inflammation as affected mice only exhibited marginal hepatocyte ballooning. The absence of conspicuous hepatocyte ballooning is in accordance with a recent comprehensive histological

scoring study concluding that obese rodent models of NASH do not entirely meet the histomorphological criteria for human hepatocyte ballooning[47]. As is seen in the clinic, DIO-NASH mice represented all stages of NAFLD and fibrosis for any dieting period ⩾ 20 wk, which confirms the highly individual fibrosis progression in this model[9,19]. Notably, up to 30% of the animals failed to develop steatohepatitis and fibrosis, and the severity in histopathology did not become more homogenous by extending AMLN dieting periods. Similar disease variability has been reported in other DIO mouse models of NASH[12,13,48], which therefore likely generalizes to all obese mouse models of fibrotic steatohepatitis. Therefore, the use of a prebiopsy for selection and stratification of in DIO-NASH models not only substantiates the efficacy readouts, but also allows for the employment of clinically relevant inclusion criteria and stratification procedures.

In the present pharmacological study, inherent differences in NASH pathology were therefore considered by introducing liver biopsy-based histology for evaluating NASH severity in all individual mice prior to introduction of treatment. Only mice with biopsy-confirmed fibrotic NASH were included in the study, and randomization and stratification procedures were applied to equalize mean levels of baseline NAS and fibrosis stage across treatment groups. The present study evaluated the pharmacodynamics of three individual compounds in current advanced clinical development for NASH. The selected compounds are representative of different drug classes and therapeutic concepts and included agonists for the GLP-1 receptor (liraglutide), FXR (OCA) and PPAR-α/δ (elafibranor)[20-22]. We have recently reported a comparative liver biopsy study on DIO-NASH and *ob/ob*-NASH mice, which confirmed that *ob/ob*-NASH mice generally display more marked fibrotic steatohepatitis[19]. Thus, potential differences in therapeutic efficacies as a function of overall severity in hepatopathology were addressed by applying identical treatment protocols to both DIO-NASH and *ob/ob*-NASH mice.

The GLP-1 analog, liraglutide, which is currently approved for the treatment of type 2 diabetes and obesity[24,25], reduced weight gain in both DIO-NASH and *ob/ob*-NASH mice with concurrent improvements in whole-body fat mass, hepatomegaly, liver lipid deposition, and hypercholesterolemia, which is consistent with findings in other obese mouse models of NASH[33,41]. The intrahepatic lipid-lowering effects of liraglutide are likely secondary to the progressive weight loss promoted by the GLP-1 agonist[49]. This is relevant, as weight loss *per se* is known to mediate benefits on NAFLD endpoints[50]. The present findings are also in agreement with a previous study assessing the effect of an exendin-4 analogue in *ob/ob*-NASH mice[10]. Liraglutide showed most marked effects on hepatic gene transcriptional signatures associated to the canonical effects of GLP-1 receptor agonists on hepatic glucose metabolism and production. The liver transcriptome analyses in DIO-NASH mice also suggested that liraglutide-induced improvements in lipid metabolism was linked to activation of signaling pathways involved in fatty acid degradation, oxidative phosphorylation and cholesterol handling. Perturbations in these signaling pathways could therefore potentially trigger gene expression programs that favored reduced hepatic free fatty acid uptake, as well as improving the clearance of cholesterol and fatty acids, all of which have been implicated in the pathogenesis of NASH. In contrast to OCA and elafibranor, liraglutide did not improve composite NAS in *ob/ob*-NASH mice. In addition, liraglutide treatment did not influence fibrosis and low-grade hepatocyte ballooning in either model, indicating that GLP-1 receptor mediated amelioration of hepatic lipid overload was perhaps not sufficient to reduce morphological indices of more advanced NASH. In contrast, total hepatic galectin-3 and Col1a1 levels were significantly lowered in both DIO-NASH and *ob/ob*-NASH mice after liraglutide treatment, consistent with the reduction in hepatomegaly. Overall, the pharmacodynamics of liraglutide in the DIO-NASH mice are in general agreement with a recent phase-II (LEAN) trial for NASH, where liraglutide treatment promoted a significant weight loss (approximately 5%) and improved NAS (lowered steatosis score) without worsening of fibrosis stage[20]. GLP-1 receptor agonists have not shown significant effects on liver fibrosis morphology in various mouse models of NASH[8]. Future studies must therefore aim to clarify if extended dosing periods are required for detecting antifibrotic efficacy of liraglutide, or whether the lack of a direct hepatic action could be a limiting factor for influencing liver fibrosis in obese mouse models of NASH.

OCA is a first-in-class selective synthetic FXR agonist that is approximately 100-fold more potent than its natural bile acid homologue[27]. Nuclear FXRs are abundantly expressed in the liver, intestine, and adipose tissue, serving as primary sensors for regulating enterohepatic bile acid flow. In the present study, OCA reduced hepatomegaly and NAS scores in both DIO-NASH and *ob/ob*-NASH mice. FXR agonists, including OCA, have shown similar effects in genetic and methinonine-choline deficient (MCD) dietary models of NASH[13,15,51]. The improvement of steatohepatitis in DIO-NASH mice corresponded to reduced expression of genes that are important transcriptional targets of FXRs and regulate hepatocyte lipid metabolism and macrophage activity[52]. Whereas several genes involved in cholesterol and lipoprotein metabolism are transcriptional targets of hepatocyte FXRs[53], it is not resolved whether FXR stimulation directly activates master transcription factors that controls the expression of genes involved in fatty acid biosynthesis[54]. As FXRs also suppress transcriptional activity of several carbohydrate responsive genes, it is assumed that FXR reduces TG levels mainly through increasing plasma lipoprotein clearance and improving hepatic insulin resistance[52-54]. The anti-inflammatory effects of FXR are well-established. Accordingly, several

studies have reported that FXR agonists, including OCA, attenuate hepatic inflammation in high-fat fed obese rodents[15,51,55,56], and *Fxr*-null mice are highly sensitive to develop severe steatohepatitis when fed an obesogenic diet[57]. OCA treatment also reversed mild-stage hepatocyte ballooning in affected *ob/ob*-NASH mice. OCA has previously been reported to reverse low-grade hepatocyte ballooning in mice fed an atherogenic diet[13], and a different semisynthetic FXR agonist (INT-767) has shown a similar effect in non-fibrotic *db/db* mice[51]. Interestingly, enhanced hepatocyte ballooning is also reported in FXR-deficient hypercholesterolemic mice[57], thus lending further support to FXR-dependent hepatocyte protective effects. As for liraglutide, OCA treatment did not influence fibrosis morphometry, but reduced total hepatic Col1a1 expression due to reduced liver weight. A recent study in *ob/ob*-NASH mice (fed AMLN diet for 8 wk) and treated with a similar daily dose of OCA for 4 wk also indicated no effect on liver fibrosis[58]. In contrast, antifibrotic effects of synthetic FXR agonists, including OCA, have been demonstrated in more aggressive models of fibrotic NASH[15,59]. It should, however, be noted that OCA reduced all NAS components in *ob/ob*-NASH mice, suggesting that prolonged OCA treatment might lead to improved fibrosis stage in this model. The present data are in accordance with a recent phase-II (FLINT) trial on OCA treatment for NASH[21], reporting significant improvements of all NAS components without worsening of fibrosis. The FLINT trial also indicated no anti-obesity potential of OCA, analogous to the observations in the present study.

PPARs constitute another family of ligand-activated nuclear receptors. PPARs are abundantly expressed in the liver (PPAR-α, PPAR-β/δ) and adipose tissue (PPAR-δ, PPAR-γ), being prominent regulators of lipid and glucose metabolism, but are also functional in immune cells, including monocytes and macrophages (PPAR-γ)[60]. Several subtype-selective PPAR agonists have been demonstrated to reduce experimental fibrotic steatohepatitis, particularly in MCD mice[8]. In contrast, there is a sparsity in studies addressing effects of PPAR agonists in more translational mouse models of NASH. In DIO-NASH mice, elafibranor showed similar efficacy in reducing body weight and steatosis compared to liraglutide, however, the metabolic effects of elafibranor were not accompanied by improvements in liver weight. Accordingly, hepatomegaly was either accentuated (DIO-NASH mice) or unaltered (*ob/ob*-NASH mice) with elafibranor treatment. RNA sequencing analysis indicated stimulation of PPAR and peroxisomal signaling pathways in DIO-NASH mice, and hepatocyte peroxisome proliferation and tumorigenesis have been consistent findings in rodent studies with PPAR-α agonists (including elafibranor)[30], but not in humans[61]. Notably, elafibranor improved NAS scores with concomitant reductions in fibrosis stage, also supported by corresponding liver transcriptome changes. In contrast, total Col1a1 and galectin-3 immunoreactivity was unaffected in elafibranor-treated DIO-NASH mice due to the liver hypertrophic effect. Elafibranor treatment also promoted marked effects on hepatic signaling pathways associated with lipid metabolism, mitochondrial energy harvesting, inflammation, fibrogenesis and execution of cell death programs. Other PPAR agonists, including fibrates (bezafibrate, Wy-14,463; PPAR-α ligands), thiazolidinediones (rosiglitazone, PPAR-γ ligand) and GW501516 (PPAR-β/δ ligand), have been reported to reduce fibrotic steatohepatitis in MCD mice[14,62,63]. PPAR stimulation is suggested to ameliorate NASH primarily by enhancing β-oxidation associated hepatic fatty acid disposal, but anti-inflammatory and antifibrotic mechanisms might also contribute to improvements in liver histology independent on reduced hepatocyte lipid accumulation[63,64]. In the present study, dual PPAR-α/δ stimulation by elafibranor may thus improve fibrosis stage in DIO-NASH and *ob/ob*-NASH mice by resolving intrahepatic lipid deposition but also through engagement of lipid metabolism-independent signaling pathways. The pharmacokinetics of elafibranor has not been reported in detail, but a preliminary study in rats indicated elafibranor excretion in the bile suggestive of extensive enterohepatic cycling[29]. Elafibranor may therefore be considered liver-targeted, which could enhance treatment efficacy in DIO-NASH and *ob/ob*-NASH mice. The present data are in overall agreement with a recent clinical phase-II study (GOLDEN-505) on elafibranor treatment for NASH[22]. Interestingly, the improvements in mean NAS (approximately 2.5 points) and fibrosis score (approximately 0.5 points) in elafibranor-treated NASH patients achieving the modified primary outcome (no fibrosis worsening) was on par with the reductions in NAS and fibrosis scores determined in DIO-NASH and *ob/ob*-NASH mice. In contrast to the weight neutral effect of elafibranor in NASH patients, elafibranor markedly reduced body weight in both DIO-NASH and *ob/ob*-NASH mice. Whereas body weight loss has not been reported with PPAR agonist treatment in humans[65], stimulated PPAR-α and PPAR-δ function has been associated with weight loss, appetite suppression and reduced tissue lipid deposition in obesity-prone mice[66-68], which could imply species-dependent metabolic effects of PPAR agonists.

In conclusion, the present comparative pharmacological study in diet-induced and genetically obese mouse models of biopsy-confirmed NASH indicated both shared and distinct anti-NASH effects of liraglutide, OCA, and elafibranor. The anti-NASH effects of the compounds corresponded well to their individual modes of action, and were also in concordance to histological findings in clinical trials for NASH. The present data therefore further supports the clinical translatability and utility of DIO-NASH and *ob/ob*-NASH mouse models of NASH in preclinical drug development.

ARTICLE HIGHLIGHTS

Research background

Although various diet-induced obese mouse models of nonalcoholic steatohepatitis (NASH) are highly applicable in preclinical drug development, none of these models have so far been systematically evaluated with respect to comparing individual pharmacodynamics of several important compound classes in current clinical development for NASH.

Research motivation

Comparison of preclinical treatment effects of potential anti-NASH compounds is currently hampered by the absence of head-to-head pharmacological studies in experimental models of NASH. Moreover, baseline NASH disease heterogeneity is often overlooked in pharmacological studies which may introduce unintentional variability in treatment responses, thereby narrowing the window for detection of therapeutic effects of potential anti-NASH compounds.

Research objectives

The present study aimed to characterize within-subject treatment responses to liraglutide, obeticholic acid and elafibranor in two obese mouse models of biopsy-confirmed NASH.

Research methods

Comparative treatment studies were conducted in male wild-type mice (DIO-NASH) and $Lep^{ob/ob}$ (*ob/ob*-NASH) mice fed a diet high in trans-fat, fructose and cholesterol. Liver biopsy was applied for stratification of liver steatosis and fibrosis, using the nonalcoholic fatty liver disease activity score (NAS) and fibrosis staging system. Individual biopsy-confirmed histopathology also allowed for evaluation of within-subject treatment responses based on differences in baseline vs. endpoint histomorphometry. DIO-NASH and *ob/ob*-NASH mice were treated with vehicle, liraglutide, obeticholic acid, or elafibranor for 8 weeks. Metabolic, histomorphological and quantitative histological effects of each compound were compared in the two models of biopsy-confirmed NASH.

Research results

Only liraglutide and elafibranor reduced body weight in DIO-NASH and *ob/ob*-NASH mice. Liraglutide improved steatosis scores in DIO-NASH mice only. Whereas elafibranor and OCA both reduced hepatic steatosis and inflammation scores in both models, only elafibranor also improved fibrosis stage. Owing to a marked reduction in liver weight, liraglutide and OCA lowered total liver fat, collagen 1a1 and galectin-3 content. Individual drug effects on NASH histological endpoints were supported by global gene expression (RNA sequencing) and liver lipid biochemistry.

Research conclusions

DIO-NASH and *ob/ob*-NASH mice show good clinical translatability with respect to disease etiology, histopathology and therapeutic effects of compounds in late-stage clinical development for NASH.

Research perspectives

The present data supports the utility of DIO-NASH and *ob/ob*-NASH mice for preclinical evaluation of the treatment efficacy of potential novel anti-NASH compounds. As also applied in clinical trials for NASH, biopsy-confirmed histopathology in the two obese mouse models of NASH allows for stratification of disease severity prior to treatment start and improves detection of treatment efficacy of test compounds by considering within-subject responses.

ACKNOWLEDGEMENTS

The authors would like to thank Louise D Fensholdt, Dan Hemmingsen, Martin Illemann, Rasmus Lind and Chen Zhang for skillful technical assistance.

REFERENCES

1 **Bedossa P**. Pathology of non-alcoholic fatty liver disease. *Liver Int* 2017; **37** Suppl **1**: 85-89 [PMID: 28052629 DOI: 10.1111/liv.13301]
2 **Rosso N**, Chavez-Tapia NC, Tiribelli C, Bellentani S. Translational approaches: from fatty liver to non-alcoholic steatohepatitis. *World J Gastroenterol* 2014; **20**: 9038-9049 [PMID: 25083077 DOI: 10.3748/wjg.v20.i27.9038]
3 **Berlanga A**, Guiu-Jurado E, Porras JA, Auguet T. Molecular pathways in non-alcoholic fatty liver disease. *Clin Exp Gastroenterol* 2014; **7**: 221-239 [PMID: 25045276 DOI: 10.2147/CEG.S62831]
4 **Sutti S**, Jindal A, Bruzzì S, Locatelli I, Bozzola C, Albano E. Is there a role for adaptive immunity in nonalcoholic steatohepatitis? *World J Hepatol* 2015; **7**: 1725-1729 [PMID: 26167244 DOI: 10.4254/wjh.v7.i13.1725]
5 **Ganz M**, Szabo G. Immune and inflammatory pathways in NASH. *Hepatol Int* 2013; **7** Suppl 2: 771-781 [PMID: 24587847 DOI: 10.1007/s12072-013-9468-6]
6 **Younossi ZM**, Koenig AB, Abdelatif D, Fazel Y, Henry L, Wymer M. Global epidemiology of nonalcoholic fatty liver disease-Meta-analytic assessment of prevalence, incidence, and outcomes. *Hepatology* 2016; **64**: 73-84 [PMID: 26707365 DOI: 10.1002/hep.28431]
7 **Rotman Y**, Sanyal AJ. Current and upcoming pharmacotherapy for non-alcoholic fatty liver disease. *Gut* 2017; **66**: 180-190 [PMID: 27646933 DOI: 10.1136/gutjnl-2016-312431]
8 **Hansen HH**, Feigh M, Veidal SS, Rigbolt KT, Vrang N, Fosgerau K. Mouse models of nonalcoholic steatohepatitis in preclinical drug development. *Drug Discov Today* 2017; **22**: 1707-1718 [PMID: 28687459 DOI: 10.1016/j.drudis.2017.06.007]
9 **Clapper JR**, Hendricks MD, Gu G, Wittmer C, Dolman CS, Herich J, Athanacio J, Villescaz C, Ghosh SS, Heilig JS, Lowe C, Roth JD. Diet-induced mouse model of fatty liver disease and nonalcoholic steatohepatitis reflecting clinical disease progression and methods of assessment. *Am J Physiol Gastrointest Liver Physiol* 2013; **305**: G483-G495 [PMID: 23886860 DOI: 10.1152/ajpgi.00079.2013]
10 **Trevaskis JL**, Griffin PS, Wittmer C, Neuschwander-Tetri BA, Brunt EM, Dolman CS, Erickson MR, Napora J, Parkes DG, Roth JD. Glucagon-like peptide-1 receptor agonism improves metabolic, biochemical, and histopathological indices of nonalcoholic steatohepatitis in mice. *Am J Physiol Gastrointest Liver Physiol* 2012; **302**: G762-G772 [PMID: 22268099 DOI: 10.1152/ajpgi.00476.2011]
11 **Asgharpour A**, Cazanave SC, Pacana T, Seneshaw M, Vincent R, Banini BA, Kumar DP, Daita K, Min HK, Mirshahi F, Bedossa P, Sun X, Hoshida Y, Koduru SV, Contaifer D Jr, Warncke UO, Wijesinghe DS, Sanyal AJ. A diet-induced animal model of non-alcoholic fatty liver disease and hepatocellular cancer. *J Hepatol* 2016; **65**: 579-588 [PMID: 27261415 DOI: 10.1016/j.jhep.2016.05.005]
12 **Krishnan A**, Abdullah TS, Mounajjed T, Hartono S, McConico A, White T, LeBrasseur N, Lanza I, Nair S, Gores G, Charlton M. A longitudinal study of whole body, tissue, and cellular physiology in a mouse model of fibrosing NASH with high fidelity to the human condition. *Am J Physiol Gastrointest Liver Physiol* 2017; **312**: G666-G680 [PMID: 28232454 DOI: 10.1152/ajpgi.00213.2016]
13 **Haczeyni F**, Poekes L, Wang H, Mridha AR, Barn V, Geoffrey Haigh W, Ioannou GN, Yeh MM, Leclercq IA, Teoh NC, Farrell GC. Obeticholic acid improves adipose morphometry and inflammation and reduces steatosis in dietary but not metabolic obesity in mice. *Obesity* (Silver Spring) 2017; **25**: 155-165 [PMID: 27804232 DOI: 10.1002/oby.21701]
14 **Ip E**, Farrell G, Hall P, Robertson G, Leclercq I. Administration

of the potent PPARalpha agonist, Wy-14,643, reverses nutritional fibrosis and steatohepatitis in mice. *Hepatology* 2004; **39**: 1286-1296 [PMID: 15122757 DOI: 10.1002/hep.20170]

15 **Zhang S**, Wang J, Liu Q, Harnish DC. Farnesoid X receptor agonist WAY-362450 attenuates liver inflammation and fibrosis in murine model of non-alcoholic steatohepatitis. *J Hepatol* 2009; **51**: 380-388 [PMID: 19501927 DOI: 10.1016/j.jhep.2009.03.025]

16 **Lee JH**, Kang YE, Chang JY, Park KC, Kim HW, Kim JT, Kim HJ, Yi HS, Shong M, Chung HK, Kim KS. An engineered FGF21 variant, LY2405319, can prevent non-alcoholic steatohepatitis by enhancing hepatic mitochondrial function. *Am J Transl Res* 2016; **8**: 4750-4763 [PMID: 27904677]

17 **Sanyal AJ**, Friedman SL, McCullough AJ, Dimick-Santos L; American Association for the Study of Liver Diseases; United States Food and Drug Administration. Challenges and opportunities in drug and biomarker development for nonalcoholic steatohepatitis: findings and recommendations from an American Association for the Study of Liver Diseases-U.S. Food and Drug Administration Joint Workshop. *Hepatology* 2015; **61**: 1392-1405 [PMID: 25557690 DOI: 10.1002/hep.27678]

18 **Ratziu V**, Bellentani S, Cortez-Pinto H, Day C, Marchesini G. A position statement on NAFLD/NASH based on the EASL 2009 special conference. *J Hepatol* 2010; **53**: 372-384 [PMID: 20494470 DOI: 10.1016/j.jhep.2010.04.008]

19 **Kristiansen MN**, Veidal SS, Rigbolt KT, Tølbøl KS, Roth JD, Jelsing J, Vrang N, Feigh M. Obese diet-induced mouse models of nonalcoholic steatohepatitis-tracking disease by liver biopsy. *World J Hepatol* 2016; **8**: 673-684 [PMID: 27326314 DOI: 10.4254/wjh.v8.i16.673]

20 **Armstrong MJ**, Gaunt P, Aithal GP, Barton D, Hull D, Parker R, Hazlehurst JM, Guo K; LEAN trial team, Abouda G, Aldersley MA, Stocken D, Gough SC, Tomlinson JW, Brown RM, Hübscher SG, Newsome PN. Liraglutide safety and efficacy in patients with non-alcoholic steatohepatitis (LEAN): a multicentre, double-blind, randomised, placebo-controlled phase 2 study. *Lancet* 2016; **387**: 679-690 [PMID: 26608256 DOI: 10.1016/S0140-6736(15)00803-X]

21 **Neuschwander-Tetri BA**, Loomba R, Sanyal AJ, Lavine JE, Van Natta ML, Abdelmalek MF, Chalasani N, Dasarathy S, Diehl AM, Hameed B, Kowdley KV, McCullough A, Terrault N, Clark JM, Tonascia J, Brunt EM, Kleiner DE, Doo E; NASH Clinical Research Network. Farnesoid X nuclear receptor ligand obeticholic acid for non-cirrhotic, non-alcoholic steatohepatitis (FLINT): a multicentre, randomised, placebo-controlled trial. *Lancet* 2015; **385**: 956-965 [PMID: 25468160 DOI: 10.1016/S0140-6736(14)61933-4]

22 **Ratziu V**, Harrison SA, Francque S, Bedossa P, Lehert P, Serfaty L, Romero-Gomez M, Boursier J, Abdelmalek M, Caldwell S, Drenth J, Anstee QM, Hum D, Hanf R, Roudot A, Megnien S, Staels B, Sanyal A; GOLDEN-505 Investigator Study Group. Elafibranor, an Agonist of the Peroxisome Proliferator-Activated Receptor-α and -δ, Induces Resolution of Nonalcoholic Steatohepatitis Without Fibrosis Worsening. *Gastroenterology* 2016; **150**: 1147-1159.e5 [PMID: 26874076 DOI: 10.1053/j.gastro.2016.01.038]

23 **Madsen K**, Knudsen LB, Agersoe H, Nielsen PF, Thøgersen H, Wilken M, Johansen NL. Structure-activity and protraction relationship of long-acting glucagon-like peptide-1 derivatives: importance of fatty acid length, polarity, and bulkiness. *J Med Chem* 2007; **50**: 6126-6132 [PMID: 17975905 DOI: 10.1021/jm070861j]

24 **Drucker DJ**, Dritselis A, Kirkpatrick P. Liraglutide. *Nat Rev Drug Discov* 2010; **9**: 267-268 [PMID: 20357801 DOI: 10.1038/nrd3148]

25 **Nuffer WA**, Trujillo JM. Liraglutide: A New Option for the Treatment of Obesity. *Pharmacotherapy* 2015; **35**: 926-934 [PMID: 26497479 DOI: 10.1002/phar.1639]

26 **Markham A**, Keam SJ. Obeticholic Acid: First Global Approval. *Drugs* 2016; **76**: 1221-1226 [PMID: 27406083 DOI: 10.1007/s40265-016-0616-x]

27 **Pellicciari R**, Fiorucci S, Camaioni E, Clerici C, Costantino G, Maloney PR, Morelli A, Parks DJ, Willson TM. 6alpha-ethyl-chenodeoxycholic acid (6-ECDCA), a potent and selective FXR agonist endowed with anticholestatic activity. *J Med Chem* 2002; **45**: 3569-3572 [PMID: 12166927 DOI: 10.1021/jm025529g]

28 **Asgharpour A**, Kumar D, Sanyal A. Bile acids: emerging role in management of liver diseases. *Hepatol Int* 2015; **9**: 527-533 [PMID: 26320013 DOI: 10.1007/s12072-015-9656-7]

29 **Cariou B**, Hanf R, Lambert-Porcheron S, Zaïr Y, Sauvinet V, Noël B, Flet L, Vidal H, Staels B, Laville M. Dual peroxisome proliferator-activated receptor α/δ agonist GFT505 improves hepatic and peripheral insulin sensitivity in abdominally obese subjects. *Diabetes Care* 2013; **36**: 2923-2930 [PMID: 23715754 DOI: 10.2337/dc12-2012]

30 **Staels B**, Rubenstrunk A, Noel B, Rigou G, Delataille P, Millatt LJ, Baron M, Lucas A, Tailleux A, Hum DW, Ratziu V, Cariou B, Hanf R. Hepatoprotective effects of the dual peroxisome proliferator-activated receptor alpha/delta agonist, GFT505, in rodent models of nonalcoholic fatty liver disease/nonalcoholic steatohepatitis. *Hepatology* 2013; **58**: 1941-1952 [PMID: 23703580 DOI: 10.1002/hep.26461]

31 **Kleiner DE**, Brunt EM, Van Natta M, Behling C, Contos MJ, Cummings OW, Ferrell LD, Liu YC, Torbenson MS, Unalp-Arida A, Yeh M, McCullough AJ, Sanyal AJ; Nonalcoholic Steatohepatitis Clinical Research Network. Design and validation of a histological scoring system for nonalcoholic fatty liver disease. *Hepatology* 2005; **41**: 1313-1321 [PMID: 15915461 DOI: 10.1002/hep.20701]

32 **Wang XX**, Wang D, Luo Y, Myakala K, Dobrinskikh E, Rosenberg AZ, Levi J, Kopp JB, Field A, Hill A, Lucia S, Qiu L, Jiang T, Peng Y, Orlicky D, Garcia G, Herman-Edelstein M, D'Agati V, Henriksen K, Adorini L, Pruzanski M, Xie C, Krausz KW, Gonzalez FJ, Ranjit S, Dvornikov A, Gratton E, Levi M. FXR/TGR5 Dual Agonist Prevents Progression of Nephropathy in Diabetes and Obesity. *J Am Soc Nephrol* 2018; **29**: 118-137 [PMID: 29089371 DOI: 10.1681/ASN.2017020222]

33 **Rahman K**, Liu Y, Kumar P, Smith T, Thorn NE, Farris AB, Anania FA. C/EBP homologous protein modulates liraglutide-mediated attenuation of non-alcoholic steatohepatitis. *Lab Invest* 2016; **96**: 895-908 [PMID: 27239734 DOI: 10.1038/labinvest.2016.61]

34 **Henderson SJ**, Konkar A, Hornigold DC, Trevaskis JL, Jackson R, Fritsch Fredin M, Jansson-Löfmark R, Naylor J, Rossi A, Bednarek MA, Bhagroo N, Salari H, Will S, Oldham S, Hansen G, Feigh M, Klein T, Grimsby J, Maguire S, Jermutus L, Rondinone CM, Coghlan MP. Robust anti-obesity and metabolic effects of a dual GLP-1/glucagon receptor peptide agonist in rodents and non-human primates. *Diabetes Obes Metab* 2016; **18**: 1176-1190 [PMID: 27377054 DOI: 10.1111/dom.12735]

35 **Hanf R**, Millatt LJ, Cariou B, Noel B, Rigou G, Delataille P, Daix V, Hum DW, Staels B. The dual peroxisome proliferator-activated receptor alpha/delta agonist GFT505 exerts anti-diabetic effects in db/db mice without peroxisome proliferator-activated receptor gamma-associated adverse cardiac effects. *Diab Vasc Dis Res* 2014; **11**: 440-447 [PMID: 25212694 DOI: 10.1177/1479164114548027]

36 **Dobin A**, Davis CA, Schlesinger F, Drenkow J, Zaleski C, Jha S, Batut P, Chaisson M, Gingeras TR. STAR: ultrafast universal RNA-seq aligner. *Bioinformatics* 2013; **29**: 15-21 [PMID: 23104886 DOI: 10.1093/bioinformatics/bts635]

37 **Love MI**, Huber W, Anders S. Moderated estimation of fold change and dispersion for RNA-seq data with DESeq2. *Genome Biol* 2014; **15**: 550 [PMID: 25516281 DOI: 10.1186/s13059-014-0550-8]

38 **Yu G**, Wang LG, Han Y, He QY. clusterProfiler: an R package for comparing biological themes among gene clusters. *OMICS* 2012; **16**: 284-287 [PMID: 22455463 DOI: 10.1089/omi.2011.0118]

39 **Honda Y**, Imajo K, Kato T, Kessoku T, Ogawa Y, Tomeno W, Kato S, Mawatari H, Fujita K, Yoneda M, Saito S, Nakajima A. The Selective SGLT2 Inhibitor Ipragliflozin Has a Therapeutic Effect on Nonalcoholic Steatohepatitis in Mice. *PLoS One* 2016; **11**: e0146337 [PMID: 26731267 DOI: 10.1371/journal.pone.0146337]

40 **Henkel J**, Coleman CD, Schraplau A, Johrens, Weber D, Castro JP, Hugo M, Schulz TJ, Krämer S, Schürmann A, Püschel GP. Induction of steatohepatitis (NASH) with insulin resistance in wildtype B6 mice by a western-type diet containing soybean oil

and cholesterol. *Mol Med* 2017; **23**: Epub ahead of print [PMID: 28332698 DOI: 10.2119/molmed.2016.00203]

41 **Mells JE**, Fu PP, Sharma S, Olson D, Cheng L, Handy JA, Saxena NK, Sorescu D, Anania FA. Glp-1 analog, liraglutide, ameliorates hepatic steatosis and cardiac hypertrophy in C57BL/6J mice fed a Western diet. *Am J Physiol Gastrointest Liver Physiol* 2012; **302**: G225-G235 [PMID: 22038829 DOI: 10.1152/ajpgi.00274.2011]

42 **Tetri LH**, Basaranoglu M, Brunt EM, Yerian LM, Neuschwander-Tetri BA. Severe NAFLD with hepatic necroinflammatory changes in mice fed trans fats and a high-fructose corn syrup equivalent. *Am J Physiol Gastrointest Liver Physiol* 2008; **295**: G987-G995 [PMID: 18772365 DOI: 10.1152/ajpgi.90272.2008]

43 **Ma K**, Malhotra P, Soni V, Hedroug O, Annaba F, Dudeja A, Shen L, Turner JR, Khramtsova EA, Saksena S, Dudeja PK, Gill RK, Alrefai WA. Overactivation of intestinal SREBP2 in mice increases serum cholesterol. *PLoS One* 2014; **9**: e84221 [PMID: 24465397 DOI: 10.1371/journal.pone.0084221]

44 **Rinella ME**. Nonalcoholic fatty liver disease: a systematic review. *JAMA* 2015; **313**: 2263-2273 [PMID: 26057287 DOI: 10.1001/jama.2015.5370]

45 **Reccia I**, Kumar J, Akladios C, Virdis F, Pai M, Habib N, Spalding D. Non-alcoholic fatty liver disease: A sign of systemic disease. *Metabolism* 2017; **72**: 94-108 [PMID: 28641788 DOI: 10.1016/j.metabol.2017.04.011]

46 **Neuschwander-Tetri BA**. Non-alcoholic fatty liver disease. *BMC Med* 2017; **15**: 45 [PMID: 28241825 DOI: 10.1186/s12916-017-0806-8]

47 **Liang W**, Menke AL, Driessen A, Koek GH, Lindeman JH, Stoop R, Havekes LM, Kleemann R, van den Hoek AM. Establishment of a general NAFLD scoring system for rodent models and comparison to human liver pathology. *PLoS One* 2014; **9**: e115922 [PMID: 25535951 DOI: 10.1371/journal.pone.0115922]

48 **Farrell GC**, Mridha AR, Yeh MM, Arsov T, Van Rooyen DM, Brooling J, Nguyen T, Heydet D, Delghingaro-Augusto V, Nolan CJ, Shackel NA, McLennan SV, Teoh NC, Larter CZ. Strain dependence of diet-induced NASH and liver fibrosis in obese mice is linked to diabetes and inflammatory phenotype. *Liver Int* 2014; **34**: 1084-1093 [PMID: 24107103 DOI: 10.1111/liv.12335]

49 **Kanoski SE**, Hayes MR, Skibicka KP. GLP-1 and weight loss: unraveling the diverse neural circuitry. *Am J Physiol Regul Integr Comp Physiol* 2016; **310**: R885-R895 [PMID: 27030669 DOI: 10.1152/ajpregu.00520.2015]

50 **Patel NS**, Doycheva I, Peterson MR, Hooker J, Kisselva T, Schnabl B, Seki E, Sirlin CB, Loomba R. Effect of weight loss on magnetic resonance imaging estimation of liver fat and volume in patients with nonalcoholic steatohepatitis. *Clin Gastroenterol Hepatol* 2015; **13**: 561-568.e1 [PMID: 25218667 DOI: 10.1016/j.cgh.2014.08.039]

51 **McMahan RH**, Wang XX, Cheng LL, Krisko T, Smith M, El Kasmi K, Pruzanski M, Adorini L, Golden-Mason L, Levi M, Rosen HR. Bile acid receptor activation modulates hepatic monocyte activity and improves nonalcoholic fatty liver disease. *J Biol Chem* 2013; **288**: 11761-11770 [PMID: 23460643 DOI: 10.1074/jbc.M112.446575]

52 **Kuipers F**, Bloks VW, Groen AK. Beyond intestinal soap--bile acids in metabolic control. *Nat Rev Endocrinol* 2014; **10**: 488-498 [PMID: 24821328 DOI: 10.1038/nrendo.2014.60]

53 **Fiorucci S**, Mencarelli A, Palladino G, Cipriani S. Bile-acid-activated receptors: targeting TGR5 and farnesoid-X-receptor in lipid and glucose disorders. *Trends Pharmacol Sci* 2009; **30**: 570-580 [PMID: 19758712 DOI: 10.1016/j.tips.2009.08.001]

54 **Li Y**, Jadhav K, Zhang Y. Bile acid receptors in non-alcoholic fatty liver disease. *Biochem Pharmacol* 2013; **86**: 1517-1524 [PMID: 23988487 DOI: 10.1016/j.bcp.2013.08.015]

55 **Ma Y**, Huang Y, Yan L, Gao M, Liu D. Synthetic FXR agonist GW4064 prevents diet-induced hepatic steatosis and insulin resistance. *Pharm Res* 2013; **30**: 1447-1457 [PMID: 23371517 DOI: 10.1007/s11095-013-0986-7]

56 **Cipriani S**, Mencarelli A, Palladino G, Fiorucci S. FXR activation reverses insulin resistance and lipid abnormalities and protects against liver steatosis in Zucker (fa/fa) obese rats. *J Lipid Res* 2010; **51**: 771-784 [PMID: 19783811 DOI: 10.1194/jlr.M001602]

57 **Kong B**, Luyendyk JP, Tawfik O, Guo GL. Farnesoid X receptor deficiency induces nonalcoholic steatohepatitis in low-density lipoprotein receptor-knockout mice fed a high-fat diet. *J Pharmacol Exp Ther* 2009; **328**: 116-122 [PMID: 18948497 DOI: 10.1124/jpet.108.144600]

58 **Jouihan H**, Will S, Guionaud S, Boland ML, Oldham S, Ravn P, Celeste A, Trevaskis JL. Superior reductions in hepatic steatosis and fibrosis with co-administration of a glucagon-like peptide-1 receptor agonist and obeticholic acid in mice. *Mol Metab* 2017; **6**: 1360-1370 [PMID: 29107284 DOI: 10.1016/j.molmet.2017.09.001]

59 **Zhang DG**, Zhang C, Wang JX, Wang BW, Wang H, Zhang ZH, Chen YH, Lu Y, Tao L, Wang JQ, Chen X, Xu DX. Obeticholic acid protects against carbon tetrachloride-induced acute liver injury and inflammation. *Toxicol Appl Pharmacol* 2017; **314**: 39-47 [PMID: 27865854 DOI: 10.1016/j.taap.2016.11.006]

60 **Chinetti G**, Fruchart JC, Staels B. Peroxisome proliferator-activated receptors: new targets for the pharmacological modulation of macrophage gene expression and function. *Curr Opin Lipidol* 2003; **14**: 459-468 [PMID: 14501584 DOI: 10.1097/00041433-200310000-00006]

61 **Gonzalez FJ**, Shah YM. PPARalpha: mechanism of species differences and hepatocarcinogenesis of peroxisome proliferators. *Toxicology* 2008; **246**: 2-8 [PMID: 18006136 DOI: 10.1016/j.tox.2007.09.030]

62 **Nagasawa T**, Inada Y, Nakano S, Tamura T, Takahashi T, Maruyama K, Yamazaki Y, Kuroda J, Shibata N. Effects of bezafibrate, PPAR pan-agonist, and GW501516, PPARdelta agonist, on development of steatohepatitis in mice fed a methionine- and choline-deficient diet. *Eur J Pharmacol* 2006; **536**: 182-191 [PMID: 16574099 DOI: 10.1016/j.ejphar.2006.02.028]

63 **Pawlak M**, Baugé E, Bourguet W, De Bosscher K, Lalloyer F, Tailleux A, Lebherz C, Lefebvre P, Staels B. The transrepressive activity of peroxisome proliferator-activated receptor alpha is necessary and sufficient to prevent liver fibrosis in mice. *Hepatology* 2014; **60**: 1593-1606 [PMID: 24995693 DOI: 10.1002/hep.27297]

64 **Tanaka N**, Aoyama T, Kimura S, Gonzalez FJ. Targeting nuclear receptors for the treatment of fatty liver disease. *Pharmacol Ther* 2017; **179**: 142-157 [PMID: 28546081 DOI: 10.1016/j.pharmthera.2017.05.011]

65 **Savkur RS**, Miller AR. Investigational PPAR-gamma agonists for the treatment of Type 2 diabetes. *Expert Opin Investig Drugs* 2006; **15**: 763-778 [PMID: 16787140 DOI: 10.1517/13543784.15.7.763]

66 **Wang YX**, Zhang CL, Yu RT, Cho HK, Nelson MC, Bayuga-Ocampo CR, Ham J, Kang H, Evans RM. Regulation of muscle fiber type and running endurance by PPARdelta. *PLoS Biol* 2004; **2**: e294 [PMID: 15328533 DOI: 10.1371/journal.pbio.0020294]

67 **Harrington WW**, S Britt C, G Wilson J, O Milliken N, G Binz J, C Lobe D, R Oliver W, C Lewis M, M Ignar D. The Effect of PPARalpha, PPARdelta, PPARgamma, and PPARpan Agonists on Body Weight, Body Mass, and Serum Lipid Profiles in Diet-Induced Obese AKR/J Mice. *PPAR Res* 2007; **2007**: 97125 [PMID: 17710237 DOI: 10.1155/2007/97125]

68 **Rachid TL**, Penna-de-Carvalho A, Bringhenti I, Aguila MB, Mandarim-de-Lacerda CA, Souza-Mello V. Fenofibrate (PPARalpha agonist) induces beige cell formation in subcutaneous white adipose tissue from diet-induced male obese mice. *Mol Cell Endocrinol* 2015; **402**: 86-94 [PMID: 25576856 DOI: 10.1016/j.mce.2014.12.027]

P- Reviewer: Balaban YH, Murotomi K, Pan Q, Sutti S, Tanaka N
S- Editor: Gong ZM **L- Editor**: A **E- Editor**: Ma YJ

World Journal of Gastroenterology

Submit a Manuscript: http://www.f6publishing.com

World J Gastroenterol 2018 January 14; 24(2): 195-210

DOI: 10.3748/wjg.v24.i2.195

ISSN 1007-9327 (print) ISSN 2219-2840 (online)

ORIGINAL ARTICLE

Basic Study

INT-767 improves histopathological features in a diet-induced *ob/ob* mouse model of biopsy-confirmed non-alcoholic steatohepatitis

Jonathan D Roth, Michael Feigh, Sanne S Veidal, Louise KD Fensholdt, Kristoffer T Rigbolt, Henrik H Hansen, Li C Chen, Mathieu Petitjean, Weslyn Friley, Niels Vrang, Jacob Jelsing, Mark Young

Jonathan D Roth, Mark Young, Intercept Pharmaceuticals, Intercept Pharmaceuticals, San Diego, CA 92121, United States

Michael Feigh, Sanne S Veidal, Louise KD Fensholdt, Kristoffer T Rigbolt, Henrik H Hansen, Niels Vrang, Jacob Jelsing, Gubra, Hoersholm DK-2970, Denmark

Li C Chen, Mathieu Petitjean, PharmaNest, Genesis Imaging Services, Princeton, NJ 08540, United States

Weslyn Friley, Qualyst Transporter Solutions, Durham, NC 27713, United States

ORCID number: Jonathan D Roth (0000-0002-8804-8193); Michael Feigh (0000-0001-5274-8799); Sanne S Veidal (0000-0003-1240-2034); Louise KD Fensholdt (0000-0002-9762-3903); Kristoffer T Rigbolt (000 0-0002-9470-0993); Henrik H Hansen (0000-0002-3732-0281); Li C Chen (0000-0002-3458-1830); Mathieu Petitjean (0000-00 03-3468-7114); Weslyn Friley (0000-0002-6992-8726); Niels Vrang (0000-0002-7203-9532); Jacob Jelsing (0000-0 002-4583-1022); Mark Young (0000-0002-9503-6211).

Author contributions: Studies were designed by Roth JD, Feigh M, Petitjean M and Young M; Fensholdt LKD Fensholdt, Veidal SS, Rigbolt KT, Chen LC and Friley W performed the majority of experiments; Hansen HH and Roth JD wrote the paper with significant contributions to data analyses and editing by all co-authors.

Institutional animal care and use committee statement: All animal experiments conformed to the internationally accepted principles for the care and use of laboratory animals (licence no. 2013-15-2934-00784, The Animal Experiments Inspectorate, Denmark).

Conflict-of-interest statement: Jonathan Roth and Mark Young are employed by and hold equity in Intercept Pharmaceuticals, Inc. All other authors have nothing to disclose.

Data sharing statement: No additional data are available.

Manuscript source: Invited manuscript

Correspondence to: Henrik H Hansen, PhD, Principal Scientist, Pharmacology, Gubra, Kongevej 11B, Hoersholm DK-2970, Denmark. hbh@gubra.dk
Telephone: +45-23-1522651

Received: October 23, 2017
Peer-review started: October 25, 2017
First decision: November 14, 2017
Revised: November 24, 2017
Accepted: December 5, 2017
Article in press: December 5, 2017
Published online: January 14, 2018

Abstract

AIM

To characterize the efficacy of the dual FXR/TGR5 receptor agonist INT-767 upon histological endpoints in a rodent model of diet-induced and biopsy-confirmed non-alcoholic steatohepatitis (NASH).

METHODS

The effects of INT-767 on histological features of NASH were assessed in two studies using *Lep*$^{ob/ob}$ (*ob/ob*) NASH mice fed the AMLN diet (high fat with trans-fat, cholesterol and fructose). In a proof-of-concept

study, *Lep*$^{ob/ob}$ (*ob/ob*) NASH mice were first dosed with INT-767 (3 or 10 mg/kg for 8 wk). A second *ob/ob* NASH study compared INT-767 (3 and 10 mg/kg) to obeticholic acid (OCA) (10 or 30 mg/kg; 16 wk). Primary histological endpoints included qualitative and quantitative assessments of NASH. Other metabolic and plasma endpoints were also assessed. A comparative assessment of INT-767 and OCA effects on drug distribution and hepatic gene expression was performed in C57Bl/6 mice on standard chow. C57Bl/6 mice were orally dosed with INT-767 or OCA (1-30 mg/kg) for 2 wk, and expression levels of candidate genes were assessed by RNA sequencing and tissue drug levels were measured by liquid chromatography tandem-mass spectrometry.

RESULTS

INT-767 dose-dependently (3 and 10 mg/kg, PO, QD, 8 wk) improved qualitative morphometric scores on steatohepatitis severity, inflammatory infiltrates and fibrosis stage. Quantitative morphometric analyses revealed that INT-767 reduced parenchymal collagen area, collagen fiber density, inflammation (assessed by Galectin-3 immunohistochemistry) and hepatocyte lipid droplet area following INT-767 treatment. In a comparative study (16 wk), the FXR agonists OCA (10 and 30 mg/kg) and INT-767 (3 and 10 mg/kg) both improved NASH histopathology, with INT-767 exerting greater therapeutic potency and efficacy than OCA. Mechanistic studies suggest that both drugs accumulate similarly within the liver and ileum, however, the effects of INT-767 may be driven by enhanced hepatic, but not ileal, FXR function.

CONCLUSION

These findings confirm the potential utility of FXR and dual FXR/TGR5 activation as disease intervention strategies in NASH.

Key words: Non-alcoholic steatohepatitis; INT-767; Obeticholic acid; Liver biopsy; FXR; TGR5; Mouse model

Core tip: The studies contained herein evaluated the preclinical efficacy of INT-767, a dual FXR/TGR5 agonist, in a mouse model of diet-induced and biopsy-confirmed non-alcoholic steatohepatitis (NASH). Rigorous analyses for NASH histological endpoints and markers were conducted including blinded qualitative and quantitative scoring using standard microscopy as well as advanced morphometric fibrosis and steatosis features using second harmonic generation imaging and two-photon fluorescence excitation. INT-767 promoted dose-dependent improvements in fibrosis, steatosis, inflammation and ballooning degeneration. The effects of INT-767 and obeticholic acid (OCA) were also compared for histological efficacy, gene expression and tissue distribution. The preclinical data suggest that INT-767 is a more potent FXR receptor agonist, and is expected to have therapeutic effects at lower doses than OCA.

Roth JD, Feigh M, Veidal SS, Fensholdt LKD, Rigbolt KT, Hansen HH, Chen LC, Petitjean M, Friley W, Vrang N, Jelsing J, Young M. INT-767 improves histopathological features in a diet-induced *ob/ob* mouse model of biopsy-confirmed non-alcoholic steatohepatitis. *World J Gastroenterol* 2018; 24(2): 195-210 Available from: URL: http://www.wjgnet.com/1007-9327/full/v24/i2/195.htm DOI: http://dx.doi.org/10.3748/wjg.v24.i2.195

INTRODUCTION

Nonalcoholic fatty liver disease (NAFLD) is considered the hepatic manifestation of the metabolic syndrome, a cluster of closely related clinical features linked to visceral obesity and characterized by insulin resistance, dyslipidemia, and hypertension. While steatosis can be considered a relatively benign liver disease, for reasons that are still incompletely understood, a subgroup of NAFLD patients go on to develop non-alcoholic steatohepatitis (NASH), which is marked by hepatocellular injury, inflammation, and progressive fibrosis. It is estimated that the prevalence of progression from NAFLD to NASH is 10% to 20% in the general population; 37% in the high-risk, severe obese population; and 40% to 55% in patients at tertiary care centers[1]. Several factors have been implicated in the development of NAFLD, including sensitization due to excessive liver triglyceride accumulation coupled with insulin resistance[2].

In addition to their roles in dietary lipid absorption and cholesterol homeostasis, bile acids activate many signaling pathways, including the ligand-activated nuclear farnesoid X receptor FXR[3] and the plasma membrane-bound G protein-coupled receptor TGR5[4,5]. FXR and TGR5 represent attractive targets for the treatment of metabolic and chronic liver diseases. FXR is predominantly expressed in the liver, kidney and intestine, with a major role in controlling bile acid homeostasis. FXR activation suppresses NF-κB–regulated pro-inflammatory genes in hepatocytes and vascular cells, as well as inflammatory mediators such as cyclooxygenase-2 (COX-2) and inducible nitric oxide synthase (iNOS)[6-8]. FXR activation also inhibits production of tumour necrosis factor-alpha (TNF-α) by human peripheral blood mononuclear cells and human monocytes, and inhibits differentiation of human monocytes into dendritic cells[8]. Furthermore, FXR activation inhibits production of TNF-α, interleukin (IL)-17, and interferon gamma (IFN-γ) in lymphocyte-enriched human intestinal lamina propria cells, suggesting that FXR function participates in preserving the intestinal barrier[9]. Although not expressed in hepatocytes, TGR5 is detected in many liver cell types

where it could directly or indirectly modulate hepatic lipid metabolism[10]. TGR5 is highly expressed in Kupffer cells, which are resident liver macrophages[11], and their proinflammatory cytokine secretion has been implicated in the progression of NAFLD[12]. In Kupffer cells, bile acids inhibit lipopolysaccharide-induced cytokine expression *via* TGR5-cAMP-dependent pathways[11]. The increased TGR5 expression in Kupffer cells after bile duct ligation suggests a protective role for TGR5 in obstructive cholestasis, preventing excessive proinflammatory cytokine production and thereby reducing liver injury[11].

INT-767 is a semisynthetic bile acid derivative[13] being developed for the treatment of liver and metabolic diseases and is the first compound described that potently and selectively activates both bile acid receptors (FXR, EC_{50} of approximately 30 nmol/L; TGR5, EC_{50} of 0.6 μmol/L). INT-767 is approximately 300-fold more potent at FXR than the natural homologue, chenodeoxycholic acid (CDCA), and 4- to 12-fold more potent at TGR5 than the natural TGR5 agonist lithocholic acid (LCA)[13]. INT-767 has been profiled in several animal models and shown to improve metabolism and decrease inflammation and fibrosis. For example, INT-767 reduced atherosclerotic plaque formation by preventing hyperlipidemia and inhibiting pro-inflammatory cytokine production in macrophages in a mouse model of hypercholesterolemia[14]. INT-767 also prevented proteinuria, podocyte injury, fibronectin accumulation and TGF-α accumulation associated with age-related kidney disease[15]. Most relevant to NASH was the finding that INT-767 treatment of obese *db/db* mice with NAFLD improved liver histopathology, and modulated intrahepatic macrophage populations to a less inflammatory phenotype[16].

While these results are encouraging, prior studies have not explicitly assessed the effects of INT-767 in mice with biopsy-confirmed histological features of NASH. *Lep*$^{ob/ob}$ (*ob/ob*) mice have been shown to be consistently prone to fibrosis when cholesterol (2%) and trans-fatty acids (45% of total fat amount) are added to a high-caloric diet (termed AMLN diet; Trevaskis, 2012; based on the American Lifestyle-Induced Obesity Syndrome mouse model developed by Tetri and colleagues[17]). With reference to standard clinical practice, biopsy-confirmation procedures have successfully been applied to *ob/ob* mice fed the AMLN diet (hereafter referred to as *ob/ob*-NASH mice) for staging of baseline liver pathology to equalize NASH severity in the experimental groups and perform within-subject comparisons during the course of drug treatment[18,19]. Thus, the present studies evaluated the efficacy of INT-767, administered for 8 wk in *ob/ob*-NASH mice. Rigorous analyses for NASH histological endpoints and markers were conducted including blinded qualitative and quantitative scoring using standard microscopy as well as advanced morphometric fibrosis and steatosis features using second harmonic generation imaging and two-photon fluorescence excitation (SHG/2-PE). The effects of INT-767 and obeticholic acid (OCA) were also compared in a longer-term (16 wk) head-to-head study, as well as in shorter studies (2 wk) comparing hepatic and ileal tissue drug concentration and gene expression profiles.

MATERIALS AND METHODS

Animals

All animal experiments conformed to the internationally accepted principles for the care and use of laboratory animals (license no. 2013-15-2934-00784, The Animal Experiments Inspectorate, Denmark). C57Bl6/J and B6.V-Lep^{ob}/JRj (*ob/ob*) mice (5-6 wk-old) were from Janvier Labs (Le Genest Saint Isle, France) and housed in a controlled environment (12 h light/dark cycle, light on at 3 AM, 21 ℃ ± 2 ℃, humidity 50% ± 10%). Each animal was identified by an implantable microchip (PetID Microchip, E-vet, Haderslev, Denmark). Mice had *ad libitum* access to tap water and either regular rodent chow (C57Bl6/J mice, Altromin 1324, Brogaarden, Hoersholm, Denmark), or a diet high in fat (*ob/ob* mice, 40%, containing 18% trans-fat), 40% carbohydrates (20% fructose) and 2% cholesterol (AMLN diet; D09100301, Research Diets, New Brunswick, NJ)[19]. *ob/ob* mice (n = 87) were fed the AMLN diet for 9 or 15 wk prior to treatment start and during drug treatment. All *ob/ob* animals underwent liver biopsy prior to treatment, see below.

Baseline liver biopsy

The biopsy procedure was applied to all mice approximately three weeks before completion of the dieting period, as detailed previously[19]. In brief, mice were anesthetized with isoflurane, a small abdominal incision in the midline was made, and the left lateral lobe of the liver was exposed. A cone-shaped wedge of liver tissue (50-100 mg) was excised from the distal part of the lobe. The cut surface of the liver was closed by electrosurgical bipolar coagulation. The liver was returned to the abdominal cavity, the abdominal wall was sutured and skin stapled. Carprofen (Rimadyl®, 5 mg/mL, 0.01 mL/10 g; Pfizer, NY) and enrofloxazin (5 mg/mL, 1 mL/kg, *i.p.*) were administered at the time of surgery and at post-operative day one and two. Animals were single-housed after the procedure and recovered for three weeks prior to treatment.

Drug treatment

INT-767 and OCA (Intercept Pharmaceuticals, New York, NY, United States) were dissolved in 0.5% carboxymethyl cellulose, and orally administered in a dosing volume of 5 mL/kg. Animals were stratified (n = 11-12 per group) based on mean fibrosis as assessed by collagen 1a1 staining. In one study, after 15 wk on diet mice were treated with INT-767 (3.0 or 10 mg/kg) for 8 wk. In a second study, after 9 wk on

diet mice were treated with either vehicle, INT-767 (3.0 or 10 mg/kg), or OCA (10 or 30 mg/kg) for 16 wk. A longer duration of administration was selected for this second study to (a) examine the durability of INT-767 NASH histological improvements, and (b) because in our experience OCA requires extended dosing (*e.g.*, at least 12 wk at 10-30 mg/kg) to elicit histological anti-fibrotic responses (data on file) and shorter treatment periods with OCA are not always sufficient to promote antifibrotic effects in *ob/ob*-NASH mice[20]. For analysis of liver and intestinal compound levels, as well as hepatic gene expression, lean C57Bl6 mice received INT-767 (1-3-10-30 mg/kg, PO, QD) or OCA (1-3-10-30 mg/kg, PO, QD) for 14 d.

Body weight and body composition analysis

Body weight was monitored once daily during the intervention period. Whole-body fat mass was analyzed at baseline (week -1) and week 8 of the intervention period by non-invasive EchoMRI scanning using EchoMRI-900 (EchoMRI, Houston, TX).

Plasma and liver biochemistry

Plasma and liver biochemistry was assessed according to methods described in detail previously[19]. Baseline and terminal blood samples from non-fasted mice were assayed for blood glucose levels as well as plasma concentrations of alanine aminotransferase (ALT), aspartate aminotransferase (AST), triglycerides (TG), total cholesterol (TC), and insulin. Terminal liver samples (about 100 mg) were analyzed for TG and TC content.

Oral glucose tolerance test

An oral glucose tolerance test (OGTT) was performed in week 4 of the treatment period according to previously reported procedures[19]. In brief, animals were fasted for 4 h prior to the OGTT. At t = 0 an oral glucose load (2 g glucose/kg) was administered via oral gavage. Succesive blood samples for measuring blood glucose (BG) were collected from the tail vein at t = 0, 15, 30, 60 and 120 min. Glucose area-under-the-curve (AUC) was determined from the sampling period of 0 to 120 min.

Liver histology and digital image analysis

Baseline liver biopsy and terminal samples (both from the left lateral lobe) were fixed overnight in 4% paraformaldehyde. Liver tissue was paraffin-embedded and sectioned (3 μm thickness). Sections were stained with hematoxylin-eosin (HE), PicroSirius Red (PSR, Sigma-Aldrich, Broendby, Denmark), anti-type I collagen (Col1a1; cat. 1310-01, Southern Biotech, Birmingham, AL), anti-galectin-3 (cat. 125402, Biolegend, San Diego, CA, United States), or anti-laminin (cat. Z0097, Agilent Technologies, Glostrup, Denmark) using standard procedures[19]. The NAFLD activity score (NAS) and fibrosis staging system was applied for scoring of steatosis (score 0-3), lobular inflammation (score 0-3), hepatocyte ballooning (score 0-2), and fibrosis (stage 0-4)[21]. Mice with fibrosis stage $\geqslant$ 1 and steatosis score $\geqslant$ 2 were included in the study. Liver sections stained for fat, Col1a1, galectin-3 and laminin were analyzed using digital imaging software (Visiomorph®, Visiopharm, Hørsholm, Denmark). Immunoreactive fractional area was expressed relative (%) to total parenchymal area by subtracting corresponding fat area determined on adjacent HE-sections. In addition, deparaffinized and unstained tissue sections of similar thickness where imaged by second harmonic generation (SHG, label free, specific to collagen 1 and 3, in transmission at 780 nm) and concurrently by 2-photon fluorescence excitation (2-PE at 780 nm, collected at 550 ± 88 nm to delineate the tissue structure). Both optical methods were performed on a mid-throughput, fully automated, nonlinear optical imaging system at 20 X objective and 0.39 μm resolution (Genesis 200®, HistoIndex, Singapore), as described previously[22]. Fat droplets appear as circular dark objects (no intrinsic fluorescence) and can thus be segregated from the parenchyma and quantified (droplet count, area, eccentricity, and size), Collagen fiber data (area, density, reticulation index) were expressed relative (%) to corresponding parenchymal area. The collagen fiber network complexity (reticulation index) was expressed, as the ratio of skeleton fibers nodes to the total length of the equivalent skeleton. Imaging parameters (laser intensity, photomultiplier tube gains, scanning) and image analysis parameters (signal intensity and morphometric thresholding and pruning) where kept constant for the entire study after optimization. SHG was optimized to use the full 8-bit dynamic range of the instrument and avoid saturation. All histological assessments were performed by pathologists and operators blinded to the experimental groups.

LC/MS/MS determination of compound levels in liver and ileum

A mass dependent volume of homogenization solution (seven volumes of 80/20 ACN/HBSS) was added to each tube containing a pre-weighed, intact tissue specimen. Tissue samples were homogenized using an Omni Bead Ruptor 24 tissue homogenizer set to 4 m/s for two cycles of 30 s each. Sample tubes were centrifuged at 3500 rcf for 3 min and a 200 μL aliquot of supernatant was transferred to a 96 deep-well plate. Samples were dried down under nitrogen and reconstituted in 60/40 methanol/10 mmol/L ammonium acetate containing 25 nmol/L of d5-GCA internal standard. Reconstituted samples were transferred to a Millipore 0.45 μm filter plate (Millipore MSHVN45) and filtered into a Costar 3957 plate by centrifugation and sealed with a silicone capmat prior to LC-MS/MS analysis. This extract was injected onto an UHPLC system equipped with a ultra-

Table 1 Effect of 8 wk of treatment with INT-767 on metabolic parameters, non-alcoholic fatty liver disease activity score/fibrosis stage, body weight/composition, and liver weight in *ob/ob*-NASH mice

	Vehicle, (n = 10)	INT-767, 3 mg/kg (n = 10)	INT-767, 10 mg/kg (n = 10)
Baseline plasma ALT (U/L)	577 ± 43.4	552 ± 36.1	498 ± 27.3
Terminal plasma ALT (U/L)	670 ± 58.9	478 ± 33.9	250 ± 21.6[b,f]
Baseline plasma AST (U/L)	436 ± 36.7	421 ± 16.7	359 ± 15.6
Terminal plasma AST (U/L)	552 ± 49.4	447 ± 38.8	257 ± 42.3[e,f]
Baseline plasma TC (mmol/L)	10.3 ± 0.8	10.3 ± 0.8	11.1 ± 0.3
Terminal plasma TC (mmol/L)	10.7 ± 0.5	9.2 ± 0.3	7.2 ± 0.4[e,f]
Baseline plasma TG (mmol/L)	0.8 ± 0.0	0.8 ± 0.1	0.8 ± 0.1
Terminal plasma TG (mmol/L)	0.7 ± 0.0	0.6 ± 0.0	0.6 ± 0.1
Terminal liver TC (mg/g tissue)	32.9 ± 1.7	24.0 ± 1.1[d]	18.0 ± 1.5[f]
Terminal liver TG (mg/g tissue)	233 ± 12.3	229 ± 15.4	149 ± 14.0[d]
Fasting blood glucose (week 4, mmol/L)	7.6 ± 0.1	8.2 ± 0.2	8.0 ± 0.3
OGTT, glucose AUC (week 4, mmol/L × min)	1318 ± 61	1304 ± 38	1417 ± 78
Fed blood glucose (week 8, mmol/L)	7.1 ± 0.2	6.8 ± 0.2	7.3 ± 0.3
Fed plasma insulin (week 8, pmol/L)	567 ± 133	482 ± 122	799 ± 229
Baseline steatosis score	3.0 ± 0.0	2.9 ± 0.1	2.9 ± 0.1
Terminal steatosis score	3.0 ± 0.0	3.0 ± 0.0	1.8 ± 0.2[f]
Baseline inflammation score	2.5 ± 0.1	3.0 ± 0.0	3.0 ± 0.0
Terminal inflammation score	2.3 ± 0.1	2.2 ± 0.2	1.0 ± 0.1[f]
Baseline ballooning degeneration score	0.6 ± 0.1	0.7 ± 0.1	0.8 ± 0.1
Terminal ballooning degeneration score	0.9 ± 0.1	0.7 ± 0.1	0.2 ± 0.1[f]
Baseline NAFLD activity score (NAS)	6.1 ± 0.2	6.3 ± 0.2	6.4 ± 0.2
Terminal NAFLD activity score (NAS)	6.2 ± 0.2	5.9 ± 0.2	3.0 ± 0.3[f]
Baseline fibrosis stage	2.7 ± 0.2	2.6 ± 0.1	2.6 ± 0.1
Terminal fibrosis stage	2.7 ± 0.1	2.5 ± 0.1	1.6 ± 0.1[f]
Terminal steatosis (% area)	41.1 ± 1.0	40.6 ± 1.6	24.8 ± 2.3[f]
Terminal fibrosis (% area)	15.9 ± 0.9	13.6 ± 0.8	8.9 ± 0.6[f]
Baseline BW (g)	49.8 ± 0.7	48.2 ± 1.0	49.4 ± 1.3
Terminal BW (g)	54.6 ± 0.8	52.6 ± 0.8	51.3 ± 1.8
Body weight change (%, relative to day 0)	109 ± 1.3	107 ± 2.1	103 ± 2.3
Baseline whole-body lean mass (g)	14.0 ± 0.4	14.6 ± 0.3	14.4 ± 0.4
Terminal whole-body lean mass (g)	17.3 ± 0.4	17.6 ± 0.5	17.2 ± 0.2
Baseline whole-body lean mass (% of BW)	28.2 ± 0.6	30.3 ± 0.6	29.1 ± 0.6
Terminal whole-body lean mass (% of BW)	31.9 ± 0.6	33.9 ± 0.9	33.6 ± 0.8
Baseline whole-body fat mass (g)	18.5 ± 0.4	18.5 ± 0.7	19.5 ± 0.7
Terminal whole-body fat mass (g)	22.5 ± 0.4	21.0 ± 0.7	19.3 ± 0.7[e]
Baseline whole-body fat mass (% of BW)	37.2 ± 0.7	38.4 ± 1.2	39.4 ± 0.6
Terminal whole-body fat mass (% of BW)	41.4 ± 0.5	40.4 ± 0.9	37.5 ± 0.7[e]
Terminal liver weight (g)	5.4 ± 0.2	4.9 ± 0.1	4.1 ± 0.1[f]
Terminal liver weight (% of BW)	9.8 ± 0.3	9.4 ± 0.2	8.0 ± 0.3[d]

Morphometric scores were analyzed by a χ^2 test compared to vehicle. All other data were analyzed by a two-way ANOVA with Bonferroni's *post-hoc* test ([a]P < 0.05, [b]P < 0.01, [e]P < 0.001; *vs* baseline. [c]P < 0.05, [d]P < 0.01, [f]P < 0.001, *vs* vehicle).

high resolution, accurate mass, mass spectrometer (UHRAM) (Thermo Fisher Scientific *Q* Exactive with Ion Max M2 with HESI-Ⅱ probe) detector operated in negative electrospray mode. Separation of test article from extracted matrix materials was accomplished using a Thermo Fisher Hypersil Gold C18 column (1 mm x 100 mm, 1.9 μm particle size) operating at 45 ℃. The gradient mobile phase system consisted of 0.25 mmol/L ammonium acetate in 40% methanol (mobile phase A) and 0.25 mmol/L ammonium acetate in 95% methanol (mobile phase B) at a total flow rate of 0.100 mL/min.

Twenty analytical runs were performed during the study sample analysis. Calibration standards, prepared in matrix matched mouse control tissues purchased from BioreclamationIVT (Baltimore, MD), were used to construct standard curves for all analytes. Typically, quadratic weighted (1/x) regression analysis of peak area ratio *vs* theoretical concentration was used to produce calibration curves.

RNA sequencing

Hepatic and ileal transcriptome analysis was performed by RNA sequencing on RNA extracts from terminal liver samples, as described[19]. RNA sequence libraries were prepared with NeoPrep (Illumina, San Diego, CA, United States) using Illumina TruSeq stranded mRNA Library kit for NeoPrep (Illumina, San Diego, CA, United States) and sequenced on the NextSeq 500 (Illumina, San Diego, CA, United States) with NSQ 500 hi-Output KT v2 (75 CYS, Illumina, San Diego, CA, United States). Reads were aligned to the GRCm38 v84 Ensembl Mus musculus genome using STAR v.2.5.2a with default parameters[23]. Differential gene

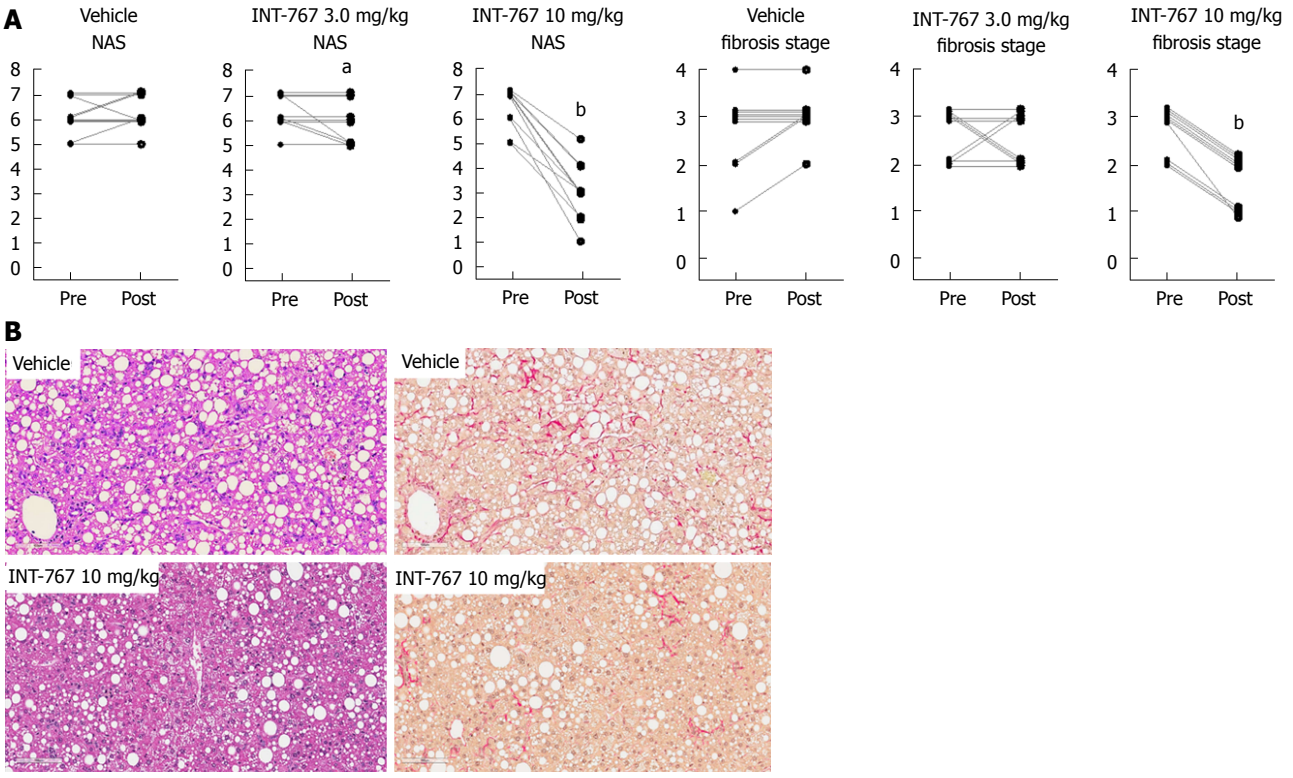

Figure 1 INT-767 treatment for 8 wk improves liver histopathology in *ob/ob*-NASH mice with biopsy-confirmed liver pathology. A: Composite NAS and fibrosis stage before and after treatment intervention; B: Representative HE and PSR stainings. $^{a}P < 0.05$, $^{b}P < 0.001$ (χ^2 test, *vs* vehicle controls).

expression analysis was performed with DEseq215[24].

Statistical analysis

All data were analyzed using GraphPad Prism 5.0 (GraphPad Software, La Jolla, CA, United States). Results are presented as mean ± SE. A chi-square (χ^2) test was used to test for within-subject changes in qualitative histology scores before and after treatment, compared to vehicle controls. Responders were defined as having a $\geqslant$ 1 point change in the indicated score. An unpaired two-tailed *t-test* was applied to quantitative histological analyses after treatment. A two-way ANOVA with Bonferroni's post-hoc test was used for analysis of changes in gene expression and quantitative histology analytes (fractional area of fat, galectin-3, and Col1a1) before and after treatment, compared to vehicle controls. A *P*-value less than 0.05 was considered statistically significant.

RESULTS

INT-767 improves liver histopathology after 8 wk of treatment in ob/ob-NASH mice

All *ob/ob*-NASH mice included in the experiment had liver biopsy-confirmed NASH (NAS 5-7) and fibrosis (stage 1-4) prior to initiation of treatment (Table 1).

INT-767 promoted dose-dependent improvements in liver histopathology after eight wk of treatment in *ob/ob*-NASH mice. INT-767 10 mg/kg significantly reduced steatosis, inflammation and hepatocyte ballooning degeneration scores compared to vehicle controls (Table 1). All INT-767 (10 mg/kg) treated mice exhibited reductions in NAS and fibrosis stage (Figure 1, Table 1). In contrast, *ob/ob*-NASH control mice maintained composite NAS and fibrosis scores compared to pre-treatment levels. INT-767 also reduced quantitative hepatic collagen and fat, as indicated by lowered Col1a1 immunoreactivity (Figure 2B) and liver fat area (Figure 3B). This reduction of collagen and fat by INT-767 was also shown in the IHC staining images (Figures 2A and 3A, respectively) and confirmed by label free SHG/2-PE images and processed images for fat content (Figures 2C and 3C, respectively).

SHG/2-PE morphometric assessments of collagen were positively correlated with Col1a1 assessment by immunohistochemistry (r^2 = 0.88, P <0.0001) and demonstrated that INT-767 predominantly impacted collagen fiber density, but not collagen fiber network complexity (reticulation index, Figure 2D). With respect to steatosis, INT-767 reduced mean fat droplet area, but not droplet count (Figure 3D). The size distribution of fat droplets in INT-767 treated *ob/ob*-NASH mice were left-shifted, suggesting a vesicular fat redistribution towards a less macro-steatotic phenotype (Figure 4).

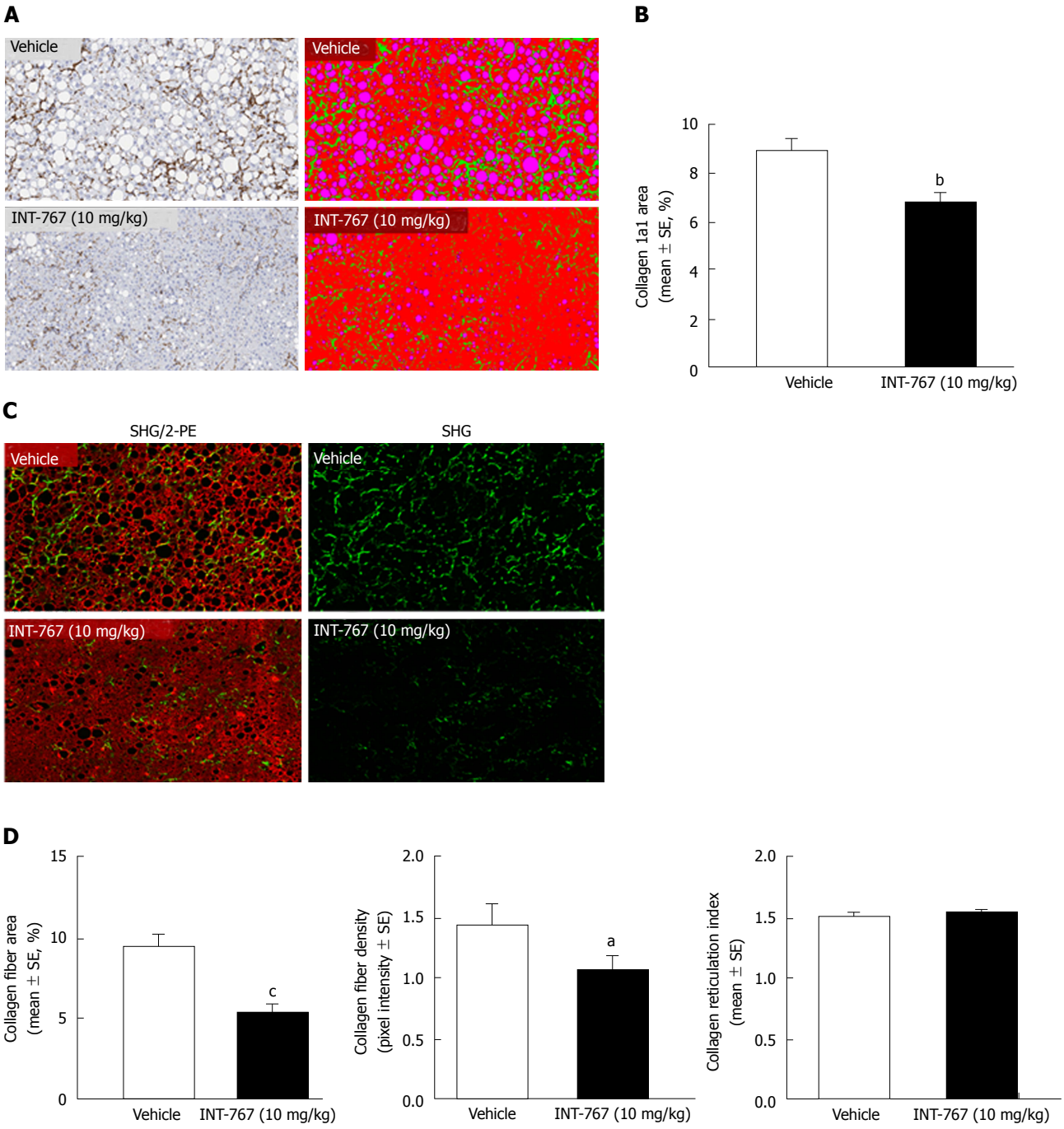

Figure 2 INT-767 treatment for 8 wk reduces hepatic collagen deposition in *ob/ob*-NASH mice with biopsy-confirmed liver pathology. A: Collagen 1a1 (immunohistochemistry); B: Fractional area of collagen (immunohistochemistry); C: Label free SHG/2-PE images for collagen fiber deposition (green) in hepatic parenchyma (red). Data are expressed as % of total parenchymal area (subtraction of fat area); D: Fractional area of collagen fiber, collagen fiber density, and collagen fiber reticulation index (SHG analysis). $^{a}P < 0.05$, $^{b}P < 0.01$, $^{c}P < 0.001$ (unpaired *t*-test).

In line with these morphometric changes, and similar to PPAR agonists[25], INT-767 10 mg/kg significantly reduced mRNA levels of cell death-inducing DNA fragmentation factor alpha-like effector c (CIDEC; a lipid-droplet associated protein that promotes intracellular storage) relative to vehicle (in RPKM, 109.4 ± 10 (vehicle) *vs* 40.8 ± 10.8 (INT-767), $P = 0.0018$).

The liver histological changes with INT-767 (10 mg/kg) treatment were accompanied by significant improvements in liver enzymes (ALT and AST). INT-767 also reduced whole-body fat mass (without changing body weight), hepatomegaly and intrahepatic concentrations of TC and TG (Table 1). In addition, INT-767 reduced terminal liver concentrations of TC and TG, and plasma TC (Table 1).

INT-767 and obeticholic acid show similar hepatic and ileal distribution in C57Bl6 mice

Hepatic and ileal concentrations of INT-767 and OCA

Table 2 INT-767 and obeticholic acid improve liver histomorphology in *ob/ob*-NASH steatohepatitis mice with biopsy-confirmed liver pathology

Treatment	Fibrosis stage			NAS		
	No improvement	With improvement	% improving[1]	No improvement	With improvement	% improving[1]
Vehicle (n = 11)	11	0	0%	11	0	0%
OCA 10 mg/kg (n = 12)	10	2	17%	8	4	33%
OCA 30 mg/kg (n = 11)	7	4	36%[a]	0	11	100%[a]
INT-767 3.0 mg/kg (n = 12)	12	0	0%	7	5	42%[a]
INT-767 10 mg/kg (n = 11)	2	9	82%[a]	0	11	100%[a]

Subjects (%) achieving > [1]points improvement in score from baseline; [a]$P < 0.05$ *vs* vehicle (χ^2 test).

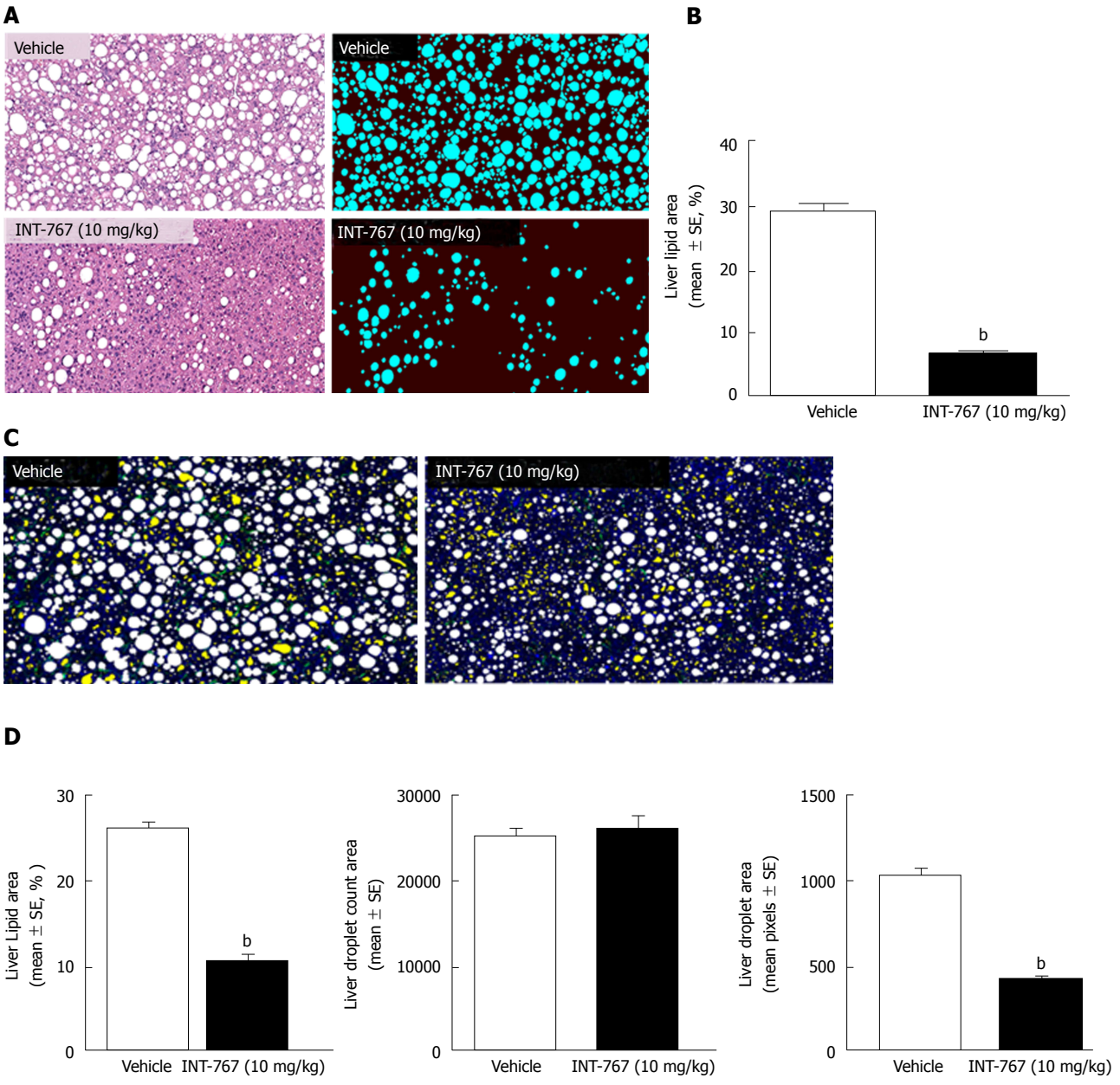

Figure 3 INT-767 treatment for 8 wk reduces hepatic lipid deposition in *ob/ob*-NASH mice with biopsy-confirmed liver pathology. A: Liver lipid (HE staining); B: Fractional area of liver fat (HE staining); C: Processed (color coded) images to display hepatic lipid content. Lipid droplets (white), rejected structures (yellow), collagen (green), auto-fluorescence (blue); D: Fractional area of liver lipid area ratio (%), lipid droplet number (count in 15 mm^2 tissue area), and lipid droplet area (1 pixel = 0.39 μm, 2-PE analysis). [b]$P < 0.001$ (unpaired t-test).

Table 3 INT-767 and obeticholic acid improve quantitative liver histopathology in *ob/ob*-NASH mice

Treatment	Lipid (steatosis)		Galectin-3 (inflammation)		Collagen 1a1 (fibrosis)	
	% fractional area					
	Before treatment	After treatment	Before treatment	After treatment	Before treatment	After treatment
Vehicle (n = 11)	33.0 ± 0.9	30.4 ± 0.9	5.7 ± 0.5	7.8 ± 0.5	1.2 ± 0.3	12.1 ± 0.4
OCA 10 mg/kg (n = 12)	33.4 ± 0.8	31.8 ± 0.4	5.5 ± 0.3	5.0 ± 0.2[a]	0.9 ± 0.1	9.0 ± 0.6[a]
OCA 30 mg/kg (n = 11)	32.2 ± 1.1	22.7 ± 1.0[a]	5.5 ± 0.4	4.0 ± 0.4[a]	1.2 ± 0.2	8.0 ± 0.7[a]
INT-767 3.0 mg/kg (n = 12)	33.0 ± 0.9	29.4 ± 1.3[a]	5.6 ± 0.5	5.4 ± 0.2[a]	1.2 ± 0.2	8.5 ± 0.6[a]
INT-767 10 mg/kg (n = 11)	33.7 ± 0.8	12.5 ± 1.5[a]	5.6 ± 0.3	2.9 ± 0.1[a]	0.9 ± 0.2	5.0 ± 0.3[a]

Fractional area (mean ± SE) at the end of study; [a]P < 0.05 *vs* vehicle (two-way ANOVA, Bonferroni's *post-hoc* test).

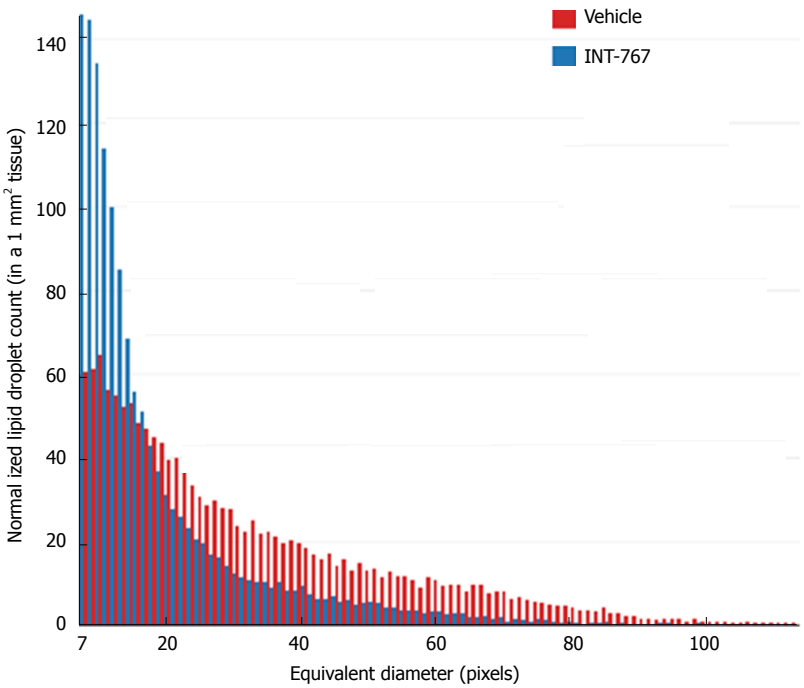

Figure 4 Histogram depicting lipid droplet size distribution in INT-767 *vs* vehicle treated *ob/ob*-NASH mice. The "equivalent diameter" is the diameter of a circle of equivalent area as the one measured on the image (often not a perfect circle). Unit is in pixels, with 1 pixel = 0.39 μm.

were determined after 14 d of dosing (1-30 mg/kg, PO) in chow-fed C57Bl6 mice only. Both compounds showed similar dose-dependent increases in hepatic and ileal exposure. For both compounds, ileal drug concentrations were approximately two-fold higher compared to the liver (Figure 5).

Impact on INT-767 and obeticholic acid on ileal and hepatic FXR target gene expression in C57Bl6 mice

Based on RNAseq data, prototypic FXR target genes were selected for analysis upon acute dosing of INT-767 and OCA (1-30 mg/kg, PO) in C57Bl6 mice. Both INT-767 and OCA regulated hepatic FXR genes, however, INT-767 more strongly regulated these genes at the highest dose administered (Figure 6A-D). By contrast, within the ileum, OCA had more pronounced effects that INT-767 to stimulate SHP and FGF-15 (Figure 6E and F).

INT-767 shows greater efficacy than obeticholic acid on liver histopathology after 16 wk of treatment in ob/ob-NASH mice

Given that INT-767 showed similar efficacy on hepatic FXR target gene expression, albeit at a lower dose compared to OCA (see above), a comparative study on the pharmacodynamics of potency-adjusted doses of INT-767 (3.0, 10 mg/kg) and OCA (10, 30 mg/kg) was performed in *ob/ob*-NASH mice. To better capture effects on progression of fibrosis, treatment was initiated in *ob/ob*-NASH mice fed AMLN diet for 6 wk (*vs* 12 wk in the previous study) and these mice presented with milder baseline NASH (NAS ⩾ 4, fibrosis ⩾ stage 1). All tested doses of INT-767 and OCA significantly reduced composite NAS, as compared to baseline (Figure 7 and 8). Administration of the highest doses of each compound effectively reduced NAS in all treated *ob/ob*-NASH mice (Table 2), but also significantly

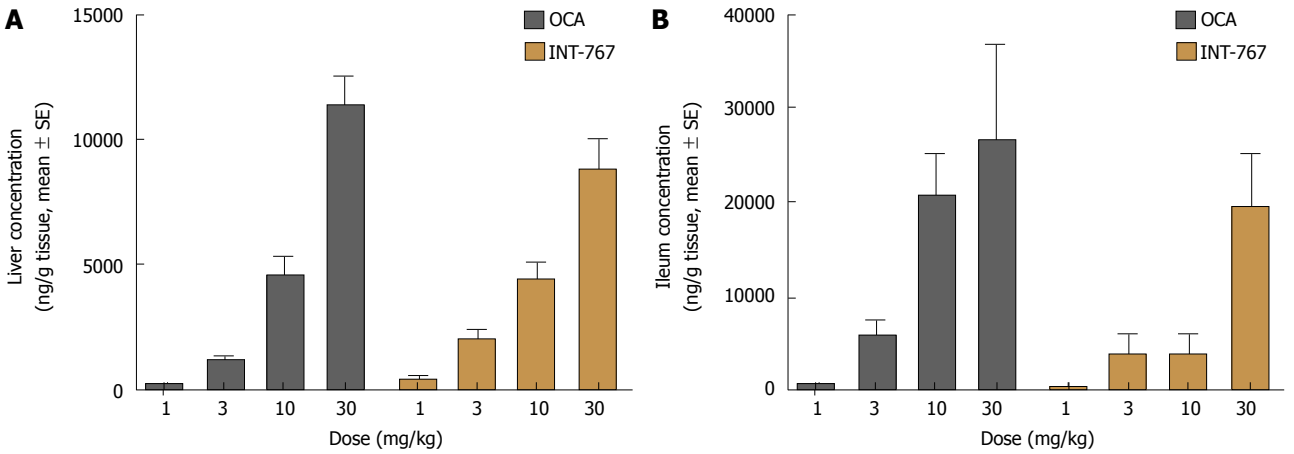

Figure 5 INT-767 and obeticholic acid (OCA) distribute similarly in the liver and ileum after 2 wk of administration in lean C57Bl/6 mice. A: Liver concentration; B: Ileum concentration.

reduced fibrosis scores in the animals (Figure 7 and 8). The ratio of mice achieving > 1 points improvement in score from baseline were 82% (9/11 animals, INT-767 10 mg/kg) and 57% (4/7 animals, OCA 30 mg/kg), see Table 2.

INT-767 and OCA showed corresponding effects on quantitative measures (fractional area) of hepatic steatosis (lipid %), inflammation (galectin-3 %), and collagen deposition (Col1a1 %) in *ob/ob*-NASH mice. INT-767 showed consistently greater maximal effects on all three parameters, as compared to OCA (Figure 9, Table 3).

DISCUSSION

Multiple methods were used to rigorously characterize the effects of INT-767 on liver histopathology in a preclinical mouse model of NASH, alone and in comparison, with OCA, and to determine potential mechanisms underlying INT-767 efficacy on NASH pathology.

The NAS system and fibrosis staging (developed by the NASH Clinical Research Network[21]) is a validated morphometric system for monitoring histopathological changes in clinical trials for NASH. In the clinic, the incorporation of a baseline biopsy affords the opportunity to further characterize within-subject changes in these parameters, and therefore also applied to *ob/ob*-NASH mice in the present study. Hepatopathology was evident in *ob/ob*-NASH mice maintained on AMLN diet for 12 wk. Consistent with previous publications using this model[18,19,26], *ob/ob*-NASH mice present with marked steatosis and inflammation, mild-stage ballooning and moderate-marked grades of fibrosis.

In the initial 8-wk dose-response study, INT-767 10 mg/kg reduced fibrosis stage (approximately 1 point) and total NAS (approximately 3 points). There was a high responder rate for improvement of steatosis (8/10 mice), inflammation (10/10 mice), hepatocyte ballooning (6/10 mice) scores, and fibrosis stage (10/10 mice). Eight weeks of treatment with INT-767 3 mg/kg was a subthreshold dose for eliciting changes in liver histology in *ob/ob*-NASH mice, which is consistent with low levels of hepatic and ileal exposure of INT-767 (see below) and minimal transcriptional regulation of FXR target genes. Although 3 mg/kg INT-767 was ineffective when initiated after 12 wk on the diet, some efficacy was noted when this lower dose was initiated after 6 wk on the diet and over a longer duration in *ob/ob*-NASH mice (OCA *vs* INT-767 comparison study). In sum, blinded qualitative histological assessments of NAS and fibrosis confirmed the efficacy of INT-767 in diet-induced and biopsy-confirmed NASH mice.

Although not validated for preclinical use, the human NAS system is largely reproducible in NAFLD mouse models and has been applied in the preclinical assessment of liver histological responses to test compounds[27]. Despite widespread use, inherent limitations of this method are associated with the subjective qualitative scoring technique (*e.g.*, intra- and inter-observer error, mistaking stage scores for measurements), misapplication of statistical analyses (*e.g.*, ANOVAs on non-numerical data), and categorical data tend to provide a relative narrow window for detecting treatment effects[28]. Additionally, qualitative scoring of disease stage largely assesses architectural changes but is not a quantitative measurement of the degree of fibrosis. Given the link between fibrosis progression and long-term outcomes in NASH[29], more detailed and quantitative assessments of fibrosis are warranted.

To gain further insight into INT-767-induced histological improvements in *ob/ob*-NASH mice, morphometric features of fibrosis were measured using SHG/2-PE microscopy[22]. SHG-2PE is a label-free sensitive imaging method for the detection of tissue structural dissymmetry and for imaging and quantitative assessment of collagen fiber specifically with non-centrosymmetric structures like collagen 1 and 3 which

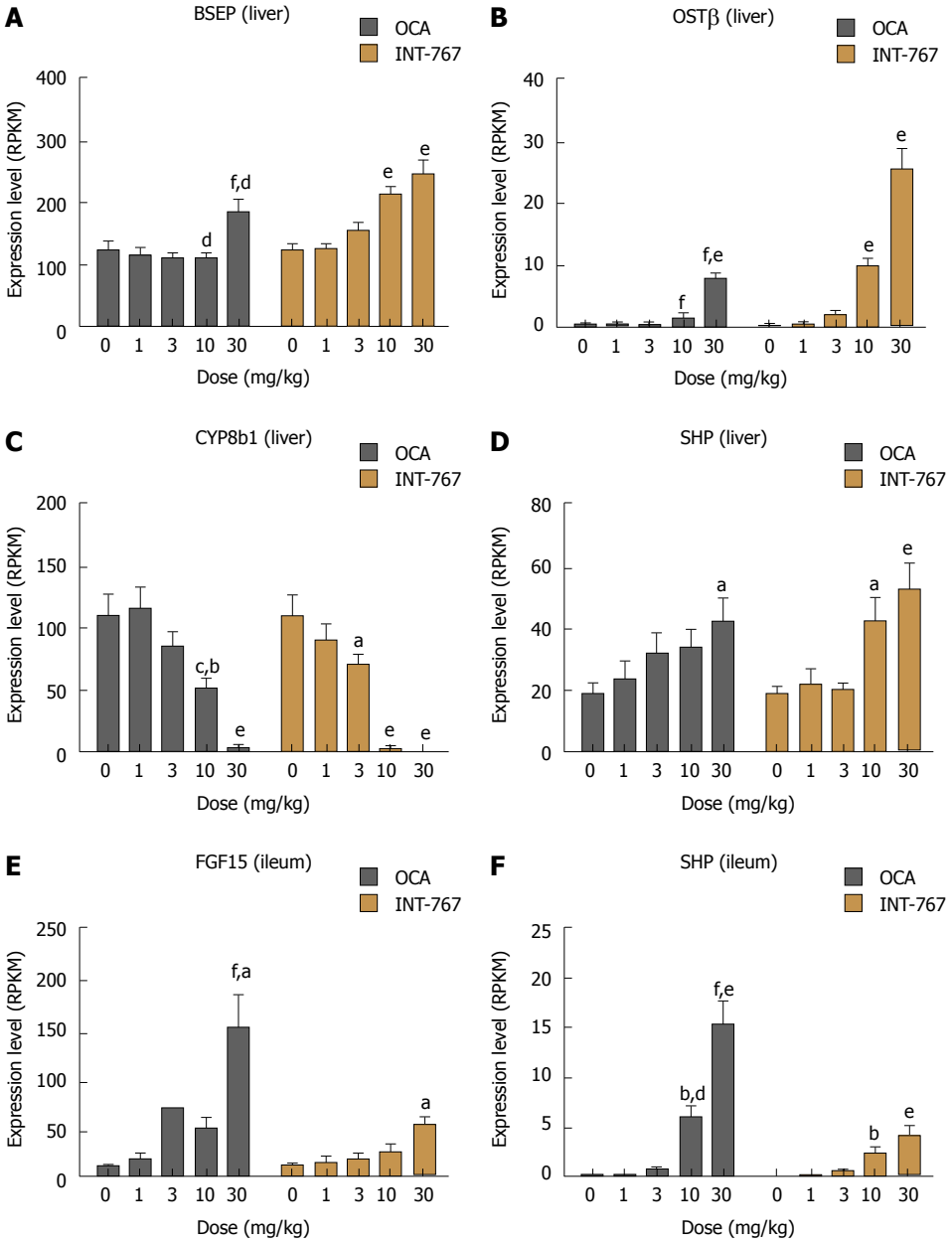

Figure 6 Obeticholic acid (OCA) and INT-767 modulate ileal and hepatic FXR target gene expression to a similar degree after 2 wk of dosing in lean C57Bl/6 mice. A-D: Hepatic expression of BSEP, OST, CYP8b1, and SHP; E and F: Ileal mRNA expression of FGF-15 and SHP. [a]$P < 0.05$, [b]$P < 0.01$, [e]$P < 0.001$ *vs* no treatment (dose = 0); [c]$P < 0.05$, [d]$P < 0.01$, [f]$P < 0.001$ *vs* corresponding INT-767 dose (two-way ANOVA with Bonferroni's *post-hoc* test).

are key contributors for hepatic fibrosis[30]. Accordingly, a significant correlation was observed between quantitative liver collagen levels (expressed as percent collagen area of total parenchymal area) using label free SHG and the collagen 1a1 immunoreactivity. SHG imaging also demonstrated that INT-767 reduced the intensity of the collagen fiber signal (collagen fiber density), but did not affect collagen network complexity (reticulation index).

The present studies also included biochemical assessments, HE staining and label-free SHG/2-PE analyses to determine effects of INT-767 on hepatic lipid parameters. INT-767 dose-dependently reduced hepatic total cholesterol and liver triglyceride levels. In addition to improving steatosis scores, liver lipid fractional area (HE staining) was also markedly reduced by INT-767. Quantitative morphometric analyses by SHG/2-PE imaging confirmed this observation, and revealed that INT-767 significantly reduced vesicular lipid droplet size with a clear shift towards smaller size lipid droplet across the range of possible droplet diameters. These findings are consistent with FXR/TGR5 stimulation of hepatic fatty acid β-oxidation and reduced triglyceride synthesis, and mirror anti-steatotic effects of INT-767 reported within other models of NAFLD[13,16] and are reminiscent of some of the lipid-lowering effects of PPARs. As macrovesicular steatosis positively correlated to the severity of lobular inflammation in NASH patients[31], as well as impaired hepatic microcirculation in experimental NASH[32], the lowering of lipid droplet

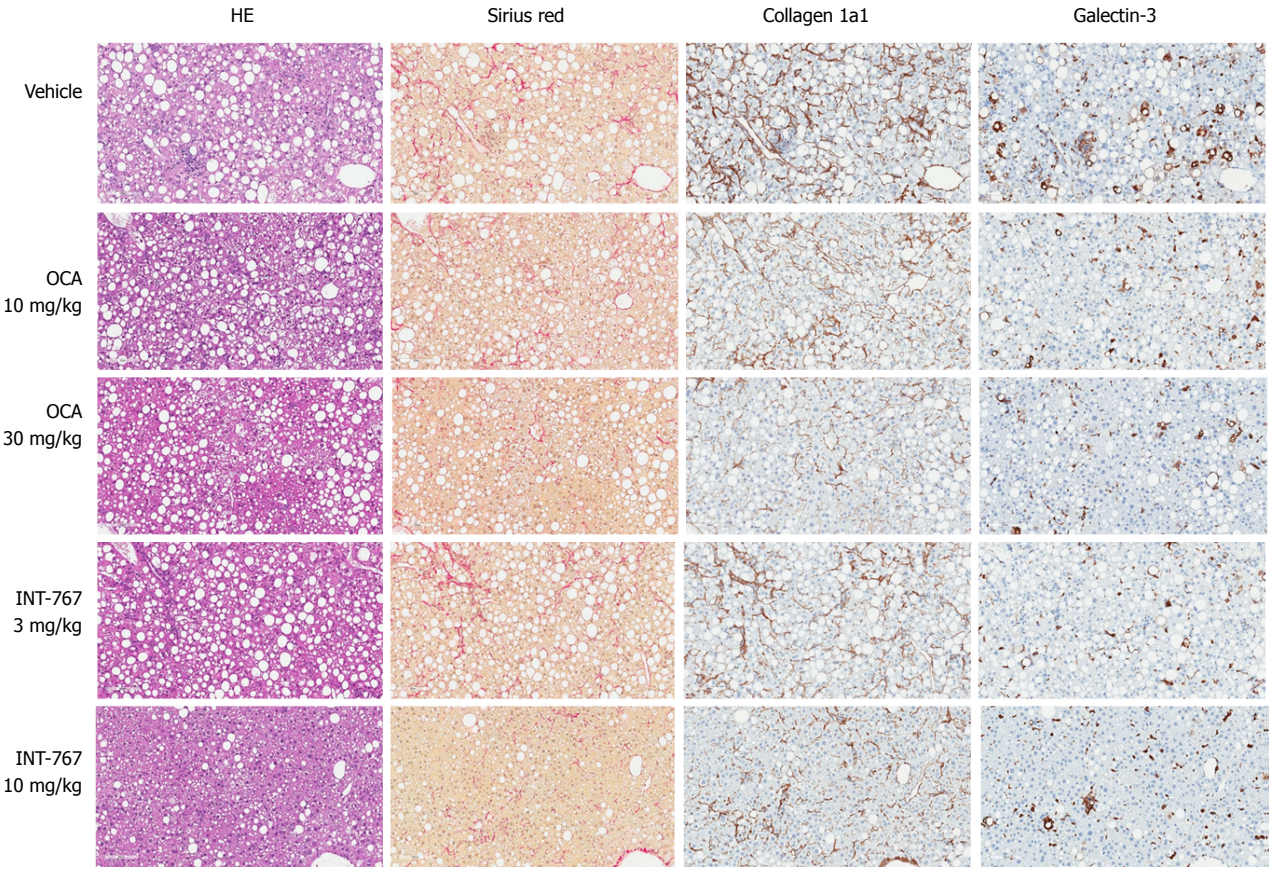

Figure 7 INT-767 and obeticholic acid (OCA) treatment for 16 wk improves liver histopathology in *ob/ob*-NASH mice with biopsy-confirmed liver pathology. Representative hematoxylin-eosin (HE), picro-Sirius red, collagen 1a1 and galectin-3 stainings; NASH: Non-alcoholic steatohepatitis.

area (diameters) by INT-767 is suggestive of improved liver function in *ob/ob*-NASH mice.

The mechanism of action and relative efficacy of INT-767 and OCA was explored. When drawing mechanistic conclusions an important first step is to account for the distribution of each drug within target tissues. INT-767 and OCA are semisynthetic bile acids and exhibits a similar pharmacokinetic profile as endogenous bile acids. These compounds are absorbed from the small intestine, transported into the liver where they undergo biliary excretion and enterohepatic recirculation and are ultimately excreted in the feces. Both compounds were administered to lean mice once daily for two weeks (a duration sufficient to achieve steady-state) and drug levels within the liver and ileum were measured. Both drugs achieved similar levels within similar dose ranges. Likewise, except for the 10 mg/kg dose, levels of INT-767 and OCA were similar within the ileum. Thus, interpretation of differences in hepatic and ileal gene expression within these samples are unlikely to be explained by differences in INT-767 *vs* OCA distribution.

In vivo gene expression studies revealed that relative to OCA, INT-767 regulated hepatic FXR target genes to a greater degree at equivalent doses. These include upregulation of the bile salt efflux transporter *BSEP*, critically involved in the secretion of bile salts into bile, and the organic solute transporter *OSTβ*, which mediates both cellular efflux and uptake of bile acids. Additionally, the cytochrome P450 Family 8 Subfamily B Member 1 (*Cyp8b1*, whose catalytic activity determines solubility of cholesterol in bile by controlling the ratio of cholic acid over CDCA synthesis) was more potently downregulated by INT-767 relative to OCA. These findings are not surprising, given that *in vitro*, INT-767 (EC_{50} approximately 30 nmol/L) is about 300-fold more potent than CDCA and 3-fold more potent than OCA at the FXR receptor[13].

Likewise, for TGR5, INT-767 (EC_{50} approximately 0.63 μmol/L) is about 12-fold more potent than the endogenous TGR5 agonist LCA (EC_{50} approximately 8 μmol/L) and comparable to the selective TGR5 agonist INT-777 (EC_{50} 0.9 μmol/L[13]). Unfortunately, we were unable to demonstrate specific functional or differential activation of TGR5 with INT-767 and OCA; TGR5 hepatic and ileal mRNA target genes are non-specific and future studies should consider examining effects in other TGR5 expressing tissues, such as brown adipose, pancreas or colon, using techniques more appropriate for assessing GPCR activation[5].

Intestinal FXR activation also impacts hepatic signaling events, and liver transcriptome analysis in chow-fed C57Bl6/J mice revealed an important difference between INT-767 and OCA. Fibroblast growth

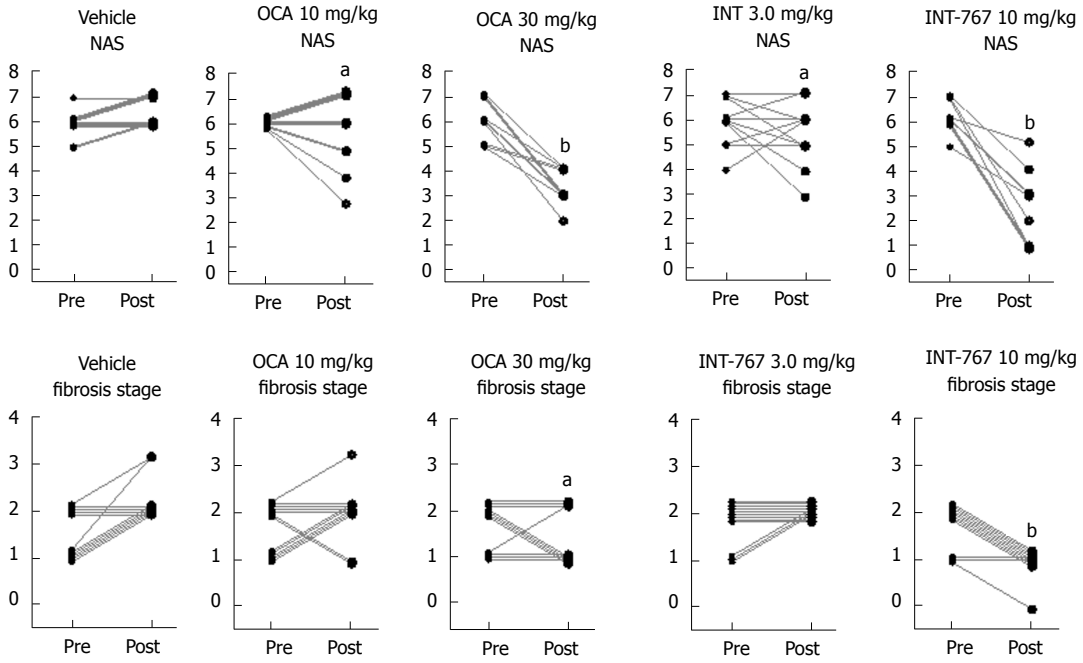

Figure 8 INT-767 and obeticholic acid (OCA) treatment for 16 wk improves liver histopathology in *ob/ob*-NASH mice with biopsy-confirmed liver pathology. Composite NAS and fibrosis stage before and after treatment intervention. [a]$P < 0.05$, [b]$P < 0.001$ (χ^2 test, *vs* vehicle controls), NASH: Non-alcoholic steatohepatitis.

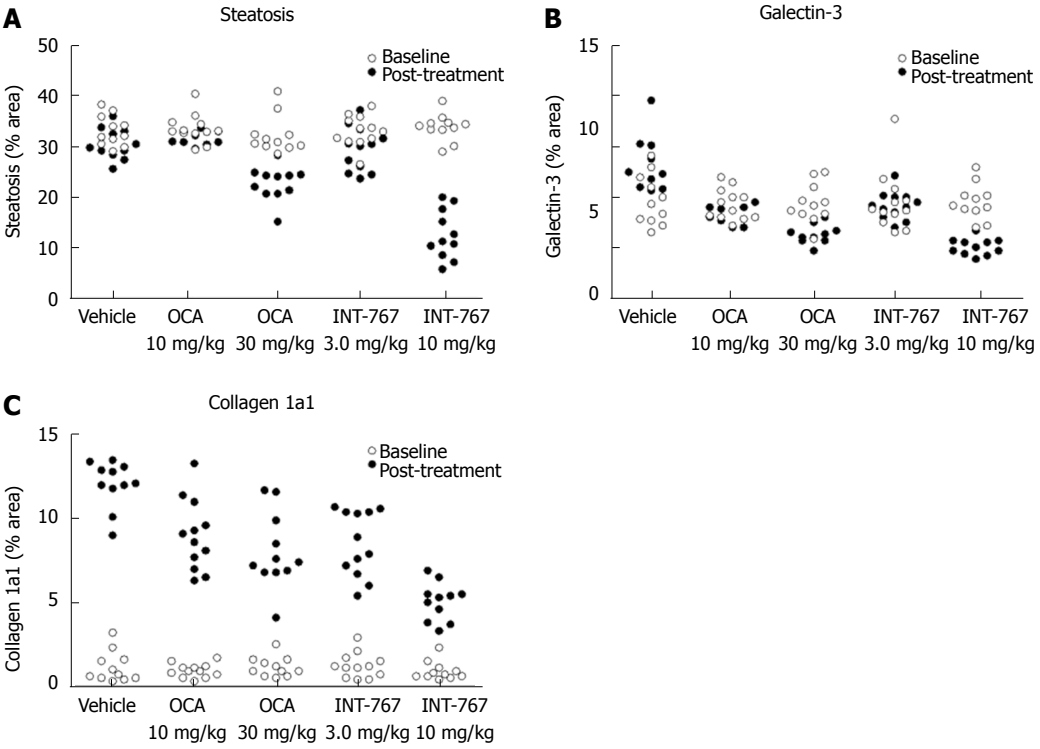

Figure 9 INT-767 or obeticholic acid treatment for 16 wks improves hepatic fat deposition, collagen 1a1 and galectin-3 levels in *ob/ob*-NASH mice with biopsy-confirmed liver pathology. Data are indicated before (baseline) and after treatment intervention. A: Fractional area of fat (HE staining); B: Galectin-3; C: Collagen 1a1. Data are expressed as % of total parenchymal area (subtraction of fat area); NASH: Non-alcoholic steatohepatitis.

factor 15 (FGF-15, equivalent to human FGF-19) is highly expressed the small intestine and upon secretion, circulates to the liver and attenuates bile acid production *via* binding to the β-Klotho receptors located on the surface of hepatocytes and other endothelial cells[33]. It is therefore argued that enhanced gut-liver FGF-15/19 signaling could contribute to anti-NASH effects of bile acid sensing receptors[34,35]. However, the same mice that experienced robust hepatic activation, INT-767 only modestly increased ileal FGF-15 mRNA compared to OCA. These findings suggest that relative to OCA, hepatic FXR signaling may be a greater driver

of INT-767 induced anti-NASH effects. At present, we do not have a mechanistic explanation as to why INT-767 exerts divergent effects on ileal FXR target genes despite being more potent than OCA and demonstrating clear accumulation within the target tissue.

An extended dosing period (16 wk) was employed in *ob/ob*-NASH mice to assess the durability of INT-767-induced anti-NASH efficacy as well as comparing the efficacy of INT-767 and OCA at equipotent doses for FXR activation. After 16 wk of treatment OCA and INT-767 significantly improved all histological parameters relative to vehicle control. In general, the drug treatment effects were dose dependent and the high dose of INT-767 outperformed the high dose of OCA. These findings confirm durable histological benefits of INT-767 with continued drug administration in a preclinical model of NASH and suggest that INT-767 may exert greater efficacy than OCA at both matched and (*in vitro*) potency-adjusted doses.

The therapeutic armamentarium for NAFLD and NASH is limited largely to lifestyle modifications and treatment of concurrent conditions, such as diabetes and obesity, with no currently approved medical treatments for the disease. Based on the nonclinical data presented herein, INT-767 is a more potent FXR receptor agonist, and is expected to have a therapeutic effect at lower doses than OCA. Ongoing clinical studies will allow a more comprehensive assessment of the benefit-risk profile of INT-767 for the treatment of NASH.

ARTICLE HIGHLIGHTS

Research background

Studies within this manuscript detail the efficacy of the dual *in vitro* FXR/TGR5 agonist INT-767 upon multiple histological endpoints in a mouse model of diet-induced non-alcoholic steatohepatitis (NASH). Prior pharmacology studies using INT-767 had not been conducted in models of established and biopsy-confirmed NASH with sufficient fibrosis.

Research motivation

INT-767 is in early clinical development for NASH. These preclinical studies provide proof-of-concept for efficacy in NASH and preclinical superiority relative to obeticholic acid (OCA; an FXR agonist in late stage development for NASH). The present studies also aimed to shed light on the impact of INT-767 on morphometric features of steatosis (droplet size and number) and fibrosis (fiber density) using quantitative histological methods.

Research objectives

The primary objective was to characterize improvements in NASH histopathology using qualitative (*e.g.*, NAS stage scoring for steatosis, inflammation, and ballooning and fibrosis) and quantitative (percent fractional area; %FA) endpoints. The secondary objective was to understand the relative efficacy of INT-767 to and mechanistic differences from OCA. This objective was achieved by comparing drug distribution and gene expression profiles in the liver and ileum.

Research methods

Therapeutic effects in NASH were measured using blinded qualitative (HE stained sections) and quantitative (%FA of IHC-stained sections) methods. The inclusion of a biopsy at both baseline and endpoint is unique and enabled a within-subjects, repeated-measures study design. Most studies do not include a biopsy and rely on endpoint measurements only. Morphometric assessments were also performed using label-free second harmonic generation imaging (for fibrosis) and two-photon emission (for steatosis) which are novel in NASH. The rigor of measuring the same samples using multiple histological techniques also allows the reader to consider how well these methods correlate with one another. mRNA levels of FXR regulated candidate genes were measured using RNA sequencing. LC/MS/MS was used to determine compound levels in liver and ileum.

Research results

In an 8-wk monotherapy study, INT-767 significantly improved qualitative features of NASH as demonstrated by a blinded assessment of NAS and fibrosis stage scores. Quantitatively, INT-767 significantly improved %FA for steatosis, inflammation (assessed by galectin-3 immunohistochemistry; IHC), fibrosis (Col1a1 IHC) and key components of basement membrane formation (laminin IHC). In a 16-wk comparative treatment study, NASH mice treated with INT-767 (3 and 10 mg/kg) exerted greater therapeutic potency and efficacy than OCA (10 and 30 mg/kg). Mechanistically, both OCA and INT-767 accumulate to a similar extent within the liver and ileum. INT-767 drives hepatic, but not ileal, FXR gene expression profiles more strongly than OCA, implying that the liver is a key site of action for INT-767.

Research conclusions

INT-767 improved key histological features of diet-induced and biopsy-confirmed NASH across studies using multiple methods and was shown to be more potent and efficacious than OCA. Novel insights from morphometric analyses include: (1) not only does INT-767 improve fibrosis %FA, but also the intensity of the collagen fiber signal consistent with reducing fiber density; and (2) in addition to reducing steatosis %FA, INT-767 induced a clear shift to reduce vesicular lipid droplet size believed to be more a healthful form of steatosis. Together, these preclinical findings confirm durable histological benefits with INT-767 dosing and suggest that INT-767 may exert greater efficacy than OCA.

Research perspectives

The present studies confirm and extend upon the extant literature validating FXR as a pharmacological target for NASH. Future research should consider (1) the mechanistic contribution of TGR5 to the *in vivo* effects of INT-767, and (2) the necessity and sufficiency of activating hepatic *vs* ileal FXR when targeting NASH, as INT-767 was more efficacious than OCA yet elicited only minimal ileal FXR activation. Finally, other models of diet- or toxin-induced NASH should consider incorporating a baseline biopsy to exclude mice that did not develop the desired phenotype prior to treatment initiation and gain a deeper mechanistic understanding of any pharmacologic intervention. Ongoing research continues to elucidate the role of FXR agonism on features of the basement membrane in NASH.

REFERENCES

1 **Review Team**, LaBrecque DR, Abbas Z, Anania F, Ferenci P, Khan AG, Goh KL, Hamid SS, Isakov V, Lizarzabal M, Peñaranda MM, Ramos JF, Sarin S, Stimac D, Thomson AB, Umar M, Krabshuis J, LeMair A; World Gastroenterology Organisation. World Gastroenterology Organisation global guidelines: Nonalcoholic fatty liver disease and nonalcoholic steatohepatitis. *J Clin Gastroenterol* 2014; **48**: 467-473 [PMID: 24921212]

2 **Farrell GC**, Larter CZ. Nonalcoholic fatty liver disease: from steatosis to cirrhosis. *Hepatology* 2006; **43**: S99-S112 [PMID: 16447287 DOI: 10.1002/hep.20973]

3 **Lefebvre P**, Cariou B, Lien F, Kuipers F, Staels B. Role of bile acids and bile acid receptors in metabolic regulation. *Physiol Rev* 2009; **89**: 147-191 [PMID: 19126757 DOI: 10.1152/physrev.00010.2008]

4 **Maruyama T**, Miyamoto Y, Nakamura T, Tamai Y, Okada H, Sugiyama E, Nakamura T, Itadani H, Tanaka K. Identification of membrane-type receptor for bile acids (M-BAR). *Biochem Biophys Res Commun* 2002; **298**: 714-719 [PMID: 12419312 DOI: 10.1016/S0006-291X(02)02550-0]

5 **Kawamata Y**, Fujii R, Hosoya M, Harada M, Yoshida H, Miwa

M, Fukusumi S, Habata Y, Itoh T, Shintani Y, Hinuma S, Fujisawa Y, Fujino M. A G protein-coupled receptor responsive to bile acids. *J Biol Chem* 2003; **278**: 9435-9440 [PMID: 12524422 DOI: 10.1074/jbc.M209706200]

6 **Li YT**, Swales KE, Thomas GJ, Warner TD, Bishop-Bailey D. Farnesoid x receptor ligands inhibit vascular smooth muscle cell inflammation and migration. *Arterioscler Thromb Vasc Biol* 2007; **27**: 2606-2611 [PMID: 18029909 DOI: 10.1161/ATVBAHA.107.152694]

7 **Wang YD**, Chen WD, Wang M, Yu D, Forman BM, Huang W. Farnesoid X receptor antagonizes nuclear factor kappaB in hepatic inflammatory response. *Hepatology* 2008; **48**: 1632-1643 [PMID: 18972444 DOI: 10.1002/hep.22519]

8 **Gadaleta RM**, Oldenburg B, Willemsen EC, Spit M, Murzilli S, Salvatore L, Klomp LW, Siersema PD, van Erpecum KJ, van Mil SW. Activation of bile salt nuclear receptor FXR is repressed by pro-inflammatory cytokines activating NF-κB signaling in the intestine. *Biochim Biophys Acta* 2011; **1812**: 851-858 [PMID: 21540105 DOI: 10.1016/j.bbadis.2011.04.005]

9 **Gadaleta RM**, van Erpecum KJ, Oldenburg B, Willemsen EC, Renooij W, Murzilli S, Klomp LW, Siersema PD, Schipper ME, Danese S, Penna G, Laverny G, Adorini L, Moschetta A, van Mil SW. Farnesoid X receptor activation inhibits inflammation and preserves the intestinal barrier in inflammatory bowel disease. *Gut* 2011; **60**: 463-472 [PMID: 21242261 DOI: 10.1136/gut.2010.212159]

10 **Mells JE**, Anania FA. The role of gastrointestinal hormones in hepatic lipid metabolism. *Semin Liver Dis* 2013; **33**: 343-357 [PMID: 24222092 DOI: 10.1055/s-0033-1358527]

11 **Keitel V**, Donner M, Winandy S, Kubitz R, Häussinger D. Expression and function of the bile acid receptor TGR5 in Kupffer cells. *Biochem Biophys Res Commun* 2008; **372**: 78-84 [PMID: 18468513 DOI: 10.1016/j.bbrc.2008.04.171]

12 **Baffy G**. Kupffer cells in non-alcoholic fatty liver disease: the emerging view. *J Hepatol* 2009; **51**: 212-223 [PMID: 19447517 DOI: 10.1016/j.jhep.2009.03.008]

13 **Rizzo G,** Passeri D, De Franco F, Ciaccioli G, Donadio L, Orlandi S, et al. Functional Characterization of the Semi-synthetic bile acid derivative INT-767, a dual FXR and TGR5 agonist. *Hepatology* 2010; **52**: 595A-Abstract 66.

14 **Miyazaki-Anzai S**, Masuda M, Levi M, Keenan AL, Miyazaki M. Dual activation of the bile acid nuclear receptor FXR and G-protein-coupled receptor TGR5 protects mice against atherosclerosis. *PLoS One* 2014; **9**: e108270 [PMID: 25237811 DOI: 10.1371/journal.pone.0108270]

15 **Wang X,** Herman-Edelstein M, Levi J, Gafter U, Rosenberg A, Kopp JB, et al. Dual activation of FXR and TGR5 by INT-767 mediates protection from diabetic nephropathy and retinopathy. *Am J Soc Nephrol*. 2015; **26**:169A.

16 **McMahan RH**, Wang XX, Cheng LL, Krisko T, Smith M, El Kasmi K, Pruzanski M, Adorini L, Golden-Mason L, Levi M, Rosen HR. Bile acid receptor activation modulates hepatic monocyte activity and improves nonalcoholic fatty liver disease. *J Biol Chem* 2013; **288**: 11761-11770 [PMID: 23460643 DOI: 10.1074/jbc.M112.446575]

17 **Tetri LH**, Basaranoglu M, Brunt EM, Yerian LM, Neuschwander-Tetri BA. Severe NAFLD with hepatic necroinflammatory changes in mice fed trans fats and a high-fructose corn syrup equivalent. *Am J Physiol Gastrointest Liver Physiol* 2008; **295**: G987-G995 [PMID: 18772365 DOI: 10.1152/ajpgi.90272.2008]

18 **Clapper JR**, Hendricks MD, Gu G, Wittmer C, Dolman CS, Herich J, Athanacio J, Villescaz C, Ghosh SS, Heilig JS, Lowe C, Roth JD. Diet-induced mouse model of fatty liver disease and nonalcoholic steatohepatitis reflecting clinical disease progression and methods of assessment. *Am J Physiol Gastrointest Liver Physiol* 2013; **305**: G483-G495 [PMID: 23886860 DOI: 10.1152/ajpgi.00079.2013]

19 **Kristiansen MN**, Veidal SS, Rigbolt KT, Tølbøl KS, Roth JD, Jelsing J, Vrang N, Feigh M. Obese diet-induced mouse models of nonalcoholic steatohepatitis-tracking disease by liver biopsy. *World J Hepatol* 2016; **8**: 673-684 [PMID: 27326314 DOI: 10.4254/wjh.v8.i16.673]

20 **Jouihan H**, Will S, Guionaud S, Boland ML, Oldham S, Ravn P, Celeste A, Trevaskis JL. Superior reductions in hepatic steatosis and fibrosis with co-administration of a glucagon-like peptide-1 receptor agonist and obeticholic acid in mice. *Mol Metab* 2017; **6**: 1360-1370 [PMID: 29107284 DOI: 10.1016/j.molmet.2017.09.001]

21 **Kleiner DE**, Brunt EM, Van Natta M, Behling C, Contos MJ, Cummings OW, Ferrell LD, Liu YC, Torbenson MS, Unalp-Arida A, Yeh M, McCullough AJ, Sanyal AJ; Nonalcoholic Steatohepatitis Clinical Research Network. Design and validation of a histological scoring system for nonalcoholic fatty liver disease. *Hepatology* 2005; **41**: 1313-1321 [PMID: 15915461 DOI: 10.1002/hep.20701]

22 **Liu F**, Chen L, Rao HY, Teng X, Ren YY, Lu YQ, Zhang W, Wu N, Liu FF, Wei L. Automated evaluation of liver fibrosis in thioacetamide, carbon tetrachloride, and bile duct ligation rodent models using second-harmonic generation/two-photon excited fluorescence microscopy. *Lab Invest* 2017; **97**: 84-92 [PMID: 27918557 DOI: 10.1038/labinvest.2016.128]

23 **Dobin A**, Davis CA, Schlesinger F, Drenkow J, Zaleski C, Jha S, Batut P, Chaisson M, Gingeras TR. STAR: ultrafast universal RNA-seq aligner. *Bioinformatics* 2013; **29**: 15-21 [PMID: 23104886 DOI: 10.1093/bioinformatics/bts635]

24 **Love MI**, Huber W, Anders S. Moderated estimation of fold change and dispersion for RNA-seq data with DESeq2. *Genome Biol* 2014; **15**: 550 [PMID: 25516281 DOI: 10.1186/s13059-014-0550-8]

25 **Langhi C**, Baldán Á. CIDEC/FSP27 is regulated by peroxisome proliferator-activated receptor alpha and plays a critical role in fasting- and diet-induced hepatosteatosis. *Hepatology* 2015; **61**: 1227-1238 [PMID: 25418138 DOI: 10.1002/hep.27607]

26 **Trevaskis JL**, Griffin PS, Wittmer C, Neuschwander-Tetri BA, Brunt EM, Dolman CS, Erickson MR, Napora J, Parkes DG, Roth JD. Glucagon-like peptide-1 receptor agonism improves metabolic, biochemical, and histopathological indices of nonalcoholic steatohepatitis in mice. *Am J Physiol Gastrointest Liver Physiol* 2012; **302**: G762-G772 [PMID: 22268099 DOI: 10.1152/ajpgi.00476.2011]

27 **Liang W**, Lindeman JH, Menke AL, Koonen DP, Morrison M, Havekes LM, van den Hoek AM, Kleemann R. Metabolically induced liver inflammation leads to NASH and differs from LPS- or IL-1β-induced chronic inflammation. *Lab Invest* 2014; **94**: 491-502 [PMID: 24566933 DOI: 10.1038/labinvest.2014.11]

28 **Standish RA**, Cholongitas E, Dhillon A, Burroughs AK, Dhillon AP. An appraisal of the histopathological assessment of liver fibrosis. *Gut* 2006; **55**: 569-578 [PMID: 16531536 DOI: 10.1136/gut.2005.084475]

29 **Angulo P**, Kleiner DE, Dam-Larsen S, Adams LA, Bjornsson ES, Charatcharoenwitthaya P, Mills PR, Keach JC, Lafferty HD, Stahler A, Haflidadottir S, Bendtsen F. Liver Fibrosis, but No Other Histologic Features, Is Associated With Long-term Outcomes of Patients With Nonalcoholic Fatty Liver Disease. *Gastroenterology* 2015; **149**: 389-397.e10 [PMID: 25935633 DOI: 10.1053/j.gastro.2015.04.043]

30 **Leeming DJ**, Byrjalsen I, Jiménez W, Christiansen C, Karsdal MA. Protein fingerprinting of the extracellular matrix remodelling in a rat model of liver fibrosis--a serological evaluation. *Liver Int* 2013; **33**: 439-447 [PMID: 23279004 DOI: 10.1111/liv.12044]

31 **Chalasani N**, Wilson L, Kleiner DE, Cummings OW, Brunt EM, Unalp A; NASH Clinical Research Network. Relationship of steatosis grade and zonal location to histological features of steatohepatitis in adult patients with non-alcoholic fatty liver disease. *J Hepatol* 2008; **48**: 829-834 [PMID: 18321606 DOI: 10.1016/j.jhep.2008.01.016]

32 **Rosenstengel S**, Stoeppeler S, Bahde R, Spiegel HU, Palmes D. Type of steatosis influences microcirculation and fibrogenesis in different rat strains. *J Invest Surg* 2011; **24**: 273-282 [PMID:

22047200 DOI: 10.3109/08941939.2011.586094]
33 **Xie MH**, Holcomb I, Deuel B, Dowd P, Huang A, Vagts A, Foster J, Liang J, Brush J, Gu Q, Hillan K, Goddard A, Gurney AL. FGF-19, a novel fibroblast growth factor with unique specificity for FGFR4. *Cytokine* 1999; **11**: 729-735 [PMID: 10525310 DOI: 10.1006/cyto.1999.0485]
34 **Shin DJ**, Osborne TF. FGF15/FGFR4 integrates growth factor signaling with hepatic bile acid metabolism and insulin action. *J Biol Chem* 2009; **284**: 11110-11120 [PMID: 19237543 DOI: 10.1074/jbc.M808747200]
35 **Fu T**, Kim YC, Byun S, Kim DH, Seok S, Suino-Powell K, Xu HE, Kemper B, Kemper JK. FXR Primes the Liver for Intestinal FGF15 Signaling by Transient Induction of β-Klotho. *Mol Endocrinol* 2016; **30**: 92-103 [PMID: 26505219 DOI: 10.1210/me.2015-1226]

P- Reviewer: Murotomi K, Villela-Nogueira CA **S- Editor**: Chen K
L- Editor: A **E- Editor**: Ma YJ

World Journal of Gastroenterology

Submit a Manuscript: http://www.f6publishing.com

World J Gastroenterol 2018 January 14; 24(2): 211-215

DOI: 10.3748/wjg.v24.i2.211

ISSN 1007-9327 (print) ISSN 2219-2840 (online)

ORIGINAL ARTICLE

Basic Study

Novel concept of endoscopic device delivery station system for rapid and tight attachment of polyglycolic acid sheet

Hirohito Mori, Hideki Kobara, Noriko Nishiyama, Tsutomu Masaki

Hirohito Mori, Hideki Kobara, Noriko Nishiyama, Tsutomu Masaki, Departments of Gastroenterology and Neurology, Kagawa University, Kagawa 761-0793, Japan

ORCID number: Hirohito Mori (0000-0002-1691-2085); Hideki Kobara (0000-0002-8508-827X); Noriko Nishiyama (000-0003-3707-9317); Tsutomu Masaki (0000-0002-8425-0685).

Author contributions: Mori H was responsible for devising the research and writing the manuscript; Kobara H and Nishiyama N participated equally in the work; Masaki T provided a critical revision of the manuscript for intellectual content and was responsible for final approval of the manuscript.

Supported by The Translational Research Program and the Strategic Promotion for Practical Applications of Innovative Medical Technology (TR-SPRINT) from the Japan Agency for Medical Research and Development (AMED).

Institutional review board statement: This Animal experiment was approved by Animal Laboratory Regulations of Kagawa University according to the Regulations and Guidelines of animal experiment of Kagawa University. [See the supplement PDF file of Institutional Review Board Approval Form (Approval No: A34) of Kagawa University.]

Conflict-of-interest statement: All authors declare that they have no conflicts of interest, and no corporate financing was received.

Institutional animal care and use committee statement: Animal experiments were performed based on Preclinical Animal Laboratory of Kagawa University according to the guidelines of animals by Kagawa University.

Data sharing statement: Technical procedures and dataset are available from the corresponding author at [hiro4884@med.kagawa-u.ac.jp].

Manuscript source: Unsolicited manuscript

Correspondence to: Hirohito Mori, MD, PhD, Associate Professor, Department of Gastroenterology and Neurology, Kagawa University School of Medicine, 1750-1 Ikenobe, Miki, Kita, Kagawa 761-0793, Japan. hiro4884@med.kagawa-u.ac.jp
Telephone: +81-87-891-2156
Fax: +81-87-891-2158

Received: November 6, 2017
Peer-review started: November 7, 2017
First decision: November 14, 2017
Revised: November 27, 2017
Accepted: December 5, 2017
Article in press: December 5, 2017
Published online: January 14, 2018

Abstract

AIM

To evaluate appropriate and rapid polyglycolic acid sheet (PGAs) covering time using device delivery station system (DDSS).

METHODS

This pilot basic study was conducted to evaluate the potential of accurate and rapid PGAs delivery using DDSS. Three 11-month-old female Beagle dogs were used in this study. Two endoscopic submucosal dissections (ESDs) 4cm in diameter were performed in lesser curvature of middle gastric body and greater curvature of antrum (total 6 ESDs performed). DDSS (3 cm length, 12 mm in outer diameter) has 2 chambers which 16 cm^2 large 2 PGAs were stored, and DDSS was attached post ESD ulcers, respectively. Beriplast P® (CSL Behring K.K., Tokyo, Japan) (combination of fibrin

glue and thrombin) was applied equally to the artificial ulcer, and tight attachment of 2 PGAs with DDSS were completed. The evaluation items were covering times, post ESD bleeding and perforation during ESD.

RESULTS

The covering time of PGAs (defined as the duration from the beginning of endoscope insertion into the mouth to the end of the fibrin glue coating process) was 6.07 (4.86-8.29) min. There was no post-ESD bleeding (1-7 d after ESD), and there was no perforation during ESD.

CONCLUSION

DDSS was very useful for rapid delivering and tight attachment of PGAs, and has potentials of multi-purpose delivery station system.

Key words: Post-endoscopic submucosal dissection ulcers; Bleeding; Polyglycolic acid sheet; Rapidly delivery; Tightly attachment

Core tip: Although mechanical closures of larger artificial ulcer floor are effective to prevent post-endoscopic submucosal dissection (ESD) bleeding, mechanical closures might create a mucosal bridge which reduces the efficacy of prevention of post-ESD bleeding. Although covering with polyglycolic acid sheet (PGAs) is a more ideal treatment, it is difficult to deliver thin PGAs by pan-endoscope. Therefore, novel concept to deliver various devices and materials were developed.

Mori H, Kobara H, Nishiyama N, Masaki T. Novel concept of endoscopic device delivery station system for rapid and tight attachment of polyglycolic acid sheet. *World J Gastroenterol* 2018; 24(2): 211-215 Available from: URL: http://www.wjgnet.com/1007-9327/full/v24/i2/211.htm DOI: http://dx.doi.org/10.3748/wjg.v24.i2.211

INTRODUCTION

There were several reports of treatments for large artificial post-endoscopic submucosal dissection (ESD) ulcers, such as natural ulcer healing, ulcer closure using an Over-The-Scope Clip system (Ovesco Endoscopy GmbH, Tüebingen, Germany)[1] and covering an ulcer with a polyglycolic acid sheet (PGAs) (Gunze Co., Kyoto, Japan). PGAs has been used to prevent post-ESD bleeding[2]. Although mechanical closures of larger artificial ulcer floor are somewhat effective to prevent post-ESD bleeding, mechanical closures might create a mucosal bridge which reduces the efficacy of prevention of post-ESD bleeding. Therefore, covering with PGAs is a more ideal treatment. However, as it is difficult to deliver thin PGAs by pan-endoscope, PGAs delivery is one of the main problems of treating post-ESD ulcers[3,4].

Since the delivery method of such a thin membrane like PGAs into the stomach without getting wet with water has not been reported yet, the efficacy of PGAs covering perforation of gastric ulcer by sealed 2 balloon method [endoscopic injection sclerotherapy (EIS) balloon, TOP co., Tokyo, Japan] (11 mm in diameter, 50 mm length) was already reported as new method[5]. Based on the 2 EIS balloon method, we developed the new concept to deliver various endoscopic devices and materials named device delivery station system (DDSS).

This animal study assessed usefulness and future perspectives of the DDSS.

MATERIALS AND METHODS

Three 11-month-old female Beagle dogs were used in this study. This pilot basic study was conducted to evaluate the potential of accurate and rapid PGAs delivery using DDSS. This Animal experiment was approved by Animal Laboratory Regulations of Kagawa University according to the Regulations and Guidelines of animals experiment of Kagawa University. [See the supplement PDF file of Institutional Review Board Approval Form (Approval No: A34) of Kagawa University.] Two endoscopic submucosal dissections (ESDs) 4cm in diameter were performed in lesser curvature of middle gastric body and greater curvature of antrum (total 6 ESDs performed). The evaluation items were covering times, post ESD bleeding and perforation during ESD. DDSS (3 cm length, 12 mm in outer diameter) has 2 chambers which 16 cm^2 large 2 PGAs were stored (Figure 1), and DDSS was easily mounted (Figure 2) and detached by pulling the thread connected with lock-pin (Figure 3) (Video). After endoscope mounting DDSS was inserted into dog's stomach, DDSS was detached by pulling out the lock-pin with grasping forceps which was retrieved through endoscopic channel. Two PGAs were pulled out from each 2 chambers (Figure 4) and attached post ESD ulcers, respectively (Figure 5). Beriplast P® (CSL Behring K.K., Tokyo, Japan) (combination of fibrin glue and thrombin) was applied equally to the artificial ulcer, and tight attachment of 2 PGAs with DDSS were completed. In this study, 0.5 mL Indigo Carmine was mixed with transparent Beriplast P® for visualization of uniformly spraying onto ulcer floor (Figure 6) (Video).

Devices

Endoscopes: GIF TYPE Q260J (Olympus Co., Tokyo, Japan). Incisional knife: Dual knife® (KD-650 L), IT knife 2® (KD-611L) (Olympus Co., Tokyo, Japan). Incisional generator device: ERBE VIO300D (Elektromedizin, Tübingen, Germany). CO2 insufflation

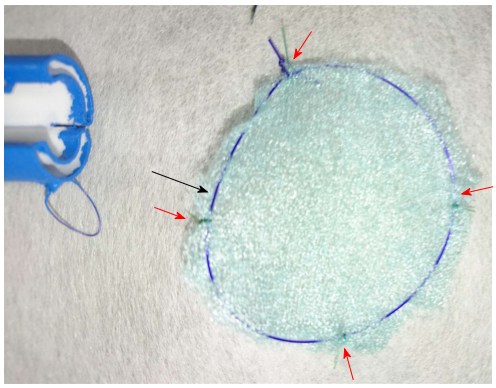

Figure 1 Preparation of polyglycolic acid sheets. Polyglycolic acid sheets (PGAs) was able to be expanded by ring-shaped 1-0 polydioxanone (PDS) which have strong expansive force (black arrow). Ring-shaped 1-0 PDS was fixed with 4-0 PDS at 4 point to prevent PGAs from slipping out of place (red arrows).

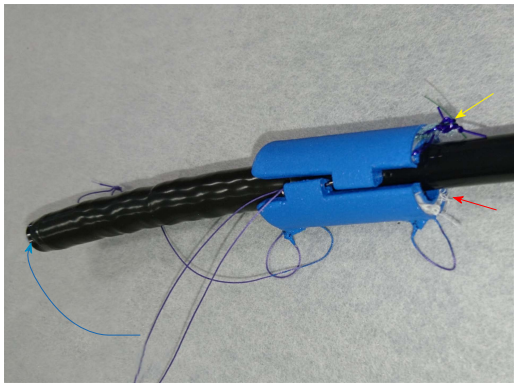

Figure 2 Mount device delivery station system on pan endoscope. Device delivery station system (DDSS) was mounted on pan endoscope with 2 chambers in which 16 cm^2 large polyglycolic acid sheets (yellow arrow) and gauze (red arrow) were stored. It is possible for DDSS to store various kinds of surgical materials in its several chambers. It is very easy to open and detach DDSS by pulling the thread connected with tiny pin by grasping forceps through endoscopic channel (blue curved arrow).

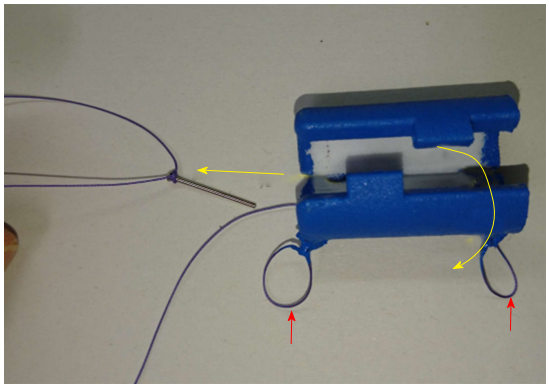

Figure 3 Detachable of device delivery station system. Device delivery station system (DDSS) is able to be opened and detached (yellow curved arrow) by pulling the thread connected with tiny pin (yellow arrow). Two ring-shaped threads are used to fix DDSS on the gastric wall (2 red arrows).

device: OLYMPUS UCR (Olympus Co., Tokyo, Japan). PGAs (Gunze Co., Kyoto, Japan).

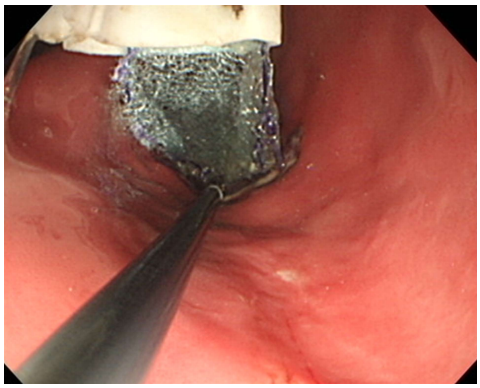

Figure 4 Delivery of dry polyglycolic acid sheet from device delivery station system. Polyglycolic acid sheets was delivered and pulled out from device delivery station system chamber without getting wet with water.

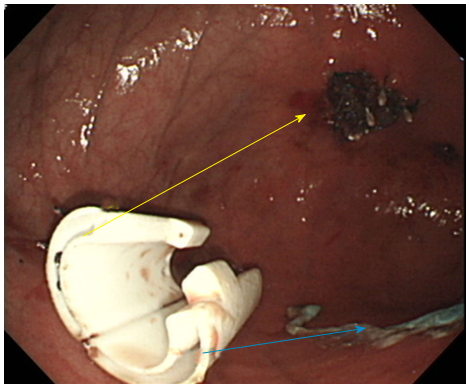

Figure 5 Simultaneous deliveries of two polyglycolic acid sheet to two post-endoscopic submucosal dissections artificial ulcers. Two polyglycolic acid sheets were pulled out from each 2 chambers and attached 2 post ulcers, respectively (yellow and blue arrows).

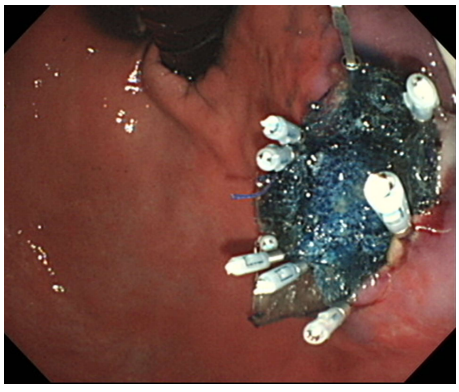

Figure 6 Mixture of Indigo Carmine and Beriplast P® for visualization. 0.5 mL Indigo Carmine mixed with transparent Beriplast P® for visualization of uniformly spraying onto ulcer floor made it possible to make tight attachment of polyglycolic acid sheets.

RESULTS

The covering time of PGAs (defined as the duration from the beginning of endoscope insertion into the mouth to the end of the fibrin glue coating process)

was 6.07 (4.86-8.29) min. There was no post-ESD bleeding (1-7 d after ESD), and there was no perforation during ESD. DDSS was the most effective way to deliver PGAs to post-ESD ulcer floor accurately and rapidly. There was no adverse event or complications at all during delivery of PGAs by DDSS.

DISCUSSION

PGAs are widely used in bio-absorbable sutures in the surgical field. In healing process, PGAs have anti-inflammatory effects with rich granulation tissue. PGAs also have the migration effects of epidermal cells. Early anti-inflammatory effects and rich granulation tissue contribute to protecting the ulcer floor[6].

Protection mechanism of PGAs seem to be same that of steroid local injection to prevent stenosis[7,8]. The tight attachment of PGAs to post-ESD ulcer is necessary to obtain a sufficient hemostatic effect. Therefore, DDSS was very useful for rapidly delivery and tightly attachment of PGAs onto post ESD artificial ulcer. Tight attachment of PGAs by DDSS might enable us to decrease post-ESD bleeding[9,10]. Post-ESD bleeding is one of serious adverse events for patients who take antiplatelet and/or anti coagulation agents. There were some reports that post bleeding events occurred within 7- 14 d after ESD. PGAs could prevent the post-ESD bleeding among patients using antithrombotic agents[11], and contribute to reduce the medical cost. In addition, there was no adverse event or complications at all during delivery of PGAs by DDSS.

Moreover, DDSS might be able to deliver much more devices and materials such as gauze, hemoclips and so on. DDSS has potential to considerably change the endoscopic treatment. However, prospective randomized control study is needed to confirm the advantages of DDSS and potential adverse events.

ARTICLE HIGHLIGHTS

Research background

Post-Endoscopic submucosal dissections (ESD) bleeding is one of crucial adverse events for patients who take anti-thrombotic agents.

Research motivation

Although there were several reports with regard to polyglycolic acid sheet (PGAs) to prevent post-ESD bleeding, it is difficult to deliver and cover the post-ESD ulcer floor with PGAs. Developing new measurement or device to deliver PGAs is necessary to perform safer ESD.

Research objectives

To evaluate the efficacy of appropriate and rapid PGAs delivery method using innovative device delivery station system (DDSS).

Research methods

Beagle dogs were used in this pilot basic study. Two ESDs 4 cm in diameter were performed (total 6 ESDs performed). Covering times of PGAs only by pan-endoscope, post ESD bleedings and perforations during ESD were investigated.

Research results

DDSS made it possible to cover post-ESD ulcer rapidly and reduce the post-ESD adverse event (bleeding of 1-7 d after ESD).

Research conclusions

DDSS was very useful for rapid delivering and tight attachment of PGAs to control post-ESD bleeding. DDSS can deliver lots of endoscopic devices and surgical materials that can be placed within the digestive tract under sealed conditions.

Research perspectives

DDSS has innovative potentials of multi-purpose device delivery measurements. Multi-center prospective studies are needed to confirm the advantages of DDSS not only for PGAs delivery but also other endoscopic devices and materials.

REFERENCES

1 **Maekawa S**, Nomura R, Murase T, Ann Y, Harada M. Complete closure of artificial gastric ulcer after endoscopic submucosal dissection by combined use of a single over-the-scope clip and through-the-scope clips (with videos). *Surg Endosc* 2015; **29**: 500-504 [PMID: 25052125 DOI: 10.1007/s00464-014-3725-1]

2 **Takimoto K**, Imai Y, Matsuyama K. Endoscopic tissue shielding method with polyglycolic acid sheets and fibrin glue to prevent delayed perforation after duodenal endoscopic submucosal dissection. *Dig Endosc* 2014; **26** Suppl 2: 46-49 [PMID: 24750148 DOI: 10.1111/den.12280]

3 **Ono H**, Takizawa K, Kakushima N, Tanaka M, Kawata N. Application of polyglycolic acid sheets for delayed perforation after endoscopic submucosal dissection of early gastric cancer. *Endoscopy* 2015; **47** Suppl 1 UCTN: E18-E19 [PMID: 25603508 DOI: 10.1055/s-0034-1390730]

4 **Tsuji Y**, Ohata K, Gunji T, Shozushima M, Hamanaka J, Ohno A, Ito T, Yamamichi N, Fujishiro M, Matsuhashi N, Koike K. Endoscopic tissue shielding method with polyglycolic acid sheets and fibrin glue to cover wounds after colorectal endoscopic submucosal dissection (with video). *Gastrointest Endosc* 2014; **79:** 151-155 [PMID: 24140128 DOI: 10.1016/j.gie.2013.08.041]

5 **Mori H**, Kobara H, Rahman A, Nishiyama N, Nishiyama A, Suzuki Y, Masaki T. Innovative delivery method using a detachable device to deliver a large polyglycolic acid sheet to a gastric ulcer perforation. *Endoscopy* 2017; **49**: E165-E167 [PMID: 28525931 DOI: 10.1055/s-0043-105573]

6 **Iizuka T**, Kikuchi D, Yamada A, Hoteya S, Kajiyama Y, Kaise M. Polyglycolic acid sheet application to prevent esophageal stricture after endoscopic submucosal dissection for esophageal squamous cell carcinoma. *Endoscopy* 2015; **47**: 341-344 [PMID: 25412087 DOI: 10.1055/s-0034-1390770]

7 **Hashimoto S**, Kobayashi M, Takeuchi M, Sato Y, Narisawa R, Aoyagi Y. The efficacy of endoscopic triamcinolone injection for the prevention of esophageal stricture after endoscopic submucosal dissection. *Gastrointest Endosc* 2011; **74**: 1389-1393 [PMID: 22136782 DOI: 10.1016/j.gie.2011.07.070]

8 **Hanaoka N**, Ishihara R, Takeuchi Y, Uedo N, Higashino K, Ohta T, Kanzaki H, Hanafusa M, Nagai K, Matsui F, Iishi H, Tatsuta M, Ito Y. Intralesional steroid injection to prevent stricture after endoscopic submucosal dissection for esophageal cancer: a controlled prospective study. *Endoscopy* 2012; **44**: 1007-1011 [PMID: 22930171 DOI: 10.1055/s-0032-1310107]

9 **Matsumura T**, Arai M, Maruoka D, Okimoto K, Minemura S, Ishigami H, Saito K, Nakagawa T, Katsuno T, Yokosuka O. Risk factors for early and delayed post-operative bleeding after endoscopic submucosal dissection of gastric neoplasms, including patients with continued use of antithrombotic agents. *BMC Gastroenterol* 2014; **14**:

172 [PMID: 25280756 DOI: 10.1186/1471-230X-14-172]
10 **Shindo Y**, Matsumoto S, Miyatani H, Yoshida Y, Mashima H. Risk factors for postoperative bleeding after gastric endoscopic submucosal dissection in patients under antithrombotics. *World J Gastrointest Endosc* 2016; **8**: 349-356 [PMID: 27076874 DOI: 10.4253/wjge.v8.i7.349]
11 **Fukuda H**, Yasmaguchi N, Isomoto H, Matsushima K, Minami H, Akazawa Y, Ohnita K, Takeshima F, Shikuwa S, Nakao K. Polyglycolic Acid Felt Sealing Method for Prevention of Bleeding Related to Endoscopic Submucosal Dissection in Patients Taking Antithrombotic Agents. *Gastroenterol Res Pract* 2016; **2016**: 1457357 [PMID: 27022390 DOI: 10.1155/2016/1457357]

P- Reviewer: Dogan UB, Dinc T, Shrestha BM **S- Editor**: Chen K
L- Editor: A **E- Editor**: Ma YJ

World Journal of Gastroenterology

Submit a Manuscript: http://www.f6publishing.com

World J Gastroenterol 2018 January 14; 24(2): 216-225

DOI: 10.3748/wjg.v24.i2.216

ISSN 1007-9327 (print) ISSN 2219-2840 (online)

ORIGINAL ARTICLE

Basic Study

β-arrestin 2 attenuates lipopolysaccharide-induced liver injury *via* inhibition of TLR4/NF-κB signaling pathway-mediated inflammation in mice

Meng-Ping Jiang, Chun Xu, Yun-Wei Guo, Qian-Jiang Luo, Lin Li, Hui-Ling Liu, Jie Jiang, Hui-Xin Chen, Xiu-Qing Wei

Meng-Ping Jiang, Chun Xu, Yun-Wei Guo, Qian-Jiang Luo, Lin Li, Hui-Ling Liu, Jie Jiang, Xiu-Qing Wei, Department of Digestive Diseases, The Third Affiliated Hospital of Sun Yat-sen University, Guangzhou 510630, Guangdong Province, China

Chun Xu, Hui-Xin Chen, Department of Digestive Diseases, Huizhou Municipal Center Hospital, Huizhou 516002, Guangdong Province, China

ORCID number: Meng-Ping Jiang (0000-0003-0726-1601); Chun Xu (0000-0002-3517-8963); Yun-Wei Guo (0000-0003-1008-3228); Qian-Jiang Luo (0000-0002-1660-3864); Lin Li (0000-0002-7765-0883); Hui-Ling Liu (0000-0002-8677-1265); Jie Jiang (000-0001-9892-0507); Hui-Xin Chen (0000-0001-7655-1341); Xiu-Qing Wei (0000-0002-4614-1787)

Author contributions: Jiang MP, Xu C and Guo YW contributed equally to this work and performed most of the experiments; Luo QJ, Li L, Liu HL and Jiang J bred the animals and collected the animal material; Chen HX analyzed the data; and Wei XQ designed the study and wrote the paper.

Supported by the National Natural Science Foundation of China, No. 81470848; and the Breeding Foundation for Young Pioneers' Research of Sun Yat-sen University, No. 14ykpy27.

Institutional review board statement: The study was reviewed and approved by the Institutional Review Board of the Third Affiliated Hospital of Sun Yat-sen University.

Institutional animal care and use committee statement: All procedures were conducted in accordance with The Guide for the Care and Use of Laboratory Animals and were approved by the Institutional Animal Care and Use Committee of The Third Affiliated Hospital of Sun Yat-sen University.

Conflict-of-interest statement: The authors declare that there is no conflict of interest regarding the publication of this paper.

Data sharing statement: No additional data are available.

Manuscript source: Unsolicited manuscript

Correspondence to: Xiu-Qing Wei, MD, PhD, Department of Digestive Diseases, The Third Affiliated Hospital of Sun Yat-Sen University, No. 600, Tianhe Road, Tianhe District, Guangzhou 510630, Guangdong Province, China. weixq@mail.sysu.edu.cn
Telephone: +86-20-85252056
Fax: +86-20-85253336

Received: September 11, 2017
Peer-review started: September 12, 2017
First decision: October 18, 2017
Revised: November 3, 2017
Accepted: November 22, 2017
Article in press: November 22, 2017
Published online: January 14, 2018

Abstract

AIM

To study the role and the possible mechanism of β-arrestin 2 in lipopolysaccharide (LPS)-induced liver injury *in vivo* and *in vitro*.

METHODS

Male β-arrestin $2^{+/+}$ and β-arrestin $2^{-/-}$ C57BL/6J mice were used for *in vivo* experiments, and the mouse macrophage cell line RAW264.7 was used for *in vitro* experiments. The animal model was established *via* intraperitoneal injection of LPS or physiological sodium chloride solution. Blood samples and liver tissues were collected to analyze liver injury and levels of pro-

inflammatory cytokines. Cultured cell extracts were collected to analyze the production of pro-inflammatory cytokines and expression of key molecules involved in the TLR4/NF-κB signaling pathway.

RESULTS

Compared with wild-type mice, the β-arrestin 2 knockout mice displayed more severe LPS-induced liver injury and significantly higher levels of pro-inflammatory cytokines, including interleukin (IL)-1β, IL-6, tumor necrosis factor (TNF)-α, and IL-10. Compared with the control group, pro-inflammatory cytokines (including IL-1β, IL-6, TNF-α, and IL-10) produced by RAW264.7 cells in the β-arrestin 2 siRNA group were significantly increased at 6 h after treatment with LPS. Further, key molecules involved in the TLR4/NF-κB signaling pathway, including phospho-IκBα and phosho-p65, were upregulated.

CONCLUSION

β-arrestin 2 can protect liver tissue from LPS-induced injury *via* inhibition of TLR4/NF-κB signaling pathway-mediated inflammation.

Key words: Lipopolysaccharide; Liver injury; β-arrestin 2; TLR4/NF-κB signaling pathway; Pro-inflammatory cytokines

Core tip: The role and mechanism of β-arrestin 2 in lipopolysaccharide (LPS)-induced liver injury remain unclear. In this study, β-arrestin 2 knockout mice displayed more severe LPS-induced liver injury and significantly higher levels of pro-inflammatory cytokines than wild-type mice. Further, RAW264.7 cells treated with β-arrestin 2 siRNA expressed significantly higher pro-inflammatory cytokines and molecules involved in the TLR4/NF-κB signaling pathway (including phospho-IκBα and phosho-p65) than the control group at 6 h after treatment with LPS. Therefore, β-arrestin 2 could protect liver tissue from LPS-induced injury *via* inhibition of TLR4/NF-κB-mediated inflammation and may serve as a therapeutic target.

Jiang MP, Xu C, Guo YW, Luo QJ, Li L, Liu HL, Jiang J, Chen HX, Wei XQ. β-arrestin 2 attenuates lipopolysaccharide-induced liver injury *via* inhibition of TLR4/NF-κB signaling pathway-mediated inflammation in mice. *World J Gastroenterol* 2018; 24(2): 216-225 Available from: URL: http://www.wjgnet.com/1007-9327/full/v24/i2/216.htm DOI: http://dx.doi.org/10.3748/wjg.v24.i2.216

INTRODUCTION

Lipopolysaccharide (LPS, also called endotoxin)-induced hepatic injury is the pathological basis of varied hepatic diseases, and Kupffer cells are the key components in LPS-induced injury[1]. Researchers found that endogenous LPS derived from the intestine could promote the production of pro-inflammatory cytokines such as tumor necrosis factor (TNF)-α, interleukin (IL)-6, and IL-1β by activating Kupffer cells and accelerate the damage to the liver[2]. Meanwhile, LPS could also aggravate liver damage in nonalcoholic steatohepatitis by increasing the production of TNF-α by Kupffer cells[3]. Additionally, studies of a genetic mouse model of obesity suggested that the mice were more prone to steatohepatitis if they were constantly exposed to LPS[4,5]. When Kupffer cells were eliminated from this model, the mice showed decreased hepatic injury and lower mortality following LPS treatment[6]. LPS and Kupffer cells are the two essential key points in the development of varied hepatic diseases.

β-arrestin 2 is an important protein that plays a well-established role in regulating signaling downstream of the G-protein-coupled receptor (GPCR) pathway. Its recruitment and binding to the ligand-stimulated receptor are essential for signal transduction, sequestration, desensitization, and cell proliferation and differentiation. Recently, accumulating evidence has shown that β-arrestin 2 is a key regulator of not only GPCR-related signaling pathways but also of pathways downstream of major cell surface receptors and receptor tyrosine kinases, including insulin receptor, insulin-like growth factor type 1 receptor, epidermal growth factor receptor, and Toll-like receptor 4 (TLR4). Of these, the TLR4-related signaling pathway has gained much attention for its role in LPS-induced inflammation and host defense. Current views postulate that stimulation with LPS enhances production of pro-inflammatory cytokines from macrophages *via* the TLR4/NF-κB signaling pathway, while silencing of TLR4 or β-arrestin 2 can both inhibit this increase in pro-inflammatory cytokines and negatively regulate TLR4-mediated inflammatory reactions[7]. Based on these findings, we hypothesized that β-arrestin 2 should have great effects on LPS-induced inflammation and hepatic injury *via* a TLR4-related signaling pathway. To explore this hypothesis, we investigated the role and the possible mechanisms of β-arrestin 2 in LPS-induced hepatic injury. We found that deletion of β-arrestin 2 in mice aggravated LPS-induced liver injury by increasing macrophage production of pro-inflammatory cytokines including IL-1β, IL-6, TNF-α, and IL-10. Further, this mechanism might be involved in TLR4/NF-κB-mediated inflammation.

MATERIALS AND METHODS

Reagents and chemicals

LPS (Cat. L2630), Trizol reagent (Cat. T9424), and rat tail collagen (Cat. L2630) were purchased from Sigma (St Louis, MO, United States). Dulbecco's modified Eagle's medium (DMEM, Cat. C11995500B), Roswell Park Memorial Institute 1640 Medium (RPMI-1640, Cat. C11875500BT), fetal bovine serum (Cat. 10270-106), penicillin and streptomycin (Cat.

15140122), and Trypsin (Cat. 25200-056) were obtained from Gibco (Rockville, MD, United States). Real-time PCR Master Mix kit-SYBR Green (Cat. AQ141-04) was from Transgen (Beijing, China). siRNA-β-arrestin 2 (Cat. sc-29208), anti-glyceraldehyde-3-phosphate dehydrogenase antibody (GAPDH, Cat. sc-25778), horseradish peroxidase (HRP) conjugated goat anti-rabbit IgG secondary antibody (Cat. sc-2004), anti-p65 (Cat. sc-372), anti-phospho-IkBα (Cat. sc-8404), anti-IkBα (Cat. sc-371), and anti-TRAF6 (Cat. sc-7221) antibodies were all purchased from Santa Cruz (Santa Cruz, CA, United States). Anti-myeloperoxidase (MPO) primary antibody (Cat. ab9535), anti-β-arrestin 2 (Cat. ab54790), anti-phospho-p65 (Cat. ab86299), and anti-phospho-Akt (Cat. ab38449) antibodies were from Abcam (Abcam, Cambridge, MA, United States). Lipofectamine 3000 (Cat. L3000-015) was from Invitrogen (Invitrogen, Carlsbad, CA, United States). Heparin was from Wanbang (Xuzhou, Jiangsu, China). First Strand cDNA Synthesis Kit ReverTra Ace-α-TM (Cat. FSK-100) was from Toyobo (New York, NY, United States). Alanine transaminase (ALT, Cat. CSB-E16539m), aspartate transaminase (AST, Cat. CSB-E12649m), and TNF-α (Cat. CSB-E04741m) enzyme-linked immunosorbent assay (ELISA) kits were all from Cusabio (Wuhan, Hubei, China).

Animal model and treatments

All animal experiments were approved by the Institutional Animal Care and Use Committee of The Third Affiliated Hospital of Sun Yat-sen University (certification no.: IACUC-F3-17-0801). The original β-arrestin $2^{+/-}$ heterozygous C57BL/6J mice were a gift from Dr. Robert J Lefkowitz (Duke University Medical Center, Durham, NC). Male β-arrestin $2^{-/-}$ and β-arrestin $2^{+/+}$ mice aged 6 to 8 wk and weighing 20-25 g were randomly divided into four groups with six mice in each group. To establish an LPS-induced liver injury model, the mice were intraperitoneally injected with LPS (5 mg/kg) or physiological solution of sodium chloride. Four hours later, the mice were killed by intraperitoneal injection of 10% chloral hydrate (350 mg/kg). A 0.5 mL blood sample was collected from the inferior vena cava. Serum was stored at -20 ℃ before testing. The liver was carefully isolated from each mouse. Part of the liver tissue was immediately fixed in 10% neutral buffered formalin before embedding to prepare paraffin sections and the other part was stored at -80 ℃ for further analysis.

Cell culture and treatment

The mouse macrophage cell line RAW264.7 was obtained from American Type Culture Collection. Cells were cultured in DMEM supplemented with 10% fetal bovine serum and 1% antibiotics (penicillin and streptomycin) at 37 ℃ in a 5% CO_2-humidified incubator. Cells at 70% confluence were collected and seeded at 2 × 10^5 cells per well in a six-well plate for further experimentation. Transfections of cells with β-arrestin 2 siRNA RNAoligo and the control RNAoligo were performed with Lipofectamine 3000 according to the manufacturer's instructions. At 24 h after transfection, the medium was replaced with regular culture medium and cells were then treated with LPS (1000 ng/mL). At 6 h after administration of LPS, the cells were collected for further experiments.

Histopathology score of liver injury

Hematoxylin and eosin (HE) staining and TUNEL staining were performed to generate a histopathology score of liver injury. H&E staining was performed as described in our previous study[8] and TUNEL staining was performed using an in-situ cell death detection kit (Roche, Basel, Switzerland) according to the manufacturer's instructions. Briefly, sections were scored in a blinded manner for apoptosis and hemorrhage in five 200 × magnified fields according to Hoque's report[9]. Apoptosis was scored from 0-4 according to the rate of hepatocyte apoptosis (0: ⩽ 1%; 1: 1%-5%; 2: 5%-10%; 3: 10%-20%; and 4: ⩾ 20%) per 200 × field. Hemorrhage was also scored as 0-4 based on the hemorrhage rate (0: 0%; 1: 1%-5%; 2: 5%-20%; 3: 20%-50%; and 4: ⩾50%) per 200 × field.

Immunohistochemistry

To evaluate LPS-induced hepatic injury, immunohistochemistry was used to detect the expression of MPO in neutrophils, and the number of MPO positive cells was counted in 20 randomly selected 200 × magnified fields of each section. Immunohistochemistry was performed as previously described[10], and MPO was detected using the anti-MPO primary antibody and horseradish peroxidase (HRP) conjugated goat anti-rabbit IgG secondary antibody. The liver tissues of six mice from each group were studied.

Quantitative real-time RT-PCR

Total RNA was collected using Trizol reagent according to the manufacturer's instructions. Then, 2 μg of RNA was used for reverse transcription to produce first-strand cDNA with the First Strand cDNA Synthesis Kit ReverTra Ace-α-TM according to the manufacturer's instructions. Real-time PCR was performed for genes of interest on an ABI7700 System (Applied Biosystems, Foster City, CA) using DyNAmo SYBR Green Master Mix. β-actin was used as an internal reference to normalize the genes of interest. The melting curve for each gene was analyzed to ensure the specificity of amplification. The genes of interest and the primers are as follows: *TNF-α*: forward, 5′-TTCTGTCTACTGAACTTCGGGGTGATCGGTCC-3′ and reverse, 5′- GTATGAGATAGCAAATCGGCTGACGGTGTGGG-3′; *IL-1β*: forward, 5′-ATGGCAACTGTTCCTGAACTCAACT-3′ and reverse, 5′-CAGGACAGGTATAGATTCTTTCCTTT-3′; *IL-6*: forward, 5′-AGGATACCACTCCCAACAGACCT-3′ and reverse, 5′-CAAGTGCATCATCGTTGTTCATAC-3′; *IL-10*: forward, 5′-GCTCTTACTGACTGGCATGAG-3′ and

reverse, 5′-CGCAGCTCTAGGAGCATGTG-3′; *β-actin*: forward, 5′-GGCTGTATTCCCCTCCATCG-3′ and reverse, 5′-CCAGTTGGTAACAATGCCATGT-3′.

Western blot analysis

Western blot analysis was used to test for the expression of proteins of interest in cultured cells or liver tissues and was performed as previously described[11]. Briefly, equal amounts of protein were separated by electrophoresis and then transferred to polyvinylidene difluoride membranes. After blocking for 1 h at room temperature, the membrane was incubated with primary antibodies against β-arrestin 2, TRAF6, IKKβ, IκBα, phospho-IκBα, p65, phosho-p65, or GAPDH at 4 ℃ overnight. After washing, the membrane was then incubated with horseradish peroxidase (HRP)-conjugated secondary antibodies for 1 h at room temperature. The bands were visualized using an enhanced chemiluminescence system. Image-Pro Plus 6.0 software (Media Cybernetics, 8484 Georgia Avenue Silver Spring, MD, United States) was used for densitometry analyses.

ELISA

The levels of ALT, AST, LDH, and TNF-α in the culture supernatants and mouse serum were determined with the ELISA kits according to the manufacturer's instruction.

Statistical analysis

SPSS version 13.0 (SPSS Inc., Chicago, IL, United States) was used for statistical analyses. Data are expressed as the mean ± SD and differences between groups were assessed by Student's *t*-test or one-way analysis of variance, followed by Bonferroni's post hoc tests. A two-sided *P*-value < 0.05 was considered significant.

RESULTS

Deletion of β-arrestin 2 aggravates lipopolysaccharide-induced liver injury in vivo

To investigate the role of β-arrestin 2 in LPS-induced liver injury, we first established an animal model of LPS-induced liver injury by intraperitoneal injection of LPS (5 mg/kg) into β-arrestin 2 wild type (WT) and β-arrestin 2 knockout (KO) mice. Four hours after administration of LPS, the mice were sacrificed and liver tissues and blood were collected for histopathological scoring of liver injury and detection of ALT and AST in serum. As shown in Figure 1, we observed a significant difference in AST and ALT levels (Figure 1A and B) between β-arrestin 2 WT and β-arrestin 2 KO mice treated with LPS, whereas no significant difference was observed in the mice treated with physiological solution of sodium chloride. Similarly, histopathological scores of liver injury, including hemorrhage score (Figure 1D) and apoptosis score (Figure 1F), were significantly higher in β-arrestin 2 KO mice than in β-arrestin 2 WT mice after administration of LPS. Moreover, the MPO index (Figure 1G and H) presented similar results to the AST, ALT, and histopathology scores. These results suggested that decreased β-arrestin 2 aggravated LPS-induced liver injury.

Deletion of β-arrestin 2 facilitates the expression of lipopolysaccharide-induced inflammatory factors

As mentioned in the Introduction section, LPS-induced liver injury involves an increase in pro-inflammatory cytokines *via* activation of Kupffer cells. We therefore evaluated mRNA levels of *IL-1β*, *IL-6*, *TNF-α*, and *IL-10* in liver tissue and serum. We discovered that mRNA levels of *IL-1β*, *IL-6*, *TNF-α*, and *IL-10* were noticeably increased after treatment with LPS. The mRNA levels of the four pro-inflammatory cytokines mentioned above were significantly higher in liver tissue from β-arrestin 2 KO mice as compared with liver tissue from the β-arrestin 2 WT mice (Figure 2 A-D). Meanwhile, protein analysis of IL-6 and TNF-α in serum was consistent with the results in liver tissue (Figure 2E and F). These results indicated that increased pro-inflammatory cytokines in both liver tissue and serum might be associated with decreased β-arrestin 2.

Decreasing levels of β-arrestin 2 promote the production of pro-inflammatory factors in RAW264.7 cells in vitro

Based on the above results, we supposed that decreasing β-arrestin 2 might promote the production of pro-inflammatory factors *via* macrophage activation. To confirm this, we investigated whether a genetic reduction of β-arrestin 2 in RAW264.7 cells could increase the production of pro-inflammatory factors. As shown in Figure 3A and B, 6 h after transfection with β-arrestin 2 siRNA, expression of β-arrestin 2 was significantly down-regulated. Meanwhile, at another 6 h after treatment with LPS, RAW264.7 cells treated with β-arrestin 2 siRNA showed significantly increased production of IL-1β, IL-6, TNF-α, and IL-10 (Figure 3C-F). These results revealed that decreasing β-arrestin 2 in RAW264.7 cells promoted the *in vitro* production of pro-inflammatory factors.

Increased pro-inflammatory factors are involved in activation of the TLR4/NF-κB signaling pathway

The TLR4/NF-κB signaling pathway is considered to be involved in LPS-induced liver injury, and silencing of β-arrestin 2 can negatively regulate TLR4-mediated inflammatory reactions. To identify the mechanism whereby decreased β-arrestin 2 promotes production of pro-inflammatory factors, we then detected the expression of key molecules in the TLR4/NF-κB signaling pathway. The results showed that key molecules, including TRAF6, IKKβ, phospho-IκBα, and phospho-p65, produced by RAW264.7 cells increased noticeably after treatment with LPS for 6 h (Figure

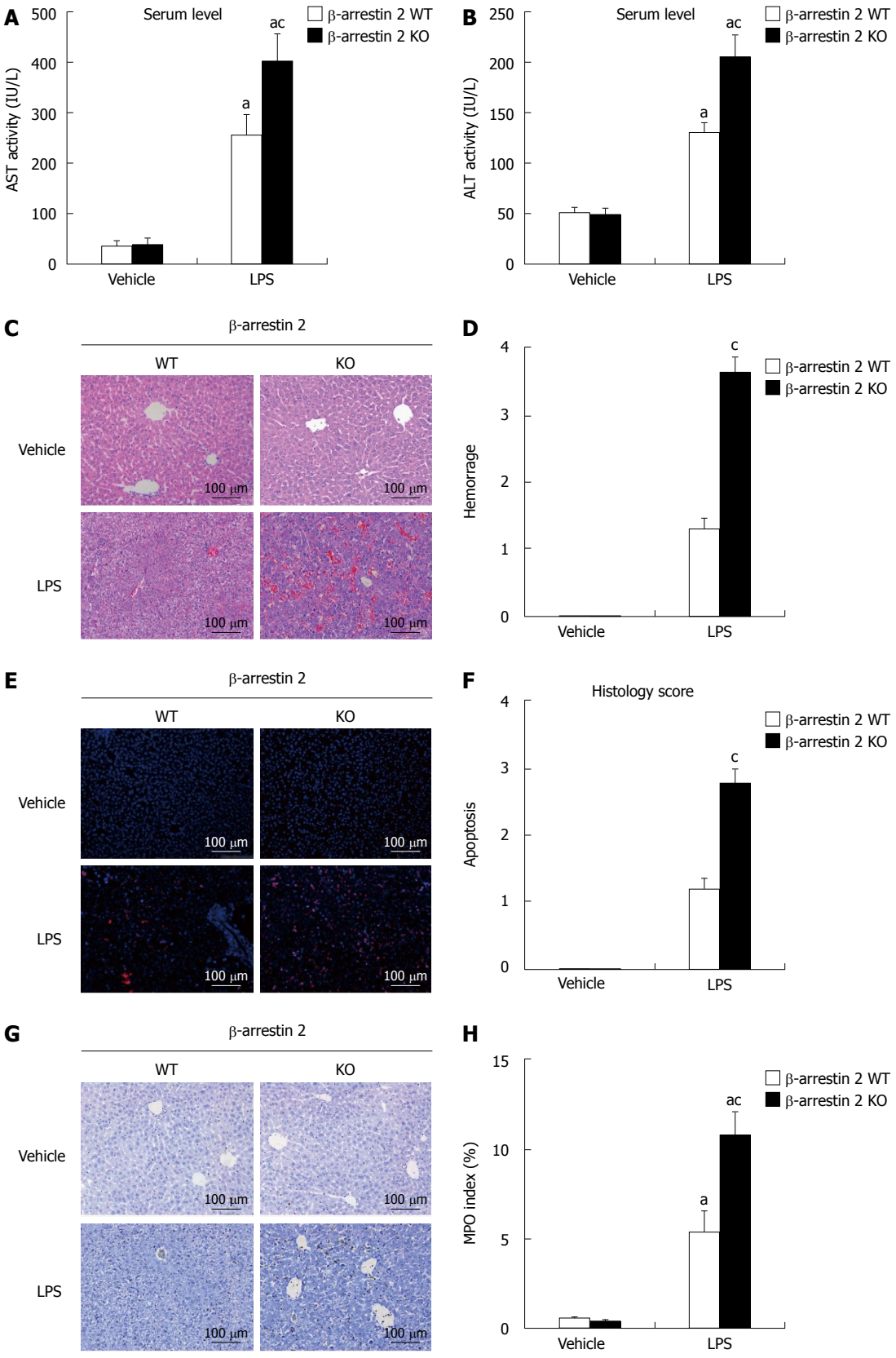

Figure 1 Evaluation of lipopolysaccharide-induced liver injury *in vivo* . A and B: Serum levels of ALT and AST were detected using ELISA kits in β-arrestin 2 WT and β-arrestin 2 KO mice treated with LPS and vehicle; C: HE staining of liver tissue (magnification, × 200); D: Histology score of hemorrhage in β-arrestin 2 WT and KO mice treated with LPS and vehicle; E: TUNEL staining of liver tissue (magnification, × 200); F: Histology score of apoptosis in β-arrestin 2 WT and KO mice treated with LPS and vehicle; G: Immunohistochemical staining for MPO expression in liver tissues from β-arrestin 2 WT and β-arrestin 2 KO mice treated with LPS and vehicle, (magnification, × 200); H: MPO index in β-arrestin 2 WT and β-arrestin 2 KO mice treated with LPS and vehicle. $^{a}P < 0.05$ *vs* vehicle control group; $^{c}P < 0.05$ *vs* β-arrestin 2 WT mice. LPS: Lipopolysaccharide.

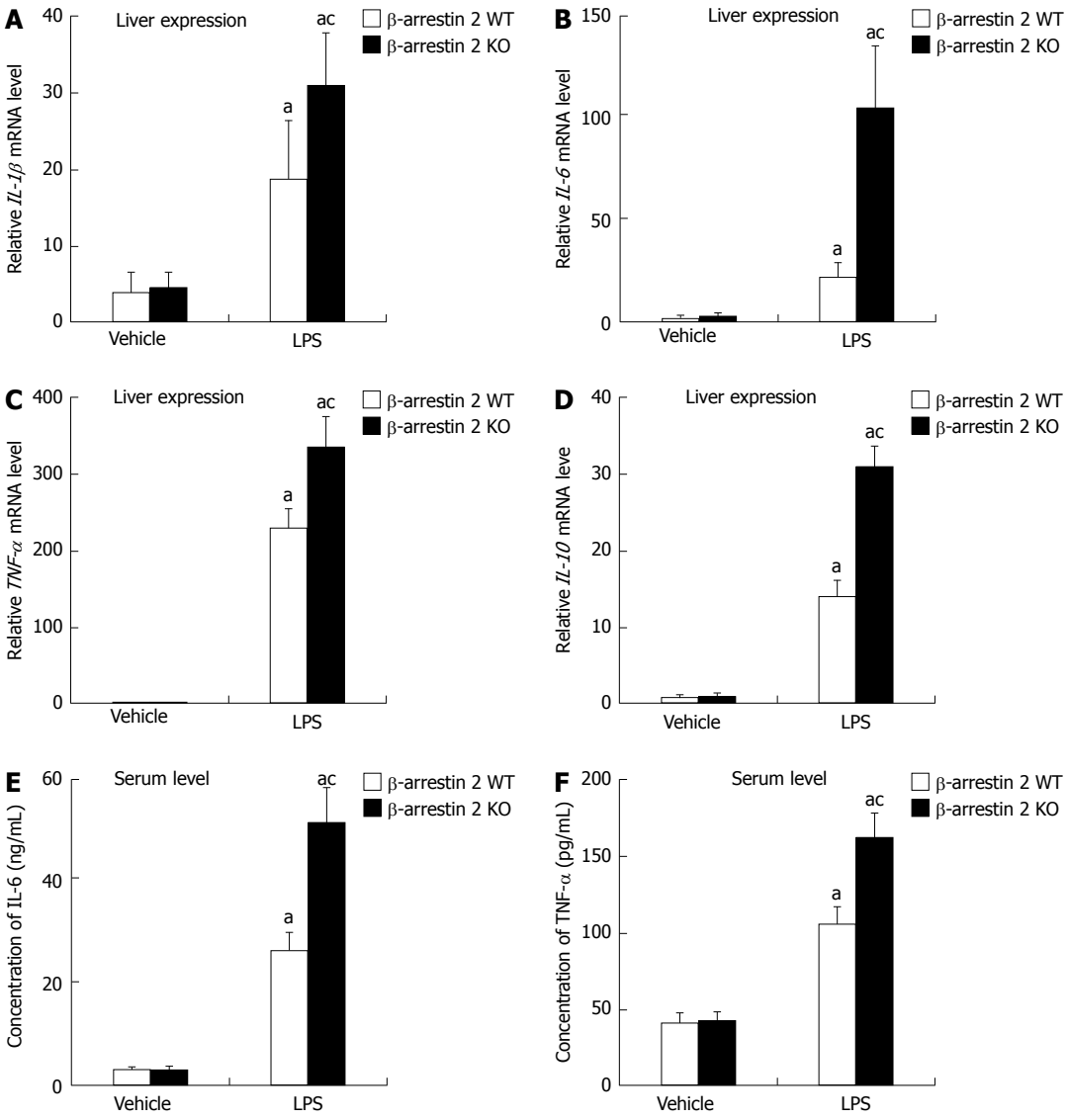

Figure 2 Expression of inflammatory factors induced by lipopolysaccharide *in vivo*. qRT-PCR was used to determine relative mRNA levels of IL-1β (A), IL-6 (B), TNF-α (C), and IL-10 (D) in liver tissues; E and F: ELISA was used to determine levels of IL-6 and TNF-α in serum. $^{a}P < 0.05$ *vs* control group; $^{c}P < 0.05$ *vs* β-arrestin 2 WT mice.

4A), suggesting that LPS-induced liver injury is related to activation of the TLR4/NF-κB signaling pathway. Moreover, phospho-IκBα and phospho-p65 (but not TRAF6 or IKKβ) were significantly increased in the cells treated with β-arrestin 2 siRNA and LPS (Figure 4B), indicating that decreased β-arrestin 2 might also be involved in activation of the TLR4/NF-κB signaling pathway, therefore promoting the production of pro-inflammatory factors in RAW264.7 cells.

DISCUSSION

LPS-induced hepatic injury is the pathological basis of varied hepatic diseases. However, the injury is considered indirect and induced by the production of pro-inflammatory cytokines from activated Kupffer cells[12]. In this current study, we found that serum levels of AST and ALT were visibly high in both β-arrestin 2 KO and WT mice treated with LPS for 4 h (Figure 1A and B). Meanwhile, the histopathology scores and count of MPO positive cells were also higher in the LPS group compared with the control group. These results showed obvious liver damage not only in β-arrestin 2 KO mice but also in WT mice, which suggested that our animal model was successful. In addition, mRNA levels of *IL-1β*, *IL-6*, *TNF-α*, and *IL-10* in liver tissue and serum levels of IL-6 and TNF-α were significantly higher after treatment with LPS, which also indicated that LPS-induced liver injury was mediated by pro-inflammatory cytokines. All these results were consistent with previous reports by Wang *et al*[13] and Seregin *et al*[14].

β-arrestin 2 is an important negative regulator of the TLR4 signaling pathway and could protect mice from TLR4-mediated endotoxic shock and lethality *via* down-regulation of inflammatory cytokines[13]. However, it is unclear whether β-arrestin 2 could attenuate LPS-induced liver injury *via* regulation of

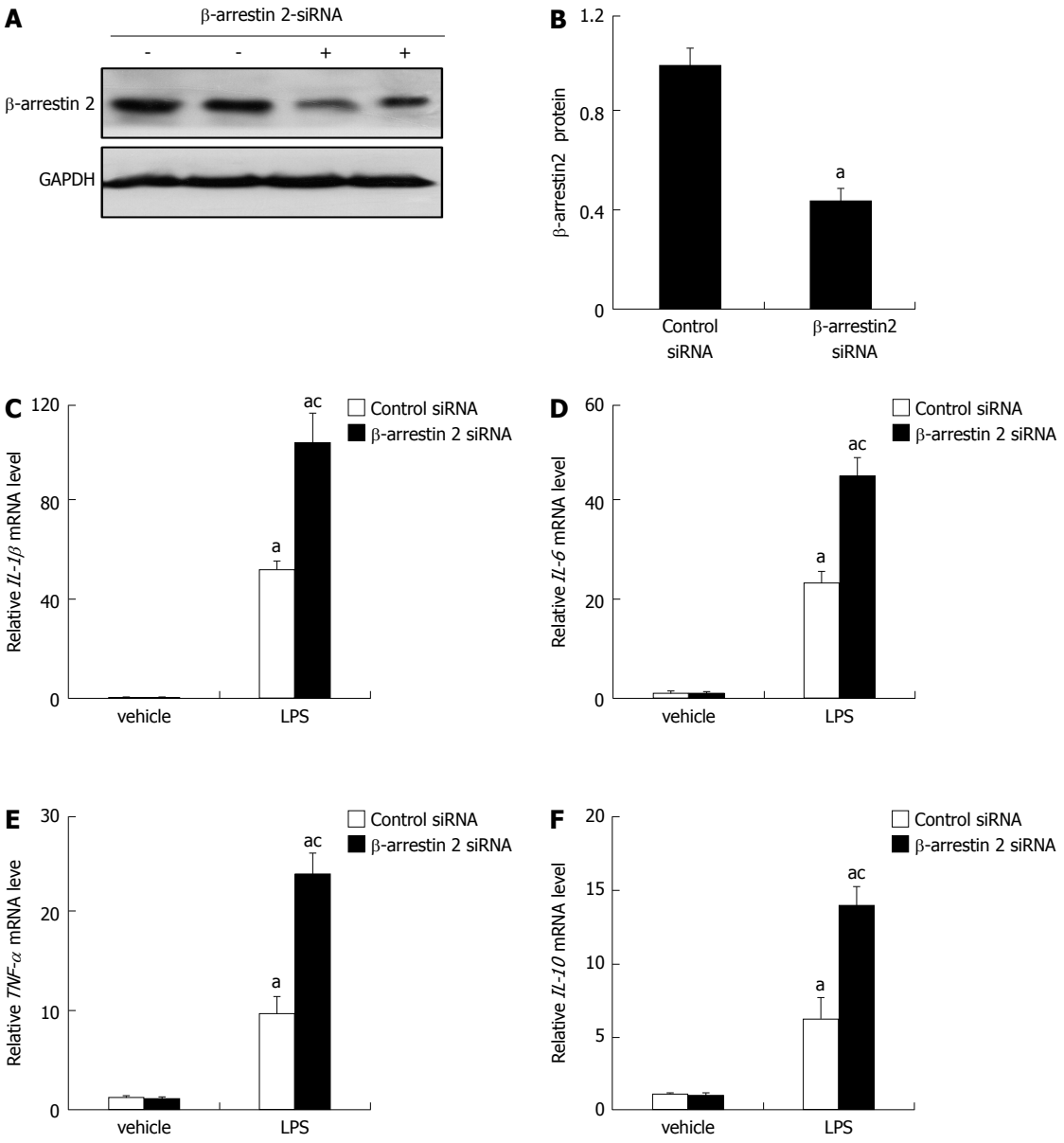

Figure 3 Expression of inflammatory factors by RAW264.7 cells *in vitro* . A: Expression of β-arrestin 2 in RAW264.7 cells was detected by Western blot. Levels of GAPDH are shown as a loading control; B: Relative quantitative evaluation of the Western blot analysis for β-arrestin 2 expression with ImageJ software, C-F: qRT-PCR was used to determine relative mRNA levels of IL-1β (C), IL-6 (D), TNF-α (E), and IL-10 (F) produced by RAW264.7 cells. $^{a}P < 0.05$ *vs* vehicle group; $^{c}P < 0.05$ *vs* control siRNA group.

pro-inflammatory cytokines. Porter *et al*[7] found that deletion of β-arrestin 2 in mice could decrease serum levels of IL-1β, IL-12p40, interferon-γ, IL-2, IL-3, IL-4, and IL-5. Thus, they hypothesized that β-arrestin 2 could reduce LPS-induced inflammation. Conversely, Li *et al*[15] found in another study that overexpression (but not deletion) of β-arrestin 2 could reduce the production of pro-inflammatory cytokines such as TNF-α and reduce experimental arthritis severity. Our results showed that ALT and AST levels and histopathology scores were higher in β-arrestin 2 KO mice than in β-arrestin 2 WT mice, which suggested that decreased β-arrestin 2 can aggravate LPS-induced liver damage. Moreover, the pro-inflammatory cytokines in both liver tissues and serum were higher in β-arrestin 2 KO mice, which revealed that decreased β-arrestin 2 might promote production of pro-inflammatory cytokines. We then investigated the correlation between decreased β-arrestin 2 and production of pro-inflammatory cytokines *in vitro* using siRNA interference technology. As we show in Figure 3, pro-inflammatory cytokines including IL-1β, IL-6, TNF-α, and IL-10 were higher in the cells treated with β-arrestin 2 siRNA and LPS, which revealed that β-arrestin 2 could attenuate LPS-induced liver injury *via* negative regulation of pro-inflammatory cytokines. Other than negative regulation of pro-inflammatory cytokines, Fong *et al*[16] found that β-arrestin 2 might modulate the CXCR4-induced chemotactic migration of lymphocytes. Moreover, Basher *et al*[17] and Fan *et al*[18] found that β-arrestin 2 inhibited chemotactic migration of neutrophils. In our study, the number of MPO

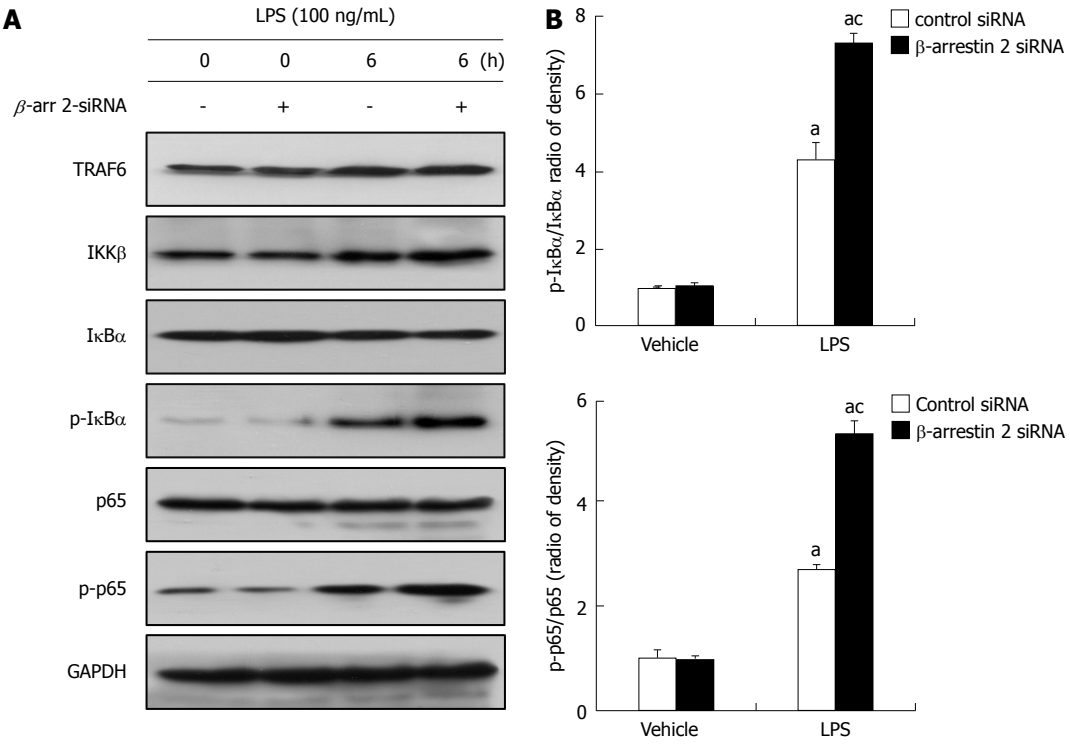

Figure 4 Expression of key molecules involved in the TLR4/NF-κB signaling pathway *in vitro*. A: Western blot analysis of the expression of key molecules involved in the TLR4/NF-κB signaling pathway. The levels of GAPDH are shown as a loading control; B: Relative gray value quantitative evaluation for p-IκBα/IκBα and p-p65/p65. $^{a}P < 0.05$ *vs* vehicle control; $^{c}P < 0.05$ *vs* control siRNA group.

positive cells was larger in liver tissues from β-arrestin 2 KO mice (Figure 1G and H), which indicated that decreased β-arrestin 2 reduce neutrophil infiltration in liver tissue. The results further revealed that inhibition of the chemotactic migration of neutrophils might be another mechanism by which β-arrestin 2 attenuates LPS-induced liver injury.

Kupffer cells are macrophages located in liver tissue, which have been identified as the major cells that produce pro-inflammatory cytokines and play a critical role in LPS-induced inflammation[19-22]. RAW264.7 macrophages are derived from leukemic mice and have similar characteristics to Kupffer cells in liver tissue. Therefore, we used RAW264.7 cells for our *in vitro* studies. Our results showed that pro-inflammatory cytokines from RAW264.7 cells obviously increased at 6 h after treatment with LPS, which revealed that RAW264.7 could act as Kupffer cells when stimulated by LPS. It is well known that β-arrestin 2 is involved in various cell signaling pathways and plays a key role in the regulation of cell signaling[23]. For example, β-arrestin 2 acts as a scaffold protein and participates in the activation of JNK and ERK in the MAPK pathway[24,25]. Further, β-arrestin 2 can directly bind to TRAF6 and reduce the phosphorylation of NF-κB through inhibition of TRAF6 oligomerization and ubiquitination, further inhibiting activation of the NF-κB pathway[13,26]. A recent study showed that β-arrestin 2 could down-regulate TLR4-mediated production of NLRP3 and IL1-1β, which are involved in inflammation induced by various factors[9]. In our study, we investigated the key molecules involved in the TLR4/NF-κB signaling pathway and found that key molecules, including TRAF6, IKKβ, phospho-IκBα, and phospho-p65, produced by RAW264.7 cells increased noticeably after treatment with LPS (Figure 4). Moreover, siRNA-mediated knockdown of β-arrestin 2 further increased levels of the key molecules mentioned above, including phospho-IκBα and phospho-p65 (Figure 4). This suggested that reductions in β-arrestin 2-induced pro-inflammatory cytokines might be associated with inhibition of the TLR4/NF-κB signaling pathway.

Altogether, our results showed that deletion of β-arrestin 2 in mice aggravated LPS-induced liver injury *via* increasing macrophage production of pro-inflammatory cytokines including IL-1β, IL-6, TNF-α, and IL-10. This mechanism might be involved in TLR4/NF-κB-mediated inflammation. We therefore concluded that β-arrestin 2 could protect liver tissue from LPS-induced injury *via* inhibition of TLR4/NF-κB-mediated inflammation. However, further study of the exact role and possible mechanism of β-arrestin 2 is needed.

ARTICLE HIGHLIGHTS

Research background

Lipopolysaccharide (LPS)-induced liver injury serves as the pathological basis of varied hepatic diseases. LPS does not directly harm hepatocytes, while Kupffer cells serve as the key components of LPS-induced injury through secretion of pro-inflammatory cytokines such as TNF-α, IL-6, and IL-1β. β-arrestin 2 is a protein that plays an important role in regulating the TLR4/NF-κB signaling pathway, which plays a critical role in inflammation. However, the

role of β-arrestin 2 in LPS-induced liver injury remains unclear.

Research motivation

The inhibition of LPS-induced inflammation *via* regulation of the TLR4/NF-κB signaling pathway may be a therapeutic method for modulating LPS-induced injury. β-arrestin 2 is a protein that plays an important role in regulating the TLR4/NF-κB signaling pathway. Therefore, we hypothesized that β-arrestin 2 can play a role in the prevention of LPS-induced liver injury.

Research objectives

The objective of this study was to investigate the role and the possible mechanism of β-arrestin 2 in LPS-induced liver injury *in vivo* and *in vitro*. This is the first study to show that β-arrestin 2 attenuated LPS-induced liver injury in a mouse model induced by injection of pure LPS. β-arrestin 2 may serve as a therapeutic target for the prevention and treatment of LPS-induced liver injury.

Research methods

The animal model was established *via* intraperitoneal injection of LPS or physiological sodium chloride solution in male β-arrestin $2^{+/+}$ and β-arrestin $2^{-/-}$ C57BL/6J mice. Blood samples and liver tissues were collected for analysis of liver injury and levels of pro-inflammatory cytokines. Extracts from the cultured mouse macrophage cell line RAW264.7 treated with various conditions were collected to analyze the production of pro-inflammatory cytokines and expression of key molecules involved in the TLR4/NF-κB signaling pathway.

Research results

The β-arrestin 2 knockout mice displayed more severe LPS-induced liver injury and significantly higher levels of pro-inflammatory cytokines, including IL-1β, IL-6, TNF-α, and IL-10, than the wild-type mice. Compared with the control group, pro-inflammatory cytokines, including IL-1β, IL-6, TNF-α, and IL-10, produced by the β-arrestin 2 siRNA-treated RAW264.7 cells were significantly higher at 6 h after treatment with LPS. The key molecules involved in the TLR4/NF-κB signaling pathway were also increased, including phospho-IκBα and phosho-p65.

Research conclusions

We hypothesized that β-arrestin 2 could protect liver tissue from LPS-induced injury *via* inhibition of TLR4/NF-κB-mediated inflammation. This hypothesis was proven using an animal model of LPS-induced liver injury in male β-arrestin 2+/+ and β-arrestin 2-/- C57BL/6J mice and a cell model using the mouse macrophage cell line RAW264.7. These findings may be helpful for the prevention and treatment of LPS-induced liver injury in future clinical practice *via* strengthening the function of β-arrestin 2. However, further study on the exact role and possible mechanism is still needed.

Research perspectives

Studies of the role of β-arrestin 2 agonists and methods of up-regulation of β-arrestin 2 in the prevention and treatment of LPS-induced liver injury should be performed.

REFERENCES

1 **Nolan JP**. The role of intestinal endotoxin in liver injury: a long and evolving history. *Hepatology* 2010; **52**: 1829-1835 [PMID: 20890945 DOI: 10.1002/hep.23917]

2 **Enomoto N**, Ikejima K, Yamashina S, Hirose M, Shimizu H, Kitamura T, Takei Y, Sato And N, Thurman RG. Kupffer cell sensitization by alcohol involves increased permeability to gut-derived endotoxin. *Alcohol Clin Exp Res* 2001; **25**: 51S-54S [PMID: 11410742 DOI: 10.1111/j.1530-0277.2001.tb02418.x]

3 **Kudo H**, Takahara T, Yata Y, Kawai K, Zhang W, Sugiyama T. Lipopolysaccharide triggered TNF-alpha-induced hepatocyte apoptosis in a murine non-alcoholic steatohepatitis model. *J Hepatol* 2009; **51**: 168-175 [PMID: 19446916 DOI: 10.1016/j.jhep.2009.02.032]

4 **Ye D**, Li FY, Lam KS, Li H, Jia W, Wang Y, Man K, Lo CM, Li X, Xu A. Toll-like receptor-4 mediates obesity-induced non-alcoholic steatohepatitis through activation of X-box binding protein-1 in mice. *Gut* 2012; **61**: 1058-1067 [PMID: 22253482 DOI: 10.1136/gutjnl-2011-300269]

5 **Yang SQ**, Lin HZ, Lane MD, Clemens M, Diehl AM. Obesity increases sensitivity to endotoxin liver injury: implications for the pathogenesis of steatohepatitis. *Proc Natl Acad Sci USA* 1997; **94**: 2557-2562 [PMID: 9122234 DOI: 10.1073/pnas.94.6.2557]

6 **Budagov RS**, Ul'ianova LP. [Effects of modulators of cytokine levels on mice and rats survival under combined radiation/thermal injuries]. *Radiats Biol Radioecol* 2004; **44**: 392-397 [PMID: 15455666]

7 **Porter KJ**, Gonipeta B, Parvataneni S, Appledorn DM, Patial S, Sharma D, Gangur V, Amalfitano A, Parameswaran N. Regulation of lipopolysaccharide-induced inflammatory response and endotoxemia by beta-arrestins. *J Cell Physiol* 2010; **225**: 406-416 [PMID: 20589830 DOI: 10.1002/jcp.22289]

8 **Guo YW**, Gu HY, Abassa KK, Lin XY, Wei XQ. Successful treatment of ileal ulcers caused by immunosuppressants in two organ transplant recipients. *World J Gastroenterol* 2016; **22**: 5616-5622 [PMID: 27350740 DOI: 10.3748/wjg.v22.i24.5616]

9 **Hoque R**, Farooq A, Ghani A, Gorelick F, Mehal WZ. Lactate reduces liver and pancreatic injury in Toll-like receptor- and inflammasome-mediated inflammation via GPR81-mediated suppression of innate immunity. *Gastroenterology* 2014; **146**: 1763-1774 [PMID: 24657625 DOI: 10.1053/j.gastro.2014.03.014]

10 **Wei XQ**, Guo YW, Liu JJ, Wen ZF, Yang SJ, Yao JL. The significance of Toll-like receptor 4 (TLR4) expression in patients with chronic hepatitis B. *Clin Invest Med* 2008; **31**: E123-E130 [PMID: 18544275 DOI: 10.25011/cim.v31i3.3469]

11 **Wei X**, Ke B, Zhao Z, Ye X, Gao Z, Ye J. Regulation of insulin degrading enzyme activity by obesity-associated factors and pioglitazone in liver of diet-induced obese mice. *PLoS One* 2014; **9**: e95399 [PMID: 24740421 DOI: 10.1371/journal.pone.0095399]

12 **Reiling J**, Bridle KR, Schaap FG, Jaskowski L, Santrampurwala N, Britton LJ, Campbell CM, Jansen PLM, Damink SWMO, Crawford DHG, Dejong CHC, Fawcett J. The role of macrophages in the development of biliary injury in a lipopolysaccharide-aggravated hepatic ischaemia-reperfusion model. *Biochim Biophys Acta* 2017 [PMID: 28709962 DOI: 10.1016/j.bbadis.2017.06.028]

13 **Wang Y**, Tang Y, Teng L, Wu Y, Zhao X, Pei G. Association of beta-arrestin and TRAF6 negatively regulates Toll-like receptor-interleukin 1 receptor signaling. *Nat Immunol* 2006; **7**: 139-147 [PMID: 16378096 DOI: 10.1038/ni1294]

14 **Seregin SS**, Appledorn DM, Patial S, Bujold M, Nance W, Godbehere S, Parameswaran N, Amalfitano A. beta-Arrestins modulate Adenovirus-vector-induced innate immune responses: differential regulation by beta-arrestin-1 and beta-arrestin-2. *Virus Res* 2010; **147**: 123-134 [PMID: 19896992 DOI: 10.1016/j.virusres.2009.10.023]

15 **Li P**, Cook JA, Gilkeson GS, Luttrell LM, Wang L, Borg KT, Halushka PV, Fan H. Increased expression of beta-arrestin 1 and 2 in murine models of rheumatoid arthritis: isoform specific regulation of inflammation. *Mol Immunol* 2011; **49**: 64-74 [PMID: 21855149 DOI: 10.1016/j.molimm.2011.07.021]

16 **Fong AM**, Premont RT, Richardson RM, Yu YR, Lefkowitz RJ, Patel DD. Defective lymphocyte chemotaxis in beta-arrestin2- and GRK6-deficient mice. *Proc Natl Acad Sci USA* 2002; **99**: 7478-7483 [PMID: 12032308 DOI: 10.1073/pnas.112198299]

17 **Basher F**, Fan H, Zingarelli B, Borg KT, Luttrell LM, Tempel GE, Halushka PV, Cook JA. beta-Arrestin 2: a Negative Regulator of Inflammatory Responses in Polymorphonuclear Leukocytes. *Int J Clin Exp Med* 2008; **1**: 32-41 [PMID: 19079685]

18 **Fan H**, Bitto A, Zingarelli B, Luttrell LM, Borg K, Halushka PV, Cook JA. Beta-arrestin 2 negatively regulates sepsis-induced inflammation. *Immunology* 2010; **130**: 344-351 [PMID: 20465566 DOI: 10.1111/j.1365-2567.2009.03185.x]

19 **Van Rooijen N**, Sanders A. Kupffer cell depletion by liposome-delivered drugs: comparative activity of intracellular clodronate, propamidine, and ethylenediaminetetraacetic acid. *Hepatology* 1996; **23**: 1239-1243 [PMID: 8621159 DOI: 10.1053/jhep.1996.

v23.pm0008621159]

20 **Su GL**, Klein RD, Aminlari A, Zhang HY, Steinstraesser L, Alarcon WH, Remick DG, Wang SC. Kupffer cell activation by lipopolysaccharide in rats: role for lipopolysaccharide binding protein and toll-like receptor 4. *Hepatology* 2000; **31**: 932-936 [PMID: 10733550 DOI: 10.1053/he.2000.5634]

21 **Seki E**, Tsutsui H, Nakano H, Tsuji N, Hoshino K, Adachi O, Adachi K, Futatsugi S, Kuida K, Takeuchi O, Okamura H, Fujimoto J, Akira S, Nakanishi K. Lipopolysaccharide-induced IL-18 secretion from murine Kupffer cells independently of myeloid differentiation factor 88 that is critically involved in induction of production of IL-12 and IL-1beta. *J Immunol* 2001; **166**: 2651-2657 [PMID: 11160328 DOI: 10.4049/jimmunol.166.4.2651]

22 **Kopydlowski KM**, Salkowski CA, Cody MJ, van Rooijen N, Major J, Hamilton TA, Vogel SN. Regulation of macrophage chemokine expression by lipopolysaccharide in vitro and in vivo. *J Immunol* 1999; **163**: 1537-1544 [PMID: 10415057]

23 **Porter-Stransky KA**, Weinshenker D. Arresting the Development of Addiction: The Role of β-Arrestin 2 in Drug Abuse. *J Pharmacol Exp Ther* 2017; **361**: 341-348 [PMID: 28302862 DOI: 10.1124/jpet.117.240622]

24 **McDonald PH**, Chow CW, Miller WE, Laporte SA, Field ME, Lin FT, Davis RJ, Lefkowitz RJ. Beta-arrestin 2: a receptor-regulated MAPK scaffold for the activation of JNK3. *Science* 2000; **290**: 1574-1577 [PMID: 11090355 DOI: 10.1126/science.290.5496.1574]

25 **Cervantes D**, Crosby C, Xiang Y. Arrestin orchestrates crosstalk between G protein-coupled receptors to modulate the spatiotemporal activation of ERK MAPK. *Circ Res* 2010; **106**: 79-88 [PMID: 19926878 DOI: 10.1161/circresaha.109.198580]

26 **Sun W**, Yang J. Molecular basis of lysophosphatidic acid-induced NF-κB activation. *Cell Signal* 2010; **22**: 1799-1803 [PMID: 20471472 DOI: 10.1016/j.cellsig.2010.05.007]

P- Reviewer: Manautou JE, Roychowdhury S **S- Editor**: Chen K
L- Editor: Wang TQ **E- Editor**: Li RF

World Journal of Gastroenterology

Submit a Manuscript: http://www.f6publishing.com

World J Gastroenterol 2018 January 14; 24(2): 226-236

DOI: 10.3748/wjg.v24.i2.226

ISSN 1007-9327 (print) ISSN 2219-2840 (online)

ORIGINAL ARTICLE

Basic Study

Hepatitis C virus core protein-induced miR-93-5p up-regulation inhibits interferon signaling pathway by targeting IFNAR1

Chang-Long He, Ming Liu, Zhao-Xia Tan, Ya-Jun Hu, Qiao-Yue Zhang, Xue-Mei Kuang, Wei-Long Kong, Qing Mao

Chang-Long He, Ming Liu, Zhao-Xia Tan, Ya-Jun Hu, Qiao-Yue Zhang, Xue-Mei Kuang, Wei-Long Kong, Qing Mao, Department of Infectious Diseases, Southwest Hospital, Third Military Medical University (Army Medical University), Chongqing 400037, China

Chang-Long He, Ming Liu, Zhao-Xia Tan, Ya-Jun Hu, Qiao-Yue Zhang, Xue-Mei Kuang, Wei-Long Kong, Qing Mao, Chongqing Key Laboratory for Research of Infectious Diseases, Chongqing 400037, China

ORCID number: Chang-Long He (0000-0002-0311-3479); Ming Liu (0000-0002-5244-2973); Zhao-Xia Tan (0000-0002-2468-2902); Ya-jun Hu (0000-0003-0024-2571); Qiao-Yue Zhang (0000-0003-2259-0155); Xue-Mei Kuang (0000-0002-4223-2243); Wei-Long Kong (0000-0002-6245-0328); Qing Mao (0000-0001-9499-8470).

Author contributions: All authors contributed to the manuscript.

Supported by National Natural Science Foundation of China, No. 81371849; and the TMMU Key Project for Clinical Research, No. 2012XLC05.

Institutional review board statement: This study was approved by the Ethics Committee of the First Affiliated Hospital of Third Military Medical University.

Conflict-of-interest statement: No potential conflicts of interest relevant to this article are reported.

Data sharing statement: No additional data are available.

Manuscript source: Unsolicited manuscript

Correspondence to: Qing Mao, MD, PhD, Doctor, Department of Infectious Diseases, Southwest Hospital, Third Military Medical University (Army Medical University), No. 30, Gaotanyan Street, Chongqing 400037, China. qingmao@tmmu.edu.cn
Telephone: +86-23-68754858
Fax: +86-23-68754858

Received: October 26, 2017
Peer-review started: October 27, 2017
First decision: November 21, 2017
Revised: December 5, 2017
Accepted: December 13, 2017
Article in press: December 13, 2017
Published online: January 14, 2018

Abstract

AIM

To investigate the mechanism by which hepatitis C virus (HCV) core protein-induced miR-93-5p up-regulation regulates the interferon (IFN) signaling pathway.

METHODS

HCV-1b core protein was exogenously expressed in Huh7 cells using pcDNA3.1 (+) vector. The expression of miR-93-5p and interferon receptor 1 (IFNAR1) was measured using quantitative reverse transcription-polymerase chain reaction and Western blot. The protein expression and phosphorylation level of STAT1 were evaluated by Western blot. The overexpression and silencing of miR-93-5p and IFNAR1 were performed using miR-93-5p agomir and antagomir, and pcDNA3.1-IFNAR1 and IFNAR1 siRNA, respectively. Luciferase assay was used to identify whether IFNAR1 is a target of miR-93-5p. Cellular experiments were also conducted.

RESULTS

Serum miR-93-5p level was increased in patients with HCV-1b infection and decreased to normal level after HCV-1b clearance, but persistently increased in those with pegylated interferon-α resistance, compared with healthy subjects. Serum miR-93-5p expression had an AUC value of 0.8359 in distinguishing patients with pegylated interferon-α resistance from those with pegylated interferon-α sensitivity. HCV-1b core protein increased miR-93-5p expression and induced inactivation of the IFN signaling pathway in Huh7 cells. Furthermore, IFNAR1 was identified as a direct target of miR-93-5p, and IFNAR1 restore could rescue miR-93-5p-reduced STAT1 phosphorylation, suggesting that the miR-93-5p-IFNAR1 axis regulates the IFN signaling pathway.

CONCLUSION

HCV-1b core protein-induced miR-93-5p up-regulation inhibits the IFN signaling pathway by directly targeting IFNAR1, and the miR-93-5p-IFNAR1 axis regulates STAT1 phosphorylation. This axis may be a potential therapeutic target for HCV-1b infection.

Key words: Hepatitis C virus; miR-93-5p; Interferon receptor 1; IFN signaling pathway

Core tip: Hepatitis C virus-1b core protein increases miR-93-5p expression and induces inactivation of the IFN signaling pathway. MiR-93-5p expression is involved in pegylated interferon-α resistance and directly targets interferon receptor 1 (IFNAR1). The miR-93-5p-IFNAR1 axis regulates STAT1 phosphorylation.

He CL, Liu M, Tan ZX, Hu YJ, Zhang QY, Kuang XM, Kong WL, Mao Q. Hepatitis C virus core protein-induced miR-93-5p up-regulation inhibits interferon signaling pathway by targeting IFNAR1. *World J Gastroenterol* 2018; 24(2): 226-236 Available from: URL: http://www.wjgnet.com/1007-9327/full/v24/i2/226.htm DOI: http://dx.doi.org/10.3748/wjg.v24.i2.226

INTRODUCTION

Hepatitis C virus (HCV) is a positive-sense single-stranded RNA virus that causes hepatitis, jaundice, and even fulminant hepatic failure at the beginning of infection, but in the majority of persons, the persistent infection with HCV causes cirrhosis and hepatocellular carcinoma (HCC)[1]. It is estimated that chronic hepatitis C impacts approximately 350 million people and constitutes a significant health burden worldwide[2,3]. In the past two decades, interferon (IFN) has served as the mainstay drug for HCV treatment, and its effect was improved by the addition of ribavirin and then by linking polyethylene glycol to the interferon molecule[4-6]. However, the outcome of IFN-based therapies depends mainly on the patients' responsiveness and the HCV genotype, especially HCV genotype 1 which has shown no sufficient response to pegylated interferon-α (IFNα)[7]. The core protein is an important component of HCV and plays a crucial role in HCV infection and pegylated IFNα resistance, but the mechanism underlying HCV core protein-induced pegylated IFNα resistance remains unclear.

MicroRNAs (miRNAs) are a class of single non-coding RNAs with a length of approximately 20 nt, which are involved in the regulation of HCV infection[8]. Several studies indicated that the expression of multiple miRNAs, such as miR-122, miR-1, miR-30, and miR-146a, was regulated by IFN in inhibiting HCV replication[9,10]. Kim *et al*[11] showed that HCV core protein promoted miR-122 destabilization in Huh7 cells, suggesting that miRNA expression was also regulated by HCV core protein. Furthermore, miRNAs can also inhibit HCV replication and infectivity, such as let-7 family miRNAs[12], suggesting that miRNAs may serve as targets for HCV therapy. The aberrant expression of miRNAs during HCV infection is involved in HCV-associated host pathways[13]. Recent studies have shown that miR-93-5p was overexpressed in HCV-associated HCC and promoted HCC progression[14,15]. However, whether miR-93-5p plays important roles in HCV core protein-associated IFN signaling pathway remains largely unclear.

In the present study, we demonstrated that serum miR-93-5p expression was higher in HCV-1b-infected patients with pegylated IFNα resistance compared with those with pegylated IFNα sensitivity. HCV-1b core protein increased miR-93-5p expression and inhibited the IFN signaling pathway in Huh7 cells. Interferon receptor 1 (IFNAR1) was identified as a direct target of miR-93-5p, and the miR-93-5p-INFAR1 axis regulated the IFN signaling pathway.

MATERIALS AND METHODS

Patients and samples

We enrolled 84 patients who had been identified to be infected with HCV-1b and 84 healthy subjects at Southwest Hospital, Third Military Medical University from July 2012 to June 2016. These patients were divided into two groups, one of which had pegylated IFNα resistance and the other had pegylated IFNα sensitivity. The clinical characteristics of individuals are described in Table 1. The collection of all samples obtained the consent from subjects according to the protocols approved by the Ethics Review Board of Southwest Hospital Institutional Review Board. Serum was isolated from blood samples within 2 h after collection according to the following steps: (1) centrifugation at 1500 rpm for 10 min, followed by transferring to new tubes; and (2) centrifugation at 12000 rpm for 2 min. These steps can prevent contamination by the cellular nucleic acids[16].

Table 1 Characteristics of patients with hepatitis C virus-1b infection

Variable	High expression of miR-93-5p	Low expression of miR-93-5p	*P* value
Gender			0.382
Male	25	20	
Female	17	22	
Age			0.189
Median			
>44	19	26	
≤44	23	16	
HCV-1b treatment			0.001
Resistance	25	9	
Sensitivity	17	33	

Differences between variables were analyzed by the χ^2 test. HCV: Hepatitis C virus.

Table 2 Primers sequences

mRNA	Sequence
β-actin forward	5′-TGTCCACCTTCCAGCAGATGT-3′
β-actin reverse	5′-TGTCACCTTCACCGTTCCAGTT-3′
IFNAR1 forward	5′-TGGTGACAGCGTGAGACTCTT-3′
IFNAR1 reverse	5′-GCAGTAGCCAGCAGCATCAG-3′
MiR-93-5p forward	5′- GCCGCCAAAGTGCTGTTC-3′
MiR-93-5p reverse	5′-CAGAGCAGGGTCCGAGGTA-3′
U6 forward	5′-CAGCACATATACTAAAATTGGAACG-3′
U6 reverse	5′-ACGAATTTGCGTGTCATCC-3′

IFNAR1: Interferon receptor 1.

Cell culture

Human hepatocellular carcinoma cell line Huh7 was purchased from ATCC, and cultured in high glucose Dulbecco's modified Eagle's medium (Hyclone, United States) supplemented with 10% fetal bovine serum (Gibco, United States) in a humidified incubator with 5% CO_2 at 37 ℃.

RNA extraction

Total RNA was isolated from cells and serum using TRI reagent (Invitrogen, Carlsbad, CA, United States) and TRIzol LS reagent (Invitrogen), respectively, according to the manufacturer's instructions. For total RNA isolated from serum, 10 μL of 0.05 μmol/L synthetic *C. elegans* miR-39 (GenePharma, Shanghai, China) was added to each sample after the samples were treated with TRIzol LS reagent. Finally, total RNA was resuspended in 45 μL of pre-heated (65 ℃) nuclease-free water and analyzed using Nanodrop1000 (Thermo, Massachusetts, United States).

Quantitative reverse transcription-polymerase chain reaction (qRT-PCR)

Reverse transcription was performed using the PrimeScript RT reagent Kit (TaKaRa, Dalian, China) according to the manufacturer's instructions. One microgram of total RNA (10 μL) was used for a reverse transcription system containing 4 μL 5 × reverse transcription buffer, 4 μL nuclease-free H_2O, 1 μL prime RT enzyme, and 1 μL RT primer. Quantitative PCR assay was conducted using the Permix Ex Taq Kit (TaKaRa) according to the manufacturer's protocols. Two microliters of cDNA was used in a qPCR system containing 10 μL SYBR Premix Ex Taq II, 0.5 μL ROX Reference Dye II, 0.5 μL reverse primer, 0.5 μL forward primer, and 6.5 μL nuclease-free H_2O. Running parameters of qPCR were: 95 ℃ for 2 min, followed by 40 cycles of 95 ℃ for 15 s and 58 ℃ for 30 s. Melt curves were collected over a range of temperatures from 58 ℃ to 95 ℃, with an increase of 0.5 ℃ per 5 s. Primer sequences are showed in Table 2.

The expression of miR-93-5p and IFNAR1 in Huh7 cells was normalized using the $2^{-\Delta\Delta Ct}$ method, with RNU6B and β-actin used as the references, respectively. Serum miR-93-5p concentration was calculated using a standard curve established by the synthetic miR-93-5p. The standard linearity of miR-93-5p quantification was generated in each qPCR reaction. Experimental qRT-PCR data were normalized using the synthetic *C. elegans* miR-39 as described previously[16].

Vector construct

DNA oligonucleotides that encode HCV core protein or *Homo sapiens* IFNAR1 protein were synthesized with flanking *Spe* Ⅰ and *Hind* Ⅲ restriction enzyme digestion sites. The synthesized DNA was inserted into pcDNA3.1 (+) vector (Addgene, United States) using T4 DNA Ligase according to the manufacturer's instructions. DNA oligonucleotides containing wild-type or mutant 3′-untranslated region (UTR) of IFNAR1 were synthesized with flanking *Spe* Ⅰ and *Hind* Ⅲ restriction enzyme digestion sites, respectively, and the synthesized DNA was inserted into psiCHECK™-2 vector (Promega, Wisconsin, United States). The sequences of the synthesized DNA are showed in Table 2.

Oligonucleotide transfection

The gain- or loss-of-function of miR-93-5p was performed using miR-93-5p agomir (RIBOBIO, Guangzhou, China) or antagomir (RIBOBIO), respectively. Lipofectamine 2000 (Invitrogen) was used for oligonucleotide transfection according to the manufacturer's instruction.

Luciferase assay

HEK293T cells were cultured in 6-well plates and the cells in each well were transfected with 200 ng wild-type psiCHECK-IFNAR1-3'-UTR or 200 ng mutant psiCHECK-IFNAR1-3'-UTR, and then miR-93-5p agomir (200 nmol/L) or antagomir (200 nmol/L) was transfected into the cells using lipofectamine 2000, respectively. Twenty-four hours after transfection, the cells were collected and lysed using the luciferase reporter assay system according to the manufacturer's instructions, followed by detection of fluorescence activity using GloMax 20/20 Luminometer.

Western blot analysis

Total protein from tissues and cells was extracted using the RIPA Lysis and Extraction Buffer (Thermo) according to the manufacturer's instructions. Western blot assay was performed according to the standard protocol. Briefly, total proteins were separated using 8% or 10% SDS-PAGE gels, followed by transfer onto PVDF membranes. Skim milk (5%) or bovine serum albumin solution (used for p-STAT1 antibody) was used to block the PVDF membranes. Anti-IFNAR1 (Abcam, Cambridge, United Kingdom), anti-STAT1 (Cell Signaling Technology, Boston, United States), anti-p-STAT1 (Cell Signaling Technology), and anti-GAPDH (Cell Signaling Technology) antibodies were used to incubate the PVDF membranes overnight. Then, a horseradish peroxidase-conjugated secondary antibody (Zhongshan Biotechnology, Beijing, China) was used to incubate the PVDF membranes for 1 h. The PVDF membranes were washed using 1 × TBST solution three times and visualized using the SuperSignal West Dura Extended Duration Substrate kit (Thermo).

Statistical analysis

All data are presented as mean ± SD. The difference between two groups was analyzed using the Mann-Whitney test or the two-tailed Student's *t*-test. One-way ANOVA was used for three or more groups. The relationship between the expression of miR-93-5p and IFNAR1 mRNA was evaluated using the Pearson's correlation. A *P*-value < 0.05 was considered statistically significant. All statistical analyses and the generation of graphs were performed using GraphPad Prism 6.0 (Graphpad Software Inc, California, United Kingdom).

RESULTS

Serum miR-93-5p expression is increased in HCV-1b-infected patients

MiR-93-5p has been shown to be overexpressed in HCV-infected HCC tissues[14]. To determine whether miR-93-5p expression is also increased in serum of HCV-infected patients, we collected 168 serum samples, including 84 samples from 84 patients with HCV-1b infection before pegylated IFNα treatment and 84 samples from the same patients after pegylated IFNα treatment for 24 wk. PCR finally confirmed that 34 patients had pegylated IFNα resistance and 50 patients had pegylated IFNα sensitivity.

To measure serum miR-93-5p concentration, we established a dynamic range of miR-93-5p quantification. The synthetic single-strand miR-93-5p was serially diluted by 10-fold from concentrations of 1 to 0.00001 fmol, and qRT-PCR experiments showed the linearity of miR-93-5p quantification (Figure 1A). For the samples before pegylated IFNα treatment, serum miR-93-5p expression was significantly increased in HCV-1b-infected patients compared with healthy subjects ($P < 0.0001$) (Figure 1B), and it was also increased in the patients with pegylated IFNα sensitivity compared with healthy subjects ($P = 0.0100$). Interestingly, serum miR-93-5p expression was higher in patients with pegylated IFNα resistance than in those with pegylated IFNα sensitivity ($P < 0.0001$) (Figure 1C). For the samples after pegylated IFNα treatment, serum miR-93-5p expression was persistently increased in patients with pegylated IFNα resistance ($P < 0.0001$) (Figure 1D), but it was decreased in patients with pegylated IFNα sensitivity, similar to that in healthy subjects (Figure 1E). These data suggest that high level of miR-93-5p in serum is involved in HCV-1b infection and pegylated IFNα resistance.

Serum miR-93-5p in patients with HCV-1b infection is involved in pegylated IFNα resistance

To determine whether serum miR-93-5p concentration can serve as a biomarker for predicting pegylated IFNα resistance, receiver operating characteristics (ROC) curve analysis was performed. The results showed an area under the curve (AUC) value of 0.8846 for serum miR-93-5p in distinguishing HCV-1b-infected patients from healthy subjects (Figure 2A), an AUC value of 0.8562 in distinguishing patients with pegylated IFNα sensitivity from healthy subjects (Figure 2B), an AUC value of 0.9265 in distinguishing patients with pegylated IFNα resistance from healthy subjects (Figure 2C), and an AUC value of 0.8359 in distinguishing patients with pegylated IFNα resistance from those with pegylated IFNαsensitivity (Figure 2D). The detailed information is showed in Table 3. These data suggest that serum miR-93-5p concentration may serve as a biomarker for pegylated IFNα resistance in HCV-1b-infected patients.

HCV-1b core protein increases miR-93-5p expression and induces inactivation of the IFN signaling pathway

HCV core protein plays an important role in HCV infection. To determine whether HCV-1b infection could regulate miR-93-5p expression, HCV-1b core protein was enforcedly expressed in Huh7 cells ($P = 0.0032$) (Figure 3A). This approach was widely used in HCV studies due to its capability in supporting HCV replication. A previous study has shown that HCV-1b core protein decreased mature miR-122 expression[11].

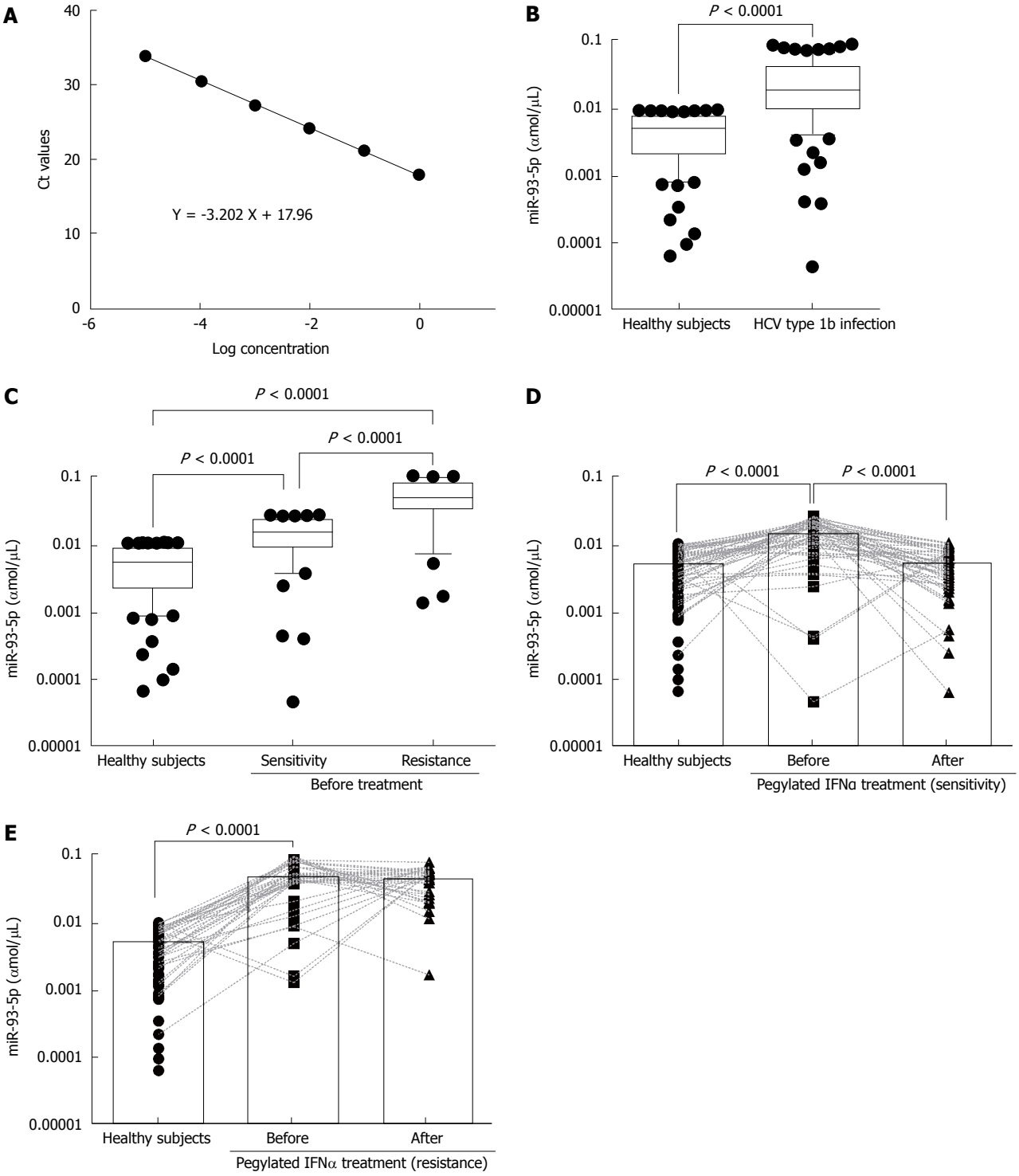

Figure 1 Serum miR-93-5p expression is increased in hepatitis C virus-1b-infected patients. A: The linearity of miR-93-5p quantification; B: Box shows serum miR-93-5p concentrations in 84 patients with HCV-1b infection, compared with 84 healthy subjects; C: Box shows serum miR-93-5p concentrations in 50 HCV-1b-infected patients with pegylated IFNα sensitivity and 34 HCV-1b-infected patients with pegylated IFNα resistance, compared with 84 healthy subjects; D: Scatter shows serum miR-93-5p concentrations in 84 healthy subjects and 50 HCV 1b-infected patients with pegylated IFNα sensitivity before or after treatment; E: Scatter shows serum miR-93-5p concentrations in 84 healthy subjects and 34 HCV 1b-infected patients with pegylated IFNα resistance before or after treatment. HCV: Hepatitis C virus; IFNα: Interferon-α.

Thus, we repeated these experiments and confirmed that HCV-1b core protein could reduce miR-122 expression (P = 0.0207) (Figure 3B), suggesting that exogenous HCV-1b core protein worked in Huh7 cells. Then, we found that HCV-1b core protein significantly increased miR-93-5p expression in Huh7 cells (P = 0.0004) (Figure 3C).

Although the treatment of pegylated IFN plus ribavirin was used, the sustained virological response (SVR) rate was around 50%-79% for HCV type 1/4

Table 3 Receiver operating characteristics curve analysis of serum miR-93-5p concentration

AUC	Sensitivity	Specificity	Cut-off value (amol/μL)
0.8846 (Infection *vs* Healthy)	0.7619	1	0.009774
0.8562 (Sensitivity *vs* Healthy)	0.7000	1	0.009774
0.9265 (Infection *vs* Resistance)	0.8529	1	0.010870
0.8359 (Resistance *vs* Sensitivity)	0.7647	1	0.030300

Infection: HCV-1b-infected patients; Healthy: Healthy subjects; Sensitivity: Patients with pegylated IFNα sensitivity; Resistance: Patients with pegylated IFNα resistance.

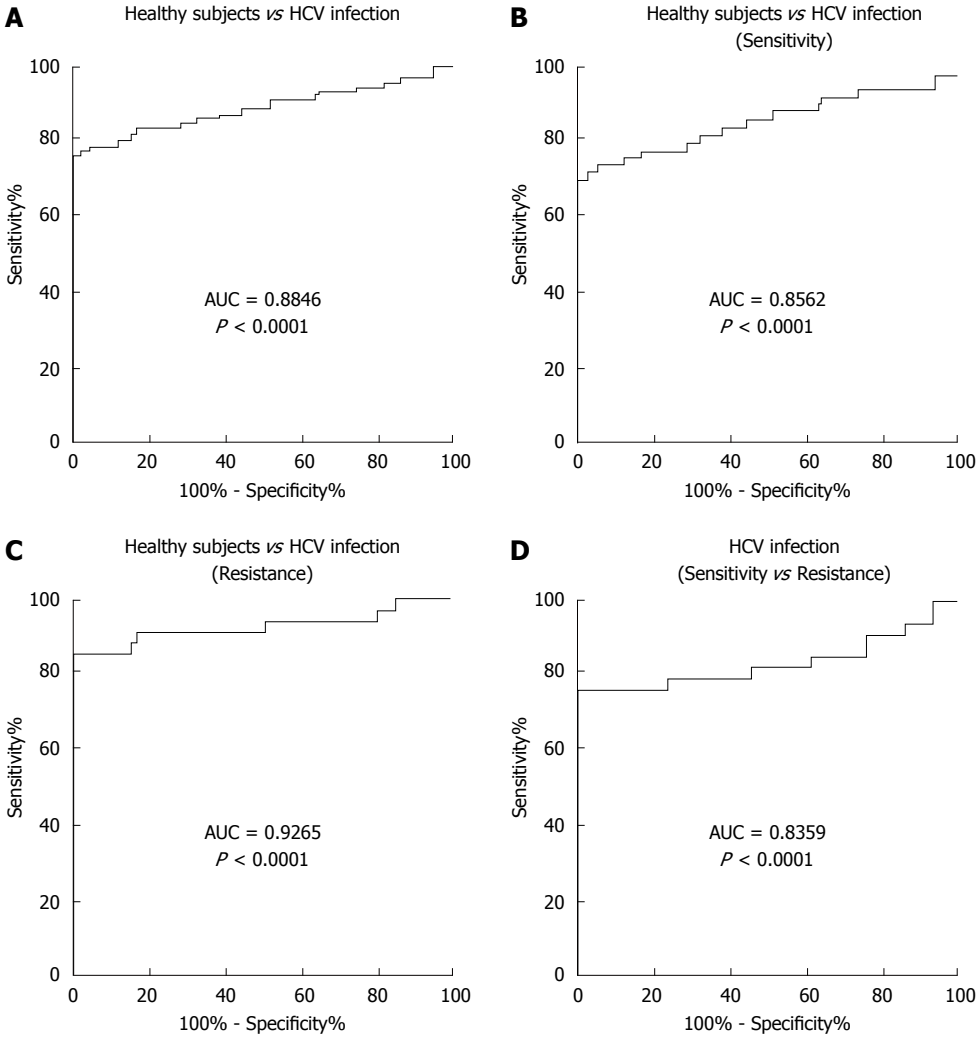

Figure 2 Serum miR-93-5p in patients with hepatitis C virus-1b infection is involved in pegylated interferon-α resistance. A: Receiver operating characteristics (ROC) curve shows an AUC value of 0.8846 for serum miR-93-5p concentration in distinguishing HCV-1b-infected patients from healthy subjects; B and C: ROC curve shows AUC values of 0.8562 and 0.9265 in distinguishing HCV-1b-infected patients with pegylated IFNα sensitivity or resistance from healthy subjects, respectively; D: ROC curve shows an AUC value of 0.8359 in distinguishing HCV-1b-infected patients with pegylated IFNα resistance from those with pegylated IFNα sensitivity. HCV: Hepatitis C virus; IFNα: Interferon-α.

and 75%-94% for HCV type 2/3[17], suggesting that IFN-α resistance largely existed in HCV-1b infection. Thus, we speculated whether HCV-1b core protein could regulate the IFN signaling pathway. We initially measured the protein expression of IFNAR1 and STAT1, as well as the phosphorylation level of STAT1. As expected, our finding showed that HCV-1b core protein significantly decreased the protein expression of IFNAR1 and the phosphorylation level of STAT1, but the protein expression of STAT1 was not changed (Figure 3D and E). These data suggest that HCV-1b core protein induces inactivation of the IFN signaling pathway.

Interferon receptor 1 is a direct target of miR-93-5p

Next, we determined whether miR-93-5p is involved in HCV-1b core protein-induced inactivation of the IFN signaling pathway. As well known that miRNA

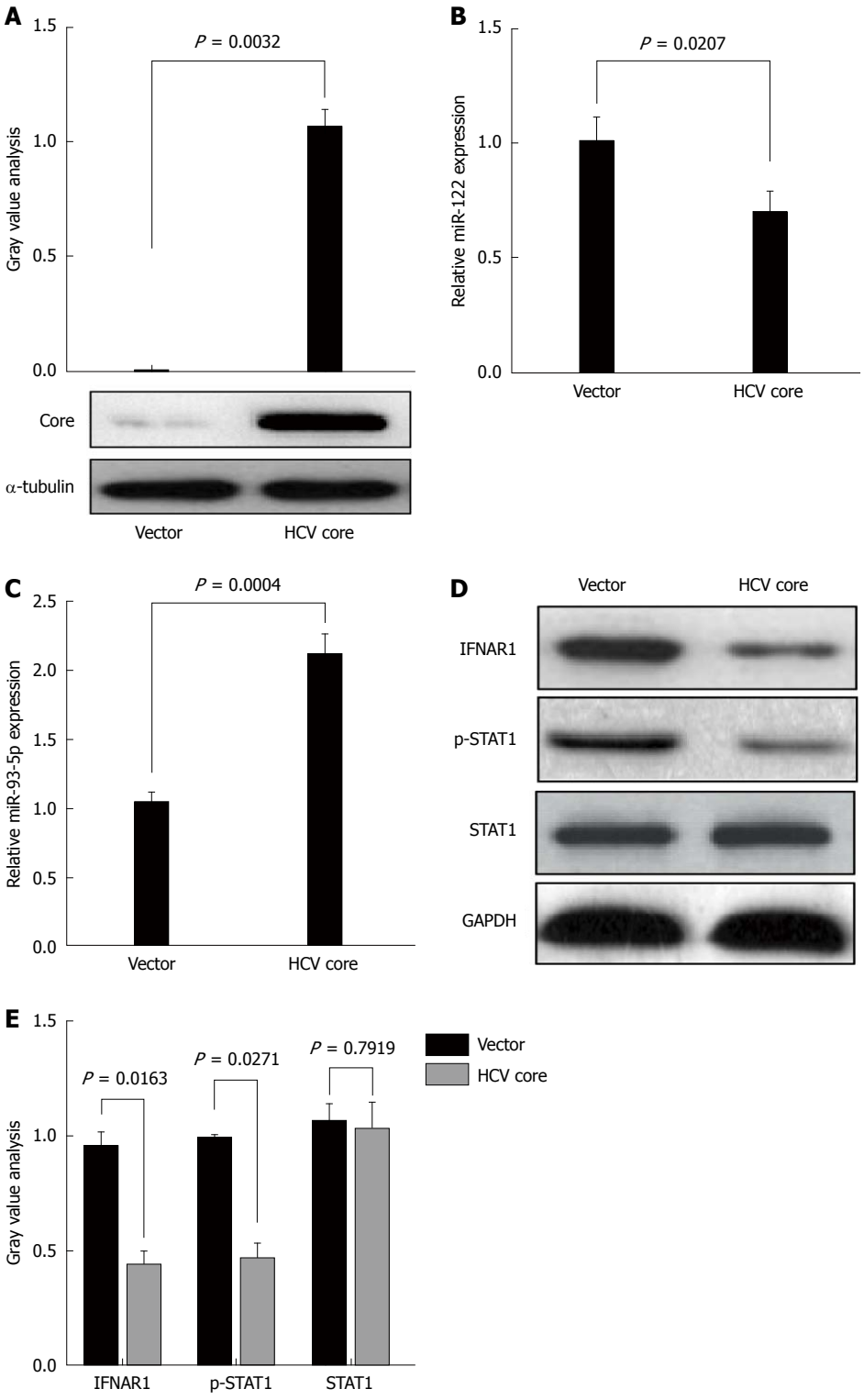

Figure 3 Hepatitis C virus-1b core protein increases miR-93-5p expression and inactivates the interferon signaling pathway. A: HCV core protein is enforcedly expressed in Huh7 cells using pcDNA3.1 (+) vector. Western blot shows HCV core protein expression. This experiment was repeated twice; B: Bar shows miR-122 expression in Huh7 cells transfected with pcDNA 3.1 (+) empty vector or HCV core-pcDNA3.1 (+) vector. U6 was used as an internal reference. This experiment was repeated three times. C: Bar shows miR-93-5p expression in Huh7 cells transfected with pcDNA 3.1 (+) empty vector or HCV core-pcDNA3.1 (+) vector. U6 was used as an internal reference. This experiment was repeated three times. D and E: Western blot shows the protein expression of IFNAR1 and STAT1, as well as the phosphorylation level of STAT1 in Huh7 cells which were transfected with pcDNA 3.1 (+) empty vector or HCV core-pcDNA3.1 (+) vector. This experiment was repeated twice. HCV: Hepatitis C virus, IFNAR1: Interferon receptor 1.

exerting its function depends on its target, we used five databases (TargetScan, PicTar, RNA22, PITA, and MiRanda) to predict the targets of miR-93-5p, and found that IFNAR1 may be a potential target of miR-93-5p. IFNAR1 mRNA has three potential binding sites for miR-93-5p in the 3'-UTR. To confirm whether

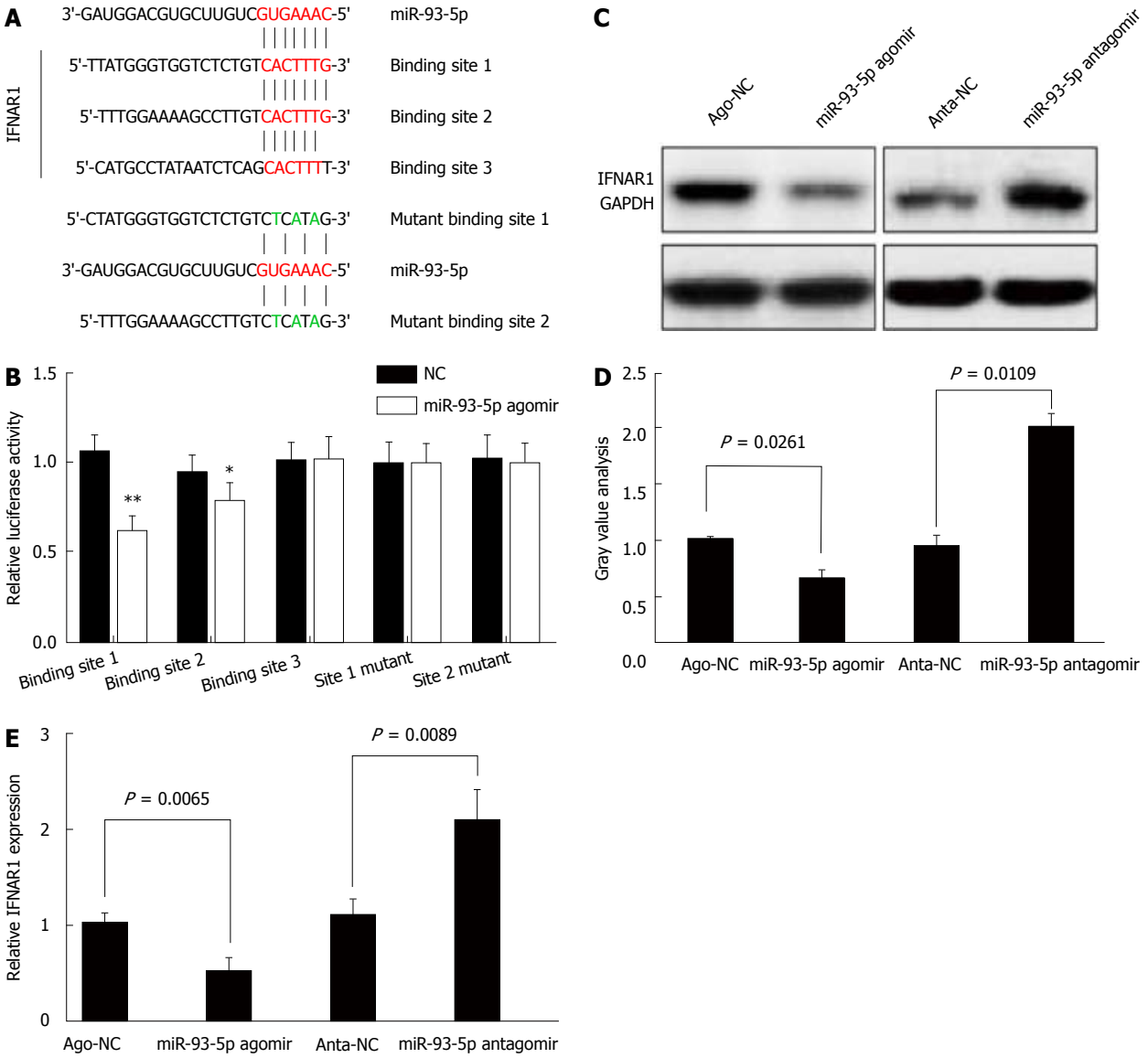

Figure 4 FNAR1 is a direct target of miR-93-5p . A: The binding sites for miR-93-5p in the IFNAR1 3'-UTR, and the design of mutant binding sites in the IFNAR1 3'-UTR for miR-93-5p; B: Luciferase assay shows that miR-93-5p agomir inhibits the relative luciferase activity in the binding site 1 or 2-expressing HEK293T cells, but not in the binding site 3- or mutant binding sites-expressing HEK293T cells. This experiment was repeated six times; C and D: Western blot shows the protein expression of IFNAR1 in Huh7 cells transfected with ago-NC (200 nmol/L), miR-93-5p agomir (200 nmol/L), anta-NC (200 nmol/L), and miR-93-5p antagomir (200 nmol/L). This experiment was repeated twice; E: qRT-PCR shows the mRNA expression of IFNAR1 in Huh7 cells transfected with ago-NC (200 nmol/L), miR-93-5p agomir (200 nmol/L), anta-NC (200 nmol/L), and miR-93-5p antagomir (200 nmol/L). β-actin was used as an internal reference. This experiment was repeated three times. IFNAR1: Interferon receptor 1.

IFNAR1 is a target of miR-93-5p, we constructed the vectors containing wild-type 3'-UTR or mutant 3'-UTR of IFNAR1 mRNA using psiCHECK vector (Figure 4A). Luciferase assay revealed that miR-93-5p agomir significantly reduced the relative luciferase activity in the presence of binding site 1 ($P < 0.0001$) or 2 ($P = 0.0173$), rather than site 3. However, the relative luciferase activity had no significant change in the presence of the mutant binding sites, compared with NC (Figure 4B). Furthermore, miR-93-5p agomir also decreased the protein ($P = 0.0261$) and mRNA ($P = 0.0065$) expression of IFNAR1 in Huh7 cells compared with NC, while opposite results were found after miR-93-5p antagomir treatment ($P = 0.0109$, $P = 0.0089$) (Figure 4C, D, and E). Together, these data suggest that IFNAR1 is a direct target of miR-93-5p.

The miR-93-5p-IFNAR1 axis regulates the IFN signaling pathway

STAT1, a transcription factor, plays a crucial role in the IFN signaling pathway. Several studies have shown that IFNAR1 regulates the phosphorylation level of STAT1[18-20]. However, it is unclear whether the miR-93-5p-IFNAR1 axis could regulate the phosphorylation level of STAT1 in Huh7 cells. Thus, we induced the enforced expression or silencing of IFNAR1 in Huh7 cells using pcDNA3.1 (+) vectors and IFNAR1 siRNA, respectively (Figure 5A). Western blot

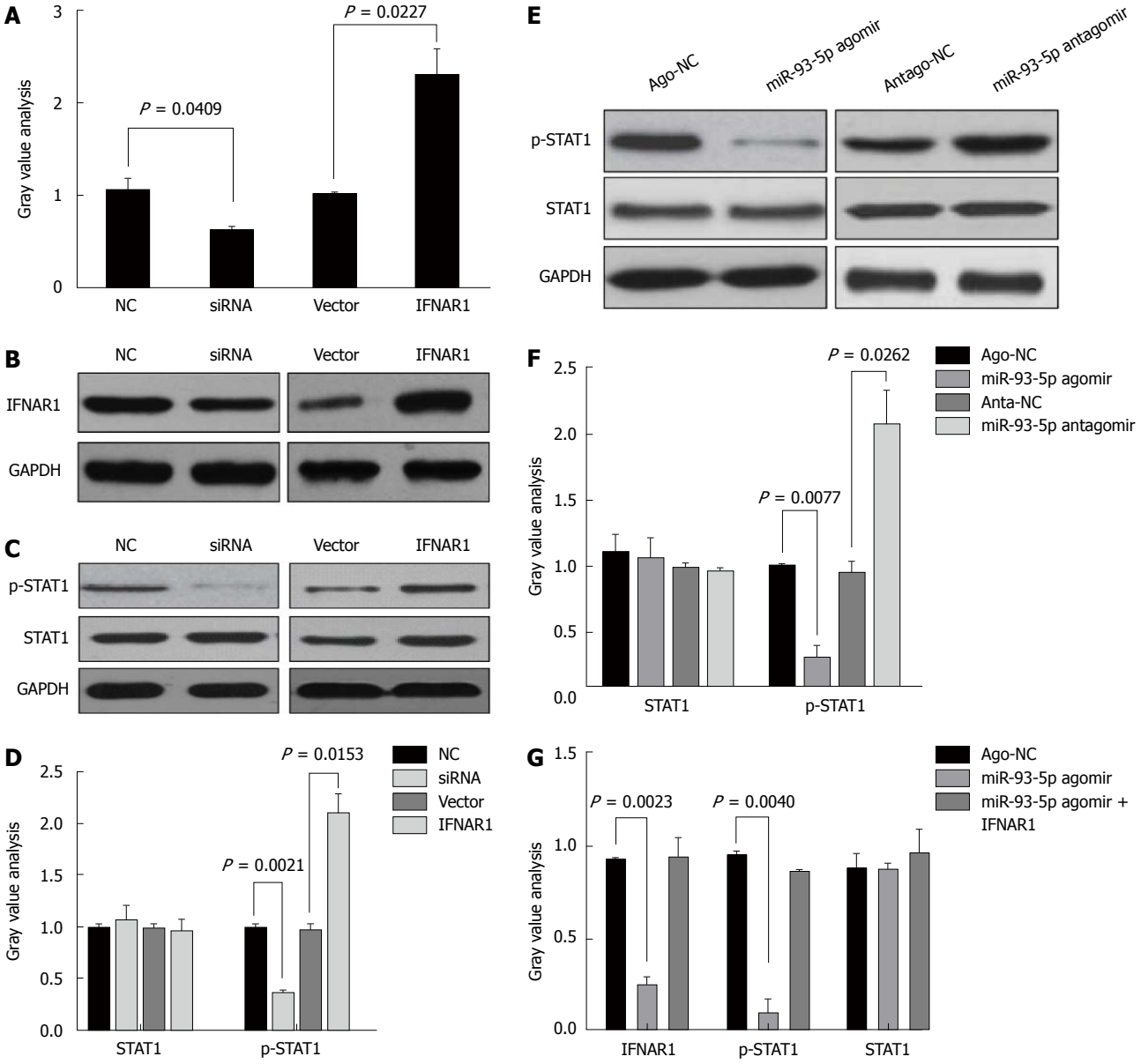

Figure 5 The miR-93-5p-IFNAR1 axis regulates the interferon signaling pathway. A: Western blot shows the protein expression of IFNAR1 in Huh7 cells transfected with NC (200 ng/mL), siRNA (200 ng/mL), vector (200 ng/mL), or IFNAR1 (200 ng/mL). This experiment was repeated twice; B and C: Western blot shows the phosphorylation level of STAT1 and the protein expression of STAT1 in Huh7 cells transfected with NC (200 ng/mL), siRNA (200 ng/mL), vector (200 ng/mL), or IFNAR1 (200 ng/mL). This experiment was repeated twice; D and E: Western blot shows the phosphorylation level of STAT1 and the protein expression of STAT1 in Huh7 cells transfected with ago-NC (200 nmol/L), miR-93-5p agomir (200 nmol/L), antago-NC (200 nmol/L), or miR-93-5p antagomir (200 nmol/L). This experiment was repeated twice; F and G: Western blot shows the phosphorylation level of STAT1 and the protein expression of STAT1 and IFNAR1 in Huh7 cells transfected with ago-NC (200 nmol/L), miR-93-5p agomir (200 nmol/L), or miR-93-5p agomir (200 nmol/L) plus IFNAR1 (200 ng/mL). IFNAR1: Interferon receptor 1.

analysis showed that IFNAR1 knockdown significantly decreased the phosphorylation level of STAT1 (P = 0.0021), but not the protein expression of STAT1, whereas IFNAR1 overexpression significantly increased the phosphorylation level of STAT1 (P = 0.0153) (Figure 5B and C). Furthermore, miR-93-5p agomir significantly decreased the phosphorylation level of STAT1 (P = 0.0077), whereas miR-93-5p inhibitors significantly increased it (P = 0.0262) (Figure 5D and E). To further confirm that the miR-93-5p-IFNAR1 axis could regulate STAT1 phosphorylation, a rescue assay was carried out. The results showed that IFNAR1 overexpression rescued miR-93-5p-induced decrease of STAT1 phosphorylation level in Huh7 cells (Figure 5F). These data suggest that the miR-93-5p-IFNAR1 axis regulates the STAT1 signaling pathway.

DISCUSSION

In the present study, we found that serum miR-93-5p expression was increased in patients with HCV-1b infection compared with healthy subjects, and was higher in HCV-1b-infected patients with pegylated IFNα resistance than in those with pegylated IFNα sensitivity. We also found that HCV-1b core protein could increase miR-93-5p expression and decrease

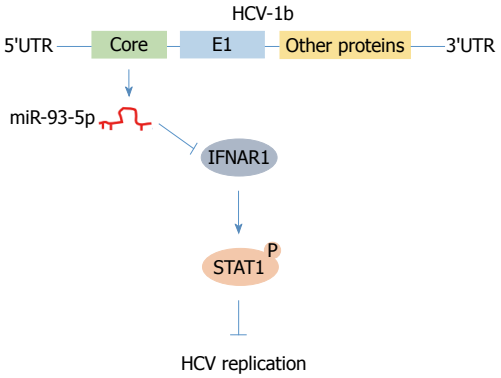

Figure 6 Schematic figure illustrating the mechanism that hepatitis C virus-1b core protein induces inactivation of the interferon signaling pathway *via* regulating miR-93-5p.

IFNAR1 expression, and further identified that IFNAR1 is a direct target of miR-93-5p. Furthermore, our findings showed that the miR-93-5p-IFNAR1 axis could regulate STAT1 phosphorylation.

MiR-93-5p belongs to the miR-106-25 cluster which plays a crucial role in cancer development. Yen *et al*[14] found that three miRNAs in the miR-106-25 cluster were overexpressed in HCC tissues and their data suggested that miR-93-5p was upregulated in HCV-associated HCC tissues. In addition, miR-93-5p overexpression was also involved in HCV-positive cirrhosis[21]. In our study, we found that miR-93-5p overexpression was associated with pegylated IFNα resistance of HCV-1b, which is the most prevalent type of HCV in China and highly resists to IFNα treatment. HCV core protein, an important component of HCV, promoted the dysregulation of miRNAs, such as miR-122[11]. However, whether HCV core protein regulates miR-93-5p expression remains largely unclear. Our findings demonstrated that HCV core protein increased miR-93-5p expression in Huh7 cells.

Ohta *et al*[15] demonstrated that miR-93 directly targets PTEN and CDKN1A, thereby activating proliferation and inhibiting apoptosis through the c-Met/PI3K/Akt pathway. In our study, we integrated five databases to find and further confirm that IFNAR1, a receptor of IFNα and IFNβ, is a potential target of miR-93-5p, implying that miR-93-5p has multiple targets in hepatocytes, but our data suggested that the miR-93-5p-IFNAR1 axis might be mainly involved in HCV-1b infection. Recently, Ma *et al*[22] showed that the miR-93-5p/IFNAR1 axis promotes gastric cancer metastasis by activating the STAT3 signaling pathway. These data strongly support our finding that IFNAR1 is a target of miR-93-5p in hepatocyte cells. We believe that similar mechanism in different types of cells may play different roles. As well known that IFNAR1 plays a crucial role in the IFN signaling pathway, our study then confirmed that the miR-93-5p-IFNAR1 axis regulates the phosphorylation level of STAT1, which is an important transcription factor in the IFN signaling pathway. Zhao *et al*[23] have confirmed that IFNAR mediates the IFN-α-triggered STAT signaling pathway, and inhibition of this pathway could increase HCV RNA replication. These data strongly support our finding that the miR-93-5p-IFNAR1 axis regulates STAT1 phosphorylation and thereby affects the therapeutic effect of pegylated IFNα.

In addition, HCV infection could reduce the protein expression of STAT1 and STAT3 by promoting proteasomal degradation[24], but our data revealed that HCV-1b infection could regulate STAT1 phosphorylation *via* the miR-93-5p-IFNAR1 axis. Although we identified the role and mechanism of miR-93-5p in regulating the IFN signaling pathway in Huh7 cells, an *in vivo* study needs to be performed in the future.

In conclusion, we found that HCV-1b core protein increased miR-93-5p expression and identified that IFNAR1 is a direct target of miR-93-5p. Moreover, the miR-93-5p-IFNAR1 axis regulated STAT1 phosphorylation, suggesting that this axis might be a novel therapeutic target for HCV-1b infection (Figure 6).

ARTICLE HIGHLIGHTS

Research background

Hepatitis C virus (HCV)-1b core protein is an important component of HCV and plays a crucial role in HCV infection and pegylated IFNα resistance, but the mechanism underlying HCV core protein-induced pegylated IFNα resistance remains unclear.

Research motivation

Our findings highlight the mechanism that HCV-1b core protein induces pegylated IFNα resistance *via* regulating the miR-93-5p-interferon receptor 1 (IFNAR1) axis. This axis may be a potential therapeutic target for HCV-1b treatment.

Research objectives

The objective of this study was to elucidate why HCV-1b causes pegylated IFNα resistance. It is partially realized and provides a clue for drug design of HCV-1b treatment.

Research methods

The research methods included cell culture, RNA extraction, qRT-PCR, vector construct, oligonucleotide transfection, luciferase assay, and Western blot. Data analysis was performed using multiple statistical methods that include the Mann-Whitney test, two-tailed Student's *t*-test, one-way ANOVA, and Pearson's correlation. Eighty-four patients with HCV-1b infection and 84 healthy subjects were enrolled in this study.

Research results

This study found that serum miR-93-5p expression was increased in patients with HCV-1b infection and HCV-1b core protein increased miR-93-5p expression, identified that IFNAR1 is a target of miR-93-5p, and further demonstrated that the miR-93-5p-IFNAR1 axis regulated the IFN signaling pathway.

Research conclusions

This study found that HCV-1b increases miR-93-5p expression, IFNAR1 is a target of miR-93-5p in hepatocyte, and miR-93-5p-IFNAR1 axis regulates the IFN signaling pathway. This study also provided some evidence that HCV-1b induces pegylated IFNα resistance by regulating the miR-93-5p-IFNAR1 axis, suggesting that the miR-93-5p-IFNAR1 axis might be a potential therapeutic target for HCV-1b infection.

Research perspectives

This study demonstrated the mechanism by which miR-93-5p inhibits the IFN

signaling pathway *in vitro*, but an *in vivo* study needs to be performed in the future. The design of siRNAs which exclusively destroy the miR-93-5p-IFNAR1 axis may be important for improving the therapeutic effect of pegylated IFNα.

REFERENCES

1 **Thomas DL**. Global control of hepatitis C: where challenge meets opportunity. *Nat Med* 2013; **19**: 850-858 [PMID: 23836235 DOI: 10.1038/nmol/L.3184]

2 **Dubuisson J**, Cosset FL. Virology and cell biology of the hepatitis C virus life cycle: an update. *J Hepatol* 2014; **61**: S3-S13 [PMID: 25443344 DOI: 10.1016/j.jhep.2014.06.031]

3 **Horsley-Silva JL**, Vargas HE. New Therapies for Hepatitis C Virus Infection. *Gastroenterol Hepatol* (NY) 2017; **13**: 22-31 [PMID: 28420944]

4 **Manns MP**, McHutchison JG, Gordon SC, Rustgi VK, Shiffman M, Reindollar R, Goodman ZD, Koury K, Ling M, Albrecht JK. Peginterferon alfa-2b plus ribavirin compared with interferon alfa-2b plus ribavirin for initial treatment of chronic hepatitis C: a randomised trial. *Lancet* 2001; **358**: 958-965 [PMID: 11583749 DOI: 10.1016/S0140-6736(01)06102-5]

5 **Palisoc AM,** Fayad J, Singh AK, Farnham IM. Induction therapy of interferon alfa-2b in combination with ribavirin as initial treatment for chronic hepatitis C genotype 1: A pilot study. *Am J Gastroenterol* 2006; **101**: S164-S164

6 **Ascione A**, De Luca M, Tartaglione MT, Lampasi F, Di Costanzo GG, Lanza AG, Picciotto FP, Marino-Marsilia G, Fontanella L, Leandro G. Peginterferon alfa-2a plus ribavirin is more effective than peginterferon alfa-2b plus ribavirin for treating chronic hepatitis C virus infection. *Gastroenterology* 2010; **138**: 116-122 [PMID: 19852964 DOI: 10.1053/j.gastro.2009.10.005]

7 **Pawlotsky JM**. New hepatitis C therapies: the toolbox, strategies, and challenges. *Gastroenterology* 2014; **146**: 1176-1192 [PMID: 24631495 DOI: 10.1053/j.gastro.2014.03.003]

8 **Lindow M**, Kauppinen S. Discovering the first microRNA-targeted drug. *J Cell Biol* 2012; **199**: 407-412 [PMID: 23109665 DOI: 10.1083/jcb.201208082]

9 **Pedersen IM**, Cheng G, Wieland S, Volinia S, Croce CM, Chisari FV, David M. Interferon modulation of cellular microRNAs as an antiviral mechanism. *Nature* 2007; **449**: 919-922 [PMID: 17943132 DOI: 10.1038/nature06205]

10 **Boldanova T**, Suslov A, Heim MH, Necsulea A. Transcriptional response to hepatitis C virus infection and interferon-alpha treatment in the human liver. *EMBO Mol Med* 2017; **9**: 816-834 [PMID: 28360091 DOI: 10.15252/emmm.201607006]

11 **Kim GW**, Lee SH, Cho H, Kim M, Shin EC, Oh JW. Hepatitis C Virus Core Protein Promotes miR-122 Destabilization by Inhibiting GLD-2. *PLoS Pathog* 2016; **12**: e1005714 [PMID: 27366906 DOI: 10.1371/journal.ppat.1005714]

12 **Cheng M**, Si Y, Niu Y, Liu X, Li X, Zhao J, Jin Q, Yang W. High-throughput profiling of alpha interferon- and interleukin-28B-regulated microRNAs and identification of let-7s with anti-hepatitis C virus activity by targeting IGF2BP1. *J Virol* 2013; **87**: 9707-9718 [PMID: 23824794 DOI: 10.1128/JVI.00802-13]

13 **Singaravelu R**, Russell RS, Tyrrell DL, Pezacki JP. Hepatitis C virus and microRNAs: miRed in a host of possibilities. *Curr Opin Virol* 2014; **7**: 1-10 [PMID: 24721496 DOI: 10.1016/j.coviro.2014.03.004]

14 **Yen CS**, Su ZR, Lee YP, Liu IT, Yen CJ. miR-106b promotes cancer progression in hepatitis B virus-associated hepatocellular carcinoma. *World J Gastroenterol* 2016; **22**: 5183-5192 [PMID: 27298561 DOI: 10.3748/wjg.v22.i22.5183]

15 **Ohta K**, Hoshino H, Wang J, Ono S, Iida Y, Hata K, Huang SK, Colquhoun S, Hoon DS. MicroRNA-93 activates c-Met/PI3K/Akt pathway activity in hepatocellular carcinoma by directly inhibiting PTEN and CDKN1A. *Oncotarget* 2015; **6**: 3211-3224 [PMID: 25633810 DOI: 10.18632/oncotarget.3085]

16 **Li BS**, Zhao YL, Guo G, Li W, Zhu ED, Luo X, Mao XH, Zou QM, Yu PW, Zuo QF, Li N, Tang B, Liu KY, Xiao B. Plasma microRNAs, miR-223, miR-21 and miR-218, as novel potential biomarkers for gastric cancer detection. *PLoS One* 2012; **7**: e41629 [PMID: 22860003 DOI: 10.1371/journal.pone.0041629]

17 **Huang CF**, Huang JF, Yang JF, Hsieh MY, Lin ZY, Chen SC, Wang LY, Juo SH, Chen KC, Chuang WL, Kuo HT, Dai CY, Yu ML. Interleukin-28B genetic variants in identification of hepatitis C virus genotype 1 patients responding to 24 weeks peginterferon/ribavirin. *J Hepatol* 2012; **56**: 34-40 [PMID: 21703176 DOI: 10.1016/j.jhep.2011.03.029]

18 **de Weerd NA**, Matthews AY, Pattie PR, Bourke NM, Lim SS, Vivian JP, Rossjohn J, Hertzog PJ. A hot spot on interferon α/β receptor subunit 1 (IFNAR1) underpins its interaction with interferon-β and dictates signaling. *J Biol Chem* 2017; **292**: 7554-7565 [PMID: 28289093 DOI: 10.1074/jbc.M116.773788]

19 **Hurtado-Guerrero I**, Pinto-Medel MJ, Urbaneja P, Rodriguez-Bada JL, León A, Guerrero M, Fernández Ó, Leyva L, Oliver-Martos B. Activation of the JAK-STAT Signaling Pathway after In Vitro Stimulation with IFNß in Multiple Sclerosis Patients According to the Therapeutic Response to IFNß. *PLoS One* 2017; **12**: e0170031 [PMID: 28103257 DOI: 10.1371/journal.pone.0170031]

20 **Chmiest D**, Sharma N, Zanin N, Viaris de Lesegno C, Shafaq-Zadah M, Sibut V, Dingli F, Hupé P, Wilmes S, Piehler J, Loew D, Johannes L, Schreiber G, Lamaze C. Spatiotemporal control of interferon-induced JAK/STAT signalling and gene transcription by the retromer complex. *Nat Commun* 2016; **7**: 13476 [PMID: 27917878 DOI: 10.1038/ncomms13476]

21 **Oksuz Z**, Serin MS, Kaplan E, Dogen A, Tezcan S, Aslan G, Emekdas G, Sezgin O, Altintas E, Tiftik EN. Serum microRNAs; miR-30c-5p, miR-223-3p, miR-302c-3p and miR-17-5p could be used as novel non-invasive biomarkers for HCV-positive cirrhosis and hepatocellular carcinoma. *Mol Biol Rep* 2015; **42**: 713-720 [PMID: 25391771 DOI: 10.1007/s11033-014-3819-9]

22 **Ma DH**, Li BS, Liu JJ, Xiao YF, Yong X, Wang SM, Wu YY, Zhu HB, Wang DX, Yang SM. miR-93-5p/IFNAR1 axis promotes gastric cancer metastasis through activating the STAT3 signaling pathway. *Cancer Lett* 2017; **408**: 23-32 [PMID: 28842285 DOI: 10.1016/j.canlet.2017.08.017]

23 **Zhao LJ**, He SF, Liu Y, Zhao P, Bian ZQ, Qi ZT. Inhibition of STAT Pathway Impairs Anti-Hepatitis C Virus Effect of Interferon Alpha. *Cell Physiol Biochem* 2016; **40**: 77-90 [PMID: 27855377 DOI: 10.1159/000452526]

24 **Stevenson NJ**, Bourke NM, Ryan EJ, Binder M, Fanning L, Johnston JA, Hegarty JE, Long A, O'Farrelly C. Hepatitis C virus targets the interferon-α JAK/STAT pathway by promoting proteasomal degradation in immune cells and hepatocytes. *FEBS Lett* 2013; **587**: 1571-1578 [PMID: 23587486 DOI: 10.1016/j.febslet.2013.03.041]

P- Reviewer: Kocazeybek B, Watanabe T **S- Editor**: Chen K
L- Editor: Wang TQ **E- Editor**: Li RF

World Journal of Gastroenterology

Submit a Manuscript: http://www.f6publishing.com

World J Gastroenterol 2018 January 14; 24(2): 237-247

DOI: 10.3748/wjg.v24.i2.237

ISSN 1007-9327 (print) ISSN 2219-2840 (online)

ORIGINAL ARTICLE

Basic Study

Transplantation of bone marrow-derived endothelial progenitor cells and hepatocyte stem cells from liver fibrosis rats ameliorates liver fibrosis

Ling Lan, Ran Liu, Ling-Yun Qin, Peng Cheng, Bo-Wei Liu, Bing-Yong Zhang, Song-Ze Ding, Xiu-Ling Li

Ling Lan, Bo-Wei Liu, Bing-Yong Zhang, Song-Ze Ding, Xiu-Ling Li, Department of Gastroenterology and Hepatology, the People's Hospital of Zhengzhou University (the Henan Provincial People's Hospital), Zhengzhou 450003, Henan Province, China

Ran Liu, Department of Oncology, Henan Provincial Rongjun Hospital, Xinxiang 453000, Henan Province, China

Ling-Yun Qin, Department of Gastroenterology and Hepatology, the Children's Hospital of Zhengzhou, Zhengzhou 450003, Henan Province, China

Peng Cheng, Intensive Care Unit, the Second Affiliated Hospital of Luohe Medical College, Luohe 462000, Henan Province, China

ORCID number: Ling Lan (0000-0001-9744-4545); Ran Liu (0000-0001-6083-8049); Ling-Yun Qin (00 00-000 1-6341-2895); Peng Cheng (0000-0001-5217-8693); Bo-Wei Liu (0 000-00 03-1664-5172); Bing-Yong Zhang (00 00-0003-4980-7246); Song-Ze Ding (0000-0002-4589-6942); Xiu-Ling Li (0000-0 002-3313-4801).

Author contributions: Lan L and Liu R contributed equally to this study and are the co-first authors; Lan L and Liu R designed the study; Lan L, Liu R, Qin LY, Cheng P and Zhang BY performed the study; Lan L, Liu R and Qin LY wrote the paper; Liu BW and Zhang BY established the rat models; Ding SZ and Li XL collected and analyzed the data.

Supported by the National Natural Science Foundation of China, No. 30900598; the Basic and Advanced Technology Research Program of Henan Province, No. 142300410380; and the Medical Science and Technology Project of Henan Province, No. 201303211.

Institutional review board statement: The study was reviewed and approved by the Institutional Review Board of Henan Provincial People's Hospital, China.

Institutional animal care and use committee statement: All procedures involving animals were reviewed and approved by the Institutional Animal Care and Use committee of the Animal Experiment Center of Henan Province, China [SCXK(Yu)2005-0001].

Conflict-of-interest statement: Potential conflicts of interest do not exist.

Data sharing statement: No additional data are available.

Manuscript source: Unsolicited manuscript

Correspondence to: Ling Lan, PhD, MD, Associate Professor, Department of Gastroenterology and Hepatology, the People's Hospital of Zhengzhou University (the Henan Provincial People's Hospital), 7 Weiwu Road, Zhengzhou 450003, Henan Province, China. lanling95@163.com
Telephone: +86-371-65580603
Fax: +86-371-6596 4376

Received: September 30, 2017
Peer-review started: October 1, 2017
First decision: October 25, 2017
Revised: November 6, 2017
Accepted: November 22, 2017
Article in press: November 22, 2017
Published online: January 14, 2018

Abstract

AIM

To explore the effectiveness for treating liver fibrosis

by combined transplantation of bone marrow-derived endothelial progenitor cells (BM-EPCs) and bone marrow-derived hepatocyte stem cells (BDHSCs) from the liver fibrosis environment.

METHODS

The liver fibrosis rat models were induced with carbon tetrachloride injections for 6 wk. BM-EPCs from rats with liver fibrosis were obtained by different rates of adherence and culture induction. BDHSCs from rats with liver fibrosis were isolated by magnetic bead cell sorting. Tracing analysis was conducted by labeling EPCs with PKH26 *in vitro* to show EPC location in the liver. Finally, BM-EPCs and/or BDHSCs transplantation into rats with liver fibrosis were performed to evaluate the effectiveness of BM-EPCs and/or BDHSCs on liver fibrosis.

RESULTS

Normal functional BM-EPCs from liver fibrosis rats were successfully obtained. The co-expression level of CD133 and VEGFR2 was 63.9% ± 2.15%. Transplanted BM-EPCs were located primarily in/near hepatic sinusoids. The combined transplantation of BM-EPCs and BDHSCs promoted hepatic neovascularization, liver regeneration and liver function, and decreased collagen formation and liver fibrosis degree. The VEGF levels were increased in the BM-EPCs (707.10 ± 54.32) and BM-EPCs/BDHSCs group (615.42 ± 42.96), compared with those in the model group and BDHSCs group ($P < 0.05$). Combination of BM-EPCs/BDHSCs transplantation induced maximal up-regulation of PCNA protein and HGF mRNA levels. The levels of alanine aminotransferase (AST), aspartate aminotransferase, total bilirubin (TBIL), prothrombin time (PT) and activated partial thromboplastin time in the BM-EPCs/BDHSCs group were significantly improved, to be equivalent to normal levels ($P > 0.05$) compared with those in the BDHSC (AST, TBIL and PT, $P < 0.05$) and BM-EPCs (TBIL and PT, $P < 0.05$) groups. Transplantation of BM-EPCs/BDHSCs combination significantly reduced the degree of liver fibrosis (staging score of 1.75 ± 0.25 *vs* BDHSCs 2.88 ± 0.23 or BM-EPCs 2.75 ± 0.16, $P < 0.05$).

CONCLUSION

The combined transplantation exhibited maximal therapeutic effect compared to that of transplantation of BM-EPCs or BDHSCs alone. Combined transplantation of autogenous BM-EPCs and BDHSCs may represent a promising strategy for the treatment of liver fibrosis, which would eventually prevent cirrhosis and liver cancer.

Key words: Bone marrow; Endothelial progenitor cells; Liver stem cell; Cell transplantation; Liver fibrosis

Core tip: In addition to liver regeneration, hepatic neovascularization and endothelial/sinusoidal remodeling are critical factors for the treatment of liver fibrosis. Bone marrow-derived endothelial progenitor cells (BM-EPCs) have been shown to play a role in hepatic angiogenesis and to be beneficial in liver fibrosis. However, BM-EPCs are all derived from healthy individuals in recent studies. Here, we evaluated the feasibility of obtaining normal BM-EPCs from rats with liver fibrosis, and the effectiveness of combined transplantation of BM-EPCs and bone marrow-derived hepatocyte stem cells for treating liver fibrosis in order to achieve the dual effects of hepatic neovascularization and liver regeneration.

Lan L, Liu R, Qin LY, Cheng P, Liu BW, Zhang BY, Ding SZ, Li XL. Transplantation of bone marrow-derived endothelial progenitor cells and hepatocyte stem cells from liver fibrosis rats ameliorates liver fibrosis. *World J Gastroenterol* 2018; 24(2): 237-247 Available from: URL: http://www.wjgnet.com/1007-9327/full/v24/i2/237.htm DOI: http://dx.doi.org/10.3748/wjg.v24.i2.237

INTRODUCTION

Liver fibrosis is the scarring process involved in the response of liver to injury. Most hepatocellular carcinoma, which is among the leading causes of cancer death worldwide, develops in the context of severe liver fibrosis and cirrhosis. Liver fibrosis is a necessary stage for cirrhosis and liver cancer. Bone marrow stem cells (BMSCs) have been recently used to treat liver fibrosis; whereas, BMSCs transplantation is not an effective treatment for liver fibrosis, due to the histopathological characteristics of liver fibrosis including deposition of excessive extracellular matrix, remodeling of abnormal vascular and sinusoid constriction[1-6]. Low levels of engraftment and proliferation of exogenous cells in the liver parenchyma[4,7], inhibition of endogenous liver regeneration[4] and lack of a role in promoting hepatic neovascularization are the potential major drawbacks of BMSC transplantation therapy[8].

Endothelial progenitor cells (EPCs) have been shown to play a function in angiogenesis and vasculogenesis[9]. EPCs have been used for the treatment of liver fibrosis/cirrhosis in rats[10-15]. Previous studies demonstrated that transplantation of bone marrow-derived EPCs (BM-EPCs) have a potential role in hepatic neovascularization, endothelial/sinusoidal remodeling and increased hepatic blood flow[10,13]. However, BM-EPCs were all derived from healthy rats in these studies. In the present study, we sought to evaluate the feasibility of clinical application of autogenous EPCs therapy by using normal BM-EPCs obtained from liver fibrosis rats.

Furthermore, loss and destruction of functional

hepatocytes is another feature of liver fibrosis[16]. BMSCs have been shown to restore and regenerate hepatic tissue[17]. Our previous study demonstrated that β_2m^-/Thy-1^+ bone marrow-derived hepatocyte stem cells (BDHSCs) derived from the pathoenvironment of liver injury in rats, which could be hepatocyte progenitors[18], promoted hepatocyte proliferation and liver regeneration in liver fibrosis rats[19]. Thus, a combined transplantation of BM-EPCs and BDHSCs may be more beneficial to liver fibrosis than transplantation of BM-EPCs or BDHSCs alone.

In the present study, we successfully obtained normal EPCs *in vitro* from bone marrow in liver fibrosis rats and evaluated the effectiveness of combined transplantation of BM-EPCs and BDHSCs *in vivo* for the treatment of liver fibrosis.

MATERIALS AND METHODS

Ethics and animals

Wistar rats (male, 8 wk, 250-300 g) (Animal Experiment Center of Henan Province, China) were housed in a standard animal laboratory. Animal studies were approved by the Animal Ethics Committee of Zhengzhou University and were in compliance with the Chinese National Regulations on the Use of Experimental Animals.

Isolation and culture of BM-EPCs and BDHSCs

The isolation and culture of BM-EPCs and BDHSCs were performed as described by Smadja *et al*[20] and Schatteman *et al*[21]. Wistar rats were subcutaneously injected with a 2:3 solution of carbon tetrachloride (CCl_4) and olive oil at a dose of 3 mL/kg body weight (double doses for the first time) twice per week for 6 wk to induce liver fibrosis. Bone marrow cells of rats with liver fibrosis were obtained by flushing femurs and humerus with DMEM/F12 medium (Gibco, New York, NY, United States). Bone marrow mononuclear cells (BMMCs) were then isolated by density gradient centrifugation with Histopaque 1077 (Sigma-Aldrich, St. Louis, MO, United States) from bone marrow cells. After washing with red blood cell lysis buffer, BMMCs were seeded into culture flasks in DMEM/F12 medium supplemented with 10% fetal bovine serum (Gibco). After 24 h, the plastic-adherent cells were removed, and the nonadherent cells were collected, washed and replated into fibronectin-coated (10 μg/mL; BD Biosciences, San Jose, CA, United States) culture flasks with the inducing medium containing DMEM/F12 medium supplemented with 10% fetal bovine serum, 20 ng/mL vascular endothelial growth factor (VEGF), 5 ng/mL basic fibroblast growth factor, 5 ng/mL epidermal growth factor (EGF) and 10 ng/mL insulin-like growth factor-1 (Peprotech, New Jersey, NJ, United States) and antibiotics (100 U/mL penicillin and 100 μg/mL streptomycin). β_2m^-/Thy-1^+ BDHSCs of rats with liver fibrosis were selected and purified by magnetic bead cell sorting as previously reported[18-22].

Flow cytometry for phenotypes of BM-EPCs

After 10 d of culture under inducing conditions, 2×10^6 BM-EPCs were incubated with the FcR blocking reagent (Miltenyi Biotec Inc., Auburn, CA, United States) and fluorescein isothiocyanate (FITC)-conjugated rabbit anti-rat CD133 antibody (BD Biosciences) and rabbit anti-rat vascular endothelial growth factor receptor 2 (VEGFR2) antibody (BD Biosciences) for 30 min at 4 ℃, respectively. Then, cells were incubated with phycoerythrin (PE)-conjugated goat anti-rabbit secondary antibody (BD Biosciences) for 30 min at 4 ℃. The phenotypic expression of BM-EPCs was analyzed by flow cytometry (FACS Scan flow cytometer; BD). BMMCs (2×10^6) cultured without induction for 10 d were used as a control.

Functional identification of BM-EPCs

BM-EPCs induced for 10 d were incubated with the inducing medium with 1,1'-dioctadecyl-3,3,3',3'-tetramethyl indocarbocyanine perchlorate-labeled acetylated low-density lipoprotein (DiI-acLDL) (Molecular Probes, Eugene, OR, United States) for 4 h at 37 ℃ in the dark. The cells were fixed with 4% paraformaldehyde for 20 min and incubated with the inducing medium with FITC-conjugated ulex europaeus agglutinin I (FITC-UEA-I) (Sigma-Aldrich) for 1 h at 37 ℃ in the dark. The cells were photographed under a fluorescence microscope.

For the analysis of capillary tube formation, Matrigel (BD Biosciences, Heidelberg, Germany) was added to the wells of a pre-cooling 24-well plate at 0 ℃, and allowed to solidify at 37 ℃ for 40 min. After 10 d of culture induction, BM-EPCs with the inducing medium were added into the wells (8×10^5 cells/well). Capillary tube formation on Matrigel was observed under an optical microscope after 24 h of incubation.

Cytokinetics of BM-EPCs

BM-EPCs induced for 10 d were seeded in a 96-well plate and divided into 3 groups: (1) the blank control group, containing only culture medium; (2) the experimental group, containing BM-EPCs from rats with liver fibrosis; and (3) the control group, containing BM-EPCs of normal rats. The cells were cultured in the incubator with 37 ℃, 5% CO_2. 2-(2-methoxy-4-nitrophenyl)-3-(4-nitrophenyl)-5-(2,4-sulfophenyl)-2*H*-tetrazole monosodium salt (WST-8) (Neuron Science and Technology Development Co., Ltd., Beijing, China) was added to the plate (10 μL/well, once/24 h) for 10 d. The values of optical density (OD) at 490 nm were detected by a microplate reader and the cytokinetics of BM-EPCs were analyzed.

Labeling and tracing of BM-EPCs in the liver

BM-EPCs were labeled with PKH26 (Sigma-Aldrich), according to the manufacturer's instructions. PKH26-

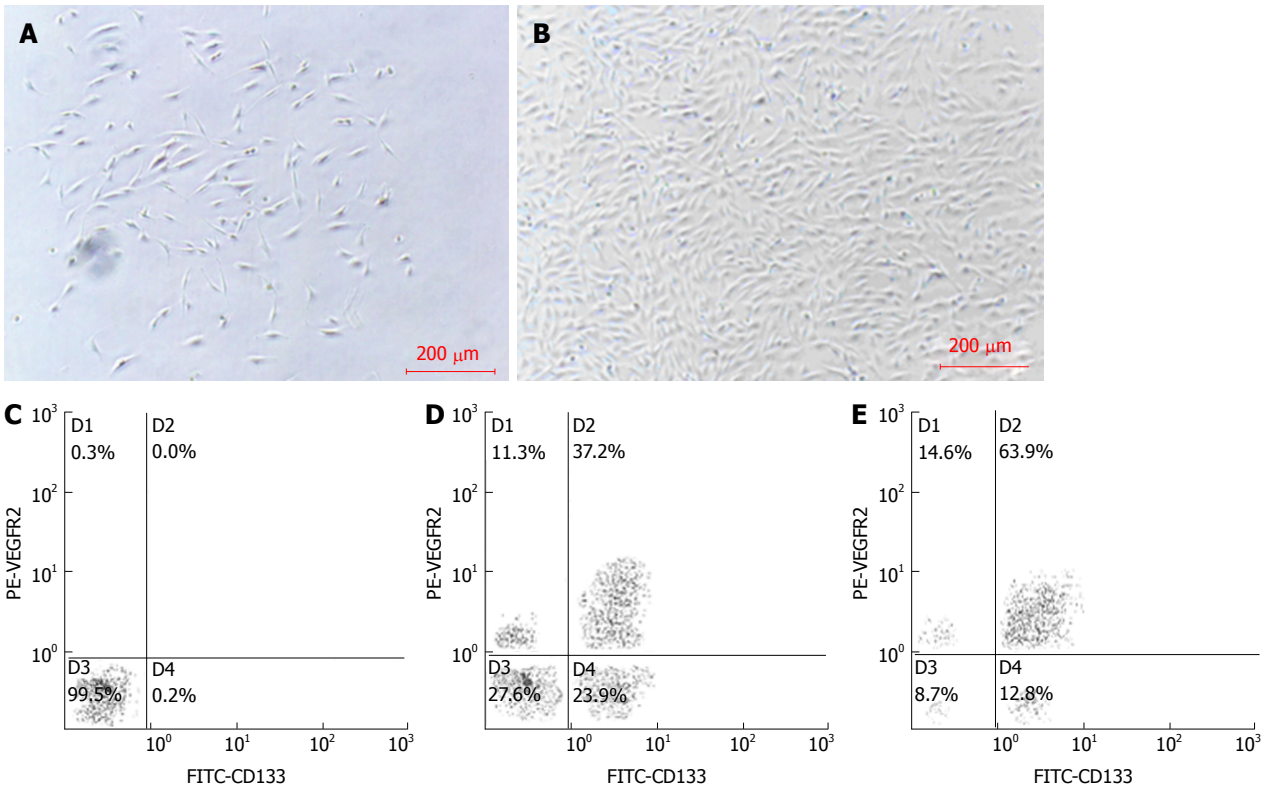

Figure 1 Morphology and phenotypes of BM-EPCs of rats with liver fibrosis, as shown by flow cytometry. A: Adherent cells cultured with induction for 4 d; B: Cell colonies cultured with induction for 10 d; C: Negative control without fluorescence-labeled BM-EPCs; D: Cells cultured without induction for 10 d; E: BM-EPCs cultured with induction for 10 d. Bars: 200 μm.

labeled BM-EPCs were transfused into rats *via* the tail vein after the rats were treated with CCl_4 for 3 and 5 wk. After 6 wk of modeling, the liver tissues were excised, and frozen sections were prepared. PKH26-positive cells were examined by using a fluorescence microscope. The liver sections of CCl_4-treated rats transfused with PBS served as a negative control.

CCl_4-induced liver fibrosis rat models and transplantation experiments

Liver fibrosis rat models were induced with CCl_4 as described above. The same volume of olive oil was used as a control. Forty rats were randomly divided into five groups (8 rats/group) as follows: (1) the negative group, rats treated with olive oil were transfused with PBS after 3, 4 and 5 wk of modeling; (2) the positive control group, rats treated with CCl_4 were transfused with PBS after 3, 4 and 5 wk; (3) the BDHSCs group, rats treated with CCl_4 were transfused with PBS containing BDHSCs after 3, 4 and 5 wk of CCl_4 induction; (4) the BM-EPCs group, rats treated with CCl_4 were transfused with PBS containing BM-EPCs after 3, 4 and 5 wk; and (5) the BM-EPCs/BDHSCs group, rats treated with CCl_4 were transfused with PBS containing BDHSCs after 4 wk of induction, and BM-EPCs after 3 and 5 wk. The transfusion after 4 wk of induction was 2×10^5 cells *via* the branch of portal vein, and transfusion after 3 or 5 wk was 2×10^6 cells *via* the tail vein. Rats were sacrificed after 6 wk of CCl_4 induction. The blood samples were collected from celiac artery for immediate biochemical detection. The liver tissues were stored at -80 ℃ or fixed in 10% formaldehyde for future analysis.

Masson's trichrome collagen staining of the liver

The liver tissues fixed with formaldehyde were embedded in paraffin, and then stained with Masson's trichrome collagen staining. The stages of liver fibrosis were graded by the semiquantitative staging scores as follows: 0, no collagen fibers; 1, slight fibrosis, collagen fibers located in the central liver lobule; 2, moderate fibrosis, widened central collagen fibers; 3, severe fibrosis, collagen fibers extended to the edge of liver lobule; 4, liver cirrhosis, pseudolobuli formation[23].

Immunohistochemistry for VEGF and proliferating cell nuclear antigen (PCNA) in the liver

The liver tissue paraffin-embedded sections were blocked with 0.3% H_2O_2 in methanol for endogenous peroxidase activity, incubated with mouse anti-rat VEGF or PCNA monoclonal antibody (Santa Cruz Biotechnology, Dallas, TX, United States) and peroxidase-conjugated rabbit anti-mouse IgG (Santa Cruz Biotechnology). The sections were stained with diaminobenzidine and counterstained with hematoxylin. Quantification of PCNA expression was carried out by measuring the integrated optical density (IOD) of positive staining area using the ImagePro plus

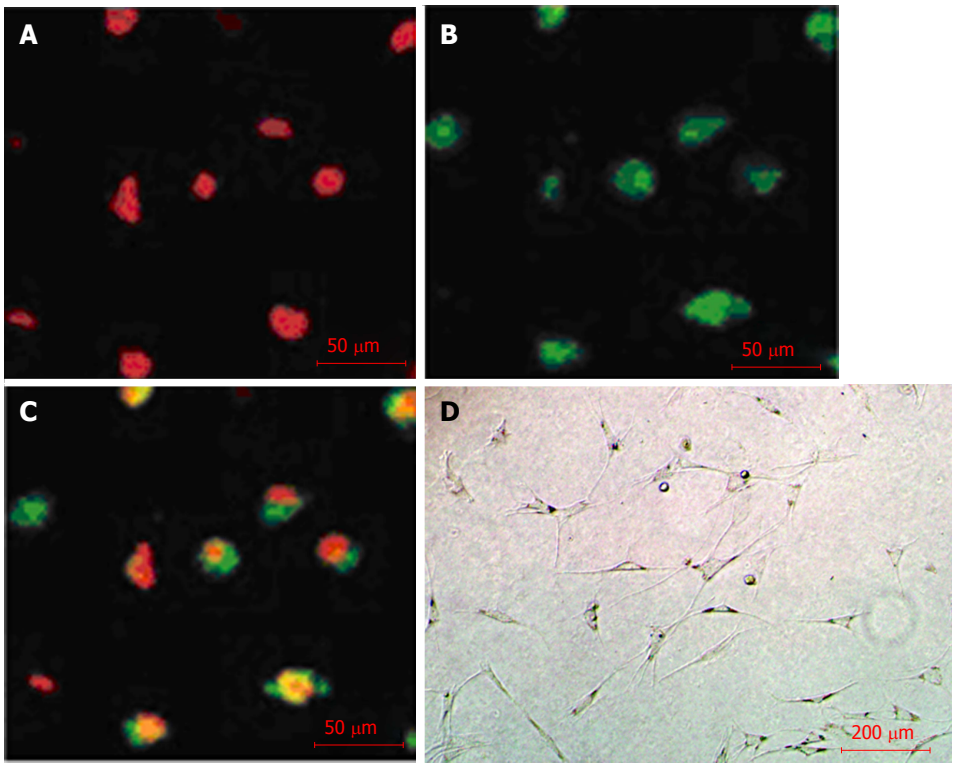

Figure 2 Phagocytosis and vasculogenesis functions of BM-EPCs of liver fibrosis rats. A: Bone marrow-derived endothelial progenitor cells uptake of Dil-ac-LDL (red); B: BM-EPCs binding with FITC-UEA-1 (green); C: Merge of A and B (yellow); D: Vascular network-like structures of BM-EPCs on Matrigel. Bars: 50 μm (A-C); 200 μm (D); BM-EPCs: Bone marrow-derived endothelial progenitor cells.

Table 1 Semiquantitative staging scores of liver fibrosis by Masson staining

Group	*n*	Stage, *n*					Score
		0	1	2	3	4	
Normal	8	8	0	0	0	0	0
Model	8	0	0	1	6	1	3.00 ± 0.19^{a}
BDHSCs	8	0	0	2	5	1	2.88 ± 0.23^{a}
BM-EPCs	8	0	0	2	6	0	2.75 ± 0.16^{a}
BM-EPCs/BDHSCs	8	0	3	4	1	0	$1.75 \pm 0.25^{a,c,e,g}$

Scores are presented as mean ± SD. $^{a}P < 0.05$ *vs* normal group; $^{c}P < 0.05$ *vs* model group; $^{e}P < 0.05$ *vs* BDHSCs group; $^{g}P < 0.05$ *vs* BM-EPCs group.

image analysis software. Three random areas were selected per slide from two slides per sample.

Enzyme-linked immunosorbent assay for VEGF in the liver

The wet liver tissues (100 mg per sample) were homogenized in 1 mL PBS in the presence of 1% protease inhibitors (Sigma-Aldrich). The supernatant fractions of liver homogenates were used to measure the VEGF levels according to the manufacturer's instructions using Rat VEGF Quantikine Enzyme-linked immunosorbent assay (ELISA) Kits (R&D Systems, Minneapolis, MN, United States).

Real-time quantitative reversely transcribed polymerase chain reaction for hepatocyte growth factor in the liver

The extracted total RNA of liver tissues was reverse transcribed into cDNA using ExScriptTM RT reagent Kit (Takara, Kusatsu, Japan). Real-time quantitative polymerase chain reaction (PCR) was performed using SYBR green Ⅱ (Takara) on a Light Cycler (Roche Diagnostics GmbH, Penzberg, Germany). The forward and reverse primers were as follows: HGF (NM_017017, 122 bp), 5′-TTTCCCGTTGTGAAGGAGAT-3′ and 5′-CCCTACTGTTGTTTGTGTTGGA-3′; GAPDH (NM_017008, 92 bp), 5′-GACATGCCGCCTGGAGAAAC-3′ and 5′-AGCCCAGGATGCCCTTTAGT-3′. Real-time PCR was performed at 95 ℃ for 10 min, followed by 40 cycles of 95 ℃ for 10 s, 60 ℃ for 60 s. To ensure specific amplification, a melting curve was generated at the end of the PCR for each sample. Hepatocyte growth factor (HGF) mRNA quantities were determined by comparative CT method by the Light Cycler software.

Liver biochemical assays in the blood

The biochemical indices of liver function, including alanine aminotransferase aspartate (ALT), aspartate aminotransferase (AST) and total bilirubin (TBIL) in serum, and prothrombin time (PT) and activated partial thromboplastin time (APTT) in plasma, were detected by using an automated analyzer (LX20; Beckman Coulter, Brea, CA, United States).

Statistical analysis

All data were presented as means ± SD and analyzed using SPSS 17.0 statistical software. The differences between the mean values of each group were compared by the one-way analysis of variance (ANOVA) or Kruskal-Wallis test as appropriate, and considered to

Table 2 Biochemical indexes of liver function in the blood

Group	*n*	ALT, IU/L	AST, IU/L	TBIL, μmol/L	PT, s	APTT, s
Normal	8	62.5 ± 12.7	153.5 ± 13.6	6.6 ± 0.3	16.6 ± 1.0	21.9 ± 1.5
Model	8	144.8 ± 61.5[a]	269.6 ± 83.3[a]	17.3 ± 2.6[a]	20.5 ± 1.1[a]	26.2 ± 2.8[a]
BDHSCs	8	70.4 ± 19.5[c]	260.4 ± 84.2[a]	13.5 ± 1.8[ac]	19.5 ± 1.3[a]	20.1 ± 2.7[c]
BM-EPCs	8	65.8 ± 26.5[c]	159.3 ± 41.3[c]	14.3 ± 2.3[ag]	19.4 ± 1.4[a]	19.9 ± 2.2[c]
BM-EPCs/BDHSCs	8	61.6 ± 13.3[c]	135.0 ± 33.3[ce]	6.5 ± 1.1[ceg]	16.6 ± 1.0[ceg]	19.8 ± 2.3[c]

Data are presented as mean ± SD. [a]$P < 0.05$ *vs* normal group; [c]$P < 0.05$ *vs* model group; [e]$P < 0.05$ *vs* BDHSCs group; [g]$P < 0.05$ *vs* BM-EPCs group.

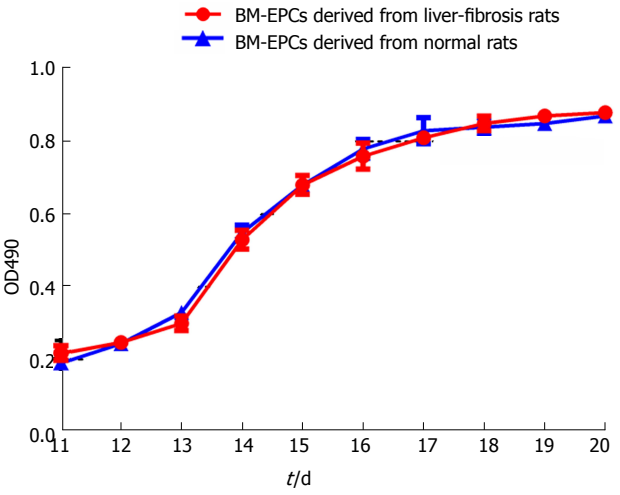

Figure 3 Growth curves of BM-EPCs. Between days 11 and 20 of culture induction, the growth curve (OD490 values) of BM-EPCs of liver fibrosis rats (red) was similar to that of BM-EPCs of normal rats (blue); BM-EPCs: Bone marrow-derived endothelial progenitor cells.

be statistically significant when the adjusted *P* values were < 0.05 (two-tailed).

RESULTS

Phenotype and purity of BM-EPCs

After 4 d of culture inductions, BM-EPCs were adherent (Figure 1A). After 10 d, BM-EPCs formed colonies (Figure 1B), and expression of CD133 and VEGFR2 were detected (Figure 1E). The co-expression level was 63.9% ± 2.15%, which was significantly higher than that of cells cultured without induction (37.2% ± 1.35%, $P < 0.05$) (Figure 1D).

Phagocytosis and vasculogenesis functions of BM-EPCs

After 10 d of culture induction, uptake of Dil-ac-LDL (red in Figure 2A) and binding with FTIC-UEA-1 (green in Figure 2B) to BM-EPCs were observed. The cells with yellow double-fluorescence were differentiating EPCs (Figure 2C). Furthermore, BM-EPCs formed a stable vascular network-like structure on Matrigel (Figure 2D).

Cytokinetics of BM-EPCs and localization of BM-EPCs in the liver

The growth curve of BM-EPCs from rats with liver fibrosis was similar to that of BM-EPCs of normal rats from day 11 to day 20 post induction. The logarithmic growth phase of cells was 3-7 d. The cells grew slowly and plateaued at day 18 (Figure 3). We implanted BM-EPCs in rats with fibrotic liver. We did not detect significant red fluorescence in the fibrotic liver tissue without implantation. BM-EPCs labeled with PKH26 were implanted in the fibrotic liver, and BM-EPCs were located primarily in/near hepatic sinusoids as indicated by nuclear staining with DAPI (data not shown).

Location of BM-EPCs in the liver

BM-EPCs labeled with PKH26 implanted in the fibrotic liver (red in Figure 4B). The DAPI nuclear staining result showed that BM-EPCs were located primarily in/near hepatic sinusoids (Figure 4C).

Collagen formation and improvement of liver fibrosis degree

Masson staining results showed there were significant numbers of collagen fibers (green) formed in the liver tissue of liver fibrosis rats in comparison to that in normal liver tissue (Figure 5A and B), and the staging score of liver fibrosis was 3.00 ± 0.19, which was dramatically higher than that in normal rats (0, $P < 0.05$). Transplantations of BDHSCs or BM-EPCs alone and combination of both suppressed the formation of collagen fibers (Figure 5C-E). There was no significant difference between the staging scores of liver fibrosis in the BDHSCs (2.88 ± 0.23) or BM-EPCs (2.75 ± 0.16) groups and that of the model group with only CCl_4 treatment ($P > 0.05$). However, transplantation of BM-EPCs/BDHSCs combination, significantly reduced the degree of liver fibrosis (staging score of 1.75 ± 0.25, $P < 0.05$) (Table 1).

Increase of VEGF levels in the liver

Immunohistochemistry (Figure 6A-E) and ELISA (Figure 6F) results showed that VEGF levels in the liver tissues in the model group with CCl_4 treatment alone were higher than that in the normal group (440.95 pg/mL ± 65.11 pg/mL *vs* 349.70 pg/mL ± 56.50 pg/mL per 100 mg liver tissue, $P < 0.05$). There were no significant differences between those in the model group and the BDHSCs group (461.28 ± 23.78, $P > 0.05$). The VEGF levels were increased in the BM-EPCs (707.10 ± 54.32) and BM-EPCs/BDHSCs group (615.42 ± 42.96), compared with those in the model group and BDHSCs group ($P < 0.05$). BM-EPCs transplantation slightly increased VEGF level but not significantly, as compared with that of combined transplantation of

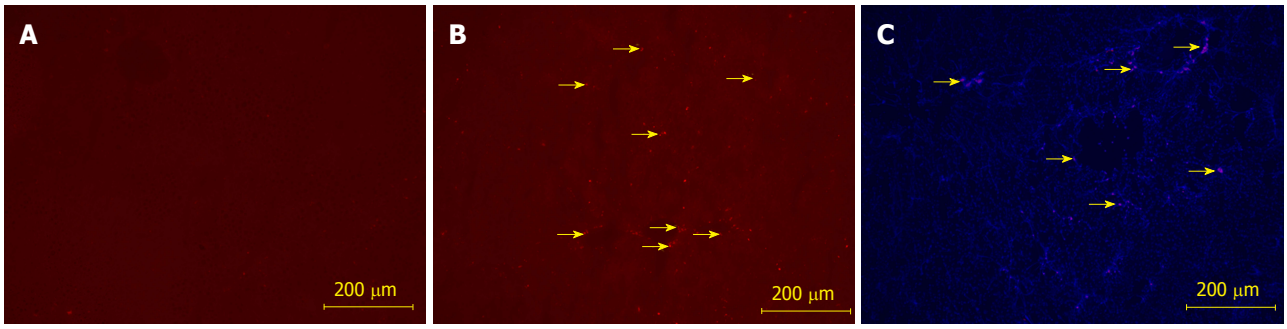

Figure 4 Location of BM-EPCs of liver fibrosis rats in the fibrotic liver. A: Autofluorescence of the fibrotic liver tissue; B: BM-EPCs labeled with PKH26 (red) implanted in the fibrotic liver tissue (yellow arrow); C: BM-EPCs (red) located in/near hepatic sinusoids (yellow arrow) on the background of DAPI staining (blue). Bars: 200 μm; BM-EPCs: Bone marrow-derived endothelial progenitor cells.

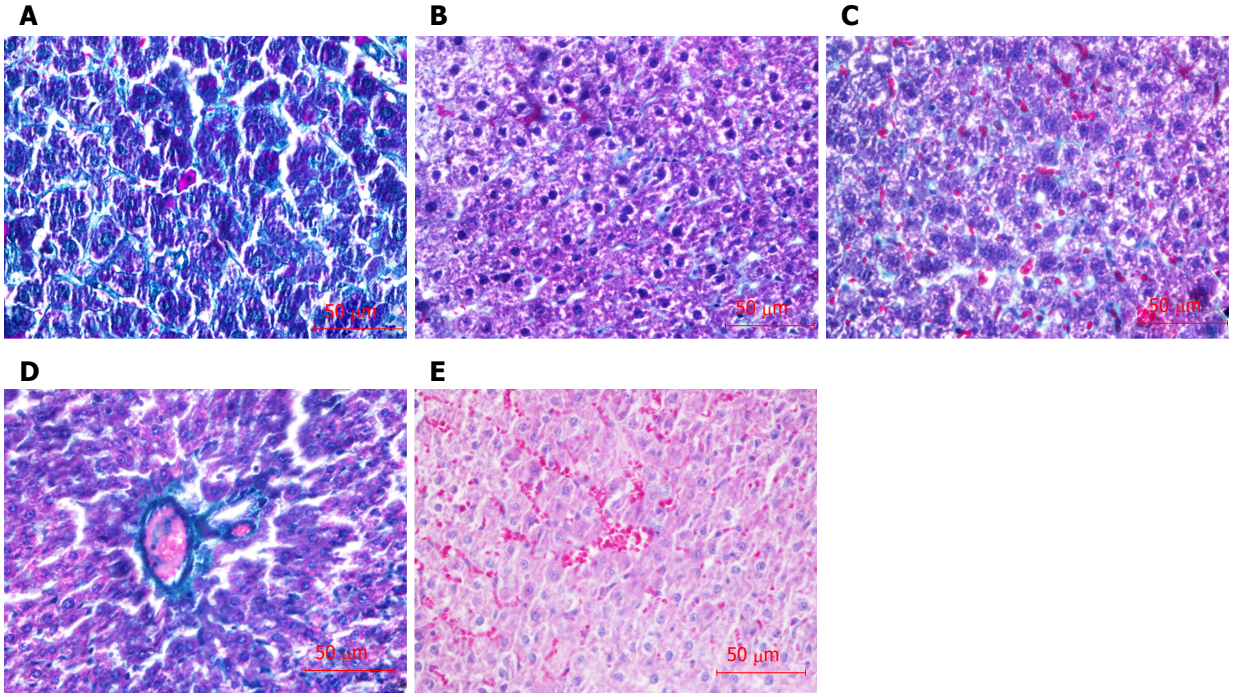

Figure 5 Collagen formation in the liver shown by masson staining (green). A: Normal group; B: Model group; C: Bone marrow-derived hepatocyte stem cells group; D: Bone marrow-derived endothelial progenitor cells group (BM-EPCs); E: BM-EPCs/BDHSCs group. Bars: 50 μm.

BM-EPCs and BDHSCs ($P > 0.05$).

Enhancement of liver regeneration

We evaluated liver regeneration after transplantation by detecting the expressions of PCNA protein and HGF gene in the liver. We found that compared with those in the normal group, the expressions of PCNA protein (Figure 7A-F) and HGF mRNA (Figure 8) in the model group was slightly but not significantly increased ($P > 0.05$). Significant increases in the levels of PCNA protein and HGF mRNA were observed in the BDHSCs, BM-EPCs and BM-EPCs/BDHSCs compared with those in the model group ($P < 0.05$), and combination of BM-EPCs/BDHSCs transplantation induced maximal up-regulation of PCNA protein and HGF mRNA levels.

Improvement of liver function

As shown in Table 2, the levels of ALT, AST, TBIT, PT and APTT were increased in the model group, compared with those in the normal group ($P < 0.05$). Compared with the model group, transplantation of BDHSCs reduced the levels of ALT, TBIL and APTT ($P < 0.05$), but failed to improve the levels of AST and PT ($P > 0.05$). Furthermore, levels of ALT, AST and APTT in the group with BM-EPCs transplantation were lower than that in the model group ($P < 0.05$), but there was no significant difference in levels of TBIL and PT between the two groups. The levels of ALT, AST, TBIT, PT and APTT in the BM-EPCs/BDHSCs group were significantly improved, to be equivalent to normal levels ($P > 0.05$) compared with those in the BDHSC (AST, TBIL and PT, $P < 0.05$) and BM-EPCs (TBIL and PT, $P < 0.05$) groups (Table 2).

DISCUSSION

Hepatic neovascularization and endothelial/sinusoidal remodeling are critical for the treatment of liver fibrosis, in addition to liver regeneration[24,25], and EPCs have been shown to play this role in liver fibrosis[10,13]. The

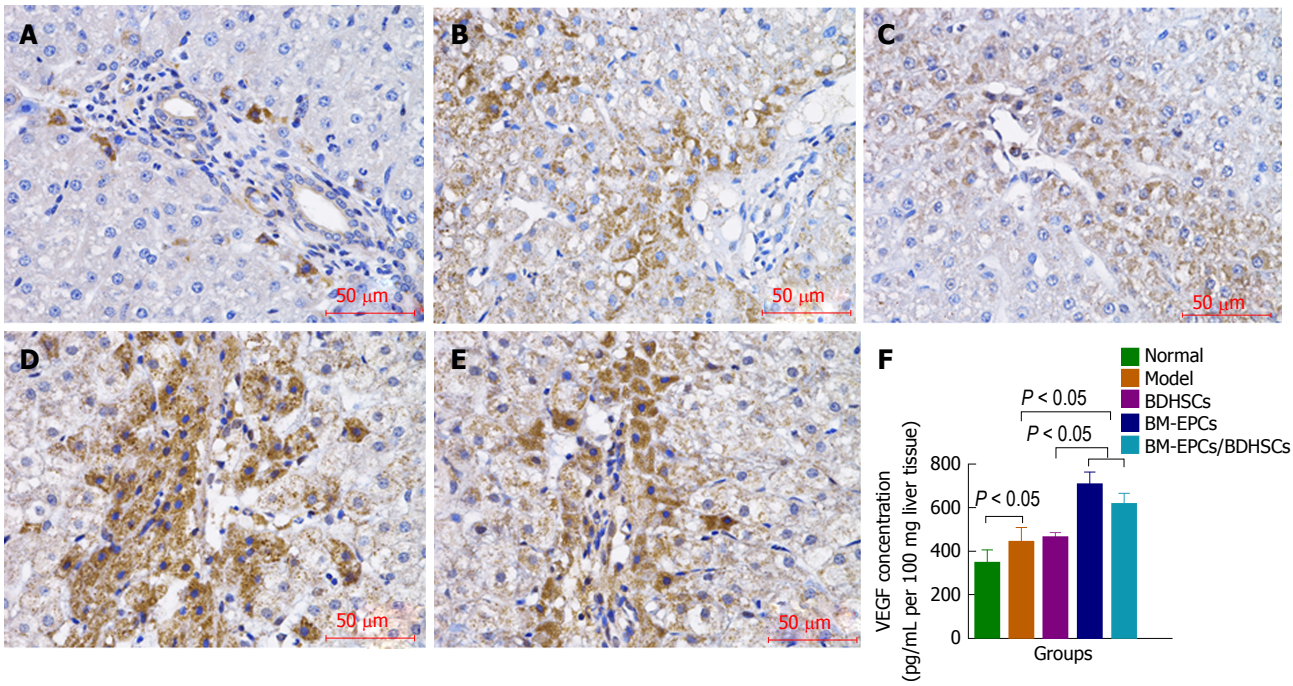

Figure 6 Vascular endothelial growth factor levels in the liver. A-E: VEGF protein expressions shown by immunohistochemistry (brown). A: Normal group; B: Model group; C: BDHSCs group; D: BM-EPCs group; E: BM-EPCs/BDHSCs group; F: VEGF concentration detected by ELISA. *n* = 8; VEGF: Vascular endothelial growth factor; BM-EPCs: Bone marrow-derived endothelial progenitor cells; BDHSCs: Bone marrow-derived hepatocyte stem cells.

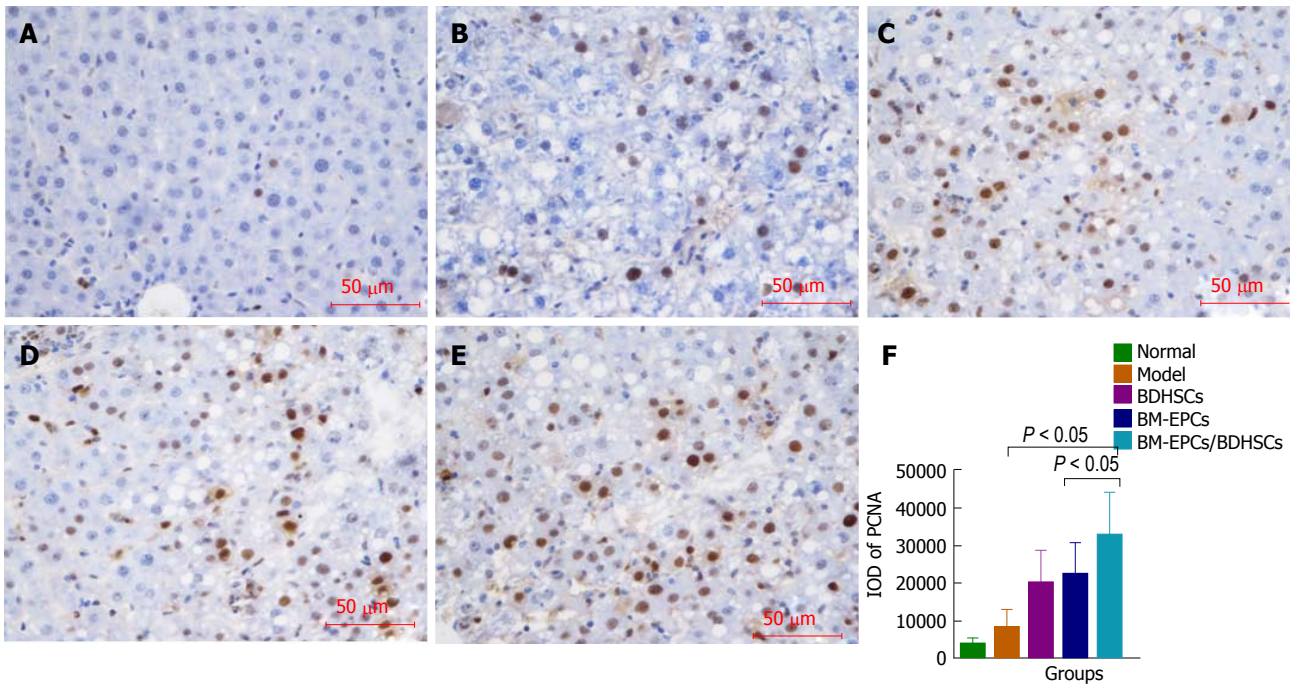

Figure 7 Proliferating cell nuclear antigen protein expression shown by immunohistochemistry (brown). A: Normal group; B: Model group; C: BDHSCs group; D: BM-EPCs group; E: BM-EPCs/BDHSCs group; F Quantitative analysis of PCNA expression by IOD. (*n* = 8); BM-EPCs: Bone marrow-derived endothelial progenitor cells; BDHSCs: Bone marrow-derived hepatocyte stem cells.

majority of EPCs exist in bone marrow and peripheral blood. EPCs are rare in blood, since their proportion is only 0.005%-0.01% of that of white blood cells in blood[26]. Bone marrow contains numerous hematopoietic stem cells and mesenchymal stem cells, which can differentiate into EPCs[27]. Therefore, bone marrow may be the major source of EPCs in potential clinical treatment of liver fibrosis. BM-EPCs used in recent therapeutic studies were derived from healthy individuals[11-15]. Thus, the clinical application of EPCs transplantation is limited, due to rare EPCs in peripheral blood and shortage of normal allogeneic bone marrow.

Whether sufficient normal EPCs can be obtained from

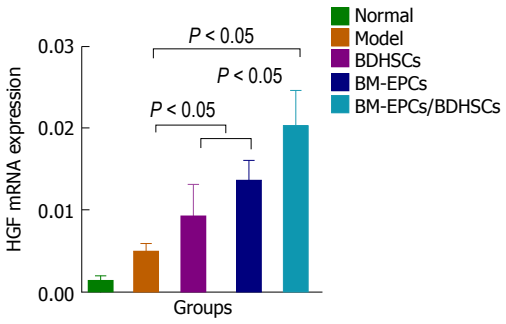

Figure 8 Hepatocyte growth factor mRNA expression detected by real-time quantitative polymerase chain reaction. *n* = 8; BM-EPCs: Bone marrow-derived endothelial progenitor cells; BDHSCs: Bone marrow-derived hepatocyte stem cells; HGF: Hepatocyte growth factor.

bone marrow cells in liver fibrosis pathoenvironment is a critical issue for the clinical application of autogenous EPCs therapy. A recent study showed that the functional homeostasis of bone marrow-derived c-Kit$^+$, Sca-1$^+$ and Lin$^-$ (BM-KSL) cells, as a stem cell fraction of BM-EPCs, was disrupted in liver fibrosis, indicating a weakened regenerative capability and decreased differentiation potential in liver fibrosis mice[28]. It is predicted that disturbed EPC differentiation might give rise to inadequate production for angiogenesis and tissue regeneration[28].

Whether normal EPCs can be obtained by *in vitro* culture from bone marrow in liver fibrosis rats remains uncertain. In the present study, abundant EPCs that possess specific phenotypes (VEGFR2 and CD133) and functions (phagocytosis and vasculogenesis) as well as normal proliferation and differentiation abilities were successfully obtained from bone marrow in liver fibrosis rats by collection and culture induction of plastic-nonadherent cells *in vitro*. EPCs do not easily attach on the bottom of surface of a culture plate, and thus different-rate adherent culture is a way to obtain EPC-differentiated cells[27,28]. BM-KSL cells are only a small portion of plastic-nonadherent cells[29]. Therefore, only some of the BMSCs in the liver fibrosis pathoenvironment might be hypophrenic. These hypophrenic cells in BMSCs could be eliminated automatically in the process of different-speed adherent and culture induction *in vitro*.

In the present study, transplanted BM-EPCs were located primarily in/near hepatic sinusoids, suggesting in the *in vivo* pathoenvironment of liver fibrosis, exogenous BM-EPCs derived from liver fibrosis rats had the ability to reside at sites of vessels in the liver.

In order to achieve the dual effects of hepatic neovascularization and liver regeneration, we next compared the effects of transplantations of BM-EPCs, BDHSCs and the combination of both on liver fibrosis. The increased levels of VEGF were observed in both BM-EPCs and BM-EPCs/BDHSCs groups, but not in the BDHSCs group. It has been reported that EPCs release vasoactive substances that promote angiogenesis by autocrine and paracrine signaling, such as VEGF, EGF and platelet-derived growth factor[11,14]. Among them, VEGF plays an essential role in both the neovascularization and the enhancement of sinusoidal density in the liver[27]. Studies have shown that the release of VEGF is essential for permeabilization of liver sinusoidal endothelial cells and integration of transplanted cells in the liver parenchyma[30,31]. Conversely, this study has shown that the effect of BM-EPCs transplantation on promoting VEGF secretion was slightly stronger than that of combined transplantation of BM-EPCs and BDHSCs. This result suggested that the release of VEGF in the liver might be controlled mainly by EPCs, but not BDHSCs.

Furthermore, an enhancement of liver regeneration manifested by increased HGF levels was observed in the rats with combined transplantation of BM-EPCs and BDHSCs[32], and this effect was greater than that of transplantation of BDHSCs or BM-EPCs alone. We deduced that BDHSCs might promote self-proliferation and mobilize endogenous liver regeneration through secretion of growth factors such as HGF[33,34], and EPCs can restore the permeabilization of the endothelial barrier interposed between liver sinusoids and parenchyma by releasing vasoactive substances and vasodilator-related molecules[30,31].

The integral effect of BM-EPCs transplantation on suppression of hepatic fibrogenesis and improvement of liver function was similar to that of BDHSCs transplantation. However, the combined effect of transplantation of BM-EPCs and BDHSCs exceeded individual transplantations significantly.

In summary, our study demonstrated that it was feasible to obtain normal EPCs from bone marrow in liver fibrosis rats and that combined transplantation of BM-EPCs and BDHSCs are effective for treating liver fibrosis. These findings highlight the clinical value of EPCs autotransplantation and the potential application of a novel strategy of therapy for liver fibrosis that involves combined transplantation of BM-EPCs and BDHSCs. Further studies are need to be carried out to explore the reciprocal mechanism of BM-EPCs and BDHSCs in liver fibrosis. In addition, whether BM-EPCs might promote tumor angiogenesis and cause potential tumor growth[2] in the process of treating liver fibrosis should also be evaluated in further study.

ARTICLE HIGHLIGHTS

Research background

Hepatic neovascularization and endothelial/sinusoidal remodeling are critical for the treatment of liver fibrosis, in addition to liver regeneration. Transplantation of bone marrow-derived endothelial progenitor cells (BM-EPCs) has potential roles in hepatic neovascularization, endothelial/sinusoidal remodeling and increased hepatic blood flow for the treatment of liver fibrosis. However, BM-EPCs were all derived from healthy rats in these studies. We sought to evaluate the feasibility of clinical application of autogenous EPCs therapy by using normal BM-EPCs obtained from liver fibrosis rats, and evaluated the effectiveness of combined transplantation of BM-EPCs and BDHSCs *in vivo* for the treatment of

liver fibrosis.

Research motivation

The author observed the feasibility of obtaining normal BM-EPCs from the liver fibrosis environment in rats. We evaluated the effectiveness for treating liver fibrosis by combined transplantation of BM-EPCs and bone marrow-derived hepatocyte stem cells (BDHSCs) in order to achieve the dual effects of hepatic neovascularization and liver regeneration. These findings highlight the clinical value of EPCs autotransplantation, and potential application of a novel strategy of therapy for liver fibrosis that involves combined transplantation of BM-EPCs and BDHSCs.

Research objectives

Our research objectives were to explore the feasibility of obtaining normal BM-EPCs from the liver fibrosis environment and the effectiveness for treating liver fibrosis by combined transplantation of BM-EPCs and BDHSCs. The significance of realizing these objectives were to highlight the clinical value of EPCs autotransplantation and potential application of a novel strategy of therapy for liver fibrosis that involves combined transplantation of BM-EPCs and BDHSCs.

Research methods

For the treatment of liver fibrosis, BDHSCs, which can promote hepatic cell regeneration, combined with BM-EPCs, which can promote hepatic revascularization, were transplanted into rats with liver fibrosis. The normal functional BM-EPCs and BDHSCs were both successfully obtained from liver fibrosis rats. Tracing analysis was conducted by labeling EPCs with PKH26 *in vitro* to show EPCs' location in the liver. After transplantation of BM-EPCs, BDHSCs or both into liver fibrosis rats, the indicators of hepatic neovascularization, liver regeneration, collagen formation, liver fibrosis degree and liver function were observed and detected.

Research results

Normal functional BM-EPCs from liver fibrosis rats were successfully obtained. The co-expression level of CD133 and VEGFR2 was 63.9% ± 2.15%. Transplanted BM-EPCs were located primarily in/near hepatic sinusoids. The combined transplantation of BM-EPCs and BDHSCs promoted hepatic neovascularization, liver regeneration and liver function, and decreased collagen formation and liver fibrosis degree.

Research conclusions

This study demonstrated that it was feasible to obtain normal BM-EPCs "filtered" by *in vivo* pathological environment from bone marrow of a liver fibrosis rat model. The combined transplantation of BM-EPCs and BDHSCs was performed in order to achieve the dual effects of hepatic neovascularization and liver regeneration for liver fibrosis. The combined transplantation exhibited maximal therapeutic effect compared to that of transplantation of BM-EPCs or BDHSCs alone. These findings highlight the clinical value of EPCs autotransplantation and the potential application of a novel strategy of therapy for liver fibrosis that involves combined transplantation of BM-EPCs and BDHSCs.

Research perspectives

Our research is still at the stage of animal experiments. Further studies are needed to explore the reciprocal mechanism of BM-EPCs and BDHSCs in liver fibrosis. Clinical experiments should be carry out gradually. In addition, whether BM-EPCs might promote tumor angiogenesis and cause potential tumor growth in the process of treating liver fibrosis should also be evaluated in further study.

ACKNOWLEDGMENTS

The authors are grateful to Dr. Zheng-Guo Liu (Department of Pathology, the People's Hospital, Zhengzhou University, Zhengzhou, China) and Dr. Xiu-Hua Ren (Basic Medical College, Zhengzhou University, Zhengzhou, China) for their contributions in staining and examination of the liver tissue sections. The authors also appreciate Dr. Adam Clemens (Division of Biology and Biomedical Sciences, Washington University, St. Louis, MO, United States) for his critical reading of the manuscript.

REFERENCES

1 **Rautou PE**. Endothelial progenitor cells in cirrhosis: the more, the merrier? *J Hepatol* 2012; **57**: 1163-1165 [PMID: 22989564 DOI: 10.1016/j.jhep.2012.09.001]

2 **Shackel N**, Rockey D. In pursuit of the "Holy Grail"--stem cells, hepatic injury, fibrogenesis and repair. *Hepatology* 2005; **41**: 16-18 [PMID: 15690475 DOI: 10.1002/hep.20551]

3 **Russo FP**, Alison MR, Bigger BW, Amofah E, Florou A, Amin F, Bou-Gharios G, Jeffery R, Iredale JP, Forbes SJ. The bone marrow functionally contributes to liver fibrosis. *Gastroenterology* 2006; **130**: 1807-1821 [PMID: 16697743 DOI: 10.1053/j.gastro.2006.01.036]

4 **Nussler A**, Konig S, Ott M, Sokal E, Christ B, Thasler W, Brulport M, Gabelein G, Schormann W, Schulze M, Ellis E, Kraemer M, Nocken F, Fleig W, Manns M, Strom SC, Hengstler JG. Present status and perspectives of cell-based therapies for liver diseases. *J Hepatol* 2006; **45**: 144-159 [PMID: 16730092 DOI: 10.1016/j.jhep.2006.04.002]

5 **Oyagi S**, Hirose M, Kojima M, Okuyama M, Kawase M, Nakamura T, Ohgushi H, Yagi K. Therapeutic effect of transplanting HGF-treated bone marrow mesenchymal cells into CCl4-injured rats. *J Hepatol* 2006; **44**: 742-748 [PMID: 16469408 DOI: 10.1016/j.jhep.2005.10.026]

6 **Sakaida I**, Terai S, Yamamoto N, Aoyama K, Ishikawa T, Nishina H, Okita K. Transplantation of bone marrow cells reduces CCl4-induced liver fibrosis in mice. *Hepatology* 2004; **40**: 1304-1311 [PMID: 15565662 DOI: 10.1002/hep.20452]

7 **Forbes SJ**, Gupta S, Dhawan A. Cell therapy for liver disease: From liver transplantation to cell factory. *J Hepatol* 2015; **62**: S157-S169 [PMID: 25920085 DOI: 10.1016/j.jhep.2015.02.040]

8 **Ishikawa T**, Terai S, Urata Y, Marumoto Y, Aoyama K, Sakaida I, Murata T, Nishina H, Shinoda K, Uchimura S, Hamamoto Y, Okita K. Fibroblast growth factor 2 facilitates the differentiation of transplanted bone marrow cells into hepatocytes. *Cell Tissue Res* 2006; **323**: 221-231 [PMID: 16228231 DOI: 10.1007/s00441-005-0077-0]

9 **Khoo CP**, Pozzilli P, Alison MR. Endothelial progenitor cells and their potential therapeutic applications. *Regen Med* 2008; **3**: 863-876 [PMID: 18947309 DOI: 10.2217/17460751.3.6.863]

10 **Sakamoto M**, Nakamura T, Torimura T, Iwamoto H, Masuda H, Koga H, Abe M, Hashimoto O, Ueno T, Sata M. Transplantation of endothelial progenitor cells ameliorates vascular dysfunction and portal hypertension in carbon tetrachloride-induced rat liver cirrhotic model. *J Gastroenterol Hepatol* 2013; **28**: 168-178 [PMID: 22849788 DOI: 10.1111/j.1440-1746.2012.07238.x]

11 **Nakamura T**, Torimura T, Sakamoto M, Hashimoto O, Taniguchi E, Inoue K, Sakata R, Kumashiro R, Murohara T, Ueno T, Sata M. Significance and therapeutic potential of endothelial progenitor cell transplantation in a cirrhotic liver rat model. *Gastroenterology* 2007; **133**: 91-107.e1 [PMID: 17631135 DOI: 10.1053/j.gastro.2007.03.110]

12 **Lian J**, Lu Y, Xu P, Ai A, Zhou G, Liu W, Cao Y, Zhang WJ. Prevention of liver fibrosis by intrasplenic injection of high-density cultured bone marrow cells in a rat chronic liver injury model. *PLoS One* 2014; **9**: e103603 [PMID: 25255097 DOI: 10.1371/journal.pone.0103603]

13 **Nakamura T**, Torimura T, Iwamoto H, Masuda H, Naitou M, Koga H, Abe M, Hashimoto O, Tsutsumi V, Ueno T, Sata M. Prevention of liver fibrosis and liver reconstitution of DMN-treated rat liver by transplanted EPCs. *Eur J Clin Invest* 2012; **42**: 717-728

[PMID: 22224757 DOI: 10.1111/j.1365-2362.2011.02637.x]
14 **Taniguchi E**, Kin M, Torimura T, Nakamura T, Kumemura H, Hanada S, Hisamoto T, Yoshida T, Kawaguchi T, Baba S, Maeyama M, Koga H, Harada M, Kumashiro R, Ueno T, Mizuno S, Ikeda H, Imaizumi T, Murohara T, Sata M. Endothelial progenitor cell transplantation improves the survival following liver injury in mice. *Gastroenterology* 2006; **130**: 521-531 [PMID: 16472604 DOI: 10.1053/j.gastro.2005.10.050]
15 **Liu F**, Liu ZD, Wu N, Cong X, Fei R, Chen HS, Wei L. Transplanted endothelial progenitor cells ameliorate carbon tetrachloride-induced liver cirrhosis in rats. *Liver Transpl* 2009; **15**: 1092-1100 [PMID: 19718641 DOI: 10.1002/lt.21845]
16 **Friedman SL**. Mechanisms of hepatic fibrogenesis. *Gastroenterology* 2008; **134**: 1655-1669 [PMID: 18471545 DOI: 10.1053/j.gastro.2008.03.003]
17 **García-Bravo M**, Morán-Jiménez MJ, Quintana-Bustamante O, Méndez M, Gutiérrez-Vera I, Bueren J, Salido E, Segovia JC, Fontanellas A, de Salamanca RE. Bone marrow-derived cells promote liver regeneration in mice with erythropoietic protoporphyria. *Transplantation* 2009; **88**: 1332-1340 [PMID: 20029329 DOI: 10.1097/TP.0b013e3181bce00e]
18 **Yu L**, Chen S, Luo N, He S. The C-terminus domain of the hepatitis B virus x protein stimulates the proliferation of mouse foetal hepatic progenitor cells, although it is not required for the formation of spheroids. *Int J Mol Med* 2017; **40**: 400-410 [PMID: 28627604 DOI: 10.3892/ijmm.2017.3026]
19 **Lan L**, Chen Y, Sun C, Sun Q, Hu J, Li D. Transplantation of bone marrow-derived hepatocyte stem cells transduced with adenovirus-mediated IL-10 gene reverses liver fibrosis in rats. *Transpl Int* 2008; **21**: 581-592 [PMID: 18282246 DOI: 10.1111/j.1432-2277.2008.00652.x]
20 **Inderbitzin D**, Avital I, Gloor B, Keogh A, Candinas D. Functional comparison of bone marrow-derived liver stem cells: selection strategy for cell-based therapy. *J Gastrointest Surg* 2005; **9**: 1340-1345 [PMID: 16332492 DOI: 10.1016/j.gassur.2005.06.010]
21 **Wu XL**, Zeng WZ, Wang PL, Lei CT, Jiang MD, Chen XB, Zhang Y, Xu H, Wang Z. Effect of compound rhodiola sachalinensis A Bor on CCl4-induced liver fibrosis in rats and its probable molecular mechanisms. *World J Gastroenterol* 2003; **9**: 1559-1562 [PMID: 12854163 DOI: 10.3748/wjg.v9.i7.1559]
22 **Thabut D**, Shah V. Intrahepatic angiogenesis and sinusoidal remodeling in chronic liver disease: new targets for the treatment of portal hypertension? *J Hepatol* 2010; **53**: 976-980 [PMID: 20800926 DOI: 10.1016/j.jhep.2010.07.004]
23 **Ueno T**, Nakamura T, Torimura T, Sata M. Angiogenic cell therapy for hepatic fibrosis. *Med Mol Morphol* 2006; **39**: 16-21 [PMID: 16575510 DOI: 10.1007/s00795-006-0311-1]
24 **Fadini GP**, Losordo D, Dimmeler S. Critical reevaluation of endothelial progenitor cell phenotypes for therapeutic and diagnostic use. *Circ Res* 2012; **110**: 624-637 [PMID: 22343557 DOI: 10.1161/CIRCRESAHA.111.243386]
25 **Casamassimi A**, Balestrieri ML, Fiorito C, Schiano C, Maione C, Rossiello R, Grimaldi V, Del Giudice V, Balestrieri C, Farzati B, Sica V, Napoli C. Comparison between total endothelial progenitor cell isolation versus enriched Cd133+ culture. *J Biochem* 2007; **141**: 503-511 [PMID: 17308344 DOI: 10.1093/jb/mvm060]
26 **Shirakura K**, Masuda H, Kwon SM, Obi S, Ito R, Shizuno T, Kurihara Y, Mine T, Asahara T. Impaired function of bone marrow-derived endothelial progenitor cells in murine liver fibrosis. *Biosci Trends* 2011; **5**: 77-82 [PMID: 21572251 DOI: 10.5582/bst.2011.v5.2.77]
27 **Smadja DM**, Cornet A, Emmerich J, Aiach M, Gaussem P. Endothelial progenitor cells: characterization, in vitro expansion, and prospects for autologous cell therapy. *Cell Biol Toxicol* 2007; **23**: 223-239 [PMID: 17370127 DOI: 10.1007/s10565-007-0177-6]
28 **Schatteman GC**, Dunnwald M, Jiao C. Biology of bone marrow-derived endothelial cell precursors. *Am J Physiol Heart Circ Physiol* 2007; **292**: H1-18 [PMID: 16980351 DOI: 10.1152/ajpheart.00662.2006]
29 **Medina J**, Arroyo AG, Sánchez-Madrid F, Moreno-Otero R. Angiogenesis in chronic inflammatory liver disease. *Hepatology* 2004; **39**: 1185-1195 [PMID: 15122744 DOI: 10.1002/hep.20193]
30 **Bahde R**, Kapoor S, Viswanathan P, Spiegel HU, Gupta S. Endothelin-1 receptor A blocker darusentan decreases hepatic changes and improves liver repopulation after cell transplantation in rats. *Hepatology* 2014; **59**: 1107-1117 [PMID: 24114775 DOI: 10.1002/hep.26766]
31 **Bahde R**, Kapoor S, Bandi S, Bhargava KK, Palestro CJ, Gupta S. Directly acting drugs prostacyclin or nitroglycerine and endothelin receptor blocker bosentan improve cell engraftment in rodent liver. *Hepatology* 2013; **57**: 320-330 [PMID: 22899584 DOI: 10.1002/hep.26005]
32 **Al-Rasheed NM**, Attia HA, Mohamad RA, Al-Rasheed NM, Al Fayez M, Al-Amin MA. Date fruits inhibit hepatocyte apoptosis and modulate the expression of hepatocyte growth factor, cytochrome P450 2E1 and heme oxygenase-1 in carbon tetrachloride-induced liver fibrosis. *Arch Physiol Biochem* 2017; **123**: 78-92 [PMID: 27960551 DOI: 10.1080/13813455.2016.1251945]
33 **Luk JM**, Wang PP, Lee CK, Wang JH, Fan ST. Hepatic potential of bone marrow stromal cells: development of in vitro co-culture and intra-portal transplantation models. *J Immunol Methods* 2005; **305**: 39-47 [PMID: 16150456 DOI: 10.1016/j.jim.2005.07.006]
34 **Yannaki E**, Athanasiou E, Xagorari A, Constantinou V, Batsis I, Kaloyannidis P, Proya E, Anagnostopoulos A, Fassas A. G-CSF-primed hematopoietic stem cells or G-CSF per se accelerate recovery and improve survival after liver injury, predominantly by promoting endogenous repair programs. *Exp Hematol* 2005; **33**: 108-119 [PMID: 15661404 DOI: 10.1016/j.exphem.2004.09.005]

P- Reviewer: Skrypnyk IN, Sugimura H **S- Editor**: Gong ZM
L- Editor: Filipodia **E- Editor**: Ma YJ

World Journal of Gastroenterology

Submit a Manuscript: http://www.f6publishing.com

World J Gastroenterol 2018 January 14; 24(2): 248-256

DOI: 10.3748/wjg.v24.i2.248

ISSN 1007-9327 (print) ISSN 2219-2840 (online)

ORIGINAL ARTICLE

Case Control Study

Genetic variants of interferon regulatory factor 5 associated with chronic hepatitis B infection

Bui Tien Sy, Nghiem Xuan Hoan, Hoang Van Tong, Christian G Meyer, Nguyen Linh Toan, Le Huu Song, Claus-Thomas Bock, Thirumalaisamy P Velavan

Bui Tien Sy, Nghiem Xuan Hoan, Hoang Van Tong, Christian G Meyer, Nguyen Linh Toan, Le Huu Song, Thirumalaisamy P Velavan, Vietnamese-German Center of Excellence in Medical Research, Hanoi, Vietnam

Bui Tien Sy, Nghiem Xuan Hoan, Le Huu Song, Institute of Clinical Infectious Diseases, 108 Military Central Hospital, Hanoi, Vietnam

Nghiem Xuan Hoan, Christian G Meyer, Claus-Thomas Bock, Thirumalaisamy P Velavan, Institute of Tropical Medicine, University of Tübingen, Tübingen 72074, Germany

Claus-Thomas Bock, Department of Infectious Diseases, Robert Koch Institute, Berlin 13302, Germany

Nguyen Linh Toan, Hoang Van Tong, Thirumalaisamy P Velavan, Department of Pathophysiology, Vietnam Military Medical University, Hanoi, Vietnam

ORCID number: Bui Tien Sy (0000-0002-4615-0114); Nghiem Xuan Hoan (0000-0002-6426-7818); Hoang Van Tong (0000-0002-7170-8810); Christian G Meyer (0000-0001-5561-2985); Nguyen Linh Toan (0000-0001-785 0-3896); Le Huu Song (0000-0003-2056-8499); Claus-Thomas Bock (0000-0002-2773-486X); Thirumalaisamy P Velavan (0000-0002-9809-9883).

Author contributions: Velavan TP and Sy BT designed study; Sy BT, Tong HV and Hoan NX performed the experiments; Song LH, Toan NL and Hoan NX are involved in patient recruitment; Bock CT and Velavan TP contributed to study materials and consumables; Hoan NX, Tong HV and Sy BT performed the statistical analyses and interpreted the data; Hoan NX, Sy BT, Tong HV, Meyer CG and Velavan TP wrote the manuscript; Sy BT, Hoan NX and Tong HV contributed equally to this work.

Supported by NAFOSTED, No. 108.02-2017.15; and BMBF, No. 01DP17047.

Institutional review board statement: The study was approved by the institutional review board of the 108 Military Central Hospital and the 103 Military Hospital of the Vietnam Military Medical University, Hanoi, Vietnam.

Informed consent statement: Informed written consent was obtained after explanation of the study at the time of sampling from all participants.

Conflict-of-interest statement: All authors have no conflicts of interest to declare.

Manuscript source: Unsolicited manuscript

Correspondence to: Thirumalaisamy P Velavan, PhD, Professor, Molecular Genetics of Infectious Diseases, Institute of Tropical Medicine, University of Tübingen, Wilhelmstrasse 27, Tübingen 72074, Germany. velavan@medizin.uni-tuebingen.de
Telephone: +49-7071-2985981
Fax: +49-7071-294684

Received: October 16, 2017
Peer-review started: October 17, 2017
First decision: November 14, 2017
Revised: November 15, 2017
Accepted: November 28, 2017
Article in press: November 28, 2017
Published online: January 14, 2018

Abstract

AIM

To investigate possible effects of IRF5 polymorphisms in the 3' UTR region of the *IFR5* locus on susceptibility

to hepatitis B virus (HBV) infection and progression of liver diseases among clinically classified Vietnamese patients.

METHODS

Four *IFR5* SNPs (rs13242262A/T, rs77416878C/T, rs10488630A/G, and rs2280714T/C) were genotyped in clinically classified HBV patients [chronic hepatitis B (CHB). *n* = 99; liver cirrhosis (LC), *n* = 131; hepatocellular carcinoma (HCC), *n* = 149] and in 242 healthy controls by direct sequencing and TaqMan real-time PCR assays.

RESULTS

Comparing patients and controls, no significant association was observed for the four *IFR5* variants. However, the alleles *rs13242262T* and *rs10488630G* contributed to an increased risk of liver cirrhosis (LC *vs* CHB: OR = 1.5, 95%CI: 1.1-2.3, adjusted *P* = 0.04; LC *vs* CHB: OR = 1.7, 95%CI: 1.1-2.6, adjusted *P* = 0.019). Haplotype *IRF5*TCGT* constructed from 4 SNPs was observed frequently in LC compared to CHB patients (OR = 2.1, 95%CI: 1.2-3.3, adjusted *P* = 0.008). Haplotype *IRF5*TCAT* occurred rather among CHB patients than in the other HBV patient groups (LC *vs* CHB: OR = 0.4, 95%CI: 0.2-0.8, adjusted *P* = 0.03; HCC *vs* CHB: OR = 0.3, 95%CI: 0.15-0.7, adjusted *P* = 0.003). The *IRF5*TCAT* haplotype was also associated with increased levels of ALT, AST and bilirubin.

CONCLUSION

Our study shows that *IFR5* variants may contribute as a host factor in determining the pathogenesis in chronic HBV infections.

Key words: Hepatitis B virus infection; Liver diseases; IRF5; *IFR5* polymorphisms; *IFR5* haplotypes

Core tip: *IFR5* is expressed in immune cells and mediates Toll-like receptor signal transduction, playing a vital role in the induction of antiviral and inflammatory response. So far, multiple *IFR5* single nucleotide polymorphisms have been shown to be associated with autoimmune diseases. This study investigated the effects of four *IFR5* variants on susceptibility to hepatitis B virus (HBV) infection and liver disease outcomes in HBV infected patients. Two *IFR5* variants (rs13242262, rs10488630) and constructed haplotypes (*TCGT*, *TCAT*) were associated with clinical outcomes suggesting that *IFR5* variants may contribute to determine the pathogenesis of HBV infection.

Sy BT, Hoan NX, Tong HV, Meyer CG, Toan NL, Song LH, Bock CT, Velavan TP. Genetic variants of interferon regulatory factor 5 associated with chronic hepatitis B infection. *World J Gastroenterol* 2018; 24(2): 248-256 Available from: URL: http://www.wjgnet.com/1007-9327/full/v24/i2/248.htm DOI: http://dx.doi.org/10.3748/wjg.v24.i2.248

INTRODUCTION

Hepatitis B virus (HBV) infection is a major health concern affecting approximately two billion individuals worldwide. 350 million people are chronically infected, putting them at risk to develop liver cirrhosis (LC) and hepatocellular carcinoma (HCC)[1]. The clinical outcome of HBV infection is heterogeneous and a consequence of the complex interaction between viral and host factors. The host´s genetic background is crucial for the outcome of the disease. Evidence for a host genetic effects are based on a twin study[2] and genome wide association studies (GWASs)[3-5]. GWASs examine possible associations of large number of genetic variants across the entire human genome, taking into account distinct disease phenotypes of HBV infection[6]. Many important candidate genes have been shown to be significantly associated with susceptibility to HBV infection and the progression of HBV-related liver diseases[6-8].

HBV is a noncytopathic virus as observed in a number of asymptomatic HBV carriers who have minimal hepatocellular injury and liver necroinflammation despite high levels of HBV replication[9]. Thus, hepatocellular injury is strongly dependent on the host immune responses[10]. Induction of type I interferons (IFNs) by viruses is crucial for innate immunity, which is primarily controlled by several transcriptional factors, in particular by interferon regulatory factors (IRFs)[11]. The IRF family comprises of nine members (IRF1 to IRF9), which are characterized by two major domains, a highly conserved amino (N)-terminal DNA binding domain and a C-terminal IFR association domain (IAD)[12]. These regions are important in mediating the interaction with transcription co-activators[13]. IRF5, a member of the IRF family, is expressed in B cells and innate immune cells and mediates Toll-like receptor signal transduction, leading to production of several inflammatory cytokines such as interleukin 12 and IFN-α[14-16]. Therefore, IRF5 plays a vital role in the induction of antiviral and inflammatory response [17,18].

So far, multiple *IRF5* single nucleotide polymorphisms (SNPs) have been shown to be associated with autoimmune diseases, including systemic lupus erythematosus and rheumatoid arthritis[19,20]. However, there are so far no data available on associations of *IRF5* variants with susceptibility to HBV infection and the clinical course of HBV-related liver diseases. This study aims to investigate possible effects of *IRF5* polymorphisms on susceptibility to HBV infection and progression of liver diseases among HBV patients in a Vietnamese population.

MATERIALS AND METHODS

Study subjects

379 unrelated Vietnamese HBV-infected patients were randomly recruited in a case-control design at the 108 Military Central Hospital and the 103 Military Hospital of the Vietnam Military Medical University, Hanoi, Vietnam.

Patients were assigned to subgroups of disease based on clinical manifestations and liver function tests. Subgroups included chronic hepatitis (CHB, *n* = 99), liver cirrhosis (LC, *n* = 131) and hepatocellular carcinoma (HCC, *n* = 149). The diagnostic criteria have previously been described[21]. Based on clinical manifestations and laboratory parameters, patients were assigned to the different clinical subgroups as previously described. Briefly, the CHB patients were characterized based upon clinical syndromes such as fatigue, anorexia, jaundice, hepatomegaly, hard density of the liver, splenomegaly, hyperbilirubinemia, elevated levels of AST and ALT, HBsAg positive for longer than 6 mo. The HBV-related LC patients were characterized as patients infected with HBV (HBsAg positive) showing the clinical manifestations such as anorexia, nausea, vomiting, malaise, weight loss, abdominal distress, jaundice, edema, cutaneous arterial "Spider" angiomas, palma erythema, ascites, shrunken liver, splenomegaly, hyperbilirubinemia, elevated levels of AST and ALT, prolonged serum prothrombin time, and decreased serum albumin. The HBV-related hepatocellular carcinoma patients were characterized as patients infected with chronically HBV (HBsAg positive), abdominal pain, an abdominal mass in the right upper quadrant, blood-tinged ascites, weight loss, anorexia, fatigue, jaundice, prolonged serum prothrombin time, hyperbilirubinemia, elevated levels of AST, ALT and serum a-fetoprotein (AFP), ultrasound showed tumor, liver biopsy and histopathology showing tumor cells. None of the patients were under any antivirals during sampling. None of the patients had a history of alcohol or drug abuse. All participants were confirmed to be negative for anti-HCV and anti-HIV antibodies by ELISA assays. Liver function tests including the assessment of alanine transaminase (ALT), aspartate transaminase (AST), total bilirubin and direct bilirubin, albumin and prothrombin levels were performed using an autoanalyser (AU640 Chemistry Analyzer, Beckman Coulter, CA, United States). 242 blood samples from healthy individuals (HC) were collected from blood banks as the control group. All 242 control individuals were negative for HBsAg, anti-HCV and anti-HIV antibodies. All specimens were frozen at -20 ℃ until use.

IRF5 SNP selection

The four *IRF5* SNPs rs13242262A/T, rs77416878C/T, rs10488630A/G, and rs2280714G/A located closely at the 3′ downstream regions of the *IRF5* locus were selected for this study. Two SNPs (rs13242262, and rs2280714) have been shown to be associated with *IRF5* mRNA expression and activation of the interferon α pathway in different world populations[22].

IRF5 variant genotyping

Genomic DNA was isolated from 200 μL of whole blood using a DNA purification kit (Qiagen, Hilden, Germany). The fragments containing the SNPs rs13242262A/T and rs77416878C/T were amplified by PCR using the primer pairs IRF5-F1: 5′-AGG CCT GTG CAG TTC TAC TCC C-3′ and IRF5-R1: 5′-CCT CAC ACT GGC CTG CCT TTA C-3′. PCR amplifications were carried out in 25 μL reaction volumes containing: 1 x PCR buffer, 0.2 mmol/L dNTPs, 1 mmol/L MgCl2, 0.15 mmol/L of each primer, 1 unit of Taq polymerase and 50 ng of genomic DNA. Cycling conditions: denaturation at 95 ℃ for 5 min, followed by 35 cycles of three-step cycling with denaturation at 94 ℃ for 40 s, annealing at 61 ℃ for 40 s, and extension at 72 ℃ for 45 s and a final extension at 72 ℃ for 7 min.

PCR products were purified using the Exo-SAP-IT PCR Product Cleanup Reagent (Affymetrix Santa Clara, mmol/L) 5 μL of purified PCR products were used as templates. Sequencing was performed using the BigDye terminator v.1.1 cycle sequencing kit (Applied Biosystems, Foster City, CA, United States) on an ABI 3130XL DNA sequencer according to the manufacturer's instructions. The polymorphisms were identified by assembling DNA sequences with the reference sequence of the *IFR5* gene obtained from the NCBI database (GenBank accession number: NC-00007). In addition, the two SNPs rs10488630A/G, and rs2280714G/A were genotyped using TaqMan® SNP genotyping assays according to the instruction of the manufacturer.

Statistical analysis

The data were analyzed using R version 3.1.2 (http://www.r-project.org). Permutation tests were used to compare groups for quantitative variables permuted for 1000 iterations. Genotype and haplotype frequencies were analyzed by gene counting and expectation-maximum (EM) algorithms and the significance of deviation from Hardy-Weinberg equilibrium was tested using the random-permutation procedure as implemented in the Arlequin v. 3.5.1.2 software (http://lgb.unige.ch/arlequin). We used a binary logistic regression model adjusted for age and gender to analyze associations of *IRF5* variants and haplotypes with HBV-related liver diseases. The false discovery rate correction method was used for multiple comparisons[23] and adjusted *P* values are given. The level of significance was set at a value of $P < 0.05$ and all reported *P* values are two-sided.

RESULTS

Baseline characteristics of study participants

The baseline characteristics of the 379 HBV-infected patients from the different subgroups with well-characterized clinical profiles and from the 242 healthy controls are described in Table 1**.** Most patients and controls were male (81% and 64%). The median age of patients increased according to progression of liver disease; healthy controls were younger than the patients. The levels of ALT, AST and bilirubin were

Table 1 Clinical profiles of 242 healthy individuals and 379 hepatitis B virus-infected patients

Characteristics	HC (*n* = 242)	CHB (*n* = 99)	LC (*n* = 131)	HCC (*n* = 149)	*P* values
Age (yr)	39 (18-79)	41 (19-78)	52 (17-78)	53 (18-79)	< 0.0001
Gender (Male/Female)	156/86	82/17	105/26	119/30	< 0.0001
AST (IU/L)	NR	219 (17-3732)	74 (12-720)	59 (16-513)	< 0.0001
ALT (IU/L)	NR	158 (12-4593)	59 (9-1354)	47 (13-471)	< 0.0001
Total bilirubin (μmol/L)	NR	46.6 (1.8-795)	31 (1.2-722)	17 (2-290)	< 0.0001
Direct bilirubin (μmol/L)	NR	29.9 (1-512)	17 (1-450)	7.1 (1.2-189)	< 0.0001
Albumin (g/L)	NR	42 (23-48)	30 (20-47)	39 (27-49)	< 0.0001
Prothrombin (% of standard)	NR	85 (50-120)	47.5 (15-101)	80 (31-115)	< 0.0001
HBV-DNA (copies/mL)	NA	1.8×10^5 (4×10^2-8.1×10^6)	8.3×10^4 (2×10^2-4.1×10^6)	9.4×10^4 (2.9×10^2-1.0×10^5)	NS
Alfa Feto Protein (IU/L)	NR	4.3 (1.5-300)	8.6 (1.2-400)	196 (1.1- 438)	< 0.0001

CHB: Chronic hepatitis B; LC: Liver cirrhosis; HCC: Hepatocellular carcinoma; PLT: Platelets; AST and ALT: Aspartate and alanine amino transferase; IU: International unit; NS: Not significant; NA: Not applicable; NR: Normal range.

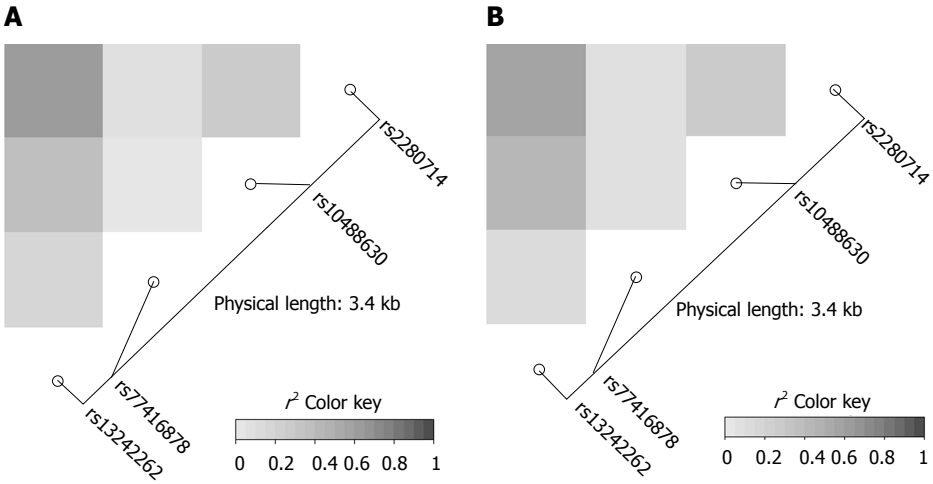

Figure 1 *IRF5* linkage disequilibrium maps. Pairwise r^2 between 4 polymorphisms in the *IRF5* locus in the 3' UTR region in Vietnamese hepatitis B virus infected patients (A) and in healthy controls (B) are presented. The color scale from white to dark indicates r^2 values from 0 to 1. The blocks of grey and dark grey represent SNPs that are all in high linkage disequilibrium with each other.

significantly higher in patients with CHB compared to the other subgroups ($P < 0.0001$). As expected, the albumin and prothrombin levels as well as platelet counts were significantly lower in patients with LC compared to patients without LC ($P < 0.001$). Alpha-fetoprotein (AFP) levels were higher in HCC patients with or without LC compared to CHB and LC groups ($P < 0.0001$). Viral loads did not differ significantly between HBV virus subgroups ($P > 0.05$).

Association IRF5 variants with HBV-related liver diseases

The genotype frequencies of the four *IRF5* variants rs13242262A/T, rs10488630A/G, rs77416878C/T, rs2280714T/C in HBV patients and in HCs were in Hardy-Weinberg equilibrium ($P > 0.05$). Linkage disequilibrium analysis revealed strong allelic combinations between rs13242262 and rs2280714; rs13242262 and rs10488630; rs10488630 and rs2280714 for both HBV infected patients and HCs (Figure 1). Genotype and allele frequencies of the *IRF5* SNPs in patients and HCs as well as the comparisons between different subgroups are given in Tables 2 and 3.

Genotype and allele frequencies of the four *IRF5* SNPs did not differ between HBV patients or subgroups and controls, indicating that *IRF5* SNPs are not associated with HBV infection *per se.* Among chronic HBV carriers, *rs13242262TT* and *rs10488630GG* genotype were significantly more frequent among LC patients compared to CHB patients (*rs13242262TT*: OR = 3.1, 95%CI: 1.2-7.8, adjusted $P = 0.014$; *rs10488630GG*, OR = 3.0, 95%CI: 1.0-9.5, adjusted $P = 0.045$, Table 2). A similar trend was observed for *rs13242262T* (OR = 1.5, 95%CI: 1.1-2.3, adjusted $P = 0.04$) and *rs10488630G* (OR = 1.7, 95%CI: 1.1-2.6, adjusted $P = 0.019$; Table 2). For SNPs rs77416878C/T, and rs2280714T/C all comparisons between patient subgroups using binary logistic model adjusted for age and gender did not indicate any significant difference (Table 3). These results show that, of the four SNPs genotyped, the two variants rs13242262 and rs10488630 are associated with liver disease progression.

Association of IRF5 haplotypes with HBV-infected liver diseases

Haplotypes were constructed based on the four SNPs. Among nine *IRF5* haplotypes detected, the five common

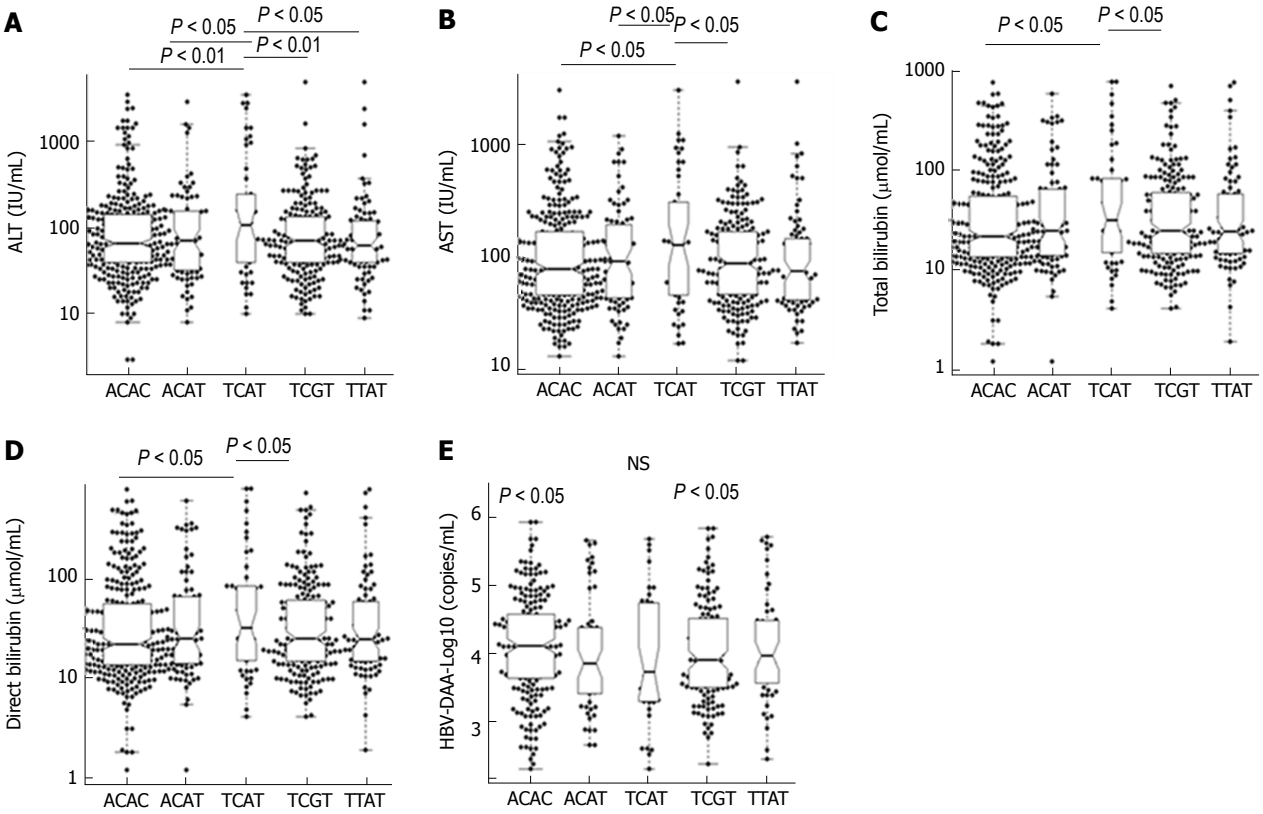

Figure 2 Association of *IRF5* haplotypes with clinical parameters in hepatitis B virus patients. Box-plots illustrate median values with 25 and 75 percentiles with whiskers to 10 and 90 percentiles; the distribution of *IRF5* haplotypes to liver enzymes, bilirubin and hepatitis B virus viral load was executed using pairwise permutation tests. Adjusted *P* values are presented under the false discovery rate correction method applied for multiple comparisons. NS: Not significant; AST and ALT: Aspartate and alanine amino transferase.

haplotypes rs13242262/rs77416878/rs10488630/rs2280714 *ACAC, TCGT, TCAT, ACAT,* and *TTAT* were observed in both HCs and HBV patients. Their frequencies are summarized in Table 4. We compared the haplotype frequencies between HCs and all HBV patients as well as the disease subgroups (HC *vs* all HBV; HC *vs* LC; HC *vs* CHB; HC *vs* HCC). The results did not indicate any significant difference (data not shown).

We further compared haplotype frequencies between the HBV subgroups. Haplotype *TCGT* was found more frequently among LC compared to CHB patients (LC *vs* CHB: OR = 2.1, 95%CI: 1.2-3.3, adjusted *P* = 0.008), indicating that this haplotype may contribute significantly to an increased risk of LC in HBV carriers. However, a contradictory finding was observed for the haplotype *TCAT*, which was observed significantly more frequent in CHB compared to LC and HCC patients (LC *vs* CHB: OR = 0.4, 95%CI: 0.2-0.8, adjusted *P* = 0.037 and HCC *vs* CHB: OR = 0.3, 95%CI: 0.15-0.7, adjusted *P* = 0.003). This haplotype appears to partly protect from the risk of the advanced clinical manifestations LC and HCC in chronic HBV carriers. There were no differences in comparisons of the *TCGT* and *TCAT* haplotype frequencies between LC and HCC patients. Also, no significant difference was observed when frequencies of other haplotypes were compared (Table 4).

Association of IRF5 polymorphisms and haplotypes with clinical parameters

To explore the possible impact of the four SNPs on disease outcomes, the SNP frequencies were correlated with several liver function tests, a cancer marker, and viral loads. No significant associations of *IRF5* genotypes with the parameters ALT, AST, total and direct bilirubin, prothrombin, AFP and HBV-DNA loads were observed (adjusted *P* > 0.05).

We further examined the association of five common *IRF5* haplotypes with clinical outcomes of HBV infection. Patients with haplotype *TCAT* had higher levels of AST, ALT, total bilirubin and direct bilirubin compared to the other haplotypes (Figure 2). No significant differences of viral loads, prothrombin and AFP levels among five common haplotypes were observed.

DISCUSSION

IRF5 is a particularly interesting member of the IRF family, which are crucial in the innate immune response with a variety of activities like activation of type I IFN genes, inflammatory cytokines and tumor suppressors[24,25]. Therefore, IRF5 is involved in many conditions, including autoimmune diseases, viral infections and cancers[11,19,20]. In this study, we studied the role of *IRF5* polymorphisms in HBV

Table 2 Association of IRF5 rs13242262A/T and rs10488630A/G with hepatitis B virus-related liver cirrhosis *n* (%)

IRF5 variants	HC, *n* = 242	CHB, *n* = 99	LC, *n* = 131	HCC, *n* = 149	LC *vs* CHB	
					OR (95%CI)	*P* value
rs13242262 A/T						
AA	67 (27.7)	27 (27.3)	32 (24.4)	45 (30.2)	Reference	
AT	119 (49.2)	59 (59.6)	65 (49.6)	77 (51.7)	1.0 (0.5-2.0)	NS
TT	56 (23.1)	13 (13.1)	34 (26.0)	27 (18.1)	3.1 (1.2-7.8)	0.014
Allele						
A	253 (52.3)	113 (57)	129 (49.2)	165 (55.3)	Reference	
T	231 (47.7)	85 (43)	133 (50.8)	133 (44.7)	1.5 (1.1-2.3)	0.040
Dominant						
AA	67 (27.7)	27 (27.3)	32(24.4)	45 (30.2)	Reference	
AT + TT	175 (72.3)	72 (72.7)	99 (75.6)	104 (69.8)	1.3 (0.7-2.6)	NS
Recessive						
AA + AT	186 (76.9)	86 (87)	97 (74.0)	122 (81.9)	Reference	
TT	56 (23.1)	13 (13)	34 (26.0)	27 (18.1)	2.8 (1.3-5.9)	0.0057
rs10488630 A/G						
AA	115 (47.5)	58 (58.6)	59 (45.1)	73 (49.0)	Reference	
AG	104 (43.0)	36 (36.4)	56 (42.7)	63 (42.3)	1.6 (0.9-2.9)	0.100
GG	23 (9.5)	5 (5.0)	16 (12.2)	13 (8.7)	3.0 (1.0-9.5)	0.045
Allele						
A	334 (69)	152 (76.8)	174 (66.4)	209 (72.3)	Reference	
G	150 (31)	46 (23.2)	88 (33.6)	89 (27.7)	1.7 (1.1-2.6)	0.019
Dominant						
AA	115 (47.5)	58 (58.6)	59 (45.0)	73 (49)	Reference	
AG + GG	127 (52.5)	41 (41.4)	72 (55.0)	76 (51)	1.8 (1.0-3.2)	0.035
Recessive						
AA + AG	219 (90.5)	94 (94.9)	115 (87.8)	136 (91.3)	Reference	
GG	23 (9.5)	5 (5.1)	16 (12.2)	13 (7.8)	2.4 (0.8-7.2)	0.100

HC: Healthy controls; CHB: Chronic hepatitis B; LC: Liver cirrhosis; HCC: Hepatocellular carcinoma.

Table 3 Allele and genotype frequencies of *IRF5* rs77416878C/T and rs2280714T/C in Vietnamese patients with hepatitis B virus-related liver diseases *n* (%)

IRF5 variants	HC, *n* = 242	CHB, *n* = 99	LC, *n* = 131	HCC, *n* = 149
rs77416878				
CC	192 (79.4)	79 (79.8)	98 (74.8)	115 (77.2)
CT	48 (19.8)	19 (19.2)	32 (24.4)	31 (20.8)
TT	2 (0.8)	1 (1)	1 (0.8)	3 (2)
Allele				
C	432 (89.3)	177 (89.4)	228 (87)	261 (87.6)
T	52 (10.7)	21 (10.6)	34 (13)	37 (12.4)
Dominant				
CC	192 (79.4)	79 (79.8)	98 (74.8)	115 (77.2)
CT + TT	50 (20.6)	20 (20.2)	33 (24.4)	34 (22.8)
Recessive				
CC + CT	240 (99.2)	98 (99)	130 (99.2)	146 (98)
TT	2 (0.8)	1 (1)	1 (0.8)	3 (2)
rs2280714				
TT	84 (34.7)	31 (31.3)	47 (35.9)	39 (26.2)
TC	114 (47.1)	52 (52.5)	69 (52.7)	87 (58.4)
CC	44 (18.2)	16 (16.2)	15 (11.4)	23 (15.4)
Allele				
T	282 (58.3)	114 (57.6)	163 (62.2)	165 (55.4)
C	202 (41.7)	84 (42.4)	99 (37.8)	133 (44.6)
Dominant				
TT	84 (34.7)	31 (31.3)	47 (35.9)	39 (26.2)
TC + TT	158 (65.3)	78 (68.7)	84 (64.1)	110 (73.8)
Recessive				
TT + TC	198 (81.8)	83 (83.8)	116 (88.6)	126 (84.6)
CC	44 (18.2)	16 (16.2)	15 (11.4)	23 (15.4)

HC: Healthy controls; CHB: Chronic hepatitis B; LC: Liver cirrhosis; HCC: Hepatocellular carcinoma. All comparisons between groups using binary logistic model adjusted for age and gen did not indicate a significant difference (adjusted $P > 0.05$, data not shown in this table).

infected patients. *IRF5* variants are associated with LC progression in patients with CHB while the constructed haplotypes are associated with LC and HCC progression in CHB patients. In addition, *IRF5* variants and their constructed haplotypes are associated with clinical outcomes of HBV infection. For the first time we provide evidence of the functional role of *IRF5* in immune response to the clinical outcome of HBV infection.

Host immune factors are crucial to the pathogenesis of HBV infection through genetic and epigenetic modifications and *via* the effects of cytokines[26]. Interferons are produced by the host in response to certain viral infections in order to inhibit viral replication. Induction of *IFN* is required for the defense against hepatitis viruses and further progression of related liver disease[27]. IRF5 is a transcriptional factor that can induce type I interferons and, therefore, appears to play an important role in the clinical course of HBV infection. To the best of our knowledge, this study is the first exploratory investigation of *IRF5* polymorphisms addressing the clinical outcome of HBV-related liver diseases. Among four SNPs studied here, rs13242262A/T and rs10488630A/G appeared were with liver cirrhosis. In addition, the *IRF5* haplotypes *TCGT* and *TCAT* are associated with liver cirrhosis in patients with chronic hepatitis B. SNP rs10488631 located in the same region was identified to be associated with primary biliary cirrhosis in populations of European descent[28]. However, this SNP was homogeneous in Asian populations and therefore excluded from analyses in this study. In addition, SNPs rs3807306

Table 4 Haplotype distribution among chronic hepatitis B virus carriers and the association of IRF5 haplotypes with hepatitis B virus-infected liver diseases *n* (%)

Haplotypes	HC, *n* = 484	CHB, *n* = 198	LC, *n* = 298	HCC, *n* = 262	LC *vs* CHB		HCC *vs* CHB		HCC *vs* LC	
					OR (95% CI)	*P* value	OR (95% CI)	*P* value	OR (95%CI)	*P* value
ACAC	196 (40.6)	83 (41.9)	98 (37.4)	132 (44.3)	Reference		Reference		Reference	
TCGT	141 (29.0)	37 (18.7)	86 (32.7)	81 (27.2)	2.1 (1.2-3.3)	0.008		NS	0.7 (0.4-1.1)	0.08
TCAT	33 (6.8)	27 (13.6)	12 (4.6)	13 (4.4)	0.4 (0.2-0.8)	0.037	0.3 (0.15-0.7)	0.003		NS
ACAT	54 (11.2)	24 (12)	30 (11.5)	31 (10.4)		NS		NS		NS
TTAT	49 (10.2)	18 (9.1)	34 (13)	33 (11.1)		NS		NS		NS
ACGC	2 (0.4)	1 (0.5)	0 (0)	1 (0.3)		NS		NS		NS
ACGT	5 (1)	5 (2.5)	1 (0.4)	3 (1)		NS		NS		NS
TCGC	2 (0.4)	0 (0)	1 (0.4)	0 (0)		NS		NS		NS
TTGT	2 (0.4)	3 (1.5)	0 (0)	4 (1.3)		NS		NS		NS

HCC: Hepatocellular carcinoma. Comparison between HC *vs* HBV patient group did not indicate any significant difference (data not shown in this table). OR and *P* values were calculated by using binary logistic model adjusted for age and gender, CHB: Chronic hepatitis B; LC: Liver cirrhosis.

and rs4728142 in the *IRF5* gene have been implicated as susceptibility loci for primary biliary cirrhosis[29].

The process of liver cirrhosis in HBV infection is a results of the interplay between viral factors and host immune responses through activation of inflammatory cytokines[30]. A recent study has shown that among several *IRF5* SNPs, the variants rs13242262, rs2280714 and rs10488630 in the 3'UTR region are associated with increased *IRF5* mRNA expression[22]. Studies have indicated that a variety of cytokines are dependent on IRF5[24,31]. Several *IRF5*-modulated genes (*e.g.*, *ISGs* and *STATs)* involved in the type I IFN signaling pathway are significantly over-expressed in response to viral infection[18]. This supports the findings of our study, namely that these SNPs may contribute to progression of HBV-related liver diseases through regulating *IRF5* expression and subsequent activation of genes in the type I IFN signaling pathway like *ISG15* as seen in our study[7]. Furthermore, although all four studied SNPs were not associated with HCC, the haplotype *TCAT* contributes to a decreased risk of HCC development in patients with chronic hepatitis B. Data concerning the association between *IRF5* and HCC are scarce. Nevertheless, methylation of *IRF5* has been suggested to be associated with HCC in a Korean study[32]. The role of *IRF5* in the development of HBV-related HCC needs to be explored further.

Although SNPs rs77416878C/T and rs2280714T/C are not associated with HBV-related liver disease and no significant association of all four SNPs studied with clinical parameters, constructed haplotypes are associated with clinical outcomes. Notably, the haplotype *TCAT* was observed significantly more frequent in CHB compared to LC and HCC patients, suggesting that this haplotype appears to partly protect from the risk of the advanced clinical manifestations LC and HCC in chronic HBV carriers. However, patients with the haplotype *TCAT* had higher levels of AST, ALT, total bilirubin and direct bilirubin compared to the other haplotypes. In fact, the clinical outcome or clinical progression of liver diseases in HBV infected patients are affected by several factors and are considered as a result of viral-host interaction. Therefore, we believe that haplotype *TCAT* is an important host factor in HBV infection but this haplotype only may not be a host factor in determining the overall clinical outcome of disease.

Until now, most studies have identified distinct *IRF5* haplotypes to be associated with high serum IFN-α activity and with systemic lupus erythematosus[33-36]. In addition, the *IRF5* risk haplotype *TCC*, which contains the risk alleles rs13242262, rs10488631 and rs2280714 are associated with increased IRF5, IFN-α, and IFN-inducible chemokine expression in healthy individuals[22]. However, our study did not assess the relationship of the *IRF5* risk haplotypes *ACAC, TCAT, TCGT* with IRF5 expression, IFN-α activity and other related *IFN*-α gene. This is one of the study's limitations; in fact the function of IRF5 in HBV infection needs further investigations. Nevertheless, we assume that the *IRF5* risk haplotypes may affect the expression of multiple downstream genes in the IFN-α signaling pathway and certain inflammatory cytokines in HBV infection.

In conclusion, *IRF5* variants rs13242262A/T and rs10488630A/G are associated with LC progression in patients with CHB. *IRF5* haplotypes appear to influence the outcome of HBV infection. Further studies in this direction will provide insights into a role of *IRF5* variants as prognostic markers of HBV-related liver diseases.

ARTICLE HIGHLIGHTS

Research background

Hepatitis B virus (HBV) infection is a major health concern in Vietnam. Investigations were carried out to determine IRF5 polymorphisms in the 3' UTR region of the *IFR5* locus on susceptibility to HBV infection and progression of liver diseases among clinically classified Vietnamese patients.

Research motivation

IRF5 is a particularly interesting member of the IRF family, which are crucial in the innate immune response with a variety of activities like activation of type I *IFN* genes, inflammatory cytokines and tumor suppressors. There are so far no data available on associations of IRF5 variants with susceptibility to HBV

infection and the clinical course of HBV-related liver diseases.

Research objectives

This study aims to investigate possible effects of IRF5 polymorphisms on susceptibility to HBV infection and progression of liver diseases among clinically classified Vietnamese patients.

Research methods

The four *IRF5* SNPs rs13242262A/T, rs77416878C/T, rs10488630A/G, and rs2280714G/A located closely at the 3' downstream regions of the *IRF5* locus were selected for this study. *IRF5* variant genotyping was performed by direct sanger sequencing and by application of TaqMan® SNP genotyping assays.

Research results

Three hundred seventy-nine unrelated Vietnamese HBV-infected patients were randomly recruited in a case-control design. *IRF5* variants are associated with LC progression in patients with CHB while the constructed haplotypes are associated with LC and HCC progression in CHB patients. In addition, *IRF5* variants and their constructed haplotypes are associated with clinical outcomes of HBV infection.

Research conclusions

Host immune factors are crucial to the pathogenesis of HBV infection. For the first time the authors provide evidence of the functional role of human *IRF5* in immune response to the clinical outcome of HBV infection. *IRF5* variants rs13242262A/T and rs10488630A/G are associated with LC progression in patients with CHB. *IRF5* haplotypes appear to influence the outcome of HBV infection.

Research perspectives

Further studies in this direction will provide insights into a role of *IRF5* variants as prognostic markers of HBV-related liver diseases.

REFERENCES

1 **Trépo C**, Chan HL, Lok A. Hepatitis B virus infection. *Lancet* 2014; **384**: 2053-2063 [PMID: 24954675 DOI: 10.1016/S0140-6736(14)60220-8]

2 **Lin TM**, Chen CJ, Wu MM, Yang CS, Chen JS, Lin CC, Kwang TY, Hsu ST, Lin SY, Hsu LC. Hepatitis B virus markers in Chinese twins. *Anticancer Res* 1989; **9**: 737-741 [PMID: 2764519]

3 **Hu Z**, Liu Y, Zhai X, Dai J, Jin G, Wang L, Zhu L, Yang Y, Liu J, Chu M, Wen J, Xie K, Du G, Wang Q, Zhou Y, Cao M, Liu L, He Y, Wang Y, Zhou G, Jia W, Lu J, Li S, Liu J, Yang H, Shi Y, Zhou W, Shen H. New loci associated with chronic hepatitis B virus infection in Han Chinese. *Nat Genet* 2013; **45**: 1499-1503 [PMID: 24162738 DOI: 10.1038/ng.2809]

4 **Jiang DK**, Sun J, Cao G, Liu Y, Lin D, Gao YZ, Ren WH, Long XD, Zhang H, Ma XP, Wang Z, Jiang W, Chen TY, Gao Y, Sun LD, Long JR, Huang HX, Wang D, Yu H, Zhang P, Tang LS, Peng B, Cai H, Liu TT, Zhou P, Liu F, Lin X, Tao S, Wan B, Sai-Yin HX, Qin LX, Yin J, Liu L, Wu C, Pei Y, Zhou YF, Zhai Y, Lu PX, Tan A, Zuo XB, Fan J, Chang J, Gu X, Wang NJ, Li Y, Liu YK, Zhai K, Zhang H, Hu Z, Liu J, Yi Q, Xiang Y, Shi R, Ding Q, Zheng W, Shu XO, Mo Z, Shugart YY, Zhang XJ, Zhou G, Shen H, Zheng SL, Xu J, Yu L. Genetic variants in STAT4 and HLA-DQ genes confer risk of hepatitis B virus-related hepatocellular carcinoma. *Nat Genet* 2013; **45**: 72-75 [PMID: 23242368 DOI: 10.1038/ng.2483]

5 **Li S**, Qian J, Yang Y, Zhao W, Dai J, Bei JX, Foo JN, McLaren PJ, Li Z, Yang J, Shen F, Liu L, Yang J, Li S, Pan S, Wang Y, Li W, Zhai X, Zhou B, Shi L, Chen X, Chu M, Yan Y, Wang J, Cheng S, Shen J, Jia W, Liu J, Yang J, Wen Z, Li A, Zhang Y, Zhang G, Luo X, Qin H, Chen M, Wang H, Jin L, Lin D, Shen H, He L, de Bakker PI, Wang H, Zeng YX, Wu M, Hu Z, Shi Y, Liu J, Zhou W. GWAS identifies novel susceptibility loci on 6p21.32 and 21q21.3 for hepatocellular carcinoma in chronic hepatitis B virus carriers. *PLoS Genet* 2012; **8**: e1002791 [PMID: 22807686 DOI: 10.1371/journal.pgen.1002791]

6 **Thursz M**, Yee L, Khakoo S. Understanding the host genetics of chronic hepatitis B and C. *Semin Liver Dis* 2011; **31**: 115-127 [PMID: 21538279 DOI: 10.1055/s-0031-1276642]

7 **Hoan NX**, Van Tong H, Giang DP, Toan NL, Meyer CG, Bock CT, Kremsner PG, Song LH, Velavan TP. Interferon-stimulated gene 15 in hepatitis B-related liver diseases. *Oncotarget* 2016; **7**: 67777-67787 [PMID: 27626177 DOI: 10.18632/oncotarget.11955]

8 **Hu L**, Zhai X, Liu J, Chu M, Pan S, Jiang J, Zhang Y, Wang H, Chen J, Shen H, Hu Z. Genetic variants in human leukocyte antigen/DP-DQ influence both hepatitis B virus clearance and hepatocellular carcinoma development. *Hepatology* 2012; **55**: 1426-1431 [PMID: 22105689 DOI: 10.1002/hep.24799]

9 **Chang JJ**, Lewin SR. Immunopathogenesis of hepatitis B virus infection. *Immunol Cell Biol* 2007; **85**: 16-23 [PMID: 17130898 DOI: 10.1038/sj.icb.7100009]

10 **Rehermann B**, Nascimbeni M. Immunology of hepatitis B virus and hepatitis C virus infection. *Nat Rev Immunol* 2005; **5**: 215-229 [PMID: 15738952 DOI: 10.1038/nri1573]

11 **Tamura T**, Yanai H, Savitsky D, Taniguchi T. The IRF family transcription factors in immunity and oncogenesis. *Annu Rev Immunol* 2008; **26**: 535-584 [PMID: 18303999 DOI: 10.1146/annurev.immunol.26.021607.090400]

12 **Chen W**, Royer WE Jr. Structural insights into interferon regulatory factor activation. *Cell Signal* 2010; **22**: 883-887 [PMID: 20043992 DOI: 10.1016/j.cellsig.2009.12.005]

13 **Chen W**, Lam SS, Srinath H, Jiang Z, Correia JJ, Schiffer CA, Fitzgerald KA, Lin K, Royer WE Jr. Insights into interferon regulatory factor activation from the crystal structure of dimeric IRF5. *Nat Struct Mol Biol* 2008; **15**: 1213-1220 [PMID: 18836453 DOI: 10.1038/nsmb.1496]

14 **Chang Foreman HC**, Van Scoy S, Cheng TF, Reich NC. Activation of interferon regulatory factor 5 by site specific phosphorylation. *PLoS One* 2012; **7**: e33098 [PMID: 22412986 DOI: 10.1371/journal.pone.0033098]

15 **Lien C**, Fang CM, Huso D, Livak F, Lu R, Pitha PM. Critical role of IRF-5 in regulation of B-cell differentiation. *Proc Natl Acad Sci USA* 2010; **107**: 4664-4668 [PMID: 20176957 DOI: 10.1073/pnas.0911193107]

16 **Savitsky DA**, Yanai H, Tamura T, Taniguchi T, Honda K. Contribution of IRF5 in B cells to the development of murine SLE-like disease through its transcriptional control of the IgG2a locus. *Proc Natl Acad Sci USA* 2010; **107**: 10154-10159 [PMID: 20479222 DOI: 10.1073/pnas.1005599107]

17 **Fang CM**, Roy S, Nielsen E, Paul M, Maul R, Paun A, Koentgen F, Raval FM, Szomolanyi-Tsuda E, Pitha PM. Unique contribution of IRF-5-Ikaros axis to the B-cell IgG2a response. *Genes Immun* 2012; **13**: 421-430 [PMID: 22535200 DOI: 10.1038/gene.2012.10]

18 **Barnes BJ**, Richards J, Mancl M, Hanash S, Beretta L, Pitha PM. Global and distinct targets of IRF-5 and IRF-7 during innate response to viral infection. *J Biol Chem* 2004; **279**: 45194-45207 [PMID: 15308637 DOI: 10.1074/jbc.M400726200]

19 **Tang L**, Chen B, Ma B, Nie S. Association between IRF5 polymorphisms and autoimmune diseases: a meta-analysis. *Genet Mol Res* 2014; **13**: 4473-4485 [PMID: 25036352 DOI: 10.4238/2014.June.16.6]

20 **Li Y**, Chen S, Li P, Wu Z, Li J, Liu B, Zhang F, Li Y. Association of the IRF5 rs2070197 polymorphism with systemic lupus erythematosus: a meta-analysis. *Clin Rheumatol* 2015; **34**: 1495-1501 [PMID: 26233721 DOI: 10.1007/s10067-015-3036-5]

21 **Hoan NX**, Tong HV, Hecht N, Sy BT, Marcinek P, Meyer CG, Song le H, Toan NL, Kurreck J, Kremsner PG, Bock CT, Velavan TP. Hepatitis E Virus Superinfection and Clinical Progression in Hepatitis B Patients. *EBioMedicine* 2015; **2**: 2080-2086 [PMID: 26844288 DOI: 10.1016/j.ebiom.2015.11.020]

22 **Rullo OJ**, Woo JM, Wu H, Hoftman AD, Maranian P, Brahn BA, McCurdy D, Cantor RM, Tsao BP. Association of IRF5 polymorphisms with activation of the interferon alpha pathway.

Ann Rheum Dis 2010; **69**: 611-617 [PMID: 19854706 DOI: 10.1136/ard.2009.118315]
23 Benjamini Y. Discovering the false discovery rate. *J R Stat Soc* 2010; **72**: 405-416 [DOI: 10.1111/j.1467-9868.2010.00746.x]
24 **Yanai H**, Chen HM, Inuzuka T, Kondo S, Mak TW, Takaoka A, Honda K, Taniguchi T. Role of IFN regulatory factor 5 transcription factor in antiviral immunity and tumor suppression. *Proc Natl Acad Sci USA* 2007; **104**: 3402-3407 [PMID: 17360658 DOI: 10.1073/pnas.0611559104]
25 **Barnes BJ**, Moore PA, Pitha PM. Virus-specific activation of a novel interferon regulatory factor, IRF-5, results in the induction of distinct interferon alpha genes. *J Biol Chem* 2001; **276**: 23382-23390 [PMID: 11303025 DOI: 10.1074/jbc.M101216200]
26 **Li X**, Liu X, Tian L, Chen Y. Cytokine-Mediated Immunopathogenesis of Hepatitis B Virus Infections. *Clin Rev Allergy Immunol* 2016; **50**: 41-54 [PMID: 25480494 DOI: 10.1007/s12016-014-8465-4]
27 **Rijckborst V**, Janssen HL. The Role of Interferon in Hepatitis B Therapy. *Curr Hepat Rep* 2010; **9**: 231-238 [PMID: 20949114 DOI: 10.1007/s11901-010-0055-1]
28 **Hirschfield GM**, Liu X, Han Y, Gorlov IP, Lu Y, Xu C, Lu Y, Chen W, Juran BD, Coltescu C, Mason AL, Milkiewicz P, Myers RP, Odin JA, Luketic VA, Speiciene D, Vincent C, Levy C, Gregersen PK, Zhang J, Heathcote EJ, Lazaridis KN, Amos CI, Siminovitch KA. Variants at IRF5-TNPO3, 17q12-21 and MMEL1 are associated with primary biliary cirrhosis. *Nat Genet* 2010; **42**: 655-657 [PMID: 20639879 DOI: 10.1038/ng.631]
29 **Juran BD**, Hirschfield GM, Invernizzi P, Atkinson EJ, Li Y, Xie G, Kosoy R, Ransom M, Sun Y, Bianchi I, Schlicht EM, Lleo A, Coltescu C, Bernuzzi F, Podda M, Lammert C, Shigeta R, Chan LL, Balschun T, Marconi M, Cusi D, Heathcote EJ, Mason AL, Myers RP, Milkiewicz P, Odin JA, Luketic VA, Bacon BR, Bodenheimer HC Jr, Liakina V, Vincent C, Levy C, Franke A, Gregersen PK, Bossa F, Gershwin ME, deAndrade M, Amos CI; Italian PBC Genetics Study Group, Lazaridis KN, Seldin MF, Siminovitch KA. Immunochip analyses identify a novel risk locus for primary biliary cirrhosis at 13q14, multiple independent associations at four established risk loci and epistasis between 1p31 and 7q32 risk variants. *Hum Mol Genet* 2012; **21**: 5209-5221 [PMID: 22936693 DOI: 10.1093/hmg/dds359]
30 **Zhou WC**, Zhang QB, Qiao L. Pathogenesis of liver cirrhosis. *World J Gastroenterol* 2014; **20**: 7312-7324 [PMID: 24966602 DOI: 10.3748/wjg.v20.i23.7312]
31 **Takaoka A**, Yanai H, Kondo S, Duncan G, Negishi H, Mizutani T, Kano S, Honda K, Ohba Y, Mak TW, Taniguchi T. Integral role of IRF-5 in the gene induction programme activated by Toll-like receptors. *Nature* 2005; **434**: 243-249 [PMID: 15665823 DOI: 10.1038/nature03308]
32 **Shin SH**, Kim BH, Jang JJ, Suh KS, Kang GH. Identification of novel methylation markers in hepatocellular carcinoma using a methylation array. *J Korean Med Sci* 2010; **25**: 1152-1159 [PMID: 20676325 DOI: 10.3346/jkms.2010.25.8.1152]
33 **Graham RR**, Kozyrev SV, Baechler EC, Reddy MV, Plenge RM, Bauer JW, Ortmann WA, Koeuth T, González Escribano MF; Argentine and Spanish Collaborative Groups, Pons-Estel B, Petri M, Daly M, Gregersen PK, Martín J, Altshuler D, Behrens TW, Alarcón-Riquelme ME. A common haplotype of interferon regulatory factor 5 (IRF5) regulates splicing and expression and is associated with increased risk of systemic lupus erythematosus. *Nat Genet* 2006; **38**: 550-555 [PMID: 16642019 DOI: 10.1038/ng1782]
34 **Graham RR**, Kyogoku C, Sigurdsson S, Vlasova IA, Davies LR, Baechler EC, Plenge RM, Koeuth T, Ortmann WA, Hom G, Bauer JW, Gillett C, Burtt N, Cunninghame Graham DS, Onofrio R, Petri M, Gunnarsson I, Svenungsson E, Rönnblom L, Nordmark G, Gregersen PK, Moser K, Gaffney PM, Criswell LA, Vyse TJ, Syvänen AC, Bohjanen PR, Daly MJ, Behrens TW, Altshuler D. Three functional variants of IFN regulatory factor 5 (IRF5) define risk and protective haplotypes for human lupus. *Proc Natl Acad Sci USA* 2007; **104**: 6758-6763 [PMID: 17412832 DOI: 10.1073/pnas.0701266104]
35 **Niewold TB**, Kelly JA, Flesch MH, Espinoza LR, Harley JB, Crow MK. Association of the IRF5 risk haplotype with high serum interferon-alpha activity in systemic lupus erythematosus patients. *Arthritis Rheum* 2008; **58**: 2481-2487 [PMID: 18668568 DOI: 10.1002/art.23613]
36 **Niewold TB**, Kelly JA, Kariuki SN, Franek BS, Kumar AA, Kaufman KM, Thomas K, Walker D, Kamp S, Frost JM, Wong AK, Merrill JT, Alarcón-Riquelme ME, Tikly M, Ramsey-Goldman R, Reveille JD, Petri MA, Edberg JC, Kimberly RP, Alarcón GS, Kamen DL, Gilkeson GS, Vyse TJ, James JA, Gaffney PM, Moser KL, Crow MK, Harley JB. IRF5 haplotypes demonstrate diverse serological associations which predict serum interferon alpha activity and explain the majority of the genetic association with systemic lupus erythematosus. *Ann Rheum Dis* 2012; **71**: 463-468 [PMID: 22088620 DOI: 10.1136/annrheumdis-2011-200463]

P- Reviewer: Silva LD, Sipos F, Waheed Y **S- Editor**: Ma YJ
L- Editor: A **E- Editor**: Ma YJ

World Journal of Gastroenterology

Submit a Manuscript: http://www.f6publishing.com

World J Gastroenterol 2018 January 14; 24(2): 257-265

DOI: 10.3748/wjg.v24.i2.257

ISSN 1007-9327 (print) ISSN 2219-2840 (online)

ORIGINAL ARTICLE

Retrospective Study

Timing of surgery after neoadjuvant chemotherapy for gastric cancer: Impact on outcomes

Yi Liu, Ke-Cheng Zhang, Xiao-Hui Huang, Hong-Qing Xi, Yun-He Gao, Wen-Quan Liang, Xin-Xin Wang, Lin Chen

Yi Liu, Ke-Cheng Zhang, Xiao-Hui Huang, Hong-Qing Xi, Yun-He Gao, Wen-Quan Liang, Xin-Xin Wang, Lin Chen, Department of General Surgery & Institute of General Surgery, Chinese People's Liberation Army General Hospital, Beijing 100853, China

ORCID number: Yi Liu (0000-0002-0973-4241); Ke-Cheng Zhang (0000-0002-9257-5607); Xiao-Hui Huang (0000-0002-4284-1559); Hong-Qing Xi (0000-0002-0472-8299); Yun-He Gao (0000-0002-1848-2955); Wen-Quan Liang (0000-0002-8667-0958), Xin-Xin Wang (0000-0002-9915-3327); Lin Chen (0000-0002-3507-673X).

Author contributions: Liu Y and Zhang KC designed the study and wrote the manuscript; Xi HQ and Huang XH contributed to the patient material; Liu Y collected the clinical data; Gao YH and Liang WQ contributed to data analysis and validation; all authors have reviewed and approved the final manuscript.

Supported by the Beijing Municipal Science and Technology Plan, No. D141100000414002; and the National Natural Science Foundation of China, No. 81272698, No. 81672319, and No. 81602507.

Institutional review board statement: The study was approved by the Chinese People's Liberation Army General Hospital Research Ethics Committee.

Informed consent statement: Informed consent was not required because all the study participants had signed a consent form prior to neoadjuvant chemotherapy and the analysis used anonymous clinical data.

Conflict-of-interest statement: All the authors have no conflict of interest.

Data sharing statement: All data from which the conclusion could be drawn are presented in the manuscript. No additional data are available.

Manuscript source: Unsolicited manuscript

Correspondence to: Lin Chen, MD, PhD, Professor, Chief, Department of General Surgery & Institute of General Surgery, Chinese People's Liberation Army General Hospital, 28 Fuxing Road, Beijing 100853, China. chenlinbj301@163.com
Telephone: +86-10-66938128
Fax: +86-10-68181689

Received: November 20, 2017
Peer-review started: November 21, 2017
First decision: December 6, 2017
Revised: December 8, 2017
Accepted: December 13, 2017
Article in press: December 13, 2017
Published online: January 14, 2018

Abstract

AIM

To evaluate whether the neoadjuvant chemotherapy (NACT)-surgery interval time significantly impacts the pathological complete response (pCR) rate and long-term survival.

METHODS

One hundred and seventy-six patients with gastric cancer undergoing NACT and a planned gastrectomy at the Chinese PLA General Hospital were selected from January 2011 to January 2017. Univariate and multivariable analyses were used to investigate the impact of NACT-surgery interval time (< 4 wk, 4-6 wk, and > 6 wk) on pCR rate and overall survival (OS).

RESULTS

The NACT-surgery interval time and clinician T stage were independent predictors of pCR. The interval time > 6 wk was associated with a 74% higher odds of pCR as compared with an interval time of 4-6 wk (P = 0.044), while the odds ratio (OR) of clinical T_3 *vs* clinical T_4 stage for pCR was 2.90 (95%CI: 1.04-8.01, P = 0.041). In Cox regression analysis of long-term survival, post-neoadjuvant therapy pathological N (ypN) stage significantly impacted OS (N_0 *vs* N_3: HR = 0.16, 95%CI: 0.37-0.70, P = 0.015; N_1 *vs* N_3: HR = 0.14, 95%CI: 0.02-0.81, P = 0.029) and disease-free survival (DFS) (N_0 *vs* N_3: HR = 0.11, 95%CI: 0.24-0.52, P = 0.005; N_1 *vs* N_3: HR = 0.17, 95%CI: 0.02-0.71, P = 0.020). The surgical procedure also had a positive impact on OS and DFS. The hazard ratio of distal gastrectomy *vs* total gastrectomy was 0.12 (95%CI: 0.33-0.42, P = 0.001) for OS, and 0.13 (95%CI: 0.36-0.44, P = 0.001) for DFS.

CONCLUSION

The NACT-surgery interval time is associated with pCR but has no impact on survival, and an interval time > 6 wk has a relatively high odds of pCR.

Key words: Gastric cancer; Timing of surgery; Neo-adjuvant chemotherapy

Core tip: The impact of interval time between completion of neoadjuvant chemotherapy and surgery on pathological complete response (pCR) had been proved in colorectal cancer and esophageal cancer. However, no such research was found in gastric cancer. To evaluate whether the interval time impacts efficiency of neoadjuvant chemotherapy, 176 patients with gastric cancer were recruited. The interval time and clinical T stage were proved predictors of pCR. Post-neoadjuvant therapy pathological N stage and surgical procedure have a significant impact on the long-term survival. An interval time > 6 wk was associated with a higher odds of pCR.

Liu Y, Zhang KC, Huang XH, Xi HQ, Gao YH, Liang WQ, Wang XX, Chen L. Timing of surgery after neoadjuvant chemotherapy for gastric cancer: Impact on outcomes. *World J Gastroenterol* 2018; 24(2): 257-265 Available from: URL: http://www.wjgnet.com/1007-9327/full/v24/i2/257.htm DOI: http://dx.doi.org/10.3748/wjg.v24.i2.257

INTRODUCTION

Surgery is the only curative treatment for gastric cancer (GC). Although standard surgery has been performed in recent years, overall survival (OS) at 5 years for GC patients remains at 20%-30%[1]. Since more and more clinical trials have validated the survival benefit of preoperative chemotherapy[2-4], neoadjuvant chemotherapy (NACT) has been gradually accepted by clinicians.

Making patients experience significant tumor downstaging and even a pathologic complete response (pCR) is the most important goal of NACT. It has been proven that patients who have a pCR may achieve superior OS and fewer local or systemic recurrence than those with a partial or no response[5,6]. Therefore, every potential way has been explored to maximize the possibility of attaining a pCR. Since the Lyon R90-01 trial found that patients undergoing surgery at an interval of 6-8 wk after NACT showed improvement in clinical tumor response and pathologic downstaging compared with a 2-3-wk interval[7], a growing number of studies have proven that a longer interval is significantly related to increased pCR rates, increased tumor downstaging, and potential superior OS in rectal cancer[8-11]. However, in esophageal cancer, results are conflicting. Some studies found that a longer interval was associated with higher pCR rates that might improve the prognosis[12,13]; even intervals beyond 12 wk have been thought to be safe[14]. Yet, other studies failed to validate the connection between longer intervals and pCR rates, and found that longer intervals were disadvantageous to long-term OS[15,16]. To our knowledge, the optimal timing of performing surgery after NACT has never been studied in GC. An interval time of 4-6 wk was first practiced in some NACT clinical trials[17,18]. However, an interval of 4-6 wk has never been validated as being optimal. Thus, the aim of this study was to assess the link between NACT-surgery interval time and pCR rates and/or OS.

MATERIALS AND METHODS

Study patients

This was a retrospective study for which we recruited 216 patients with GC who underwent NACT at the Chinese PLA General Hospital from January 2011 to January 2017. The criteria for inclusion were: (1) GC was diagnosed using endoscopy and a biopsy; (2) Patients who underwent NACT and a planned gastrectomy; and (3) All clinical pathological information was available, including NACT relevant information, surgical parameters, imaging information, pathological diagnosis, perioperative therapy, and follow-up data. The exclusion criteria were: (1) Patients older than 75 years; and (2) Patients who ever received chemoradiotherapy. Finally, only 176 patients were included (Figure 1). Before NACT, endoscopic ultrasound (EUS) and contrast-enhanced computed tomography (CE-CT) had been performed to assess clinical stage and confirm that patients had $T_{2-4}N_{0-3}M_0$ GC, according to the Japanese classification of gastric carcinoma[19].

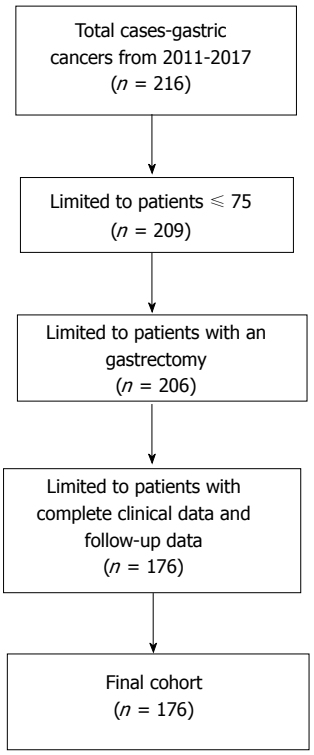

Figure 1 Flow diagram of patient inclusion.

NACT and surgery

Most patients (*n* = 167) received 2-4 cycles of a SOX regimen (S-1 80 mg/m^2 per day, PO, days 1-14, and oxaliplatin 130 mg/m^2 per day, Ⅳ, infusion on day 1), which is widely used in Asia[20]; the remaining patients (*n* = 9) received a XELOX regimen (capecitabine 1000 mg/m^2 per day, PO, days 1-14, and oxaliplatin 130 mg/m^2 per day, IV, infusion on day 1). After two cycles of chemotherapy, the curative effect was evaluated using EUS and CT according to RECIST1.1[21]. A gastrectomy was carried out immediately when imaging showed an observable increase in tumor size or tumor disappearance. If imaging indicated a decrease in tumor size, another one or two cycles of chemotherapy could be performed. The planned operations after NACT were conducted by experienced surgeons. Patients without evidence of metastasis underwent a gastrectomy with a D2 lymphadenectomy. For other patients, the type of operation was decided by a multidisciplinary team. The location of the primary tumor determined whether a proximal, distal, or total gastrectomy was selected.

Histopathology analysis and follow-up

The same pathologist microscopically analyzed all resected specimens. Patients with post-neoadjuvant therapy pathological (yp)T0N0M0 GC were defined as having a pCR and all others were defined as not having a pCR[11]. Clinical examinations and abdominal CT were performed every 6 mo for 3 years. Digestive endoscopy was performed at least once a year. In March 2017, we confirmed the survival status of patients and the median follow-up time was 42 mo (range, 2-74 mo). Follow-up data were completed for all recruited patients.

Primary and secondary objectives

The primary objective was to evaluate the impact of NACT-surgery interval time on pCR rate and the optimal timing of operation. The secondary objective was to determine the association between NACT-surgery interval time and 3-year OS or disease-free survival (DFS). For that purpose, of the 171 patients who were admitted from January 2011 to March 2014, 121 were selected.

Statistical analysis

We used the Chi-squared test or Fisher's exact test for binary and categorical variables, and ANOVA or *t*-tests for continuous variables, as appropriate. Patient and tumor characteristics were compared between the three groups at baseline and postsurgery. A bivariate analysis of patients, tumors and surgical characteristics, and pCR status was conducted. Tumor or treatment characteristics that achieved a *P*-value < 0.2 in univariate analysis were included in the multivariable analysis. Logistic regression was used to model the effects of optimal interval time on the odds of having a pCR, and factors independently associated with pCR were determined using a stepwise procedure. The Kaplan-Meier method was used to estimate survivor functions and the log-rank test was used for the comparison of survival curves. Multivariate analysis using Cox proportional hazards regression analysis with a stepwise procedure was performed to investigate independent factors of survival.

All the statistical analyses were performed using IBM SPSS Statistics version 22.0 software. The hazard ratio (HR) and 95% confidence interval (95%CI) were reported and used to assess the relationship between pCR rate and survival for each independent factor.

RESULTS

Among the 176 patients, 111 (63%) had an NACT-surgery interval time < 4 wk, 48 (27%) had an interval time of 4-6 wk, and 17 (9.7%) had an interval time > 6 wk. The median age was 57 years (range, 21-75 years) and the male to female ratio was 3.5/1. Characteristics of the study cohort are summarized in Table 1. Patient characteristics, tumor characteristics, and surgical procedure were compared among the three groups (< 4 wk, 4-6 wk, and > 6 wk). Age (*P* = 0.014), tumor differentiation (before NACT) (*P* = 0.000), clinical T stage (*P* = 0.006), and ypT stage (*P* = 0.045) were significantly different among the three groups. Forty (22.7%) patients had achieved a pCR; the pCR rate was 67.5% for those with a NACT-surgery interval time < 4 wk, 15% for those with a

Table 1 Demographic and tumor characteristics according to the neoadjuvant chemotherapy-surgery interval time and pathological complete response status *n* (%)

	< 4 wk (*n* = 111)	4-6 wk (*n* = 48)	> 6 wk (*n* = 17)	*P* value	pCR (*n* = 40)	No pCR (*n* = 136)	*P* value
Age, yr, mean ± SD	55.5585 ± 10.8079	59.7916 ± 9.7891	61.5882 ± 9.5985	0.014	57.375 ± 9.862354	57.27206 ± 10.88013	0.908
Sex				0.974			0.174
Male	87 (78.38)	37 (77.08)	13 (76.47)		28 (70.00)	109 (80.15)	
Female	24 (21.62)	11 (22.92)	4 (23.53)		12 (3.00)	27 (19.85)	
Chemotherapy cycles				0.692			1.000
< 4	39 (35.14)	17 (35.42)	4 (23.53)		14 (35.00)	46 (33.82)	
⩾ 4	72 (64.86)	31 (64.58)	13 (76.47)		26 (65.00)	90 (66.18)	
ASA, yr, mean ± SD				0.083			0.467
1	8 (7.21)	1 (2.8)	2 (11.76)		4 (10.00)	7 (5.15)	
2	97 (87.39)	39 (81.25)	15 (88.24)		32 (80.00)	119 (87.50)	
3	6 (5.40)	8 (16.67)	0		4 (10.00)	10 (7.35)	
Histology (before NACT)				0.398			0.658
Tubular adenocarcinoma	90 (81.08)	40 (83.33)	15 (88.24)		34 (85.00)	111 (81.62)	
Mucinous	10 (9.01)	1 (2.08)	0 (0.00)		1 (2.50)	10 (7.35)	
Signet ring cell	9 (9.11)	4 (8.33)	1 (5.88)		3 (7.50)	11 (8.09)	
mixed type[1]	2 (1.80)	3 (6.25)	1 (5.88)		2 (5.00)	4 (2.94)	
Differentiation (before NACT)				0.000			0.032
Well	2 (1.80)	0 (0.00)	15 (88.24)		2 (5.00)	0 (0.00)	
Moderate	28 (25.23)	10 (20.83)	1 (5.88)		10 (25.00)	35 (25.74)	
Poor	81 (72.97)	38 (79.17)	1 (5.88)		28 (79.00)	101 (74.26)	
Clinical T stage				0.006			0.027
2	31 (27.93)	17 (35.42)	6 (35.29)		15 (37.50)	39 (28.68)	
3	24 (21.62)	19 (39.58)	8 (47.06)		16 (40.00)	35 (19.85)	
4	56 (50.45)	12 (25.00)	3 (17.65)		9 (22.50)	62 (51.47)	
Clinical N stage				0.170			0.012
Positive	89 (80.18)	33 (68.75)	11 (64.71)		24 (60.00)	109 (88.97)	
Negative	22 (19.82)	15 (31.25)	6 (35.29)		16 (40.00)	27 (11.03)	
Tumor location				0.650			0.044
Upper	45 (40.54)	23 (47.92)	6 (35.29)		10 (25.00)	64 (47.06)	
Middle	16 (14.41)	7 (14.58)	2 (11.76)		6 (15.00)	19 (13.97)	
Lower	45 (40.54)	14 (29.17)	7 (41.18)		22 (55.00)	44 (32.35)	
Diffuse type[2]	5 (4.51)	4 (8.33)	2 (11.76)		2 (5.00)	9 (6.62)	
Tumor diameter (before NACT)				0.134			0.069
⩽ 2 cm	15 (13.51)	8 (16.67)	2 (11.76)		7 (17.50)	18 (2.21)	
2-5 cm	50 (45.05)	21 (43.75)	13 (76.47)		24 (60.00)	60 (69.85)	
⩾ 5 cm	46 (41.44)	19 (39.58)	2 (11.76)		9 (12.50)	58 (27.94)	
Surgical procedure				0.363			0.002
Proximal gastrectomy	21 (18.92)	10 (20.83)	2 (11.76)		9 (22.50)	24 (17.65)	
Distal gastrectomy	32 (28.83)	10 (20.83)	8 (47.06)		19 (47.50)	31 (22.79)	
Total gastrectomy	58 (52.25)	28 (58.33)	7 (41.18)		12 (30.00)	81 (59.56)	
NACT-surgery interval time							0.043
< 4 wk					27 (67.50)	84 (61.76)	
4-6 wk					6 (15.00)	42 (30.88)	
> 6 wk					7 (17.50)	10 (7.35)	
ypT stage				0.045			
0	27 (24.32)	6 (12.50)	7 (41.18)				
1	7 (6.31)	9 (18.75)	3 (17.65)				
2	25 (22.52)	6 (12.50)	2 (11.76)				
3	38 (34.23)	15 (31.25)	4 (23.53)				
4	14 (12.61)	12 (25.00)	1 (5.88)				
ypN stage				0.187			
0	67 (60.30)	23 (47.92)	14 (82.35)				
1	7 (6.31)	7 (14.58)	2 (11.76)				
2	16 (14.41)	5 (10.42)	1 (5.88)				
3a	14 (12.61)	8 (16.67)	0				
3b	7 (6.31)	5 (10.42)	0				

[1]Mixed type: the tumor contains at least two kinds of cancer cell with different pathological classification, and the proportion of cancer cells in each type is similar; [2]Diffuse type: the region of tumor is beyond one part of the stomach (three parts of the stomach: cardiac and gastric fundus, gastric body, and pylorus and gastric antrum). pCR: Pathological complete response; NACT: Neoadjuvant chemotherapy.

NACT-surgery interval time of 4-6 wk, and 17.5% for those with a NACT-surgery interval time > 6 wk.

Impact of NACT-surgery interval time on pCR

Table 1 also shows the bivariate association between

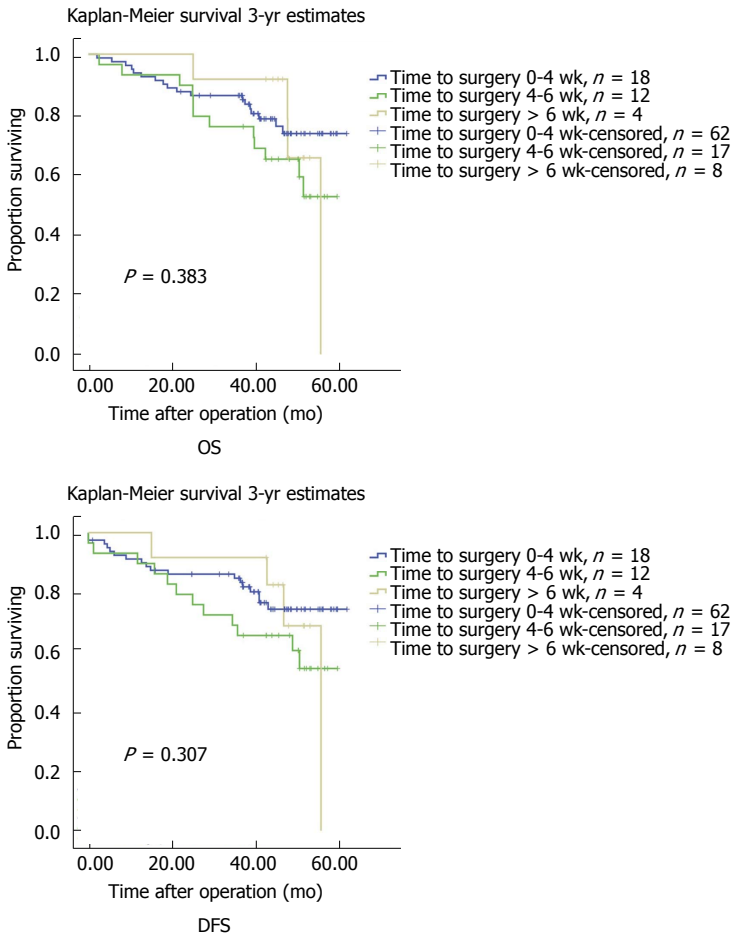

Figure 2 Overall survival and disease-free survival curves of the three groups. OS: Overall survival; DFS: Disease-free survival.

Table 2 Multivariate logistic analysis identifying independent predictors of pathological complete response

Factor	OR	95%CI	*P* value
Sex			
Male vs female	1.76	0.74-4.18	0.201
NACT-Surgery interval time			
< 4 wk *vs* > 6 wk	0.69	0.22-2.13	0.521
4-6 wk *vs* > 6 wk	0.26	0.07-0.96	0.044
Clinical T stage			
T2 *vs* T4	1.99	0.70-5.68	0.200
T3 *vs* T4	2.90	1.04-8.01	0.041
Clinical N stage			
Positive *vs* negative	2.12	0.90-4.97	0.086
Tumor diameter (before NACT)			
≤ 2 cm *vs* ≥ 5 cm	1.60	0.44-5.80	0.472
2-5 cm *vs* ≥ 5 cm	1.58	0.60-4.14	0.354

NACT: Neoadjuvant chemotherapy.

pCR and patient characteristics, tumor characteristics, and surgical procedure. NACT-surgery interval time (P = 0.043), tumor differentiation (before NACT) (P = 0.032), clinical T stage (P = 0.027), clinical N stage (P = 0.012), tumor location (P = 0.044), and surgical procedure (P = 0.002) were significantly different between patients with and without pCR.

Factors that have achieved a P-value < 0.2 in univariate analysis were selected for multivariate analysis, including gender, NACT-surgery and interval time, clinical T stage, clinical N stage, tumor diameter. The multivariate analysis (Table 2) showed that a NACT-surgery interval time of 4-6 wk was associated with a 74% lower change of having a pCR as compared with an NACT-surgery interval time > 6 wk (P = 0.044), while the OR of clinical T_3 *vs* clinical T_4 stage for pCR was 2.90 (95%CI: 1.04-8.01, P = 0.041).

Impact of NACT-surgery interval time on OS and DFS

Kaplan-Meier analyses for 3-year OS and DFS are presented in Figure 2. There was no significant difference among the three survival curves for both OS and DFS according to the log-rank test. The median OS was 41.5 mo (range, 20.0-61.8 mo) and median DFS was 39.5 mo (range, 0-61.8 mo).

Recurrence was experienced by 29.5% of patients. As shown in Table 3, NACT-surgery interval time was not found to be independently associated with OS or DFS. Independent factors associated with OS were ypN stage (N_0 *vs* N_3: HR = 0.16, 95%CI: 0.37-0.70, P

Table 3 Multivariable analysis identifying independent predictors of overall survival and disease-free survival

Independent predictor	3-yr estimate (overall survival)			3-yr estimate (disease-free survival)		
	HR	95%CI	*P* value	HR	95%CI	*P* value
NACT-Surgery interval time						
< 4 wk *vs* > 6 wk	0.49	0.11-2.129	0.340	0.43	0.10-1.85	0.258
4-6 wk *vs* > 6 wk	0.99	0.24-4.06	0.985	0.93	0.23-3.80	0.922
Age						
⩽ 60 *vs* > 60	0.90	0.34-2.37	0.833	0.84	0.32-2.19	0.720
Sex						
Female *vs* male	1.27	0.40-4.04	0.688	1.24	0.39-3.99	0.716
Histology (before NACT)						
Tubular adenocarcinoma *vs* mixed type	2.56	0.24-26.94	0.433	2.25	0.22-22.56	0.491
Mucinous *vs* mixed type	3.79	0.21-70.55	0.372	3.12	0.18-53.99	0.435
Signet ring cell *vs* mixed type	5.71	0.40-81.22	0.199	4.99	0.37-66.54	0.224
Differentiation (before NACT)						
Well and moderate *vs* poor	2.49	0.99-6.24	0.052	2.45	0.98-6.11	0.054
Clinical T stage						
T2 *vs* T4	1.51	0.42-5.39	0.524	1.67	0.48-5.84	0.422
T3 *vs* T4	0.99	0.31-3.16	0.980	0.98	0.31-3.11	0.968
Clinical N stage						
Positive *vs* negative	0.45	0.13-1.62	0.221	0.49	0.14-1.74	0.270
Tumor diameter (before NACT)						
⩽ 2 cm *vs* ⩾ 5 cm	3.16	0.61-16.45	0.171	2.88	0.57-14.65	0.202
2-5 cm *vs* ⩾ 5 cm	1.91	0.72-5.10	0.196	1.74	0.65-4.65	0.267
Tumor location						
Upper *vs* diffuse type	1.04	0.15-7.33	0.973	0.99	0.14-6.98	0.989
Middle *vs* diffuse type	1.11	0.16-7.78	0.915	1.16	0.17-8.05	0.879
Lower *vs* diffuse type	4.41	0.78-25.18	0.095	3.94	0.69-22.50	0.123
Surgical procedure						
Proximal gastrectomy *vs* total gastrectomy	0.69	0.17-2.73	0.593	0.79	0.20-3.07	0.729
Distal gastrectomy *vs* total gastrectomy	0.12	0.33-0.42	0.001	0.13	0.36-0.44	0.001
ypT stage						
T0 *vs* T4	1.04	0.15-7.20	0.968	1.27	0.18-9.08	0.811
T1 *vs* T4	0.57	0.09-4.14	0.601	0.588	0.86-4.04	0.589
T2 *vs* T4	1.15	0.24-5.53	0.858	1.29	0.26-6.46	0.756
T3 *vs* T4	0.60	0.15-2.09	0.387	0.59	0.16-2.18	0.425
ypN stage						
N0 *vs* N3	0.16	0.37-0.70	0.015	0.11	024-0.52	0.005
N1 *vs* N3	0.14	0.02-0.81	0.029	0.17	0.02-0.71	0.020
N2 *vs* N3	0.47	0.11-1.98	0.302	0.40	0.09-1.67	0.208

NACT: Neoadjuvant chemotherapy.

= 0.015; N_1 *vs* N_3: HR = 0.14, 95%CI: 0.02-0.81, *P* = 0.029) and surgical procedure (distal gastrectomy *vs* total gastrectomy: HR = 0.12, 95%CI: 0.33-0.42, *P* = 0.001). For DFS, independent factors were also ypN stage and surgical procedure.

DISCUSSION

The impact of the NACT-surgery interval on pCR and survival has been proven in rectal cancer and esophageal cancer[8,14]. However, the optimal NACT-surgery interval time and its association with survival, to the best of our knowledge, have never been investigated in GC. Similar to what was found in rectal cancer, the results of the present study suggest that a NACT-surgery interval time > 6 wk had a positive impact on pCR compared with either 4-6 wk or < 4 wk. However, the NACT-surgery interval time did not have an impact on either OS or DFS.

To determine the cutoff level, we plotted a curve of cumulative proportion of pCR by interval weeks (Figure 3). The curve shows that the slope is highest when the interval time is < 4 wk, and 4 and 6 wk are points of inflection. Meanwhile, the NACT-surgery interval time is commonly 4-6 wk, which is what clinicians in China have adopted. Thus, to prove whether a NACT-surgery interval time of 4-6 wk is optimal, after taking all factors into consideration, we divided the population into three groups by the cutoff levels of 4 and 6 weeks.

The impact of NACT-surgery interval time on pCR is the primary objective that we wanted to address. We defined pCR as T0N0M0, and partial response (PR) was not included in this study. This is because PR, which is confirmed using imaging according to RECIST[21], is more subjective and hence, more difficult to confirm than CR. In Table 1, age and tumor differentiation (before NACT) were significantly different among the three groups. The average age is highest in the > 6 wk group and lowest in the < 4 wk group. The result suggests that older patients may need a longer recovery

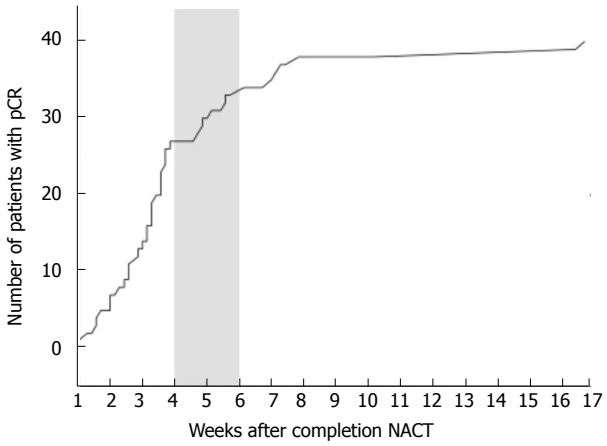

Figure 3 Cumulative frequency of pathological complete remission by neoadjuvant chemotherapy to surgery interval time. NACT: Neoadjuvant chemotherapy.

period from NACT. In the subsequent univariate and multivariable analyses, age was shown to have no impact on pCR and long-term outcomes. With respect to tumor differentiation, previous studies showed that the more differentiated a tumor, the higher the pathology response rate when patients were treated with a XELOX regimen[22,23]. However, results from our univariate analysis contradict these previous findings. The NACT-surgery interval time, tumor differentiation (before NACT), clinical T stage, clinical N stage, tumor location, and surgical procedure were significantly different between the pCR group and the no-pCR group. We had not included surgical procedure into univariate analysis, for the reason that the pCR status had been determined before surgery. The subsequent multivariable analysis proved that NACT-surgery interval time and cT stage was independent factors associated with having a pCR. Compared with clinical T_4 stage, patients with lower clinical T_2 or T_3 stage were more likely to achieve a pCR, although there was no significant difference between clinical T_2 and T_3 stages. This result is consistent with a previous study[24], which showed that lower T and N stages were linked with higher likelihood of pCR. Patients with a NACT-surgery interval time of 4-6 wk had a lower odds of having a pCR than those with an interval time > 6 wk (P = 0.044). Although a NACT-surgery interval time < 4 wk was associated with a 49% lower chance of having a pCR as compared with an interval time > 6 wk, the result was not statistically significant (P = 0.521). From these outcomes and the associations among them, we can conclude that the NACT-surgery interval time > 6 wk was the optimal interval time and had a positive impact on pCR as compared with the other groups.

This result is consistent with those from previous rectal and esophageal cancer studies[25-28], and it may be a common rule in gastrointestinal malignancies. Although many studies have shown that there is a positive impact from delaying the NACT-surgery interval time on pCR rate and short-term outcomes, the underlying mechanism has never been discussed. We speculate that it may be the result of multiple factors, including the ongoing effect of radiochemotherapy, changes in the tumor microenvironment, and recovery of immunity from chemotherapy. Additional basic medical studies may be needed to explain it.

The association between NACT-surgery interval time and long-term outcomes was also investigated. The survival curves of the three groups intersected at certain points and the log-rank test did not find any statistical significance among the curves (Figure 2). For both OS and DFS, Cox regression analysis showed that the NACT-surgery interval time and pCR (reflected by ypT_0 status) had no impact on survival. This result is contrary to our expectation because pCR is deemed to have a positive impact on survival. Meredith *et al*[29] and Abdul-Jalil *et al*[30] both reported that pCR was an independent factor for OS and DFS. We thought that the small sample size may be the limitation. Regarding the NACT-surgery interval time, many previous studies in esophageal cancer proved that the interval time did not have any effect on survival[13,15,31], while some studies in rectal cancer reached an opposite conclusion[26,28]. Our result is consistent with studies in esophageal cancer. Our finding that ypN stage had a significant impact on OS and DFS aligns with those from previous studies[32,33]. The surgical procedure was found to be also an independent factor that can influence OS and DFS. Patients on whom a distal gastrectomy was performed had a significant difference in survival compared with patients on whom a total gastrectomy was performed. The reason for this result may be that patients who undergo a distal gastrectomy have a greater chance of having a pCR, and also, may be the difference of surgical method itself.

There were some limitations to our study. Its retrospective nature may induce some bias. Our relatively short follow-up time for survival (3-year estimates) and the absence of information regarding diseases not treated at the PLA General Hospital after the operation may have impacted our results. Also, our single institute research cannot avoid sampling bias and may not be representative. The small sample size was the biggest limitation, and the number of patients with interval time > 6 wk was not sufficient to explore more timing groups or the maximum interval time (such as 6-8 wk, 8-12 wk, and > 12 wk). A future multi-center randomized control trial with a larger sample size may be needed to validate our results.

To conclude, the NACT-surgery interval time > 6 wk can increase the chance of a pCR, but the NACT-surgery interval time does not have an impact on long-term survival.

ARTICLE HIGHLIGHTS

Research background

The impact of the interval time from the completion of neoadjuvant

chemotherapy (NACT) to surgery on pathological complete response (pCR) and survival has been proved in rectal cancer and esophageal cancer. However, the optimal NACT-surgery interval time and its association with survival, to the best of our knowledge, have never been investigated in gastric cancer. This study can provide evidence for the timing of surgery and patients with neoadjuvant chemotherapy may benefit from it.

Research motivation

To investigate whether the interval time between NACT and surgery have an impact on pCR was our main topic. The investigation lays a foundation for the further RCT research.

Research objectives

There were two objectives in this study. The primary objective was to evaluate the impact of NACT-surgery interval time on pCR rate and the optimal timing of operation. The secondary objective was to determine the association between NACT-surgery interval time and 3-year OS or disease-free survival (DFS). If the impacts are existent, more studies will focus on the investigation of optimal interval time and this evidence will bring a change in treatment plan for GC patients with neoadjuvant chemotherapy.

Research methods

This is a retrospective study, in which we realized our objectives through data analysis using bivariate analysis, logistic regression analysis, and Cox proportion hazards regression. These methods are routinely used in studies and have high stability.

Research results

The impact of the NACT-surgery interval time on pCR has been proved and the interval time > 6 wk can increase the chance of a pCR. Clinical T stage also have an impact on pCR. The independent predictors of long-term survival are ypN stage and surgical procedure. These findings for the first time proved the impact of the NACT-surgery interval time on pCR in gastric cancer and give a reference for the optimal interval time. The further investigations of accurate optimal interval time are needed.

Research conclusions

The authors for the first time investigated and found the impact of the NACT-surgery interval time on pCR, and the optimal interval time may be > 6 wk. This result is consistent with those from previous rectal and esophageal cancer studies, and we speculate that it may be the result of multiple factors, including the ongoing effect of radiochemotherapy, changes in the tumor microenvironment, and recovery of immunity from chemotherapy. Additional basic medical studies may be needed to explain it.

Research perspectives

Further studies, either retrospective or prospective, are needed to investigate more interval time groups with a large sample size. Also, it is meaningful to investigate the mechanism of this finding through basic medical studies.

REFERENCES

1 **Patel SH**, Kooby DA. Gastric adenocarcinoma surgery and adjuvant therapy. *Surg Clin North Am* 2011; **91**: 1039-1077 [PMID: 21889029 DOI: 10.1016/j.suc.2011.06.009]

2 **Cunningham D**, Allum WH, Stenning SP, Thompson JN, Van de Velde CJ, Nicolson M, Scarffe JH, Lofts FJ, Falk SJ, Iveson TJ, Smith DB, Langley RE, Verma M, Weeden S, Chua YJ, MAGIC Trial Participants. Perioperative chemotherapy versus surgery alone for resectable gastroesophageal cancer. *N Engl J Med* 2006; **355**: 11-20 [PMID: 16822992 DOI: 10.1056/NEJMoa055531]

3 **Ychou M**, Boige V, Pignon JP, Conroy T, Bouché O, Lebreton G, Ducourtieux M, Bedenne L, Fabre JM, Saint-Aubert B, Genève J, Lasser P, Rougier P. Perioperative chemotherapy compared with surgery alone for resectable gastroesophageal adenocarcinoma: an FNCLCC and FFCD multicenter phase III trial. *J Clin Oncol* 2011; **29**: 1715-1721 [PMID: 21444866 DOI: 10.1200/JCO.2010.33.0597]

4 **Xiong BH**, Cheng Y, Ma L, Zhang CQ. An updated meta-analysis of randomized controlled trial assessing the effect of neoadjuvant chemotherapy in advanced gastric cancer. *Cancer Invest* 2014; **32**: 272-284 [PMID: 24800782 DOI: 10.3109/07357907.2014.911877]

5 **Martin ST**, Heneghan HM, Winter DC. Systematic review and meta-analysis of outcomes following pathological complete response to neoadjuvant chemoradiotherapy for rectal cancer. *Br J Surg* 2012; **99**: 918-928 [PMID: 22362002 DOI: 10.1002/bjs.8702]

6 **Cho H**, Nakamura J, Asaumi Y, Yabusaki H, Sakon M, Takasu N, Kobayashi T, Aoki T, Shiraishi O, Kishimoto H, Nunobe S, Yanagisawa S, Suda T, Ueshima S, Matono S, Maruyama H, Tatsumi M, Seya T, Tanizawa Y, Yoshikawa T. Long-term survival outcomes of advanced gastric cancer patients who achieved a pathological complete response with neoadjuvant chemotherapy: a systematic review of the literature. *Ann Surg Oncol* 2015; **22**: 787-792 [PMID: 25223927 DOI: 10.1245/s10434-014-4084-9]

7 **Francois Y**, Nemoz CJ, Baulieux J, Vignal J, Grandjean JP, Partensky C, Souquet JC, Adeleine P, Gerard JP. Influence of the interval between preoperative radiation therapy and surgery on downstaging and on the rate of sphincter-sparing surgery for rectal cancer: the Lyon R90-01 randomized trial. *J Clin Oncol* 1999; **17**: 2396 [PMID: 10561302 DOI: 10.1200/JCO.1999.17.8.2396]

8 **Tulchinsky H**, Shmueli E, Figer A, Klausner JM, Rabau M. An interval >7 weeks between neoadjuvant therapy and surgery improves pathologic complete response and disease-free survival in patients with locally advanced rectal cancer. *Ann Surg Oncol* 2008; **15**: 2661-2667 [PMID: 18389322 DOI: 10.1245/s10434-008-9892-3]

9 **de Campos-Lobato LF**, Geisler DP, da Luz Moreira A, Stocchi L, Dietz D, Kalady MF. Neoadjuvant therapy for rectal cancer: the impact of longer interval between chemoradiation and surgery. *J Gastrointest Surg* 2011; **15**: 444-450 [PMID: 21140237 DOI: 10.1007/s11605-010-1197-8]

10 **Wolthuis AM**, Penninckx F, Haustermans K, De Hertogh G, Fieuws S, Van Cutsem E, D'Hoore A. Impact of interval between neoadjuvant chemoradiotherapy and TME for locally advanced rectal cancer on pathologic response and oncologic outcome. *Ann Surg Oncol* 2012; **19**: 2833-2841 [PMID: 22451236 DOI: 10.1245/s10434-012-2327-1]

11 **Probst CP**, Becerra AZ, Aquina CT, Tejani MA, Wexner SD, Garcia-Aguilar J, Remzi FH, Dietz DW, Monson JR, Fleming FJ; Consortium for Optimizing the Surgical Treatment of Rectal Cancer (OSTRiCh). Extended Intervals after Neoadjuvant Therapy in Locally Advanced Rectal Cancer: The Key to Improved Tumor Response and Potential Organ Preservation. *J Am Coll Surg* 2015; **221**: 430-440 [PMID: 26206642 DOI: 10.1016/j.jamcollsurg.2015.04.010]

12 **Ruol A**, Rizzetto C, Castoro C, Cagol M, Alfieri R, Zanchettin G, Cavallin F, Michieletto S, Da Dalt G, Sileni VC, Corti L, Mantoan S, Zaninotto G, Ancona E. Interval between neoadjuvant chemoradiotherapy and surgery for squamous cell carcinoma of the thoracic esophagus: does delayed surgery have an impact on outcome? *Ann Surg* 2010; **252**: 788-796 [PMID: 21037434 DOI: 10.1097/SLA.0b013e3181fc7f86]

13 **Shaikh T**, Ruth K, Scott WJ, Burtness BA, Cohen SJ, Konski AA, Cooper HS, Astsaturov I, Meyer JE. Increased time from neoadjuvant chemoradiation to surgery is associated with higher pathologic complete response rates in esophageal cancer. *Ann Thorac Surg* 2015; **99**: 270-276 [PMID: 25440267 DOI: 10.1016/j.athoracsur.2014.08.033]

14 **Shapiro J**, van Hagen P, Lingsma HF, Wijnhoven BP, Biermann K, ten Kate FJ, Steyerberg EW, van der Gaast A, van Lanschot JJ; CROSS Study Group. Prolonged time to surgery after neoadjuvant chemoradiotherapy increases histopathological response without affecting survival in patients with esophageal or junctional cancer. *Ann Surg* 2014; **260**: 807-813; discussion 813-814 [PMID: 25379852 DOI: 10.1097/SLA.0000000000000966]

15 **Tessier W**, Gronnier C, Messager M, Hec F, Mirabel X, Robb WB, Piessen G, Mariette C. Does timing of surgical procedure after neoadjuvant chemoradiation affect outcomes in esophageal cancer? *Ann Thorac Surg* 2014; **97**: 1181-1189 [PMID: 24529482 DOI:

10.1016/j.athoracsur.2013.12.026]
16 **Lin G**, Han SY, Xu YP, Mao WM. Increasing the interval between neoadjuvant chemoradiotherapy and surgery in esophageal cancer: a meta-analysis of published studies. *Dis Esophagus* 2016; **29**: 1107-1114 [PMID: 26542065 DOI: 10.1111/dote.12432]
17 **Hashemzadeh S**, Pourzand A, Somi MH, Zarrintan S, Javad-Rashid R, Esfahani A. The effects of neoadjuvant chemotherapy on resectability of locally-advanced gastric adenocarcinoma: a clinical trial. *Int J Surg* 2014; **12**: 1061-1069 [PMID: 25157992 DOI: 10.1016/j.ijsu.2014.08.349]
18 **Oki E**, Emi Y, Kusumoto T, Sakaguchi Y, Yamamoto M, Sadanaga N, Shimokawa M, Yamanaka T, Saeki H, Morita M, Takahashi I, Hirabayashi N, Sakai K, Orita H, Aishima S, Kakeji Y, Yamaguchi K, Yoshida K, Baba H, Maehara Y. Phase II study of docetaxel and S-1 (DS) as neoadjuvant chemotherapy for clinical stage III resectable gastric cancer. *Ann Surg Oncol* 2014; **21**: 2340-2346 [PMID: 24604583 DOI: 10.1245/s10434-014-3594-9]
19 **Japanese Gastric Cancer Association.**. Japanese classification of gastric carcinoma: 3rd English edition. *Gastric Cancer* 2011; **14**: 101-112 [PMID: 21573743 DOI: 10.1007/s10120-011-0041-5]
20 **Yamada Y**, Higuchi K, Nishikawa K, Gotoh M, Fuse N, Sugimoto N, Nishina T, Amagai K, Chin K, Niwa Y, Tsuji A, Imamura H, Tsuda M, Yasui H, Fujii H, Yamaguchi K, Yasui H, Hironaka S, Shimada K, Miwa H, Hamada C, Hyodo I. Phase III study comparing oxaliplatin plus S-1 with cisplatin plus S-1 in chemotherapy-naïve patients with advanced gastric cancer. *Ann Oncol* 2015; **26**: 141-148 [PMID: 25316259 DOI: 10.1093/annonc/mdu472]
21 **Watanabe H**, Okada M, Kaji Y, Satouchi M, Sato Y, Yamabe Y, Onaya H, Endo M, Sone M, Arai Y. [New response evaluation criteria in solid tumours-revised RECIST guideline (version 1.1)]. *Gan To Kagaku Ryoho* 2009; **36**: 2495-2501 [PMID: 20009446]
22 **Wu ZF**, Cao QH, Wu XY, Chen C, Xu Z, Li WS, Yao XQ, Liu FK. Regional Arterial Infusion Chemotherapy improves the Pathological Response rate for advanced gastric cancer with Short-term Neoadjuvant Chemotherapy. *Sci Rep* 2015; **5**: 17516 [PMID: 26620627 DOI: 10.1038/srep17516]
23 **Sun LB**, Zhao GJ, Ding DY, Song B, Hou RZ, Li YC. Comparison between better and poorly differentiated locally advanced gastric cancer in preoperative chemotherapy: a retrospective, comparative study at a single tertiary care institute. *World J Surg Oncol* 2014; **12**: 280 [PMID: 25200958 DOI: 10.1186/1477-7819-12-280]
24 **Al-Sukhni E**, Attwood K, Mattson DM, Gabriel E, Nurkin SJ. Predictors of Pathologic Complete Response Following Neoadjuvant Chemoradiotherapy for Rectal Cancer. *Ann Surg Oncol* 2016; **23**: 1177-1186 [PMID: 26668083 DOI: 10.1245/s10434-015-5017-y]
25 **Panagiotopoulou IG**, Parashar D, Qasem E, Mezher-Sikafi R, Parmar J, Wells AD, Bajwa FM, Menon M, Jephcott CR. Neoadjuvant Long-Course Chemoradiotherapy for Rectal Cancer: Does Time to Surgery Matter? *Int Surg* 2015; **100**: 968-973 [PMID: 26414816 DOI: 10.9738/INTSURG-D-14-00192.1]
26 **Garrer WY**, El Hossieny HA, Gad ZS, Namour AE, Abo Amer SM. Appropriate Timing of Surgery after Neoadjuvant ChemoRadiation Therapy for Locally Advanced Rectal Cancer. *Asian Pac J Cancer Prev* 2016; **17**: 4381-4389 [PMID: 27797248]
27 **Lee A**, Wong AT, Schwartz D, Weiner JP, Osborn VW, Schreiber D. Is There a Benefit to Prolonging the Interval Between Neoadjuvant Chemoradiation and Esophagectomy in Esophageal Cancer? *Ann Thorac Surg* 2016; **102**: 433-438 [PMID: 27154156 DOI: 10.1016/j.athoracsur.2016.02.058]
28 **Mihmanlı M**, Kabul Gürbulak E, Akgün İE, Celayir MF, Yazıcı P, Tunçel D, Bek TT, Öz A, Ömeroğlu S. Delaying surgery after neoadjuvant chemoradiotherapy improves prognosis of rectal cancer. *World J Gastrointest Oncol* 2016; **8**: 695-706 [PMID: 27672428 DOI: 10.4251/wjgo.v8.i9.695]
29 **Meredith KL**, Weber JM, Turaga KK, Siegel EM, McLoughlin J, Hoffe S, Marcovalerio M, Shah N, Kelley S, Karl R. Pathologic response after neoadjuvant therapy is the major determinant of survival in patients with esophageal cancer. *Ann Surg Oncol* 2010; **17**: 1159-1167 [PMID: 20140529 DOI: 10.1245/s10434-009-0862-1]
30 **Abdul-Jalil KI**, Sheehan KM, Kehoe J, Cummins R, O'Grady A, McNamara DA, Deasy J, Breathnach O, Grogan L, O'Neill BD, Faul C, Parker I, Kay EW, Hennessy BT, Gillen P. The prognostic value of tumour regression grade following neoadjuvant chemoradiation therapy for rectal cancer. *Colorectal Dis* 2014; **16**: O16-O25 [PMID: 24119076 DOI: 10.1111/codi.12439]
31 **Ranney DN**, Mulvihill MS, Yerokun BA, Fitch Z, Sun Z, Yang CF, D'Amico TA, Hartwig MG. Surgical resection after neoadjuvant chemoradiation for oesophageal adenocarcinoma: what is the optimal timing? *Eur J Cardiothorac Surg* 2017; **52**: 543-551 [PMID: 28498967 DOI: 10.1093/ejcts/ezx132]
32 **Guillem JG**, Chessin DB, Cohen AM, Shia J, Mazumdar M, Enker W, Paty PB, Weiser MR, Klimstra D, Saltz L, Minsky BD, Wong WD. Long-term oncologic outcome following preoperative combined modality therapy and total mesorectal excision of locally advanced rectal cancer. *Ann Surg* 2005; **241**: 829-836; discussion 836-838 [PMID: 15849519 DOI: 10.1097/01.sla.0000161980.46459.96]
33 **Das P**, Skibber JM, Rodriguez-Bigas MA, Feig BW, Chang GJ, Hoff PM, Eng C, Wolff RA, Janjan NA, Delclos ME, Krishnan S, Levy LB, Ellis LM, Crane CH. Clinical and pathologic predictors of locoregional recurrence, distant metastasis, and overall survival in patients treated with chemoradiation and mesorectal excision for rectal cancer. *Am J Clin Oncol* 2006; **29**: 219-224 [PMID: 16755173 DOI: 10.1097/01.coc.0000214930.78200.4a]

P- Reviewer: Espinel J, Ilhan E, Tanabe S **S- Editor**: Gong ZM **L-Editor**: Wang TQ **E- Editor**: Ma YJ

World Journal of Gastroenterology

Submit a Manuscript: http://www.f6publishing.com

World J Gastroenterol 2018 January 14; 24(2): 266-273

DOI: 10.3748/wjg.v24.i2.266

ISSN 1007-9327 (print) ISSN 2219-2840 (online)

ORIGINAL ARTICLE

Retrospective Study

Predictive and prognostic value of serum AFP level and its dynamic changes in advanced gastric cancer patients with elevated serum AFP

Ya-Kun Wang, Lin Shen, Xi Jiao, Xiao-Tian Zhang

Ya-Kun Wang, Lin Shen, Xi Jiao, Xiao-Tian Zhang, Department of Gastrointestinal Oncology, Key Laboratory of Carcinogenesis and Translational Research (Ministry of Education), Peking University Cancer Hospital and Institute, Beijing 100142, China

ORCID number: Ya-Kun Wang (0000-0001-5579-2998); Lin Shen (0000-0002-1205-049X); Xi Jiao (0000-0002-5588-5657); Xiao-Tian Zhang (0000-0001-5267-7871).

Author contributions: Wang KY collected and analyzed the data and wrote the manuscript; Jiao X collected the data and revised the manuscript; Shen L and Zhang XT were in charge of the project and revised the manuscript.

Supported by the National Key Research and Development Program of China, No. 2017YFC1308900; Beijing Natural Science Foundation, No. 7161002; and Capital Health Improvement and Research Funds, No. 2016-1-1021.

Institutional review board statement: This study was approved by the Ethics Committee of Beijing University Cancer Hospital.

Informed consent statement: Patients were not required to give informed consent for this study because the analysis used anonymous clinical data that were obtained after each patient agreed to treatment by written consent.

Conflict-of-interest statement: None of the authors has declared any conflict of interest.

Data sharing statement: No additional data are available.

Manuscript source: Unsolicited manuscript

Correspondence to: Xiao-Tian Zhang, MD, Professor, Department of Gastrointestinal Oncology, Key Laboratory of Carcinogenesis and Translational Research (Ministry of Education), Peking University Cancer Hospital and Institute, No. 52, Fucheng Road, Haidian District, Beijing 100142, China. zhangxiaotianmed@163.com
Telephone: +86-10-88196561
Fax: +86-10-88196561

Received: October 26, 2017
Peer-review started: October 27, 2017
First decision: November 14, 2017
Revised: November 18, 2017
Accepted: December 5, 2017
Article in press: December 5, 2017
Published online: January 14, 2018

Abstract

AIM

To investigate predictive and prognostic value of serum alpha-fetoprotein (AFP) level and its dynamic changes in patients with advanced gastric cancer with elevated serum AFP (AFPAGC).

METHODS

One hundred and five patients with AFPAGC were enrolled in the study, and all of them underwent at least one cycle of systemic chemotherapy at our institute and had serum AFP $\geqslant$ 20 ng/mL at diagnosis or recurrence. Clinicopathologic features, serum AFP level at diagnosis and changes during treatment, first-line chemotherapy regimens, efficacy and toxicity, and survival information were collected. A Person's χ^2 or Fisher's exact test was used to measure the differences between variables. Survival prognostic factors were investigated using the Kaplan-Meier method and Cox regression.

RESULTS

Median serum AFP level was 161.7 ng/mL (range, 22.9-2557110 ng/mL). Objective response rates (ORR) was significantly lower in the AFP ⩾ 160 ng/mL group than in the AFP < 160 ng/mL group (30.4% *vs* 68.3%, $P < 0.001$). ORR to doublet regimens was significantly lower in the AFP ⩾ 160 ng/mL group, whereas ORR to triplet regimens was similar between the two groups. Liver metastasis rate was significantly higher in the AFP ⩾ 160 ng/mL group than in the AFP < 160 ng/mL (69.8% *vs* 50.0%, $P < 0.001$). Overall survival (OS) in the two cohorts did not show any significant difference ($P = 0.712$). Dynamic changes of AFP were consistent with response to chemotherapy, and median OS of patients with a serum AFP decline ⩾ 50% and those with a serum AFP decline < 50% was 17.5 m and 10.0 m, respectively ($P = 0.003$). Hepatic ($P = 0.005$), peritoneal ($P < 0.001$), non-regional lymph node metastasis ($P < 0.001$), and portal vein tumor thrombus (PVTT) ($P = 0.042$) were identified as independent prognostic factors for AFPAGC.

CONCLUSION

Real-time examination of AFP has great predictive and prognostic value for managing AFPAGC. For those with markedly elevated AFP, triplet regimens may be a better choice.

Key words: Alpha-fetoprotein; AFP-producing gastric cancer; Predictive factor; Prognostic factor; Triplet regimen

Core tip: Alpha-fetoprotein (AFP)-producing gastric cancer is a rare and aggressive subtype of gastric cancer, characterized by frequent liver metastasis and poor prognosis. We measured AFP and its changes over time during treatment, which revealed that AFP, as a biomarker of advanced gastric cancer with elevated serum AFP (AFPAGC), is significantly associated with response to chemotherapy. The decline in AFP after chemotherapy was found to be related to good prognosis for AFPAGC. We finally attempted to find an optimal treatment regimen for AFPAGC, which suggests that for those with markedly elevated AFP, triplet regimens may be a better choice.

Wang YK, Zhang XT, Jiao X, Shen L. Predictive and prognostic value of serum AFP level and its dynamic changes in advanced gastric cancer patients with elevated serum AFP. *World J Gastroenterol* 2018; 24(2): 266-273 Available from: URL: http://www.wjgnet.com/1007-9327/full/v24/i2/266.htm DOI: http://dx.doi.org/10.3748/wjg.v24.i2.266

INTRODUCTION

Gastric cancer (GC) remains the second leading cause of cancer-related death worldwide. Alpha-fetoprotein (AFP)-producing GC (AFPGC) is rare, accounting for 2.3%-7.1% of all GCs[1]. In 1970, Bourreille's group first reported a case of AFPGC, and its pathological specimen was immunohistochemically positive for AFP[2]. Previous work suggests that AFPGC is associated with a poor prognosis due to frequent liver metastasis[3,4]. However, most studies of AFPGC were based on surgically resected samples and many patients with advanced GC with elevated serum AFP (AFPAGC) have already missed an opportunity for surgical resection[5], with palliative chemotherapy having been a mainstay treatment. AFP is the most representative biomarker for AFPAGC, but how it is involved in the development and progression of AFPAGC remains known. On the other hand, due to the rarity of this special form of cancer, there is limited data in the literature about its optimal treatment.

In the present study, we studied whether AFP can be used to predict prognosis, and measured its dynamic changes over time during treatment, with an aim to find an optimal treatment regimen for AFPAGC and identify prognostic factors for this subtype of advanced GC.

MATERIALS AND METHODS

Patient selection

From 2006 to 2016, 2047 patients were diagnosed with advanced gastric adenocarcinoma at our institute. Subjects were enrolled if they were diagnosed with primary gastric adenocarcinoma; had no chance for surgery at diagnosis or had relapsed after radical resection (relapse types included anastomotic recurrence and distant metastasis); underwent at least one cycle of systemic chemotherapy at our institute (total number of chemotherapy cycles ranged from one to seven, with a median number of cycles of four in this study); and had serum AFP ⩾ 20 ng/mL at diagnosis or recurrence. The exclusion criteria were concomitant liver diseases, such as hepatitis, cirrhosis, fatty liver, or alcoholic liver, and concomitant second or multiple primary tumors. We chose 105 patients and measured pre-treatment serum AFP using radioimmunoassay (normal range: < 7 ng/mL).

Data collection

We collected data including age, gender, primary lesion site, histological type, Lauren classification, human epidermal growth factor receptor-2 (HER2) status, metastasis site, serum AFP level at diagnosis and changes during treatment, first-line chemotherapy regimen, efficacy and toxicity, local treatment for liver metastasis, and survival information.

Evaluation and follow-up

All patients were regularly followed from the date of first hospitalization at our center. Laboratory examinations were performed every 1 or 2 wk,

Table 1 Univariate prognostic analysis of clinicopathological features *n* (%)

Variable	AFPAGC (*n* = 105)	Median OS (mo)	*P* value
Sex			
Male	82 (78.1)	15.0	0.144
Female	23 (21.9)	11.3	
Age (yr)			
⩾ 60	49 (46.7)	15.0	0.189
< 60	56 (53.3)	12.0	
Serum AFP level (ng/mL)			
⩾ 500	37 (35.2)	13.0	0.806
< 500	68 (64.5)	14.6	
Primary lesion site			
EGJ	41 (39.8)	15.0	0.245
Non-EGJ	62 (60.2)	12.0	
Differentiation degree			
Well	30 (29.4)	15.4	0.496
Poor	66 (64.7)	12.9	
HAS	6 (5.9)	4.5	
Lauren classification			
Intestinal	45 (57.0)	15.4	0.352
Non-intestinal	34 (43.0)	14.6	
HER2 status			
Positive	20 (24.4)	17.5	0.583
Negative	62 (75.6)	14.6	
LM			
Present	63 (60.0)	12.0	0.048[a]
Absent	42 (40.0)	16.7	
Peritoneal metastasis			
Present	16 (15.4)	6.17	0.001[a]
Absent	88 (84.6)	15.2	
Non-regional LNM			
Present	56 (53.3)	11.0	0.042[a]
Absent	49 (46.7)	17.9	
Other hematogenous metastasis			
Present	27 (25.7)	10.5	0.004[a]
Absent	78 (74.3)	17.5	
PVTT			
Present	13 (12.4)	8.3	0.011[a]
Absent	92 (87.6)	15.0	
First-line regimen			
Doublet regimen	89 (88.1)	14.6	0.850
Triplet regimen	12 (11.9)	15.1	
Evaluation			
PR	42 (48.3)	17.6	0.007[a]
SD + PD	45 (51.7)	11.1	
AFP decline degree			
⩾ 50%	49 (55.7)	17.5	0.003[a]
< 50%	39 (44.3)	10.0	
Local treatment for LM			
Yes	19 (18.1)	17.9	0.215
No	86 (81.9)	12.9	

[a]*P* < 0.05. GEJ: Gastroesophageal junction; HER2: Human epidermal growth factor receptor-2; AFP: α-fetoprotein; LM: Liver metastasis; LNM: Lymph node metastasis; PVTT: Portal vein tumor thrombus.

and enhanced computed tomography or magnetic resonance imaging was performed to evaluate therapeutic efficacy every 6 wk during chemotherapy. Objective response rate (ORR) was evaluated using RECIST version 1.0 (before 2009) and RECIST version 1.1, and adverse reactions were recorded. Overall survival (OS) was defined as the time from diagnosis to death from any cause or last follow-up.

Statistical analysis

A Person's χ^2 test was used to measure the differences among variables, and a Fisher's exact test was used when the sample size was less than five. To identify prognostic factors for APFAGC, survival durations were calculated using the Kaplan-Meier method and Cox regression. For all tests, a *P*-value < 0.05 was considered significant. SPSS software (version 21.0; SPSS, Chicago, IL, United States) was used for analyses. GraphPad Prism 6 (GraphPad Software, Inc, La Jolla, CA, United States) was used for graphing.

RESULTS

Clinicophathological features of 105 AFPAGC cases

A total of 105 AFPAGC patients were evaluated. They ranged in age from 27 to 78 years, with a median age of 59 years. Most of the patients were diagnosed with locally advanced or metastatic GC at the initial diagnosis. Only eight patients who had recurrent disease after radical gastrectomy were involved in this study, including three cases with non-regional lymph node metastasis, six cases with liver metastasis, one case with peritoneal metastasis, and one case with anastomotic recurrence. Median serum AFP level was 161.7 ng/mL (range, 22.9-2557110 ng/mL). Nearly two-thirds (64.5%) of the patients had serum AFP < 500 ng/mL at the time of diagnosis. With regard to immunohistochemical staining (IHC) for AFP, IHC results were available in only 14 patients, of whom eight were AFP positive.

As for the primary lesion site, 41 (39.8%) tumors were located at the gastroesophogeal junction (GEJ). In histological examination, 29.4% and 64.7% patients were identified as well-differentiated and poorly differentiated adenocarcinoma, respectively. Notably, six (5.9%) patients were diagnosed with hepatoid adenocarcinoma, which was defined as a special subtype of primary gastric adenocarcinoma characterized histologically by "hepatocellular carcinoma (HCC) like differentiation"[6]. Besides, 45 (57.0%) patients had intestinal type based on the Lauren classification, and 20 (24.4%) patients HER2 positive.

As expected, 60.0% of patients were detected with liver metastasis, while only 15.4% with peritoneal dissemination. Also, portal vein tumor thrombus (PVTT) in AFPAGC had an occurrence rate of 12.4% in this study. The clinicopathological features of AFPAGC are detailed in Table 1.

Comparison of efficacy and toxicity of first-line chemotherapy regimens

In the treatment of inoperable locally advanced and/or metastatic (stage IV) GC, doublet combinations of platinum and fluoropyrimidines were frequently used, and most of triplet regimes were given to those who had potential opportunity for surgery and

Table 2 Comparison of objective response rates to different chemotherapy regimens *n* (%)

Regimen	Platinum-based doublet regimen (*n* = 58)	Taxane-based doublet regimen (*n* = 17)	Triplet regimen (*n* = 11)	*P* value
Overall population				0.201
PR	31 (53.4)	5 (29.4)	6 (54.5)	
SD + PD	27 (46.6)	12 (76.4)	5 (45.5)	
AFP ⩾ 160 ng/mL				0.067
PR	10 (32.3)	0 (0.0)	4 (57.1)	
SD + PD	21 (67.7)	7 (100.0)	3 (42.9)	
AFP < 160 ng/mL				0.193
PR	21 (77.8)	5 (50.0)	2 (50.0)	
SD + PD	6 (22.2)	5 (50.0)	2 (50.0)	

PR: Partial response; SD: Stable disease; PD: Progressive disease.

Table 3 Severe adverse events of different chemotherapy regimens *n* (%)

Regimen	Platinum-based doublet regimen (*n* = 72)	Taxane-based doublet regimen (*n* = 17)	Triplet regimen (*n* = 12)	*P* value
⩾ G3 AEs	11 (15.3)	4 (23.5)	7 (58.3)	0.004

AEs: Adverse events.

good performance status in this study. Among the original 105 patients who received first-line systemic chemotherapy, 87 (82.9%) were evaluable for their response. The majority (66.7%, *n* = 58) received platinum-based doublet regimens, including oxaliplatin + capecitabine in 36 patients, oxaliplatin + S-1 in 7, cisplatin + capecitabine in 12, cisplatin + S-1 in 1, oxaliplatin + 5-FU in 1 , and cisplatin + 5-FU in 1. Seventeen (19.5%) patients received taxane-based doublet regimens, including paclitaxel + capecitabine in 11 patients, paclitaxel + S-1 in 4, paclitaxel + 5-FU in 1, and docetaxel + capecitabine in 1. Eleven (12.6%) patients received triplet regimens, including POS (paclitaxel + oxaplatin + S-1) in 6 patients, DCF (docetaxel + cisplatin + 5-FU) in 4, and PCF (paclitaxel + cisplatin + 5-FU) in 1. In addition, 12 of 20 HER2 positive patients received anti-HER2 therapies, including trastuzumab in 11 patients and lapatinib in 1.

Overall ORR to first-line chemotherapy was 48.3%. ORR to platinum-based doublet regimens was similar to that to triplet regimens (53.4% *vs* 54.5%), but much higher than that to taxane-based doublet regimens (29.4%). The differences between either of them did not reach statistical significance (Table 2).

As for toxicity, there were totally 22 (21.0%) patients who suffered severe (⩾ grade 3) adverse events (AEs) during first-line systemic chemotherapy, with most frequently occurring severe AEs being bone marrow suppression (13.3%), hand foot syndrome (4.8%), and digestive tract reaction (3.8%). Notably, patients who received triplet regimens had a significantly higher rate of severe AEs (58.3% *vs* 15.3-23.5%, *P* = 0.004) (Table 3).

Table 4 Comparison of response, liver metastasis rate, and overall survival between alpha-fetoprotein ⩾ 160 ng/mL and alpha-fetoprotein < 160 ng/mL groups *n* (%)

Variable	AFP ⩾ 160 ng/mL	AFP < 160 ng/mL	*P* value
Overall ORR			
PR	14 (30.4)	28 (68.3)	< 0.001[a]
SD + PD	32 (69.6)	13 (31.7)	
ORR to doublet regimens			
PR	10 (26.3)	26 (70.3)	< 0.001[a]
SD + PD	28 (73.7)	11 (30.7)	
ORR to triplet regimens			
PR	4 (57.1)	2 (50.0)	0.652
SD + PD	3 (42.9)	2 (50.0)	
Liver metastasis rate	69.8%	50.0%	0.030[a]
Median OS	13.0 mo	14.8 mo	0.712

[a]*P* < 0.05. PR: Partial response; SD: Stable disease; PD: Progressive disease; ORR: Objective response rate; OS: Overall survival.

With regard to second-line chemotherapy, treatment data were available in 57 patients in this study. Thirty-two patients received second-line systemic chemotherapy, regimens mainly involved taxanes alone or combined with fluorouracil drugs. Nine patients had no chance for second-line treatment due to bad performance status. Moreover, 16 patients received local treatment instead of systemic chemotherapy due to progression after first-line treatment, including transarterial chemoembolization in 11 patients, radiotherapy in 2, ablation in 1, and pleural or intraperitoneal perfusion chemotherapy in 2.

Predictive and prognostic value of serum AFP level and its dynamic changes during treatment

Serum AFP level at diagnosis ranged from 22.9 to 2557110 ng/mL, with a median value of 161.7 ng/mL. As AFP is considered the most representative marker for AFPAGC, we next investigated the association between AFP level and response to chemotherapy, occurrence of liver metastasis, and survival. We chose the median value 160 ng/mL as a cutoff value.

The χ^2 test showed that overall ORR in the AFP ⩾ 160 ng/mL group was significantly lower than that of the AFP < 160 ng/mL group (30.4% *vs* 68.3%, *P* < 0.001). Furthermore, ORR to doublet regimens was significantly lower in the AFP ⩾ 160 ng/mL group, whereas ORR to triplet regimens was similar between the two groups (Table 4).

The ROC curve analysis for the predictive value of serum AFP is shown in Figure 1. The sensitivity and specificity were 71.1% and 69.0%, respectively, at a cut-off value of 164.8 ng/mL.

In addition, we found that liver metastasis rate was significantly higher in the AFP ⩾ 160 ng/mL group than in the AFP < 160 ng/mL group (69.8% *vs* 50.0%, *P* < 0.001), although OS did not show any significant difference (*P* = 0.712, Table 4). We measured serum AFP levels in 81 patients at the time of evaluation,

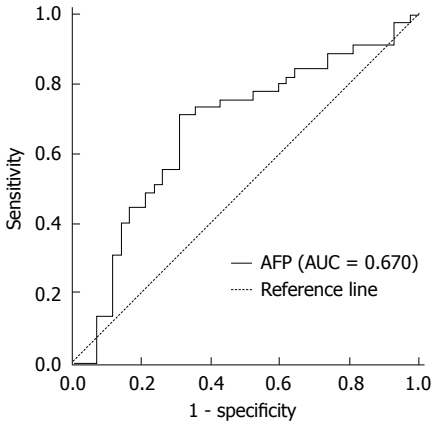

Figure 1 The receiver operating characteristic curve analysis for predictive value of serum alpha-fetoprotein level. The area under the curve is 0.670.

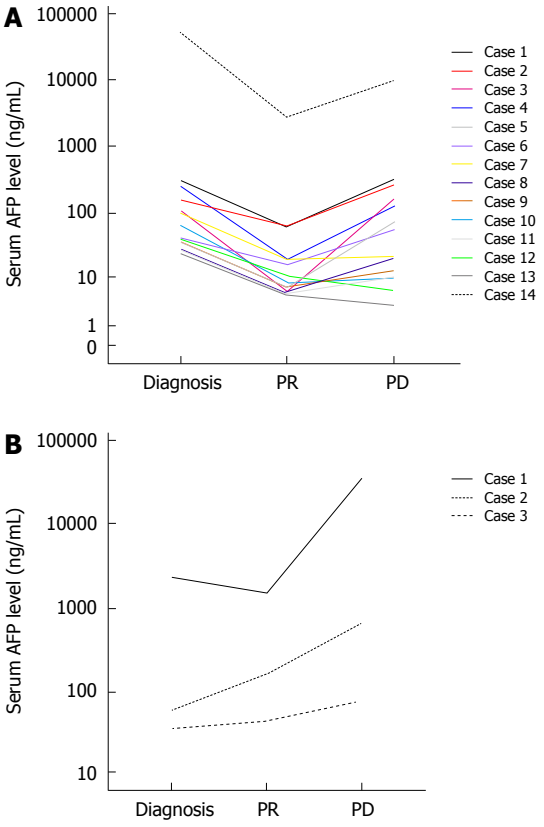

Figure 2 Changes of serum alpha-fetoprotein levels at the time of diagnosis, evaluation, and progression. A: Dynamic changes of serum AFP in patients whose AFP declined by ⩾ 50% when evaluated as PR; B: Dynamic changes of serum AFP in patients whose AFP declined by < 50% when evaluated as PR. PR: Partial response; PD: Progressive disease.

and the patients were sub-classified into two cohorts according to the decline degree of AFP: (1) ⩾ 50%(n = 47); and (2) < 50% (including those who had elevated AFP after chemotherapy) (n = 34). A significant correlation was observed between AFP decline degree and response to chemotherapy (72.3% *vs* 14.7%, P < 0.001, Table 5).

Among the 39 patients who achieved partial response (PR), serum AFP levels were exactly measured

Table 5 Correlation between decline degree of serum alpha-fetoprotein and response *n* (%)

Variable	AFP decline ⩾ 50%	AFP decline < 50%	*P* value
Response			
PR	34 (72.3)	5 (14.7)	<0.001
SD + PD	13 (27.7)	29 (85.3)	

SD: Stable disease; PD: Progressive disease; OS: Overall survival; PR: Partial response

Table 6 Multiple Cox regression analysis of prognostic factors

Factor	HR	95%CI	*P* value
LM (present)	2.809	1.363-5.788	0.005[a]
PM (present)	4.243	2.026-8.883	< 0.001[a]
Non-regional LNM (present)	3.743	1.928-7.268	< 0.001[a]
Other hematogenous metastasis (present)	1.479	0.692-3.161	0.312
PVTT (present)	2.341	1.030-5.320	0.048[a]
Response (SD + PD)	1.92	0.953-3.867	0.068
AFP decline degree (< 50%)	1.876	0.980-3.589	0.057

[a]*P* value < 0.05. LM: Liver metastasis; PM: Peritoneal metastasis; LNM: Lymph node metastasis; PVTT: Portal vein tumor thrombus; SD: Stable disease; PD: Progressive disease; HR: Hazard ratio.

in 17 patients until the time of progression. Among them, serum AFP declined by ⩾ 50% in 14 patients when evaluated as PR, but re-elevated back to the pre-treatment levels when progressed. No re-evaluation of serum AFP levels was also observed in several patients (Figure 2A). By contrast, serum AFP level did not decline that much in three patients when evaluated as PR, and with the tumor progressed, AFP levels of all these patients elevated markedly, even much higher than the pre-treatment levels (Figure 2B).

Survival analysis of AFPAGC

The 1-year survival for AFPAGC patients was 41.9% and median OS was 13.9 mo. Potential prognosis-related factors including sex, age, primary tumor features, serum AFP level, liver and extrahepatic metastasis, treatment, and response were examined. Univariate analysis showed that metastasis status (liver metastasis, peritoneal metastasis, non-regional lymph node metastasis, and other hematogenous metastasis), PVTT, response to chemotherapy, and serum AFP decline degree were associated with prognosis (Table 1, Figures 3 and 4). Multivariate analysis showed that hepatic (P = 0.005), peritoneal (P < 0.001), and non-regional lymph node metastasis (P < 0.001), and PVTT (P = 0.042) were independent prognostic factors (Table 6).

DISCUSSION

We found that monitoring serum AFP over time had predictive and prognostic value in the management of AFPAGC. AFP is a fetal serum protein produced by fetal

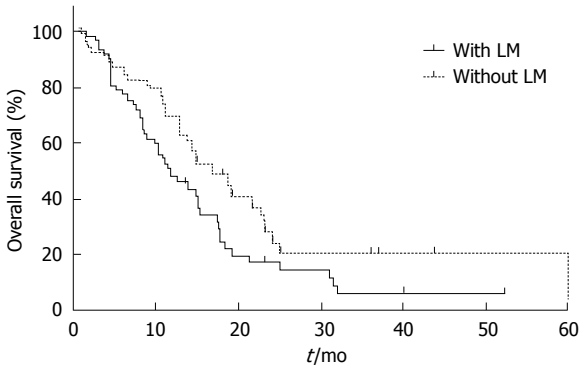

Figure 3 The median overall survival of patients with liver metastasis and those without was 16.7 m and 12.0 m, respectively (*P* = 0.048).

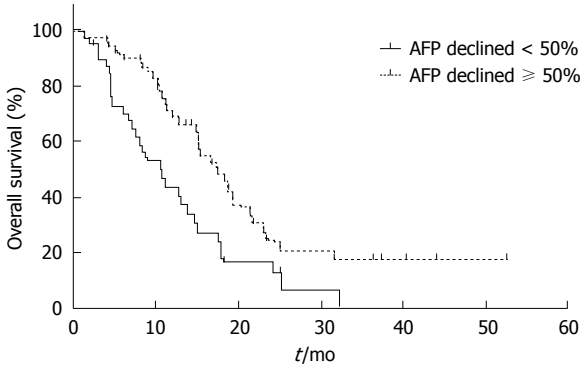

Figure 4 The median overall survival of patients with a ⩾ 50% serum alpha-fetoprotein level decline and those with a < 50% decline was 17.5 mo and 10.0 mo, respectively (*P* = 0.003).

and yolk sac cells and its level rapidly decreases after birth. Although AFP is a well-known tumor marker for hepatocellular carcinoma and yolk sac tumors[7], it is also elevated in various extrahepatic tumors, including gastrointestinal tract tumors, as well as pancreatic, gallbladder, lung, and bladder cancers[8].

The definition of AFPGC varies across studies, and elevation of serum AFP or immunohistochemical staining for AFP is often used[1,3,9,10]. As a rare subgroup of GC, AFPGC was reported to be more aggressive than that without AFP production, and to have more liver metastasis, even after radical D2 gastrectomy[5]. Therefore, systemic chemotherapy is a first-line approach for treatment of this special subtype of GC.

Previous studies focused on AFPGC after radical gastrectomy, and few data exist about optimal treatment for AFPAGC. Thus, we studied the treatment, therapeutic response, and outcomes of AFPAGC, and elucidated the predictive and prognostic value of serum AFP in the management of this special cancer. Considering many factors that can cause a mild increase in AFP, such as liver metastasis sites, we selected a threshold of AFP ⩾ 20 ng/mL as the inclusion criterion in this study.

Our study revealed that AFP, a biomarker of AFPAGC, was associated with response to chemotherapy. ORR in the AFP ⩾ 160 ng/mL group was significantly lower than that of the AF*P* < 160 ng/mL group (30.4% *vs* 68.3%, *P* < 0.001). This may be partially explained by the fact that AFP-producing gastric cell lines were resistant to many drugs[11]. We have known that AFP is not only a product of tumor, but also contributes to tumor aggression as well as regulation of hepatocellular growth and tumorigenesis[12]. Similar to that in HCC[13], AFP also has a crucial role in the proliferation, apoptosis, and angiogenesis of AFPGC cells[14]. Therefore, we speculate that AFP may play a significant role in primary drug resistance in AFPAGC and this warrants more study.

Besides the serum AFP level at diagnosis, we measured the dynamic changes of AFP over time after treatment, and this helped us to predict the efficacy of treatment and early relapse. It is noteworthy to mention that serum AFP does not always increase after tumor recurrence due to high heterogeneity of AFPAGC[15-17], which has been reported in a previous study[18]. Although serum AFP itself cannot be definitely associated with survival, we found AFP decline was significantly associated with prognosis, suggesting the need of real-time assay of AFP during management of AFPAGC. Furthermore, monitoring AFP changes after first-line chemotherapy may suggest tumor behavior and assist with subsequent treatment choices.

To explore optimal treatment regimens for AFPAGC, we analyzed ORR and toxicity of different regimens, and found that platinum-based doublet regimens and triplet regimens had similar ORR in AFPAGC. In the treatment of inoperable locally advanced and/or metastatic (stage IV) GC, doublet combinations of platinum and fluropyrimidines are often used, with an ORR of 52.2%-58.7%[19]. However, triplet regimens are not routinely used in China and Japan[20]. ORR to doublet regimens was significantly lower for subjects with markedly elevated serum AFP in the present study (26.3% *vs* 56.1%), so triplet regimens may be better for this subgroup compared with doublet regimens, despite frequent ⩾ grade 3 adverse events (58.3%). Due to extremely aggressive biological behavior, more aggressive therapy using triplet regimens may be considered for those with high serum AFP level. Optimizing triplet regimens also needs further study.

Targeted therapy may also offer a key to striding over primary drug resistance to some extent. Next-generation sequencing has been applied to GC and the Cancer Genome Altas (TCGA) Research Network defined four major genomic subtypes of GC: Epstein-Barr (EBV)-infected tumors; microsatellite instability (MSI) tumors; genomically stable (GS) tumors; and chromosomally unstable (CIN) tumors[21]. EBV-infected and MSI tumors were identified as potential candidates for immune checkpoint inhibitors[22]. Recent studies suggest that most TCGA tumors with elevated AFP expression were categorized as CIN subtypes, characterized by frequent amplifications of receptor tyrosine kinases, many of which are amenable to blockade by agents in current use or

in development[23]. Recurrent amplification of the gene encoding ligand vascular endothelial growth factor A was notable given the activity of the vascular endothelial growth factor-receptor 2 (VEGF-R2) targeted antibody ramucirumab in GC[24,25]. Due to increased VEGF expression and rich neovascularization in AFPGC, which is consistent with high incidence of PVTT (12.4% in our study), anti-angiogenic therapy is thought to be effective. In a case report of a patient with chemotherapy-resistant recurrent AFPGC, after six doses of ramucirumab, metastatic lymph nodes were centrally necrotic, and serum AFP decreased from 1280 to 225 ng/mL[26]. What's more, apatinib, a small molecular tyrosine kinase inhibitor targeting VEGF-R2, is also anti-angiogenic. Another case report of targeted therapy with apatinib in a patient with advanced AFPGC showed that PFS was achieved in 5 mo[27]. Similarly, in our present study, we also found that serum AFP in one patient decreased from 2000 ng/mL to 400 ng/mL with apatinib. Also, multi-target tyrosine kinase inhibitors, including sorafenib, which was approved for first-line treatment of HCC, were reported to be effective for this type of GC[28], indicating a correlation between the carcinogenesis of AFPGC and HCC.

Therefore, we suspect that anti-angiogenic drugs and multi-target tyrosine kinase inhibitors may have great potential for treating this aggressive subtype of GC, and AFP production may predict response. Thus, combined chemotherapy and molecular targeted treatment should be studied. Overall, AFPAGC is associated with a relatively poor prognosis, and it is a heterogeneous cancer with different clinical outcomes, biological behaviors, and genetic alterations. However, not all AFPAGC patients have a prognosis as poor as we previously thought.

In conclusion, real-time examination of AFP has great predictive and prognostic value in managing AFPAGC. High AFP is associated with poor response to chemotherapy, and AFP decline after chemotherapy is considered related to good prognosis in AFPAGC. Liver metastasis, peritoneal metastasis, non-regional lymph node metastasis, and PVTT are independent prognostic factors for this special cancer. For those with markedly elevated serum AFP, triplet regimens may be a better choice.

ARTICLE HIGHLIGHTS

Research background

Alpha-fetoprotein (AFP)-producing gastric cancer (AFPGC) is a special subgroup of gastric cancer (GC), and there are robust data confirming the poor prognosis for this population, especially for those with resected disease. However, due to aggressive biological behavior and high frequency of liver metastasis, most AFPGC patients were considered as inoperable at the initial diagnosis and there is limited data in the literature about management of AFP-producing advanced GC.

Research motivation

As the precise underlying mechanism of AFPGC remains to be elucidated, the optimal treatment approach requires further consideration, especially for advanced gastric cancer with elevated serum AFP (AFPAGC). Therefore, we performed this study to seek better management regimen for AFPAGC, with an aim to improve the prognosis of this special aggressive cancer.

Research objectives

The main objectives of this study were: (1) to elucidate predictive and prognostic value of serum AFP level and its dynamic changes during management of AFPAGC; and (2) to discover optimal treatment modality for AFPAGC. This would also allow risk stratification for patients with gastric cancer in future clinical trials.

Research methods

Patient data in this study were obtained by reviewing electronic medical charts. Statistical analyses were performed with SPSS 21.0 software. A Person's χ^2 test was used to measure the differences among variables. To identify prognostic factors for APFAGC, survival durations were calculated using the Kaplan-Meier method and Cox regression.

Research results

Our results revealed that for AFPAGC, serum AFP level was associated with liver metastasis rate and response to chemotherapy. Serum AFP decline degree was associated with response to chemotherapy and survival. Furthermore, we investigated optimal chemotherapy regimen for this special population, which revealed that for those with marked AFP elevation, triplet regimens could offer a better objective response rates (ORR) than doublet regimens, but the toxicity is a problem that remains to be solved. Finally, hepatic ($P = 0.005$), peritoneal ($P < 0.001$), non-regional lymph node metastasis ($P < 0.001$), and PVTT ($P = 0.042$) were identified as independent prognostic factors for AFPAGC.

Research conclusions

This is the first study to elucidate the great predictive and prognostic value of real-time examination of serum AFP in managing AFPAGC. We also suggest that for GCs with markedly elevated AFP, triplet regimens may be a better choice. This would also allow risk stratification for patients with gastric cancer in future clinical trials.

Research perspectives

Since AFPAGC is rare, for which large prospective clinical trials are not feasible, it is very significant to summarize clinical experience retrospectively. Although our results showed that triplet regimens may offer a better ORR, there remains controversy regarding the utility of triplet regimens due to their toxicity. Therefore, it will be necessary to optimize triplet regimens and find new therapeutic targets in future studies. Next generation sequencing may bring us new insight in the future.

REFERENCES

1 **Wang D**, Li C, Xu Y, Xing Y, Qu L, Guo Y, Zhang Y, Sun X, Suo J. Clinicopathological characteristics and prognosis of alpha-fetoprotein positive gastric cancer in Chinese patients. *Int J Clin Exp Pathol* 2015; **8**: 6345-6355 [PMID: 26261510]

2 **Alpert E**, Pinn VW, Isselbacher KJ. Alpha-fetoprotein in a patient with gastric carcinoma metastatic to the liver. *N Engl J Med* 1971; **285**: 1058-1059 [PMID: 4106197 DOI: 10.1056/nejm197111042851905]

3 **Liu X**, Cheng Y, Sheng W, Lu H, Xu Y, Long Z, Zhu H, Wang Y. Clinicopathologic features and prognostic factors in alpha-fetoprotein-producing gastric cancers: analysis of 104 cases. *J Surg Oncol* 2010; **102**: 249-255 [PMID: 20740583 DOI: 10.1002/jso.21624]

4 **Hirajima S**, Komatsu S, Ichikawa D, Kubota T, Okamoto K, Shiozaki A, Fujiwara H, Konishi H, Ikoma H, Otsuji E. Liver metastasis is the only independent prognostic factor in AFP-producing gastric cancer. *World J Gastroenterol* 2013; **19**: 6055-6061 [PMID: 24106406 DOI: 10.3748/wjg.v19.i36.6055]

5 **Adachi Y**, Tsuchihashi J, Shiraishi N, Yasuda K, Etoh T, Kitano S. AFP-producing gastric carcinoma: multivariate analysis of prognostic factors in 270 patients. *Oncology* 2003; **65**: 95-101

[PMID: 12931013]
6 **Nagai E**, Ueyama T, Yao T, Tsuneyoshi M. Hepatoid adenocarcinoma of the stomach. A clinicopathologic and immunohistochemical analysis. *Cancer* 1993; **72**: 1827-1835 [PMID: 7689918]
7 **El-Bahrawy M**. Alpha-fetoprotein-producing non-germ cell tumours of the female genital tract. *Eur J Cancer* 2010; **46**: 1317-1322 [PMID: 20185298 DOI: 10.1016/j.ejca.2010.01.028]
8 **Su JS**, Chen YT, Wang RC, Wu CY, Lee SW, Lee TY. Clinicopathological characteristics in the differential diagnosis of hepatoid adenocarcinoma: a literature review. *World J Gastroenterol* 2013; **19**: 321-327 [PMID: 23372352 DOI: 10.3748/wjg.v19.i3.321]
9 **Lin HJ**, Hsieh YH, Fang WL, Huang KH, Li AF. Clinical manifestations in patients with alpha-fetoprotein-producing gastric cancer. *Curr Oncol* 2014; **21**: e394-e399 [PMID: 24940098 DOI: 10.3747/co.21.1768]
10 **Reim D**, Choi YS, Yoon HM, Park B, Eom BW, Kook MC, Ryu KW, Choi IJ, Joo J, Kim YW. Alpha-fetoprotein is a significant prognostic factor for gastric cancer: Results from a propensity score matching analysis after curative resection. *Eur J Surg Oncol* 2017; **43**: 1542-1549 [PMID: 28511775 DOI: 10.1016/j.ejso.2017.04.005]
11 **Chang YC**, Nagasue N, Kohno H, Ohiwa K, Yamanoi A, Nakamura T. Xenotransplantation of alpha-fetoprotein-producing gastric cancers into nude mice. Characteristics and responses to chemotherapy. *Cancer* 1992; **69**: 872-877 [PMID: 1370917]
12 **Li M**, Li H, Li C, Wang S, Jiang W, Liu Z, Zhou S, Liu X, McNutt MA, Li G. Alpha-fetoprotein: a new member of intracellular signal molecules in regulation of the PI3K/AKT signaling in human hepatoma cell lines. *Int J Cancer* 2011; **128**: 524-532 [PMID: 20473866 DOI: 10.1002/ijc.25373]
13 **Sauzay C,** Petit A, Bourgeois A-M, Barbare J-C, Chauffert B, Galmiche A, Houessinon A. Alpha-foetoprotein (AFP): A multi-purpose marker in hepatocellular carcinoma. Clinica Chimica Acta 2016; 463: 39-44 [DOI: 10.1016/j.cca.2016.10.006]
14 **Koide N**, Nishio A, Igarashi J, Kajikawa S, Adachi W, Amano J. Alpha-fetoprotein-producing gastric cancer: histochemical analysis of cell proliferation, apoptosis, and angiogenesis. *Am J Gastroenterol* 1999; **94**: 1658-1663 [PMID: 10364040 DOI: 10.1111/j.1572-0241.1999.01158.x]
15 **He L**, Ye F, Qu L, Wang D, Cui M, Wei C, Xing Y, Lee P, Suo J, Zhang DY. Protein profiling of alpha-fetoprotein producing gastric adenocarcinoma. *Oncotarget* 2016; **7**: 28448-28459 [PMID: 27057629 DOI: 10.18632/oncotarget.8571]
16 **Motoyama T**, Aizawa K, Watanabe H, Fukase M, Saito K. alpha-Fetoprotein producing gastric carcinomas: a comparative study of three different subtypes. *Acta Pathol Jpn* 1993; **43**: 654-661 [PMID: 7508672]
17 **Eom BW**, Jung SY, Yoon H, Kook MC, Ryu KW, Lee JH, Kim YW. Gastric choriocarcinoma admixed with an alpha-fetoprotein-producing adenocarcinoma and separated adenocarcinoma. *World J Gastroenterol* 2009; **15**: 5106-5108 [PMID: 19860007 DOI: 10.3748/wjg.15.5106]
18 **Tomiyama K**, Takahashi M, Fujii T, Kunisue H, Kanaya Y, Maruyama S, Yokoyama N, Shimizu N, Soda M. A rare case of recurrent alpha-fetoprotein-producing gastric cancer without re-elevation of serum AFP. *J Int Med Res* 2006; **34**: 109-114 [PMID: 16604831 DOI: 10.1177/147323000603400114]
19 **Yamada Y**, Higuchi K, Nishikawa K, Gotoh M, Fuse N, Sugimoto N, Nishina T, Amagai K, Chin K, Niwa Y, Tsuji A, Imamura H, Tsuda M, Yasui H, Fujii H, Yamaguchi K, Yasui H, Hironaka S, Shimada K, Miwa H, Hamada C, Hyodo I. Phase III study comparing oxaliplatin plus S-1 with cisplatin plus S-1 in chemotherapy-naïve patients with advanced gastric cancer. *Ann Oncol* 2015; **26**: 141-148 [PMID: 25316259 DOI: 10.1093/annonc/mdu472]
20 **Shen L**, Shan YS, Hu HM, Price TJ, Sirohi B, Yeh KH, Yang YH, Sano T, Yang HK, Zhang X, Park SR, Fujii M, Kang YK, Chen LT. Management of gastric cancer in Asia: resource-stratified guidelines. *Lancet Oncol* 2013; **14**: e535-e547 [PMID: 24176572 DOI: 10.1016/s1470-2045(13)70436-4]
21 **Cancer Genome Atlas Research Network.**. Comprehensive molecular characterization of gastric adenocarcinoma. *Nature* 2014; **513**: 202-209 [PMID: 25079317 DOI: 10.1038/nature13480]
22 **Ma C**, Patel K, Singhi AD, Ren B, Zhu B, Shaikh F, Sun W. Programmed Death-Ligand 1 Expression Is Common in Gastric Cancer Associated With Epstein-Barr Virus or Microsatellite Instability. *Am J Surg Pathol* 2016; **40**: 1496-1506 [PMID: 27465786 DOI: 10.1097/pas.0000000000000698]
23 **Arora K**, Bal M, Shih A, Moy A, Zukerberg L, Brown I, Liu X, Kelly P, Oliva E, Mullen J, Ahn S, Kim KM, Deshpande V. Fetal-type gastrointestinal adenocarcinoma: a morphologically distinct entity with unfavourable prognosis. *J Clin Pathol* 2017; Epub ahead of print [PMID: 28814568 DOI: 10.1136/jclinpath-2017-204535]
24 **Fuchs CS**, Tomasek J, Yong CJ, Dumitru F, Passalacqua R, Goswami C, Safran H, Dos Santos LV, Aprile G, Ferry DR, Melichar B, Tehfe M, Topuzov E, Zalcberg JR, Chau I, Campbell W, Sivanandan C, Pikiel J, Koshiji M, Hsu Y, Liepa AM, Gao L, Schwartz JD, Tabernero J; REGARD Trial Investigators. Ramucirumab monotherapy for previously treated advanced gastric or gastro-oesophageal junction adenocarcinoma (REGARD): an international, randomised, multicentre, placebo-controlled, phase 3 trial. *Lancet* 2014; **383**: 31-39 [PMID: 24094768 DOI: 10.1016/s0140-6736(13)61719-5]
25 **Wilke H**, Muro K, Van Cutsem E, Oh SC, Bodoky G, Shimada Y, Hironaka S, Sugimoto N, Lipatov O, Kim TY, Cunningham D, Rougier P, Komatsu Y, Ajani J, Emig M, Carlesi R, Ferry D, Chandrawansa K, Schwartz JD, Ohtsu A; RAINBOW Study Group. Ramucirumab plus paclitaxel versus placebo plus paclitaxel in patients with previously treated advanced gastric or gastro-oesophageal junction adenocarcinoma (RAINBOW): a double-blind, randomised phase 3 trial. *Lancet Oncol* 2014; **15**: 1224-1235 [PMID: 25240821 DOI: 10.1016/s1470-2045(14)70420-6]
26 **Arakawa Y**, Tamura M, Aiba K, Morikawa K, Aizawa D, Ikegami M, Yuda M, Nishikawa K. Significant response to ramucirumab monotherapy in chemotherapy-resistant recurrent alpha-fetoprotein-producing gastric cancer: A case report. *Oncol Lett* 2017; **14**: 3039-3042 [PMID: 28928842 DOI: 10.3892/ol.2017.6514]
27 **Zhu XR**, Zhu ML, Wang Q, Xue WJ, Wang YW, Wang RF, Chen SY, Zheng LZ. A case report of targeted therapy with apatinib in a patient with advanced gastric cancer and high serum level of alpha-fetoprotein. *Medicine* (Baltimore) 2016; **95**: e4610 [PMID: 27631210 DOI: 10.1097/md.0000000000004610]
28 **Fang YU**, Wang L, Yang N, Gong X, Zhang YU, Qin S. Successful multimodal therapy for an α-fetoprotein-producing gastric cancer patient with simultaneous liver metastases. *Oncol Lett* 2015; **10**: 3021-3025 [PMID: 26722283 DOI: 10.3892/ol.2015.3731]

P- Reviewer:Kanat O, Kimura A, **S- Editor**: Chen K
L- Editor: Wang TQ **E- Editor**: Wang CH

World Journal of Gastroenterology

Submit a Manuscript: http://www.f6publishing.com

World J Gastroenterol 2018 January 14; 24(2): 274-289

DOI: 10.3748/wjg.v24.i2.274

ISSN 1007-9327 (print) ISSN 2219-2840 (online)

SYSTEMATIC REVIEWS

Neoadjuvant chemotherapy for gastric cancer. Is it a must or a fake?

Rossella Reddavid, Silvia Sofia, Paolo Chiaro, Fabio Colli, Renza Trapani, Laura Esposito, Mario Solej, Maurizio Degiuli

Rossella Reddavid, Silvia Sofia, Renza Trapani, Laura Esposito, Mario Solej, Maurizio Degiuli, Surgical Oncology and Digestive Surgery, Department of Oncology, University of Turin, San Luigi University Hospital, Orbassano, Turin 10049, Italy

Paolo Chiaro, Fabio Colli, Department of Surgical Sciences, Digestive and Oncological Surgery, University of Turin, Molinette Hospital, Turin 10126, Italy

ORCID number: Rossella Reddavid (0000-0003-0603-9953); Silvia Sofia (0000-0003-1145-078X); Renza Trapani (0000-0002-0816-2288); Paolo Chiaro (0000-0003-0045-892X); Fabio Colli (0000-0003-2978-5975); Laura Esposito (0000-0002-3188-9960); Mario Solej (0000-0002-4334-3295); Maurizio Degiuli (0000-0002-9812-7020).

Author contributions: Degiuli M designed the study; Degiuli M and Reddavid R edited and revised the study; Chiaro P, Colli F, Reddavid R, Solej M, Esposito L, Sofia S and Trapani R reviewed the literature and drafted the study; all authors equally contributed to this paper for the final approval of the final version.

Conflict-of-interest statement: All authors declare they have no conflicts of interest related to the work submitted for publication.

Manuscript source: Invited manuscript

Correspondence to: Maurizio Degiuli, MD, Associate Professor, Head, Surgical Oncology and Digestive Surgery, Department of Oncology, University of Turin, San Luigi University Hospital, Regione Gonzole 10, Orbassano 10049, Turin, Italy. maurizio.degiuli@unito.it
Telephone: +39 335 8111286

Received: November 19, 2017
Peer-review started: November 19, 2017
First decision: November 30, 2017
Revised: December 13, 2017
Accepted: December 20, 2017
Article in press: December 20, 2017
Published online: January 14, 2018

Abstract

AIM

To investigate the neoadjuvant chemotherapy (NAC) effect on the survival of patients with proper stomach cancer submitted to D2 gastrectomy.

METHODS

We proceeded to a review of the literature with PubMed, Embase, ASCO and ESMO meeting abstracts as well as computerized use of the Cochrane Library for randomized controlled trials (RCTs) comparing NAC followed by surgery (NAC + S) with surgery alone (SA) for gastric cancer (GC). The primary outcome was the overall survival rate. Secondary outcomes were the site of the primary tumor, extension of node dissection according to Japanese Gastric Cancer Association (JGCA) performed in both arms, disease-specific (DSS) and disease-free survival (DFS) rates, clinical and pathological response rates and resectability rates after perioperative treatment.

RESULTS

We identified a total of 16 randomized controlled trials comparing NAC + S (n = 1089) with SA (n = 973) published in the period from January 1993 - March 2017. Only 6 of these studies were well-designed, structured trials in which the type of lymph node (LN) dissection performed or at least suggested in the trial protocol was reported. Two out of three of the RCTs with D2 lymphadenectomy performed in almost all cases failed to show survival benefit in the NAC arm. In

the third RCT, the survival rate was not even reported, and the primary end points were the clinical outcomes of surgery with and without NAC. In the remaining three RCTs, D2 lymph node dissection was performed in less than 50% of cases or only recommended in the "Study Treatment" protocol without any description in the results of the procedure really perfomed. In one of the two studies, the benefit of NAC was evident only for esophagogastric junction (EGJ) cancers. In the second study, there was no overall survival benefit of NAC. In the last trial, which documented a survival benefit for the NAC arm, the chemotherapy effect was mostly evident for EGJ cancer, and more than one-fourth of patients did not have a proper stomach cancer. Additionally, several patients did not receive resectional surgery. Furthermore, the survival rates of international reference centers that provide adequate surgery for homogeneous stomach cancer patients' populations are even higher than the survival rates reported after NAC followed by incomplete surgery.

CONCLUSION

NAC for GC has been rapidly introduced in international western guidelines without an evidence-based medicine-related demonstration of its efficacy for a homogeneous population of patients with only stomach tumors submitted to adequate surgery following JGCA guidelines with extended (D2) LN dissection. Additional larger sample-size multicentre RCTs comparing the newer NAC regimens including molecular therapies followed by adequate extended surgery with surgery alone are needed.

Key words: Gastric cancer; Neoadjuvant chemotherapy; Perioperative chemotherapy; D2 lymphadenectomy; Randomized control trial

Core tip: Neoadjuvant chemotherapy (NAC) for resectable locally advanced gastric cancer has been rapidly introduced in international western guidelines without an evidence-based medicine-related demonstration of its efficacy for a homogeneous population of patients with stomach tumors who received adequate surgery following Japanese Gastric Cancer Association guidelines with an extended (D2) lymph nodes dissection. Additional randomized controlled trials with a larger sample size comparing the newer NAC regimens, including molecular therapies followed by adequate extended surgery with surgery alone are necessary.

Reddavid R, Sofia S, Chiaro P, Colli F, Trapani R, Esposito L, Solej M, Degiuli M. Neoadjuvant chemotherapy for gastric cancer. Is it a must or a fake? *World J Gastroenterol* 2018; 24(2): 274-289 Available from: URL: http://www.wjgnet.com/1007-9327/full/v24/i2/274.htm DOI: http://dx.doi.org/10.3748/wjg.v24.i2.274

INTRODUCTION

Gastric cancer (GC) is the third most common cancer-related cause of death[1]. Worldwide, approximately 1 million new cases of gastric cancer are diagnosed every year[2]. In 2016, nearly 13000 new cases are expected to be diagnosed in Italy with 7400 (56.9%) cases in males and 5300 (40.7%) cases in females[3].

The main prognostic factors for gastric cancer patients who receive radical surgery are the number of metastatic lymph nodes (LN) and the LN-ratio (the ratio between metastatic LN and LN removed).

The 5-year overall survival for resectable GC is approximately 20% to 30% worldwide, but, surprisingly, it is 70% in Japan and in other eastern countries, where the high incidence of the disease is managed with screening programs to find tumors at an earlier stage, and patients receive adequate surgery, including extended LN dissection (D2 gastrectomy)[4].

The therapeutic role of LN dissection has been a matter of discussion for a long period. In eastern countries, D2 lymphadenectomy has been considered the standard procedure for many decades[5-7]. In western countries, a more limited LN dissection has been performed until the last decade due to the low incidence of this tumor and the resulting limited experience with this complex and challenging procedure that has substantial learning curves[8-10].

Nevertheless, at the end of the 90s, the Italian Gastric Cancer Study Group (IGCSG) randomized controlled trial (RCT) showed that when a D2 lymphadenectomy with a pancreas-preserving technique is performed in references centers, it is a reproducible and safe procedure for the radical treatment of GC in western countries as well[11].

Later, Dutch and IGCSG trials also documented a survival benefit of the extended procedure in patients with advanced disease[12,13]. Consequently, the survival rates for western reference centers adopting D2 gastrectomy as the standard procedure for gastric cancer were comparable to the rates reported in Japan and Korea. Therefore, in international western guidelines for the diagnosis and treatment of gastric cancer, D2 gastrectomy is currently the recommended surgical choice for cases of resectable advanced disease.

Although surgery is the treatment of choice for GC, in western countries, prognosis remains poor outside reference centers even after curative resection, especially for the high rate of recurrence and the poor efficacy of adjuvant therapy[14]. Many trials have investigated the impact of adjuvant treatment by comparing surgery alone with surgery followed by adjuvant chemotherapy, but there is no definitive evidence of any survival advantage[15].

Moreover, in the western world, one-third of patients diagnosed with GC have unresectable diseases[16].

Therefore, in the last decade, a multimodal approach of GC has been suggested with the adoption of neoadjuvant (preoperative or perioperative) treatment

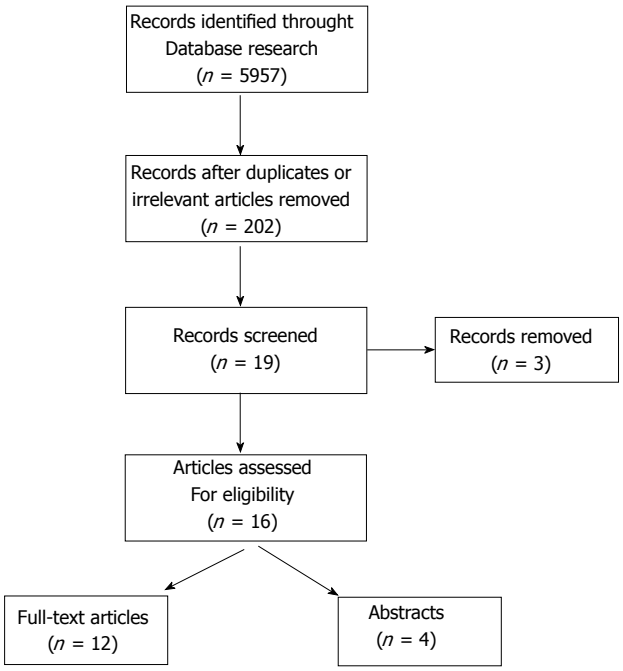

Figure 1 Literature selection flowchart.

(NAC). Based on the reason that, at least theoretically, this treatment may reduce tumor volume, improve the R0 resection rate, and kill micro metastases, NAC has been recently introduced in the national guidelines of many countries, especially after publication of the Medical Research Council Adjuvant Gastric Infusional Chemotherapy (MAGIC) and the Federation Nationale des Centres de Lutte contre le Cancer (FNCLCC) -Federation Francophone de Cancerologie Digestive (FFCD) RCTs, without a clear and evidence-based medicine (EBM)-related demonstration of a survival benefit compared to controlled surgery with proper enlarged LN dissection in patients with only stomach tumors[15,17,18].

Effectively the MAGIC and FNCLCC-FFCD RCTs have shown a survival advantage of NAC + surgery *vs* surgery alone, but surgery performed in these patients did not include a proper extended lymphadenectomy in the majority of cases, and many patients had lower esophagus (LE) or esophagogastric junction (EGJ) cancer instead of only GC. Therefore, it is possible that a proper radical surgery (gastrectomy with D2 LN dissection) may nullify the survival benefit of NAC described after incomplete surgery and also that the location of the tumor outside the stomach (EGJ and LE), may amplify the response to preoperative treatment.

To document a possible benefit of NAC after adequate D2 gastrectomy for only stomach cancer, we proceeded to review the literature on neoadjuvant treatment for resectable gastric cancer by mainly investigating these variables.

MATERIALS AND METHODS

Literature search

We proceeded to conduct a complete review of the literature with the support of the Federate Library of Medicine of Turin. The body of evidence for this review was primarily comprised of mature RCT data and meta-analyses of RCTs.

We searched PubMed, Embase, American Society of Clinical Oncology (ASCO) and European society of Medical Oncology (ESMO) meeting abstracts as well as the Cochrane Library by computer for non-randomized and randomized works published from 1993 to March 2017 (Figure 1).

Keywords were matched and included "NAC or neoadjuvant chemotherapy or neo-adjuvant chemotherapy or neo-adjuvant chemo-therapy or neoadjuvant chemo-therapy or preoperative chemotherapy or pre-operative chemotherapy or preoperative chemo-therapy or pre-operative chemo-therapy or perioperative chemotherapy or peri-operative chemotherapy or peri-operative chemo-therapy or perioperative chemo-therapy ", "GC or gastric cancer or stomach cancer or stomach neoplasm or gastric neoplasm or gastric adenocarcinoma or stomach adenocarcinoma", and "RCT or randomized controlled trial or randomised controlled trial".

All published trials comparing NAC-containing procedures *vs* no treatment before surgery in patients with gastric cancer (or gastric cancer + cardia cancer + lower-esophagus cancer) were included earlier in our analysis. Blinding the trial conditions was not necessary. There was no language restriction.

Inclusion criteria

We screened titles and abstracts of all identified papers (5957) and included only trials that satisfied the following criteria: patient populations with gastric cancer (diagnosed and classified according to 6th or 7th TNM and/or Japanese Gastric Cancer Association) without age, gender and racial limitations[19-21]; intervention and a comparative intervention that was clearly documented (NAC + surgery -NAC+S versus surgery alone -SA) for GC regardless of the detailed NAC regimens that were administered, surgical techniques performed (type of gastrectomy and LN dissection), pathological classification, location and stage of the disease. All patients needed to have a history of potentially curative surgery.

NAC could be performed through oral or intravenous (Ⅳ), intraperitoneal (IP) and intra-arterial (IA) infusion.

Esophagogastric junction and lower esophagus cancer patients were considered only if they were enrolled together with proper gastric cancer patients in the same study[15,17,18,22]. In these cases, the results of tests for heterogeneity effects according to the site of the primary tumor were documented when reported

by the authors.

When results were reported or updated in more than one publication, only the most recent paper was used.

At the end of the process, only RCTs were included in this review (Figure 1).

Exclusion criteria

We included only GC patients according to the theory of site-dependent differences in tumor genomics and biology[23]. Therefore, studies recruiting lower-esophagus and cardia cancers without gastric cancer were excluded. Studies including GC and diseases other than GC (lower esophageal cancer, esophagogastric junction tumor) were also excluded unless analyses were conducted separately.

Studies of preoperative radiotherapy or immunotherapy were excluded if they were not associated with chemotherapy.

We excluded patients with history of prior treatment before entering the trial as well.

Types of interventions

Any chemotherapy regimen performed before resective surgery with or without postoperative adjuvant treatment was included and located in the NAC-arm.

For the surgery alone-arm (SA-arm), we enrolled all types of gastrectomy and lymphadenectomy that were performed (D0, D1, D1plus, D2, D3).

Studies in which GC was associated with another synchronous malignancy or studies containing multivisceral resections were excluded.

Outcomes of interest and definitions

The primary outcomes were the overall survival rates (time from random assignment to the last follow-up or death) and/or disease-free survival rates (DFS) (time from random assignment to tumor recurrence or death) and/or disease-specific survival rates (DSS) (time from random assignment to death from disease). Secondary outcomes included the perioperative response rates, the R0 (margin negative) resection rate after perioperative treatment, and OS or DFS or DSS according to the type of lymph node dissection performed (D1, D2, others) following Japanese Gastric Cancer Treatments Guidelines[21]. Preoperative tumor stages were all recorded following TNM classification of malignant tumors (mostly from the 6th edition[19]).

The objective response to NAC was evaluated as either complete response (CR), partial response (PR), stable disease (SD) or progressive disease (PD) according to the indications of the Japanese Gastric Cancer Association[21].

Some trials assessed the down-staging effect of NAC by separating out patients with negative nodes from patients with positive nodes on pathological examinations after surgery.

Quality assessment of RCTs

The quality of the included RCTs was assessed using modified Jadad's scoring system[24] and Cochrane reviewers' handbook 5.0.1 RCT criteria[25]. The assessment was based on the randomization methods, the report of dropout rates, allocation concealment, the use of intention-to-treat (ITT) analysis, and losses to follow-up, the extent to which valid results were depicted. Based on these criteria, the studies were divided into high quality group (score $\geqslant$ 4) and low quality group (score < 4) (Table 1).

RESULTS

Study selection and population

Figure 1 shows the literature trial selection flowchart. In brief, 5957 studies were identified from the literature search. Out of all these studies, a total of 202 relevant papers documenting the results of any comparison of NAC + S *vs* SA for gastric cancer were selected. Then, we proceeded to a further selection of 19 papers reporting the results of controlled trials that were described as randomized in the title, (6 abstracts and 13 full-text papers). Nevertheless, a more detailed examination showed that in 3 of these studies, patient allocation had in fact not been conducted randomly[26-28]. Therefore, only 16 papers were proper randomized controlled trials that fulfilled our research criteria and were included in this review.

These RCTs were published between 1993 and 2011 with a 24 to 83 mo follow-up period. A total of 2062 patients was included in the analysis with 1089 receiving NAC (52.81%) and 973 (47.18%) undergoing SA.

Characteristics of included studies

In Yonemura's trial[29] (1993), fifty-five patients with far advanced gastric cancer (TNM stage IV) were enrolled with 29 who received neoadjuvant treatment and 26 who underwent surgery alone (Table 2). NAC patients were treated with a PMUE regimen, a combination of cisplatin (CDDP) 75 mg/m^2, mitomycin C (MMC) 10 mg/body, etoposide 150 mg/body, and 400 mg/d UFT. The author reported response rates, resectability rates with curative intent and a survival rate advantage in the NAC group, but, overall, this was not statistically significant. Furthermore, the type of lymph node dissection performed in both arms was not reported.

In 1995, Shchepotin *et al*[30] included 146 GC patients in a RCT in which the tumor stage was not specified (Table 2). Fifty patients were treated with surgery alone, and 96 patients were submitted to NAC. Out of these patients, 49 received intravenous (systemic) chemotherapy (IVCH) and 47 received super selective intra-arterial chemotherapy (IACH). The chemotherapy regimen was not mentioned. Only IACH + S showed a response rate and a survival rate advantage over

Table 1 Quality assessment of all the 16 randomized controlled trials found in literature and included in this study

Study	Randomization	Allocation concealment	Blind	Withdrawal and dropout	Jadad score	ITT
Yonemura *et al*[29], 1993	Adequate	Inadequate	Adequate	Well reported	5	NR
Shchepotin *et al*[30], 1995	Unclear	Unclear	Inadequate	NR	1	NR
Kang *et al*[31], 1996	Unclear	Unclear	Inadequate	Well reported	3	NR
Lygidakis *et al*[32], 1999	Inadequate	Unclear	Inadequate	Well reported	2	NR
Takiguchi *et al*[33], 2000	Unclear	Inadequate	inadequate	Well reported	2	NR
Wang *et al*[22], 2000	Unclear	Unclear	Inadequate	Well reported	3	NR
Kobayashi *et al*[35], 2000	Adequate	Adequate	Inadequate	Well reported	5	NR
Hartgrink *et al*[4], 2004	Adequate	Adequate	Inadequate	Well reported	5	NR
Nio *et al*[36], 2004	Inadequate	Inadequate	Inadequate	Well reported	1	NR
Zhao *et al*[37], 2006	unclear	Unclear	Inadequate	Well reported	3	NR
Cunningham *et al*[17], 2006	Adequate	Adequate	Adequate	Well reported	7	YES
Schuhmacher *et al*[15], 2010	Unclear	Unclear	Unclear	Well reported	4	YES
Imano *et al*[38], 2010	unclear	unclear	Unclear	Well reported	4	NR
Biffi *et al*[39], 2010	Unclear	Unclear	Unclear	Well reported	4	YES
Qu *et al*[40], 2010	Adequate	Unclear	Unclear	NR	4	NR
Ychou *et al*[18], 2011	Adequate	Well reported	Unclear	Well reported	6	YES

NR: Not reported; ITT: Intention-to-treat analysis.

surgery alone, and this survival benefit was statistically significant ($P < 0.01$). Patient selection and the type of lymph node dissection performed were not reported.

The Kang *et al*[31] trial enrolled 107 patients with operable gastric cancer at TNM stages Ⅲ and Ⅳ. Fifty-four patients received surgery alone and 53 received NAC with a PEF regimen followed by surgery. The response rate was not specified. The curative resection rate was higher in the NAC + S group than in the SA group. However, there was no significant difference in overall survival between the two arms ($P = 0.114$). The type of lymph node dissection that was performed was not reported (Table 2).

Lygidakis *et al*[32] recruited 58 patients with resectable gastric cancer at all stages. Patients were randomly assigned to 3 groups. Group A (No. 20) patients received preoperative hypoxic upper abdominal chemotherapy using mitomycin-C, 5-fluorouracil, leucovorin, and farmorubicin combined with adjuvant systemic chemotherapy; Group B (No 19) patients received preoperative hypoxic upper abdominal chemotherapy without systemic chemotherapy; and Group C (No 19) patients received surgery alone. Improved survival was reported by combining hypoxic upper abdominal perfusion NAC with surgery compared to surgery alone. Response rate, resectability rate and type of LN dissection were not documented (Table 2).

Two-hundred-sixty-two patients with resectable GC mostly with serosal invasion were treated by Takiguchi *et al*[33] with either SA (239 patients) or NAC (123) between May 1993 and May 1998. NAC patients received 5-FU (F group, $n = 39$) until the day before surgery or 5-FU combined with CDDP (FP Group, $n = 84$). NAC with 5-FU combined with low-dose CDDP was reported to reduce the rate of intraperitoneal positive cytology, increase the rate of successful resections and improve OS without statistical significance. The extension of the lymph node dissection was not described (Table 2).

In 2000, Wang *et al*[22] published the results of an RCT that included sixty patients with gastric cardia cancer that were randomly assigned to surgery alone (No. 30) or to NAC with 5-FU (No. 30). As Siewert Ⅲ cancers are nowdays considered as proper gastric cancers, this study was included in the study despite our inclusion criteria[34]. The 5-year OS rate was improved in the NAC group but this survival benefit was not statistically significant. The resectability rate and type of node dissection performed in both groups were not reported (Table 2).

Kobayashi *et al*[35] performed a multicenter randomized clinical trial by recruiting 171 patients with advanced gastric cancer (a more detailed TNM tumor stage was not specified). These patients were randomized either to NAC with oral 5'-DFUR (No 91) followed by surgery and adjuvant therapy with iv MMC and oral 5'-FUDR or for surgery alone (No. 80) followed by the same adjuvant therapy. This clinical trial failed to demonstrate any survival benefit of preoperative chemotherapy over surgery alone. Response rate, resectability rate and the type of node dissection performed in both arms were not documented (Table 2).

In 2004, Hartgrink *et al*[4] reported the long-term results of the Dutch randomized FAMTX trial. In this trial, 59 AGC patients were recruited with no further details about the stage of the disease. Of these patients, 29 were allocated to the FAMTX regimen prior to surgery, while 30 patients received surgery alone. The resectability rates were equal for both groups. A complete or partial response was registered in 32% of the FAMTX group. The median survival since randomization was 18 mo in the FAMTX group *vs* 30 mo in the SA group ($P = 0.17$). Therefore, the trial could not show a beneficial effect of preoperative FAMTX. The standard surgical procedure included a limited (D1) lymphadenectomy. The authors concluded that surgery alone is the best treatment for operable gastric cancer (Table 2).

In 2004, Nio *et al*[36] published the results of a RCT in

Table 2 Positive human epidermal growth factor receptor 2 status by immunohistochemistry and/or fluorescence in situ hybridization for the patients enrolled in the ToGA trial[10,11,27]

Author Countries	Year, Type of publication	N° patients randomization	Site Stage	Regimen	Response rate	Resectability rate	Survival rate (HR; p)	Node dissection (D1,D2, others)
Yonemura *et al*[29] Japan	1993 Abstract	55 Tot 29 NAC + S 26 S	GC IV	PMUE	Adv NAC + S	Adv NAC + S	Adv NAC+S Rates NR	NR
Shchepotin *et al*[30] Ukraine	1995 Abstract	146 Tot 50 S 49 IVCH + S 47 IACH + S	GC NR	NR	Adv IACH + S	Adv IACH + S	Adv IACH + S $P < 0.001$	NR
Kang *et al*[31] South Korea	1996 Abstract	107 Tot 54 S 53 NAC + S	GC III/IV	PEF	NR	Adv NAC + S	No difference $P = 0.114$	NR
Lygidakis *et al*[32] Greece	1999 Paper	59 Tot 19 S 20 NAC + S + IVCH 20 NAC + S	GC All stages	Mitomycin-C + 5-FU + FA + Farmorubicin	NR	NR	Adv NAC + S + IVCH	NR
Takiguchi *et al*[33] Japan	2000 Abstract	262 Tot 139 S 123 NAC + S	GC III/IV	5FU + CDDP	Adv NAC + S	Adv NAC+S	Adv NAC + S $P = 0.0996$	NR
Wang *et al*[22] China	2000 Paper	60 Tot 30 S 30 NAC + S	EGJ NR	5FU	Adv NAC + S	NR	Adv NAC + S $P = 0.17$	NR
Kobayashi *et al*[35] Japan	2000 Paper	171 Tot 80 S 91 NAC + S	AGC	FUDR	NR	NR	Adv S $P = 0.010$	NR
Hartgrink *et al*[4] The Netherlands	2004 Paper	59 Tot 30 S 29 NAC + S	Proper AGC (not EGC)	FAMTX	32% CR or PR	EQUAL	Adv S 34% S *vs* 21% NAC + S $P = 0.017$	At least 15 nodes
Nio *et al*[36] Japan	2004 Paper	295 Tot 193 S 102 NAC + S	GC All stages > 50% stage I	UFT	NR	NR	Overall No Adv. NAC + S $P = 0.6878$ stage II/III -pN + Adv. NAC + S $P = 0.0486$	D2 48% S 56% NAC + S
Zhao *et al*[37] China	2006 Paper	60 Tot 20 5′-DFUR 20 5FU + CF 20 S	GC All stages	5′-DFUR Or 5FU+CF	5′-DFUR and 5FU + CF increase AI and reduce PI	NR	NR	NR
Cunningham *et al*[17] United Kingdom	2006 Paper	503 Tot 250 S 253 NAC + S	GC, EGJ, LE All stages	Epirubicin Cisplatinum 5-FU	Diameter 5 cm *vs* 3 cm $P < 0.001$ T1 + T2 stages > NAC + S $P = 0.002$	NR	Adv NAC + S OS/DFS 23% S 36.3%/ NAC+S HR 0.75/0.66 $P =$ 0.009/0.001 more evident for EGJ	D2 40% S 42% NAC + S
Schumacher *et al*[15] Germany	2010 Paper	282/144 Tot 72 S 72 NAC + S	GC, EGJ (Siewert II, III) stages III, IV	Cisplatinum + FF	Adv in S Tumor length, thickness and width and P Stages more	R0 67% S 81.9% NAC + S $P = 0.036$ LN + 76.5% S 61.4% NAC + S $P = 0.018$	No Adv NAC + S 52 ms S 64 ms NAC + S HR = 0.84 $P = 0.46$	D2 94% 92.6% S 95.7% NAC + S
Imano *et al*[38] Japan	2010 Paper	63 Tot 16 S 15 CDDP 16 5-FU 16 5-FU + CDDP	GC NR	5FU or CDDP or 5F +CDDP	5-FU + CDDP Increases AI Reduces PI	NR	No differences in 4 arms	D2 in all arms
Biffi *et al*[39] Italy	2010 Paper	240/70 Tot 35 S 34 NAC + S	EGJ (Siewert II, III), AG	TCF	65% CR + PR	Adv NAC + S (P value NR)	not evaluated premature interruption for low accrual	D2 in almost all cases

Qu *et al*[40] China	2010 Paper	78 Tot 39 S 39 NAC + S	AGC	Paclitaxel and FOLFOX4	Adv NAC + S *P* = 0.001	Adv NAC + S *P* = 0.025	Adv NAC+S *P* = 0.006 at 2 yr	NR
Ychou *et al*[18] France	2011 Paper	224 Tot 111 S 113 NAC + S	LE,EGJ,GC All stages	CDDP + 5FU	Adv NAC + S *P* = 0.054	Adv NAC + S *P* = 0.04	OS (NAC + S/S) = 38/24 HR = 0.69 *P* = 0.02 DFS (NAC + S/S) = 34/19 HR= 0.65 *P* = 0.003 more evident for EGJ	D2 recommended No data on the effect of D2 *vs* other LN dissection

GC: Gastric cancer; NAC: Neoadjuvant chemotherapy; S: Surgery; EGC: Early gastric cancer; AGC: Advanced gastric cancer; EGJ: Esophagogastric junction; LE: Lower esophagus; OS: Overall survival; DFS: Disease free survival; LN: Lymph node; D2: D2 lymphadenectomy; FA: Folinic acid; CR: Complete response; PR: Partial response; 5-FU: 5-fluorouracil; PMUE: Cisplatin + mitomycin C + etoposide +1-(2-tetrahydrofuryl)- + uracil; IVCH: Intravenous (systemic) chemotherapy; IACH: Super selective intra-arterial chemotherapy; PEF: Low dose cisplatinum + epirubicin + 5-fluorouracil; CDDP: Low dose cisplatinum; 5'-DFUR: 5'-deoxy-5-fluorouridine; FAMTX: 5-fluorouracil + doxorubicin + methotrexate; UFT: Tegafur + 5-fluorouracil; FF: d-L-folinic acid+fluouracile; TCF: Docetaxel + cisplatin + fluorouracil; FOLFOX4: 5-fluorouracil + leucovorin + oxaliplatin; Adv: Advantage; NR: Not reported; Tot: Total; AI: Apoptosis index; PI: Cell proliferation index; HR: Hazard ratio.

which 295 patients with GC of all stages were included (more than 50% were stage I). Overall, 193 patients were randomly allocated to the SA-arm and 102 were allocated to the NAC-arm with the UFT regimen (Tegafur + 5-FU). The response rate to NAC was 33.3%. The resectability rate was not reported. There were no significant differences in the OS rates between the NAC and SA groups. A survival benefit of NAC over SA was documented only in stages 2 and 3 and was higher in stage 2 and 3 patients with a complete or partial response to NAC compared to non-responders. The type of LN dissection performed was D2 only in 48% in the SA arm and 56% in the NAC-arm.

Zhao *et al*[37] studied the apoptosis induced by preoperative oral 5'-FUDR administration in GC and its mechanism of action. Sixty patients with gastric cancer of all TNM stages were randomly assigned to 3 groups (20 each group) before surgery. Group one patients received a NAC treatment with 5'-DFUR oral administration; group two patients received 5-FU + CF by venous drip for 3-5 d; and group three patients received surgery alone. The authors documented a significant increase in the apoptosis of gastric carcinoma cells and a decrease in the tumor cell proliferation index in group one patients after oral 5'-FUDR administration compared to groups 2 and 3. Nevertheless, preoperative NAC did not improve patient prognosis. The resectability rate and type of lymph node dissection were not reported.

In the most known RCT on NAC (MAGIC Trial) published in 2006 in the *New England Journal of Medicine (NEJM)*, Cunningham *et al*[17] studied the effects of preoperative treatment on 503 recruited patients with all stages of resectable adenocarcinoma of the stomach, esophagogastric junction, or the lower esophagus (Table 2). Patients were randomly assigned to either a perioperative treatment (250 patients) followed by surgery or surgery alone (253 patients). Perioperative chemotherapy consisted of three preoperative and three postoperative cycles of i.v. epirubicin (50 mg/m^2) and cisplatin (60 mg/m^2) on day 1 as well as a continuous i.v. infusion of fluorouracil (200 mg/m^2 per day) for 21 d. The resected tumors were significantly smaller and less advanced in the perioperative-chemotherapy group ($P < 0.001$), and among patients undergoing resection, there was a greater proportion of stage T1 and T2 tumors in the perioperative-chemotherapy arm compared to the surgery alone arm ($P = 0.002$). Compared with the surgery alone arm, the perioperative chemotherapy arm had a higher likelihood of overall survival (hazard ratio for death, 0.75; 95 percent confidence interval, 0.60 to 0.93; $P = 0.009$; five-year survival rate, 36% *vs* 23%) and progression-free survival (hazard ratio for progression, 0.66; 95 percent confidence interval, 0.53 to 0.81; $P < 0.001$). Nevertheless, the tumor was located in the stomach in 74% of cases in the NAC- arm and 73.9% in the surgery alone-arm; the tumor originated from the lower esophagus or from the esophago-gastric junction in the ramaining cases. D2 lymphadenectomy was performed only in 40% of patients in the SA arm and in 42% of patients in the NAC arm. Furthermore, according to tests for heterogeneity of the treatment effects related to the baseline characteristics of patients, the survival benefit of perioperative chemotherapy was stronger for the esophagogastric junction and the lower esophagus site of the primary tumor compared to the proper stomach site. Resectability rates were not significantly different among the two groups.

Schuhmacher *et al*[15] in 2010 reported the preliminary results of the European Organisation for Research and Treatment of Cancer (EORTC) randomized trial Nr. 40954 that compared NAC to SA for locally advanced cancer of the GC and EGJ (Table 2). The original trial design required that 360 patients with locally advanced (UICC stages Ⅲ and Ⅳ cM0) adenocarcinoma of the stomach or esophagogastric junction (Sievert Ⅱ and Ⅲ) were randomly assigned to

preoperative chemotherapy with cisplatin, d-L-folinic acid and fluorouracil after surgery or surgery alone. This trial was stopped for poor accrual after 144 patients were enrolled, including 72 patients in the surgery alone arm and 72 in the perioperative-chemotherapy treatment arm. More than half of patients had tumors located in the proximal third of the stomach, including EGJ Siewert type Ⅱ and Ⅲ. The trial showed a significantly increased R0 resection and pN0 rates in the NAC arm (P = 0.036) compared to the SA arm, but failed to demonstrate a survival benefit of perioperative treatment. In this trial, adequate surgery with D2 lymph node dissection was performed in 92.6% of SA arm patients and in 95.7% of NAC + S arm patients. The survival rates at 2 years were 72.7% (95%CI: 60.7%-81.7%) and 69.9% (95%CI: 57.7%-79.2%) in the neoadjuvant and surgery-only arms, respectively. The better outcome than expected after surgery alone was ascribed to the high quality of surgery and nodal dissection that was performed.

Imano *et al*[38] in 2010 reported the results of a four-arm randomized trial designed to evaluate the effects of short-term NAC (chemotherapy performed for 72 h before surgery) on the proliferative ability of cancer cells in gastric cancer. Sixty-three patients with gastric cancer were randomly assigned to 4 groups as follows: Group F, which had a single administration of 5-FU (16 patients); Group C, which had a single administration of CDDP (15 patients); Group FC, which had administration of both 5-FU and CDDP; and the Control Group, which had surgery alone (16 patients). Gastric cancer TNM or UICC stages were not reported. The D2 lymph node dissection was performed in all patients. The authors found that the combination of CDDP and 5-FU reduced proliferative ability and increased cellular apoptosis in gastric cancer cells. Nevertheless, there were no differences in overall survival rates between each group. Resectability and R0 resection rates were not reported (Table 2).

A group from the European Institute of Oncology in Milan[39] published the data of a multicenter RCT in which the objective was the non-inferiority of preoperative NAC with TCF regimen followed by surgery (Arm A) compared to surgery followed by the same chemotherapy regimen (Arm B) on clinical outcomes (morbidity and mortality of surgery) in GC patients (Table 2). Based on the initial design, a target sample size of 240 patients with locally advanced GC was required. Nevertheless, this trial was prematurely stopped at 69 randomized patients due to insufficient accrual with 34 in Arm A and 35 in Arm B, D2 lymphadenectomy was performed in almost all cases in both arms. The resectability rate was greater in the Arm A compared to the Arm B. In conclusion, preoperative TCF was safe and had similar morbidity compared to surgery followed by a TCF regimen. Furthermore, due to its early discontinuation for slow accrual, this study did not provide information about the efficacy of preoperative TCF, and no survival results were reported.

Qu *et al*[40] enrolled 78 patients with cTNM stage Ⅲ or Ⅳ (M0) gastric cancer (Table 2). Thirty-nine of these patients were randomized to the NAC arm (paclitaxel combined with FOLFOX4 regimen) and 39 to the surgical arm. The clinical response rate was 66% in the NAC arm. The R0 resection rate was significantly higher, and the number of lymph node metastases was significantly lower in the NAC arm compared to the SA arm. In addition, the 2-year survival rate was higher in NAC- than in the surgery alone-arm. The location of the disease and type of lymph node dissection performed were not described. The sample size was very small.

The results of the FNCLCC *and* FFCD multicenter Phase Ⅲ trial[18] were published in the *Journal of Clinical Oncology* in 2011 (Table 2). In this trial, 224 patients with resectable adenocarcinoma of the lower esophagus, gastroesophageal junction (EGJ), or stomach were randomly assigned to either perioperative chemotherapy with cisplatin and a fluorouracil regimen (NAC arm, n = 113) followed by surgery or surgery alone (SA arm, n=111). The curative resection rate was significantly higher in the NAC arm compared to that in the SA arm (84% *vs* 73%, P = 0.04). A non-significant decrease of lymph node metastases in the NAC arm compared to that of the SA arm was reported (67% *vs* 80%; P = 0.54). Compared to the SA group, the NAC group showed a better OS (5-year rate 38% *vs* 24%; HR for death 0.69; P = 0.02) and a better disease-free survival (5-year rate: 34% *vs* 19%; HR for death 0.65; P = 0.003). Nevertheless, in this trial, only 25% of patients had a tumor located in the stomach, while in 64% of cases, the tumor site was the esophagogastric junction, and another 11% of patients had cancer of the lower esophagus. While an extended lymphadenectomy (D2) was recommended in the "Study Treatment" protocol, the lymph node dissections performed in both arms were not described in the results. The authors concluded that compared to surgery alone, perioperative chemotherapy using a combination of cisplatin and fluorouracil significantly improved the curative resection rate, OS and DFS of patients with adenocarcinoma of the lower esophagus, EGJ and stomach. Nevertheless, this strong conclusion is an evident contrast to their previous comment reported in the "RESULTS" section of this paper where they stated that although the multivariable analysis showed the two significant prognostic factors for OS were the administration of a preoperative chemotherapy (P = 0.01) and tumor site (P < 0.01), the chemotherapy effect was only significant in the esophagogastric junction subgroup, which included around two-thirds of the patients. The two other subgroups (lower esophagus and stomach) were too small to distinguish between no effect and a small effect. Should these comments have been emphasized in the conclusion of the paper as well?

DISCUSSION

Actually, curative resection (R0) with D2 lymphadenectomy is the recommended standard procedure for advanced gastric cancer according to the Japanese[21], Korean[41], British[42], German[43], and Italian[44] guidelines, as well as the guidelines of the European Society for Medical Oncology (ESMO)[45] and the joint ESMO-ESSO (European Society of Surgical Oncology) ESTRO (European Society of Radiotherapy and Oncology)[46]. Recently, the National Comprehensive Cancer Network (NCCN) recommended D2 gastrectomy in the United States as well[47].

Following the results of the MAGIC[17] and FNCLCC-FFCD[18] trials, which documented an overall survival and a disease free survival benefit after NAC compared to surgery alone (from 23% to 36%, $P = 0.009$ and from 24% to 38%, $P = 0.02$, respectively), the same reported national and international guidelines suggested the adoption of preoperative or perioperative chemotherapy, mostly in cases in which lymph node metastasis is clinically suspected (cN+) or there is a clinical TNM stage 3 or higher (cT3+). In some experiences NAC has been employed for earlier T stage as well (cT2+)[47].

We deeply believe that the conclusions drawn after the publication and circulation of those two trials have been too strong in influencing the decision of several medical-oncology societies to adopt unconditionally preoperative or perioperative chemotherapy regimens for locally advanced resectable gastric cancer. We have tried to demonstrate that the survival benefits reported in MAGIC and FNCLCC-FFCD trials are significant in those series, but the 5-year OS rate of NAC-arms in both trials is even lower than OS rates reported in series from other eastern and western reference centers for gastric cancer treatment after only adequate curative surgery with extended lymph node dissection[48-52]. In fact, these reported benefits come from unbalanced series regarding the extent of nodal dissection. Furthermore, subsite analysis of both study populations clearly shows that chemotherapy effects on patient survival claimed in the published reports are mostly related to the site of tumor. In both trials, the chemotherapy effect is strongly evident in the EGJ subgroup.

Consequently, we did a massive literature search to investigate the eventual demonstration of any survival benefit of preoperative or preoperative chemotherapy in patient populations with tumors properly located only in the stomach and treated with adequate surgery, including complete D2 lymph node dissection as described by JGCA guidelines and recommended by international guidelines.

In this literature search, we found only 16 randomized controlled trials that compared neoadjuvant chemotherapy followed by surgery *vs* surgery alone in gastric cancer. Ten of these 16 papers were low sample-size single-center trials in which the extension of LN dissection was not described at all (Table 2). When reported, there was very little evidence of the effects of NAC on clinical and pathological responses. Very often, the eventual chemotherapy effect on those responses was not accomplished by any survival advantage, and in cases of survival benefit, this was not significant, or its level of significance was decreased by the low sample size of the study population.

Only 6 articles accurately described the extension of LN dissection performed on the patient population (Table 3).

A proper D2 lymph node dissection was documented in only 3 published RCTs[15,38,39]. Two of these trials with complete D2 dissection performed in almost all cases did not show any survival benefit in the NAC arm[15,38]. In the third RCT with adequate surgery and extended lymph node dissection, the primary end points were morbidity and mortality of surgery. Furthermore, due to low accrual with early discontinuation of the trial, no information on the efficacy of preoperative chemotherapy was provided, and no survival results were reported[39].

In the remaining 3 RCTs[17,18,36], a proper D2 nodal dissection was performed in less than 50% of patients or was recommended in the "Study Treatment" protocol but not described in the results.

In one of these trials[18], subsite analysis according to the site of the tumor showed that the favourable chemotherapy effect on OS reported in the conclusion of the trial for all groups of tumor site (lower esophagus, EGJ, stomach) was actually strongly evident only for EGJ cancers, which represented 64% of all cancers of the study population, while the other two subgroups (lower esophagus and stomach, 11% and 25%, respectively) were too small to distinguish between no effect and a small effect. Furthermore, the 5-year OS and DFS rates reported in the trial for the SA arm were 24% and 19%, respectively and were too low compared to rates commonly reported in other series from either eastern or western reference centers for gastric cancer care and research[13,48,50,51,54].

In the randomized trial published by Nio *et al*[36], there were no significant differences in overall survival rates between the NAC and SA groups in the whole study population. A survival benefit of NAC over surgery alone was documented only in subsite analysis according to the UICC stage of disease. This benefit was reported for UICC stage II and III, and it was higher in stage II and III patients with complete or partial response to NAC compared to non-responders.

Finally, the MAGIC trial[17] also contains several critical points. Despite the reported significant OS benefit for the NAC arm, more than one-fourth of patients had a cancer located outside the stomach (i.e., lower esophagus or esophagogastric junction) and D2 lymphadenectomy was performed in only 40.4% of patients of the SA group and in only 42.5% of patients of the perioperative-chemotherapy group. Furthermore, non-resectional surgery was performed in

Tab 3 Characteristics and outcomes of randomized controlled trial describing the type of lymph node dissection and the site of primary tumor in both arms

Ref.	No. patients randomization	Site of primary tumor	Node dissection (D1, D2, others)	Survival rate (HR, p)	HR for site of primary tumor
Nio *et al*[36], 2004	295 Tot 193 S 102 NAC + S	Stomach	D2 in less than 50% overall 48% S 56% NAC + S	Overall No Adv NAC + S *P* = 0.6878 stage II/III -pN+ Adv NAC + S *P* = 0.0486	NR
Cunningham *et al*[17], 2006	503 Tot 250 S 253 NAC + S	Stomach 73.9% EGJ 11.5% LE 14.6%	D2 in less than 50% 40% S 42% NAC + S	Adv NAC + S OS/DFS 5 yr-SR 23%/NR S 36.3%/NR NAC + S HR = 0.75/0.66 *P* = 0.009/0.001	HR LE 0.7 EGJ: 0.5 Stomach: 0.8
Schumacher *et al*[15], 2010	282/144 Tot 72 S 72 NAC + S	Stomach 47.2% EGJ 52.8% (Siewert II, III)	Proper D2 in 94% overall 92.6% S 95.7% NAC+S	No adv NAC + S 52 ms S 64 ms NAC + S HR = 0.84 *P* = 0.46	NR
Imano *et al*[38], 2010	63 Tot 16 S 15 CDDP 16 5-FU 16 5-FU + CDDP	Stomach	Proper D2 in all patients of both arms	No differences for all arms	NR
Biffi *et al*[39], 2010	240/70 Tot 35 S 34 NAC + S	Stomach 59% EGJ 41% (Siewert II, III)	Proper D2 in almost all cases	not evaluated premature interruption for low accrual	NR
Ychou *et al*[18], 2011	224 Tot 111 S 113 NAC + S	LE 11%, EGJ 64%, Stomach 25%	D2 recommended No data on LND performed	OS (NAC + S/S) 38/24 HR = 0.69 *P* = 0.02 DFS (NAC + S/S) 34/19 HR = 0.65 *P* = 0.003	HR LE 1.14 EGJ 0.57 Stomach 0.92

S: Surgery; NAC: Neoadjuvant chemotherapy; Adv: Advantage; LND: Lymph node dissection; OS: Overall survival; DFR: Disease free survival; HR: Hazard ratio; LN+: Lymph node positive; D2: D2 lymph node dissection; NR: Not reported; LE: Lower esophagus; EGJ: Esophagogastric junction; pN+: Positive lymph nodes at pathological examinations.

16.8 and 13.2% of patients in the SA and NAC groups, respectively. As a result of the inadequacy of surgical treatment and lymph node dissection administered to patients, the rate of overall survival and progression-free survival at 5 years after the operation was extremely low in the SA group (23% and 18%, respectively), and in the NAC group the chemotherapy effect on prognosis produced survival rates that remained lower than those reported in worldwide reference centers after adequate extended surgery without any neoadjuvant treatment. Furthermore, although non statistically significant, tests for heterogeneity effects according to the site of the primary tumor showed that the perioperative chemotherapy effect was much more prevalent for esophagogastric junction cancer (HR for mortality 0.5) and much smaller for stomach cancer (HR for mortality 0.8).

Therefore, did preoperative or perioperative chemotherapy make up for all shortcomings of incomplete surgery that did not respect the adequacy of cure and extension of nodal dissection? Could neoadjuvant treatment be a valid support for inadequate surgery alone in those centers where it is performed without a complete D2 lymph node dissection? Furthermore, could neoadjuvant treatment combined with adequate surgery increase survival rates to the rates found by eastern authors?

The only well-designed clinical trials with controlled D2 surgery performed in almost all cases in both arms were prematurely ended for low accrual[15,39]. One of the studies did not even consider survival as a primary end point, and the objective of the study was the effect of preoperative drugs on clinical outcomes of surgery (morbidity and mortality) and on pathological response[39]. The EORTC trial effectively aimed to detect an improvement in median survival after administration of a neoadjuvant treatment, but when it was stopped for poor accrual, despite a significant increase in curative resection, it failed to demonstrate a survival benefit[15]. The authors themselves concluded that the high quality of surgery performed with extended resection of regional lymph nodes outside the perigastric area was responsible for the better than expected outcome after radical surgery alone. In fact, the survival rates at 2 and

Table 4 Survival results after surgery alone in reference centers

Study, country	Period	Setup	No. of patients	Node dissection	5-yr OS rates
Cunningham *et al*[17] United Kingdom	1994-2002	MC RCT	503	D2 in 40% S/42% NAC	NAC + S 36.3% Surgery alone 23%
Ychou *et al*[18] France	1995-2003	MC RCT	224	No data on type of LND	NAC + S 38% Surgery alone 24%
Maruyama *et al*[48] Japan	1991-2009	MC Retr	11261	D2	AJCC Stage Ⅱ 73.1% AJCC stage Ⅲ 44.5%
Wu *et al*[53] Taiwan	1993-1999	MC RCT	110/111	D1 *vs* D3	D1 53.6%/ D3 59.5%
Kim *et al*[49] South Korea	2009-2011	MC Retr	1561	D2	AJCC Stage Ⅱ 86.5% AJCC Stage Ⅲ 63.7%
Siewert *et al*[50] Germany	1986-1989	MC Prosp	1096	D2	46.60%
Sue-Ling *et al*[51] United Kingdom	1970-1989	SI Prosp	207	D2	55%
Viste *et al*[54] Norway	1980-1990	SI Retr	105	D2	47%
Robertson *et al*[55] Hong Kong	1987-1991	SI RCT	25/30	D1 *vs* D2	D1 45%/D2 35%
Dent *et al*[56] South Africa	1982-1985	SS RCT	22/21	D1 *vs* D2	D1 69%/D2 67%
Bonenkamp *et al*[57] The Netherlands	1989-1993	MC RCT	380/331	D1 *vs* D2	D1/D2: 45%/47% D2, pT2: 44% D2, pT3: 22% D2, LN-/LN+: 69%/30%
Degiuli *et al*[13] Italy	1998-2006	MC RCT	133/134	D1 *vs* D2	D1 /D2: 66.5%/64.2% D2 pT2-T4: 59% D2 pT2-pT4 N+: 51%

MC: Multicenter; RCT: Randomized control trial; Retr: Retrospective study; NAC: Neoadjuvant chemoterapy; S: Surgery; Prosp: Prospective study; SI: Single institution; SS: Single surgeon; LND: Lymph node dissection; OS: Overall survival; AJCC: American Joint Committee on Cancer; LN+: Lymph node positive; LN-: Lymph node negative; D1: D1 lymph node dissection; D2: D2 lymph node dissection; D3: D3 lymph node dissection; NR: Not reported; pT2: Pathological TNM T2 stage; pT3: Pathological TNM T3 stage.

5 years were surprisingly high at approximately 70 and 50%, respectively, without any differences in the two arms of the study.

Survival results after surgery alone in reference centers

As already reported above, several studies from either eastern or western countries have reported survival rates after adequate surgery with extended nodal dissection that were significantly higher than rates reported both in the MAGIC[17] and FNCLCC-FFCD[18] trials after neoadjuvant treatment followed by incomplete surgery. Furthermore, these studies consider only cancer arising from the stomach, while the two RCTs included the lower esophagus and EGJ cancers as well (Table 4).

Recently, Maruyama *et al*[48] reported an overall 5-year survival rate of 70.1% among all UICC stages of the disease (data from Japanese Nationwide Registry of 11.261 gastric patients over the period 1991-2009) after surgery alone with accurate D2 lymph node dissection. Removing data for Stage Ⅰ patients, which usually do not have indications for preoperative treatment, the rates referring to UICC stage Ⅱ and Ⅲ, which are commonly submitted to NAC according to the current guidelines, were 73% and 44.5, respectively and were still significantly higher with respect to figures reported in the neoadjuvant settings discussed above (Table 4).

In a recent RCT from Taiwan, Wu *et al*[53] observed an overall 5-year survival of 59.5% after extended surgery, and the rate of T1 patients in this study population was 26% (Table 4).

In 2017, Kim *et al*[49] published survival data as observed in high volume centers in Korea. Overall, the 5-year survival was surprisingly very high at approximately 80% in all patients, but AJCC stage Ⅰ represented 63% of the study population. Anyway, the 5-year survival rates for stage Ⅱ and Ⅲ were still 86.5% and 63.7%, respectively (Table 4).

Survival rates after SA higher than those published in MAGIC and FNCLCC-FFCD neoadjuvant settings have been reported also in the western world, both in non-randomized and randomized studies on D2 gastrectomy. In historical non-randomized trials published in the 80s and 90s in Germany[50], England[51] and Norway[54], the 5-year OS rates coming from reference centers after extended procedures were reported as 46.5, 55% and 47%, respectively. In all these study populations, T1 cancers represented less than 10% of all patients (Table 4).

In historical randomized trials from Honk-Kong[55] and South Africa[56], despite evident limitations due to the low accrual, OS after D2 gastrectomy were reported as 35% and 67%, respectively (Table 4).

Additionally, in more recent RCTs coming from Europe, the Dutch[57] and the IGCSG[13] trials, the rates of overall survival observed after proper D2 gastrectomy alone were at least comparable to the results reported by Cunningham and Ychou in the MAGIC and FNCLCC-FFCD RCTs after chemotherapy followed by incomplete surgery. The results of the Dutch trials were first published in the NEJM in 1999. The 5-year OS rate after extended nodal dissection was 47% in all patients. It was 77%, 44% and 22% in T1, T2 and T3 patients, respectively, and 69% and 30% in lymph node-negative or lymph node-positive patients, respectively[57] (Table 4).

The survival results of the IGCSG RCT were published in 2014 in the British Journal of Surgery[13]. The overall 5-year survival and the 5-year disease-specific survival rates were 64.2% and 72.6%, respectively, for the whole cohort of patients submitted to D2 lymphadenectomy. Tumors were stratified by the depth of invasion and by lymph node involvement, and both the OS and DSS were calculated for pT2-pT4 patients and for pT2-pT4 with node-positive patients. In these two subsites of patients (which represent a common indication for neoadjuvant treatments), the 5-year OS and DSS were 59% and 69%, respectively. The observed morbidity and mortality were extremely low (24% and 2.2%, respectively), and therefore, they did not negatively impact the effects of extended surgery on survival, in contrast to what was described previously by Cuschieri *et al*[58] and Bonenkamp *et al*[57] in their studies. This trial is a clear demonstration that adequate surgery with proper extended nodal dissection with low complications and mortality can provide impressive survival results that are even significantly higher than those reported in trials adopting neoadjuvant treatments in a similar patient population (Table 4).

On the other hand, due to the high rates of morbidity and mortality, the MAGIC trial designed by Cuschieri to demonstrate the superiority of the extended gastrectomy over the standard D1 procedure in Great Britain failed to document a survival advantage[58,59].

In fact, the OS reported by Cuschieri 5 years after surgery was low with 33% in the D2 arm and 35% in the D1 arm, which was only comparable to the results observed in the MAGIC and FNCLCC-FFCD trials when taking all patients into consideration. It was even lower if we removed AJCC Stage Ⅰ patients. In fact, in the remaining AJCC stage Ⅱ and stage Ⅲ patients, it was 31% and 11%, respectively. These poor survival rates have been related to a combination of the observed severe morbidity and mortality with the inadequacy of the procedures performed, including many protocol violations, especially due to high rates of noncompliance (*e.g.*, non-removal of several Ln stations that were expected to be removed during lymph node dissections). A few years later, the positive results of the MAGIC trial on NAC do seem a direct consequence of this lack of quality and adequacy of surgical treatment provided to gastric cancer patients in many upper GI centers from Great Britain until the revolutionary centralization of treatments adopted since recent years. The chemotherapy effect was more evident when the quality of surgery was lower.

In conclusion, neoadjuvant (preoperative or perioperative) chemotherapy for GC has been rapidly introduced in international western guidelines without evidence-based medicine related demonstrations of its efficacy for proper stomach cancer in patients who receive a complete extended (D2) lymph node dissection. The currently available data support the adoption of NAC procedures in several national guidelines based on low-volume study populations with mixed sites of the primary disease (lower esophagus, esophagogastric junction and stomach), and statistical tests have often shown evidence of the heterogeneity of chemotherapy effects according to the site of the primary tumor. In both MAGIC and FNCLCC-FFCD trials, tests for heterogeneity showed that perioperative chemotherapy effects were much more evident for esophagogastric junction cancer and much less for stomach cancer. Furthermore, in both these RCTs supporting the adoption of NAC, surgery provided to patients was incomplete because extended nodal dissection was performed in less than 50% of patients or not described, and no results on the LN yield were documented to warrant its adequacy. The only well-designed RCT with extended surgery performed in almost all cases was prematurely ended for poor accrual, but at the moment of its closure, it failed to demonstrate a survival benefit for NAC.

Moreover, in national reference centers for gastric cancer care and research, OS and DSS rates of subsites of patients theoretically fit for NAC submitted to surgery alone with complete D2 dissection and performed for cancers located in the stomach only, are even higher than those reported after NAC followed by incomplete surgery provided to a patient population with mixed sites of the primary tumor.

We think additional high volume sample-size multicenter (and eventually multinational) RCTs comparing newer treatment regimens of neoadjuvant settings (capecitabine, oxaliplatin, docetaxel) combined with molecular therapies (epidermal growth factor receptor inhibitors or antiangiogenic agents) followed by controlled D2 surgery with controlled D2 surgery alone are necessary to investigate the survival effects of modern preoperative chemotherapy in patients with only stomach cancer who receive proper extended surgery.

ARTICLE HIGHLIGHTS

Research background

Actually, curative surgery with complete D2 lymph node dissection is the treatment of choice for gastric cancer (GC). In high-volume reference centers surgery alone gives excellent survival rates. Anyway, in western countries,

prognosis remains poor outside reference centers even after curative resection, especially for the high rate of recurrence mainly due to incomplete nodal dissection. Many trials have investigated the impact of adjuvant treatment by comparing surgery alone with surgery followed by adjuvant chemotherapy, but there is no definitive evidence of any survival advantage.

Therefore, in the last decade, a multimodal approach of GC has been suggested with the adoption of preoperative or perioperative treatment (NAC). The problem is that NAC has been introduced in the national guidelines of many countries, especially after publication of MRC and French RCTs, without a clear and evidence-based medicine (EBM)-related demonstration of a survival benefit compared to controlled surgery with proper enlarged LN dissection in patients with only stomach tumors.

In fact, MAGIC and FNCLCC-FFCD RCTs have shown a survival advantage of NAC + surgery vs surgery alone, but surgery performed in these patients did not include a proper extended lymphadenectomy in the majority of cases, and many patients had lower esophageal or cardia cancer instead of only GC. Therefore, it is possible that a proper radical surgery (gastrectomy with D2 LN dissection) may nullify the survival benefit of NAC described after incomplete surgery and also that the location of the tumor outside the stomach (cardia and lower esophagus), may amplify the response to preoperative treatment.

To document a possible benefit of NAC after adequate D2 gastrectomy for only stomach cancer, we proceeded to review the literature on neoadjuvant treatment for resectable gastric cancer by mainly investigating these variables.

Research motivation

Neoadjuvant (pre- or peri-operative) chemotherapy has been recently introduced in the national guidelines of many countries mainly after publication of MRC and French RCTs, without a clear and evidence-based medicine (EBM)-related demonstration of a survival benefit compared to controlled surgery with proper enlarged LN dissection in patients with only stomach tumors. The advantage reported after NAC seems mostly related to incomplete nodal dissection performed in both arms of these trials and to heterogeneous recruitment of lower esophagus and esophago-gastric junction cancer together with proper stomach cancer. Are there any trials among RCTs available in Literature investigating the effect of NAC over an homogeneous population of patients with only-stomach cancer treated with complete D2 lymph node dissection in both arms? Otherwise we could not exclude that: 1) a proper radical surgery (gastrectomy with D2 LN dissection) may nullify the survival benefit of NAC described after incomplete surgery and 2) the location of the tumor outside the stomach (esophago-gastric junction and lower esophagus) may amplify the response to preoperative treatment. In other words, NAC could be unuseful in proper gastric cancer submitted to curative complete D2 dissection.

Research objectives

The main objective was to investigate whether a possible survival benefit (OS and/or DSS and/or DFS) of NAC after adequate D2 gastrectomy for only stomach cancer was documented in all RCTS available in Literature till now. Secondary outcomes included the perioperative response rates, the R0 (margin negative) resection rate, and OS or DFS or DSS according to the type of lymph node dissection performed (D1, D2, others) after neoadjuvant treatment. We realized that no RCTs available till now could document a survival benefit of NAC over surgery alone for homogeneous population of patients with tumor of the only stomach treated with complete D2 gastrectomy and that a further large volume randomized trial is needed.

Research methods

We proceeded to conduct a complete review of the literature with the support of the Federate Library of Medicine of Turin. The body of evidence for this review was primarily comprised of mature randomized controlled trial (RCT) data. All published randomized trials comparing NAC-containing procedures *vs* no treatment before surgery in patients with gastric cancer (or gastric cancer + cardia cancer + lower-esophagus cancer) were included in our analysis. Blinding the trial conditions was not necessary. There was no language restriction. Esophagogastric junction and lower esophageal cancer patients were considered only if they were enrolled together with proper gastric cancer patients in the same study. The reason for considering also esophago-gastric junction and lower esophageal cancers in the recruitment process was that these locations represented a consistent part of the study population of the main RCTs actually claimed to be the basis for NAC treatment in gastric cancer. At the end of the process, only RCTs were included in this review. As we wanted to include all RCTS available in Literature at the moment, any chemotherapy regimen performed before resective surgery with or without postoperative adjuvant treatment was included and located in the NAC-arm as well as in the surgery alone-arm (SA-arm) we enrolled all types of gastrectomy and lymphadenectomy that were performed (D0, D1, D1plus, D2, D3). The quality of the included RCTs was assessed usin nodified JADAD's scoring system and Cochrane reviewers' andbook 5.0.1 RCT criteria.

Research results

The currently available data support the adoption of NAC procedures in several national guidelines based on low-volume study populations with mixed sites of the primary disease (lower esophagus, esophago-gastric junction and stomach). Statistical tests have often shown evidence of the heterogeneity of chemotherapy effects according to the site of the primary tumor. In fact, in both Magic and FNCLCC-FFCD trials, tests for heterogeneity showed that perioperative chemotherapy effects were much more evident for esophago-gastric junction cancer and much less for stomach cancer.

Furthermore, in both these RCTs supporting the adoption of NAC, surgery provided to patients was incomplete because extended nodal dissection was performed in less than 50% of patients or not described, and no results on the LN yield were documented to warrant its adequacy. The only well-designed RCT with extended surgery performed in almost all cases was prematurely ended for poor accrual, but at the moment of its closure, it failed to demonstrate a survival benefit for NAC.

Moreover, in national reference centers for gastric cancer care and research, OS and DSS rates of subsites of patients theoretically fit for NAC submitted to surgery alone with complete D2 dissection and performed for cancers located in the stomach only, are even higher than those reported after NAC followed by incomplete surgery provided to a patient population with mixed sites of the primary tumor.

Research conclusions

This study documented that the adoption of NAC procedures in several national guidelines is actually based on low-volume study populations with mixed sites of the primary disease (lower esophagus, esophago-gastric junction and stomach) and with inadequate surgery as concern the extent of nodal dissection (incomplete D2 dissection). In fact, statistical tests reported in these trials have shown evidence of the heterogeneity of chemotherapy effects according to the site of the primary tumor, documented a major effect mainly over esophagogastric junction cancer. Moreover, survival rates reported in Surgery-Alone arm by main RCTs claimed to be fundamental for supporting the adoption of NAC (MRC and French trials) are really too low as compared to rates documented in reference centers study population after proper D2 gastrectomy without preoperative chemotherapy. Effectively, in these surgical series coming from high volume referral centres, survival rates after extended surgery without NAC are even higher than those reported after NAC followed by incomplete surgery.

Our hypothesis is that, with current data available it 's not possible to exclude that: (1) The location of the tumor outside the stomach (esophago-gastric junction and lower esophagus) may amplify the response to preoperative treatment. (2) A proper radical surgery (gastrectomy with D2 LN dissection) may nullify the survival benefit of NAC described after incomplete surgery. (3) On the contrary, NAC effect on survival is more likely to be evident after incomplete surgery. In other words, NAC could be unuseful in cancer of the only stomach submitted to curative complete D2 dissection.

Research perspectives

We think additional high volume sample-size multicenter (and eventually multinational) RCTs comparing newer treatment regimens of neoadjuvant settings (capecitabine, oxaliplatin, docetaxel) combined with molecular therapies (epidermal growth factor receptor inhibitors or antiangiogenic agents) followed by controlled D2 surgery with controlled D2 surgery alone are necessary to investigate the survival effects of modern preoperative chemotherapy in patients with gastric cancer only who receive proper extended surgery. This is the ony way to investigate if neoadjuvant therapy can positively impact survival

also in homogeneous population of gastric cancer patients without any biases related to location of the tumor and adequacy of surgery administered.

REFERENCES

1 **Inghelmann R**, Grande E, Francisci S, Verdecchia A, Micheli A, Baili P, Capocaccia R, De Angelis R. Regional estimates of stomach cancer burden in Italy. *Tumori* 2007; **93**: 367-373 [PMID: 17899867]

2 **Russo A**, Li P, Strong VE. Differences in the multimodal treatment of gastric cancer: East versus west. *J Surg Oncol* 2017; **115**: 603-614 [PMID: 28181265 DOI: 10.1002/jso.24517]

3 **Pinto C**, Mangone L. [Epidemiology of cancer in Italy: from real data to the need for cancer networks.] *Recenti Prog Med* 2016; **107**: 505-506 [PMID: 27782224 DOI: 10.1701/2454.25696]

4 **Hartgrink HH**, van de Velde CJ, Putter H, Songun I, Tesselaar ME, Kranenbarg EK, de Vries JE, Wils JA, van der Bijl J, van Krieken JH; Cooperating Investigators of The Dutch Gastric Cancer Group. Neo-adjuvant chemotherapy for operable gastric cancer: long term results of the Dutch randomised FAMTX trial. *Eur J Surg Oncol* 2004; **30**: 643-649 [PMID: 15256239 DOI: 10.1016/j.ejso.2004.04.013]

5 **de Steur WO**, Dikken JL, Hartgrink HH. Lymph node dissection in resectable advanced gastric cancer. *Dig Surg* 2013; **30**: 96-103 [PMID: 23867585 DOI: 10.1159/000350873]

6 **Japanese Gastric Cancer Association Registration Committee**, Maruyama K, Kaminishi M, Hayashi K, Isobe Y, Honda I, Katai H, Arai K, Kodera Y, Nashimoto A. Gastric cancer treated in 1991 in Japan: data analysis of nationwide registry. *Gastric Cancer* 2006; **9**: 51-66 [PMID: 16767357 DOI: 10.1007/s10120-006-0370-y]

7 **Sasako M**, Saka M, Fukagawa T, Katai H, Sano T. Modern surgery for gastric cancer--Japanese perspective. *Scand J Surg* 2006; **95**: 232-235 [PMID: 17249270 DOI: 10.1177/145749690609500404]

8 **Jiang L**, Yang KH, Chen Y, Guan QL, Zhao P, Tian JH, Wang Q. Systematic review and meta-analysis of the effectiveness and safety of extended lymphadenectomy in patients with resectable gastric cancer. *Br J Surg* 2014; **101**: 595-604 [PMID: 24668465 DOI: 10.1002/bjs.9497]

9 **Giuliani A**, Miccini M, Basso L. Extent of lymphadenectomy and perioperative therapies: two open issues in gastric cancer. *World J Gastroenterol* 2014; **20**: 3889-3904 [PMID: 24744579 DOI: 10.3748/wjg.v20.i14.3889]

10 **Verlato G**, Giacopuzzi S, Bencivenga M, Morgagni P, De Manzoni G. Problems faced by evidence-based medicine in evaluating lymphadenectomy for gastric cancer. *World J Gastroenterol* 2014; **20**: 12883-12891 [PMID: 25278685 DOI: 10.3748/wjg.v20.i36.12883]

11 **Degiuli M**, Sasako M, Ponti A, Soldati T, Danese F, Calvo F. Morbidity and mortality after D2 gastrectomy for gastric cancer: results of the Italian Gastric Cancer Study Group prospective multicenter surgical study. *J Clin Oncol* 1998; **16**: 1490-1493 [PMID: 9552056 DOI: 10.1200/JCO.1998.16.4.1490]

12 **Songun I**, Putter H, Kranenbarg EM, Sasako M, van de Velde CJ. Surgical treatment of gastric cancer: 15-year follow-up results of the randomised nationwide Dutch D1D2 trial. *Lancet Oncol* 2010; **11**: 439-449 [PMID: 20409751 DOI: 10.1016/S1470-2045(10)70070-X]

13 **Degiuli M**, Sasako M, Ponti A, Vendrame A, Tomatis M, Mazza C, Borasi A, Capussotti L, Fronda G, Morino M; Italian Gastric Cancer Study Group. Randomized clinical trial comparing survival after D1 or D2 gastrectomy for gastric cancer. *Br J Surg* 2014; **101**: 23-31 [PMID: 24375296 DOI: 10.1002/bjs.9345]

14 **Xu W**, Beeharry MK, Liu W, Yan M, Zhu Z. Preoperative Chemotherapy for Gastric Cancer: Personal Interventions and Precision Medicine. *Biomed Res Int* 2016; **2016**: 3923585 [PMID: 28105420 DOI: 10.1155/2016/3923585]

15 **Schuhmacher C**, Gretschel S, Lordick F, Reichardt P, Hohenberger W, Eisenberger CF, Haag C, Mauer ME, Hasan B, Welch J, Ott K, Hoelscher A, Schneider PM, Bechstein W, Wilke H, Lutz MP, Nordlinger B, Van Cutsem E, Siewert JR, Schlag PM. Neoadjuvant chemotherapy compared with surgery alone for locally advanced cancer of the stomach and cardia: European Organisation for Research and Treatment of Cancer randomized trial 40954. *J Clin Oncol* 2010; **28**: 5210-5218 [PMID: 21060024 DOI: 10.1200/JCO.2009.26.6114]

16 **Greenlee RT**, Howe HL. County-level poverty and distant stage cancer in the United States. *Cancer Causes Control* 2009; **20**: 989-1000 [PMID: 19199061 DOI: 10.1007/s10552-009-9299-x]

17 **Cunningham D**, Allum WH, Stenning SP, Thompson JN, Van de Velde CJ, Nicolson M, Scarffe JH, Lofts FJ, Falk SJ, Iveson TJ, Smith DB, Langley RE, Verma M, Weeden S, Chua YJ, MAGIC Trial Participants. Perioperative chemotherapy versus surgery alone for resectable gastroesophageal cancer. *N Engl J Med* 2006; **355**: 11-20 [PMID: 16822992 DOI: 10.1056/NEJMoa055531]

18 **Ychou M**, Boige V, Pignon JP, Conroy T, Bouché O, Lebreton G, Ducourtieux M, Bedenne L, Fabre JM, Saint-Aubert B, Genève J, Lasser P, Rougier P. Perioperative chemotherapy compared with surgery alone for resectable gastroesophageal adenocarcinoma: an FNCLCC and FFCD multicenter phase III trial. *J Clin Oncol* 2011; **29**: 1715-1721 [PMID: 21444866 DOI: 10.1200/JCO.2010.33.0597]

19 **Sobin LH,** Wittekind C. International Union Against Cancer (UICC) TNM classification of malignant tumours. 6. New York: Wiley; 2002

20 **Sobin LH,** Gospodarowicz MK, Wittekind C. International Union Against Cancer (UICC) TNM classification of malignant tumours. 7. New York: Wiley-Liss; 2010 [DOI: 10.1002/9780471420194.tnmc09.pub2]

21 **Japanese Gastric Cancer Association**. Japanese gastric cancer treatment guidelines 2014 (ver. 4). *Gastric Cancer* 2017; **20**: 1-19 [PMID: 27342689 DOI: 10.1007/s10120-016-0622-4]

22 **Wang XL**, Wu GX, Zhang MD, Guo M, Zhang H, Sun XF. A favorable impact of preoperative FPLC chemotherapy on patients with gastric cardia cancer. *Oncol Rep* 2000; **7**: 241-244 [PMID: 10671664 DOI: 10.3892/or.7.2.241]

23 **Shah MA**, Khanin R, Tang L, Janjigian YY, Klimstra DS, Gerdes H, Kelsen DP. Molecular classification of gastric cancer: a new paradigm. *Clin Cancer Res* 2011; **17**: 2693-2701 [PMID: 21430069 DOI: 10.1158/1078-0432.CCR-10-2203]

24 **Jadad AR**, Moore RA, Carroll D, Jenkinson C, Reynolds DJ, Gavaghan DJ, McQuay HJ. Assessing the quality of reports of randomized clinical trials: is blinding necessary? *Control Clin Trials* 1996; **17**: 1-12 [PMID: 8721797 DOI: 10.1016/0197-2456(95)00134-4]

25 **Higgins JP,** Green S. Cochrane Handbook for Systematic Reviews of Interventions, Version 5.0.1 (Updated September 2008). e Cochrane Collaboration 2008. Available from: URL: http://www.cochrane-handbook.org_

26 **Masuyama M**, Taniguchi H, Takeuchi K, Miyata K, Koyama H, Tanaka H, Higashida T, Koishi Y, Mugitani T, Yamaguchi T. [Recurrence and survival rate of advanced gastric cancer after preoperative EAP-II intra-arterial infusion therapy]. *Gan To Kagaku Ryoho* 1994; **21**: 2253-2255 [PMID: 7944452]

27 **Nishioka B**, Ouchi T, Watanabe S, Umehara M, Yamane E, Yahata K, Muto F, Kojima O, Nomiyama S, Sakita M, Fujita Y, Majima S. [Follow-up study of preoperative oral administration of an antineoplastic agent as an adjuvant chemotherapy in stomach cancer]. *Gan To Kagaku Ryoho* 1982; **9**: 1427-1432 [PMID: 6764116]

28 **Zhang CW**, Zou SC, Shi D, Zhao DJ. Clinical significance of preoperative regional intra-arterial infusion chemotherapy for advanced gastric cancer. *World J Gastroenterol* 2004; **10**: 3070-3072 [PMID: 15378797 DOI: 10.3748/wjg.v10.i20.3070]

29 **Yonemura Y**, Sawa T, Kinoshita K, Matsuki N, Fushida S, Tanaka S, Ohoyama S, Takashima T, Kimura H, Kamata T. Neoadjuvant chemotherapy for high-grade advanced gastric cancer. *World J Surg* 1993; **17**: 256-61; discussion 261-2 [PMID: 8511923 DOI: 10.1007/bf01658939]

30 **Shchepotin I**, Evans S, Chorny V, Ugrinov O, Osinsky S, Galakchin K, Troitsky I, Buras R, Shabahang M, Nauta R.

Preoperative superselective intraarterial chemotherapy in the combined treatment of gastric-carcinoma. *Oncol Rep* 1995; **2**: 473-479 [PMID: 21597762 DOI: 10.3892/or.2.3.473]

31 **Kang YK,** Choi DW, Im YH, Kim CM, Lee JI , Moon NM, Lee JO. A phase III randomized comparison of neoadjuvant chemotherapy followed by surgery versus surgery for locally advanced stomach cancer. Abstract 503 presented at the ASCO Annual Meeting, 1996

32 **Lygidakis NJ**, Sgourakis G, Aphinives P. Upper abdominal stop-flow perfusion as a neo and adjuvant hypoxic regional chemotherapy for resectable gastric carcinoma. A prospective randomized clinical trial. *Hepatogastroenterology* 1999; **46**: 2035-2038 [PMID: 10430393]

33 **Takiguchi N,** Oda K, Suzuki H, Wakatsuki K, Nunomora M, Kouda K, Saito N, Nakajima N. Neoadjuvant chemotherapy with 5-uorouracil (5-FU) or low dose cis-platinum (CDDP) + 5-FU in the treatment of gastric carcinoma with serosal invasion. *Proc Am Soc Clin Oncol* 2000; **19**: A1178

34 **Brierley JD,** Gospodarwicz MK, Wittekind C, Amin MB. TNM classification of maligant tumours. 8th ed. Oxford: Wiley Blackwell; 2017

35 **Kobayashi T**, Kimura T. [Long-term outcome of preoperative chemotherapy with 5'-deoxy-5-fluorouridine (5'-DFUR) for gastric cancer]. *Gan To Kagaku Ryoho* 2000; **27**: 1521-1526 [PMID: 11015996]

36 **Nio Y**, Koike M, Omori H, Hashimoto K, Itakura M, Yano S, Higami T, Maruyama R. A randomized consent design trial of neoadjuvant chemotherapy with tegafur plus uracil (UFT) for gastric cancer--a single institute study. *Anticancer Res* 2004; **24**: 1879-1887 [PMID: 15274369]

37 **Zhao WH**, Wang SF, Ding W, Sheng JM, Ma ZM, Teng LS, Wang M, Wu FS, Luo B. Apoptosis induced by preoperative oral 5'-DFUR administration in gastric adenocarcinoma and its mechanism of action. *World J Gastroenterol* 2006; **12**: 1356-1361 [PMID: 16552801 DOI: 10.3748/wjg.v12.i9.1356]

38 **Imano M**, Itoh T, Satou T, Sogo Y, Hirai H, Kato H, Yasuda A, Peng YF, Shinkai M, Yasuda T, Imamoto H, Okuno K, Shiozaki H, Ohyanagi H. Prospective randomized trial of short-term neoadjuvant chemotherapy for advanced gastric cancer. *Eur J Surg Oncol* 2010; **36**: 963-968 [PMID: 20638818 DOI: 10.1016/j.ejso.2010.06.012]

39 **Biffi R**, Fazio N, Luca F, Chiappa A, Andreoni B, Zampino MG, Roth A, Schuller JC, Fiori G, Orsi F, Bonomo G, Crosta C, Huber O. Surgical outcome after docetaxel-based neoadjuvant chemotherapy in locally-advanced gastric cancer. *World J Gastroenterol* 2010; **16**: 868-874 [PMID: 20143466 DOI: 10.3748/wjg.v16.i7.868]

40 **Qu JJ**, Shi YR, Liu FR, Ma SQ, Ma FY. [A clinical study of paclitaxel combined with FOLFOX4 regimen as neoadjuvant chemotherapy for advanced gastric cancer]. *Zhonghua Wei Chang Wai Ke Za Zhi* 2010; **13**: 664-667 [PMID: 20878572]

41 **Lee JH**, Kim JG, Jung HK, Kim JH, Jeong WK, Jeon TJ, Kim JM, Kim YI, Ryu KW, Kong SH, Kim HI, Jung HY, Kim YS, Zang DY, Cho JY, Park JO, Lim DH, Jung ES, Ahn HS, Kim HJ. Clinical practice guidelines for gastric cancer in Korea: an evidence-based approach. *J Gastric Cancer* 2014; **14**: 87-104 [PMID: 25061536 DOI: 10.5230/jgc.2014.14.2.87]

42 **Allum WH**, Blazeby JM, Griffin SM, Cunningham D, Jankowski JA, Wong R; Association of Upper Gastrointestinal Surgeons of Great Britain and Ireland, the British Society of Gastroenterology and the British Association of Surgical Oncology. Guidelines for the management of oesophageal and gastric cancer. *Gut* 2011; **60**: 1449-1472 [PMID: 21705456 DOI: 10.1136/gut.2010.228254]

43 **Meyer HJ**, Hölscher AH, Lordick F, Messmann H, Mönig S, Schumacher C, Stahl M, Wilke H, Möhler M. [Current S3 guidelines on surgical treatment of gastric carcinoma]. *Chirurg* 2012; **83**: 31-37 [PMID: 22127381 DOI: 10.1007/s00104-011-2149-x]

44 **De Manzoni G**, Marrelli D, Baiocchi GL, Morgagni P, Saragoni L, Degiuli M, Donini A, Fumagalli U, Mazzei MA, Pacelli F, Tomezzoli A, Berselli M, Catalano F, Di Leo A, Framarini M, Giacopuzzi S, Graziosi L, Marchet A, Marini M, Milandri C, Mura G, Orsenigo E, Quagliuolo V, Rausei S, Ricci R, Rosa F, Roviello G, Sansonetti A, Sgroi G, Tiberio GA, Verlato G, Vindigni C, Rosati R, Roviello F. The Italian Research Group for Gastric Cancer (GIRCG) guidelines for gastric cancer staging and treatment: 2015. *Gastric Cancer* 2017; **20**: 20-30 [PMID: 27255288 DOI: 10.1007/s10120-016-0615-3]

45 **Okines A**, Verheij M, Allum W, Cunningham D, Cervantes A; ESMO Guidelines Working Group. Gastric cancer: ESMO Clinical Practice Guidelines for diagnosis, treatment and follow-up. *Ann Oncol* 2010; **21 Suppl 5**: v50-v54 [PMID: 20555102 DOI: 10.1093/annonc/mdq164]

46 **Waddell T**, Verheij M, Allum W, Cunningham D, Cervantes A, Arnold D; European Society for Medical Oncology (ESMO); European Society of Surgical Oncology (ESSO); European Society of Radiotherapy and Oncology (ESTRO). Gastric cancer: ESMO-ESSO-ESTRO Clinical Practice Guidelines for diagnosis, treatment and follow-up. *Ann Oncol* 2013; **24 Suppl 6**: vi57-vi63 [PMID: 24078663 DOI: 10.1093/annonc/mdt344]

47 **Ajani JA**, Bentrem DJ, Besh S, D'Amico TA, Das P, Denlinger C, Fakih MG, Fuchs CS, Gerdes H, Glasgow RE, Hayman JA, Hofstetter WL, Ilson DH, Keswani RN, Kleinberg LR, Korn WM, Lockhart AC, Meredith K, Mulcahy MF, Orringer MB, Posey JA, Sasson AR, Scott WJ, Strong VE, Varghese TK Jr, Warren G, Washington MK, Willett C, Wright CD, McMillian NR, Sundar H; National Comprehensive Cancer Network. Gastric cancer, version 2.2013: featured updates to the NCCN Guidelines. *J Natl Compr Canc Netw* 2013; **11**: 531-546 [PMID: 23667204]

48 **Maruyama K**, Katai H. Surgical treatment of gastric cancer in Japan, trend from standardization to individualization. *Chirurgia (Bucur)* 2014; **109**: 722-730 [PMID: 25560493]

49 **Kim EY**, Song KY, Lee J. Does Hospital Volume Really Affect the Surgical and Oncological Outcomes of Gastric Cancer in Korea? *J Gastric Cancer* 2017; **17**: 246-254 [PMID: 28970955 DOI: 10.5230/jgc.2017.17.e31]

50 **Siewert JR**, Böttcher K, Roder JD, Busch R, Hermanek P, Meyer HJ. Prognostic relevance of systematic lymph node dissection in gastric carcinoma. German Gastric Carcinoma Study Group. *Br J Surg* 1993; **80**: 1015-1018 [PMID: 8402053 DOI: 10.1002/bjs.1800800829]

51 **Sue-Ling HM**, Johnston D, Martin IG, Dixon MF, Lansdown MR, McMahon MJ, Axon AT. Gastric cancer: a curable disease in Britain. *BMJ* 1993; **307**: 591-596 [PMID: 8401015 DOI: 10.1136/bmj.307.6904.591]

52 **Degiuli M**, Sasako M, Ponti A, Calvo F. Survival results of a multicentre phase II study to evaluate D2 gastrectomy for gastric cancer. *Br J Cancer* 2004; **90**: 1727-1732 [PMID: 15150592 DOI: 10.1038/sj.bjc.6601761]

53 **Wu CW**, Hsiung CA, Lo SS, Hsieh MC, Chen JH, Li AF, Lui WY, Whang-Peng J. Nodal dissection for patients with gastric cancer: a randomised controlled trial. *Lancet Oncol* 2006; **7**: 309-315 [PMID: 16574546 DOI: 10.1016/S1470-2045(06)70623-4]

54 **Viste A**, Svanes K, Janssen CW Jr, Maartmann-Moe H, Søreide O. Prognostic importance of radical lymphadenectomy in curative resections for gastric cancer. *Eur J Surg* 1994; **160**: 497-502 [PMID: 7849169]

55 **Robertson CS**, Chung SC, Woods SD, Griffin SM, Raimes SA, Lau JT, Li AK. A prospective randomized trial comparing R1 subtotal gastrectomy with R3 total gastrectomy for antral cancer. *Ann Surg* 1994; **220**: 176-182 [PMID: 8053740 DOI: 10.1097/00000658-199408000-00009]

56 **Dent DM**, Madden MV, Price SK. Randomized comparison of R1 and R2 gastrectomy for gastric carcinoma. *Br J Surg* 1988; **75**: 110-112 [PMID: 3349293 DOI: 10.1002/bjs.1800750206]

57 **Bonenkamp JJ**, Hermans J, Sasako M, van de Velde CJ, Welvaart K, Songun I, Meyer S, Plukker JT, Van Elk P, Obertop H, Gouma DJ, van Lanschot JJ, Taat CW, de Graaf PW, von Meyenfeldt MF, Tilanus H; Dutch Gastric Cancer Group. Extended lymph-node dissection for gastric cancer. *N Engl J Med* 1999; **340**: 908-914

[PMID: 10089184 DOI: 10.1056/NEJM199903253401202]

58 **Cuschieri A**, Weeden S, Fielding J, Bancewicz J, Craven J, Joypaul V, Sydes M, Fayers P. Patient survival after D1 and D2 resections for gastric cancer: long-term results of the MRC randomized surgical trial. Surgical Co-operative Group. *Br J Cancer* 1999; **79**: 1522-1530 [PMID: 10188901 DOI: 10.1038/sj.bjc.6690243]

59 **Cuschieri A**, Fayers P, Fielding J, Craven J, Bancewicz J, Joypaul V, Cook P. Postoperative morbidity and mortality after D1 and D2 resections for gastric cancer: preliminary results of the MRC randomised controlled surgical trial. The Surgical Cooperative Group. *Lancet* 1996; **347**: 995-999 [PMID: 8606613 DOI: 10.1016/s0140-6736(96)90144-0]

P- Reviewer: Aoyagi K, Fujita T, Fukuchi M, Petrucciani N
S- Editor: Gong ZM **L- Editor**: A **E- Editor**: Ma YJ

World Journal of Gastroenterology

Submit a Manuscript: http://www.f6publishing.com

World J Gastroenterol 2018 January 14; 24(2): 290-296

DOI: 10.3748/wjg.v24.i2.290

ISSN 1007-9327 (print) ISSN 2219-2840 (online)

CASE REPORT

Clinically diagnosed late-onset fulminant Wilson's disease without cirrhosis: A case report

Takahiro Amano, Tokuhiro Matsubara, Tsutomu Nishida, Hiromi Shimakoshi, Akiyoshi Shimoda, Aya Sugimoto, Kei Takahashi, Kaori Mukai, Masashi Yamamoto, Shiro Hayashi, Sachiko Nakajima, Koji Fukui, Masami Inada

Takahiro Amano, Tokuhiro Matsubara, Tsutomu Nishida, Hiromi Shimakoshi, Akiyoshi Shimoda, Aya Sugimoto, Kei Takahashi, Kaori Mukai, Masashi Yamamoto, Shiro Hayashi, Sachiko Nakajima, Koji Fukui, Masami Inada, Department of Gastroenterology and Hepatology, Toyonaka Municipal Hospital, Toyonaka, Osaka 560-8565, Japan

ORCID number: Takahiro Amano (0000-0002-0489-7519); Tokuhiro Matsubara (0000-0002-3222-7758); Tsutomu Nishida (0000-0003-4037-9003); Hiromi Shimakoshi (0000-0002-4638-2273); Akiyoshi Shimoda (0000-0003-4397-6583); Aya Sugimoto (0000-0001-5852-2475); Kei Takahashi (0000-0002-6804-8313); Kaori Mukai (0000-0002-6928-7666); Masashi Yamamoto (0000-0002-1107-6858); Shiro Hayashi (0000-0003-4533-2976); Sachiko Nakajima (0000-0002-9088-6882); Koji Fukui (0000-0002-0562-466X); Masami Inada (0000-0003-1822-9017).

Author contributions: Matsubara T, Amano T and Nishida T conceived and designed the study, acquired and analyzed the data, drafted the article; Shimakoshi H, Shimoda A, Sugimoto A and Takahashi K interpreted the data; All authors gave final approval of the manuscript.

Conflict-of-interest statement: The authors have no conflicts of interest to declare.

Manuscript source: Unsolicited manuscript

Correspondence to: Tokuhiro Matsubara, MD, PhD, Department of Gastroenterology and Hepatology, Toyonaka Municipal Hospital, 4-14-1 Shibahara, Toyonaka, Osaka 560-8565, Japan. tmatsubara@chp.toyonaka.osaka.jp
Telephone: +81-6-68430101
Fax: +81-6-68583531

Received: October 16, 2017
Peer-review started: October 16, 2017
First decision: November 8, 2017
Revised: November 23, 2017
Accepted: November 28, 2017
Article in press: November 28, 2017
Published online: January 14, 2018

Abstract

A 64-year-old woman was referred to our hospital with jaundice of the bulbar conjunctiva and general fatigue. After admission, she developed hepatic encephalopathy and was diagnosed with fulminant hepatitis based on the American Association for the Study of Liver Disease (AASLD) position paper. Afterwards, additional laboratory findings revealed that serum ceruloplasmin levels were reduced, urinary copper levels were greatly elevated and Wilson's disease (WD)-specific routine tests were positive, but the Kayser-Fleischer ring was not clear. Based on the AASLD practice guidelines for the diagnosis and treatment of WD, the patient was ultimately diagnosed with fulminant WD. Then, administration of penicillamine and zinc acetate was initiated; however, the patient unfortunately died from acute pneumonia on the 28th day of hospitalization. At autopsy, the liver did not show a bridging pattern of fibrosis suggestive of chronic liver injury. Here, we present the case of a patient with clinically diagnosed late-onset fulminant WD without cirrhosis, who had positive disease-specific routine tests.

Key words: Wilson's disease; Fulminant hepatitis; Late-onset; Liver cirrhosis; Copper

Core tip: A 64-year-old woman was referred to our

hospital with hepatopathy. After admission, she developed hepatic encephalopathy. Laboratory findings revealed that serum ceruloplasmin levels were reduced, serum and urinary copper levels were greatly elevated and Wilson's disease (WD)-specific routine tests were positive. She was diagnosed with fulminant WD based on the American Association for the Study of Liver Disease practice guidelines. At autopsy, the liver did not show a bridging pattern of fibrosis suggestive of chronic liver injury. Here, we present the first case of a patient with clinically diagnosed late-onset fulminant WD without cirrhosis.

Amano T, Matsubara T, Nishida T, Shimakoshi H, Shimoda A, Sugimoto A, Takahashi K, Mukai K, Yamamoto M, Hayashi S, Nakajima S, Fukui K, Inada M. Clinically diagnosed late-onset fulminant Wilson's disease without cirrhosis: A case report. *World J Gastroenterol* 2018; 24(2): 290-296 Available from: URL: http://www.wjgnet.com/1007-9327/full/v24/i2/290.htm DOI: http://dx.doi.org/10.3748/wjg.v24.i2.290

INTRODUCTION

Wilson's disease (WD) was initially described by Kinnier Wilson in 1912 as a congenital copper metabolism disorder disease with autosomal recessive inheritance and obstructed copper metabolic pathways from hepatocytes to bile[1]. The gene responsible for WD is ATP7B on chromosome 13q14[2]. Additionally, it has been reported that WD is an infrequent cause of chronic liver disease, with an estimated incidence of 1 per 30000, and its heterozygote rates are approximately 1 in 90 people worldwide[3]. There are two types of WD-induced hepatic failure: acute onset type, in which patients often develop fulminant hepatitis; and chronic type, which gradually progresses to cirrhosis. Furthermore, WD is identified in less than 5% of acute hepatic failure patients worldwide and is particularly dominant in young females[4,5].

Kidneys of patients with fulminant WD may be protected from copper-mediated tubular damage until transplantation by performing plasmapheresis, hemofiltration and exchange transfusion, hemofiltration or dialysis. Nevertheless, this disease is fatal without urgent liver transplantation. However, early diagnosis is difficult because of a lack of disease-specific symptoms, such as a Kayser-Fleischer ring or neuro-symptoms[4,6]; however, there is typically histological evidence involving copper deposition and bridging fibrosis or cirrhosis[7].

A few reports of patients with late-onset fulminant WD in the elderly population exist; this population usually develops fulminant hepatitis from chronic liver disease or cirrhosis. Here, we report a patient with clinically diagnosed late-onset fulminant WD without cirrhosis, who had positive disease-specific routine tests.

CASE REPORT

A 64-year-old woman became conscious of bulbar conjunctiva 2 d prior to admission. Afterwards, she was referred to our hospital with a low-grade fever and hepatopathy, complaining of jaundice of the bulbar conjunctiva and general fatigue, and she received emergency hospitalization. She had no medical history of drinking, consanguineous marriage, or oral use of dietary supplements, and her body mass index was 24. Regarding her family, her elder sister died from hepatic failure of unknown causes in her thirties. A physical examination showed normal abdominal findings and consciousness level, but her laboratory studies revealed abnormal liver function, including an elevated serum total bilirubin (T-Bil) level of 33.9 mg/dL [upper limit of normal (ULN): 1.2 mg/dL], direct bilirubin level of 25.5 mg/dL (ULN: 0.3 mg/dL) with an elevated ammonia (NH_3) level of 143 μg/dL (ULN: 66 μg/dL), reduced serum prothrombin time of 19% (lower limit of normal: 70%) and anemia (hemoglobin, 6.1 g/dL) (Table 1). Contrast computerized tomography (CT) showed hepato-splenomegaly without mass lesion and dilatation of the hepatic duct in the liver (Figure 1). Based on these findings, she was diagnosed with acute hepatic failure on admission.

After hospitalization, she was treated with transfusion of 6 fresh frozen plasma units. Her plasma was exchanged with 32 fresh frozen plasma units for 3 d under continuous hemofiltration because of anuria after 2 d in the hospital; however, her liver function did not recover. Furthermore, both hemoglobin and platelet levels gradually decreased with higher reticulocyte [175‰ (ULN: 20%)] and low levels of haptoglobin (below the scale, < 10 mg/dL), but both direct and indirect Coombs tests were negative. Based on these laboratory findings, we first diagnosed Coombs-negative hemolytic anemia with hepatic failure of unknown cause. Additional specific laboratory findings associated with acute hepatic failure did not suggest related causes, such as viral hepatitis, autoimmune hepatitis or primary biliary cirrhosis (Table 1). Then, we attempted to perform a liver biopsy but were unsuccessful because of the progression of liver failure.

On day 4 of hospitalization, the patient progressed to a precoma stage with flapping tremor and confusion. On neurological examination, she fell into hepatic encephalopathy with greatly elevated NH_3 levels (168 μg/dL). According to the 2014 American Association for the Study of Liver Disease (AASLD) and European Association for study of the liver (EASL) guidelines[8], her hepatic encephalopathy was characterized as type A, overt, grade Ⅱ, episodic, and precipitated. On day 5 of hospitalization, we performed bone marrow examination, which showed hemophagocytosis in the bone marrow and diagnosed the cause of pancytopenia. The Histiocyte Society HLH-2004 diagnostic criteria (available at http://www.histiocytesociety.org/) were fulfilled (Figure 2). Based

Table 1 Laboratory data on admission

Biochemical data		Fe, μg/dL	130
WBC, /μL	26200	ferritin, ng/mL	7817
RBC, $\times 10^4$/μL	163	IgG, mg/dL	1678
Hb, g/dL	6.1	IgM, mg/dL	86
Platelets, $\times 10^4$/μL	20.2	IgA, mg/dL	505
MCV, fL	122.7	ANA	< 40
MCH, pg	37.4	AMA-M2, index	2
MCHC, g/dL	30.5	sIL2-R, U/mL	1130
PT, %	19	Direct Coombs	-
PT-INR	2.43	Indirect Coombs	-
D-dimer, μg/mL	1.8	Vitamin B12, pg/mL	> 1500
AST, U/L	164	Folic acid, ng/mL	4
ALT, U/L	15	Erythropoietin, IU/mL	367
LDH, U/L	609	Reticulocytes, %	175
ALP, U/L	26	**Viral markers**	
γGTP, U/L	371	HBsAg, IU/mL	0.02
Alb, g/dL	2.3	HBeAg, S/CO	< 0.5
T-Bil, mg/dL	33.99	HBeAb, %	< 35
D-Bil, mg/dL	25.51	HBcAb, S/CO	0.23
BUN, mg/dL	36	HBsAb, mIU/mL	0
Cr, mg/dL	0.75	HCVAb, S/CO	0.1
UA, mg/dL	2.2	CMV-IgM	0.58
Na, mEq/L	133	CMV-IgG	> 128
K, mEq/L	4.6	EBV-IgM	< 10
T-CHO, mg/dL	83	EBV-IgA	< 10
CRP, mg/dL	2.62	EBV-IgG	80
NH_3, μg/dL	138	HAVAb-IgM, S/CO	< 0.5
Immunological and other data		HAVAb	< 0.4
Fe, μg/dL	130	HSV-CF	< 4
Ferritin, ng/mL	7817		

ULN of AST: 10-31 U/L; ULN of ALT: 4-31 U/L; ULN of ALP: 98-328 U/L; ULN of γGTP: 8-45 U/L. Alb: Albumin; ALP: Alkaline phosphatase; ALT: Alanine aminotransferase; ANA: Antinuclear antibody; AST: Aspartate aminotransferase; BUN: Blood urea nitrogen; CMV: Cytomegalovirus; Cr: Creatinine; CRP: C-reactive protein; D-Bil: Direct bilirubin; EBV: Epstein-Barr virus; Fe: Iron; γGTP: Gamma-glutamyl transpeptidase; HAVAb: Hepatitis A virus antibody; Hb: Hemoglobin; HBcAb: Hepatitis B core antibody; HBeAg/Ab: Hepatitis B envelope antigen/antibody; HBsAg/Ab: Hepatitis B surface antigen/antibody; HCVAb: Hepatitis C virus antibody; HSV-CF: Herpes simplex virus-complement fixation; IgG/IgA/IgM: Immunoglobulin G/A/M; K: Potassium; LDH: Lactate dehydrogenase; Na: sodium; NH3: Ammonia; PT: Prothrombin time; RBC: Red blood cell; sIL2-R: Soluble interleukin 2-receptor; T-Bil: Total bilirubin; T-CHO: Total cholesterol; UA: Uric acid; ULN: Upper limit of normal; WBC: White blood cell.

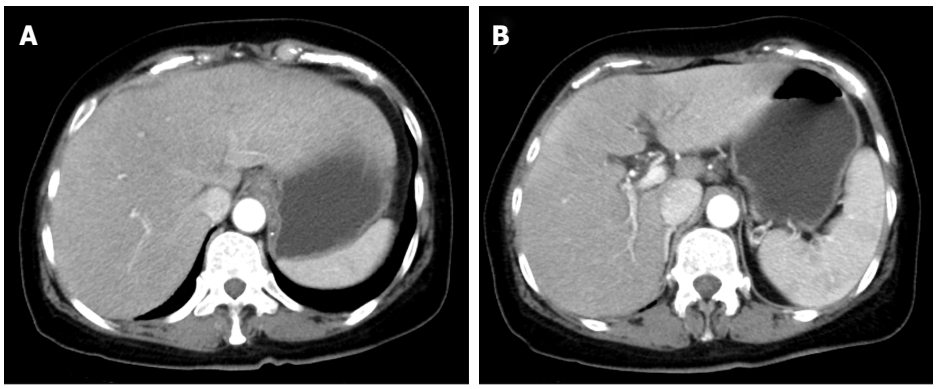

Figure 1 Contrast computerized tomography before the treatment. A: CT revealed hepatomegaly with no mass or dilatation of the intrahepatic duct in the liver; B: CT revealed splenomegaly. CT: Computerized tomography.

on the AASLD position paper[9], we diagnosed acute hepatic failure as fulminant hepatitis with unidentified hemophagocytic syndrome.

Figure 3 shows the time course of T-Bil, alanine aminotransferase (ALT), aspartate aminotransferase (AST), prothrombin time, hemoglobin, NH_3 and platelets. Then, we performed steroid pulse therapy (methylprednisolone of 1 g/d, intravenously) for 3 d, followed by oral methylprednisolone (0.6 mg/kg). Then, steroids were tapered to 5 mg weekly. After steroid therapy, it was found that serum ceruloplasmin levels declined to 16.7 mg/dL and urinary copper levels were greatly elevated, up to 17900 μg/dL (895 μg/d); however, serum copper levels did not increase (105 μg/dL)

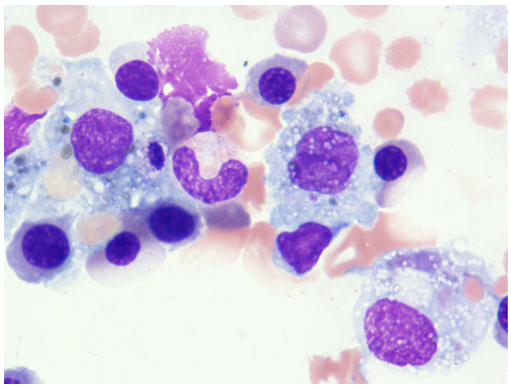

Figure 2 Bone marrow examination revealed macrophages phagocytizing blood cells.

and the Kayser-Fleischer ring was not clear. Based on the AASLD[7] and EASL clinical practice guidelines[3] for the diagnosis and treatment of WD, the patient met the diagnostic criteria for WD. From these findings, she was finally diagnosed fulminant WD.

Then, administration of penicillamine (900 mg/d) and zinc acetate (150 mg/d) was started from a gastric tube on day 9 of hospitalization. Additionally, we considered liver transplantation; however, the patient died from hepatic failure with acute pneumonia on day 28 of hospitalization. We obtained approval from her family and then performed pathological anatomy. The liver (weight of 1580 g) was bile stained and soft (Figure 4A). The capsule was wrinkled. Microscopically, the liver showed massive necrosis and collapse of the intervening parenchyma (Figure 4B, C). Rhodanine staining unclearly depicted copper deposition in the scattered residual hepatocytes because of massive necrosis and collapse of the intervening parenchyma (not shown), and a bridging pattern of fibrosis suggestive of chronic liver injury was not found (Figure 4D, E). Histopathological examinations confirmed the diagnosis of fulminant hepatitis. Additionally, we obtained approval from her son and examined ATP7B on chromosome 13, but no genetic defect associated with WD was found. In summary, we here report a patient with sporadic, late-onset fulminant WD without cirrhosis.

DISCUSSION

WD is an autosomal recessive inherited disease with copper metabolism disorder in the liver that results in excessive copper deposition in many organs and tissues. Generally, WD is recognized as a slow, progressive chronic disease with young-onset in children or young adults, but age at onset of WD is widely variable. The presenting feature of WD is hepatic dysfunction, which is shown in more than half of patients. It develops as acute hepatitis involving three major patterns: (1) chronic active hepatitis; (2) cirrhosis, which is the most common initial presentation; and (3) fulminant hepatitis.

Most cases of WD develop in persons less than 40-years-old, and late-onset fulminant WD is quite rare. Some cases of patients who developed WD at over 40 years of age have been reported; however, the diagnosis of WD varied[10,11]. Ferenci *et al*[10] suggested that more attention is paid to the identification of older patients with WD. Almost all patients with fulminant WD died rapidly, without urgent liver transplantation over time; therefore, early diagnosis is necessary. However, the diagnosis of WD is quite difficult because clinical features of WD-like hepatic failure or neuropsychiatric disturbances vary widely and the clinical condition varies from asymptomatic states to fulminant hepatic failure[2]. If all available tests without genetic tests are applied, 20% of the cases in patients over 40 years old were missed[10,11]. There were several reasons why elderly WD subjects were overlooked due to diagnostic criteria limitations based on clinical symptoms and laboratory findings. Ferenci *et al*[10] also demonstrated that WD should be considered in patients presenting unidentified hepatic or neurologic disease. Increased awareness of WD and the use of a recently proposed diagnostic algorithm could lead to greater detection in elderly patients.

Recently, predictive markers for the diagnosis of WD-induced acute hepatic failure have been reported: reduced hemoglobin (< 10 g/dL), elevated serum copper levels (> 200 μg/dL), decreased ratios of alkaline phosphatase (ALP) to T-Bil (< 4) and elevated ratios of AST to ALT (> 2.2). The sensitivity/specificity of reduced hemoglobin and elevated serum copper levels was 94%/74% and 75%/96%, respectively. Additionally, the sensitivity/specificity of ALP to T-Bil ratio and AST to ALT ratio was 94%/96% and 94%/86%, respectively. Consequently, the combination of ALP to T-Bil ratio and AST to ALT ratio provided a diagnostic sensitivity and specificity of 100%[4]. In the present case, serum copper and hemoglobin on admission were 105 μg/dL and 6.1 g/dL, respectively. Unfortunately, we had a difficult time with early diagnosis, but disease-specific routine tests were positive in this case; the ratio of ALP to T-Bil was 1.3 and that of AST to ALT was 10.9. Screening for a diagnosis of WD in the setting of acute hepatic failure with ceruloplasmin measurements is generally unreliable. Disease-specific routine tests were useful to accurately distinguish WD patients with acute liver failure and were an acceptable and rapidly available alternative.

According to the AASLD practice guidelines on the diagnosis and treatment of WD, classical diagnosis of WD includes recognition of corneal Kayser-Fleischer rings, identification of reduced concentrations of serum ceruloplasmin (< 20 mg/dL), and increased 24-h urine copper (> 40 μg/d), in addition to quantitative copper levels in percutaneous liver biopsy specimens (> 250 μg/g dry weight). In the present case, concentrations of serum ceruloplasmin and 24-h urine copper were 16.7 mg/dL and 895 μg/d, respectively. Although low serum levels of ceruloplasmin and high levels

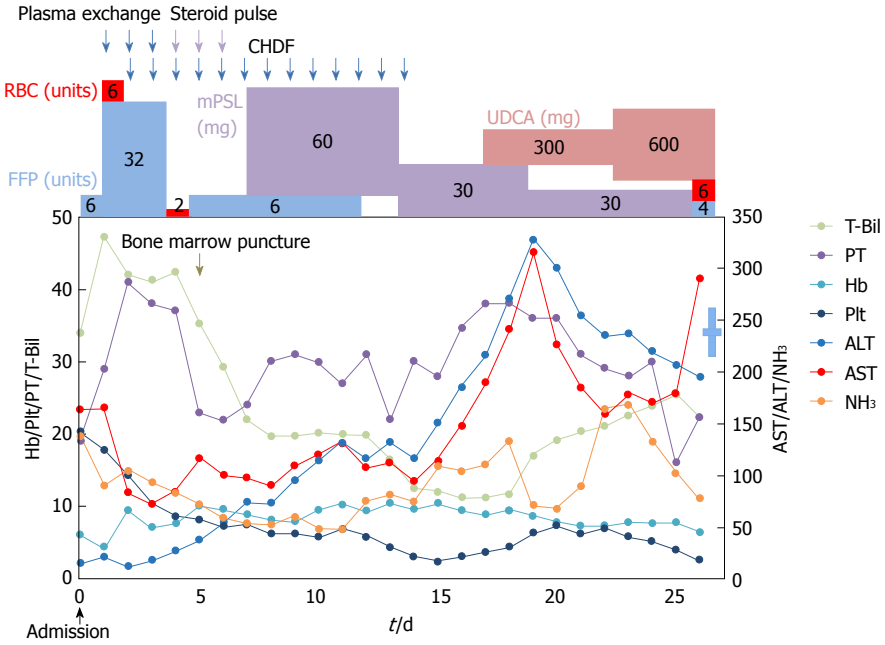

Figure 3 Time courses of laboratory data and treatment. ALT (U/L): Alanine aminotransferase; AST (U/L): Aspartate aminotransferase; CHDF: Continuous hemodiafiltration; FFP: Fresh frozen plasma; Hb (g/dL): Hemoglobin; mPSL: Methylprednisolone; NH_3 (μg/dL): Ammonia; PT (%): Prothrombin time; Plt (×10^4/μL): Platelet; RBC: Red blood cell; T-Bil (mg/dL): Total bilirubin; UDCA: Ursodeoxycholic acid.

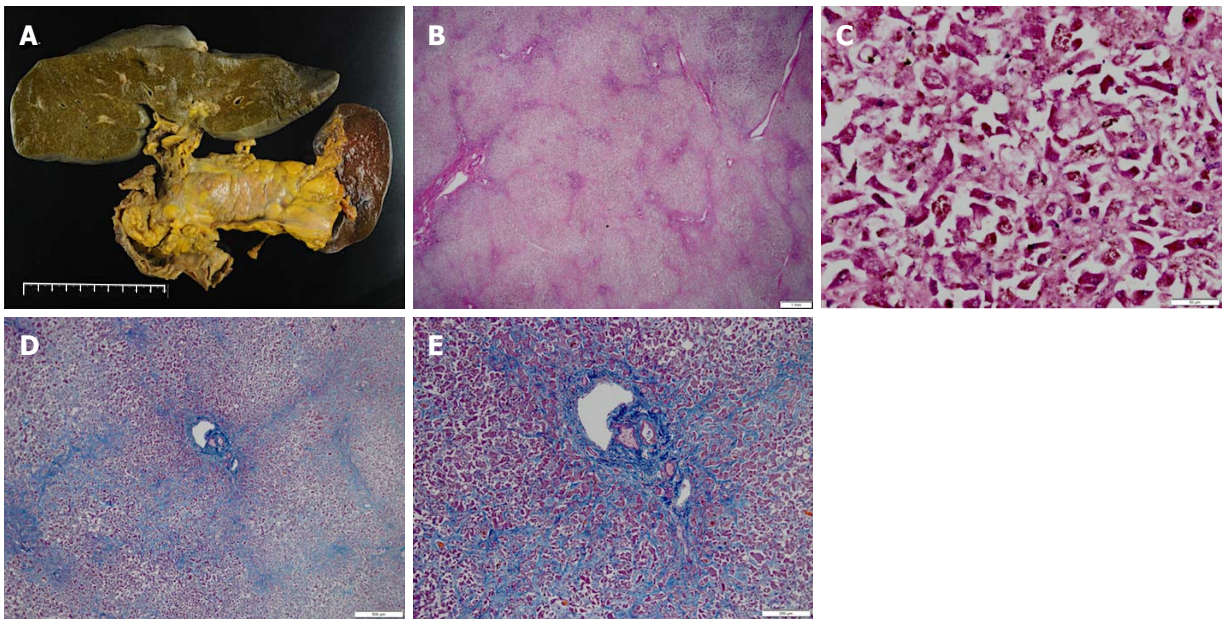

Figure 4 Pathological findings in the liver. A: The liver (1580 g) was bile stained and soft; B: Low power field: The capsule was wrinkled in HE staining; C: High power field: Microscopically, the liver showed massive necrosis and collapse of the intervening parenchyma in HE staining; D: Low power field in AZAN staining; E: High power field in AZAN staining: Bridging pattern of fibrosis suggestive of chronic liver injury was not found. HE: Hematoxylin-eosin.

of cupriuria may be observed in acute liver failure due to other causes, we ruled out other acute liver injuries, such as viral infection, autoimmune and drug-induced hepatic damage, despite the possibility of other unknown hepatitis. In addition, all of the above predictive markers (reduced hemoglobin, elevated serum copper levels, decreased ratios of ALP to T-Bil and elevated ratios of AST to ALT) met the criteria for diagnosis of WD-induced acute hepatic failure. Hence, we reached a diagnosis of acute liver failure due to WD. We believe that WD-induced acute hepatic failure first developed, and then hemophagocytosis followed, which allowed hepatic failure to rapidly deteriorate without developing cirrhosis.

There are, however, limitations to our report of WD diagnosis. First, it was difficult to retrospectively weigh the precise copper levels in the liver because all liver tissues were fixed in formalin. Then, we evaluated

copper deposition in the liver using rhodanine staining. We, however, believe that copper deposition was difficult to examine with rhodanine staining in the scattered residual hepatocytes because of massive necrosis and collapse of the intervening parenchyma. Some reports have suggested that immunohistochemistry staining is inadequate for examining copper deposition[12,13].

Liver biopsy is a useful method to confirm WD diagnosis and almost all patients with WD-induced acute hepatic failure have advanced fibrosis. However, no presence of bridging fibrosis and cirrhosis in the liver was found during autopsy in the present case. According to the AASLD and EASL clinical practice guidelines on the diagnosis and treatment of WD, the patient ultimately met the diagnostic criteria, which are accurate in approximately 85% of cases with clinical symptoms and laboratory findings. In addition, genetic testing is necessary to diagnose WD. Unfortunately, gene testing was not performed on the patient due to her rapid clinical course, but her son was negative for the ATP7B gene by DNA analysis. However, it was reported that 13% of patients with WD did not have a mutation and 28.8% showed only one mutation[9]. Based on these reports and her clinical course, we diagnosed the patient with late-onset fulminant WD. To the best of our knowledge, the present case is the first report of a patient diagnosed with late-onset fulminant WD without cirrhosis, who had positive disease-specific routine tests.

ARTICLE HIGHLIGHTS

Case characteristics

A 64-year-old woman was referred to our hospital with jaundice of the bulbar conjunctiva and general fatigue.

Clinical diagnosis

A physical examination showed normal abdominal findings but Kayser-Fleischer ring was not clear. The authors first diagnosed hepatic failure of unknown cause.

Differential diagnosis

Malignant tumors (hepatocellular carcinoma, cholangiocarcinoma and metastatic tumors) and hepatic failure-related causes, such as viral hepatitis, autoimmune hepatitis or primary biliary cirrhosis, drug-induced hepatic damage.

Laboratory diagnosis

Laboratory studies revealed the diagnostic criteria for Wilson's disease based on the American Association for the Study of Liver Disease (AASLD) and European Association for study of the liver (EASL) clinical practice guidelines; declined serum ceruloplasmin levels (16.7 mg/dL) and elevated urinary copper levels [17900 μg/dL (895 μg/d)], and Wilson's disease-specific routine tests; reduced hemoglobin (6.1 g/dL), decreased ratios of alkaline phosphatase (ALP) to total bilirubin (T-Bil) (1.3) and elevated ratios of aspartate aminotransferase (AST) to alanine aminotransferase (ALT) (10.9).

Imaging diagnosis

Contrast computerized tomography (CT) showed hepato-splenomegaly without mass lesion and dilatation of the hepatic duct in the liver.

Pathological diagnosis

At autopsy, the liver did not show a bridging pattern of fibrosis suggestive of chronic liver injury.

Treatment

Administration penicillamine and zinc acetate were started.

Related reports

Regarding predictive markers for the diagnosis of Wilson's disease-induced acute hepatic failure, the sensitivity/specificity of reduced hemoglobin, elevated serum copper levels, ALP to T-Bil ratio, AST to ALT ratio and the combination of ALP to T-Bil ratio were 94%/74%, 75%/96%, 94%/96%, 94%/86% and 100%, respectively.

Term explanation

To the best of our knowledge, the present case is the first report of a patient diagnosed with late-onset fulminant WD without cirrhosis who had positive disease-specific routine tests.

Experiences and lessons

Generally, WD is recognized as a slow, progressive chronic disease with young-onset in children or young adults, but this case reports a patient with sporadic, late-onset fulminant WD without cirrhosis. In addition, predictive markers (reduced hemoglobin, elevated serum copper levels, decreased ratios of ALP to T-Bil and elevated ratios of AST to ALT) were useful in the diagnosis of WD.

REFERENCES

1 **Compston A**. Progressive lenticular degeneration: a familial nervous disease associated with cirrhosis of the liver, by S. A. Kinnier Wilson, (From the National Hospital, and the Laboratory of the National Hospital, Queen Square, London) Brain 1912: 34; 295-509. *Brain* 2009; **132**: 1997-2001 [PMID: 19634211 DOI: 10.1093/brain/awp193]

2 **Rodriguez-Castro KI**, Hevia-Urrutia FJ, Sturniolo GC. Wilson's disease: A review of what we have learned. *World J Hepatol* 2015; **7**: 2859-2870 [PMID: 26692151 DOI: 10.4254/wjh.v7.i29.2859]

3 **European Association for Study of Liver**. EASL Clinical Practice Guidelines: Wilson's disease. *J Hepatol* 2012; **56**: 671-685 [PMID: 22340672 DOI: 10.1016/j.jhep.2011.11.007]

4 **Korman JD**, Volenberg I, Balko J, Webster J, Schiodt FV, Squires RH Jr, Fontana RJ, Lee WM, Schilsky ML; Pediatric and Adult Acute Liver Failure Study Groups. Screening for Wilson disease in acute liver failure: a comparison of currently available diagnostic tests. *Hepatology* 2008; **48**: 1167-1174 [PMID: 18798336 DOI: 10.1002/hep.22446]

5 **Ostapowicz G**, Fontana RJ, Schiødt FV, Larson A, Davern TJ, Han SH, McCashland TM, Shakil AO, Hay JE, Hynan L, Crippin JS, Blei AT, Samuel G, Reisch J, Lee WM; U.S. Acute Liver Failure Study Group. Results of a prospective study of acute liver failure at 17 tertiary care centers in the United States. *Ann Intern Med* 2002; **137**: 947-954 [PMID: 12484709 DOI: 10.7326/0003-4819-137-12-200212170-00007]

6 **Roberts EA**, Schilsky ML; Division of Gastroenterology and Nutrition, Hospital for Sick Children, Toronto, Ontario, Canada. A practice guideline on Wilson disease. *Hepatology* 2003; **37**: 1475-1492 [PMID: 12774027 DOI: 10.1053/jhep.2003.50252]

7 **Roberts EA**, Schilsky ML; American Association for Study of Liver Diseases (AASLD). Diagnosis and treatment of Wilson disease: an update. *Hepatology* 2008; **47**: 2089-2111 [PMID: 18506894 DOI: 10.1002/hep.22261]

8 **Vilstrup H**, Amodio P, Bajaj J, Cordoba J, Ferenci P, Mullen KD, Weissenborn K, Wong P. Hepatic encephalopathy in chronic liver disease: 2014 Practice Guideline by the American Association for the Study of Liver Diseases and the European Association for the Study of the Liver. *Hepatology* 2014; **60**: 715-735 [PMID: 25042402 DOI: 10.1002/hep.27210]

9 **Polson J**, Lee WM; American Association for the Study of Liver Disease. AASLD position paper: the management of acute liver failure. *Hepatology* 2005; **41**: 1179-1197 [PMID: 15841455 DOI: 10.1002/hep.20703]

10 **Ferenci P**, Członkowska A, Merle U, Ferenc S, Gromadzka G, Yurdaydin C, Vogel W, Bruha R, Schmidt HT, Stremmel W. Late-onset Wilson's disease. *Gastroenterology* 2007; **132**: 1294-1298 [PMID: 17433323 DOI: 10.1053/j.gastro.2007.02.057]
11 **Weitzman E**, Pappo O, Weiss P, Frydman M, Haviv-Yadid Y, Ben Ari Z. Late onset fulminant Wilson's disease: a case report and review of the literature. *World J Gastroenterol* 2014; **20**: 17656-17660 [PMID: 25516681 DOI: 10.3748/wjg.v20.i46.17656]
12 **Lindquist RR**. Studies on the pathogenesis of hepatolenticular degeneration. II. Cytochemical methods for the localization of copper. *Arch Pathol* 1969; **87**: 370-379 [PMID: 5766764]
13 **Pilloni L**, Lecca S, Van Eyken P, Flore C, Demelia L, Pilleri G, Nurchi AM, Farci AM, Ambu R, Callea F, Faa G. Value of histochemical stains for copper in the diagnosis of Wilson's disease. *Histopathology* 1998; **33**: 28-33 [PMID: 9726045 DOI: 10.1046/j.1365-2559.1998.00455.x]

P- Reviewer: Aizawa Y, Iorio R, Manesis EKK, Xie Q, Yalniz M
S- Editor: Ma YJ **L- Editor**: Filipodia **E- Editor**: Li RF

World Journal of Gastroenterology

Submit a Manuscript: http://www.f6publishing.com

World J Gastroenterol 2018 January 14; 24(2): 297-302

DOI: 10.3748/wjg.v24.i2.297

ISSN 1007-9327 (print) ISSN 2219-2840 (online)

CASE REPORT

Mass forming chronic pancreatitis mimicking pancreatic cystic neoplasm: A case report

Keum Nahn Jee

Keum Nahn Jee, Department of Radiology, Dankook University Hospital, Chungcheongnam-do 330-715, South Korea

ORCID number: Keum Nahn Jee: (0000-0003-2669-4381).

Author contributions: Jee KN designed the report, collected the patient's clinical data, drafting the article and reviewed the manuscript and approved the final manuscript as submitted.

Informed consent statement: This study was reviewed and approved the retrospective case review by Institutional Review Board of Dankook University Hospital, Cheonan, South Korea, with informed consent from the patient waived.

Conflict-of-interest statement: There are no potential conflicts (financial, professional, or personal) of interest relevant to this article to disclose by the author.

Manuscript source: Unsolicited manuscript

Correspondence to: Keum Nahn Jee, MD, PhD, Professor, Department of Radiology, Dankook University Hospital, Mang-hyang Street 201, Anseo-dong, Dongnam-gu, Cheonan, Chungcheongnam-do 330-715, South Korea. jkn1303@dkuh.co.kr
Telephone: +82-41-5506921
Fax: +82-41-5529674

Received: October 19, 2017
Peer-review started: October 20, 2017
First decision: November 8, 2017
Revised: November 15, 2017
Accepted: November 22, 2017
Article in press: November 22, 2017

Published online: January 14, 2018

Abstract

Mass forming chronic pancreatitis is very rare. Diagnosis could be done by the pathologic findings of focal inflammatory fibrosis without evidence of tumor in pancreas. A 34-year-old man presented with right upper abdominal pain for a few weeks and slightly elevated bilirubin level on clinical findings. Radiological findings of multidetector-row computed tomography, magnetic resonance (MR) imaging with MR cholangiopancreatography and endoscopic ultrasonography revealed focal branch pancreatic duct dilatation with surrounding delayed enhancing solid component at uncinate process and head of pancreas, suggesting branch duct type intraductal papillary mucinous neoplasm. Surgery was done and pathology revealed the focal chronic inflammation, fibrosis, and branch duct dilatation. Herein, I would like to report the first case report of mass forming chronic pancreatitis mimicking pancreatic cystic neoplasm.

Key words: Chronic pancreatitis; Pseudotumor; Computed tomography; Magnetic resonance imaging; Endoscopic ultrasound

Core tip: Extremely unusual radiological manifestation of mass forming chronic pancreatitis mimicking pancreatic cystic neoplasm is the first case report in the English-written medical literature.

Jee KN. Mass forming chronic pancreatitis mimicking pancreatic cystic neoplasm: A case report. *World J Gastroenterol* 2018;

24(2): 297-302 Available from: URL: http://www.wjgnet.com/1007-9327/full/v24/i2/297.htm DOI: http://dx.doi.org/10.3748/wjg.v24.i2.297

INTRODUCTION

Chronic pancreatitis represents a recurrent, prolonged inflammatory process and progressive fibrosis of the pancreas. These results in irreversible morphologic change of the pancreas, clinical symptoms of abdominal pain, and insufficiency of exocrine and endocrine function[1-3]. On computed tomography (CT) and magnetic resonance (MR) image, dilatation of the main pancreatic duct, parenchymal atrophy, pancreatic calcification or stone, focal pancreatic enlargement or inflammatory pancreatic mass, bile duct dilatation, attenuation change of peripancreatic fat and fluid collection are frequent findings[4-6].

Inflammatory mass in chronic pancreatitis retain a large degree of fibrosis like pancreatic carcinoma[7-9], and both lesions are shown as a gradual progressive enhancement on contrast-enhanced CT and dynamic MR imaging, making the discrimination of the two entities difficult[5,6,10].

In the case of mass forming chronic pancreatitis, diagnosis of inflammatory pancreatic mass could be almost impossible if associated radiological findings of chronic pancreatitis is not shown.

This paper presents a very unique case of mass forming chronic pancreatitis mimicking pancreatic cystic neoplasm.

CASE REPORT

A 34-year-old man complained for right upper abdominal pain for a few days. His laboratory findings including white blood cell count, C-reactive protein, alkaline phosphatase, liver enzyme level and tumor markers of carbohydrate antigen 19-9 and carcinoembryonic antigen were within normal range except slight elevation of total bilirubin (1.3 mg/dL, normal range of 0.2-1.2), gamma-glutamyl transferase (108 IU/L, normal range of 8-60) and lipase (90 U/L, normal range of 30-60). The patient had past medical history of admission due to acute alcoholic pancreatitis 13 years ago and social history of daily alcohol consumption for 15 years and having smoked 20 pack years.

Unenhanced abdomen CT image showed slight low attenuating lesion involving pancreatic uncinate process and head (Figure 1A). Contrast-enhanced abdominal CT images showed a delayed enhancing solid portion surrounding a few tubular cystic attenuating lesion sized about 2.5 cm × 2.1 cm in pancreatic uncinate process and head, and mild dilatation of common bile duct (CBD) and gallbladder (Figure 1B and C). MR cholangiopancreatography showed branch pancreatic duct dilation in head and uncinate process causing extrinsic indentation and tapering of distal CBD, and mild dilatation of proximal CBD and gallbladder (Figure 2A). Fat-saturated T2-weighted MR image showed a slight high signal intensity solid component surrounding bright signal intensity branch duct dilatation in pancreatic uncinate process and head, with the lesion sized about 2.6 cm × 2.2 cm (Figure 1B). Fat-suppressed T1-weighted MR image showed a well-demarcated low signal intensity lesion in head and uncinate process of pancreas (Figure 2C), and delayed contrast-enhancing solid component surrounding low signal intensity branch-duct dilation in pancreatic uncinate process and head was shown on fat-suppressed T1-weighted dynamic gadolinium-enhanced MR images (Figure 2D and E). Diffusion-weighted MR images showed higher signal intensity on low *b* factor (b = 20 s/m^2) image and low signal intensity on high *b* factor (b = 800 s/m^2) image, suggesting no diffusion restriction on apparent diffusion coefficient map (Figure 2H), which reflecting the large area of cystic component of the lesion. Endoscopic ultrasonography (EUS) showed pruning pattern, anechoic branch duct dilatation containing a few small hyperechoic mural nodules (Figure 3A and B).

The lesion located in uncinate process and head of pancreas with indenting distal CBD and dilatation of proximal CBD, without dilatation of main pancreatic duct due to anatomic variation of pancreatic divisum which was detected on MR image (Figure 2B). Radiological diagnostic impression was branch duct type intraductal papillary mucinous neoplasm (IPMN) of pancreas. However, some worrisome features of delayed contrast-enhancing solid component around the wall of dilated branch duct on CT and MR images and small mural nodules in dilated branch ducts on EUS were shown. EUS guided fine needle aspiration (FNA) cytology was obtained from the solid component along the wall of dilated duct and suggested the possibility of intraductal-growing epithelial neoplasm.

The patient underwent pylorus-preserving pancreaticoduodenectomy, due to considering FNA finding, imaging findings of CT, MRI, and EUS and aggravated right upper abdominal pain and persistent mild elevation of bilirubin and gamma-glutamyl transferase levels without response to conservative medical treatment for four weeks. The gross pathology of resected specimen showed whitish hard infiltrating lesion in pancreatic uncinate process and head portion (Figure 4A). The histopathologic report revealed periductal inflammation with fibrosis and mild dilatation of branch pancreatic ducts and intralobular fibrosis, consistent with chronic pancreatitis (Figure 4B).

DISCUSSION

Chronic pancreatitis is defined as inflammatory and fibrotic disease of pancreatic tissue, characterized by irreversible functional and morphologic change.

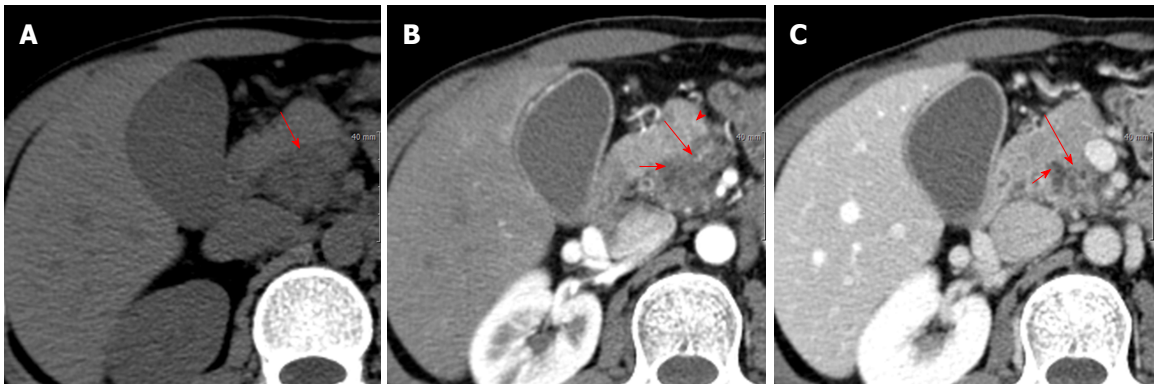

Figure 1 Findings from computed tomography. A: Unenhanced computed tomography (CT) image shows a slight low attenuating lesion (arrow) in pancreatic uncinated process and head and dilatation of gallbladder; B: Contrast-enhanced arterial phase CT image shows minimal enhancing low attenuating lesion (long arrow) surrounding a few tubular low cystic attenuating structures (short arrow), and homogenous highly enhancing normal pancreas (arrowhead); C: Contrast-enhanced portal venous phase CT image shows delayed enhancing lesion (long arrow) containing a few tubular cystic structures (short arrow).

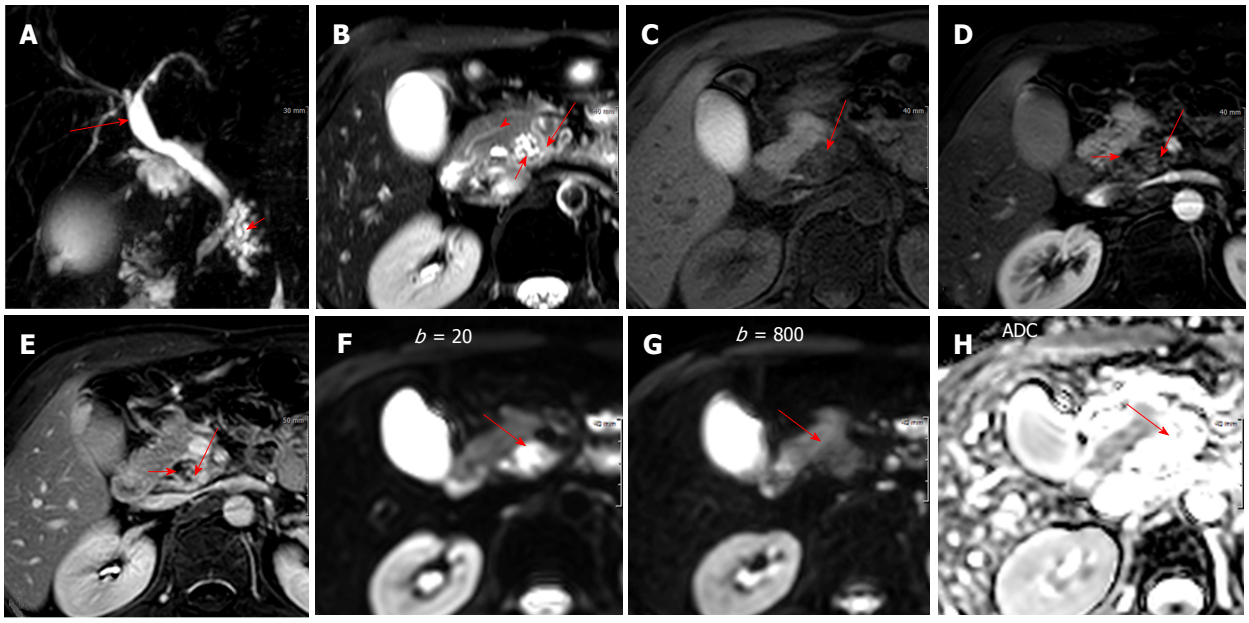

Figure 2 Findings from magnetic resonance image. A: Magnetic resonance (MR) cholangiopancreatography shows localized branch pancreatic duct dilatation (short arrow) in head of pancreas with tapering of distal common bile duct and dilatation of proximal common duct (long arrow); B: T2-weighted MR image shows slight high signal intensity lesion (long arrow) containing bright intensity branch duct dilatation (short arrow) in head and uncinate process of pancreas, and incidental finding of pancreatic divisum (arrowhead); C: Fat-suppressed T1-weighted MR image shows a well-demarcated low signal intensity lesion (long arrow) in uncinate process and head of pancreas; D-E: Fat-suppressed T1-weighted gadolinium-enhanced arterial- (D) and delayed-phase (E) MR images show delayed highly enhancing solid mass-like lesion (long arrows) containing non-enhancing dark intensity branch duct dilatation (short arrows) in pancreatic head; F: The higher signal intensity lesion (arrow) on diffusion-weighted image obtained with b = 20 s/m^2 shows as low signal intensity (arrow) on diffusion-weighted image obtained with b = 800 s/m^2 and as higher (arrow) apparent diffusion coefficient (ADC) without diffusion restriction.

Alcohol abuse is the most common (70%-80%) cause of chronic pancreatitis in the developed countries[1,2,3,7]. In addition, smoking, gene mutations, autoimmune syndromes, metabolic disturbances, environmental conditions and anatomical abnormalities are suggested as other associated factors with occurrence of the disease[3,11,12].

The pathology of advanced alcoholic chronic pancreatitis revealed a firm consistency of pancreas with an irregular contour without the normal lobulation[13]. The fibrosis may diffusely affect the entire gland, but occasionally it is unevenly distributed, with preserved normal lobular pattern in some areas. The severity of the duct changes depends on the extent of the surrounding fibrosis. Thus, the main duct may be focally or diffusely involved with obstruction, irregular dilatation and distortion[14,15]. Fibrosis in the pancreas head may cause a tapering stenosis of CBD[16].

In this case, initial clinical symptom of right upper abdominal pain was developed due to dilatation of gallbladder by stenosis of distal CBD, and the causative lesion of CBD obstruction was a focal mass lesion,

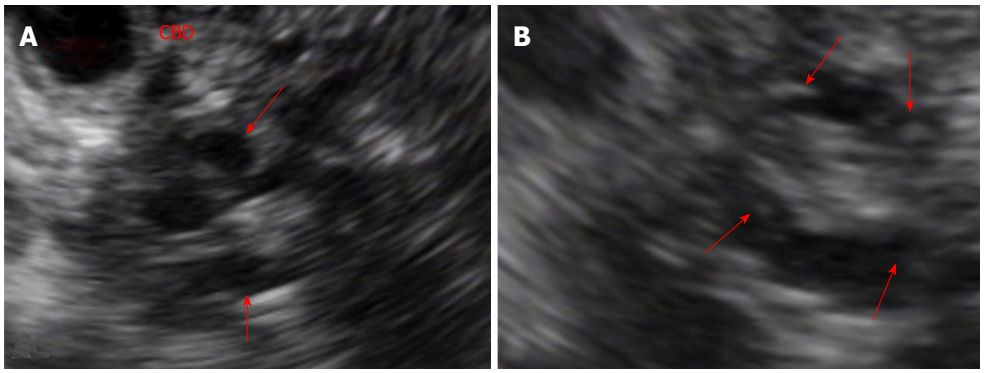

Figure 3 Findings from endoscopic ultrasound. A: EUS shows a few anechoic tubular structures (arrows), causing indentation of distal CBD and dilatation of proximal bile duct; B: EUS shows small hyperechoic mural nodules (arrows) in the dilated branch pancreatic ducts. EUS: Endoscopic ultrasound; CBD: Common bile duct.

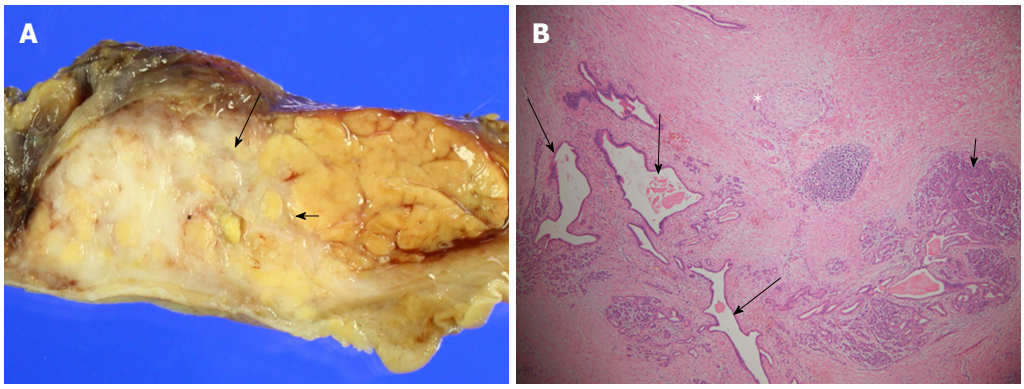

Figure 4 Macroscopic and microscopic findings of resected specimen. A: Gross specimen shows whitish hard infiltrating mass-like lesion (arrows) focally replaced head and uncinate process of pancreas; B: Microscopy (hematoxylin and eosin, x 40) shows perilobular and intralobular fibrosis (asterisk) replaces normal pancreatic acini with focal perivascular lymphocyte infiltration (short arrow) and dilated branch ducts (long arrows).

including branch duct dilatation with surrounding solid component in uncinate process and head of pancreas, detected on CT, MRI and EUS findings. The diagnostic impression based on radiological imaging findings was branch duct type IPMN most likely and serous cystadenoma as a possible differential diagnosis. In thinking of branch duct type IPMN, analyses of imaging findings included the "worrisome features" of contrast-enhancing ductal margin on CT and MRI and mural nodules in dilated duct on EUS[17-19]. In addition, FNA suggested intraductal-growing epithelial neoplasm though scant cellularity. Surgery was the best choice at that time, considering aggravated clinical symptom, radiological findings, opinion of FNA, and patient's young age. However, final pathologic result revealed interlobular and intralobular inflammation and fibrosis associated with branch duct dilatation, compatible with chronic pancreatitis. It was a totally unexpected one, even though considering patient's past medical history of severe alcoholic pancreatitis and social history of frequent alcohol consumption and heavy smoking.

There have been many reports for the differentiation mass forming chronic pancreatitis from pancreatic adenocarcinoma such as dynamic enhancement of CT and MR imaging, Perfusion CT imaging, duel energy CT in spectral imaging mode, 18F fluorodeoxyglucose positron emission tomography/CT combined with carbohydrate antigen 19-9, and quantitative endoscopic ultrasound elastography, but still it is very difficult to distinguish accurately between the two[5,10,20-24]. MRI is much better than CT for detection and characterization of focal pancreatic lesion, but it could not differentiate mass forming chronic pancreatitis from pancreatic carcinoma, even using diffusion-weighted functional MR imaging technique[5,10,25,26]. In addition, none of the above mentioned papers included a case of a solid mass containing cystic lesion like this in their research of differentiation between mass forming pancreatitis and pancreatic carcinoma.

Among the papers on relationship between main pancreatic duct (MPD) and the mass, the "duct-penetrating" sign of MPD on MR cholangiopancreatography was reported to be helpful with relatively high sensitivity and specificity, and the result was smoothly stenotic or normal MPD penetrating a mass was seen more frequently in inflammatory pancreatic mass than in pancreatic carcinoma[27]. However, in this peculiar case, inflammatory mass possessed dilated branch pancreatic duct without stenosis.

In this very unique case, it could be comprehended

uneven fibrosis and inflammation developed in localized area of uncinate process and head of pancreas, focal severe perilobular and interlobular fibrosis caused stricture and dilatation of branch pancreatic duct in uncinate process, and the these outbreaks led to very distinctive and peculiar radiological features of mass forming chronic pancreatitis and clinical symptoms of bile duct obstruction.

There has been no literature about focal fibrotic mass forming chronic pancreatitis containing branch duct dilatation, and incidentally this lesion showed almost typical imaging findings of pancreatic cystic neoplasm.

ARTICLE HIGHLIGHTS

Case characteristics

A 34-year-old man was referred to our hospital with right upper abdominal pain, and a pancreatic solid and cystic lesion found on computed tomography (CT), magnetic resonance (MR) image with MR cholangiography, and endoscopic ultrasonography (EUS).

Clinical diagnosis

Branch duct type intraductal papillary mucinous neoplasm.

Differential diagnosis

Serous cystadenoma among solid and cystic pancreatic neoplasms.

Laboratory diagnosis

Abnormal laboratory results included slightly elevated level of total bilirubin (1.3 mg/dL, normal range of 0.2-1.2) and gamma-glutamyl transferase (108 IU/L, normal range of 8-60).

Imaging diagnosis

CT and MR imaging showed a delayed contrast-enhanced solid lesion containing pruning-pattern branch duct dilatation in uncinate process and head of pancreas, with small hyperechoic mural nodules in the dilated branch ducts on EUS.

Pathological diagnosis

Microscopic findings of resected specimen revealed mass forming chronic pancreatitis including branch duct dilatation.

Treatment

The patient was treated with pylorus-preserving pancreaticoduodenectomy.

Related reports

There have been many reports for the discrimination between mass forming chronic pancreatitis and pancreatic adenocarcinoma using various imaging modalities.

Term explanation

There are no non-standard medical terms used in this manuscript.

Experiences and lessons

The author presents this case to share the very unusual but important knowledge that mass forming chronic pancreatitis might include the branch duct dilatation.

ACKNOWLEDGEMENTS

I wish to thank to Drs. Sung Ho Cho (Department of Surgery, Dankook University Hospital) and Won-Ae Lee (Department of Pathology, Dankook University Hospital) for their comments and discussions about the case.

REFERENCES

1 **Steer ML**, Waxman I, Freedman S. Chronic pancreatitis. *N Engl J Med* 1995; **332**: 1482-1490 [PMID: 7739686 DOI: 10.1056/NEJM199506013322206]
2 **Muniraj T**, Aslanian HR, Farrell J, Jamidar PA. Chronic pancreatitis, a comprehensive review and update. Part I: epidemiology, etiology, risk factors, genetics, pathophysiology, and clinical features. *Dis Mon* 2014; **60**: 530-550 [PMID: 25510320 DOI: 10.1016/j.disamonth.2014.11.002]
3 **Etemad B**, Whitcomb DC. Chronic pancreatitis: diagnosis, classification, and new genetic developments. *Gastroenterology* 2001; **120**: 682-707 [PMID: 11179244 DOI: 10.1053/gast.2001.22586]
4 **Luetmer PH**, Stephens DH, Ward EM. Chronic pancreatitis: reassessment with current CT. *Radiology* 1989; **171**: 353-357 [PMID: 2704799 DOI: 10.1148/radiology.171.2.2704799]
5 **Kim T**, Murakami T, Takamura M, Hori M, Takahashi S, Nakamori S, Sakon M, Tanji Y, Wakasa K, Nakamura H. Pancreatic mass due to chronic pancreatitis: correlation of CT and MR imaging features with pathologic findings. *AJR Am J Roentgenol* 2001; **177**: 367-371 [PMID: 11461864 DOI: 10.2214/ajr.177.2.1770367]
6 **McNulty NJ**, Francis IR, Platt JF, Cohan RH, Korobkin M, Gebremariam A. Multi--detector row helical CT of the pancreas: effect of contrast-enhanced multiphasic imaging on enhancement of the pancreas, peripancreatic vasculature, and pancreatic adenocarcinoma. *Radiology* 2001; **220**: 97-102 [PMID: 11425979 DOI: 10.1148/radiology.220.1.r01jl1897]
7 **Imamura T**, Iguchi H, Manabe T, Ohshio G, Yoshimura T, Wang ZH, Suwa H, Ishigami S, Imamura M. Quantitative analysis of collagen and collagen subtypes I, III, and V in human pancreatic cancer, tumor-associated chronic pancreatitis, and alcoholic chronic pancreatitis. *Pancreas* 1995; **11**: 357-364 [PMID: 8532652 DOI: 10.1097/00006676-199511000-00007]
8 **Longnecker DS**. Pancreas. Anderson's Pathology. 10th ed. St. Louis: Mosby-Year Book; 1996; 1891-1916.
9 **Ritchie AC.** Pancreas. Boyd's textbook of pathology, 9th ed. Philadelphia: Lea & Febiger; 1990; 1202-1234.
10 **Johnson PT**, Outwater EK. Pancreatic carcinoma versus chronic pancreatitis: dynamic MR imaging. *Radiology* 1999; **212**: 213-218 [PMID: 10405744 DOI: 10.1148/radiology.212.1.r99jl16213]
11 **Maisonneuve P**, Lowenfels AB, Müllhaupt B, Cavallini G, Lankisch PG, Andersen JR, Dimagno EP, Andrén-Sandberg A, Domellöf L, Frulloni L, Ammann RW. Cigarette smoking accelerates progression of alcoholic chronic pancreatitis. *Gut* 2005; **54**: 510-514 [PMID: 15753536 DOI: 10.1136/gut.2004.039263]
12 **Ammann RW**. The natural history of alcoholic chronic pancreatitis. *Intern Med* 2001; **40**: 368-375 [PMID: DOI: 11393404 10.2169/internalmedicine.40.368]
13 **Klöppel G**, Maillet B. The morphological basis for the evolution of acute pancreatitis into chronic pancreatitis. *Virchows Arch A Pathol Anat Histopathol* 1992; **420**: 1-4 [PMID: 1539444 DOI: 10.1007/BF01605976]
14 **Ammann RW**, Heitz PU, Klöppel G. Course of alcoholic chronic pancreatitis: a prospective clinicomorphological long-term study. *Gastroenterology* 1996; **111**: 224-231 [PMID: 8698203 DOI: 10.1053/gast.1996.v111.pm8698203]
15 **Klöppel G**. Chronic pancreatitis of alcoholic and nonalcoholic origin. *Semin Diagn Pathol* 2004; **21**: 227-236 [PMID: 16273941 DOI: 10.1053/j.semdp.2005.07.002]
16 **Yadegar J**, Williams RA, Passaro E Jr, Wilson SE. Common duct stricture from chronic pancreatitis. *Arch Surg* 1980; **115**: 582-586 [PMID: 7377960 DOI: 10.1001/archsurg.1980.01380050012004]
17 **Tanaka M**, Fernández-del Castillo C, Adsay V, Chari S, Falconi M, Jang JY, Kimura W, Levy P, Pitman MB, Schmidt CM, Shimizu M, Wolfgang CL, Yamaguchi K, Yamao K; International

Association of Pancreatology. International consensus guidelines 2012 for the management of IPMN and MCN of the pancreas. *Pancreatology* 2012; **12**: 183-197 [PMID: 22687371 DOI: 10.1016/j.pan.2012.04.004]

18 **Goh BK**, Tan DM, Ho MM, Lim TK, Chung AY, Ooi LL. Utility of the sendai consensus guidelines for branch-duct intraductal papillary mucinous neoplasms: a systematic review. *J Gastrointest Surg* 2014; **18**: 1350-1357 [PMID: 24668367 DOI: 10.1007/s11605-014-2510-8]

19 **Castellano-Megías VM**, Andrés CI, López-Alonso G, Colina-Ruizdelgado F. Pathological features and diagnosis of intraductal papillary mucinous neoplasm of the pancreas. *World J Gastrointest Oncol* 2014; **6**: 311-324 [PMID: 25232456 DOI: 10.4251/wjgo.v6.i9.311]

20 **Yin Q**, Zou X, Zai X, Wu Z, Wu Q, Jiang X, Chen H, Miao F. Pancreatic ductal adenocarcinoma and chronic mass forming pancreatitis: Differentiation with dual-energy MDCT in spectral imaging mode. *Eur J Radiol* 2015; **84**: 2470-2476 [PMID: 26481480 DOI: 10.1016/j.ejrad.2015.09.023]

21 **Yadav AK**, Sharma R, Kandasamy D, Pradhan RK, Garg PK, Bhalla AS, Gamanagatti S, Srivastava DN, Sahni P, Upadhyay AD. Perfusion CT - Can it resolve the pancreatic carcinoma versus mass forming chronic pancreatitis conundrum? *Pancreatology* 2016; **16**: 979-987 [PMID: 27568845 DOI: 10.1016/j.pan.2016.08.011]

22 **Lu N**, Feng XY, Hao SJ, Liang ZH, Jin C, Qiang JW, Guo QY. 64-slice CT perfusion imaging of pancreatic adenocarcinoma and mass forming chronic pancreatitis. *Acad Radiol* 2011; **18**: 81-88 [PMID: 20951612 DOI: 10.1016/j.acra.2010.07.012]

23 **Gu X**, Liu R. Application of 18F-FDG PET/CT combined with carbohydrate antigen 19-9 for differentiating pancreatic carcinoma from chronic mass forming pancreatitis in Chinese elderly. *Clin Interv Aging* 2016; **11**: 1365-1370 [PMID: 27729779 DOI: 10.2147/CIA.S115254]

24 **Kim SY**, Cho JH, Kim YJ, Kim EJ, Park JY, Jeon TJ, Kim YS. Diagnostic efficacy of quantitative endoscopic ultrasound elastography for differentiating pancreatic disease. *J Gastroenterol Hepatol* 2017; **32**: 1115-1122 [PMID: 27862278 DOI: 10.1111/jgh.13649]

25 **Wang Y**, Miller FH, Chen ZE, Merrick L, Mortele KJ, Hoff FL, Hammond NA, Yaghmai V, Nikolaidis P. Diffusion-weighted MR imaging of solid and cystic lesions of the pancreas. *Radiographics* 2011; **31**: E47-E64 [PMID: 21721197 DOI: 10.1148/rg.313105174]

26 **Barral M**, Taouli B, Guiu B, Koh DM, Luciani A, Manfredi R, Vilgrain V, Hoeffel C, Kanematsu M, Soyer P. Diffusion-weighted MR imaging of the pancreas: current status and recommendations. *Radiology* 2015; **274**: 45-63 [PMID: 25531479 DOI: 10.1148/radiol.14130778]

27 **Ichikawa T**, Sou H, Araki T, Arbab AS, Yoshikawa T, Ishigame K, Haradome H, Hachiya J. Duct-penetrating sign at MRCP: usefulness for differentiating inflammatory pancreatic mass from pancreatic carcinomas. *Radiology* 2001; **221**: 107-116 [PMID: 11568327 DOI: 10.1148/radiol.2211001157]

P- Reviewer: Agrawal S, Tandon RK **S- Editor**: Chen K
L- Editor: A **E- Editor**: Ma YJ

World Journal of Gastroenterology

Submit a Manuscript: http://www.f6publishing.com

World J Gastroenterol 2018 January 14; 24(2): 303-309

DOI: 10.3748/wjg.v24.i2.303

ISSN 1007-9327 (print) ISSN 2219-2840 (online)

CASE REPORT

Successful treatment of a giant ossified benign mesenteric schwannoma

Ying-Sheng Wu, Shao-Yan Xu, Jing Jin, Ke Sun, Zhen-Hua Hu, Wei-Lin Wang

Ying-Sheng Wu, Shao-Yan Xu, Jing Jin, Zhen-Hua Hu, Wei-Lin Wang, Division of Hepatobiliary and Pancreatic Surgery, Department of Surgery, First Affiliated Hospital, School of Medicine, Zhejiang University, Hangzhou 310003, Zhejiang Province, China

Ying-Sheng Wu, Shao-Yan Xu, Jing Jin, Zhen-Hua Hu, Wei-Lin Wang, Key Laboratory of Combined Multi-Organ Transplantation, Ministry of Public Health, Hangzhou 310003, Zhejiang Province, China

Ying-Sheng Wu, Shao-Yan Xu, Jing Jin, Zhen-Hua Hu, Wei-Lin Wang, Key Laboratory of Organ Transplantation, Hangzhou 310003, Zhejiang Province, China

Ying-Sheng Wu, Shao-Yan Xu, Jing Jin, Zhen-Hua Hu, Wei-Lin Wang, Key Laboratory of Precision Diagnosis and Treatment for Hepatobiliary and Pancreatic Tumor of Zhejiang Province, Hangzhou 310003, Zhejiang Province, China

Ying-Sheng Wu, Shao-Yan Xu, Jing Jin, Zhen-Hua Hu, Wei-Lin Wang, Collaborative Innovation Center for Diagnosis and Treatment of Infectious Diseases, First Affiliated Hospital, School of Medicine, Zhejiang University, Hangzhou 310003, Zhejiang Province, China

Ke Sun, Department of Pathology, First Affiliated Hospital, School of Medicine, Zhejiang University, Hangzhou 310003, Zhejiang Province, China

ORCID number: Ying-Sheng Wu (0000-0002-9406-9169); Shao-Yan Xu (0000-0001-8016-0917); Jing Jin (0000-0001-8706-4979); Ke Sun (0000-0002-3789-3143); Zhen-Hua Hu (0000-0002-8636-0757); Wei-Lin Wang (0000-0001-9432-2649).

Author contributions: Wu YS and Xu SY contributed equally to this work; Wu YS, Xu SY and Jing Jin collected case data, prepared the photos and wrote the manuscript; Sun K proofread the pathologic materials; Hu ZH and Wang WL proofread and revised the manuscript; all of the authors approved the final version to be published.

Supported by the National Natural Science Foundation of China, No. 81572307.

Informed consent statement: Informed consent was obtained from the patient.

Conflict-of-interest statement: The authors declare that there is no conflict of interest related to this report.

Manuscript source: Unsolicited manuscript

Correspondence to: Wei-Lin Wang, PhD, MD, Division of Hepatobiliary and Pancreatic Surgery, Department of Surgery, First Affiliated Hospital, School of Medicine, Zhejiang University, 79# Qingchun road, Hangzhou 310003, Zhejiang Province, China. wam@zju.edu.cn
Telephone: +86-571-87236466
Fax: +86-571-87236466

Received: August 30, 2017
Peer-review started: August 31, 2017
First decision: September 20, 2017
Revised: October 3, 2017
Accepted: October 26, 2017
Article in press: October 26, 2017
Published online: January 14, 2018

Abstract

Primary benign schwannoma of the mesentery is extremely rare. To date, only 9 cases have been reported in the English literature, while mesenteric schwannoma with ossified degeneration has not been reported thus far. In the present study, we present the first giant ossified benign mesenteric schwannoma in a 58-year-

old female. Ultrasound, computed tomography and magnetic resonance imaging were used, but it was still difficult to determine the definitive location and diagnose the mass. By laparotomy, a 10.0 cm × 9.0 cm × 9.0 cm giant mass was found in the mesentery and was then completely resected. Microscopically, the tumour located in the mesentery mainly consisted of spindle-shaped cells with a palisading arrangement. Some areas of the tumour were ossified, and a true metaplastic bone formation was observed, with the presence of bone lamellae and osteoblasts. Immunohistochemical investigation of the tumour located in the mesentery showed that the staining for the S-100 protein was strongly positive, while the stainings of SMA, CD34, CD117 and DOG-1 were negative. The cell proliferation index, measured with Ki67 staining, was less than 3%. Finally, a giant ossified benign mesenteric schwannoma was diagnosed. After surgery, the patient was followed up for a period of 43 mo, during which she remained well, with no evidence of tumour recurrence.

Key words: Schwannoma; Mesentery; Ossification; Laparotomy; S-100

Core tip: To date, only 9 cases of mesenteric schwannomas have been reported in the English literature; an ossified mesenteric schwannoma has not been reported. In the present study, we present the first giant ossified benign mesenteric schwannoma. It was challenging to determine the location and obtain a precise diagnosis of the mesenteric schwannoma prior to surgery. We completely resected the mesenteric schwannoma by laparotomy. In this paper, a literature review was conducted to deepen our understanding of mesenteric schwannomas.

Wu YS, Xu SY, Jin J, Sun K, Hu ZH, Wang WL. Successful treatment of a giant ossified benign mesenteric schwannoma. *World J Gastroenterol* 2018; 24(2): 303-309 Available from: URL: http://www.wjgnet.com/1007-9327/full/v24/i2/303.htm DOI: http://dx.doi.org/10.3748/wjg.v24.i2.303

INTRODUCTION

Schwannomas are mesenchymal neoplasms of the peripheral nerve sheath[1], which mainly develop in young to middle-aged patients with no obvious gender difference. Schwannomas are usually solitary sporadic lesions. About 3% occurred in patients with NF-2, 2% in those with schwannomatosis, and 5% in association with multiple meningiomas with or wthout NF2. Most of schwannomas, whether sporadic or inherited, display inactivating germline mutations of the tumour suppressor gene *NF2* located on chromosome 22 which encodes the protein merlin or schwannomin[2]. This protein, localized to regions of the cell membrane engaged in cell contact and mobility, is expressed in Schwann cells, meningeal cells and the lens of the eye. The mechanism by which the loss of this protein results in tumorigenesis is not well understood. Schwannomas are usually benign (> 90%) and occupy approximately 5% of benign soft-tissue neoplasms[3,4]. The tumour can sometimes show secondary degenerative changes, including cyst formation, hyalinization, haemorrhage and calcification[5]. Schwannomas usually occur in the head, neck and extremities[6], while schwannomas in the bowel mesentery are extremely rare. To our knowledge, only nine cases of schwannomas located in the bowel mesentery have been reported[7-15]. In addition, mesenteric schwannoma with ossified degeneration has not been reported thus far. In the present study, we present the first giant ossified benign mesenteric schwannoma.

CASE REPORT

On January 14, 2014, a 58-year-old woman visited our department due to a lesion detected incidentally in her abdominal cavity during a routine health examination in the local hospital. On physical examination, a lesion was palpable in her upper left abdomen, sized 12 cm × 6 cm, and she felt slight tenderness. Four years previously, she had undergone resection of a lipoma in her back. Blood test findings, including tumour markers, were unremarkable. Ultrasound (US) revealed a solid lesion in the upper left abdomen, with clear margin, and also showed some cystic and strong echo areas in the lesion. Color doppler flow imagings (CDFIs) showed blood signals in the lesion. In a native computed tomography (CT) scan, the lesion in the upper left abdomen appeared well-defined and was 9.6 cm in diameter, while regions of high density were visible, compatible with calcification and/or ossification (Figure 1A). Contrast-enhanced CT study revealed a lesion with slight and inhomogeneous enhancement (Figure 1B). On T1-weighted images, the upper left abdominal lesion appeared hypointense, while appeared inhomogeneous and hyperintense on T2-weighted images (Figure 2). According to these imaging results, the abdominal lesion was primarily considered to be a teratoma.

After sufficient pre-surgical preparation, an exploratory laparotomy was performed. We found a giant mass originating from the mesentery and surrounded by a fibrous capsule. The territory of tumour blood supply was the branch of superior mesenteric artery. We carefully separated tissues around the tumour, ligated the vessels supplying the tumour and resected the tumour completely from the mesentery. Intraoperative frozen pathology revealed an ossified mesenteric schwannoma.

Macroscopically, the mass was 10.0 cm × 9.0 cm × 9.0 cm in size and yellowish-white in colour. Microscopically, in the mesenteric tumour, both

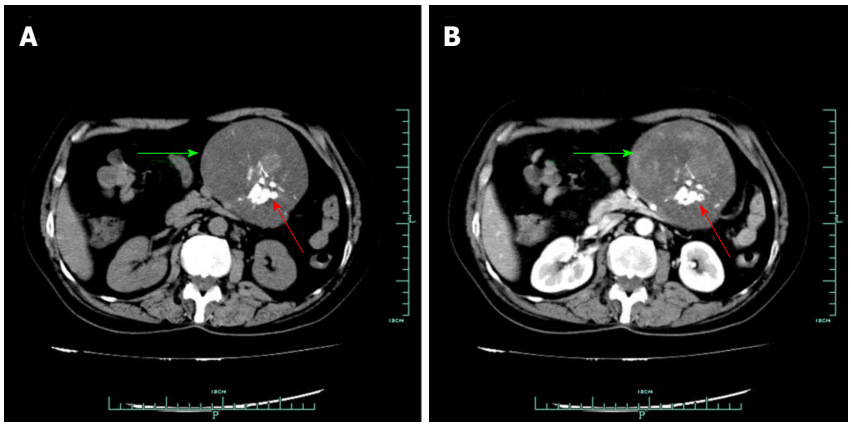

Figure 1 Computed tomography findings. A: In a native CT scan, the mass in the upper left abdomen appeared well defined (green arrow), while regions of high density were visible (red arrow); B: On the contrast-enhanced CT, the mass was inhomogeneous and slightly enhanced, and regions of high density were also visible (green arrow). CT: Computed tomography.

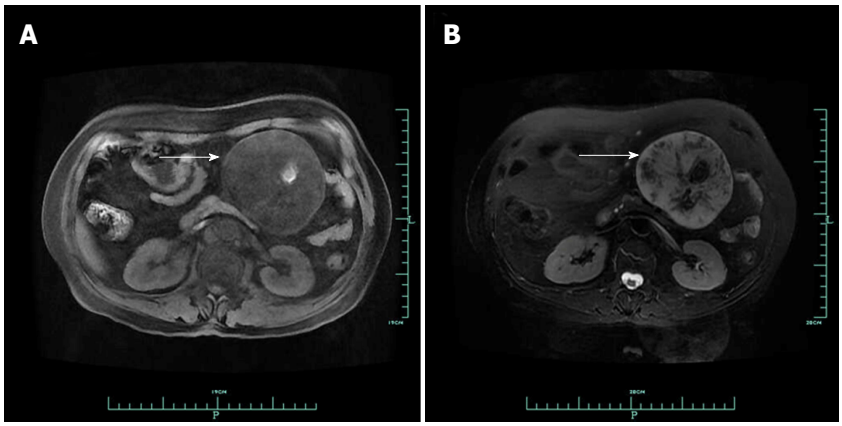

Figure 2 Magnetic resonance imaging findings. A: On MRI, the mass (white arrow) in the upper left abdominal cavity appeared hypointense on T1-weighted images; B: The mass (white arrow) appeared inhomogeneous hyperintense on T2-weighted images. MRI: Magnetic resonance imaging.

hypercellular and hypocellular areas were visible. The tumour mainly consisted of spindle-shaped cells with a palisading arrangement; atypical cells or signs of malignancy were not observed (Figure 3A). Some areas of the tumour were ossified, and a true metaplastic bone formation could be seen, with the presence of bone lamellae and osteoblasts (Figure 3B). Immunohistochemical investigation of the tumour showed a strong positivity for S-100 protein (Figure 4), while SMA, CD34, CD117 and DOG-1 were negative. The cell proliferation index, measured with Ki67 staining, was less than 3%. Finally, a giant benign ossified mesenteric schwannoma was diagnosed. After surgery, the patient recovered smoothly and left the hospital 8 d later. She was followed up for a period of 43 mo, during which she was well, with no evidence of tumour recurrence during the follow-up time.

DISCUSSION

Schwannoma is an encapsulated tumour arising from Schwann cells[16]. Malignant peripheral sheath nerve tumours (MPNSTs) are uncommon and are always associated with von Recklinghausen's disease[17]. Schwannomas mostly develop in young to middle-aged patients[18] and typically arise in the head, neck, and extremities[19]. The tumours in the ligament[20], mesentery[10] and intra-abdominal organs[21-23] are extremely rare. Secondary degenerative changes, including cyst formation, calcification, haemorrhage, and hyalinization, can sometimes be shown. However, mesenteric schwannoma with ossified degeneration has not been reported thus far, and to our knowledge, only nine cases of schwannomas in the bowel mesentery have been reported[7-15]. In the present study, we present a giant ossified benign mesenteric schwannoma. Brief clinical characteristics of ten cases of mesenteric schwannoma in the English-language literature, including our case, are outlined in Table 1 and the summarized clinical characteristics are present in Table 2. The mean age of these patients was 52.89 ± 12.89 years (range 38-80 years), and the male-female ratio was 4:5. Most patients were asymptomatic (70.00%). The mean tumour size was

Table 1 Clinical characteristics of the 10 patients with mesenteric schwannomas

Ref.	Year	Sex/Age	Symptom	Imaging method	Size(cm)	Preoperative diagnosis	Treatment	Histology	Follow-up (mo)	Status
Present case	2017	F/58	Asymptomatic	US, CT, MRI	10 × 9 × 9	Teratoma	Surgery	Benign	43	Survived
Medina-Gallardo *et al*[7]	2017	F/80	Asymptomatic	CT	NA	NA	Laparoscopic operation	Benign	NA	NA
Tepox Padrón *et al*[8]	2017	F/38	Asymptomatic	MRI	11.3 × 8.4 × 4.1	NA	Surgery	Benign	24	Survived
Wang *et al*[8]	2014	M/54	Abdominal pain and hematochezia	CT, Colonoscopy	NA	NA	Ascending, transverse and splenic flexure colectomy	Benign	12	Survived
Tang *et al*[8]	2014	F/43	Mild abdominal pain	CT	4.0 × 4.0 × 1.9	GIST or leiomyoma	Laparoscopic operation	Benign	10	Survived
Lao *et al*[8]	2011	M/45	Asymptomatic	CT, MRI and Angiography	2.2 × 1.7	NA	Surgical excision	Benign	NA	NA
Kilicoglu *et al*[8]	2006	M/56	Nausea, vomiting, abdominal pain, and constipation	US	22 × 19 × 4	Intra-abdominal mass	Surgery	Benign	11	Survived
Minami *et al*[8]	2005	F/54	Asymptomatic	CT, MRI	8.0 × 7.0 × 4.8	Benign solid tumour	Enucleation	Benign	5	Survived
Ramboer *et al*[8]	1998	NA	Asymptomatic	MRI	NA	NA	NA	Benign	NA	NA
Murakami *et al*[8]	1998	M/48	Asymptomatic	United States, CT, MRI	4.5 × 4.0 × 4.0	Benign solid tumour	Laparotomy	Benign	24	Survived

M: Male; F: Female; NA: Not available; US: Ultrasound; CT: Computed tomography; MRI: Magnetic resonance imaging; GIST: Gastrointestinal stromal tumour.

8.86 ± 6.68 cm (range 2-22 cm). All of the tumours were benign.

Obtaining an accurate preoperative diagnosis of a mesenteric schwannoma prior to surgery is nearly impossible. The final diagnosis is based on the histo-pathological examinations of resected specimen[8]. Microscopically, these tumours present two morphologic features: Antoni type A areas and Antoni type B areas[24]. Antoni type A areas consist of closely packed spindle cells, with occasional nuclear palisading. Antoni type B areas are hypocellular and contain more mixoid tissue with high water content[18,25], which can be cystic, haemorrhagic, calcified and even ossified[5,24]. In the present study, some areas of the tumour were ossified, and a true metaplastic bone formation could be seen, with the presence of bone lamellae and osteoblasts, just as reported by Gurzu *et al*[26]. Schwannomas show strong immunoreactivity for S-100 protein, while CD34, CD117, DOG-1 and SMA are negative[27]. In all these cases, immunohistochemical staining is crucial to confirm the differentiation of the tumour cells. In the present study, the tumour located in the mesentery showed a strong positivity for S-100 protein, while SMA, CD34, CD117 and DOG-1 were negative. The cell proliferation index, measured with Ki67 staining, was less than 3%. Ki67 staining is potentially useful in distinguishing benign peripheral nerve sheath tumours from malignant peripheral nerve sheath tumours, particularly in differentiating problematic cases of cellular schwannoma and malignant peripheral nerve sheath tumours. Ki-67 labelling indices $\geqslant$ 20% are highly predictive of malignant peripheral nerve sheath tumours[28]. The main differential diagnosis for schwannomas is gastrointestinal stromal tumours (GISTs). GISTs are composed of spindled mesenchymal cells, which show a diffuse growth pattern and, frequently, positivity for CD34, CD117 and DOG-1[29]. Negative immunohistochemical staining for CD34, CD117 and DOG-1 can exclude the possibility of GIST.

Multiple imaging modalities, including US, CT, MRI, are helpful for establishing a probable diagnosis; however, an accurate preoperative diagnosis of the schwannoma is still difficult to obtain[9]. On US, schwannomas are usually well-defined hypodense lesions[12]. Plain CT scan shows a well-defined hypodense mass. Cystic, haemorrhagic, calcified and even ossified degeneration sometimes can be seen. On dynamic CT, Antoni A areas of schwannomas are typically well enhanced. Because of the loose stroma and low cellularity, schwannomas with Antoni B areas generally show low density and can be cystic[9,11]. On T1-weighted images, schwanommas appeared hypointense, while appeared inhomogeneous and hyperintense on T2-weighted images[14,30]. Celiac angiography is important to determine the arteries supplying the tumour[11]. Fine-needle aspiration cytology, accompanied by immunohistochemical staining, may play an important role in defining the appropriate treatment procedure and prognosis[31].

Surgery is curative for mesenteric schwannomas. In the present case, by laparotomy, a giant mass was found that had originated from the mesentery and was surrounded by a fibrous capsule. The patient was followed up for a period of 43 mo, during which she remained well, with no evidence of tumour recurrence.

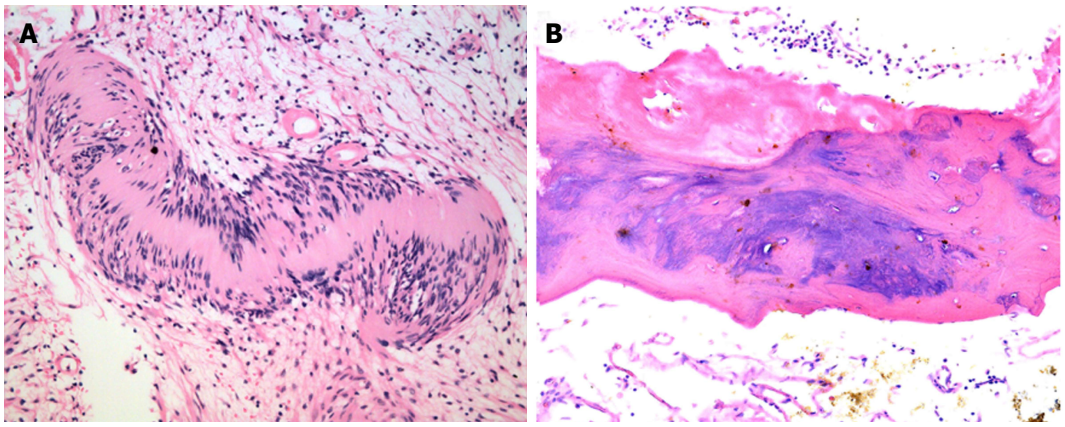

Figure 3 Microscopic examination. A: Microscopically, in the mesenteric tumour, both hypercellular and hypocellular areas were visible. The tumour mainly consisted of spindle-shaped cells with a palisading arrangement; atypical cells or signs of malignancy were not observed (HE × 40); B: Some areas of the tumour were ossified, and a true metaplastic bone formation could be seen, with the presence of bone lamellae and osteoblasts (HE × 200). HE: Hematoxylin and eosin.

Table 2 Summary of clinical data from all 10 cases of mesenteric schwannomas

	n (%) or mean ± SD (range)
Age (yr) (*n* = 8)	
Mean	52.89 ± 12.14 (38-80)
Sex (male/female), (male %) (*n* = 9)	4/5 (44.44%)
Symptoms (*n* = 10)	
Asymptomatic	7 (70.00)
Symptomatic	
Abdominal pain	3 (30.00)
Hematochezia	1 (10.00)
Nausea	1 (10.00)
Vomiting	1 (10.00)
Constipation	1 (10.00)
Mean size (cm) (*n* = 7)	8.86 ± 6.68 (2-22)
Operation (*n* = 9)	
Laparotomy	6 (66.67)
Laparoscopic operation	2 (22.22)
Enucleation	1 (11.11)
Histology (*n* = 10)	
Benign	10 (100.00)
Malignant	0 (0.00)
Follow-up (mo) (*n* = 8)	18.43 ± 12.00 (5-43)
Survived	7 (100.00)

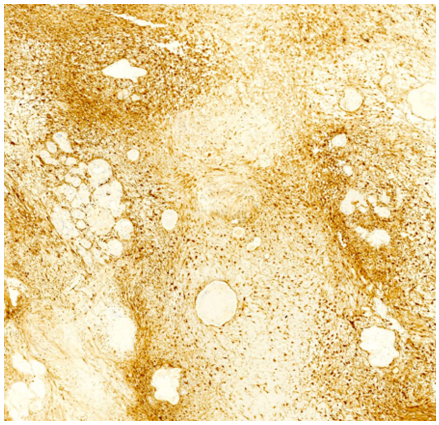

Figure 4 Immunohistochemical staining. The mesenteric tumour was strongly positive for S-100 (× 40).

In conclusion, a schwannoma located in the mesentery is extremely rare. To our knowledge, our study presents the tenth reported mesenteric schwannoma. In addition, a mesenteric schwannoma with ossified degeneration has not been reported thus far. In the present study, we present the first giant benign mesenteric schwannoma with ossified degeneration. It was difficult to acquire an accurate diagnosis of the mesenteric schwannoma preoperatively, because of the lack of specific symptoms, radiological characteristics and tumour markers.

ARTICLE HIGHLIGHTS

Case characteristics

A 58-year-old woman visited our department due to a lesion detected incidentally in her abdominal cavity during a routine health examination in the local hospital.

Clinical diagnosis

A lesion, palpable in the her upper left abdomen, was sized 12 cm × 6 cm, and she felt slight tenderness.

Differential diagnosis

Gastrointestinal stromal tumour, intra-abdominal teratoma, sarcoma and neurogenic tumour.

Laboratory diagnosis

Blood test findings, including tumour markers, were unremarkable.

Imaging diagnosis

Ultrasound revealed a solid lesion in the upper left abdomen, with clear margin, and also showed some cystic and strong echo areas in the lesion. Color doppler flow imagings (CDFIs) showed blood signals in the lesion. In a native computed tomography (CT) scan, the lesion in the upper left abdomen appeared well-defined and was 9.6 cm in diameter, while regions of high density were visible, compatible with calcification and/or ossification. Contrast-enhanced CT study revealed a lesion with slight and inhomogeneous enhancement. On T1-weighted images, the upper left abdominal lesion appeared hypointense, while appeared inhomogeneous and hyperintense on T2-weighted images (Figure 2). According to these imaging results, the abdominal lesion was primarily considered to be a teratoma.

Pathological diagnosis

Macroscopically, the mass was 10.0 cm × 9.0 cm × 9.0 cm in size and yellowish-

white in colour. Microscopically, in the mesenteric tumour, both hypercellular and hypocellular areas were visible. The tumour mainly consisted of spindle-shaped cells with a palisading arrangement; atypical cells or signs of malignancy were not observed. Some areas of the tumour were ossified, and a true metaplastic bone formation could be seen, with the presence of bone lamellae and osteoblasts. Immunohistochemical investigation of the tumour showed a strong positivity for S-100 protein , while SMA, CD34, CD117 and DOG-1 were negative. The cell proliferation index, measured with Ki67 staining, was less than 3%. Finally, a giant benign ossified mesenteric schwannoma was diagnosed.

Treatment

The authors completely resected the mass located in the mesentery by laparotomy.

Related reports

Schwannomas in the bowel mesentery are extremely rare. To our knowledge, only 9 cases of schwannomas located in the bowel mesentery have been reported. In addition, mesenteric schwannoma with ossified degeneration has not been reported thus far.

Experiences and lessons

In the present study, the authors present the first giant ossified benign mesenteric schwannoma. It was difficult to obtain an accurate diagnosis of the mesenteric schwannoma preoperatively, because of the lack of specific symptoms, radiological characteristics and tumour markers.

REFERENCES

1 **Le Guellec S**. [Nerve sheath tumours]. *Ann Pathol* 2015; **35**: 54-70 [PMID: 25541115 DOI: 10.1016/j.annpat.2014.11.008]
2 **J D**, R S, K C, Devi NR. Pancreatic schwannoma - a rare case report. *J Clin Diagn Res* 2014; **8**: FD15-FD16 [PMID: 25177575 DOI: 10.7860/JCDR/2014/8465.4642]
3 **Ariel IM**. Tumors of the peripheral nervous system. *CA Cancer J Clin* 1983; **33**: 282-299 [PMID: 6413007 DOI: 10.3322/canjclin.33.5.282]
4 **Pilavaki M**, Chourmouzi D, Kiziridou A, Skordalaki A, Zarampoukas T, Drevelengas A. Imaging of peripheral nerve sheath tumors with pathologic correlation: pictorial review. *Eur J Radiol* 2004; **52**: 229-239 [PMID: 15544900 DOI: 10.1016/j.ejrad.2003.12.001]
5 **Xu SY**, Sun K, Xie HY, Zhou L, Zheng SS, Wang WL. Hemorrhagic, calcified, and ossified benign retroperitoneal schwannoma: First case report. *Medicine (Baltimore)* 2016; **95**: e4318 [PMID: 27472709 DOI: 10.1097/MD.0000000000004318]
6 **Das Gupta TK**, Brasfield RD. Tumors of peripheral nerve origin: benign and malignant solitary schwannomas. *CA Cancer J Clin* 1970; **20**: 228-233 [PMID: 4316984 DOI: 10.3322/canjclin.20.4.228]
7 **Medina-Gallardo A**, Curbelo-Peña Y, Molinero-Polo J, Saladich-Cubero M, De Castro-Gutierrez X, Vallverdú-Cartie H. Mesenteric intranodal schwannoma: uncommon case of neurogenic benign tumor. *J Surg Case Rep* 2017; **2017**: rjx008 [PMID: 28458819 DOI: 10.1093/jscr/rjx008]
8 **Tepox Padrón A**, Ramírez Márquez MR, Cordóva Ramón JC, Cosme-Labarthe J, Carrillo Pérez DL. Mesenteric schwannoma: an unusual cause of abdominal mass. *Rev Esp Enferm Dig* 2017; **109**: 76-78 [PMID: 28081612 DOI: 10.17235/reed.2016.4202/2016]
9 **Wang QM**, Jiang D, Zeng HZ, Mou Y, Yi H, Liu W, Zeng QS, Wu CC, Tang CW, Hu B. A case of recurrent intestinal ganglioneuromatous polyposis accompanied with mesenteric schwannoma. *Dig Dis Sci* 2014; **59**: 3126-3128 [PMID: 24927799 DOI: 10.1007/s10620-014-3232-1]
10 **Tang SX**, Sun YH, Zhou XR, Wang J. Bowel mesentery (meso-appendix) microcystic/reticular schwannoma: case report and literature review. *World J Gastroenterol* 2014; **20**: 1371-1376 [PMID: 24574814 DOI: 10.3748/wjg.v20.i5.1371]
11 **Lao WT**, Yang SH, Chen CL, Chan WP. Mesentery neurilemmoma: CT, MRI and angiographic findings. *Intern Med* 2011; **50**: 2579-2581 [PMID: 22041360 DOI: 10.2169/internalmedicine.50.6198]
12 **Kilicoglu B**, Kismet K, Gollu A, Sabuncuoglu MZ, Akkus MA, Serin-Kilicoglu S, Ustun H. Case report: mesenteric schwannoma. *Adv Ther* 2006; **23**: 696-700 [PMID: 17142203 DOI: 10.1007/BF02850308]
13 **Minami S**, Okada K, Matsuo M, Hayashi T, Kanematsu T. Benign mesenteric schwannoma. *J Gastrointest Surg* 2005; **9**: 1006-1008 [PMID: 16137598 DOI: 10.1016/j.gassur.2005.04.018]
14 **Ramboer K**, Moons P, De Breuck Y, Van Hoe L, Baert AL. Benign mesenteric schwannoma: MRI findings. *J Belge Radiol* 1998; **81**: 3-4 [PMID: 9563265]
15 **Murakami R**, Tajima H, Kobayashi Y, Sugizaki K, Ogura J, Yamamoto K, Kumazaki T, Egami K, Maeda S. Mesenteric schwannoma. *Eur Radiol* 1998; **8**: 277-279 [PMID: 9477282 DOI: 10.1007/s003300050379]
16 **Das Gupta TK**, Brasfield RD, Strong EW, Hajdu SI. Benign solitary Schwannomas (neurilemomas). *Cancer* 1969; **24**: 355-366 [PMID: 5796779 DOI: 10.1002/1097-0142(196908)24:2<355::AID-CNCR2820240218>3.0.CO;2-2]
17 **Móller Pedersen V**, Hede A, Graem N. A solitary malignant schwannoma mimicking a pancreatic pseudocyst. A case report. *Acta Chir Scand* 1982; **148**: 697-698 [PMID: 7170905]
18 **Xu SY**, Wu YS, Li JH, Sun K, Hu ZH, Zheng SS, Wang WL. Successful treatment of a pancreatic schwannoma by spleen-preserving distal pancreatectomy. *World J Gastroenterol* 2017; **23**: 3744-3751 [PMID: 28611527 DOI: 10.3748/wjg.v24.i20.3744]
19 **Abell MR**, Hart WR, Olson JR. Tumors of the peripheral nervous system. *Hum Pathol* 1970; **1**: 503-551 [PMID: 4330996]
20 **Bayraktutan U**, Kantarci M, Ozgokce M, Aydinli B, Atamanalp SS, Sipal S. Education and Imaging. Gastrointestinal: benign cystic schwannoma localized in the gastroduodenal ligament; a rare case. *J Gastroenterol Hepatol* 2012; **27**: 985 [PMID: 22515807 DOI: 10.1111/j.1440-1746.2012.06960.x]
21 **Liu LN**, Xu HX, Zheng SG, Sun LP, Guo LH, Wu J. Solitary schwannoma of the gallbladder: a case report and literature review. *World J Gastroenterol* 2014; **20**: 6685-6690 [PMID: 24914396 DOI: 10.3748/wjg.v20.i21.6685]
22 **Nishikawa T**, Shimura K, Tsuyuguchi T, Kiyono S, Yokosuka O. Contrast-enhanced harmonic EUS of pancreatic schwannoma. *Gastrointest Endosc* 2016; **83**: 463-464 [PMID: 26341855 DOI: 10.1016/j.gie.2015.08.041]
23 **Xu SY**, Guo H, Shen Y, Sun K, Xie HY, Zhou L, Zheng SS, Wang WL. Multiple schwannomas synchronously occurring in the porta hepatis, liver, and gallbladder: first case report. *Medicine (Baltimore)* 2016; **95**: e4378 [PMID: 27537565 DOI: 10.1097/MD.0000000000004378]
24 **Tao L**, Xu S, Ren Z, Lu Y, Kong X, Weng X, Xie Z, Hu Z. Laparoscopic resection of benign schwannoma in the hepatoduodenal ligament: A case report and review of the literature. *Oncol Lett* 2016; **11**: 3349-3353 [PMID: 27123115 DOI: 10.3892/ol.2016.4410]
25 **Xu SY**, Sun K, Xie HY, Zhou L, Zheng SS, Wang WL. Schwannoma in the hepatoduodenal ligament: A case report and literature review. *World J Gastroenterol* 2016; **22**: 10260-10266 [PMID: 28028376 DOI: 10.3748/wjg.v22.i46.10260]
26 **Gurzu S**, Bara T, Bara T Jr, Jung I. Metaplastic bone formation in the abdominal wall--an incidental finding in a patient with gastric cancer. Case report and hypothesis about its histogenesis. *Am J Dermatopathol* 2013; **35**: 844-846 [PMID: 24257191 DOI: 10.1097/DAD.0b013e318285db5c]
27 **Weiss SW**, Langloss JM, Enzinger FM. Value of S-100 protein in the diagnosis of soft tissue tumors with particular reference to benign and malignant Schwann cell tumors. *Lab Invest* 1983; **49**: 299-308 [PMID: 6310227]
28 **Pekmezci M**, Reuss DE, Hirbe AC, Dahiya S, Gutmann DH, von Deimling A, Horvai AE, Perry A. Morphologic and immunohistochemical features of malignant peripheral nerve sheath tumors and cellular schwannomas. *Mod Pathol* 2015; **28**: 187-200 [PMID: 25189642 DOI: 10.1038/modpathol.2014.109]
29 **Kovecsi A**, Jung I, Bara T, Bara T Jr, Azamfirei L, Kovacs Z, Gurzu S. First Case Report of a Sporadic Adrenocortical Carcinoma With Gastric Metastasis and a Synchronous Gastrointestinal Stromal

Tumor of the Stomach. *Medicine* (Baltimore) 2015; **94**: e1549 [PMID: 26376405 DOI: 10.1097/MD.0000000000001549]
30 **Xu SY**, Sun K, Owusu-Ansah KG, Xie HY, Zhou L, Zheng SS, Wang WL. Central pancreatectomy for pancreatic schwannoma: A case report and literature review. *World J Gastroenterol* 2016; **22**: 8439-8446 [PMID: 27729750 DOI: 10.3748/wjg.v22.i37.8439]
31 **Domanski HA**, Akerman M, Engellau J, Gustafson P, Mertens F, Rydholm A. Fine-needle aspiration of neurilemoma (schwannoma). A clinicocytopathologic study of 116 patients. *Diagn Cytopathol* 2006; **34**: 403-412 [PMID: 16680779 DOI: 10.1002/dc.20449]

P- Reviewer: Lee CL, Lee WJ, Maruyama H, Serio G
S- Editor: Gong ZM **L- Editor**: A **E- Editor**: Ma YJ

World Journal of Gastroenterology

Submit a Manuscript: http://www.f6publishing.com

World J Gastroenterol 2018 January 14; 24(2): 310-314

DOI: 10.3748/wjg.v24.i2.310

ISSN 1007-9327 (print) ISSN 2219-2840 (online)

LETTERS TO THE EDITOR

Candida accommodates non-culturable *Helicobacter pylori* in its vacuole - Koch's postulates aren't applicable

Farideh Siavoshi, Parastoo Saniee

Farideh Siavoshi, Department of Microbiology, School of Biology, University College of Sciences, University of Tehran, Tehran 14176-14411, Iran

Parastoo Saniee, Department of Microbiology and Microbial Biotechnology, Faculty of Life Sciences and Biotechnology, Shahid Beheshti University G.C., Tehran 19839-4716, Iran

ORCID number: Farideh Siavoshi (0000-0002-6659-1160); Parastoo Saniee (0000-0003-1729-8256)

Author contributions: Siavoshi F and Saniee P contributed equally to the literature review and writing of this letter.

Conflict-of-interest statement: The authors declare that there is no conflict of interest.

Manuscript source: Unsolicited manuscript

Correspondence to: Farideh Siavoshi, PhD, Associate Professor, Lecturer, Department of Microbiology, School of Biology, University College of Sciences, University of Tehran, Enghelab Avenue, Tehran 14176-14411, Iran. siavoshi@khayam.ut.ac.ir
Telephone: + 98-21-61112460
Fax: +98-21-66492992

Received: November 10, 2017
Peer-review started: November 11, 2017
First decision: November 30, 2017
Revised: December 8, 2017
Accepted: December 13, 2017
Article in press: December 13, 2017
Published online: January 14, 2018

Abstract

The following are the responses to the "letter to the editor" ("*Helicobacter* is preserved in yeast vacuoles! Does Koch's postulates confirm it?") authored by Nader Alipour and Nasrin Gaeini that rejected the methods, results, discussions and conclusions summarized in the review article authored by Siavoshi F and Saniee P. In the article, 7 papers, published between 1998 and 2013, were reviewed. The 7 papers had been reviewed and judged very carefully by the assigned expertise of the journals involved, including the reviewers of the *World Journal of Gastroenterology* (*WJG*), before publication. In the review article, 121 references were used to verify the methods, results and discussions of these 7 papers. The review article was edited by the trustworthy British editor of the (*WJG*), and the final version was rechecked and finally accepted by the reviewers of (*WJG*). None of the reviewers made comments like those in this "letter to the editor", especially the humorous comments, which seem unprofessional and nonscientific. Above all, the authors' comments show a lack of understanding of basic and advanced microbiology, e.g. bacterial endosymbiosis in eukaryotic cells. Accordingly, their comments all through the letter contain misconceptions. The comments are mostly based on personal conclusions, without any scientific support. It would have been beneficial if the letter had been reviewed by the reviewers of the article by Siavoshi and Saniee.

Key words: *Helicobacter pylori*; Intracellular occurrence; *Candida* yeast; 16S rDNA detection

Core tip: The authors of the "letter to the editor" "*Helicobacter* is preserved in yeast vacuoles! Does Koch's postulates confirm it?" argue that amoeba fits better than *Candida* yeast in our review. They like to

see intracellular *Helicobacter pylori* only inside amoeba, not in yeast. The questions raised are: which one can carry *H. pylori* to the human gastrointestinal tract, vagina and skin, while remaining alive and able to colonize - amoeba or yeast? Which one is recognized as a member of the microbiota of these locations - amoeba or yeast? Accordingly, the authors present their personal conclusions, without supporting references and experimental data.

Siavoshi F, Saniee P. *Candida* accommodates non-culturable *Helicobacter pylori* in its vacuole - Koch's postulates aren't applicable. *World J Gastroenterol* 2018; 24(2): 310-314 Available from: URL: http://www.wjgnet.com/1007-9327/full/v24/i2/310.htm DOI: http://dx.doi.org/10.3748/wjg.v24.i2.310

TO THE EDITOR

Response to all the comments in the "letter to the editor"[1]

Paragraph 1: Line 2: the title of the review article is written incorrectly: "Vacuoles of *Candida* yeast behave as a specialized niche for *Helicobacter pylori*" is wrong. Lines 4-10: the whole impression is incorrect. The review paper described detection of *H. pylori* inside the vacuole of *Candida* yeast, but not penetration[2]. This was demonstrated by microscopic observations of bacterium-like bodies (BLBs) inside the yeast vacuole and detection of *H. pylori*-specific genes in the whole DNA extracted from the yeast. It was proposed that the non-culturable intracellular *H. pylori*, like other non-culturable intracellular bacteria, *e.g.*, those in arbuscular mycorrhizal fungi[3], could multiply inside the vacuole of yeast cells and be transmitted to the next generation[2]. Lines 11-15: the article was a review article and therefore did not contain methods. It is not clear what methodologies the authors of the letter did not agree with. It would be better to write the same letter of criticism to those journals that published the original papers. The presence of several BLBs inside the yeast vacuole was not accepted by the authors. We have never emphasized the number of bacteria in the vacuoles. Counting the number of BLBs is not always possible and was not the aim of our studies. The letter authors presented their personal conclusions, which were not supported by published references.

Paragraph 2: One of the best-known genera of yeasts is *Candida*. Furthermore, *Candida* yeast, *Candida* species and *Candida albicans* have been used throughout the review article and the original papers. *Candida* species, especially the *C. albicans* that we studied, were isolates from the oral cavity, stomach, vagina and foods, as mentioned in all the original papers[4-10]. There are no simple biochemical tests for the identification of yeasts, like those for bacteria. Macroscopic and microscopic characteristics, growth on CHROMagar, PCR and PCR-RFLP (polymerase chain reaction-restriction fragment length polymorphism) are the methods currently used. We used colony characteristics, microscopic morphology, formation of blastoconidia and growth on CHROMagar[11] for identification of *Candida* species, as mentioned in our original papers. According to reports, *Candida* species are the inhabitants of human skin and mucosal surfaces[12-14], as also mentioned in our papers. Accordingly, we knew we were studying *Candida* yeasts, *i.e.*, yeasts belonging to the genus *Candida*. *Candida* yeast is mentioned in the title of the review article, and *C. albicans* and *Candida* species are mentioned throughout the published works.

Paragraph 3: Our studies had nothing to do with Koch's postulates. The aim of our studies was to show that the yeast cell can serve as a specialized niche and environmental reservoir for *H. pylori*. We have used standard and routine methods, as mentioned in our published papers, which have been checked and accepted by the experienced reviewers of the original papers and the review article. The authors of the letter have answered their own question about Koch's postulates (if they were applicable): because *H. pylori* was not culturable, Koch's postulates were not applicable. The authors are asked to present references that have applied Koch's postulates for *H. pylori* or any other bacteria and amoeba. The authors have presented their personal conclusions, without any support from published references.

Paragraph 4: All the immunologic methods for production of IgY-Hp and purification of antibodies were performed according to standard protocols, mentioned with the relevant reference in the original paper[15]. IgY-Hp perfectly and specifically interacted with *H. pylori* antigens, as described in the reference papers we used[16-18]. Even detection of *Campylobacter* proteins/antigens in the yeast protein pool would be another valuable finding. Both Western blot and immunofluorescent microscopy showed the immunospecificity of the IgY-Hp[8,9]. The authors have presented their personal conclusions, without supporting references, such as those describing immunologic detection of microbial antigens by human serum as a routine, commercialized, feasible and affordable method.

Paragraph 5: The discussion of bacterial tropism to yeast extract (which is a powder added to culture media) is totally unclear and has nothing to do with our work. The authors neglected to consider that "yeast extract", even yeast, if added to culture media, still goes through sterilization in the autoclave that kills all the microorganisms, including bacteria and yeast. Their

references numbered 2[19] and 3[20] cited in the letter are irrelevant. Reference number 2[19] is about adhesion of *H. pylori* to yeast cells, and not yeast extract (the powder). Reference number 3[20] is related to co-culture of *H. pylori* with free-living *Acanthamoeba castellanii*, which maintained the viability of *H. pylori* for up to 8 wk, again irrelevant. Their references numbered 4[5] and 5[21] in the letter do not correlate with the sentences given. The examination of body fluids to look for *H. pylori* is not clear and again irrelevant to yeast extract, yeast or *H. pylori*. Again, these are personal conclusions, without any scientific support.

Paragraph 6: Several papers on the intracellular occurrence of bacteria inside fungi, such as arbuscular mycorrhizal fungi, have been published. We used the details of these studies[22-25] as the main references in our original papers. The fungal cell wall as a barrier to bacterial entry to the fungal cell has been discussed in detail by Gehrig *et al*[26]. However, in our studies we did not discuss the entry of *H. pylori* into the yeast cell. We only reported the intracellular occurrence of *H. pylori* inside the yeast; bacterial entry was not the subject of our studies. The David Copperfield story mentioned by the authors is an exciting fantasy and a reminder of childhood. However, it is adulthood, knowledge, experience and hard work that give one the courage to discover the unknown fantasies in the microbial world, like the discovery that bacteria once entered primitive eukaryotic cells through phagotrophy, and ended up being digested, slaves or endosymbionts[27-29], as discussed in our original and review papers. Apparently, the authors like to see intracellular *H. pylori* only inside amoebae, but not in yeasts. The questions raised are: which one can carry *H. pylori* to the human gastrointestinal tract, vagina and skin, while remaining alive and even being able to colonize - amoeba or *Candida* yeast? Which one is recognized as a member of the microbiota of the human gastrointestinal tract, vagina and skin - amoeba or *Candida* yeast? Furthermore, the authors compared the size of amoeba and yeast and recognized amoeba as more suitable for the accommodation of several bacteria, without any supporting references.

Paragraph 7: The authors have answered their own question. Intracellular bacteria become intracellular to avoid stresses, such as the host immune response and antibiotics[30]. *H. pylori,* whether inside yeast, amoeba or epithelial cells, becomes more resistant to antibiotics. It is not known whether internalized antibiotics that reach the vacuole of eukaryotic cells, yeast or amoeba, remain intact and effective. Comparing the effects of antibiotics on *H. pylori* cells inside yeast with those in amoeba was not the concern of our studies. These are the authors' personal conclusions, with no supporting references. The location of *H. pylori* on the yeast cell is not clear. Our concern was the intracellular existence of *H. pylori* inside the yeast.

Paragraph 8: The authors' comments are not clear. The relationship between yeast-positive individuals and a higher frequency of *H. pylori* infection was not discussed in our papers. We studied the intracellular occurrence of *H. pylori* inside the vaginal yeast of expectant mothers, and proposed that transmission of vaginal yeast to newborns might increase the likelihood of oral and gastric colonization by yeasts acting as a reservoir of *H. pylori*[7]. We did not study the frequency of vaginal yeasts in normal and healthy women, which has been accurately reported by the expertise of the field[31]. The subjects of their references 5, 6 and 7[21,32,33] were not the concern of our studies, because these papers reported the frequency of yeast in special patients and not in those with *H. pylori* infection.

Paragraph 9: The contents of paragraph 9 are unclear and confusing, not being correlated with even the titles of their references 8-19 used in the "letter to the editor". In this paragraph, the authors hypothesized the transmission of *H. pylori* through water consumption and related to amoebae, which has not been documented yet. The personal conclusion of the authors was again to replace yeast with amoeba in the review paper of Siavoshi and Saniee, which was not their own research project. The reason for using at least 6 similar papers out of a total of 20 references to describe the occurrence of amoeba in water is not clear. It was again the personal conclusions of the authors, who insisted on proposing amoeba and not yeast as the reservoir of *H. pylori*, without any supporting references or personal experimental data. Their reference number 18 is a paper with plagiarized content by the letter authors that has been retracted from the journal *Helicobacter* through the appropriate authorities, which has been fully acknowledged by Nader Alipour himself.

Paragraph 10: The comment about anti-*H. pylori* therapy, including antifungal drug usage, is confusing. Extensive clinical trials might reveal whether antifungal therapy is effective against *H. pylori* or not. Their reference number 20[34] is not relevant to the subject of the review. Their reference 17[35] reports *Candida*-associated ulcer in only one patient without implication of *H. pylori* infection, so statistical analysis was not applicable. Personal conclusions have been presented, without being confirmed by supporting references.

Paragraph 11: All the arguments of the authors that have rejected the idea of yeast as the reservoir of *H. pylori* are based on their personal conclusions, without presentation of any supportive references. Copying the whole text of the review paper and only replacing the name yeast with amoeba, and also the authors' names (Siavoshi F and Saniee P) with their own names, shows that they agree with the methods that they

have rejected all through the "letter to the editor".

Paragraphs 12 and 13 (conclusions): We tried to respond to all the comments in the "letter to the editor", paragraph by paragraph. When we reached the last two paragraphs, we realized that all the arguments of the authors were based upon a paper containing plagiarized content that they had authored, and they were trying to justify their misconduct by persistently arguing that yeast must be replaced with amoeba in a research article written by other people (Siavoshi F and Saniee P). In their paper based on plagiarism, they only replaced yeast with amoeba, and changed the authors' names from Siavoshi F and Saniee P to Alipour N, Gaeini N, Taner A, Yildiz F, Masseret S and Malfertheiner P. The authors other than Alipour were not aware of the plagiarism. All other sentences in the text, photographs and references had been left unchanged. The journal *Helicobacter* retracted the article with the plagiarism through the appropriate authorities, which has been fully acknowledged by Nader Alipour himself.

REFERENCES

1 **Alipour N**, Gaeini N. Helicobacter is preserved in yeast vacuoles! Does Koch's postulates confirm it? *World J Gastroenterol* 2017; **23**: 2266-2268 [PMID: 28405156 DOI: 10.3748/wjg.v23.i12.2266]
2 **Siavoshi F**, Saniee P. Vacuoles of Candida yeast as a specialized niche for Helicobacter pylori. *World J Gastroenterol* 2014; **20**: 5263-5273 [PMID: 24833856 DOI: 10.3748/wjg.v20.i18.5263]
3 **Bianciotto V**, Genre A, Jargeat P, Lumini E, Bécard G, Bonfante P. Vertical transmission of endobacteria in the arbuscular mycorrhizal fungus Gigaspora margarita through generation of vegetative spores. *Appl Environ Microbiol* 2004; **70**: 3600-3608 [PMID: 15184163 DOI: 10.1128/AEM.70.6.3600-3608.2004]
4 **Siavoshi** F, Nourali-Ahari F, Zeinali S, Hashemi-Dogaheh M, Malekzadeh R, Massarrat S. Yeasts protects Helicobacter pylori against the enviromental stress. *Arc Iran Med* 1998; **1**: 2-8
5 **Siavoshi F**, Salmanian AH, Akbari F, Malekzadeh R, Massarrat S. Detection of Helicobacter pylori-specific genes in the oral yeast. *Helicobacter* 2005; **10**: 318-322 [PMID: 16104948 DOI: 10.1111/j.1523-5378.2005.00319.x]
6 **Salmanian AH**, Siavoshi F, Akbari F, Afshari A, Malekzadeh R. Yeast of the oral cavity is the reservoir of Heliobacter pylori. *J Oral Pathol Med* 2008; **37**: 324-328 [PMID: 18266659 DOI: 10.1111/j.1600-0714.2007.00632.x]
7 **Siavoshi F**, Taghikhani A, Malekzadeh R, Sarrafnejad A, Kashanian M, Jamal AS, Saniee P, Sadeghi S, Sharifi AH. The role of mother's oral and vaginal yeasts in transmission of Helicobacter pylori to neonates. *Arch Iran Med* 2013; **16**: 288-294 [PMID: 23641743]
8 **Saniee P**, Siavoshi F, Nikbakht Broujeni G, Khormali M, Sarrafnejad A, Malekzadeh R. Immunodetection of Helicobacter pylori-specific proteins in oral and gastric Candida yeasts. *Arch Iran Med* 2013; **16**: 624-630 [PMID: 24206402]
9 **Saniee P**, Siavoshi F, Nikbakht Broujeni G, Khormali M, Sarrafnejad A, Malekzadeh R. Localization of H.pylori within the vacuole of Candida yeast by direct immunofluorescence technique. *Arch Iran Med* 2013; **16**: 705-710 [PMID: 24329143]
10 **Salmanian** AH, Siavoshi F, Beyrami Z, Latifi-Navid S, Tavakolian A, Sadjadi A. Food borne yeasts serve as reservoirs of helicobacter pylori. *J Food Safety* 2012; **32**: 152-160 [DOI: 10.1111/j.1745-4565.2011.00362.x]
11 **Odds FC**, Bernaerts R. CHROMagar Candida, a new differential isolation medium for presumptive identification of clinically important Candida species. *J Clin Microbiol* 1994; **32**: 1923-1929 [PMID: 7989544]
12 **Soll DR**, Galask R, Schmid J, Hanna C, Mac K, Morrow B. Genetic dissimilarity of commensal strains of Candida spp. carried in different anatomical locations of the same healthy women. *J Clin Microbiol* 1991; **29**: 1702-1710 [PMID: 1761692]
13 **Soll DR**. Candida commensalism and virulence: the evolution of phenotypic plasticity. *Acta Trop* 2002; **81**: 101-110 [PMID: 11801217 DOI: 10.1016/s0001-706x(01)00200-5]
14 **Odds FC**. Candida infections: an overview. *Crit Rev Microbiol* 1987; **15**: 1-5 [PMID: 3319417 10.3109/10408418709104444]
15 **Nikbakht Brujeni G**, Jalali SA, Koohi MK. Development of DNA-designed avian IgY antibodies for quantitative determination of bovine interferon-gamma. *Appl Biochem Biotechnol* 2011; **163**: 338-345 [PMID: 20652441 DOI: 10.1007/s12010-010-9042-9]
16 **Jones** M, Johnson M, Herd T. Sensitivity of yeast vegetative cells and ascospores to biocides and environmental stress. *Lett Appl Microbial* 199; **12**: 254-257 [DOI: 10.1111/j.1472-765X.1991.tb00552.x]
17 **Bielański W**. Epidemiological study on Helicobacter pylori infection and extragastroduodenal disorders in Polish population. *J Physiol Pharmacol* 1999; **50**: 723-733 [PMID: 10695554]
18 **Phaff HJ,** Starmer WT. Yeasts associated with plants, insects and soil, in The yeasts, Rose AH, Harisson JS, Editors. Academic Press: London. 1987: 181-205
19 **Ansorg R**, Schmid EN. Adhesion of Helicobacter pylori to yeast cells. *Zentralbl Bakteriol* 1998; **288**: 501-508 [PMID: 9987188 DOI: 10.1016/s0934-8840(98)80069-8]
20 **Winiecka-Krusnell J**, Wreiber K, von Euler A, Engstrand L, Linder E. Free-living amoebae promote growth and survival of Helicobacter pylori. *Scand J Infect Dis* 2002; **34**: 253-256 [PMID: 12064686 DOI: 10.1080/00365540110080052]
21 **Dutt P**, Chaudhary S, Kumar P. Oral health and menopause: a comprehensive review on current knowledge and associated dental management. *Ann Med Health Sci Res* 2013; **3**: 320-323 [PMID: 24116306 DOI: 10.4103/2141-9248.117926]
22 **Scannerini** S, Bonfante P. Bacteria and bacteria like objects in endomycorrhizal fungi (Glomaceae). Symbiosis as Source of Evolutionary Innovation: Speciation and Morphogenesis, 1991: 273-287
23 **Bianciotto V**, Lumini E, Lanfranco L, Minerdi D, Bonfante P, Perotto S. Detection and identification of bacterial endosymbionts in arbuscular mycorrhizal fungi belonging to the family Gigasporaceae. *Appl Environ Microbiol* 2000; **66**: 4503-4509 [PMID: 11010905 DOI: 10.1128/aem.66.10.4503-4509.2000]
24 **Bianciotto V**, Bandi C, Minerdi D, Sironi M, Tichy HV, Bonfante P. An obligately endosymbiotic mycorrhizal fungus itself harbors obligately intracellular bacteria. *Appl Environ Microbiol* 1996; **62**: 3005-3010 [PMID: 8702293]
25 **MacDonald** RM, Chandler MR, Mosse B. The occurrence of bacterium-like organelles in vesicular-arbascular mycorizal fungi. *New Phytol* 1982; **90**: 659-663 [DOI: 10.1111/j.1469-8137.1982.tb03275.x]
26 **Gehrig H**, Schüssler A, Kluge M. Geosiphon pyriforme, a fungus forming endocytobiosis with Nostoc (cyanobacteria), is an ancestral member of the Glomales: evidence by SSU rRNA analysis. *J Mol Evol* 1996; **43**: 71-81 [PMID: 8660431 DOI: 10.1007/bf02352301]
27 **Haas A**, Goebel W. Microbial strategies to prevent oxygen-dependent killing by phagocytes. *Free Radic Res Commun* 1992; **16**: 137-157 [PMID: 1601328 DOI: 10.3109/10715769209049167]
28 **Cavalier-tsmith T**. The origin of nuclei and of eukaryotic cells. *Nature* 1975; **256**: 463-468 [PMID: 808732 DOI: 10.1038/256463a0]
29 **Bozue JA**, Johnson W. Interaction of Legionella pneumophila with Acanthamoeba castellanii: uptake by coiling phagocytosis and inhibition of phagosome-lysosome fusion. *Infect Immun* 1996; **64**: 668-673 [PMID: 8550225]
30 **Berk SG**, Ting RS, Turner GW, Ashburn RJ. Production of respirable vesicles containing live Legionella pneumophila cells by

two Acanthamoeba spp. *Appl Environ Microbiol* 1998; **64**: 279-286 [PMID: 9435080]
31 **Linares** L, Marín C. Frequency of yeasts of the genus Candida in humans as pathogens and as part of normal flora. In Proceedings of the IV International Conference on the Mycoses. 1978
32 **Tylenda CA**, Larsen J, Yeh CK, Lane HC, Fox PC. High levels of oral yeasts in early HIV-1 infection. *J Oral Pathol Med* 1989; **18**: 520-524 [PMID: 2575167 DOI: 10.1111/j.1600-0714.1989.tb01355.x]
33 **Hoffmann JN**, You HM, Hedberg EC, Jordan JA, McClintock MK. Prevalence of bacterial vaginosis and Candida among postmenopausal women in the United States. *J Gerontol B Psychol Sci Soc Sci* 2014; **69** Suppl 2: S205-S214 [PMID: 25360022 DOI: 10.1093/geronb/gbu105]
34 **Baingana RK**, Kiboko Enyaru J, Davidsson L. Helicobacter pylori infection in pregnant women in four districts of Uganda: role of geographic location, education and water sources. *BMC Public Health* 2014; **14**: 915 [PMID: 25190150 DOI: 10.1186/1471-2458-14-915]
35 **Sasaki K**. Candida-associated gastric ulcer relapsing in a different position with a different appearance. *World J Gastroenterol* 2012; **18**: 4450-4453 [PMID: 22969213 DOI: 10.3748/wjg.v18.i32.4450]

P- Reviewer: Engin AB, Tongtawee T, Yokota S **S- Editor**: Gong ZM
L- Editor: A **E- Editor**: Ma YJ

Published by **Baishideng Publishing Group Inc**
7901 Stoneridge Drive, Suite 501, Pleasanton, CA 94588, USA
Telephone: +1-925-223-8242
Fax: +1-925-223-8243
E-mail: bpgoffice@wjgnet.com
Help Desk: http://www.f6publishing.com/helpdesk
http://www.wjgnet.com

ISSN 1007-9327